

**CHARACTERIZATION OF THE CLINICAL
UROPATHOGENIC *Escherichia coli* ISOLATES
AND THEIR HOST-PATHOGEN INTERACTION:
A MOLECULAR PERSPECTIVE**

A Thesis submitted for The Degree of
Doctor of Philosophy (Science) Under Jadavpur University

by

SNEHASHIS KOLEY

INDEX NO. 97/19/LifeSc./26 of 2019-20

Department of Life Science and Biotechnology

Jadavpur University

Jadavpur, Kolkata – 700032

2023



TELE. ADDRESS
"TROPMED"

CALCUTTA SCHOOL OF TROPICAL MEDICINE
GOVT. OF WEST BENGAL
108, CHITTARANJAN AVENUE
KOLKATA - 700 073

Phones : 03322123695
03322123696
03322123697
Fax : 03322123698
Website : www.stmkolkata.org

THE 7th November 20 23

CERTIFICATE FROM THE SUPERVISOR

This is to certify that the thesis entitled "**CHARACTERIZATION OF THE CLINICAL UROPATHOGENIC *Escherichia coli* ISOLATES AND THEIR HOST-PATHOGEN INTERACTION: A MOLECULAR PERSPECTIVE**" Submitted by **Sri SNEHASHIS KOLEY** who got his name registered on 4th September, 2019 for the award of **Ph. D. (Science)** Degree of **Jadavpur University**, is absolutely based upon his own work under the supervision of **Dr. Mandira Mukherjee** and that neither this thesis nor any part of it has been submitted for either any degree / diploma or any other academic award anywhere before.

Date: 07.11.2023

Seal:

Dr. Mandira Mukherjee, PhD
Associate Professor
Department of Biochemistry & Medical Biotechnology
Calcutta School of Tropical Medicine
Kolkata-700 073

Mandira Mukherjee

(Signature of the Supervisor)

Name: **Dr. Mandira Mukherjee**

Designation: Associate Professor and Head

Department of Biochemistry and Medical Biotechnology,

School of Tropical Medicine, Kolkata – 73

Dedication

This thesis is dedicated to some of the most important persons in my life, without whose constant support and encouragement this work would not be possible.

Dr. Mandira Mukherjee (Research Guide)

Mr. Ashok Koley (Father)

Mrs. Archana Koley (Mother)

Mrs. Priya Kumar Koley (Wife)

Mr. Joydeb Kumar (Father-in-law)

Mrs. Tapashii Kumar (Mother-in-law)



Acknowledgment

I would like to thank God, the Almighty for blessing me and providing me the enormous strength to successfully complete my doctoral research work in the first place, with the utmost respect and humble gratitude.

*I want to express my sincere gratitude to my advisor, **Dr. Mandira Mukherjee**, the Head of the Department of Biochemistry and Medical Biotechnology, at The School of Tropical Medicine, Kolkata; for her unwavering support in terms of both professional, practical and academic assistance. I was able to complete this thesis thanks to her persistence, encouragement, excitement, vast knowledge, and faith in my abilities. Without the assistance, encouragement, and patience of the Dr. Mukherjee – not to mention her counsel and unmatched expertise in the fields of Microbiology, Molecular Biology, and Immunology – this thesis would not have been feasible. Working under her direction has increased my interest in and curiosity about conducting research. Working under her direction is a beautiful experience in and of itself. I firmly believe that the expertise, understanding, and information I have acquired in the areas of microbiology, molecular biology, and immunology during the years of my doctoral work will direct my professional path toward additional research and advancement. I have learned to think critically, choose challenges, solve them, and offer my ideas thanks to Dr. Mukherjee. For my doctoral studies, I couldn't have asked for a better advisor and mentor.*

*I would also like to thank **Prof. (Dr.) Subhasish Kamal Guha**, Director STM, Kolkata and past directors **Prof. (Dr.) Pratip Kumar Kundu** and **Prof. (Dr.) Nandita Basu (Ghorai)** for their kind support. I would also like to express sincere gratitude to the Department of Life Science and Biotechnology, Jadavpur University, Kolkata for allowing me to conduct this work. I would also like to thank **Dr. Bidhan Mondal** (Veterinarian, STM), **Dr. Santanu Munshi** (HOD, Department of Pharmacology and Experimental Biology, STM) and **Dr. Bibhuti Saha** (Dean, STM) for their constant support, whenever it was necessary.*

*I would also like to express gratitude to my mother **Mrs. Archana Koley**, my father **Mr. Ashok Koley**, and my wife **Mrs. Priya Kumar Koley** for their constant encouragement, unconditional, unambiguous, loving support. I am also extremely blessed to have consistent emotional support and encouragement from my in-laws and well-wishers.*

*I would like to specially thank my lab-mates **Dr. Shreya Basu**, **Dr. Sandip Kumar Mukherjee**, **Dr. Biplob Ghosh**, **Dr. Debojyoti Bandyopadhyay**, **Dr. Arunita Ghosh** and **Mr. Ambar Bose** for their perspective remarks, encouragement, intellectual and practical assistance.*

Abstract

In clinical practice, one of the most frequent bacterial infections is urinary tract infection (UTI), accounting for significant morbidity rates and high healthcare expenses. Pregnancy-related UTIs pose a major risk to the fetus and are frequently associated with premature birth, early membrane rupture, maternal chorioamnionitis, low birth weight, developmental retardation, or fetal necrosis. UTIs in non-pregnant population, especially in older women, can develop a number of consequences and if untreated can be fatal. 80%-90% of UTIs in both populations are caused by uropathogenic *Escherichia coli* (UPEC).

Urine culture is the gold standard for detection of UTI in human, and this time-consuming method leads to the empirical antibiotic prescription resulting in emergence of multi-drug resistance (MDR) and pose difficulty in its clinical management. Hence identification and in-depth characterization of UPEC from pregnant and non-pregnant population, with respect to their antibiotic resistance pattern, pathogenicity, colonization potential and the ability to elicit host-cytokine response is required to develop effective clinical measures against UTI.

In this study, statistically significant incidence of MDR with ESBL and carbapenemase production was observed among UPEC isolates from pregnant and non-pregnant groups. The distribution of major resistant genes (oxacillinase, cephalosporinase, carbapenemase), mobile genetic elements, plasmid replicon types, virulence factor genes were significantly prevalent among both groups. Phylogroup E, followed by novel phylotype property (NPP) were also prevalent in these two groups. Clonal heterogenicity and predominance of ST405 and CC131 were evident among isolates from both groups, with implication of zoonotic transmission. HTB-4 uroepithelial cells upon infection with UPEC isolates from pregnant population (UPECp) displayed a correlation between expression of *fimH* and *IFN γ* , *fimH* and *IL17A*, and *fimH* and *IL1 β* whereas a correlation was observed between expression of *papC* and *GCSF*, *hlyA* and *TGF β* upon infection with UPEC from non-pregnant population (UPECnp). The severity of infection was further tested *in vivo* in murine model with two different UPEC isolates from these two different groups, with different virulence scores and phylogenetic background. Upon infection in mice, they revealed highest bacterial colonization on different post-infection (p.i.) days, and displayed varying levels of cytokines; IL1 β , IL17A, GCSF and TGF- β in bladder and kidney tissues, and in serum. The IL1 β levels were significantly different amongst the two batches of mice infected with UPECp and UPECnp isolates. Hence IL-1 β might be a potent non-invasive marker to stratify the severity of UTI.

Therefore, this study revealed the necessity of cytokine profiling which is much less time-consuming in addition to urine culture and AMR analysis, to help clinicians to cease empiric treatment and formulate effective prescription policy in UTI.

Overview

“Every disease that’s with us is caused by DNA. And every disease can be fixed by DNA” – George McDonald Church (Geneticist)

“Almost all aspects of life are engineered at the molecular level, and without understanding molecules we can only have a very sketchy understanding of life itself” – Francis Crick

“I have learned more from my mistakes than from my successes” – Sir Humphry Davy

“The important thing is to never stop questioning [or learning]” – Albert Einstein

This research focuses on determining the potential of different interleukins as non-invasive markers both ex-vivo and in-vivo to get information about the infection potential of the microbes and their ability to trigger a host-cytokine response. It is hoped that, this study would be effective to establish the need of cytokine profiling in addition to urine culture and antimicrobial analysis.

Name: SNEHASHIS KOLEY

Signature: Snehashis Koley

Place: Kolkata

Date: 07.09.2023

Table of Contents

Chapter 1: Introduction	1 – 56
1.1. Urinary Tract Infection.....	2
1.2. History.....	2 – 3
1.3. Definition of terms	3 – 4
1.4. Classification of UTI.....	4 – 7
1.5. Diagnosis of UTI.....	7 – 11
1.6. Causative organisms of UTI.....	11
1.7. Uropathogenic <i>Escherichia coli</i>	12 – 13
1.8. Virulence factors associated with UPEC.....	13 – 19
1.9. UTI and pregnancy.....	19 – 26
1.10. The phylogenetic groups of <i>Escherichia coli</i>	26 – 28
1.11. Treatment of UTI.....	28 – 30
1.12. Antibiotic classifications and their mode of action.....	30 – 41
1.13. Misuse of antibiotics and Multi-drug resistance.....	41 – 45
1.14. Origin of Antibiotic resistance.....	45 – 46
1.15. Innate immune response of the host due to UTI.....	47 – 48
1.16. Adaptive immune response of the host due to UTI.....	48
1.17. References.....	48 – 56
Chapter 2: Identification and characterization of uropathogenic <i>Escherichia coli</i> from pregnant and non-pregnant population: MDR, ESBL and carbapenemase production	57 – 93
2.1. Background of the study.....	58
2.2. Objectives of the study.....	58
2.3. Materials	58 – 60
2.4. Experimental Procedures	60 – 76
2.5. Result	76 – 91
2.6. Discussion	91 – 93
2.7. References	147 – 152

Chapter 3: Characterization of MDR uropathogenic <i>Escherichia coli</i> isolates from pregnant and non-pregnant population according to acquired β-lactamase genes, mobile genetic elements and resistant plasmid replicon types.....	94 – 133
3.1. Background study	95
3.2. Objectives	95
3.3. Materials	95 – 96
3.4. Experimental Procedure	96 – 115
3.5. Result	115 – 128
3.6. Discussion	128 – 130
3.7. References	130 – 133
Chapter 4: Characterization of imipenem-resistant UPECp and UPECnp isolates according to phylogenetic background, virulence factor genes and clonal lineages.....	134 – 187
4.1. Background of the study.....	135 – 136
4.2. Objective.....	136
4.3. Materials	136 – 137
4.4. Experimental Procedure	137 – 159
4.5. Result	159 – 180
4.6. Discussion	180 – 182
4.8. References	182 – 187
Chapter 5: Host Cytokine Response upon Infection by different UPECp and UPECnp isolates with discrete virulence profile <i>ex-vivo</i>.....	188 – 223
5.1. Background study.....	189 – 190
5.2. Objectives.....	190
5.3. Materials.....	190 – 192
5.4. Experimental Procedure.....	192 – 203
5.5. Results.....	203 – 210
5.6. Discussion.....	210 – 215
5.7. Conclusion.....	215 – 216
5.8. References.....	216 – 223
Chapter 6: In-vivo experiments and analysis of cytokines to stratify the UPEC pathogenesis in mice model of UTI.....	224 – 255

6.1. Background study.....	225 – 226
6.2. Objective of the study.....	226
6.3. Materials.....	226 – 227
6.4. Experimental procedure.....	227 – 242
6.5. Results.....	242 – 252
6.6. Discussion.....	250 – 255
6.7. References.....	255 – 258
Conclusions from the study.....	259 – 260
Contributions from this study.....	261
List of Publications.....	262
Seminars and Workshops presented/attended.....	263

List of Tables

Table 1.1: Normal laboratory variables in pregnancy.....	21
Table 1.2: Different β -lactam antibiotics.....	34
Table 2.1: IMViC results for Enterobacteriaceae.....	71
Table 2.2: Triple sugar iron test results (for Enterobacteriaceae).....	73
Table 2.3: Zone of inhibitions of different antibiotics (According to CLSI guidelines 2018)	75
Table 2.4A: Growth Positivity, Gram staining results, and Biochemical test results collected from pregnant women.....	77 – 80
Table 2.4B: Growth Positivity, Gram staining results, and Biochemical test results collected from non-pregnant women.....	80 – 82
Table 2.5A: Zone of inhibition observed against different antibiotics in UPECp isolates...	83 – 84
Table 2.5B: Zone of inhibition observed against different antibiotics in UPECnp isolates...	84
Table 2.6A: Susceptible and resistance pattern against different antibiotics in UPECp isolates	84 – 85
Table 2.6B: Susceptible and resistance pattern against different antibiotics in UPECnp isolates	85 – 86
Table 2.7: Correlation of antibiotic resistance pattern in UPECp and UPECnp isolates.....	86 – 87
Table 2.8: ESBL phenotype confirmatory test results of UPECp and UPECnp isolates.....	88 – 89
Table 3.1: PCR reaction mixture.....	100

Table 3.2: Primer sequences for major oxacillinase, ESBL and carbapenemase genes identification used in this study.....	102
Table 3.3: Primer sequences for MGE identification used in this study.....	108 – 109
Table 3.4: Primer sequences for PBRT identification used in this study	114 – 115
Table 3.5A: Prevalence of aminopenicillinase, β -lactamase and carbapenemase resistance genes in UPECp isolates.....	116 – 117
Table 3.5B: Prevalence of aminopenicillinase, β -lactamase and carbapenemase resistance genes in UPECnp isolates.....	117 – 118
Table 3.6: Prevalence of mobile genetic elements in UPECp and UPECnp isolates.....	119 – 120
Table 3.7A: Prevalence of PBRTs in UPECp isolates.....	123 – 124
Table 3.7A: Prevalence of PBRTs in UPECnp isolates.....	124 – 125
Table 4.1: Primer sequences and PCR conditions for phylogenetic analysis used in this study	140 – 141
Table 4.2: Primer sequences and PCR conditions for virulence gene analysis used in this study	146 – 147
Table 4.3: Primer sequences and PCR conditions for Pathogenic island analysis used in this study	153
Table 4.4: Primer sequences and PCR conditions for MLST analysis used in this study.....	158
Table 4.5: Quadruplex PCR amplification result for UPECp and UPECnp isolates.....	159 – 160
Table 4.6: Comparison between imipenem-resistant UPECp (n=23) and UPECnp (n=29) isolates with respect to their phylogenetic background and virulence score.....	161
Table 4.7: Results of virulence genes distribution in UPECp and UPECnp isolates	163 – 164
Table 4.8: Distribution of VFG's and PAIs in imipenem-resistant UPECp an UPECnp isolates	164 – 165
Table 4.9: Results for pathogenic islands distribution in UPECp and UPECnp isolates.....	166 – 168
Table 4.10: Correlation between statistically significant prevalent PAI genes alongwith VFGs of imipenem resistant UPECp and UPECnp isolates.....	169
Table 4.11A: Virulence factor gene (VFG) scores, distribution of pathogenic islands, phylogenetic property, and resistance pattern against meropenem (MR), ertapenem (ETR) of the imipenem resistant UPECp (n=23) isolates.....	169 – 170
Table 4.11B: Virulence factor gene (VFG) scores, distribution of pathogenetic islands, phylogenetic property, and resistance pattern against meropenem (MR), ertapenem (ETR) of the imipenem-resistant UPECnp isolates.....	170
Table 4.12: Alleles of seven housekeeping genes in imipenem-resistant UPECp and UPECnp isolates along with their sequence types (ST) and clonal complexes (CC).....	176 – 178
Table 5.1: Primer sequences for virulence genes and interleukins used in this study.....	197 – 198

Table 5.2: Correlation of antibiotic resistance pattern in the UPECp and UPECnp isolates.....	204
Table 5.3: Correlation between expression of virulence genes and expression of cytokines in Uropathogenic <i>Escherichia coli</i> pregnant isolates.....	208 – 209
Table 5.4: Correlation between expression of virulence genes and expression of cytokines in Uropathogenic <i>Escherichia coli</i> non-pregnant isolates.....	209 – 210
Table 6.1: Distribution of virulence factor genes (VFGs) and phylogenetic background in <i>Escherichia coli</i> P025 and <i>Escherichia coli</i> NP105.....	242

List of Figures

Figure 1.1: Schematic representation of the Urinary Tract Infection	2
Figure 1.2: (a), (b) Pathogenesis of Urinary Tract Infection.....	8
Figure 1.3: Complicated and Uncomplicated UTIs caused by Uropathogenic <i>Escherichia coli</i> and other uropathogens worldwide.....	12
Figure 1.4: Virulence and Fitness factors of Uropathogenic <i>Escherichia coli</i>	14 – 15
Figure 1.5: GFR and Effective Renal Plasma Flow during pregnancy.....	20
Figure 1.6: Dichotomous decision tree to determine the phylogenetic group by the Clermont triplex PCR method.....	27
Figure 1.7: Dichotomous decision tree to determine the phylogenetic group by the Clermont quadruplex PCR method.....	28
Figure 1.8: Antibiotic target sites	31
Figure 1.9: Different classes of bacterial cell wall inhibitors	32
Figure 1.10: Core structure of beta-lactam antibiotics	32 – 33
Figure 1.11: Mechanism of action of beta-lactam antibiotics	33
Figure 1.12: General Mechanisms of Protein Synthesis Inhibitors	36
Figure 1.13: Mechanism of action of Aminoglycoside and Tetracycline.....	37
Figure 1.14: Core structure of Quinolone group of antibiotics	39
Figure 1.15: Mode of action of Fluoroquinolones.....	40
Figure 1.16: Global AMR death aspect by the year 2050.....	42
Figure 1.17: Distribution of <i>E. coli</i> resistance pattern to Cephalosporins and Fluoroquinolones	43
Figure 1.18: Distribution of <i>E. coli</i> resistance pattern to Aminoglycosides and Carbapenem	43
Figure 1.19: Distribution of <i>E. coli</i> resistance pattern to Aminopenicillins and Amoxicillin-clavulanate	44
Figure 1.20: Distribution of <i>E. coli</i> resistance pattern of Macrolides and Piperacillin-tazobactam	44

Figure 1.21: Country-wise consumption of antibiotics, where India is at the top of the list in antibiotic consumption in recent times.....	45
Figure 2.1: (A) Eden Hospital, MCH, Kolkata (B) School of Tropical Medicine, Kolkata (C) Carmichael Hospital of Tropical Medicine.....	61
Figure 2.2: Isolates showing clinical growth in LB broth and nutrient agar plate.....	62
Figure 2.3: Cell wall of gram-negative and gram-positive organism.....	62
Figure 2.4: Staining procedures at a glance.....	63
Figure 2.5: Gram-positive and gram-negative bacteria staining.....	63
Figure 2.6: Growth of gram-negative bacteria on MacConkey agar.....	64
Figure 2.7: Mechanism of Indole test.....	65
Figure 2.8: Indole positive and indole negative results.....	66
Figure 2.9: Methyl red positive and methyl red negative results.....	67
Figure 2.10: Mechanism of VP test.....	68
Figure 2.11: Voges Proskauer positive and negative results.....	69
Figure 2.12: Mechanism of citrate test.....	70
Figure 2.13: Citrate Utilization Test positive and negative results	70
Figure 2.14: Triple sugar iron results	72
Figure 2.15: Colonies in Eosin Methylene Blue agar plates	74
Figure 2.16: Resistance pattern against different antibiotics in UPECp and UPECnp isolates	86
Figure 2.17: Representative picture of the antibiotic susceptibility test	88
Figure 2.18: Distribution of ESBL, BLIR and non-ESBL in UPECp and UPECnp isolates..	90
Figure 2.19: Representative picture of MIC by IPM MIC strips.....	90
Figure 2.20: Representative picture of (A) MBL positive (B) MBL negative isolates.....	91
Figure 3.1: Polymerase chain reaction – An overview.....	100
Figure 3.2: The active-site serine at position 71 and position 179.....	101
Figure 3.3: Representative pictures of aminopenicillinase (<i>bla</i> _{OXA-I} , <i>bla</i> _{OXA-II} , <i>bla</i> _{OXA-III}), ESBL (<i>bla</i> _{TEM} , <i>bla</i> _{CTX-M}) and carbapenemase (<i>bla</i> _{NDM} , <i>bla</i> _{OXA-48}) genes on agarose gel electrophoresis. M represents the DNA marker lane (100bp DNA ladder)	115
Figure 3.4: Heatmap representation of β -lactamase genes in the UPEC isolates collected from (a) pregnant women (b) non-pregnant women. The cluster analysis was based on presence and absence of <i>bla</i> _{TEM} , <i>bla</i> _{CTX-M} , <i>bla</i> _{OXA-I} , <i>bla</i> _{OXA-II} , <i>bla</i> _{OXA-III} , <i>bla</i> _{NDM} , <i>bla</i> _{OXA-48} either alone or in varied combinations. Numbers	

in right side indicates sample ID of each isolates. Color key represented the variation in colors from red to white, illustrating the absence of particular gene to its presence respectively..... 118 – 119

Figure 3.5: Representative picture of integrases (*intI1*, *intI2*) and insertion sequences (*IS5*, *IS26*, *ISEcp1*) on agarose gel electrophoresis. M represents the DNA marker lane (100bp DNA ladder).. 120

Figure 3.6: Heatmap representation of different combinations of MGEs; integrons (*intI1*, *intI2*) and insertion elements (*IS5*, *IS26*, *ISEcp1*) in *bla*_{TEM} positive (a) *bla*_{TEM} negative (b) UPEC isolates collected from pregnant women. Numbers in right side indicates sample ID of each isolates. Color key represented the variation in colors from red to white, illustrating the absence of specific combination of MGEs to the presence of that particular combination respectively..... 121 – 122

Figure 3.7: Heatmap representation of different combinations of MGEs; integrons (*intI1*, *intI2*) and insertion elements (*IS5*, *IS26*, *ISEcp1*) in *bla*_{TEM} positive (a) *bla*_{TEM} negative (b) UPEC isolates collected from non-pregnant women. Numbers in right side indicates sample ID of each isolates. Color key represented the variation in colors from red to white, illustrating the absence of specific combination of MGEs to the presence of that particular combination respectively..... 121 – 122

Figure 3.8: Representative picture of Plasmid based replicon types run on Agarose gel electrophoresis. M represents the DNA marker lane (100bp DNA ladder)..... 125

Figure 3.9: Heatmap representation of multiple-replicon plasmids in the *bla*_{TEM} positive (a) *bla*_{TEM} negative (b) UPEC isolates collected from pregnant women. Numbers in right side indicates sample ID of each UPEC isolates. Color key represented the variation in colors from red to white, illustrating the absence of specific combination of multiple-replicon plasmids to presence of that particular combination respectively..... 126 – 127

Figure 3.10: Heatmap representation of multiple-replicon plasmids in the *bla*_{TEM} positive (a) *bla*_{TEM} negative (b) UPEC isolates collected from non-pregnant women. Numbers in right side indicates sample ID of each UPEC isolates. Color key represented the variation in colors from red to white, illustrating the absence of specific combination of multiple-replicon plasmids to presence of that particular combination respectively..... 127 – 128

Figure 4.1: Quadruplex genotypes and steps required for assigning *E. coli* isolates to phylo-groups 140

Figure 4.2: Representative pictures of the quadruplex genes *chuA*, *yjaA*, *TspE4.C2* and *arpA* genes, and *arpA.gpE* (for E-specific phylogroup). M represents the DNA marker lane (100 bp DNA ladder) 161

Figure 4.3: Representative pictures of adhesion genes (*fimH*, *papC*, *papEF*, *papGI*, *papGII*, *papGIII*, *sfaA*, *afaA*); toxin genes (*hlyA*, *iroN*, *chuA*, *iha*, *cnfI*, *iucD*, *cdtBU*, *vat*, *ibeA*, *usp*), capsule gene (*kpsMTII*), biofilm forming genes (*flu*, *csgA*) in agarose gel electrophoresis. M represents the DNA marker lane (100 bp DNA ladder)..... 162 – 163

Figure 4.4: Statistical representations of the correlations between twenty-one VFGs among (a) UPECp isolates and (b) UPECnp isolates. Correlations were individually computed among UPECp and UPECnps using Graphpad Prism 8 (Prism software package). Heat maps were generated on the correlation coefficient values represented by the color keys that ranged from (-) 0.5 (black) to (+)1 (white) 166

Figure 4.5: Representative pictures of PAI I₅₃₆, PAI II₅₃₆, PAI III₅₃₆, PAI IV₅₃₆, PAI I_{CFT073}, PAI II_{CFT073}, PAI I₉₆, PAI II₉₆ markers on agarose gel electrophoresis. M1 (100bp DNA ladder) and M2 (1kb DNA ladder) represents the DNA marker lane..... 168

Figure 4.6: The representative chromatograms of seven different housekeeping genes obtained after sequencing of an isolates NP048 (a) *adk* [(536bp), allele no. 35]; (b) *fumC* [(469bp), allele no. 37]; (c) *gyrB* [(460bp), allele no. 29] (d) *icd* [(518bp), allele no. 25], (e) *mdh* [(452bp), allele no. 4]; (f) *purA* [(478bp), allele no. 5] (g) *recA* [(510bp), allele no. 73]. A part of the entire chromatogram of the respective genes had been depicted above. Allele numbers were obtained from MLST data analysis mentioned in ‘experimental procedure’ section..... 171 – 174

Figure 4.7: The representative chromatograms of seven different housekeeping genes obtained after sequencing of an isolates P033 (a) *adk* [(536bp), allele no. 10]; (b) *fumC* [(469bp), allele no. 11]; (c) *gyrB* [(460bp), allele no. 4] (d) *icd* [(518bp), allele no. 8], (e) *mdh* [(452bp), allele no. 8]; (f) *purA* [(478bp), allele no. 13] (g) *recA* [(510bp), allele no. 2]. A part of the entire chromatogram of the respective genes had been depicted above. Allele numbers were obtained from MLST data analysis mentioned in ‘experimental procedure’ section..... 174 – 176

Figure 4.8: Representative pictures of *adk*, *fumC*, *gyrB*, *mdh*, *recA*, *purA*, *icd* control genes on agarose gel electrophoresis. M represents the DNA marker lane (100bp DNA ladder)..... 178 – 179

Figure 4.9: Maximum likelihood tree constructed using MEGA 11.0 based on the nucleotide sequence of seven housekeeping genes: *adk*, *gyrB*, *fumC*, *icd*, *mdh*, *purA* and *recA*, and depicting inferred phylogeny of 52 UPEC. Sequence Types (ST), clonal complexes (CC), Origins, Phylogenetic Groups were displayed to the right of the dendrogram..... 179 – 180

Figure 5.1: Representative photo of confluent monolayer T24 uroepithelial cells seen under inverted microscope at 20X magnification 193

Figure 5.2: The representative picture for seeding of HTB-4 uroepithelial cells in 24-well tissue culture plate and T-25 flasks and maintaining them at 37°C with 5% CO₂ with constant humidity.... 194

Figure 5.3: Prevalence of six virulence genes in uropathogenic *Escherichia coli* pregnant (n=21) and non-pregnant isolates (n=21)..... 205

Figure 5.4A: Relative fold change of *fimH*, *papC*, *papGIII*, *sfaA*, *hlyA*, *iroN* genes in UPECp isolates 205

Figure 5.4B: Relative fold change of *fimH*, *papC*, *papGIII*, *sfaA*, *hlyA*, *iroN* genes in UPECnp isolates 205

Figure 5.5A: Relative fold change of *IL-6*, *IL-8*, *TNF-α*, *IFN-γ*, *MCP-1*, *G-CSF*, *IL-1β*, *IL17A*, *IL-5*, *TGF-β* of HTB-4 uroepithelial cells, due to infection by UPECp isolates..... 207

Figure 5.5B: Relative fold change of *IL-6*, *IL-8*, *TNF-α*, *IFN-γ*, *MCP-1*, *G-CSF*, *IL-1β*, *IL17A*, *IL-5*, *TGF-β* of HTB-4 uroepithelial cells, due to infection by UPECnp isolates..... 207

Figure 6.1: Urinary catheter. Urinary catheters are made out of polyethylene tubing on a 30-G hypodermic syringe. An unused catheter (a) has extra tubing hanging off the end of the needle (b). The extra tubing is cut off near the bevel of the needle prior to use..... 228

Figure 6.2: BALB/C mice in a cage kept in conditions and access of food mentioned in 6.4.1.3. 229

Figure 6.3: Catheterization process in the bladder of a BALB/C mice..... 230

Figure 6.4: (From left to right) A. Position of the mice for autopsy B. Opening of the abdominal wall C. kidney and ureter extraction D. more detailed view for bladder removal..... 231

- Figure 6.5: Bacterial colonization (CFU/ml) in (A) bladder (left) and (B) kidney (right) of mice infected with *E. coli* NP105 ☒ and *E. coli* P025 ■ and were euthanized on days 5, 7, 9, 12 and 15 p.i. Data were represented as the means \pm standard deviations (SD). * $p < 0.05$, ** $p < 0.01$, *** $p < 0.001$ and **** $p < 0.0001$ above the bars indicated differences among the infected groups..... 243
- Figure 6.6: Histopathology of bladder and kidney samples of mice infected with *E. coli* P025 and *E. coli* NP105 on day 7th and day 9th p.i. Microscopic images were apprehended at 40X magnification 244
- Figure 6.7: Relative expression of *fimH* in (A) bladder and (B) kidney of *E. coli* NP 105 ☒ and *E. coli* P025 ■ and euthanized on days 5, 7, 9, 12 and 15 p.i. Data were presented as the means \pm SD. * $p < 0.05$ above the bars indicate differences in fold expression between the infected groups. Non-significant differences are represented as ‘ns’..... 245
- Figure 6.8: Relative expression of *papC* in bladder(A) and kidney(B) tissues of mice infected with *E. coli* NP 105 ☒ and *E. coli* P025 ■ and euthanized on days 5, 7, 9, 12, 15 p.i. Data are presented as the means \pm SD. * $p < 0.05$ above the bars indicate differences in fold expression between the infected groups. Non-significant are represented as ‘ns’..... 245
- Figure 6.9: Relative expression of *hlyA* in bladder (A) and kidney (B) of *E. coli* P025 ■ and euthanized on days 5, 7, 9, 12 and 15 p.i. Data are represented as the means \pm SD. * $p < 0.05$ above the columns indicate significant differences compared with the uninfected group and p values above the bars indicate differences among the infected groups..... 246
- Figure 6.10: IL-1 β levels in bladder (A), kidney (B) and serum (C) from mice that were uninfected or infected with *E. coli* NP105☒ and *E. coli* P025 ■and euthanized on days 5, 7, 9, 12 and 15 p.i. Data are represented as the means \pm SD. * $p < 0.05$, ** $p < 0.01$, and *** $p < 0.001$ indicate significant differences compared with the uninfected group..... 247 – 248
- Figure 6.11: IL-17A levels in bladder (A), kidney (B) and serum (C) from mice that were uninfected or infected with *E. coli* NP105 and *E. coli* P025 and euthanized on days 5, 7, 9, 12, and 15 p.i. Data are represented as the means \pm SD. * $p < 0.05$, ** $p < 0.01$, and *** $p < 0.001$ indicate significant differences compared with the uninfected group..... 248 – 249
- Figure 6.12: GCSF levels in bladder (A), kidney (B) and serum (C) from mice that were uninfected or infected with *E. coli* NP105 and *E. coli* P025 and euthanized on days 5, 7, 9, 12, and 15 p.i. Data are represented as the means \pm SD. * $p < 0.05$, ** $p < 0.01$, and *** $p < 0.001$ indicate significant differences compared with the uninfected group..... 250 – 251
- Figure 6.13: TGF- β levels in bladder (A), kidney (B) and serum (C) from mice that were uninfected or infected with *E. coli* NP105 and *E. coli* P025 and euthanized on days 5, 7, 9, 12, and 15 p.i. Data are represented as the means \pm SD. * $p < 0.05$, ** $p < 0.01$, and *** $p < 0.001$ indicate significant differences compared with the uninfected group..... 251 – 252

List of Abbreviations:

E. coli: *Escherichia coli* • **UPEC:** Uropathogenic *Escherichia coli* • **UTI:** Urinary Tract Infection • **IMViC test:** (I) Indole test, (M) Methyl red test, (V) Voges-Proskauer test (C) Citrate test • **TSI:** Triple Sugar Iron Test • **EMB agar:** Eosin Methylene Blue Agar • **LB:** Luria Bertani • **MH:** Mueller Hinton • **SDW:** Single Distilled Water • **DDW:** Double Distilled Water • **OD:** Optical Density • **CFU:** Colony Forming Unit • **CLSI:** Clinical and Laboratory Standard Institute • **AK:** Amikacin • **AMP:** Ampicillin • **CAZ:** Ceftazidime • **CTX:** Cefotaxime • **CIP:** Ciprofloxacin • **NIT:** Nitrofurantoin • **COT:** Co-Trimoxazole • **IPM:** Imipenem • **MRP:** Meropenem • **ETR:** Ertapenem • **CAC:** Ceftazidime-Clavulanic Acid • **CEC:** Cefotaxime-Clavulanic Acid • **CV:** Crystal Violet • **CV-I:** Crystal Violet Iodine • **MDR:** Multidrug resistant • **ESBL:** Extended spectrum β -lactamase • **BLIR:** β -lactamase inhibitor resistance • **TEM:** Temoneira • **CTX-M:** Cefotaxime-Munich • **OXA:** Oxacillinase • **NDM:** New Delhi Metallo β -lactamase • **EDTA:** Ethylenediaminetetraacetic acid • **TAE:** Tris-acetate EDTA • **PCR:** polymerase chain reaction • **DNA:** Deoxyribonucleic acid • **RNA:** Ribonucleic acid • **dNTPs:** Deoxynucleotide triphosphates • **EtBr:** Ethidium Bromide • **VFs:** Virulence Factors • **PAIs:** Pathogenicity islands • **MGE:** Mobile Genetic Elements • **int:** integrases • **IS:** Insertion sequences • **PBRT:** Plasmid based replicon typing • **IDSA:** Infectious Disease Society of America • **MSA:** Multiple sequence alignment • **MLST:** Multilocus sequence typing • **RPM:** Revolutions per minute • **ST:** Sequence types • **CC:** Clonal Complexes • **UD:** Undetected • **IL:** Interleukins • **ATCC:** American type cell culture • **BALB:** Bagg Albino • **IL-6:** Interleukin 6 • **IL-8:** Interleukin 8 • **TNF- α :** Tumor necrosis factor- α • **IFN- γ :** Interferon- γ • **MCP-1:** Monocyte Chemoattractant protein-1 • **GCSF:** Granulocyte colony stimulating factor • **IL5:** Interleukin 5 • **IL17A:** Interleukin 17A • **TGF β :** Transforming growth factor- β • **IL1 β :** Interleukin 1- β , **AMR:** Antimicrobial Resistance

Chapter 1: Introduction

1.1 Urinary Tract Infection:

- **Mayo Clinic:** A Urinary tract infection (UTI) is an infection in any part of the urinary system. The urinary system includes kidneys, ureters, bladder and urethra. Most infections involve the lower urinary tract – the bladder and the urethra.
- **Center for Disease Control and Prevention:** UTIs are common infections that happen when bacteria, often from the skin or rectum, enter the urethra and infect the urinary tract. The infections can affect several parts of the urinary tract, but the most common type is a bladder infection (cystitis). Kidney infection (pyelonephritis) is another type of UTI. They're less common, but more serious than bladder infections.
- **Cleveland Clinic:** A urinary tract infection (UTI) is an infection of your urinary system. This type of infection can involve your: urethra (urethritis), kidneys (pyelonephritis), and bladder (cystitis).
- **Urology care foundation (American Urological Association):** A urinary tract infection, or UTI, is when bacteria get into your urinary tract-kidneys, bladder, or urethra.

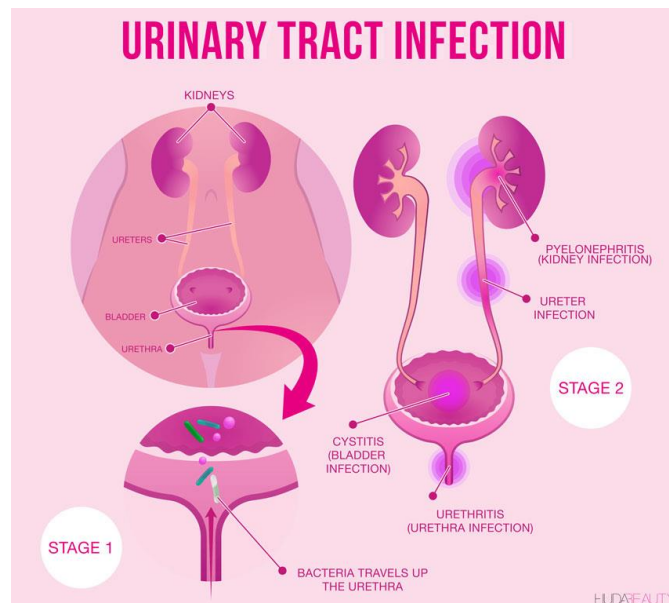


Figure 1.1: Schematic representation of the urinary tract infection

1.2 History

Urinary tract infections have been recognized since ancient times. The 'Ebers Papyrus' records that the ancient Egyptians used herbs to treat urinary tract diseases [1]. The

Roman doctors advised bed rest, diet, herbs, and narcotics for treating these infections, while the Arabs invented ‘uroscopy’. The Greeks believed that a UTI was caused by disharmony. Moreover, the Romans developed surgery for kidney stones. Almost identical methods to those used by Romans were employed by European physicians in the middle ages and until the nineteenth century, and of course, “bleeding” was also practiced. Ancient treatments for UTI were mostly palliative because they were never able to understand the root cause of the condition. Several antibacterial treatments were employed to treat UTIs before antibiotics were discovered, but their efficacy was minimal at best [2]. The mucosa layer that guards against stone disease is protected by an antibacterial effect found in herbal treatments for stone disease. (Additional mechanisms of herbs against stone disease include a diuretic effect, modifications in urine’s ionic composition, and the presence of saponins, which work by dispersing mucoproteins in urine that function by promoting crystallization and stone formation).

1.3 Definition of terms

1.3.1 Urinary Tract Infection: An UTI is described as an infectious agent adhering to, multiplying, and remaining in the urogenital system. A typical organism found in the distal urogenital tract is frequently involved in this. UTI most frequently involves a bacterial organism.

1.3.2 Microburia: It is the term used to describe the presence of microbes, usually bacteria, in urine.

1.3.3 Bacteriuria: The presence of bacteria in urine is referred to as bacteriuria. A urine sample may be contaminated by bacteria, especially if it was obtained during urethral catheterization or voiding. Urine collected using these techniques may contain bacteria from the distal urogenital tract, or urine may become contaminated after collection (e.g. during transfer to storage containers in the laboratory). Bacteriuria can be symptomatic or asymptomatic. One or more organisms have colonized a urine sample in a patient with asymptomatic bacteriuria, which is further characterized as the absence of any signs of infection. Without bacteriuria, is not an illness. An illustration would be a patient with a long-term Foley who has no symptoms but who typically has significant bacteriuria. Symptomatic bacteriuria is linked to a urinary tract infection, typically to a urinary tract infection, brought on by a single organism. Cystitis and prostatitis are examples of the lower urinary tract (UTIs), while pyelonephritis and pyonephrosis are examples of upper UTIs. Because

they affect healthy, non-pregnant women, most UTIs are regarded as basic or uncomplicated. Those with a disease or a more resistant pathogen who have complicated UTIs have the risk of not responding to therapy.

1.3.4 Funguria: Fungi in the urine are referred to as funguria. Usually, fungi are not found in the urogenital system; therefore, their discovery indicates an infection, regardless of the presence of any clinical symptoms.

1.3.5 Pyuria: Pyuria is defined as the presence of three or more white blood cells per high-power field of unspun urine, 10 or more white cells per cubic millimeter in a urine specimen, a positive Gram's staining result for an unspun urine specimen, or a positive urine dipstick test for leukocyte esterase. Sterile pyuria is identified by aerobic laboratory procedures (on a 5% sheep-blood agar plate and Macconkey agar plate) as the prolonged presence of white blood cells in the urine in the absence of bacteria [3].

1.4 Classification of UTI:

This infection targets different parts of the urinary tract and as a consequence results in the contagion of the lower and upper urinary tracts to become contagious. The name of the infection is determined by the infection site.

1.4.1 Classification based on the infection site:

1.4.1.1 Urethritis: The inflammation and swelling of the urethra. It is a lower urinary tract infection. Urethra is a fibromuscular tube through which urine (in both males and females) and semen (in males) exit the body. Urethritis has a strong association with sexually transmitted infections (STIs). The main symptom of urethritis is pain with urination (dysuria) [4]. Additionally, other symptoms include:

- Feeling the frequent or urgent need to urinate
- Difficulty starting urination
- Pain during sex
- Discharge from the urethral opening or vagina
- Blood in semen or urine (for males)
- Itching, pain, or discomfort when a person is not urinating

1.4.1.2 Cystitis: Cystitis is the medical term for an infection of the bladder or lower urinary system. It can be broadly divided into complicated and straightforward categories. Symptoms may include:

- Pressure in lower pelvis pain
- Dysuria (painful urination)
- Polyuria (frequent urination)
- Urinary urgency
- Nocturia (urination during the night)
- Haematuria (urine with traces of blood)

Based on the etiology and therapeutic approach cystitis is further classified with traumatic cystitis being the most prevalent type in females and one of the most common forms associated with bladder bruising, often followed by bacterial cystitis. Through the urethra, coliform bacteria are transported to the bladder from the bowel [5].

1.4.1.3 Pyelonephritis: Commonly referred to as upper UTI. It occurs as a complication of an ascending UTI that spreads from the bladder to the kidneys. It is also known as ‘pyelitis’. Pyonephrosis is the term for a severe occurrence that results in pus binding up around the kidneys. Symptoms usually include fever, flank pain nausea, vomiting, burning with urination, and increased frequency and urgency [5].

Acute pyelonephritis can be divided into uncomplicated and complicated. Complicated pyelonephritis includes pregnant patients, patients with uncontrolled diabetes, kidney transplants, urinary anatomical abnormalities, acute or chronic kidney failure, as well as immunocompromised patients, and those with hospital-acquired bacterial infections.

Most patients develop acute pyelonephritis as a result of ascending infection, the progression of which involves multiple steps. To reach the bladder via the urethra, bacteria must first attach to urethral mucosal epithelial cells, which can happen through instrumentation or UTI infections which occur more frequently in females. Due to shorter urethras, hormonal changes, and proximity to the anus, females experience UTIs more frequently than males. Acute pyelonephritis may also result from obstruction of the urinary tract due to a kidney stone or another similar condition. Urinary stasis and incomplete emptying due to an outflow obstruction of urine,

causes bacteria to multiply without being flushed out. Vesicoureteral reflux, a congenital disease where urine flows backward from the bladder into the kidneys, is a less frequent cause of acute pyelonephritis [6].

1.4.2 Classification based on factors that trigger the infection and the nature of occurrence:

1.4.2.1 Uncomplicated UTI: This is an outcome of bacterial infection, and it affects more women than males. This also includes the common form of infection including cystitis and pyelonephritis, affecting lower and upper urinary tracts and resulting in bladder and kidney infections [5]. If the pathogen breaks the epithelial barrier of the kidney, UTI can turn into bacteremia. Both in men and women, bacterial growth in a catheterized sample as low as 10^2 cfu/ml may be regarded as bacteremia. Rectal examination should always be done on males as part of the urologic evaluation to look for prostatic risk factors.

1.4.2.2. Complicated UTI: Both men and women can get complicated UTIs at any time in their lives, and tends to produce severe outcomes resulting in death under serious circumstances. These infections are extremely complex, difficult to cure, and persistent. It can result in structural abnormalities that impair the ability of the urinary tract to flush out urine, which in turn provides better scope for the growth of bacteria because urine is thought to be a suitable growth medium and leads to dire consequences. Urinary catheters, which are frequently used by patients and act as a common source of infection, are one type of medical device that is frequently used on patients with UTI. Other causes of complicated UTI include renal and bladder dysfunction, as well as kidney transplants. The first three months, following a kidney transplant, are extremely important, and the patient is susceptible to such issues.

1.4.2.3. Recurrent UTI: Women who have had uncomplicated UTI frequently suffer this occurrence, which is classified as re-infection and relapse. After receiving antibiotic treatment for several weeks, the patient experiences severe UTIs sometimes, known as re-infections. Relapse is a less common kind of recurrent UTI. It results from inadequate therapy and the patient encounters the condition within two weeks of initial infection. Recurrent UTIs are typically linked to pyelonephritis, which can cause kidney failure, kidney obstruction from kidney stones, and morphological anomalies from both sexes. Additionally, the classification of UTIs divides them

into symptomatic and asymptomatic UTIs based on the severity of the symptoms displayed by the patients.

1.4.3. Classification based on Symptoms:

1.4.3.1. **Asymptomatic UTI:** Asymptomatic UTI or bacteriuria is the presence of bacteria in the properly collected urine of a patient that has no signs or symptoms of a urinary tract infection. In clinical practice, it is extremely prevalent. While ABU is uncommon in newborns and young children, it becomes more common as people age. When women and men are 65 to 80 years old, the incidence can reach 15% or more, and after that age, it can reach 40% to 50%. The majority of patients with ABU never experience symptomatic urinary tract infections and would have no adverse consequences from asymptomatic bacteriuria. There is sufficient evidence to recommend treating a pregnant woman with ABU. Additionally, individuals in the first three months after a kidney transplant and those undergoing urologic procedures when mucosal bleeding is anticipated should probably receive treatment for asymptomatic bacteriuria.

1.4.3.2. **Symptomatic UTI:** Symptomatic UTI is a prevalent clinical issue in elderly populations, and it is more common in women and men who have more functional impairments, including those who have chronic indwelling urethral catheters [7]. Trautner [8] defined symptomatic UTI as an event in which women visited the clinic with dysuria, frequency, or urgency plus a positive urine culture ($\geq 10^2$ cfu/ml with a uropathogen). A subclinical UTI was defined as *Escherichia coli* bacteriuria ($\geq 10^3$ cfu/ml), pyuria, and UTI symptoms on a day in which the woman did not present for medical care for these symptoms.

1.5. Diagnosis of UTI:

1.5.1. **Medical History:** The medical history serves as the essential foundation for the clinical diagnosis of the Urinary Tract Infection. Depending on certain factors, the likelihood of a urinary tract infection may increase (\uparrow) or decrease (\downarrow) [10]. Clinical research has proven the following variables.

Dysuria, pollakisuria, nycturia (\uparrow) • Present or increased incontinence (\uparrow) • Macrohematuria (\uparrow) • Suprapubic pain (\uparrow) • “Offensive” smell, turbid urine (\uparrow) • Prior infections of the urinary tract (\uparrow) • Changed or new discharge, vaginal irritation (\downarrow)

Additionally, risk factors that are known to increase the probability of UTI, include:

Sexual intercourse within the preceding two weeks • Contraception with a vaginal diaphragm or spermicide • Contraception with DMPA (depot medroxyprogesterone acetate) • Antibiotic administration within the preceding two to four weeks • Special anatomical features or restrictions (for example, from vesicoureteral reflux, neuropathic bladder, mechanical or functional obstruction) • Diabetes Mellitus

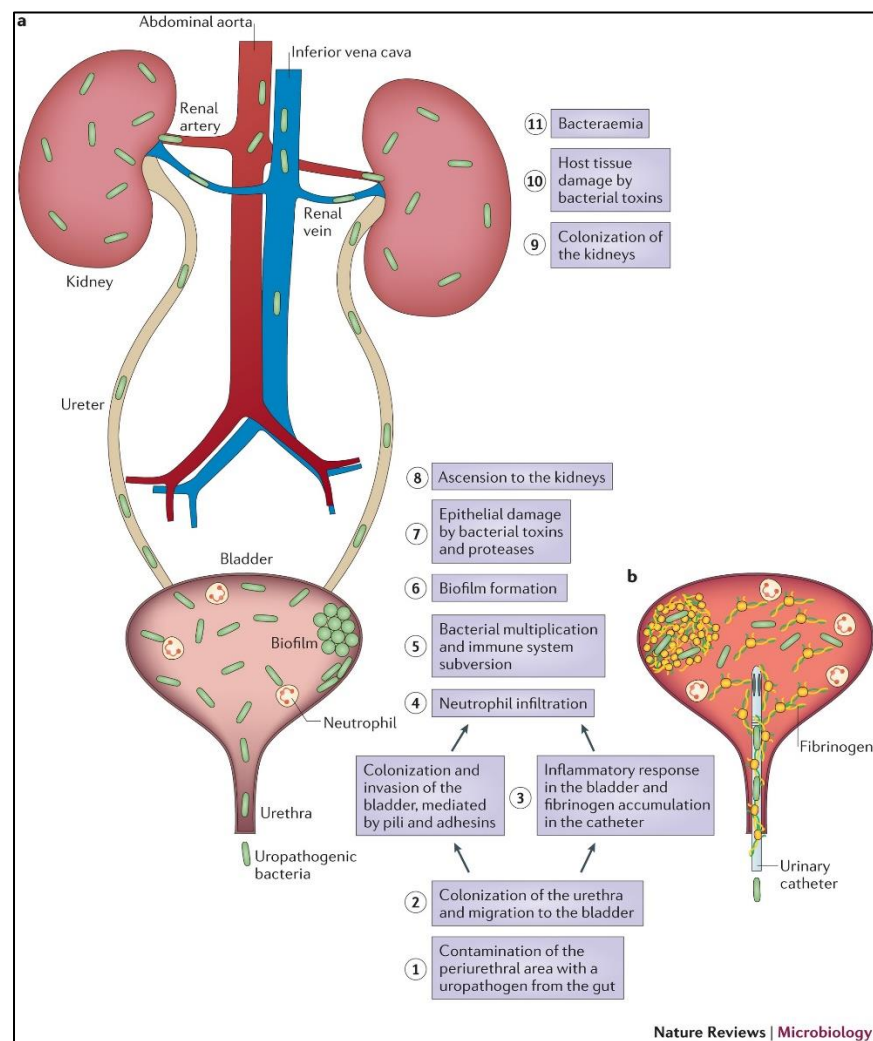


Figure 1.2: (a) & (b) Pathogenesis of urinary tract infection (Taken from Flores-Mireles et al., [9])

1.5.2 Urine Testing:

In diagnostic testing, urine testing is the second most important element.

1.5.2.1 Urine collection: The necessity of collecting midstream urine and cleaning the perineum, vulva, or glans penis has been the subject of several investigations. However, these were mostly with fairly young and otherwise healthy women, so it is not clear whether they can be transferred to normal clinical practice. Making the urine collection technique based on the clinical problem would be a pragmatic approach. Fresh spontaneous urine rather than midstream urine can be collected for a preliminary urine test using a dipstick, and genital cleaning is not essential. However, further research and urine culture call for the urine sample to be obtained and processed with the least amount of contamination possible.

1.5.2.2. Urine culture: To direct diagnostic tests, a urine culture should be acquired from all patients who show signs of UTI. The most accurate method of identifying a bacterial UTI is urine culture. Transporting and storing urine samples for aerobic bacterial culture should be done in sealed, sterilized containers, and processing should start right away. Refrigerate the sample at 4°C if laboratory processing takes more than 30 minutes.

1.5.2.3. Practical Test Methods: A bacteriological urine culture including pathogen identification, quantification, and sensitivity testing is the gold standard for a urine test. Introducing indirect approaches is frequently employed in practice to find the bacteria or inflammation (dipsticks) to determine whether the patient even has a UTI. The bacterial count may be assessed by urine microscopy and immersion culture media.

1.5.2.4. Dip Sticks: If there is clinical evidence that a patient has a UTI, urine dipsticks are one of the most often utilized diagnostic tools. Multistix is most often used, which may be able to detect nitrite (a metabolic product of typical pathogens of the urinary tract), leukocyte esterase, protein, and blood (as a marker of inflammation). A urinary tract infection is more likely to occur if nitrite is found, with an increased likelihood ratio [LR] of 2.6 to 10.6. the sensitivity is, however, not very high. On the other hand, the chance is only slightly increased (LR 1.0 to 2.6) by the presence of leukocyte esterase. The detection of blood is admittedly highly sensitive, but the specificity is low.

1.5.2.5. Urine Microscopy: Due to methodological limitations the sensitivity in detecting UTI with $\leq 10^5$ cfu/ml by gram-stained microscopy is low. Some studies have found that skilled professionals can perform diagnostic procedures with greater accuracy than urine cultures.

However, the existing microscopic investigations are heterogeneous, and all review publications conclude that it is challenging to draw broad conclusions [11].

1.5.2.6. Immersion culture media: A plastic rod coated with culture medium – typically a mixture of CLED agar and McConkey agar – is used in these immersion studies, and requires 24 hours' culture. Under the circumstances of primary care, the sensitivity and specificity levels achieved in the laboratory cannot be duplicated [12]. The sensitivity was determined to be 73% (95% confidence interval [CI] 66 – 80) and specificity was found to be 94% (CI 88 – 98) in the primary care context. The sensitivity is lowered to 65% (CI 55 – 74) in female patients who had previously had a negative nitrite test, with about the same specificity (CI 90 – 99). The accurate detection of $\leq 10^4$ cfu/ml is not possible with this method [13].

1.5.2.7. Blood Tests: A raised WBC count or C-reactive protein level is consistent with an infective illness. Blood culture positive for a known uropathogen in the absence of an alternative more likely source suggests a UTI, especially if urine culture is also positive for the same organism.

1.5.3. Diagnostic testing in special patient groups

It is frequently adequate to diagnose UTI simply based on these indirect test procedures for the (relatively frequent) case of uncomplicated UTI. An effort should typically be made to conduct a urine culture to identify the causative organisms and determine their susceptibility to various antibiotics for all complicated and therapy-resistant urinary tract infections [14].

1.5.3.1. Pregnant women: Treatment of asymptomatic bacteriuria in pregnant women decreases the occurrence of pyelonephritis and possibly also damage to the child. The dipsticks now being utilized in antenatal care testing, however, is quite insensitive. The detection rate for asymptomatic bacteriuria would be comparable to urine culture if immersion culture medium were employed frequently [15].

1.5.3.2. Female geriatric patients: In this group, the likelihood of having asymptomatic bacteriuria significantly increases. Thus, the prevalence ranges from 25% to 50% in aged care facility residents, even reaching 100% in catheterized patients. Both urine cultures and dipsticks are ineffective in verifying the clinical diagnosis of UTI in the latter group. An infection can only be ruled out by a negative urine culture. Antibiotic prescriptions in nursing homes have decreased

as a result of the development of particular diagnostic criteria for this population by an American consensus conference [16].

1.5.3.3. Female patients with diabetes mellitus: Female diabetic patients who receive medical treatment frequently display ABU or Urinary Tract Infection. The spectrum of bacteria and resistance rates are not distinct in this group. Therefore, it is legitimate to challenge the current practice of classifying this group as having complicated urinary tract infections [17].

1.5.3.4. Men: Urinary Tract Infections in men continue to be thought of as difficult infections. Urine culture testing is advised to confirm the diagnosis because dipstick testing is unreliable in this population. Unfortunately, there has not been much therapeutic or diagnostic research performed on men [18].

1.6. Causative Organisms of UTI:

Both Gram-negative and Gram-positive bacteria, as well as some fungi, are responsible for UTIs. Uropathogenic *Escherichia coli* (UPEC) is the most causative agent for both complicated and uncomplicated UTIs. *Klebsiella pneumoniae*, *Staphylococcus saprophyticus*, *Enterococcus faecalis*, Group B streptococcus (GBS), *Proteus mirabilis*, *Pseudomonas aeruginosa*, *Staphylococcus aureus*, and *Candida albicans*, followed by UPEC in terms of prevalence among the bacteria that cause uncomplicated UTI. For complicated UTI, the most frequent causative agent is UPEC, followed by *Enterococcus spp.*, *K. pneumoniae*, *Candida spp.*, *S. aureus*, *P. mirabilis*, *P. aeruginosa*, and GBS [9]. Based on the presence of genomic Pathogenicity Islands (PAI) and the expression of virulence components such as adhesins, toxins, surface polysaccharides, flagella, and iron-acquisition systems, four primary phylogroups (A, B1, B2, and D) have been identified [19].

The bladder epithelium, which is made up of umbrella cells (also known as superficial facet cells), intermediate cells, and basal cells, can attach directly to the uropathogens that cause uncomplicated UTIs, including UPEC, *K. pneumoniae*, and *S. saprophyticus*. Uroplakins, the main protein components of the umbrella cell apical membrane and which create a crystalline array shielding the human bladder tissue from harmful agents in urine, bind to UPEC and *K. pneumoniae*. Integrins, which are found on the surface of Uroepithelial cells, can act as UPEC receptors in addition to uroplakins.

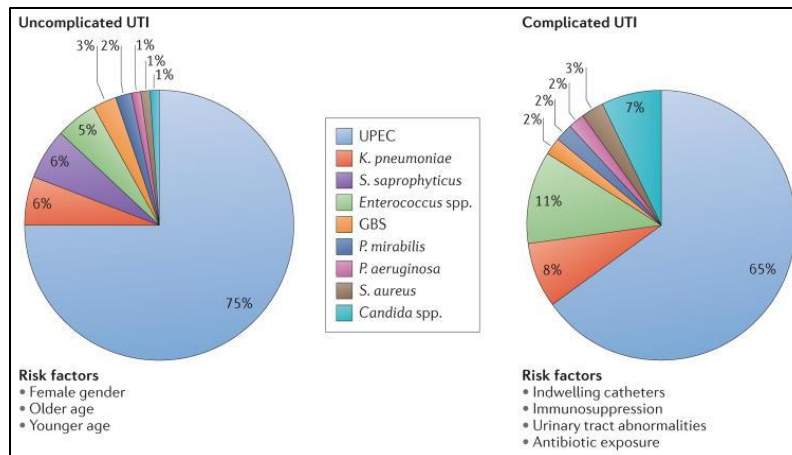


Figure 1.3: complicated and uncomplicated UTIs caused by uropathogenic *Escherichia coli* and other Uropathogens worldwide (Taken from Flores-Mireles et al., [9])

1.7 Uropathogenic *Escherichia coli* (UPEC):

Over 75% of UTI infections are caused by the common etiologic agent, uropathogenic *Escherichia coli*. Research on UPEC pathogenicity has been conducted because of its clinical importance. It turns out, as predicted, that the virulence of UPECs cannot be attributed to the presence of a specific component but rather to the coordinated expression of several genes depending on the urinary districts they colonize. Even though commensal *E. coli* and UPECs encode similarly, if not identically, UPECs are more virulent than commensals. Furthermore, due to their significant genetic similarity, it is difficult to identify these pathogens, making the discovery of *E. coli* strains in urine samples from symptomatic patients sufficient to refer to the discovery of a UPEC strain [20].

A single UPEC strain can encode more than 12 different chaperone-ushe pathway (CUP) pilus, and there are 38 different CUP pilus operons found in *E. coli* genomes. While some CUP pilus operons are present in all UPEC isolates, others are only identified in a small number of them, hence the distribution of CUP operons is not uniform. The many CUP pili encoded by UPEC are tipped with various adhesins, some of which are known to mediate unique tropisms in the lower and upper urinary tract by binding to receptors with stereochemical specificity, particularly in the bladder or kidney epithelium [9].

During UTIs, UPEC pathogenesis includes (a) UPEC colonization of the Periurethral and vaginal areas with the colonization of the urethra; (b) ascending into the bladder lumen and growth as planktonic cells in the urine; (c) adherence to the surface and interaction with the bladder epithelium defense system; (d) biofilm formation; (e) invasion and replication by forming bladder Intracellular Bacterial Communities (IBCs) where quiescent intracellular reservoirs (QIRs) form and reside in underlying urothelium; (f) kidney colonization and host tissue damage with increased risk for bacteremia/septicemia [21].

1.8. Virulence factors associated with UPEC:

The virulence factors that UPEC uses to colonize the bladder are crucial in the development of UTIs. These include surface structural components, such as lipopolysaccharides (LPS), polysaccharide capsules, flagella, outer-membrane proteins (OMPs), as well as secreted toxins, secretion systems, and TonB-dependent iron-uptake receptors. These are all intriguing prospects for the creation of novel medications and vaccines.

1.8.1. Adhesion factors: Pathogenic *E. coli* possess specific adherence factors that allow them to colonize sites that *E. coli* does not normally inhabit, such as the small intestine and urethra [22]. This is considered the first step in the colonization process, and both the host and the pathogen function in this process. For UPEC to be able to colonize, different fimbrial adhesins must be expressed.

1.8.1.1. Type-1 fimbriae: Genes that encode type-1-fimbriae are present in 99% of *E. coli* isolates [23], and by mediating an increased inflammation, they damage urinary tract cells during urinary tract infection [24]. The *fim* operon encodes type 1 pili which express a mannose-sensitive hemagglutination. Type 1 fimbriae are extremely versatile virulence factors that can maintain the attachment of the bacteria to different types of cells throughout the urinary system. Although their binding sites in Bowman's capsules and the glomerulus could not be identified, type 1 fimbriae showed a great affinity for proximal tubules and vessel walls. They bind firmly to the muscle layers and moderately to the vessel walls of the bladder. The distal tubules and collecting ducts were also revealed to contain type 1 fimbria receptors. Additionally, they can make them adhere to macrophage surfaces [25]. These fimbriae identify host proteins including mannoside and uroplakin produced by bladder epithelial cells. These adhesins, which are mostly made up of the

FimA protein along with FimF, FimG, and FimH [26], are encoded by the bacterial backbone DNA. FimH is one of the subunits of type 1 fimbria that determines the sugar specificity. Deletion of fimH reduces colonization in mouse models of ascending UTI, but the introduction of a plasmid containing the fimH gene can restore colonization [24].

1.8.1.2. P-fimbriae: Pyelonephritogenic P-fimbriated *E. coli* attach to the carbohydrate complex alpha-D-Galp-(1-4)-beta-D-Galp. They firmly adhere to Bowman's capsule, the glomerulus, and the endothelial cells that line vessel walls in the kidney. The highly organized composite structure is made up of at least six different parts. When P-fimbriae expressing *E. coli* reach the urinary tract, they establish bacteriuria. They also aid in breaking through the epithelial barrier to enter the circulation and can lead to erythrocyte hemagglutination [27]. The pap gene cluster (also known as *fso* and *fst*) encodes this kind of fimbriae, and pap⁺ strains persist longer in the gut flora than pap⁻ strains [28]. P antigens are expressed on the surface of red blood cells as well as in a variety of urinary tract lining cells.

1.8.1.3. Dr/Afa adhesins: Red blood cells have a membrane protein called Dr blood group antigen, which is found on the decay accelerating factor (DAF), which prevents autologous components from lysing or destroying red blood cells [29]. The uropathogenic *E. coli* Dr and Afa adhesin families can recognize these antigens. Adhesins come in both non-fimbrial (AFAI and AFAII) and fimbrial (F1845 and O75X) types. The Dr family of adhesins somehow mediates the immune invasion of UPEC by allowing the invaders to evade the host humoral immune response [30].

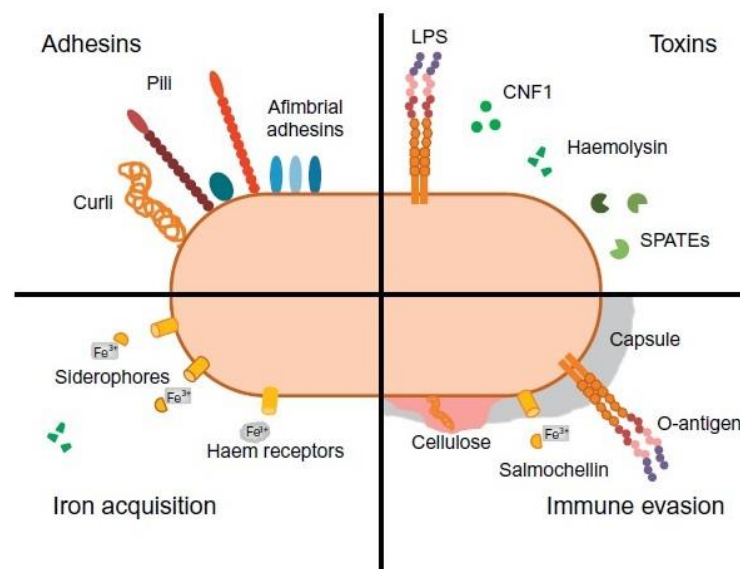


Figure 1.4: Virulence and fitness factors of uropathogenic *Escherichia coli*. (from Lüthje P, Brauner A. Virulence Factors of uropathogenic *E. coli* and their interaction with the host. *Advances in Microbial Physiology*, 2014; 65: 337 – 372)

1.8.1.4. Other fimbriae as virulence factors: A seven-gene operon called *focAICDFGH* encodes F1C, a virulence factor causing urinary tract infections. FocA is the main subunit while FocH is the tip adhesin. The muscle layer and bladder endothelium both have F1C receptors, which cannot bind to the epithelium. They bind to vascular endothelial cells, distal tubules, collecting ducts, and glomeruli. The incidence of type 1 fimbriae in UTI strains and normal fecal isolates differ little, although studies have shown a correlation between F1C fimbriae and pyelonephritis. The only genetic difference between S and F1C fimbriae is the tip adhesin SfaS. Various investigations on S fimbriae have established the requirements needed to be recognized as a virulence factor. Other adhesins, such as F9 fimbriae, are not essential for the survival of UPEC strains [30].

1.8.2. Toxins: As virulence factors in UTIs, several toxic substances or proteins secreted by uropathogenic *Escherichia coli* strains play a significant role. Toxins can, however, modify inflammatory responses and alter the host cell signaling cascade. Studies conducted both in vitro and in vivo revealed that toxins also have a role in the development of host cell death and the release of essential nutrients, which facilitate access to deeper tissues inside the urinary system [31].

1.8.2.1. α -hemolysin: One of the most significant toxins is α -hemolysin (HlyA), a lipoprotein that is a member of the RTX (repeats in toxin) toxin family [32]. HlyA is a pore-forming toxin that damages cell membranes and mediates inducible nitric-oxide-synthase (iNOS) apoptosis [33]. However, at high concentrations, HlyA can lyse erythrocytes and nucleated host cells by a process that allows UPEC, which could damage the host immune effector cells for enhanced access to the iron and nutrient stores. However, at low concentrations, HlyA can promote the exfoliation of bladder epithelial cells and induce apoptosis of target host cells [34].

1.8.2.2. Cytotoxic necrotizing factor 1 (CNF1): In addition to being involved in UTIs, cytotoxic necrotizing factor 1 (CNF1) also promotes the development of actin stress fibers and membrane ruffles, which allows *E. coli* to enter the cells in a Rho GTPase-dependent way [35]. The toxin has a notable impact on the actin skeleton of HEp-2 cells, and they create huge vacuoles in HEp-2 cells

[36]. However, several in vitro and in vivo studies revealed that this protein inhibits polymorphonuclear phagocytosis, causes bladder epithelial cells to die through apoptosis, and may also cause apoptotic death to bladder epithelial cells, and may also cause bladder cells to exfoliate, making it easier for bacteria to invade underlying tissues [37].

1.8.2.3. Secreted autotransporter toxin (SAT): SAT, which has a toxin activity against cell lines originating from the bladder or kidney, may also play a significant role in the pathogenesis of UTI. SAT is a serine protease autotransporter that falls within one subgroup of autotransporters recently classified as SPATE (Serine Protease Autotransporters of Enterobacteriaceae) family and associated with pyelonephritic *E. coli* strains [38]. The host tissue may be damaged by the cytopathic action of SAT and may enhance the propagation ability of UTI.

1.8.2.4. Cytolethal distending toxin (CDT): cytolethal distending toxin has the special ability to damage the DNA of the target cell. The pathogenesis of UTIs is assisted by this toxin, which can stop the cell cycle [39]. However, CDT is a result of an operon that codes for three proteins, CdtA, CdtB, and CdtC, which are respectively encoded by the *cdtA*, *cdtB*, and *cdtC* genes [36]. The other bacterial toxins attack the cell membrane or other targets within the cytoplasm, whereas CDT attacks DNA and has enzyme activity similar to that of DNaseI [40].

1.8.2.5. Other toxins: Other substances including cytolysin A and the protein Tcp, which contains the TIR domain of the interleukin (IL-1) receptor, are also thought to contribute to the virulence of UTIs [41, 42]. The former results in host cell death [42], whilst the latter can manipulate TLR signaling to benefit survival during UTIs [41]. However, Tcp is associated with pyelonephritis, but uncommon in environmental *E. coli*, in the fecal flora of healthy children, and in less severe types of UTI [31]. Tcp also plays a part in the human avoidance system and has a cytopathic effect on the kidney [43].

Along with these toxins, arginine succinyltransferase (AST), vacuolating autotransporter toxin (VAT), and Shigella enterotoxin-1 (ShET-1) may also contribute to UTIs. VAT has a cytotoxic effect on the bladder and kidney, while the two others are involved in the invasion of the infections [43]. VAT, a member of the SPATE protease family, is a highly protected immunogenic protein [36].

1.8.3. Siderophores: All life forms require iron, and *E. coli* utilizes it for the metabolism of peroxides, the storage, and transport of oxygen, DNA synthesis, and electron transport. However, during UTI, the amount of iron availability is reduced in the urinary tract of the host [44]. In response, *E. coli* has many functionally redundant systems that mediate iron intake by secreting siderophores, which are low-molecular-weight compounds that chelate Fe^{3+} [45]. For UPEC to colonize the urinary system, iron utilization, which is mediated by these siderophores, is essential [46]. *E. coli* has four different siderophore systems, including salmochelin, enterobactin, aerobactin, and Yersiniabactin [47].

1.8.3.1. Aerobactin: Aerobactin is a hydroxamate siderophore with a low molecular weight, most abundant at low pHs, and better Fe^{3+} -binding stability in acidic conditions. Through an outer membrane receptor protein, this siderophore absorbs Fe^{3+} from the iron-binding proteins of the host [39]. Aerobactin, which is produced by the condensation of two lysines and one citrate molecule, and is catalyzed by the enzyme aerobactin synthase, offers several advantages over other siderophores [29, 48].

1.8.3.2. Enterobactin: Another specialized widely distributed catecholate siderophore, called enterobactin, is less soluble and less stable than aerobactin. However, this siderophore can defer transferrin in an aqueous solution more rapidly than aerobactin, as it has a stronger affinity for iron [49]. However, the hydrolysis of the siderophore causes iron to be liberated from enterobactin. In addition to these, enterobactin may enable UPEC to colonize an environment that restricts iron, such as the urinary system [48].

1.8.3.3. Yersiniabactin: Widespread in Enterobacteriaceae, including *E. coli*, Yersiniabactin is a mixed-type siderophore that is encoded on the high-pathogenicity island [50]. The strong iron affinity of Yersiniabactin results in the formation of a Yersiniabactin- Fe^{3+} complex that binds to the iron molecule and identifies a particular bacterial outer membrane TonB-dependent receptor and Fyu(Psn). With the aid of the proteins embedded in the membranes, yersiniabactin in the cytosol releases the iron molecule [51].

1.8.3.4. Salmochelin: Salmochelin, a glucosylated enterobactin derivative, evades the host immunological response because it is not identified by siderocalin [50]. However, siderocalin, sometimes referred to as lipocalin 2 and neutrophil gelatinase-associated lipocalin, binds

enterobactin and inhibits its absorption. Enterobactin is modified to salmochelin by glycosylation through the activity of glucosyltransferase to get around this and to avoid being identified by lipocalin 2 [52]. The salmochelin siderophore receptor IroN, however, has recently been discovered to be involved in the invasion of urothelial cells; as a result, IroN may function as both an iron uptake receptor and an internalization factor in the development of urinary tract infections [30].

1.8.3.5. Hemin uptake system: Another method of iron acquisition is the hemin uptake pathway, which also includes ChuA and Hma, which are involved in the direct upregulation of haem receptors. Several studies have identified the significance of this mechanism in the development of bacterial biofilms and the uptake of free iron during UTIs [43, 53, 54]. Other regulatory proteins control ChuA expression, for instance, in uropathogenic *E. coli* strain 536, an increase in RfaH level triggers ChuA expression [55]. However, the other receptor Hma functions independently of ChuA and requires the residue Tyr-126 to do so. However, the consumption of hemoglobin, which is necessary for maximal kidney colonization, is a function of both ChuA and Hma [46].

1.8.4. Capsule: The primary function of a capsule is to enclose and shield the bacterium from various unfavorable conditions as well as the host immune system, which is primarily made up of polysaccharides [19]. The capsule offers defense against host engulfment, complement-mediated bactericidal effect, antimicrobial resistance, and antiserum activity [19, 43]. Certain capsules, such as K1 and K5, prevent a proper humoral immune response of the infected host by showing a molecular mimicry of tissue response [19].

1.8.5. Lipopolysaccharides (LPS): LPS are amphipathic molecules made up of fatty acids lined to an oligosaccharide core that is then bound to a long polysaccharide chain known as O-antigen. Multiple features of the UPEC life cycle are mediated by LPS structural components, including the ability to acutely colonize bladders, establish reservoirs, and elicit innate and adaptive immune responses [56]. When the amount of LPS at the cell surface is reduced, hypersensitivity to hydrophobic toxic compounds (i.e. bile salts and certain antibiotics) develops. LPS also provides resistance to hydrophobic antibiotics.

1.8.6. Motility: The organelle known as the flagellum, is in charge of bacterial movement and participates in the early adhesion stage of biofilm development [19, 57]. According to a recent

study, the migration of the infection from the bladder to the kidneys is aided by motility [58]. Flagellated UPEC accounts for roughly 70%-90% of all urinary tract infections, and pathogenesis involves contact between the bacteria and the epithelial cell surface of the urinary tract [19]. However, the ability of *E. coli* is improved by flagellar motility through adaptive reactions to appealing or repulsive environmental stimuli [59].

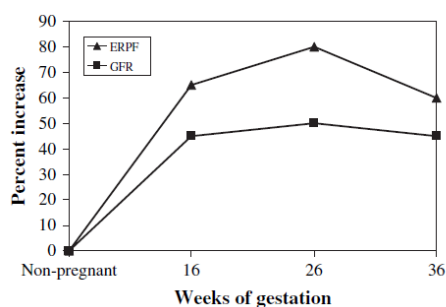
1.9. UTI and Pregnancy:

Both symptomatic and asymptomatic bacteriuria are extremely common in pregnant women, and previous history of the infection is a major risk factor. The effect of asymptomatic UTI can be subsided by employing suitable treatment which in turn prevents the adverse consequences of its progress. Poor diagnosis during pregnancy can lead to urinary tract infection, which then enhances the extent of the infection, and pregnant women under such circumstances are susceptible to serious complications. According to different studies, the occurrence of infection was around 56% during pregnancy, and the rate among pregnant women during the second trimester was up to 50%. UTI is considered the most common hospital-acquired infection constituting up to 35% of nosocomial infections and is regarded as a viral factor for the outbreak of bacteremia among hospitalized patients. Although *E. coli* is thought to be the prime perpetrator, studies have validated the significance of *S. aureus* in conferring the infection [60]. Untreated UTI might increase the chance of pyelonephritis, which can have serious consequences including transitory renal failure, acute respiratory illnesses, and hematological abnormalities [61]. It is a well-known fact that pregnancy is linked to several anatomical hormonal, and physical changes in women. These changes increase the risk of urinary stasis, which results in the retrograde flow of urine from the bladder to the ureter. This is a result of physical abnormalities that increases the likelihood of UTI in pregnant women.

1.9.1. Changes during pregnancy: The physiological changes that occur during pregnancy makes healthy women at risk for serious complications related to the urinary tract. Researchers have confirmed that one of the key reasons for the development of UTI during pregnancy is the relevance of physiological changes. The urinary system undergoes significant alterations during pregnancy due to the factors like hormonal, mechanical, and physiological changes [62]. This in turn has a significant impact on how the infection is acquired.

1.9.1.1. Anatomic changes in the upper urinary tract: Various anatomical changes to the upper urinary system occur during a typical pregnancy. Renal vascular volume and interstitial volume increase are secondary to changes in total vascular volume. Overall kidney dimension increases by roughly 1cm as a result, and renal volume rises by as much as 30%. In addition to volume increases, there is dilation of the collecting system, which includes the pelvis, ureters, and renal calyces. As a result, 80% of pregnant women experience physiologic hydronephrosis and hydroureter by mid-pregnancy. The majority of patients experience some degree of ureteral dilatation, which is most commonly on the right side and is frequently more pronounced there than on the left. Most likely, an enlarging uterus and ovarian vein plexus are the secondary causes of mechanical compression, which results in dilatation. Dilation is rarely present below the pelvic brim. It is unclear how progesterone affects these alterations and how hormones as a whole contribute to them. A study suggested that progesterone may influence smooth muscle relaxation, but other investigators have demonstrated no correlation between the degree of dilatation and progesterone or estradiol concentrations [63].

1.9.1.2. Renal hemodynamics and glomerular filtration rate during normal pregnancy: In a typical pregnancy, both the renal plasma flow (RPF) and glomerular filtration rate (GFR) significantly increase. GFR and effective RPF were enhanced by 40% to 65% and 50% to 85% respectively, in the first half of gestation, according to a thorough compilation of carefully chosen research (Figure 1.5). These studies are noteworthy in that they (1) measured GFR and RPF using the gold standard (renal clearance of inulin and para- amnio-hippurate), (2) compared first-half



GFR and RPF to pre-pregnancy or postpartum values, and (3) minimized urinary tract dead space, which causes a smaller filtration rate (filtration fraction = GFR/RPF). RPF decreases as the pregnancy progresses while GFR remains constant.

Figure 1.5: GFR and Effective renal plasma flow (ERPF)

during pregnancy. Renal plasma flow increases dramatically in the first trimester, then reaches peak levels 50% to 80% above baseline non-pregnant levels by the beginning of the third trimester, with a subsequent decline in the latter part of pregnancy toward term. GFR, which is largely determined by RPF, follows a similar pattern of increase, by about 50% with more of a plateau at term. (Data from Conrad KP, Lindheimer MD. Roberts JM, Cunningham FG, editors. Chesley's

hypertensive disorders in pregnancy. 2nd edition. Stamford (CT): Appleton and Lange; 1999. p. 263 – 326).

Creatinine clearance is utilized by clinicians to gauge GFR and evaluate renal function after collecting urine for 24 hours. Although endogenous creatinine is released by the proximal tubule of the kidney and filtered by the glomerulus, creatinine clearance is a valid indicator of GFR during pregnancy. The exception is when the GFR is significantly reduced due to a condition like renal disease and creatinine clearance may overestimate the actual GFR. During pregnancy, there is a moderate rise in creatinine clearance, which varies from 100 to 150 ml per minute. The GFR changes are shown to begin fairly early in gestation using the 24-hour urine collection approach to measure creatinine clearance and estimate GFR. GFR rise of 25% by the 4th week of pregnancy (from the last menstrual period) and 45% by the 9th week of gestation, was demonstrated by Davison and Noble. These hemodynamic alterations are among the earliest and most dramatic maternal adaptations to pregnancy [63].

Table 1.1: Normal laboratory variables in pregnancy (from Jeyabalan & Lain, 2007)

Variable	Normal Value in Pregnancy
Creatinine	0.5 mg/dl
Blood Urea Nitrogen (BUN)	9.0 mg/dl
Glomerular filtration rate (GFR)	↑ ~40% to 60% above baseline
Creatinine clearance	↑ ~25% above baseline
Uric acid	2.0 -3.0 mg/dl
Urinary protein excretion	<300 mg/24h
Urinary albumin excretion	<20 mg/24h
Sodium retention over pregnancy	900 – 950 mmol
Plasma osmolality	↓ ~10mOsm/kg H ₂ O
PCO ₂	↓ ~10mm Hg below baseline
Serum bicarbonate	18 – 20 mEq/L
Urinary glucose excretion	Variable

Serum creatinine and urea levels, because of increased GFR during pregnancy, are also decreased and they are two commonly used indicators of renal function. In comparison to non-pregnant values of 0.8 mg/dl and 13.0 mg/dl, the average blood creatinine and urea levels are 0.5 mg/dl and 9.0 mg/dl, respectively. Skeletal muscle production and urine excretion, along with relatively free filtration of creatinine through the glomerular barrier, define the levels of circulating creatinine.

While GFR is significantly increased during pregnancy, skeletal muscle synthesis of creatinine remains largely unchanged, which leads to lower levels of circulating creatinine. At the glomerulus level, urea is also freely filtered.

1.9.1.3. Mechanisms of renal hemodynamic alterations in pregnancy: The precise mechanisms causing the gestational renal hemodynamic changes remain incompletely understood. The enhanced renal blood flow and hence the increased GFR are ultimately caused by decreased renal vascular resistance. These early modifications take place in anticipation of the fetal-placental unit's future requirements and may even come before the early gestational changes in plasma volume and cardiac output.

These initial changes in renal hemodynamics have been linked to hormones. It's interesting to note that GFR and RPF increase throughout the luteal phase of the menstrual cycle even before conception. In the second half of the menstrual cycle, GFR rises by 20%, and in the early stages of pregnancy, it rises by another 40% to 65% over baseline values. These results provide support to the theory that these gestational changes in the renal system may be influenced by maternal ovarian hormones or pregnancy hormones produced by the fetal-placental unit.

Numerous hormonal changes that take place during pregnancy have been researched about renal and cardiovascular abnormalities. Studies have been done on the functions of the sex-steroid hormones progesterone and estrogen. Although it is undeniable that estrogen has a part in boosting blood flow to other reproductive and non-reproductive organs, it does not appear to affect RPF and GFR. However, the rise in RPF and GFR caused by progesterone treatment in human and animal studies was far less pronounced than that seen during pregnancy. The precise involvement of progesterone and its metabolites in pregnancy-induced renal hemodynamic alterations has to be further investigated. In this regard, peptide hormones of maternal and placental origin have also been studied. The function of Prolactin is still debatable, and placental lactogens have not been researched. It has been widely investigated in rats using the corpus luteum of the ovary as the source of relaxin, which is produced in both rats and women. Studies have shown that when recombinant human relaxin or pig relaxin is administered to conscious, chronically instrumented female non-pregnant rats, GFR and effective RPF alternations comparable to those of mid-gestation are detected. These alterations were likewise noted in female rats who had undergone

ovariectomies and even in male rats that had received relaxin. Additionally, the administration of relaxin-neutralizing antibodies to midterm pregnant rats abolished the increase in GFR and RPF.

The endothelial Endothelin-B receptor and nitric oxide pathway are responsible for pregnancy- and relaxin-induced renal vasodilation and hyper-filtration, according to extensive research. Vascular gelatinase, particularly matrix metalloproteinase-2, has recently been demonstrated to be an essential part of this renal vasodilatory process. There is some indication that relaxin may have a significant role in pregnancy-related changes to renal hemodynamics, notwithstanding the paucity of human studies. The gestational increase in GFR is lower in women who lack ovarian function with undetectable serum relaxin levels and who become pregnant through egg donation than it is in women with normal ovarian activity. Additionally, a scleroderma therapy trial involving the chronic administration of relaxin led to a 15% - 20% increase in creatinine clearance beyond expected levels. These findings from research on both humans and animals, while not conclusive, point to a significant role of relaxin in the early and profound renal changes that take place during pregnancy.

1.9.1.4. Renal handling of substrates in normal pregnancy:

1.9.1.4.1. Uric acid: In a healthy pregnancy, serum uric acid levels drop by 25% to 35%, reaching a nadir of 2 to 3 mg/dl at 24 weeks' gestation before rising approaching non-pregnant levels in the third trimester. Purine breakdown and dilatory intake are the main contributors to uric acid production, and renal excretion is the main mechanism for its elimination. A whopping 95% of the circulating acid is unbound and filters through the glomerulus. Proximal tubular reabsorption and secretion of uric acid also occur. Net uric acid reabsorption takes place in humans, with only 7% to 12% of the filtered load being excreted through the urine. Although several variables may contribute to circulating uric acid changes during pregnancy, altered renal processing is most likely the main cause. Higher GFR decreased proximal tubular reabsorption, or both may be the cause of the higher uric acid clearance by the kidney pregnancy. Pre-eclampsia is one of the conditions that can cause the plasma volume to contract, which can result in a reduction in uric acid clearance and an increase in circulating levels. In the prognosis, diagnosis, and pathogenesis of pre-eclampsia, uric acid has drawn a lot of interest.

1.9.4.1.2. **Protein:** Evaluation of urine protein excretion is crucial for identifying and tracking renal illness as well as pregnancy-related pathologic states like pre-eclampsia. Particularly, after 20 weeks of gestation, total protein excretion and urine albumin excretion increase during pregnancy in comparison to non-pregnant levels. The average 24-hour excretion of total protein and albumin is 200 mg and 12 mg, respectively, with upper limits of 300 mg per 24 hours and 20 mg per 24 hours, according to the findings of a longitudinal study that looked at women before conception, during pregnancy, and after delivery. Smaller cross-sectional studies also supported these findings. Pregnancy also results in an increase in renal tubular enzymes and low molecular weight proteins, which suggests a diminished proximal tubular resorptive capacity. The gestational proteinuria and albuminuria are also influenced by increased GFR and potential changes in glomerular charge selectivity. During a typical pregnancy, there doesn't seem to be any change in the glomerular permselectivity based on molecular weight or size.

1.9.4.1.3. **Sodium and volume homeostasis:** Systemic vascular resistance is significantly decreased during a typical pregnancy, and this is accomplished by increases in cardiac output and plasma volume. Throughout pregnancy, net sodium retention of 900 to 950 mEq results in this gradual expansion of plasma volume. A notable adaptation of this gradual expansion of plasma volume. A notable adaptation of the renal tubule during pregnancy is the net reabsorption of sodium by the renal tubule despite the significant filtered load. In the first few weeks of pregnancy, a physiological drop in plasma osmolality takes place as well. It reaches a nadir about the tenth week and remains steady the entire time the mother is pregnant. This result has been explained by a 'resetting of the osmostat', with a suitable vasopressin response around a changed threshold.

1.9.4.1.4. **Acid-base homeostasis:** The maintenance of the acid-base balance is a function of the kidney as well. An increase in minute ventilation during pregnancy leads to a relative respiratory alkalosis, which is the main acid-base change of pregnancy. Bicarbonate excretion is enhanced and serum bicarbonate levels fall as a result of the compensatory response of the kidney. This drop in serum bicarbonate could put a restriction on the buffering capacity in pregnancy.

1.9.4.1.5. **Glucose:** By a sodium-coupled active transport in the proximal tubule, glucose is readily filtered and almost entirely reabsorbed. The collecting tubule also takes in a tiny amount of glucose. Minimal glucose (<125mg/dl) is eliminated in the urine in non-pregnancy. Typically, it takes a plasma concentration of glucose more than 200 to 240 mg/dl or a threshold concentration

for glucose to show up in the urine. A tubular anomaly can cause renal glucosuria, an asymptomatic condition in which varying amounts of glucose are expelled despite normal serum glucose concentrations. An increase in the plasma volume during pregnancy causes an increase in GFR as well as a rise in tubular flow rate. The capacity of the proximal tubule to completely reabsorb glucose may be restricted by this higher flow rate, leading to physiological pregnancy-related glucosuria. In 29 otherwise healthy women, Davison and colleagues, showed less efficient glucose reabsorption during pregnancy, with a recovery to normal postpartum. Additionally, it has been suggested by animal research, that the capacity of the distal nephron to absorb glucose may be reduced. Therefore, decreased efficiency of both the proximal tubule and the collecting tubule may be a contributing factor to the rise in excreted glucose in late pregnancy. Overall, compared to the modest amount of excreted by non-pregnant individuals, the amount of excreted glucose in the third trimester is raised several-fold. The use of glycosuria as a screening for pregnancy-related glucose intolerance is not very effective due to these modifications in the renal processing of glucose and the normal appearance of glucose in the urine [63].

1.9.2. Types of urinary tract infections in pregnancy: There are three major types of UTIs during pregnancy. They are asymptomatic bacteriuria, acute cystitis, and acute pyelonephritis. The clinical presentations of these conditions vary.

Asymptomatic bacteriuria (ABU) may be present even before the mother gets pregnant. There are reports that 1.2 to 5% of young girls would demonstrate ABU at some time before puberty. The prevalence of ABU in pregnancy is about 10%. Lower serum IL-6 levels and serum antibody responses to *E. coli* antigens which occur in pregnancy have been associated with the increased incidence of ABU in pregnancy. Neonatal complications associated with ABU include intrauterine growth restriction, low birth weight, and pre-term premature rupture of the membrane. Maternal complications which are associated with ABU are hypertension, pre-eclampsia, and maternal anemia. Roughly, 30% of pregnant women, with this condition, go on to develop symptomatic cystitis without therapy, and of those, roughly 50% will eventually develop acute pyelonephritis.

Although acute cystitis relates to the infection of the urinary bladder, the urethra is also infected very often. Acute cystitis can be distinguished from ABU primarily by the presence of urgency, frequency, and dysuria. The patient typically remains afebrile. Usually, severe systemic symptoms such as nausea, vomiting, high-grade fever, and discomfort are absent. Since urgency and

frequency are frequent signs of a healthy pregnancy, the majority of women may not be aware that they are suffering from the infection.

Acute pyelonephritis is an infection of the kidney and the pelvic ureter. Being a serious systemic illness, it affects 1-2% of all pregnancies and is the most common non-obstetric cause of hospital admission during pregnancy. Complications are characterized by high-grade fever, chills and rigors, headache, nausea, vomiting, lumbar pain, and in serious cases, reduced urine output. Without treatment, it may result in maternal septicemia and preterm labor. Recurrent pyelonephritis has been implicated as a cause of intra-uterine growth and fetal death. Overall recurrence incidence is about 2–3% and it can recur during the same pregnancy [64].

1.10 The phylogenetic groups of *Escherichia coli*:

The *E. coli* species has a complex genetic structure, and over time, techniques have evolved to assess the phylogenetic relationship. Serotyping was used in the pre-molecular period to study the diversity of *E. coli*. The somatic (O) antigen, the flagellar (H) antigen, and to a lesser extent the capsular (K) antigen are useful in differentiating *E. coli* strains, according to serotyping research. The serotyping of *E. coli* is complex – there are 173 O antigens, 80 K antigens, and 56 H antigens that are known, and many of the possible combinations of O, K, and H antigens can be found in nature. This results in an extremely high ultimate number of *E. coli* serotypes, between 50000 to 100000 or more.

The determination of differences in the electrophoretic mobility of enzymes generated from various *E. coli* strains served as the foundation for the molecular studies of *E. coli* diversity [65]. The multilocus enzyme electrophoresis (MLEE) method for studying bacterial diversity became popular in the 1980s. It was discovered that *E. coli* populations evolve clonally, and that closely related strains may have different serotypes even though they are genetically distinct [66]. Four main phylogenetic groupings of *E. coli* were discovered based on the MLEE studies of 38 enzyme loci: A, B1, B2, and D [67]. A method for the quick and easy determination of the *E. coli* phylogenetic groups using a triplex PCR was developed by Clermont et al. [68]. Amplification of a 279bp fragment of the *chuA* gene, a 211bp fragment of the *yjaA* gene, and a 152bp fragment of *TspE4.C2*, a non-coding region of the genome, forms the basis of this genotyping technique. The

E. coli strains are classified into the phylogenetic groups A, B1, B2, and D based on the presence or absence of combinations of these three amplicons.

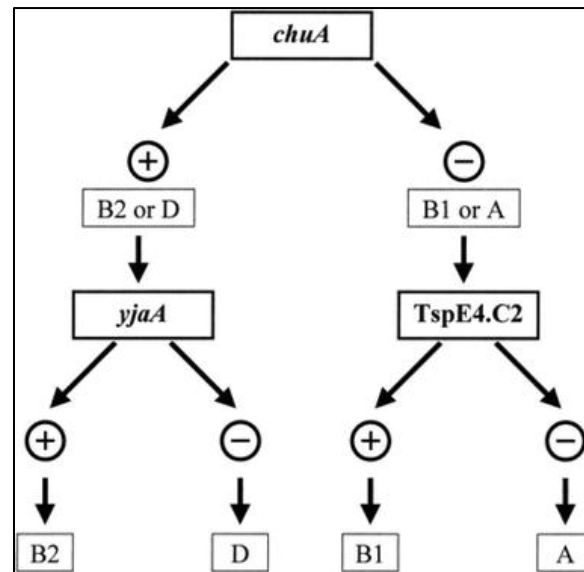


Figure 1.6: Dichotomous decision tree to determine the phylogenetic group by the Clermont triplex PCR method

However, later, new *E. coli* phylogenetic groupings were identified using multi-locus sequence typing and whole genome data. As a result, there are now eight well-identified phylogenetic groups (A, B1, B2, C, D, E, F, that belongs to *E. coli sensu stricto*, and the eighth – the *Escherichia* cryptic clade I). In order to encompass the newly described phylogenetic groups, Clermont et al., thus revised their method. The novel extended PCR phylotyping method uses an extra gene target, *arpA*, which also acts as internal DNA quality control, to make it possible to identify the F phylogenetic group. Thus, the revised PCR method is based on a quadruplex PCR, and if required, additional single PCR reactions are employed to distinguish between E and Clade I, A or C, and D or E phylo-group.

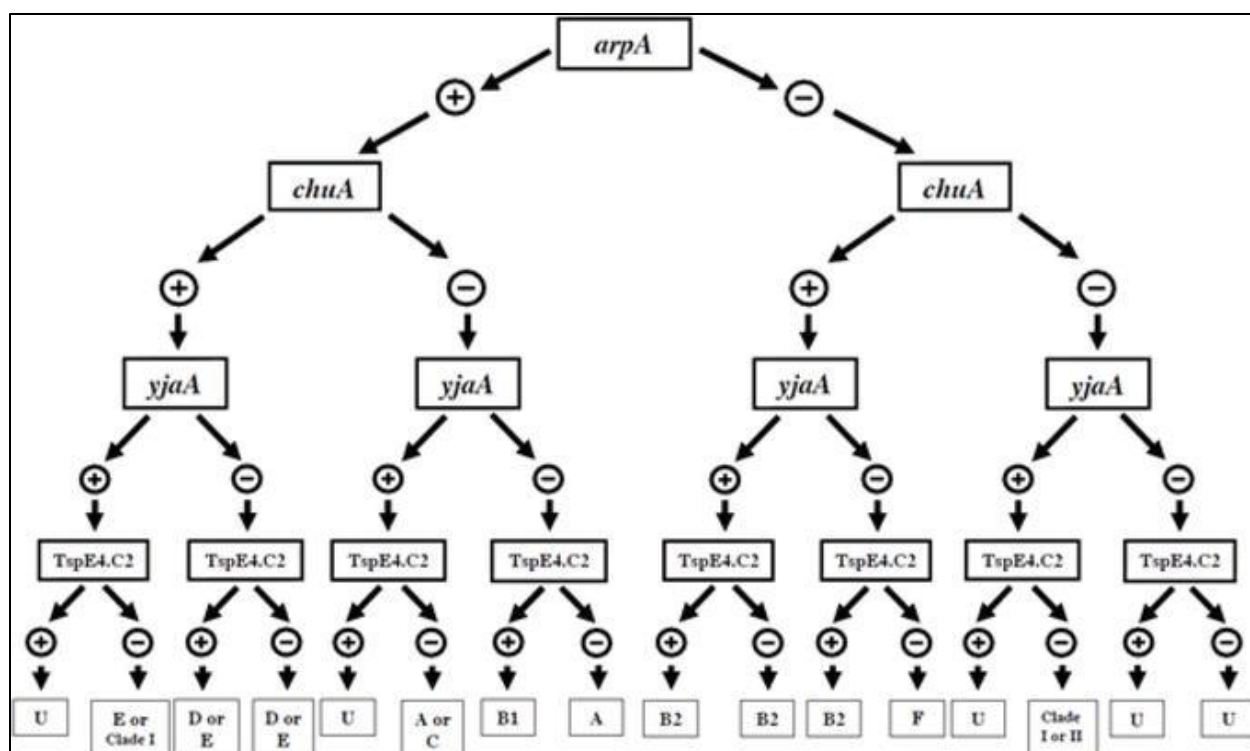


Figure 1.7: Dichotomous decision tree to determine the phylogenetic group by the Clermont quadruplex PCR method

1.11. Treatment of UTI:

UTIs result in considerable economic and public health burdens and substantially affect the life quality of affected individuals. Currently, antibiotics – such as trimethoprim-sulfamethoxazole, ciprofloxacin, and ampicillin – are the most commonly recommended therapeutics for UTIs (Flores-Mireles et al, 2015). Empiric treatments for UTIs are given below.

1.11.1. Empiric treatment regimens for urinary tract infections (excerpt from Antimicrobial use Urinary Tract Infection)

Urinary Syndrome	Drug of choice	Alternative choice	Comments
Acute Cystitis	Nitrofurantoin 100mg BD for 5 days	Cotrimoxazole DS BD or Ciprofloxacin 500mg BD for 3 days	Obtain urine cultures before antibiotics and modify therapy based on sensitivity report

Acute Pyelonephritis	Piperacillin-tazobactam 4.5gm IV q6h or Cefoperazone-sulbactam 3gm IV q12h or Ertapenem 1gm IV OD Treat for 14 days	Imipenem-cilastatin 500 mg IV q6h or meropenem 1gm IV q8h	Obtain urine cultures before antibiotics and switch to a narrow-spectrum agent based on the sensitivity report
Acute prostatitis Chronic bacterial prostatitis	Piperacillin-tazobactam 4.5 gm IV q6h or Cefoperazone-sulbactam 3gm IV q12h or Ertapenem 1gm IV OD or Ciprofloxacin 750mg PO BD	TMP/SMX DS PO q12h	Obtain urine and blood cultures before antibiotics & switch to narrow-spectrum agent based on sensitivities. Treat for 4 weeks. Therapy based on urine and prostatic message cultures obtained before antibiotic. Treat for 4-6 weeks
Community-acquired	Imipenem-cilastatin 1g IV q8h or Meropenem 1g IV q8h		Add vancomycin if S. aureus is a concern. Add colistin if high local prevalence of carbapenem-resistant organisms or previously colonized
Hospital-acquired	Imipenem 1g IV q8h or Meropenem 1g IV q8h plus Vancomycin 1g IV q12h plus Colistin 9 mu iv stat then 4.5mu iv q12h		Broaden spectrum if prior antibiotic exposure. De-escalate to a narrow-spectrum agent on receipt of sensitivities

https://main.icmr.nic.in/sites/default/files/guidelines/Treatment_Guidelines_2019_Final.pdf

1.11.2. Alternative Therapeutics/ Non-Antibiotic treatment for Urinary Tract Infections [69]:

1.11.2.1. Urinary Alkalinization: The use of oral medications, such as potassium citrate, to alkalize the urine is a method of lowering urine acidity. It is hypothesized that increasing urine pH lessens the dysuria of the patient to a greater extent.

1.11.2.2. Probiotics: It is believed that probiotic organisms, such as lactobacillus spp., create a barrier to prevent pathogenic bacteria from ascending the urinary tract and subsequently causing infection. They alter the defense system of the host by limiting pathogen adhesion, development, and colonization.

1.11.2.3. **Chinese Herbal Medicine:** The Chinese herbal medicine most commonly used, according to a 2015 Cochrane review, are Er Xian Tang, Bai Tou Weng Tang, and San Jin Wan.

1.11.2.4. **Methenamine hippurate:** In the presence of acidic urine, Methenamine hippurate is hydrolyzed to formaldehyde, and shows a bactericidal effect on *E. coli*.

1.11.2.5. **Cranberry:** It is postulated that cranberries prevent bacteria (particularly *E. coli*) from adhering to the Uroepithelial cells.

1.11.2.6. **Topical estrogen:** Vaginal atrophia is improved and vaginal lactobacilli has been increased due to the topical application of vaginal estrogen. These promote a change in vaginal pH, suppressing the growth of gram-negative bacteria.

1.11.2.7. **Hyaluronic acid:** Intravesical hyaluronic acid aims to replenish the surface glycosaminoglycan layer of the urothelium and can prevent bacterial adherence.

1.11.2.8. **Oral immuno-stimulants:** Serotypes of Uropathogens that have been heat-killed or rendered inert are found in oral immuno-stimulants, which are used to boost the immune response of the patient to urine infections. Immuno-stimulants function by boosting immune system activity rather than by granting a specific pathogen-specific acquired immunity, like a vaccination does.

1.12. Antibiotic Classifications and their mode of action:

The term antibiotic was coined from the word ‘antibiosis’ means ‘against life’. Antibiotics were once thought to be organic substances produced by one type of bacterium that is toxic to other bacteria. This idea led to the initial definition of antibiotic, which was generally defined as an organic compound produced by one microorganism or of bacterial origin that, at a low dose, can hinder the growth of or be lethal to other bacteria. Modern times have changed this concept to also include antimicrobials that are partially or entirely manufactured synthetically. While some antibiotics can completely eradicate other bacteria, others can only stop their growth. Those that kill bacteria are termed bactericidal while those that inhibit bacterial growth are termed bacteriostatic. Penicillin was the first antibiotic discovered in September 1928 by the English bacteriologist Late Sir Alexander Fleming. He accidentally discovered the antibiotic in a soil-dwelling fungus called *Penicillium notatum*, but it was not announced publicly until 1929 and human clinical trials weren’t started until 1940. Antibiotics such as β -lactams, glycopeptides,

aminoglycosides, tetracyclines, macrolides, Oxazolidinones, fluoroquinolones, and carbapenems are commonly used to treat urinary tract infections. Each type of antibiotic has a particular mode of action.

Antibacterial drug-target interactions have been extensively researched, and they primarily come into three categories: inhibition of cell wall turnover, inhibition of protein synthesis, and inhibition of DNA replication and repair.

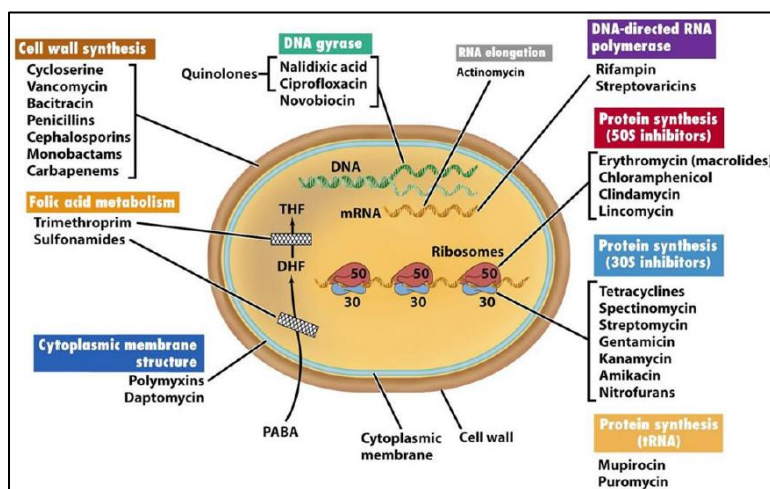
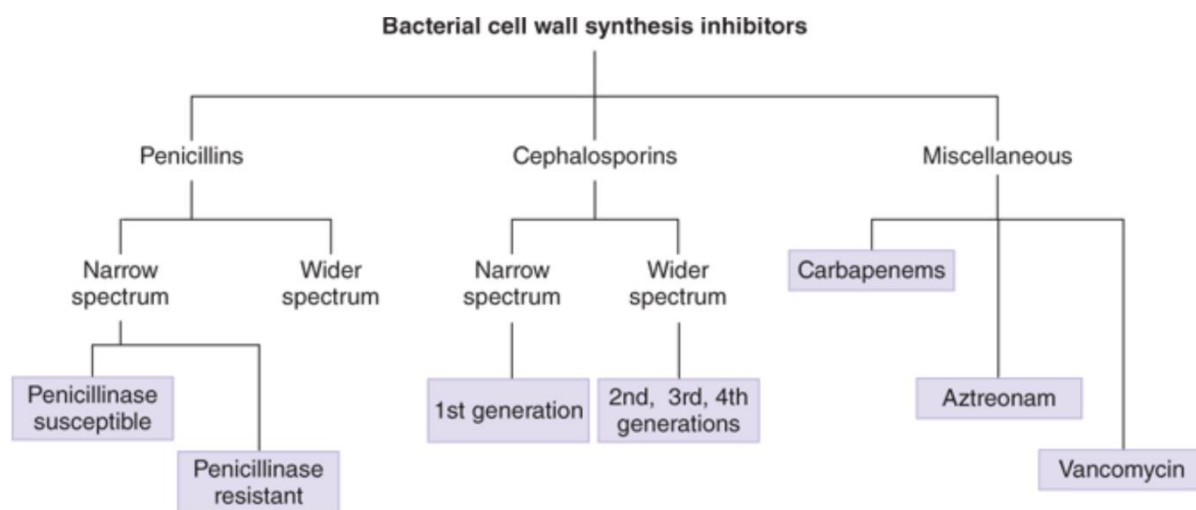


Figure 1.8: Antibiotic target sites (from Etebu E, Arikekpar I. Antibiotics: Classification and Mechanisms of Action with emphasis on molecular perspectives. IJAMBR 2016 4: 90-101.)

1.12.1. Inhibition of cell wall synthesis:

The majority of bacterial cells are encased in a rigid layer of peptidoglycan (PG), sometimes known as murein in earlier sources, which protects the cells from high osmotic pressure along with a frequently hostile environment.

Peptidoglycan has a degree of cross-linking peptide bonds called β -(1-4)-N-acetyl Hexosamine. Bacteria must produce peptidoglycan to survive, and they do this through the activity of PBPs, which are transglycosylases and transpeptidases. These two enzymes crosslink the strands of developing peptidoglycan units as well as extend the glycan stands of existing peptidoglycan molecules by adding disaccharide pentapeptides.



Source: A.J. Trevor, B.G. Katzung, M. Kruidering-Hall: Katzung & Trevor's Pharmacology: Examination & Board Review, 11th Ed.
 www.accesspharmacy.com
 Copyright © McGraw-Hill Education. All rights reserved.

Figure 1.9: Different classes of bacterial cell wall inhibitors

1.12.1.1. β -lactam chemistry:

The basic structure of every antibiotic belonging to the “beta-lactam” superfamily, is a 4-member “beta-lactam” ring. Modification of the structure of the naturally occurring penicillins (Penicillin G & V) resulted in the development of both synthetic penicillin analogs, as well as new families of beta-lactams (beginning with the cephalosporins), that have distinctly different side rings and side chains with different antibacterial spectrums of activity, greater resistance to beta-lactamases, and different pharmacokinetic properties. At present, four major beta-lactam subgroups include **A. Penicillins B. Cephalosporins C. Monobactams D. Carbapenems.**

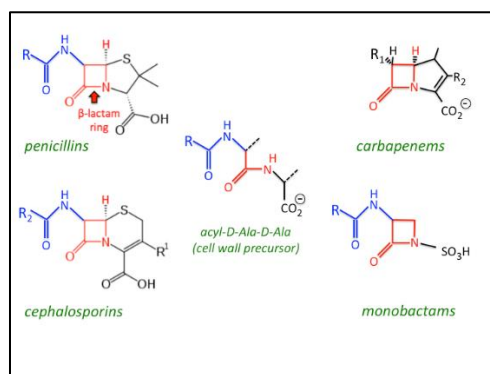


Figure 1.10: Core structure of beta-lactam antibiotics. All beta-lactam antibiotics contain the same core 4-member “beta-lactam” ring (highlighted in red). The ring mimics the terminal D-Ala-D-

Ala peptide sequence, which is the substrate for cell wall transpeptidases. This ring creates covalent bonds between various peptidoglycan chains, during periods of cell growth. Transpeptidases, often referred to as PBPs, tightly bind to the active site due to their four-ring structure and related side groups. Enzyme activity is inhibited by tight binding and consequent cell wall formation.

1.12.1.2. Mechanism of Action of β -lactam antibiotics:

The 4-member ring of beta-lactam antibiotics provides a 3D shape mimicking the D-Ala-D-Ala peptide terminus that serves as the natural substrate for transpeptidases during cell wall synthesis. The tight binding of these drugs to the transpeptidase active site inhibits cell wall synthesis, resulting in a weakened cell wall that is susceptible to lysis during the period of cell growth. One of the major driving forces of cell lysis is the very high internal osmotic pressure present in bacteria, which is caused by the presence of a high concentration of proteins and other molecules that growing bacteria need to survive.

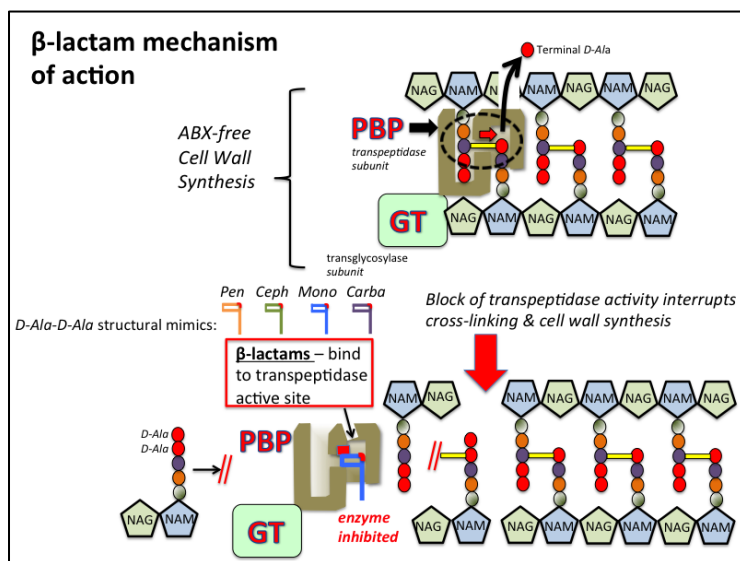


Figure 1.11: Mechanism of action of beta-lactam antibiotics. **Top:** In the absence of a drug, transpeptidase enzyme (PBP) in the cell wall catalyze cross-links between adjacent glycan chains, which involves the removal of a terminal D-alanine residue from one of the peptidoglycan precursors (highlighted by the broken oval). Glycosyltransferases (GT), which exist as either separate subunits or tightly associated with transpeptidases (e.g. as in the case of PBP-2) create covalent bonds between adjacent sugar molecules NAG & NAM. The net result of covalent bonds

between both the peptide and sugar chains creates a rigid cell wall that protects the bacterial cell from osmotic forces that would otherwise result in cell rupture. **Bottom:** Beta-lactam antibiotics, which include penicillins (Pen), Cephalosporins (Ceph), monobactams (Mono), and carbapenems (Carba) bear a structural resemblance to the natural D-Ala-D-Ala substrate for transpeptidase, and exert their inhibitory effects on cell wall synthesis by tightly binding to the active site of the transpeptidase (PBP). NAG: N-acetylglucosamine, NAM: N-acetylmuramic acid ([betalactam_pharm \[TUSOM | Pharmwiki\] \(tulane.edu\)](#)).

Table 1.2: Different β -lactam antibiotics (Penicillins, Cephalosporins, Carbapenems) and their sub-groups

Category	Parenteral Agents	Oral Agents
Penicillin		
Natural Penicillins	Penicillin G	Penicillin V
Antistaphylococcal Penicillins	Nafcillin, Oxacillin, Methicillin	Dicloxacillin
Aminopenicillins	Ampicillin	Amoxicillin, Ampicillin
Aminopenicillins + β -lactamase inhibitors	Ampicillin-sulbactam	Amoxicillin-clavulanate
Extended-spectrum Penicillins	Piperacillin, Ticarcillin	
Extended-spectrum + β -lactamase inhibitors	Piperacillin-tazobactam, Ticarcillin-clavulanate	
Cephalosporins		
First Generations	Cefazoline	Cephalexin
Second Generations	Cefotetan, Cefoxitin, Cefuroxime	Cefuroxime axetil, Cefaclor
Third Generations	Cefotaxime, Ceftazidime, Ceftriaxone	Cefixime, Cefdinir
Fourth Generations	Cefepime	
Fifth Generations	Ceftaroline	
Carbapenems		
	Imipenem/Cilastatin, Meropenem, Doripenem, Ertapenem	-

1.12.1.3. Use of β -lactam group of drugs across the world:

The prevention and treatment of bacterial infections brought on by susceptible organisms are approved uses for beta-lactam antibiotics. initially, only effective against that is now also effective against a variety of gram-negative organisms have increased the usefulness of beta-lactam

antibiotics. According to a report from an ICU in Indonesia, beta-lactams are used more frequently than aminoglycosides and macrolides to treat UTI, intraabdominal infections, infant meningitis, and pneumonia [70]. The most common class of medications used for treatment in hospitals, according to a report from a hospital in Kerala, India, is beta-lactam. Cephalosporin was identified as the beta-lactam antibiotic with the highest prevalence, followed by inhibitor combination medications such as piperacillin-tazobactam and amoxicillin-clavulanic acid [71].

1.12.1.4. Use of β -lactam group of drugs in pregnancy:

A Hungarian study monitored 38,151 pregnant women over 16 years and found that 6,554 (17.2%) women used antibiotics, which were mainly penicillin (84%) prescriptions [72]. A similar study carried out in Brazil showed 54% of women using penicillin and cephalosporins representing 23.4% of the total antibiotics used during pregnancy [73]. There is no doubt that penicillin is the most prescribed antibiotic for pregnant women [74]. Penicillins are indicated during pregnancy mainly to treat syphilis, infections in the upper respiratory tract associated with Group B streptococci, enterococcal infection, and for prophylaxis of bacterial endocarditis [75]. The use of beta-lactam agents in urinary tract infections has decreased due to the increasing rates of resistant *E. coli* strains. Usually, the major concern about beta-lactam antibiotics is not their direct toxicity, but the allergic reactions, which are almost impossible to prevent [76]. Previous studies showed alterations in penicillin pharmacokinetics in pregnant women since the maternal blood concentration markedly decreased due to increased kidney blood flow and glomerular filtration rate [77]. Due to increased blood volume and renal clearance, both causing distribution volume augmentation, the plasmatic concentration of the antibiotic can be reduced by up to 50% in pregnant women compared to non-pregnant ones [78]. Higher doses should be used to obtain antibiotic blood concentration.

The Hungarian study observed that 1.2% of women used some kind of cephalosporin. Cephalosporins are largely used in pregnant women for the prophylaxis of post-caesarean section infections, minor urinary infections caused by gram-negative rods, acute pyelonephritis, and, in some cases bacterial resistance to other antibiotics [79]. Until now, no risks of teratogenicity were observed in women using these antibiotics.

This antibiotic has been very successfully used in the treatment of post-delivery infections. However, there is little or no substantiated clinical experience about the use of imipenem in pregnancy and no reports on teratogenicity exist. It is classified as Category C by FDA. Recent studies showed that ertapenem could be useful during pregnancy to treat severe pyelonephritis or community-acquired pneumonia, which are not caused by *P. aeruginosa* [80].

1.12.2. Inhibition of Protein Synthesis:

A substance known as a protein synthesis inhibitor prevents or delays cell growth or proliferation by disrupting the procedures that directly result in the production of new proteins. Usually, it refers to those substances that have ribosome-level effects, such as antibacterial medicines. The compounds take advantage of the significant variations in ribosome size, sequence, structure, and protein-to-RNA ratios between prokaryotic and eukaryotic cells. Some antibiotics can kill bacteria by inhibiting their ribosomes while not affecting human ribosomes because of the structural differences. ([https://bio.libretexts.org/Bookshelves/Microbiology/Microbiology_\(Boundless\)/13%3A_Antimicrobial_Drugs/13.02%3A_Functions_of_Antimicrobial_Drugs/13.2D%3A_Inhibiting_Protein_Synthesis](https://bio.libretexts.org/Bookshelves/Microbiology/Microbiology_(Boundless)/13%3A_Antimicrobial_Drugs/13.02%3A_Functions_of_Antimicrobial_Drugs/13.2D%3A_Inhibiting_Protein_Synthesis))

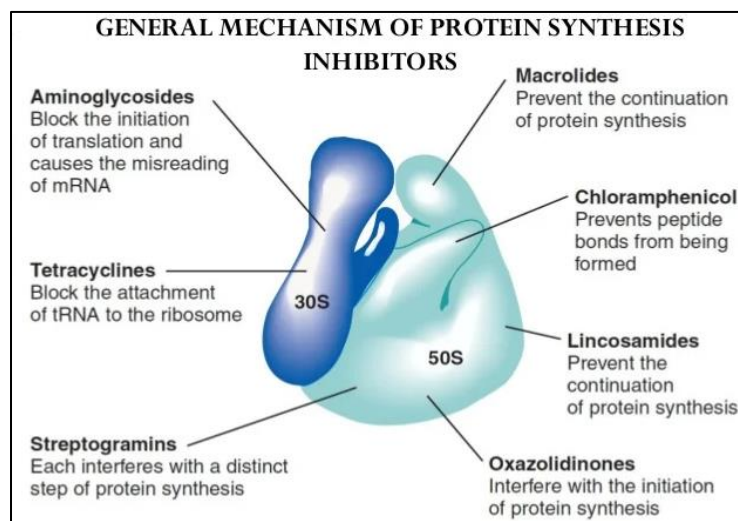


Figure 1.12: General Mechanisms of Protein Synthesis Inhibitors

1.12.2.1. Mechanism of action of protein synthesis inhibitor antibiotics:

In general, protein synthesis inhibitors work at different stages of prokaryotic mRNA translation into proteins like initiation, elongation (including aminoacyl tRNA entry, proofreading, peptidyl transfer, and ribosomal translocation), and termination.

- Linezolid acts at the initiation stage, probably by preventing the formation of an initiation complex, although the mechanism is not fully understood
- Tetracyclines and Tigercyclines (a glycylcycline related to tetracyclines) block the A site on the ribosome, preventing the binding of aminoacyl tRNAs.
- Aminoglycosides, among other potential mechanisms of action, interfere with the proofreading process, causing an increased rate of error in synthesis with premature termination.

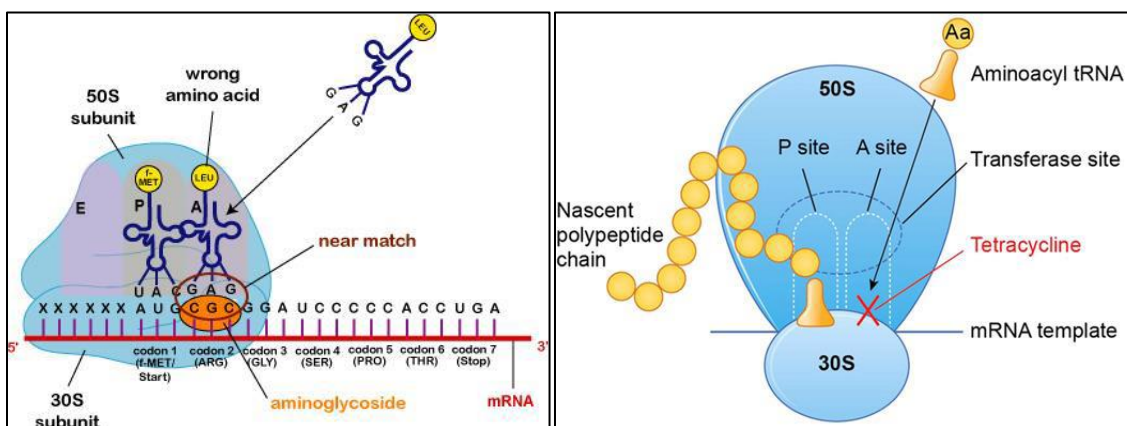


Figure 1.13: mechanism of action of (left) Aminoglycoside and (right) Tetracycline

- Chloramphenicol blocks the peptidyl transfer step of elongation on the 50S ribosomal subunit in both bacteria and mitochondria.
- Macrolides, clindamycin, and aminoglycosides have evidence of inhibition of ribosomal translocation.
- Streptogramins also cause premature release of the peptide chain.

1.12.2.2. Use of protein synthesis inhibitor antibiotics across the world:

A significant class of clinically beneficial antibacterials known as protein synthesis inhibitors includes drugs including erythromycin, tetracycline, chloramphenicol, and aminoglycosides. They avoid the 80S eukaryotic ribosome particle and only engage with the 70S bacterial ribosome. According to numerous studies, antibiotics that limit protein synthesis, like erythromycin, clarithromycin, and azithromycin, are used to treat UTI infections that are linked to biofilms [81].

1.12.2.3. Use of protein synthesis inhibitor antibiotics in pregnancy:

The use of macrolides in pregnant women is restricted to treating syphilis and upper-respiratory tract diseases in patients with allergic history to penicillin. In addition, it has been used to treat toxoplasmosis and urethritis caused by *Chlamydia trachomatis*. Erythromycin freely passes across the placental barrier, resulting in low plasmatic fetal concentration [78].

Gentamicin is the most widely used Aminoglycoside, especially used to treat pyelonephritis resistant to beta-lactam agents [79]. It freely crosses the placenta reaching fetal concentration peaks of approximately 40% of the maternal blood concentration, one or two hours after intramuscular administration [82]. As a rule, among glycosides, only gentamicin should be reserved for cases with restricted indication and they must be used in the smallest dose during the shortest time possible.

Literature regarding tetracycline is very controversial concerning its teratogenicity. Some consider tetracycline safe during the first three months of pregnancy [77], other consider that these drugs, particularly oxytetracycline, present a teratogenic risk to the fetus if they are used during the second month of pregnancy and could cause neural-tube defects, palatine cleft, and severe congenital cardiovascular abnormalities [83]. Based on FDA recommendations and controversial studies, tetracyclines are not recommended during any stage of pregnancy.

1.12.3. Inhibition of DNA replication:

Some antibacterial drugs work by inhibiting nucleic acid synthesis. The category of antibiotics that interfere with nucleic acid polymerization can be divided into two main classes: (1) those that perturb the template function of DNA; (2) those that inhibit the enzymes associated with DNA. The former category can be broken down into complex formation and chemical modification of DNA. Mitomycins are such a class that modifies DNA chemically. They exhibit very little

selectivity and bind to DNA covalently and irreversibly. They are not used as antibiotics because of their toxicity. A class of less toxic antibiotics known as bleomycin works via numerous DNA breaks in both single-stranded and double-stranded DNA. They are exclusively employed in the treatment of specific tumor types. Imidazole derivatives (including metronidazole) and nitrofurans are two other examples of antibiotics that chemically modify DNA. Metronidazole is 90%-100% effective against sexually transmitted urogenital infections caused by *Trichomonas vaginalis*. Nitrofurantoin is used in the treatment of Urinary tract infections. Both antibiotics act by inducing breakage in DNA strands via direct chemical interaction. Specifically, the nitro group of the antibiotic is converted to a nitronate radical in the cell. The radical form of the antibiotic is the activated form that attacks and breaks DNA strands.

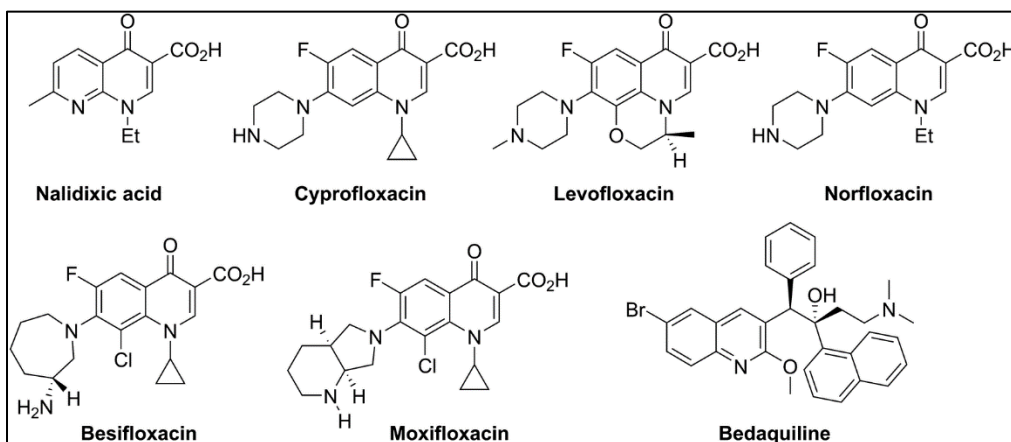


Figure 1.14: Core structure of Quinolone group of antibiotics

One member of the quinolone family, a group of synthetic antimicrobials, is nalidixic acid. It was discovered In 1962 as a byproduct during the synthesis of chloroquine, an antimalarial drug. Nalidixic acid selectively inhibits the activity of bacterial DNA gyrase, blocking DNA replication. Chemical modifications to the original quinolone backbone have resulted in the production of fluoroquinolones, like ciprofloxacin and levofloxacin, which also inhibit the activity of DNA gyrase. Ciprofloxacin and levofloxacin are effective against a broad spectrum of gram-positive or gram-negative bacteria and are among the most commonly prescribed antibiotics used to treat a wild range of infections, including urinary tract infections, respiratory infections, abdominal infections, and skin infections. However, despite their selective toxicity against DNA gyrase, side effects associated with different fluoroquinolones include phototoxicity, neurotoxicity,

cardiotoxicity, glucose metabolism dysfunction, and increased risk for tendon rupture. ([https://bio.libretexts.org/Bookshelves/Microbiology/Microbiology_\(OpenStax\)/14%3A_Antimicrobial_Drugs/14.03%3A_Drugs_Targeting_Other_Microorganisms](https://bio.libretexts.org/Bookshelves/Microbiology/Microbiology_(OpenStax)/14%3A_Antimicrobial_Drugs/14.03%3A_Drugs_Targeting_Other_Microorganisms))

1.12.3.1. Mechanism of action of Quinolones antibiotics:

Quinolones groups of antibiotics bind with DNA gyrase complex and inhibit the bacterial DNA gyrase or topoisomerase II. This enzyme introduces negative twists in DNA and helps separate its strands, inhibition of DNA gyrase disrupts DNA replication and repair, transcription bacterial chromosome separation during division, and other cell processes involving DNA.

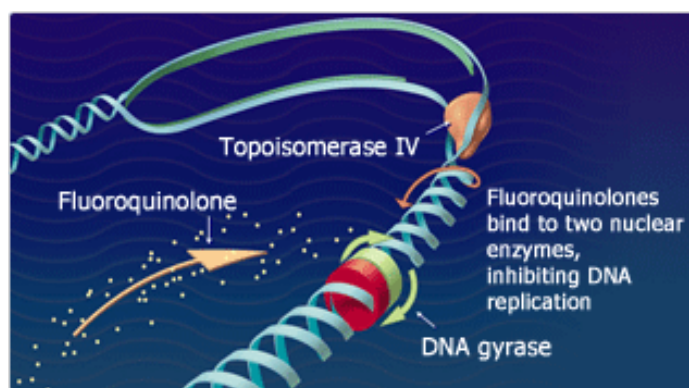


Figure 1.15: Mode of action of Fluoroquinolones

1.12.3.2. Use of Quinolone group of drugs across the world:

Quinolone group of drugs is a broad-spectrum antibiotic with a high level of effectiveness against intestinal bacteria like *E. coli*, *Klebsiella pneumoniae*, as well as various gram-positive and gram-negative bacteria including *Haemophilus*, *Neisseria*, *Pseudomonas aeruginosa*, *Mycobacterium*, *Streptococcus pyogenes*, *Staphylococcus aureus*. Urinary tract infections, Tuberculosis, sexually transmitted diseases caused by *Neisseria* and *Chlamydia*, gastrointestinal infections, respiratory tract infections, skin infections, and osteomyelitis are all treated with this class of antibiotics.

1.12.3.3. Use of Quinolone group of drugs in Pregnancy:

In the amniotic fluid and umbilical cord blood, quinolone reaches high concentrations [84]. They are used to treat persistent UTIs as they reach the urinary tract in high concentrations [85]. However, taking these medicines during pregnancy is still up for debate. Although, serious adverse

effects were observed in animal models in several studies, some other studies in human beings did not find any alterations in the joints of babies from mothers exposed to many quinolones in several periods of pregnancy [84, 86].

1.13. Misuse of antibiotics and Multi-Drug Resistance (MDR):

Antibiotics are medicines used to prevent and treat bacterial infections. The effectiveness of antibiotics, which have revolutionized medicine and saved millions of lives, is in jeopardy due to the rise of resistant bacteria throughout the world. Several decades after the first patients received antibiotic treatment, bacterial infections are once again a threat to humanity. The overuse and abuse of these drugs, as well as the pharmaceutical industry's lack of new drug research as a result of diminished economic incentives and challenging regulatory constraints, have all been linked to the challenge of antibiotic resistance. CDC has classified many bacteria as presenting urgent, serious, and concerning threats, many of which are already responsible for placing a substantial clinical and financial burden on the US healthcare system, patients, and their families. Implementing new regulations, reviving research projects, and pursuing crisis management strategies all require coordinated efforts [87].

The reasons for this problem are at least partly economic and commercial. In the case of antibiotics, the prevalence of affordable generics results in low current prices; unpredictable patterns of emerging resistance make future medical needs (and thus commercial opportunities) hard to predict, and necessary conservation measures to limit the prescribing of antibiotics would relegate new products to last-line treatments used only when nothing else works. All of this makes antibiotics appear to be less appealing from a business perspective. Therefore, economic actions are required to promote investment while preventing drug abuse.

1.13.1. Antibiotic Resistance: A Global Threat

The global burden of infections resistant to existing antimicrobial medicines is now growing at an alarming pace. Drug-resistant infections are already responsible for more than half a million deaths globally each year. Early studies commissioned by the review suggest that if the world fails to act to control resistance, this toll will exceed 10 million each year by 2050 and have cost the world over 100 trillion USD in lost output. Resistance is not an isolated phenomenon though the extent of resistance varies across different countries and regions of the world. This variation is often

linked to the extent of use in these countries or regions. For instance areas with greater use of antimicrobials are associated with greater levels of resistance. Increasing international travel means that AMR has the capability of spreading globally including to countries that are controlling their antibiotics use effectively. This makes a strong case for international coordination on AMR as no country can protect itself from resistant bacteria unless the world takes action together.

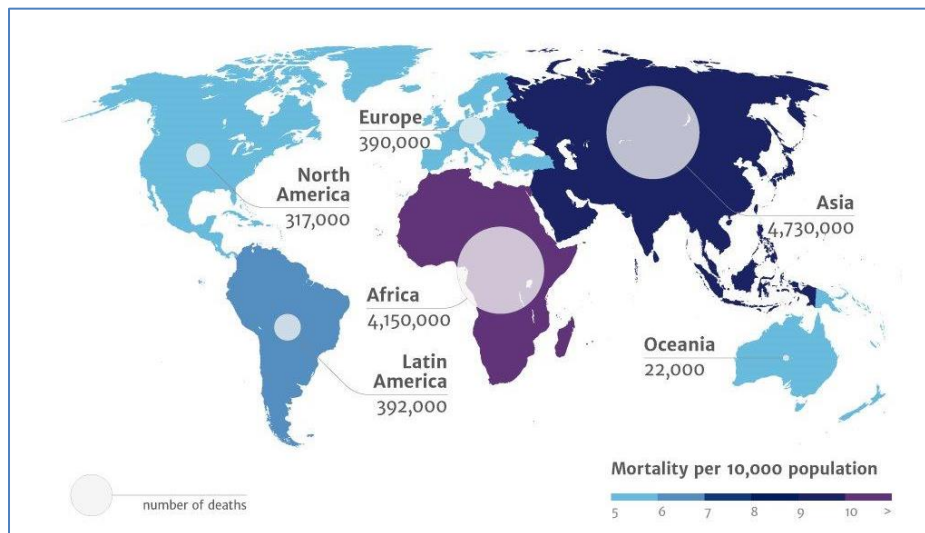


Figure 1.16: Global AMR death aspect by the year 2050 (source: <https://amr-review.org/infographics>)

Added to this issue, are the overuse and unnecessary use of antimicrobials for humans and animals which also promote the development and spread of resistance, either directly or through the environment. Much of the misuse of antimicrobials is associated with the lack of rapid diagnostics that can pin-point the exact nature of the diseases causing microbe. Doctors and prescribers, unsure of the kind of disease affecting their human or animal patient but still needing to provide treatment to them rely on empirical or treatment with broad-spectrum drugs that may or may not cure the patient but still expose microbes to a variety of drugs increasing the likelihood of resistance developing of these drugs. Figure suggest that much of the use of antibiotics in the world is for animals rather than humans and that much of this is for promoting the growth of animals rather than treating sick animals. The development and spread of drug resistance in the environment is also often overlooked. Antimicrobials can also reach the environment through waste products from the manufacturing sector that do not adequately treat the waste products and through use and excretion by humans and animals. The overuse of antimicrobials is also related to high rates of

infection and the dependence on antimicrobials as curative treatments, reducing the focus afforded to prudent measures that might prevent an infection in the first place. AMR is an issue that spans multiple areas and cannot be solved by any one solution. Nor is it an issue that any one country can address successfully by acting alone. Hence a multi-disciplined approach to solving the diverse issues and coordination among various countries is critical.

“By highlighting the vast financial and human costs that unchecked drug resistance will have, this important research underlines that this is not just a medical problem, but an economic and social one too” – Dr. Jeremy Farrar, Director, Wellcome Trust.

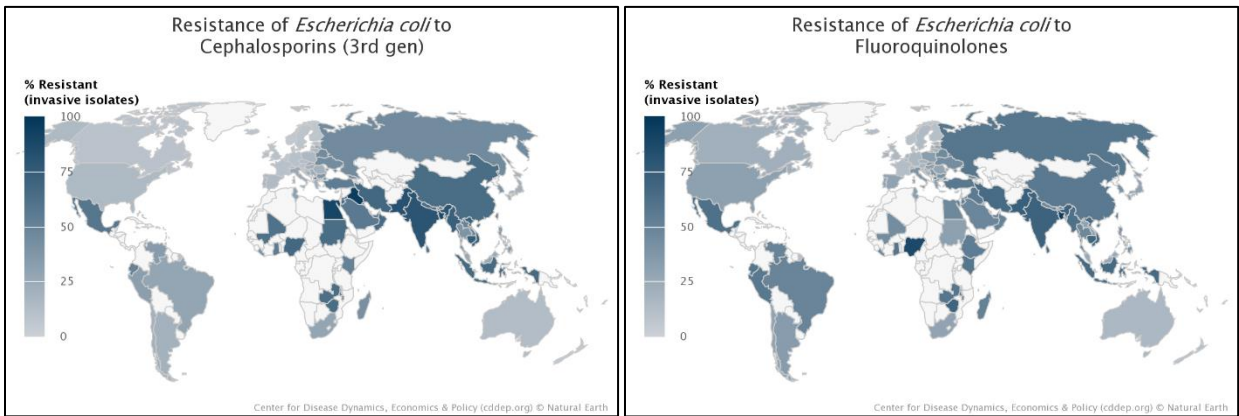


Figure1.17: Distribution of *E. coli* resistance pattern to Cephalosporins (left) and Fluoroquinolones (right)

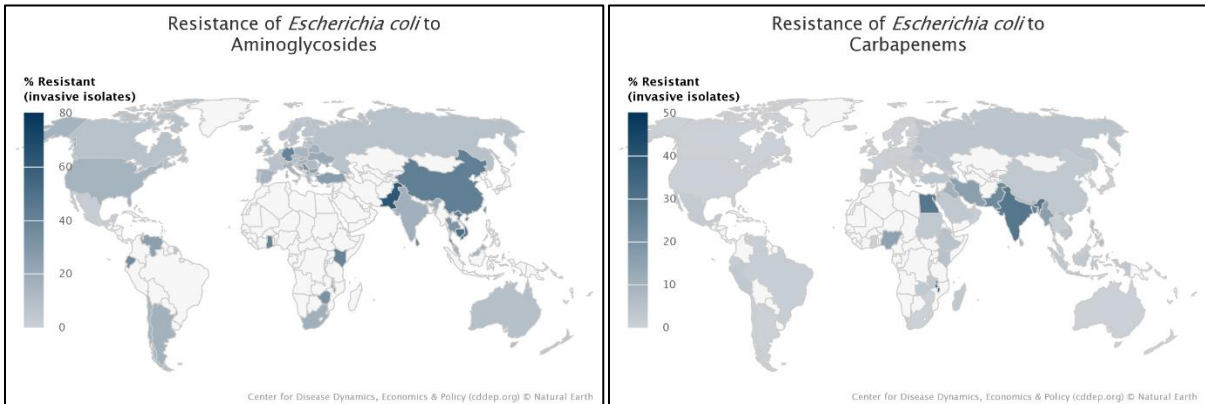


Figure1.18: Distribution of *E. coli* resistance pattern to Aminoglycosides (left) and Carbapenems (right)

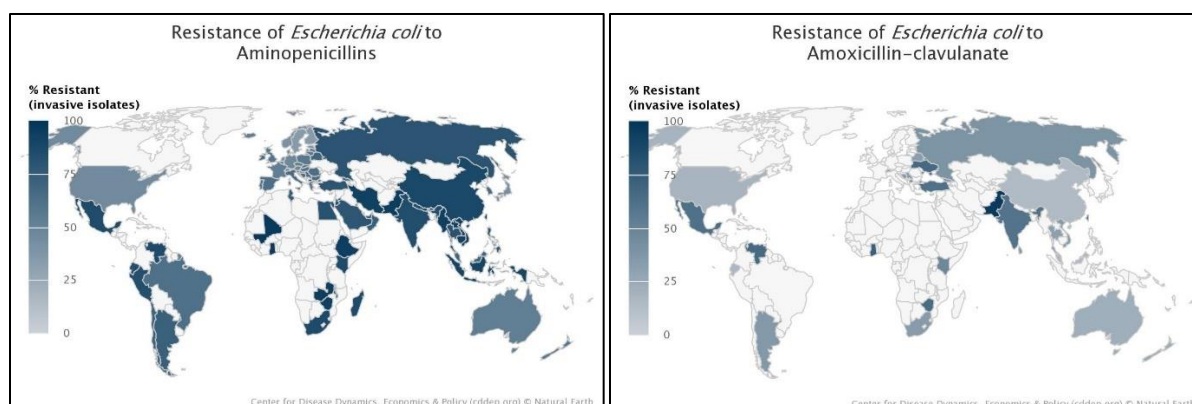


Figure 1.19: Distribution of *E. coli* resistance pattern to Aminopenicillins (left) and Amoxicillin-clavulanate (right)

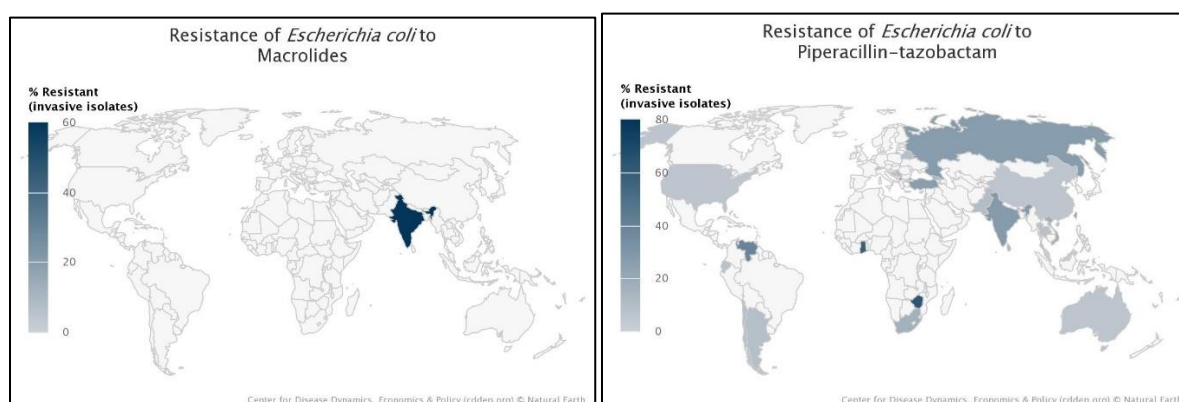


Figure 1.20: Distribution of *E. coli* resistance pattern of Macrolides (left) and Piperacillin-tazobactam (right)

1.13.2. Indian Scenario:

AMR is a major public health concern in India. The emergence of resistance is not only limited to the old and more frequently used classes of drugs but there has also been a rapid increase in resistance to the newer and more expensive drugs, like carbapenems, which is worrisome. The emergence of carbapenem-resistant *Enterobacteriaceae* (CRE) has been a major concern in developed countries, especially in the hospital/healthcare setting. Although available data indicate only a mild increase in carbapenem-resistant isolates of *E. coli* from India (from 10% in 2008 to 13% in 2013), there has been a much larger increase in carbapenem-resistant *Klebsiella pneumoniae* (from 29% in 2008 to 57% in 2014) and *Acinetobacter baumannii*[88]. India is among the nations with the highest burden of bacterial infections [89]. An estimated 410000 children aged

5 years or less die from pneumonia in India annually [90]; accounting for almost 25% of all child deaths in India [91]. Consequently, the impact of AMR is likely to be higher in the Indian setting. An indicator of the rising tide of AMR in India is the rapidly increasing proportion of isolates of *Staphylococcus aureus* that are resistant to methicillin. In 2008, about 29% of isolates were methicillin-resistant *Staphylococcus aureus* (MRSA), and by 2014, this had risen to 47% [88]. In contrast, in countries that have established effective antibiotic stewardship and/or infection prevention and control programs, the proportion of MRSA isolates has been decreasing. In India, extended-spectrum beta-lactamase (ESBL) producing strains of *Enterobacteriaceae* has emerged as a challenge in hospitalized patients as well as in the community. In a multicentric study conducted in seven tertiary care hospitals in Indian cities, 61% of *E. coli* producers. In the same study, 31 – 51% of *Klebsiella* species were carbapenem-resistant, 65% *Pseudomonas sp.* were resistant to ceftazidime, and 42% were resistant to imipenem [92]. *Acinetobacter sp.* isolated from hospitalized patients in a tertiary care hospital in New Delhi showed 57 – 80% resistance to imipenem/meropenem while 70% of isolates were resistant to Tigecycline [93].

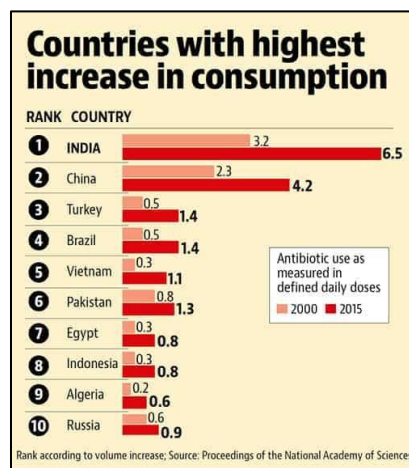


Figure 1.21: Country-wise consumption of antibiotics, where India is at the top of the list in antibiotic consumption in recent times.

1.14. Origin of Antibiotic resistance:

Bacteria as a class or species are not always equally vulnerable to or resistant to a given antibiotic. Within bacterial groups that are closely related, resistance levels might vary substantially. The least drug concentration necessary to stop bacterial growth is known as the minimum inhibitory

concentration (MIC), and it is used to determine both susceptibility and resistance. A species is deemed to have intrinsic resistance to medicine if its average MIC falls within the range of resistance [94].

1.14.1. Natural resistance: It may be intrinsic, or induced. Intrinsic may be defined as a trait that is shared universally within a bacterial species, is independent of the previous antibiotic exposure, and is not related to horizontal gene transfer [95]. The most common bacterial mechanisms involved in intrinsic resistance are reduced permeability of the outer membrane and the natural activity of efflux pumps.

1.14.2. Acquired Resistance: It is possible for bacteria to acquire genetic material that confers resistance through transformation, transposition, and conjugation (referred to as Horizontal Gene Transfer [HGT]), as well as through mutations to their own chromosomal DNA. The acquisition may either be short or long-term. The most frequent way to acquire foreign genetic material is by plasmid-mediated transmission of resistance genes; bacteriophage-borne transmission is rather uncommon. Some bacteria, including *Acinetobacter* species, are naturally competent and can thus take genetic material straight from their environment. Internally, integrins and insertion sequences may recognize genetic material, and stressors on the bacterium (starvation, UV radiation, chemicals, etc.) are frequently responsible for genetic changes (such as substitutions and deletions). Bacteria have an average mutation rate of 1 for 10^6 to 10^9 cell divisions and most of these mutations would be deleterious to the cell [96].

1.14.3. Antibiotic resistance mechanism:

Antibiotic resistance mechanisms can be divided into four primary groups: (1) decreasing medication uptake; (2) altering drug targets; (3) inactivating a drug; (4) active drug efflux. Limiting drug uptake, drug inactivation, and drug efflux are examples of intrinsic resistance strategies; drug target modification, drug inactivation, and drug efflux are examples of acquired resistance strategies. There are variances between the sorts of mechanisms used by gram-positive and gram-negative bacteria due to structural differences, among other things. Gram-positive bacteria less frequently employ restricting the uptake of a drug (don't have an LPS outer membrane) and don't have the capacity for some forms of drug efflux mechanisms, whereas gram-negative bacteria use all four primary methods [97, 98].

1.15. Innate Immune Response of the Host due to Urinary Tract Infections:

The Toll-like receptor 2 (TLR2), Toll-like receptor 4 (TLR4), Toll-like receptor 5 (TLR5), and Toll-like receptor 11 (TLR11) are just a few of the many pattern recognition receptors (PRRs) expressed by various resident and recruited cells in the urinary tract that enable early recognition of the pathogen and transduce this signal to induce a quick and powerful pro-inflammatory immune response. People who have genetic abnormalities in components of these pathways have increased susceptibility to UTIs. Even though these immune responses are crucial, they must be carefully managed to guarantee the preservation or quick restoration of the epithelial barrier [99].

1.15.1. Epithelial cells: They are the first line of defense against pathogens. They secrete a plethora of soluble compounds ranging from pro-inflammatory cytokines to antibacterial agents. Interleukin-1 (IL-1), IL-6, and IL-8 are often the first cytokines to be detected in urine following infection, and they are important for the recruitment of phagocytes into the infected bladder on kidney tissue. In response to bacterial infection, bladder epithelial cells (BECs) and α -intercalated cells function as the initial source of AMPs in the urinary tract, at a later stage, AMPs are secreted recruited neutrophils. Following UPEC's invasion of BECs, the bacteria are encapsulated in RAB27b⁺ fusiform vesicles, which intrinsically have exocytic properties, and as a consequence, BECs can expel intracellular medium without loss of viability [100]. The underlying mechanism of bacterial expulsion involves the mobilization of multiple exocytic activities within BECs. One pathway involves TLR4 signalling, other is activated when intracellular bacteria which escaped the first wave of expulsion, are recognized and captured by autophagy. A more drastic mechanism used by the bladder to reduce bacterial load is the shedding of the superficial epithelial cell layer. Observations in experimental mouse models and in patients with UTIs reveal that during the acute phases of UTIs, when the superficial BECs become heavily infected, BECs spontaneously shed in large numbers into the urine, leading to significantly reduced bacterial numbers in the bladder [101].

1.15.2. Neutrophils: They are first immune cells to be recruited to the bladder following UTIs, and they have a predominant role in the clearance of the bacteria. They respond to CXCL1 and other hemoattractants produced by superficial bladder epithelial cells, macrophages and mast cells after PRR is activated due to various bacterial products.

1.15.3. Macrophages: A substantial population of macrophages resides in the submucoas of the urinary tract, and more cells are recruited to these sites following infection. Upon activation, these macrophages produce crucial cytokines and chemokines that modulate the activity of these and other immune cells in the vicinity, which markedly influences the timing and intensity of inflammatory responses during UTIs. Following infection, CXCL1 and macrophage migration inhibitory factor (MIF) was secreted by macrophages to recruit neutrophils, and CCL2 to recruit LY6C⁺ macrophages [102]. Recruited neutrophils, upon extravasation and reaching the epithelial region, need TNF signaling to cross the basal membrane of the epithelium.

1.15.4. Mast Cells: Mast cells are another resident immune cell type located underneath the uroepithelium in close proximity to blood and lymphatic vessels that traverse the mucosal region. In the bladder mast cells are found in high numbers in the detrusor muscle region. They have a pivotal sentinel and key immunomodulatory role during UTIs, which is partly due to their ability to release many pre-stored pro-inflammatory mediators – such as TNF, histamine, and several chemokines – upon activation [103].

1.15.5. Other innate immune cells: NK cells are known to have a key role in clearing viral infections, their importance during bacterial infection is less well characterized. $\gamma\delta$ T cells are an intriguing group of resident immune cells in urinary tract. Mice lacking $\gamma\delta$ T cell receptors are prone to UTIs than wild type.

1.16. Adaptive Immune Response of the Host due to Urinary Tract Infections:

Adaptive immune responses, particularly in the bladder, is limited. UTIs that progress to the kidneys can lead to the productions of antibodies specific for the infecting agent, but patients with infections limited to the bladder inexplicably fail to induce an antibody response. This apparent defect in the antibody response of the bladder could be a major reason for the remarkable recurrence of UTIs, especially following the bladder infection [99]

1.17. References:

1. Al-Achi A. An introduction to botanical medicines: history, science, uses, and dangers. Westport, Conn: Praeger Publishers; 2008. 188 p. (The Praeger series on contemporary health and living).

2. Nickel JC. Management of urinary tract infections: Historical perspective and current strategies: Part 1 – before antibiotics. 2005. Journal of Urology. 173(1): 21 – 6.
3. Wise GJ, Schlegel PN. Sterile Pyuria. Longo DL, editor. N Engl J Med. 2015 Mar 12;372(11):1048–54.
4. Young A, Toncar A, Wray AA. Urethritis. [Updated 2022 Dec 1]. In: StatPearls [Internet]. Treasure Island (FL): StatPearls Publishing; 2023 Jan- available from: <https://www.ncbi.nlm.nih.gov/books/NBK537282/>
5. Vasudevan R. Urinary Tract Infection: An Overview of the Infection and the Associated Risk Factors. JMEN [Internet]. 2014 May 15 [cited 2023 Apr 14];1(2). Available from: <https://medcraveonline.com/JMEN/urinary-tract-infection-an-overview-of-the-infection-and-the-associated-risk-factors.html>
6. Belyayeva M, Jeong JM. Acute Pyelonephritis. [Updated 2022 Sep 18]. In: StatPearls [Internet]. Treasure Island (FL): StatPearls Publishing; 2023 Jan-. Available from: <https://www.ncbi.nlm.nih.gov/books/NBK519537/>
7. Nicolle L. Symptomatic urinary tract infection or asymptomatic bacteriuria? Improving care for the elderly. Clinical Microbiology and Infection. 2019 Jul;25(7):779–81.
8. Trautner BW. Urinary Tract Infections as a Continuum: Implications for Diagnostic and Antibiotic Stewardship. Clinical Infectious Diseases. 2021 Apr 26;72(8):1339–41.
9. Flores-Mireles AL, Walker JN, Caparon M, Hultgren SJ. Urinary tract infections: epidemiology, mechanisms of infection and treatment options. 2015. Nature Reviews Microbiology.13(5): 269 – 284.
10. Schmiemann G, Kniehl E, Gebhardt K, Matejczyk MM, Hummers-Pradier E. The Diagnosis of Urinary Tract Infection. Deutsches Ärzteblatt international [Internet]. 2010 May 28 [cited 2023 Apr 16]; Available from: <https://www.aerzteblatt.de/10.3238/arztebl.2010.0361>
11. Whiting P, Westwood M, Bojke L, Palmer S, Richardson G, Cooper J, et al. Clinical effectiveness and cost-effectiveness of tests for the diagnosis and investigation of urinary tract infection in children: a systematic review and economic model. Health Technol Assess [Internet]. 2006 Oct [cited 2023 Apr 16];10(36). Available from: <https://www.journalslibrary.nihr.ac.uk/hta/hta10360/>
12. Winkens R, Nelissen-Arets H, Stobberingh E. Validity of the urine dipslide under daily practice conditions. Family Practice. 2003 Aug;20(4):410–2.
13. Gatermann S, Fünfstück R, Handrick W, et al. In: *Harnwegsinfektion - Mikrobiologisch-infektologische Qualitätsstandards*. Mauch M, Podbielski A, Hermann M, editors. München, Jena: Urban & Fischer; 2005. pp. 8–21.
14. EAU (European Association of Urology) Guidelines on Urological Infections. European Association of Urology. <http://www.uroweb.org/nc/professional-resources/guidelines/online/>

15. McIsaac W, Carroll JC, Biringer A, Bernstein P, Lyons E, Low DE, et al. Screening for Asymptomatic Bacteriuria in Pregnancy. *Journal of Obstetrics and Gynaecology Canada*. 2005 Jan;27(1):20–4.
16. Loeb M, Bentley DW, Bradley S, Crossley K, Garibaldi R, Gantz N, et al. Development of Minimum Criteria for the Initiation of Antibiotics in Residents of Long-Term–Care Facilities: Results of a Consensus Conference. *Infect Control Hosp Epidemiol*. 2001 Feb;22(02):120–4.
17. Meiland R. Asymptomatic Bacteriuria in Women With Diabetes Mellitus: Effect on Renal Function After 6 Years of Follow-up. *Arch Intern Med*. 2006 Nov 13;166(20):2222.
18. Fernandez M, Raja U. UTI in men—is investigation required? www.bestbets.org/cgi-bin/bets.pl?record=00790
19. Bien J, Sokolova O, Bozko P. Role of uropathogenic *Escherichia coli* Virulence Factors in Development of Urinary Tract Infection and Kidney Damage. *International Journal of Nephrology*. 2012; 2012:1–15.
20. Zagaglia C, Ammendolia MG, Maurizi L, Nicoletti M, Longhi C. Urinary Tract Infections Caused by uropathogenic *Escherichia coli* Strains—New Strategies for an Old Pathogen. *Microorganisms*. 2022 Jul 14;10(7):1425.
21. Terlizzi ME, Gribaudo G, Maffei ME. UroPathogenic *Escherichia coli* (UPEC) Infections: Virulence Factors, Bladder Responses, Antibiotic, and Non-antibiotic Antimicrobial Strategies. *Front Microbiol*. 2017 Aug 15;8:1566.
22. Kaper JB, Nataro JP, Mobley HLT. Pathogenic *Escherichia coli*. *Nat Rev Microbiol*. 2004 Feb;2(2):123–40.
23. Vigil PD, Alteri CJ, Mobley HLT. Identification of *In Vivo* -Induced Antigens Including an RTX Family Exoprotein Required for uropathogenic *Escherichia coli* Virulence. Bäumler AJ, editor. *Infect Immun*. 2011 Jun;79(6):2335–44.
24. Connell I, Agace W, Klemm P, Schembri M, Märdil S, Svanborg C. Type 1 fimbrial expression enhances *Escherichia coli* virulence for the urinary tract. *Proc Natl Acad Sci USA*. 1996 Sep 3;93(18):9827–32.
25. Avalos Vizcarra I, Hosseini V, Kollmannsberger P, Meier S, Weber SS, Arnoldini M, et al. How type 1 fimbriae help *Escherichia coli* to evade extracellular antibiotics. *Sci Rep*. 2016 Jan 5;6(1):18109.
26. Klemm P, Schembri MA. Bacterial adhesins: function and structure. *International Journal of Medical Microbiology*. 2000 Mar;290(1):27–35.
27. Riegman N, van Die I, Leunissen J, Hoekstra W, Bergmans H. Biogenesis of F7(1) and F7(2) fimbriae of uropathogenic *Escherichia coli*: influence of the FsoF and FstFG proteins and localization of the Fso/FstE protein. *Mol Microbiol*. 1988 Jan;2(1):73–80.

28. Wullt B, Bergsten G, Connell H, Röllano P, Gebretsadik N, Hull R, et al. P fimbriae enhance the early establishment of *Escherichia coli* in the human urinary tract. *Mol Microbiol*. 2000 Nov;38(3):456–464.
29. Nowicki B, Labigne A, Moseley S, Hull R, Hull S, Moulds J. The Dr hemagglutinin, afimbrial adhesins AFA-I and AFA-III, and F1845 fimbriae of uropathogenic and diarrhea-associated *Escherichia coli* belong to a family of hemagglutinins with Dr receptor recognition. *Infect Immun*. 1990 Jan;58(1):279–281.
30. Spurbeck RR, Mobley HL. uropathogenic *Escherichia coli*. *Escherichia coli*. 2nd Ed. London: Academic Press; 2013:275–304.
31. Agarwal J, Srivastava S, Singh M. Pathogenomics of uropathogenic *Escherichia coli*. *Indian Journal of Medical Microbiology*. 2012 Apr;30(2):141–149.
32. Eberspächer B, Hugo F, Bhakdi S. Quantitative study of the binding and hemolytic efficiency of *Escherichia coli* hemolysin. *Infect Immun*. 1989 Mar;57(3):983–988.
33. Chen M, Jahnukainen T, Bao W, Daré E, Ceccatelli S, Celsi G. uropathogenic *Escherichia coli* Toxins Induce Caspase-Independent Apoptosis in Renal Proximal Tubular Cells via ERK Signaling. *Am J Nephrol*. 2003;23(3):140–151.
34. Russo TA, Davidson BA, Genagon SA, Warholic NM, MacDonald U, Pawlicki PD, et al. *E. coli* virulence factor hemolysin induces neutrophil apoptosis and necrosis/lysis in vitro and necrosis/lysis and lung injury in a rat pneumonia model. *American Journal of Physiology-Lung Cellular and Molecular Physiology*. 2005 Aug;289(2):L207–16.
35. Bower JM, Eto DS, Mulvey MA. Covert Operations of uropathogenic *Escherichia coli* within the Urinary Tract. *Traffic*. 2005 Jan;6(1):18–31.
36. Soltani S, Emamie AD, Dastranj M, Farahani A, Davoodabadi A, Mohajeri P. Role of toxins of uropathogenic *Escherichia coli* in development of urinary tract infection. *British Journal of Pharmaceutical Research*. 2018;21(1):e.JPRI.39188.
37. Mills M, Meysick KC, O'Brien AD. Cytotoxic Necrotizing Factor Type 1 of uropathogenic *Escherichia coli* Kills Cultured Human Uroepithelial 5637 Cells by an Apoptotic Mechanism. Barbieri JT, editor. *Infect Immun*. 2000 Oct;68(10):5869–80.
38. Guyer DM, Radulovic S, Jones FE, Mobley HLT. Sat, the Secreted Autotransporter Toxin of uropathogenic *Escherichia coli*, Is a Vacuolating Cytotoxin for Bladder and Kidney Epithelial Cells. *Infect Immun*. 2002 Aug;70(8):4539–46.
39. Tóth I, Héroult F, Beutin L, Oswald E. Production of cytolethal distending toxins by pathogenic *Escherichia coli* strains isolated from human and animal sources: Establishment of the existence of a new cdt variant (type IV). *Journal of Clinical Microbiology*. 2003;41(9):4285–4291.
40. Ladant D, Alouf JE, Popoff MR. *The Comprehensive Sourcebook of Bacterial Protein Toxins*. London: Academic Press; 2005.

41. Cirli C, Wieser A, Yadav M, Duerr S, Schubert S, Fischer H, Stappert D, Wantia N, Rodriguez N, Wagner H, Svanborg C, Miethke T. Subversion of Toll-like receptor signaling by a unique family of bacterial Toll/interleukin-1 receptor domain-containing proteins. *Nature Medicine*. 2008;14(4):399–406.
42. Lai XH, Arencibia I, Johansson A, Wai SN, Oscarsson J, Kalfas S, Sundqvist K-G, Mizunoe Y, Anders S, Uhlin BE. Cytocidal and apoptotic effects of the ClyA protein from *Escherichia coli* on primary and cultured monocytes and macrophages. *Infection and Immunity*. 2000;68(7):4363–4367.
43. Jahandeh N, Ranjbar R, Behzadi P, Behzadi E. uropathogenic *Escherichia coli* virulence genes: Invaluable approaches for designing DNA microarray probes. *Central European Journal of Urology*. 2015;68(4):452.
44. Henderson JP, Crowley JR, Pinkner JS, Walker JN, Tsukayama P, Stamm WE, Hooton TM, Hultgren SJ. Quantitative metabolomics reveals an epigenetic blueprint for iron acquisition in uropathogenic *Escherichia coli*. *PLoS Pathogens*. 2009;5(2):e1000305.
45. Olson PD, Justice SS, Hunstad D. *Escherichia coli* in urinary tract infections. *Molecular Medical Microbiology*. 2nd ed. London: Academic Press. 2015;76(7): 1373–1387.
46. Hagan EC, Mobley HLT. Haem acquisition is facilitated by a novel receptor Hma and required by uropathogenic *Escherichia coli* for kidney infection. *Molecular Microbiology*. 2008; 71(1): 79–91.
47. Neilands JB, Bindereif A, Montgomery JZ. Genetic basis of iron assimilation in pathogenic *Escherichia coli*. In: *Genetic Approaches to Microbial Pathogenicity*. Berlin, Heidelberg: Springer; 1985. Pp. 179 – 195.
48. Johnson JR. Virulence factors in *Escherichia coli* urinary tract infection. *Clinical Microbiology Reviews*. 1991;4(1):80–128.
49. Warner PJ, Williams PH, Bindereif A, Neilands JB. ColV plasmid-specific aerobactin synthesis by invasive strains of *Escherichia coli*. *Infection and Immunity*. 1981;33(2):540–545.
50. Hagberg L, Jodal U, Korhonen TK, Lidin-Janson G, Lindeberg U, Eden CS. Adhesion, hemagglutination, and virulence of *Escherichia coli* causing tract infections. *Infection and Immunity*. 1981;31(2):564–570.
51. Billips BK, Forrestal SG, Rycyk MT, Johnson JR, Klumpp DJ, Schaeffer AJ. Modulation of host innate immune response in the bladder by uropathogenic *Escherichia coli*. *Infection and Immunity*. 2007;75(11):5353 – 5360.
52. Wiles TJ, Kulesus RR, Mulvey MA. Origins and virulence mechanisms of uropathogenic *Escherichia coli*. *Experimental and Molecular Pathology*. 2008;85(1):11–19.
53. Reigstad CS, Hultgren SJ, Gordon JI. Functional genomic studies of uropathogenic *Escherichia coli* and host urothelial cells when intracellular bacterial communities are assembled. *Journal of Biological Chemistry*. 2007;282(29): 21259–21267.

54. Garcia EC, Brumbaugh AR, Mobley HL. Redundancy and specificity of *Escherichia coli* iron acquisition systems during urinary tract infection. *Infection and Immunity*. 2011;79(3):1225–1235.
55. Nagy G, Dorbindt U, Emody L, Karch H, Hacker J. Expression of hemin receptor molecule ChuA is influenced by RfaH in uropathogenic *Escherichia coli* strain 536. *Infection and Immunity*. 2001;69(3): 1924–1928.
56. Aguiniga LM, Yaggie RE, Schaeffer AJ, Klumpp DJ. Lipopolysaccharide Domains Modulate Urovirulence. *Infection and Immunity*. 2016 Nov;84(11): 3131–3140.
57. Ong CLY, Ulett GC, Mabbett AN, Beatson SA, Webb RI, Monaghan W, Nimmo GR, Looke DF, McEwan AG, Schembri MA. Identification of type 3 fimbriae in uropathogenic *Escherichia coli* reveals a role in biofilm formation. *Journal of Bacteriology*. 2008;190(3):1054–1063.
58. Lane MC, Alteri CJ, Smith SN, Mobley HL. Expression of flagella is coincident with uropathogenic *Escherichia coli* ascension to the upper urinary tract. *Proceedings of the National Academy of Sciences*. 2007;104(42): 16669–16674.
59. Emody L, Kerenyi M, Nagy G. Virulence factors of uropathogenic *Escherichia coli*. *International Journal of Antimicrobial Agents*. 2003;22: 29–33.
60. Ugbogu O, Ogbonnaya R, Nworie O. Asymptomatic bacteriuria among pregnant women in Aba. *Nigeria Journal of Microbiology*. 2010; 24: 2024–2027.
61. Obirikorang C, Quaye L, Bio FY, Amidu N, Acheampong I, Addo. Asymptomatic bacteriuria among pregnant women antenatal clinic at the University Hospital, Kumasi, Ghana. *Journal of Biomedical Science*. 2012; 1(1): 38–44.
62. Patterson TF, Andriole VT. Bacteriuria in pregnancy. *Infectious Disease Clinics of North America*. 1987; 1(4): 807–822.
63. Jeyabalan A, Lain KY. Anatomic and Functional Changes of the Upper Urinary Tract During Pregnancy. *Urology Clinics of North America*. 2007; Feb 34 (1): 1–6.
64. Loh KY, Sivalingam N. Urinary tract infections in pregnancy. *Malaysian Family Physician*. 2007; 2(2): 54–57.
65. Milkman R. Electrophoretic variation in *Escherichia coli* from natural sources. *Science*. 1973; 182: 1024 – 1026.
66. Chaudhuri RR, Henderson IR. The evolution of the *Escherichia coli* phylogeny. *Infection, Genetics and Evolution*. 2012;12:214–226
67. Herzer PJ, Inouye S, Inouye M, Whittam TS. Phylogenetic distribution of branched RNA-linked multicopy single-stranded DNA among natural isolates of *Escherichia coli*. *Journal of Bacteriology*. 1990;172:6175–6181.
68. Clermont O, Bonacorsi S, Bingen E. Rapid and simple determination of the *Escherichia coli* phylogenetic group. *Applied and Environmental Microbiology*. 2000; 66: 4555 – 4558.

69. Barclay J, Veeratterapillay R, Harding C. Non-antibiotic options for recurrent urinary tract infections in women. *BMJ*. 2017 Nov 23;j5193.
70. Wikaningtyas P, Sigit J, Sukandar EY, Gunawan I. Profile of antibiotic resistance and usage pattern in ICU of private hospital in Bandung, Indonesia.2015 *Int J Pharm Pharm Sci*. 7(2): 160-162.
71. Remesh A, Salim S, Gavathri AM, Nair U, Retnavally KG. Antibiotics prescribing pattern in the inpatient departments of a tertiary care hospital. 2013. *Archives of Pharmacy Practice*. 4(2): 71-76.
72. Czeizel AE, Rockenbauer M, Olsen J. Use of antibiotics during pregnancy. 1998. *European Journal of Obstetrics and Gynecology and Reproductive Biology*. 1998; 81: 1 – 8.
73. Fonseca MRCC, Fonseca E, Bergsten-Mendes G. Prevalence of drug use during pregnancy: a pharmacoepidemiological approach. *Revista de Saúde Pública*. 2002; 36: 205 – 212.
74. Czeizel AE, Rockenbauer M, Sorensen HT, Olsen J. A population based case-control teratologic study of ampicillin treatment during pregnancy. *American Journal of Obstetrics and Gynecology*. 2001. 185: 140 – 147.
75. Dashe J, Gilstrap LC 3rd. Antibiotic use in pregnancy. *Obstetrics and gynecology clinics of North America*. 1997 Sep; 24(3): 617 – 629.
76. Shepherd GM. Hypersensitivity reactions to drugs: evaluation and management. *Mount Sinai Journal of Medicine: A Journal of Translational and Personalized Medicine*. 2003; 70: 113 – 125.
77. Niebyl JR. Antibiotics and other anti-infective agents in pregnancy and lactation. *American Journal of Perinatology*. 2003; 20: 405 – 414.
78. Einarson A, Shuhaiber S, Koren G. Effects of antibacterials on the unborn child: what is known and how should this influence prescribing. *Paediatric Drugs*. 2001; 3: 803 – 816.
79. Christensen B. Which antibiotics are appropriate for treating bacteriuria in pregnancy? *Journal of Antimicrobial Chemotherapy*. 2000. 46, 1: 29 – 34.
80. Ortiz-Ruiz G, Vetter N, Isaacs R, Cardies A, Woods GL, Friedland I. Ertapenem versus ceftriaxone for the treatment of community-acquired pneumonia in adults: combined analysis of two multicenter randomized, double bind studies. *Journal of Antimicrobial Chemotherapy*. 2004; 53: 59 – 66.
81. Sara M.S. Importance of Biofilms in Urinary Tract Infections: New Therapeutic Approaches. *Advances in Biology*. 2014.
82. Weinstein AJ, Gibbs RS, Gallagher M. Placental transfer of clindamycin and gentamicin in term pregnancy. *American Journal of Obstetrics and Gynecology*. 1973; 124: 688 – 691.
83. Czeizel AE, Rockenbauer M. A population-based case-control teratologic study of oral oxytetracycline treatment during pregnancy. *European Journal of Obstetrics & Gynecology and Reproductive Biology*. 2000; 88: 27 – 33.

84. Loebstein R, Addis A, Ho E, Andreou R, Sage S, Donnenfeld AE, Schick B, Bonati M, Moretti M, Lalkin A, Pastuszak A, Koren G. Pregnancy outcome following gestational exposure to fluoroquinolones: a multicenter prospective controlled study. *Antimicrobial Agents and Chemotherapy*. 1998; 42: 1336 – 1339.
85. Hooton TM, Stamm WE. Diagnosis and treatment of uncomplicated urinary tract infection. *Infectious Disease Clinics of North America*. 1997; 11: 551 – 581.
86. Berkovitch M, Pastuszak A, Gazarian M, Lewis M, Koren G. Safety of the new quinolones in pregnancy. *Obstetrics and Gynecology*. 1994; 84: 535 – 538.
87. Ventola CL. The antibiotic resistance crisis: part 1: causes and threats. *Pharmacy and Therapeutics*. 2015 Apr; 40(4): 277 – 283.
88. Center for Disease Dynamics Economics and Policy. Resistance Map. (<http://resistancemap.cddep.org/resmap/c/in/India>, accessed 20 June, 2016).
89. World Health Organization. World Health Statistics 2016: Monitoring health for the SDGs. Global Health Observatory (GHO) Data. Geneva: World Health Organization; 2016. (http://www.who.int/gho/publications/world_health_statistics/2016/en/, accessed 29 July 2016).
90. Thacker N. Integrated management of neonatal and childhood illnesses: a new hope for child survival. *Indian Pediatrics*. 2007 Mar;44(3):169–171.
91. Verma R, Khanna P. Pneumococcal conjugate vaccine: a newer vaccine available in India. *Human Vaccines and Immunotherapeutics*. 2012 Sep;8(9):1317–20.
92. Mehta A, Rosenthal VD, Mehta Y, Chakravarthy M, Todi SK, Sen N, Sahu S, Gopinath R, Rodrigues C, Kapoor P, Jawali V, Chakraborty P, Raj JP, Bindhani D, Ravindra N, Hegde A, Pawar M, Venkatachalam N, Chatterjee S, Trehan N, Singhal T, Damani N. Device-associated nosocomial infection rates in intensive care units of seven Indian cities. Findings of the International Nosocomial Infection Control Consortium (INICC). *The Journal of Hospital Infection*. 2007 Oct;67(2):168–74.
93. Indian Network for Surveillance of Antimicrobial Resistance (INSAR) group,. Methicillin resistant *Staphylococcus aureus* (MRSA) in India: prevalence & susceptibility pattern. *Indian Journal of Medical Research*. 2013 Feb;137(2):363–369.
94. Reygaert WC. An overview of the antimicrobial resistance mechanisms of bacteria. *AIMS Microbiology*. 2018; 4(3): 482–501.
95. Maritnez JL. General principles of antibiotic resistance in bacteria. *Drug Discovery Today*. 2014; 11: 33 – 39.
96. Coculescu B. Antimicrobial resistance induced by genetic changes. *Journal of Medicine and Life*. 2009 Apr 15; 2(2): 114 – 123.
97. Chancey ST, Zähler D, Stephens DS. Acquired inducible antimicrobial resistance in gram-positive bacteria. *Future Microbiology*. 2012; 7: 959–978.

98. Mahon CR, Lehman DC, Manuselis G. Textbook of Diagnostic Microbiology. St. Louis: Saunders; 2014. Antimicrobial agent mechanisms of action and resistance; pp. 254 – 273.
99. Abraham SN, Miao Y. The nature of immune responses to urinary tract infections. *Nature Reviews Immunology*. 2015 Oct; 15(10): 655 – 663.
100. Bishop BL, Duncan MJ, Song J, Li G, Zaas D, Abraham SN. Cyclic AMP-regulated exocytosis of *Escherichia coli* from infected bladder epithelial cells. *Nature Medicine*. 2007 May; 13(5): 625 – 630.
101. Mulvey MA, Lopez-Boado YS, Wilson CL, Roth R, Parks WC, Heuser J, Hultgren SJ. Induction and evasion of host defenses by type-1-piliated uropathogenic *Escherichia coli*. *Science*. 1998 Nov 20; 282(5393): 1494 – 1497.
102. Schiwon M, Weisheit C, Franken L, Gutweiler S, Dixit A, Thiebes S, Quast T, Fuhrmann M, Opdenakker G, Bernhagen J, Bucala R, Panzer U, Kolanus W, Gröne HJ, Knolle PA, Kurts C, Engel DR. Crosstalk between sentinel and helper macrophages permits neutrophil migration into infected uroepithelium. *Cell*. 2014 Jan 30; 156 (3): 456 – 468.
103. Abraham SN, St John AL. Mast cell-orchestrated immunity to pathogens. *Nature Reviews Immunology*. 2010 Jun; 10(6): 440 – 452.

Chapter 2: Identification and characterization of uropathogenic *Escherichia coli* from pregnant and non-pregnant population: MDR, ESBL and carbapenemase production

2.1. Background of the Study:

The most frequent bacterial infectious disease seen in clinical practice is Urinary Tract Infection (UTI), which accounts for significant morbidity rates and high expenses of healthcare. UTIs are among the most common and significant nosocomial and community-acquired infections, with 150 million instances of these extraintestinal infections reported each year globally. Furthermore, due to its high mortality rate in humans, complications like hypertension, chronic renal failures, chronic pyelonephritis, and sharply rising drug resistance, UTI has emerged as a major public health issue worldwide, particularly in hospitals [1]. Various risk factors for UTI in women have been discovered through research. The relatively short and straight structure of urethra is one of the primary causes. The most frequent cause of acute cystitis in women is the retrograde entry of bacteria from the perineum. Its innate defense to infections is hampered by a number of UTI anomalies and factors. The factors include sex, age, hospitalization and obstruction [2]. Moreover, untreated bacteriuria in pregnancy leads to serious obstetric complications and poor maternal and perinatal outcomes, such as intrauterine growth retardation, preeclampsia, cesarean delivery, and premature delivery [3]. UTI continued to be the most frequent infections in all hospitalized patients, making up around one third of all infections in India [4]. Significant consequences for empiric therapy against pathogenic isolates as well as the potential co-selection of antibiotic resistant bacteria are associated with Multidrug-resistant (MDR) *E. coli* isolates that cause UTI. MDR was often associated with extended spectrum β -lactamase (ESBL) production as the extended spectrum cephalosporins were the drugs of first choice in UTI treatment. In recent times clinicians are compelled to treat UTI with the carbapenems due to high emergence of ESBL and β -lactamase inhibitor resistant pathogens [4].

2.2 Objective of the study:

- Isolation and biochemical characterization of uropathogenic *Escherichia coli* (UPEC) by urine culture analysis in samples collected from pregnant and non-pregnant population
- Antibigram analysis and identification of the MDR UPEC strains
- Phenotypic detection of extended spectrum β -lactamase (ESBL) and carbapenemase production amongst the MDR-UPEC strains

2.3. Materials:

2.3.1. Equipment:

Laminar Air Flow (BD Instrumentation) • Shaker-Incubator (ICT) • Autoclave • Glass spreader • Spirit Lamp • Eppendorf Tubes (1.5ml and 2ml) (Tarsons) • Microtips (0.5-10 µl, 2-20 µl, 20-200 µl, 200-2000µl) (Himedia) • Micropipettes ((0.5-10 µl, 2-20 µl, 20-200 µl, 200-2000µl) (P'Fact, Microlit, Biohit) • Cotton (Bengal Surgicals Limited) (Laxmi Healthcare Products (P) Ltd.) • 90mm Glass Petri Dish (Borosil) • Glass Culture Tubes (Touff, Borosil) • Test Tubes Racks (Tarsons) • Surgical Gloves (Pricare, Himedia) • Cryogenic Tubes 1.5ml (Tarsons) • Cooling Centrifuge (Remi) • Tabletop Centrifuge (Remi) • Weighing Machine (K Mitra) • Refrigerator (Godrej) • -20⁰C deep freezer (Cellfrost)

2.3.2. Reagents:

Luria Bertani (LB) media (SRL) • Mueller Hinton (MH) media (SRL) • Tryptone Broth (Himedia) • MRVP medium (Glucose Phosphate Broth) (Himedia) • Simons' citrate borth (Himedia) • Triple Sugar Iron Media (Himedia) • Eosin Methylene Blue (EMB) agar (Himedia) • MacConkey agar (Himedia) • Barium Chloride (Merck) • Sulphuric Acid (Merck) • 70% Ethanol (Bengal Chemical) • 95% Ethanol (Himedia) • 87% Glycerol (SRL) • Single Distilled Water (SDW) (Kemecos India Pvt. Ltd., Hospital Supply) • Double distilled water (Prepared from SDW in the distillation plant of department) • Crystal Violet (Stanbio Reagents Pvt. Ltd.) • Safranin (Stanbio Reagents Pvt. Ltd.) • Iodine (Stanbio Reagents Pvt. Ltd.) • Agar Agar (Himedia) • Antibiotic Discs (Himedia) • EZYTM MIC strips (HiMedia)

2.3.3. Preparation of Reagents:

2.3.3.1. **Luria Bertani Broth:** 20grams of LB broth powder was dissolved in 1000 ml of SDW, thoroughly mixed and autoclaved.

2.3.3.2. **Mueller Hinton Broth:** 21grams of MH broth powder was dissolved in 1000 ml of SDW, thoroughly mixed and autoclaved.

2.3.3.3. **Tryptone Broth:** 15gm tryptone powder was dissolved in 1000ml of SDW, pH was checked to be around 7.6 and then autoclaved.

2.3.3.4. **MR-VP medium Glucose Phosphate Broth:** 17gm MRVP medium was dissolved in 1000ml SDW, pH checked around 7, autoclaved.

2.3.3.5. **Simons' citrate agar:** 24 gm of media was dissolved in 1000 ml SDW, thoroughly mixed and autoclaved. The rack was secured using a ring stand and clamp so that the tubes (which contained liquid medium) have a 3cm slant with a 2-3 cm butt. To ensure sterility, it was chilled until solid and then incubated for 48 hours at 37⁰C.

2.3.3.6. **Triple Sugar Iron Test (TSI):** 65gm Tsi media was added to 1000 ml of SDW and autoclaved. The rack was secured using a ring stand and clamp so that the tubes (which contained liquid medium) have a 3cm slant with a 2-3 cm butt. To ensure sterility, it was chilled until solid and then incubated for 48 hours at 37⁰C.

2.3.3.7. **MacConkey Agar Plates:** 55.04 gm media was added in 1000ml SDW, autoclaved. Sterile media was poured in 90mm plastic petridish to get cooled and solidified.

2.3.3.8. **EMB Agar Plates:** 36gms of media was added in 1000ml SDW, autoclaved. Sterile media was poured in 90mm plastic petridish to get cooled and solidified.

2.3.3.9. **McFarland Solution:** 0.05ml of 1% Barium chloride was added to 9.95ml of 1% sulphuric acid to make 0.5 standard Mcfarland solution. OD is in the range of 0.08 – 0.1

2.3.3.10. **MH Agar Plates:** 21gm of MH media and 15gm of Agar Agar was dissolved in 1000ml of SDW, autoclaved. The sterile media was then poured in 100mm glass petridish to get cooled and solidified.

2.3.3.11. **LB Agar Plates:** 20 gm of LB media and 15 gm of Agar Agar was dissolved in 1000 ml of SDW, autoclaved. The sterile media was then poured in 100 mm glass petridish to get cooled and solidified.

2.4. Experimental Procedure:

2.4.1. Clinical Sample Collection:

2.4.1.1. **Pregnant isolates:** This study had been carried out during January, 2017 to December, 2017, on Urine samples which were obtained from the pregnant women admitted in Eden Hospital, Calcutta Medical College, Kolkata, in their 3rd trimester, and clinically suspected of having a urinary tract infection.

2.4.1.2. Non-Pregnant isolates: Urine samples obtained during January, 2017 to December, 2017, from OPD (Out Patient Department) and Indoor (Carmichael Hospital of Tropical Diseases) who were clinically suspected of having UTI, and were admitted to the hospital.



Figure 2.1. **School of Tropical Medicine, Kolkata (STM, Kolkata) (top), Carmichael Hospital of Tropical Medicine (CHTM, Kolkata) (bottom left), Eden Hospital, Medical College and Hospital, Kolkata (bottom right)**

2.4.2. Processing of clinical isolates: Fresh midstream urine samples were collected aseptically and placed in sterile containers. 1ml of the samples from each container were taken out and combined with 2ml of LB broth before being kept in a shaker-incubator at 37°C overnight. This study contained just one positive urine culture per patient that yielded considerable monomicrobial growth ($>10^5$ CFU/ml). The isolates were subjected to Gram staining for identification.

2.4.3. Gram Staining: Gram staining is a popular technique for differentiating between two broad groups of bacteria, based on their composition of their cell wall. It uses a red or violet coloring to distinguish between Gram-positive and gram-negative cells. As the cell walls of gram-positive bacteria includes a strong layer of peptidoglycan, they retain the crystal violet stain and remains violet. Gram-negative bacteria, on the other, stain red due to a weaker peptidoglycan layer in cell walls, which are unable to hold crystal violet through the decolorization process.

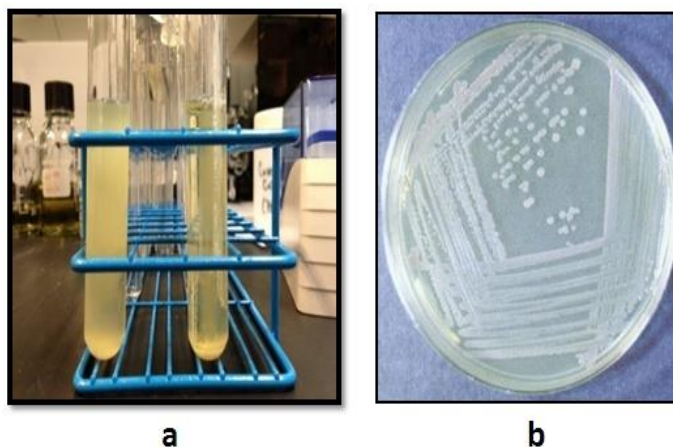


Figure 2.2. Clinical isolates showing growth in (a) LB broth (b) nutrient agar plate

2.4.3.1. Principles of Gram Staining: Some bacteria can retain the primary stain by resisting decolorization after being stained with a primary stain and fixed with a mordant, while other bacteria are decolorized by a decolorizer. Gram-positive bacteria are those that retain the primary stain, whereas Gram-negative bacteria are those that decolorized and take the counter stain.

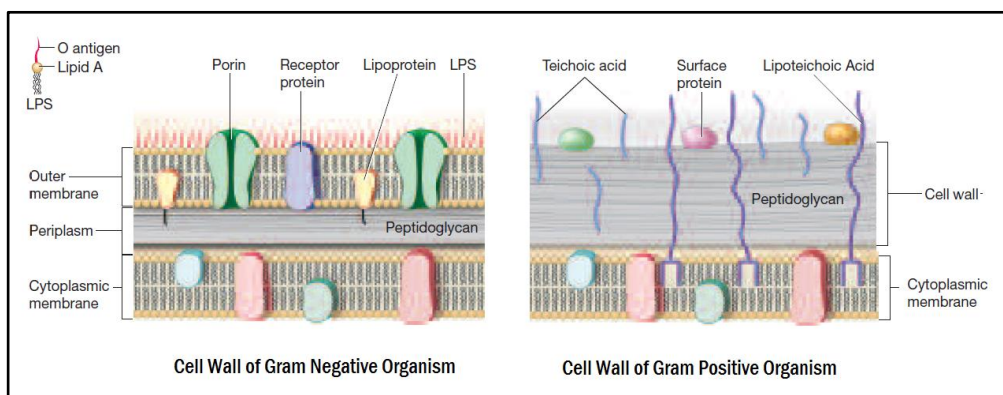


Figure 2.3. Cell wall of gram-negative and gram-positive organism

2.4.3.2. **Following steps were used to stain culture positive isolates with gram staining** (Figure 2.4.):

Samples were streaked onto microscope slides, heat fixed and dried. Crystal violet was added to sample and left to sit for 1 minute. Stain was wiped away with SDW, gram's Iodine was applied and left to sit for further 1-2 minutes. Then slides were cleaned with 95 percent ethanol or acetone, rinsed with water. Samples were sprayed with safranin, let it sit for 30-60 seconds. Slides were cleaned, dried and blotted. The stained slides were examined under a compound binocular microscope to see if gram-negative bacteria were present among the collected isolates.

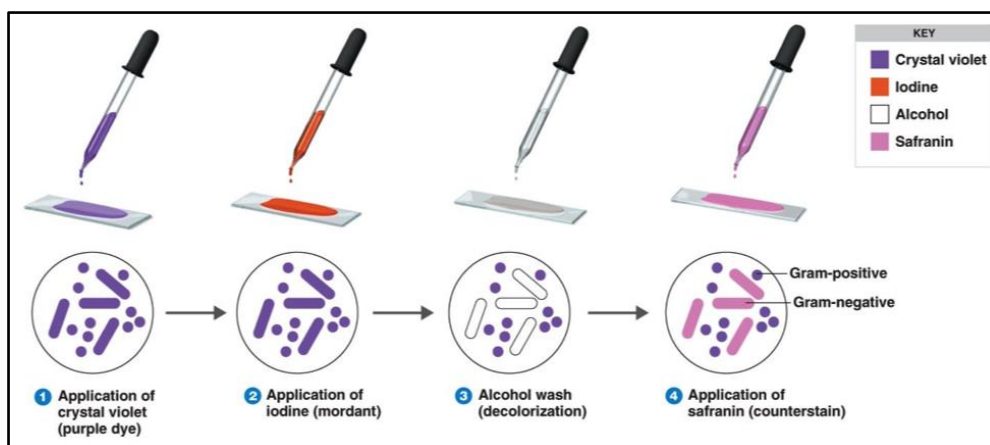


Figure 2.4. Staining procedures at a glance

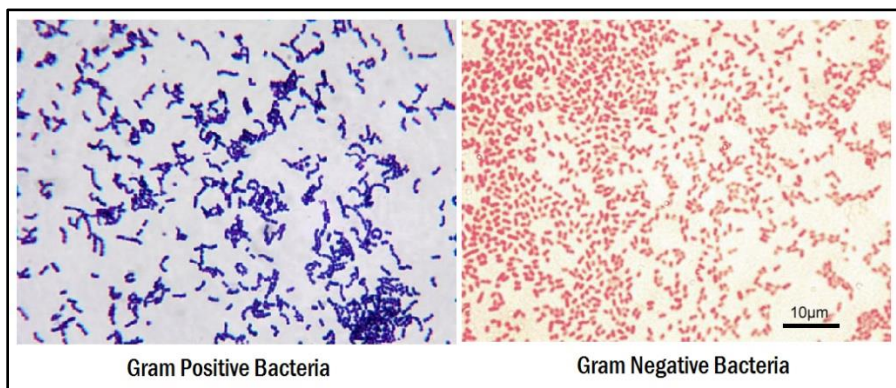


Figure 2.5: Gram-positive and gram-negative bacteria staining

2.4.4. Further processing of the samples:

- Culture positive isolates were further grown on MacConkey agar plates (Figure 2.6.)

- A single colony was then picked up by the help of a sterile loop, sub-cultured in LB media.
- On the next day, from the grown bacterial cultures, multiple glycerol stocks were prepared for further use. Biochemical tests also performed to identify the single colonies isolated from the samples.

2.4.5. Glycerol stocks preparation: Glycerol stocks were prepared with the following ratio: 87% Glycerol: Grown cells in LB broth = 1:3

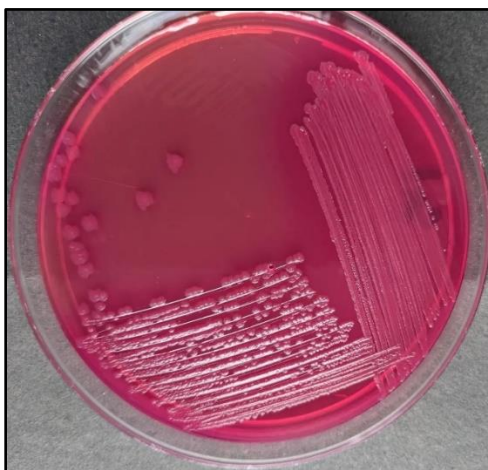


Figure 2.6: Growth of gram-negative bacteria on MacConkey agar

2.4.6. Biochemical Analysis: Biochemical techniques were used to identify *E. coli*. The Enterobacteriaceae family can be recognized using the four useful reactions that make up the IMViC reactions. The four reactions are the Indole Test, The Methyl Red Test, The Voges Proskauer Test, and The Citrate Utilization Test. The letter ‘i’ is solely used for rhyming.

2.4.6.1. Indole Test: This test demonstrates the ability of certain bacteria to decompose the amino acid tryptophane to indole, which accumulates in the medium. The test for indole synthesis is crucial for identifying enterobacteria. Tryptophan is broken down by the majority of *E. coli*, *P. vulgaris*, *P. rettgeri*, *M. morgani* and *Providencia* species, releasing indole in the process. This is accomplished via a chain of several intracellular enzymes, collectively referred to as “Tryptophanase”. It is used as part of the IMViC procedures, a test designed to distinguish among members of Enterobacteriaceae. A variation on this test using Ehrlich’s reagent (using ethyl

alcohol in place of isoamyl alcohol, developed by Paul Ehrlich) is used when performing the test on non-fermenters and anaerobes.

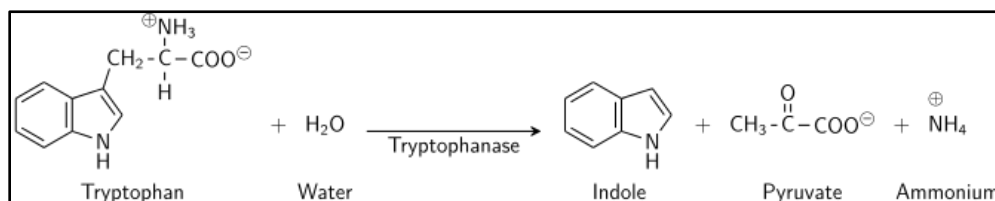


Figure 2.7: Mechanism of Indole test

2.4.6.1.1. Principle: Tryptophan is an amino acid that can undergo deamination and hydrolysis by bacteria that express tryptophanase enzyme. Indole is generated by reductive deamination from tryptophan via the intermediate molecule indole pyruvic acid. Tryptophanase catalyzes the deamination reaction, during which the amine (-NH₂) group of the tryptophan molecule is removed. Final products of the reaction are indole, pyruvic acid, ammonium (NH₄⁺) and energy. Pyridoxal phosphate is required as coenzyme. When indole is combined with Kovac's reagent (which contains hydrochloric acid and p-Dimethylaminobenzaldehyde in amyl alcohol) the solution turns from yellow to cherry red. Because amyl alcohol is not water soluble, the red coloration will form in an oily layer at the top of the broth.

2.4.6.1.2. Composition of the reagent:

Indole Kovacs Reagent	
p-Dimethylaminobenzaldehyde	50.0gm
Hydrochloric Acid, 37%	250.0ml
Amyl Alcohol	750.0ml

2.4.6.1.3. Procedure:

A sterilized test tube is taken containing 4ml of tryptophan broth. The tube is inoculated aseptically by taking the growth from 18-24 hours culture. The test tube is further incubated at 37⁰C for 24-48 hours. 0.5ml of Kovac's reagent is added to the broth culture. The presence or absence of ring is observed.

2.4.6.1.4. Interpretation:

Positive: Formation of a pink red color ('Cherry-red ring') in the reagent layer on top of the medium within seconds of adding the reagents. **Example:** *Escherichia coli*

Negative: No color change even after the addition of reagent. **Example:** *Klebsiella pneumoniae*

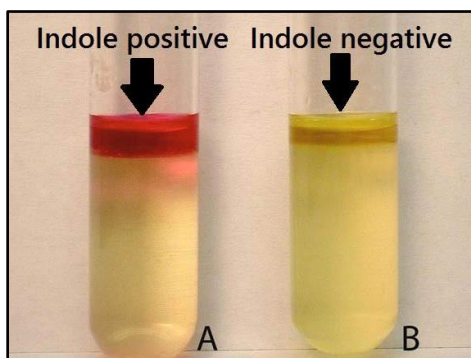


Figure 2.8: Indole positive and indole negative results

2.4.6.2. Methyl Red Test: The Methyl Red (MR) test detects the production of sufficient acid during the fermentation of glucose and the maintenance of conditions such that the pH of an old culture is sustained below a value of about 4.5, as shown by a change in the color of methyl red indicator which is added at the end of the period of incubation. By aliquoting parts to various tubes, Clark and Lubs developed MR-VP broth, which allowed both the MR and VP tests to be run from the same inoculated medium.

2.4.6.2.1. Principle: Some bacteria have the capacity to utilize glucose and transform it into an end product which is a stable acid, such as lactic acid, acetic acid or formic acid. Initially, these bacteria convert glucose to pyruvic acid, which is then metabolized by the ‘mixed acid pathway’ to produce the stable acid. The type of acid produced differs from species to species and depends on the specific enzymatic pathways present in the bacteria. The acid so produced decreases the pH to 4.5 or below, which is indicated by a change in color of methyl red from yellow to red. In the methyl red test (MR) test, the test bacteria are grown in a broth medium containing glucose. If the bacteria have the ability to utilize glucose with production of a stable acid, the color of the methyl red changes from yellow to red, when added into the broth culture. The mixed acid pathway gives 4 mol of acidic products (mainly lactic and acetic acid), 1 mol of neutral fermentation product (ethanol), 1 mol of CO₂, and 1 mol of H₂ per mol of glucose fermented. The large quantity of acids produced causes a significant decrease in the pH of the culture medium.

2.4.6.2.2. Media and Reagents used:

MRVP broth (pH 6.9) (Ingredients per liter of deionized water): buffered peptone = 7.0 gm, Glucose = 5.0 gm, Dipotassium phosphate = 5.0 gm

Methyl red solution (0.02%): 0.1gm of methyl red was dissolved in 300ml of 95% ethyl alcohol. Sufficient distilled water is added to make 500ml. Store at 4 to 8°C in a brown bottle. Solution is stable for 1 year.

2.4.6.2.3. Procedure:

Prior to inoculation, the medium should be allowed to equilibrate to room temperature. The medium should be inoculated using organisms taken from an 18-24 hours pure culture. Culture is incubated aerobically at 37°C for 24 hours. Following 24 hours of incubation, 1 ml of the broth is aliquoted to a clean test tube. The remaining broth is re-incubated for an additional 24 hours. 2 or 3 drops of methyl red indicator is added to the aliquot. Observation of red color immediately.

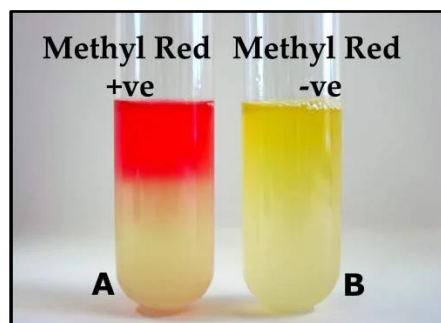


Figure 2.9: Methyl red positive and methyl red negative results

2.4.6.2.4. Interpretation:

Positive reaction: A distinct red color (A), eg. *Escherichia coli*

Negative reaction: A yellow color (B), eg. *Klebsiella pneumoniae*

2.4.6.3. **Voges-Proskauer Test:** Voges and Proskauer, in 1898, first observed the production of a red color after the addition of potassium hydroxide to cultures grown on specific media. Harden later revealed that the development of the red color was a result of acetyl-methyl carbinol production.

2.4.6.3.1. **Principle:** The VP test is used to determine if an organism produces acetyl-methyl carbinol from glucose fermentation. If present, acetyl-methyl carbinol is converted to diacetyl in the presence of α -naphthol, strong alkali (40%), and atmospheric oxygen. The α -naphthol was not part of the original procedure but was found to act as a color intensifier by Barritt and must be added first. The diacetyl and guanidine- containing compounds found in the peptones of the broth then condense to form a pinkish red polymer.

2.4.6.3.2. **Media and Reagents used:**

MRVP broth (pH 6.9) [ingredients per liter of deionized water: buffered peptone = 7.0gm, glucose = 5.0gm, dipotassium phosphate = 5.0gm]

Voges-Proskauer Reagent A (Barritt's reagent A): α -Naphthol (5%) 50gm, Absolute ethanol 1000ml

Voges-Proskauer Reagent B (Barritt's reagent B): Potassium Hydroxide 400gm, Deionized water 1000ml

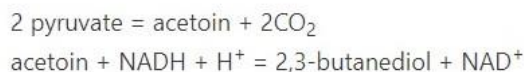


Figure 2.10: Mechanism of Voges-Proskauer test

2.4.6.3.3. **Procedure:**

Before inoculation, medium is allowed to equilibrate to room temperature. The medium is inoculated using organisms taken from an 18-24 pure culture. Organisms were incubated aerobically at 37°C for 24 hours. After 24 hours of incubation, 2ml of broth were aliquoted to a clean test tube. Remaining broth were re-incubated for an additional 24 hours. 6 drops of 5% α -naphthol were added and mixed well to aerate. 2 drops of 40% potassium hydroxide were added and mixed well to aerate. Pink-red color at the surface were observed within 30 minutes. The tubes were vigorously shaken during this 30 min period.

2.4.6.3.4. **Interpretation:**

Positive Reaction: Pink-red color at the surface. Eg. *Klebsiella*, *Enterobacter*.

Negative Reaction: A lack of pink-red color. Eg. *Escherichia coli*, *Streptococcus mitis*.

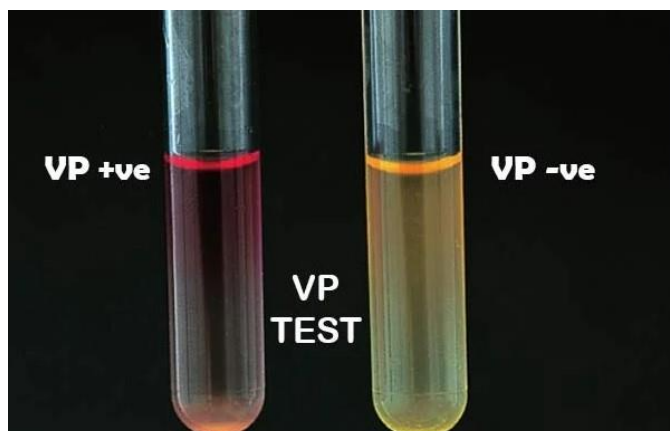


Figure 2.11: Voges Proskauer positive and negative results

2.4.6.4. Citrate Utilization Test: This test is one of a number of IMViC tests (Indole, Methyl-Red, Voges-Proskauer, and Citrate) that are used to distinguish between the distinct gram-negative bacilli of the Enterobacteriaceae family.

2.4.6.4.1. Principle: The ability of an organism to use citrate as a source of energy is examined using citrate agar. Citrate serves as the only source of carbon in the medium, and inorganic ammonium salts ($\text{NH}_4\text{H}_2\text{PO}_4$) serve as the only source of nitrogen. Citrate-permease, an enzyme that can convert citrate into pyruvate, is produced by bacteria that can thrive on this medium. The organism's metabolic cycle can then incorporate pyruvate to produce energy. Growth is indicative of utilization of citrate, an intermediate metabolite in the Krebs cycle. The ammonium salts are broken down to ammonia by the bacteria as they break down citrate, which increases alkalinity. Above pH 7.6, the change causes the bromothymol blue indicator in the medium to change from green to blue.

2.4.6.4.2. Preparation: Media is dissolved in SDW according to the manufacturer's instruction and dispensed into test tubes. It was autoclaved at 121°C at 15 psi for 15 minutes. It was further cooled in slanted position (long slant, shallow butt). Tubes should be stored in a refrigerator to ensure a shelf life of 6 to 8 weeks. Uninoculated medium would be a deep forest green due to the pH of the sample and the bromothymol blue.

2.4.6.4.3. Procedure:

The slant is streaked back and forth with a light inoculum picked from the center of a well-isolated colony. Further, slant was aerobically incubated at 35 to 37°C for up to 4 -7 days. A color change from green to blue along the slant is observed.

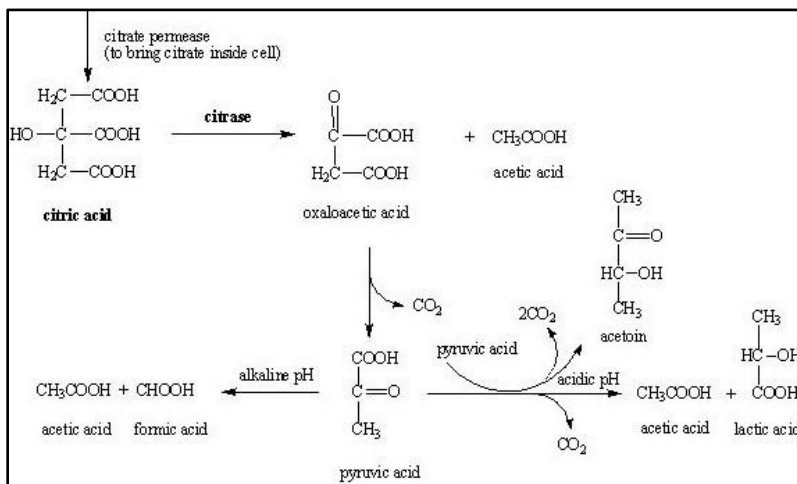


Figure 2.12: Mechanism of citrate test

2.4.6.4.4. Interpretation:

- **Positive reaction:** Growth with color change from green to intense blue along the slant. Eg. *Klebsiella*
- **Negative reaction:** No growth and no color change. Slant remains green. Eg. *Escherichia coli*.

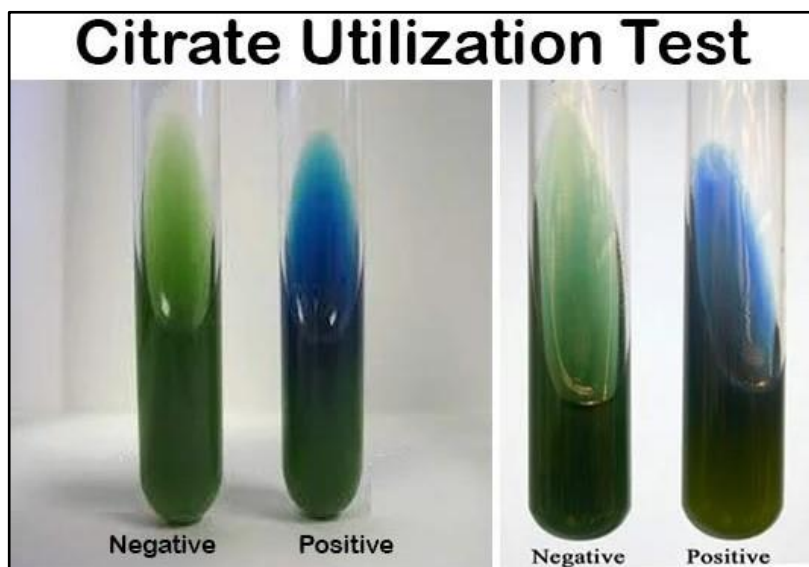


Figure 2.13: Citrate Utilization Test positive and negative results

Table 2.1: IMViC results for *Enterobacteriaceae* (urine culture positive isolates were differentiated using IMViC tests)

Species	IMViC reactions			
	I	M	Vi	C
<i>Escherichia coli</i>	+	+	-	-
<i>Edwardsiella tarda</i>	+	+	-	-
<i>Proteus vulgaris</i>	+	+	-	-
<i>Klebsiella pneumoniae</i>	-	-	+	+
<i>Klebsiella oxytoca</i>	+	-	+	+
<i>Enterobacter spp.</i>	-	-	+	+
<i>Serratia marcescens</i>	-	-	+	+
<i>Citrobacter freundii</i>	-	+	-	+
<i>Citrobacter koseri</i>	+	+	-	+
<i>Pseudomonas aeruginosa</i>	-	-	-	+
<i>Staphylococcus aureus</i>	-	+	+	-

2.4.6.5. Triple Sugar Iron Test: The distinction between the sugars that bacteria can ferment and those that it cannot is one of the characteristics of the bacteria and a key factor for identifying it. A microbiological test called Triple Sugar Iron (TSI) test can assess a microorganism's capacity to ferment sugars and generate hydrogen sulphide. The test is conducted using an agar slant of a specific medium containing a pH sensitive dye (Phenol Red), 1% Lactose, 1% Sucrose, 0.1% Glucose, Sodium Thiosulfate, and ferrous sulfate or ferrous ammonium sulfate. When all of these components are combined and allowed to solidify at an angle, an agar test tube is produced that is angled. The slanted shape of the medium offers a variety of surfaces that are either exposed to air containing oxygen to variable degrees (an aerobic environment) or are not exposed to air at all (an anaerobic environment), under which fermentation patterns of organisms are identified.

2.4.6.5.1. Principle: The triple sugar-iron agar test, which uses Triple Sugar Iron Agar, is intended to distinguish between different types of organisms based on variations in how they ferment carbohydrate and produce hydrogen sulphide. Gas production and a shift in the pH indicator's hue from red to yellow are the indicators of carbohydrate fermentation. TSI agar contains three fermentative sugars, lactose, sucrose, and glucose, all at concentrations of 1% each, to make it easier to observe patterns of carbohydrate use. The pH decreases as a result of the fermentation-induced buildup of acid. For detecting carbohydrate fermentation, which is indicated by a change

in the color of the carbohydrate medium from orange red to yellow, in the presence of acids, the acid-base indicator phenol red is incorporated. Alkaline compounds are created when peptone is decarboxylated oxidatively, and the pH increases. The transition of the medium from orange red to deep red serves as a clue. The presence of ferrous ammonium sulfate and sodium thiosulfate in the medium allows for the detection of hydrogen sulphide generation, shown by the tube's bottom turning black. The concentration of glucose is one-tenth that of lactose or sucrose to aid in the detection of microbes that only ferment glucose. The small quantity of acid produced during glucose fermentation in the tube's slant oxidizes quickly, keeping the color of the medium orange or forcing it to return to an alkaline pH. In contrast, as the butt of the tube is exposed to lower oxygen tension, the acid reaction (yellow) is maintained there. When the scarce glucose source is exhausted, organisms with the capacity to do so start using lactose or sucrose. Unrestricted air circulation must be allowed by loosely shutting the tube cap, in order to improve the alkaline state of the slant.

2.4.6.5.2. Method:

Top of a well-isolated colony was touched with a straight inoculation needle. The colony was inoculated in TSI by first stabbing through the center of the medium to the bottom of the tube and then streaking the surface of the agar slant. The cap is left loosely and tube is incubated at 35 – 37°C in ambient air for 18 to 24 hours. The reaction of the medium is examined.

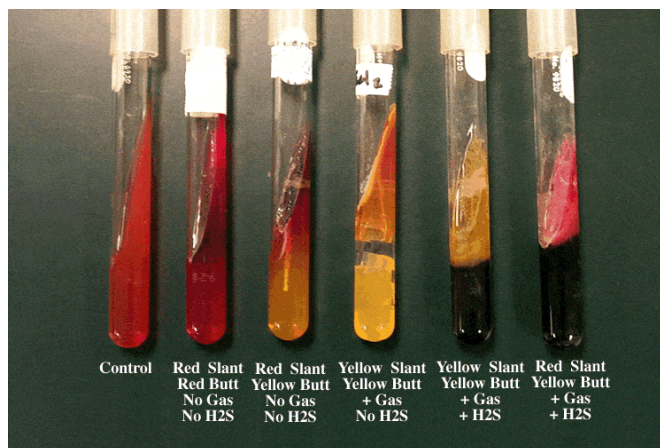


Figure 2.14: Triple sugar iron results

2.4.6.5.3. Expected results:

An alkaline/acid (red slant/yellow butt) reaction: it is indicative of dextrose fermentation only.

An acid/acid (yellow slant/yellow butt) reaction: it indicates the fermentation of dextrose, lactose and/ or sucrose.

An alkaline/alkaline (red slant/red butt) reaction: absence of carbohydrate fermentation results.

Blackening of the medium: occurs in the presence of H₂.

Gas production: bubbles or cracks in the agar indicate the production of gas (formation of CO₂ and H₂).

2.4.6.5.4. **Uses:** primarily to differentiate members of the Enterobacteriaceae family from other gram-negative rods. Also used in the differentiation among Enterobacteriaceae on the basis of their sugar fermentation patterns.

Table 2.2: Triple Sugar Iron Test results (for *Enterobacteriaceae*) [A → acidic (yellow), K → alkaline (red), Gas → + (bubble), H₂S → + (black)

Species	Triple Sugar Iron Test			
	Slant	Butt	Gas	H ₂ S
<i>Escherichia coli</i>	A	A	+	-
<i>Klebsiella pneumoniae</i>	A	A	+/-	+
<i>Klebsiella oxytoca</i>	A	A	+	-
<i>Enterobacter aerogenes</i>	A	A	+	-
<i>Enterobacter cloacae</i>	A	A	+	-
<i>Proteus vulgaris</i>	A	A	+	+
<i>Proteus mirabilis</i>	K	A	+	+
<i>Citrobacter freundii</i>	A	A	+	-/+
<i>Citrobacter koseri</i>	K/A	A	+	+
<i>Salmonella typhimurium</i>	K	A	+	+
<i>Pseudomonas aeruginosa</i>	K-	K	-	-

2.4.6.6. **Eosin Methylene Blue (EMB) agar test:** The culture medium known as Eosin Methylene Blue (EMB) agar is selective and distinct. It helps distinguish between colonies that ferment lactose and those that do not by preferentially encouraging the growth of gram-negative bacteria. Lactose and sucrose were of two types of carbohydrates that were present in the EMB agar that Holt-Harris and Teague first described. Peptone and phosphate were added, sucrose was taken out of the recipe and the amount of lactose was increased. These modifications were made by Levine to the medium.

This made it easier to distinguish between fecal and non-fecal coliform kinds. Additionally, it distinguished the coliforms from salmonellae and other non-lactose fermenters.

2.4.6.6.1. **Principle:** EMB agar contains sucrose and lactose, utilized as fermentable carbohydrates substrates, which encourage the growth of some gram-negative bacteria, especially fecal and non-fecal coliforms. Differentiation of enteric bacteria is possible due to the presence of the sugars, namely lactose and sucrose in the EMB agar and the ability of certain bacteria to ferment the lactose in the medium. The medium is acidified by lactose-fermenting gram-negative bacteria, the pH is reduced and as a result the dye produces a dark purple complex usually associated with a green metallic sheen. The vigorous lactose and/or sucrose fermentation ability of typical fecal coliforms is indicated by the metallic green sheen. Colonies appear as brown-pink due to less acid production by the slow lactose-fermenters producing organisms. Non-lactose fermenters increase the pH of the medium and produce colorless or light pink colonies by deamination of the proteins. Eosin Y and Methylene blue are pH indicator dyes that combine to form a dark purple precipitate at low pH, and inhibit the growth of most gram-positive organisms.

2.4.6.6.2. **Preparation:**

Required amount media weighed and suspended in SDW. Mixing was done to make the suspension uniform and heating given till boiling to completely dissolve the medium. Sterilizing was done by autoclaving. Labelling and storing in refrigerator was done thereafter.

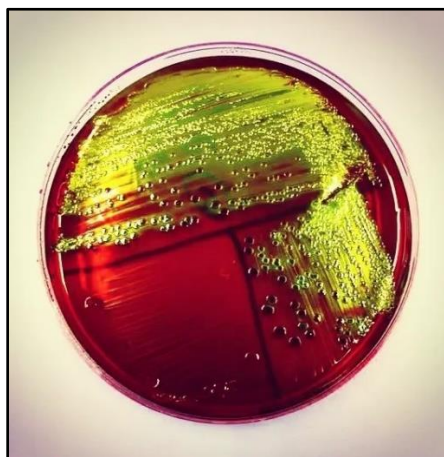


Figure 2.15: Colonies in Eosin Methylene Blue agar plates

2.4.6.6.3. **Colony Morphology:**

Escherichia coli: Colonies are 2-3mm in diameter and have a greenish metallic sheen in reflected light, dark or even black center in transmitted light.

2.4.7. Storage of confirmed uropathogenic *Escherichia coli* (UPEC) isolates: Each sample from pregnant population was assigned a number starts with P and from non-pregnant population the number starts with NP. Confirmed UPEC isolates were sub-cultured in LB broth and then glycerol stock was prepared using the ratio 87% Glycerol: Cultured broth = 3:1. **The glycerol stocks were kept in and in -20°C for day to day work and -80°C deep freezer for a long-term storage in Department of Biochemistry and Medical Biotechnology, School of Tropical Medicine, Kolkata.**

2.4.8. Antibiotic susceptibility testing: The susceptibility of uropathogenic *E. coli* isolates to various antibiotics were determined using the Kirby Bauer disc diffusion method using Mueller Hinton Agar. The antibiotics tested were Amikacin (AK; 30mcg), Ampicillin (AMP; 30mcg), Ceftazidime (CAZ; 30mcg), Cefotaxime (CTX; 30mcg), Ciprofloxacin (CIP; 10mcg), Nitrofurantoin (NIT; 300mcg), Co-trimoxazole (Trimethoprim/Sulfamethoxazole) (COT; 1.25/23.75mcg), Imipenem (IPM; 10mcg), Meropenem (MRP; 10mcg), Ertapenem (ETP; 10mcg) (HiMedia, Mumbai, India). The Clinical Laboratory Standard Institute (CLSI)s guidelines were followed to determine the zone of inhibition, *E. coli* ATCC25922 was used as a control. An isolate was assigned to be multidrug resistant (MDR) if it was resistant to ≥ 3 different classes of antibiotics.

Table 2.3: Zone of Inhibitions of different antibiotics (According to CLSI guidelines 2018):

Antibiotics	Zone of inhibition		
	Susceptible	Intermediate	Resistant
Amikacin (AK, 30mcg)	≥ 17	15-16	≤ 14
Ampicillin (AK, 10mcg)	≥ 17	14-16	≤ 13
Ceftazidime (CAZ, 30mcg)	≥ 21	18-20	≤ 17
Cefotaxime (CTX, 30mcg)	≥ 26	23-25	≤ 22
Ciprofloxacin (CIP, 5mcg)	≥ 26	22-25	≤ 21
Nitrofurantoin (NIT, 300mcg)	≥ 17	15-16	≤ 14
Co-Trimoxazole (COT, 25mcg)	≥ 16	11-15	≤ 10
Imipenem (IPM, 10mcg)	≥ 23	20-22	≤ 19
Meropenem (MRP, 10mcg)	≥ 23	20-22	≤ 19
Ertapenem (ETP, 10mcg)	≥ 22	19-21	≤ 18

2.4.9. Extended Spectrum β -lactamase (ESBL) phenotypic confirmatory test:

The Clinical and Laboratory Standards Institute (CLSI) recommends a phenotypic confirmatory combined-disk test for ESBL production in Enterobacteriaceae. It consists of measuring the growth-inhibitory zones around both cefotaxime (CTX) and ceftazidime (CAZ) discs with or without clavulanate (CA) for *Klebsiella pneumoniae*, *Klebsiella oxytoca*, *Escherichia coli* and *Proteus mirabilis* [5]. So, on 3rd GC resistant isolates, an ESBL confirmatory test was carried out using ceftazidime (CAZ, 30mcg) and Ceftazidime-Clavulanic acid (CAC, 30/10mcg); cefotaxime (CTX, 30mcg) and Cefotaxime-Clavulanic acid (CEC, 30/10mcg) combination discs. The CLSI recommends that the disc tests be performed with confluent growth on MH agar. A difference of ≥ 5 mm between the zone diameters of either of the cephalosporin discs and their respective cephalosporin/clavulanic acid disc is taken to be phenotypic confirmation of ESBL production [6].

2.4.10. **Minimal Inhibitory Concentration (MIC) study:** MIC test strips (EZYTM MIC, HiMedia, India) impregnated with a gradient concentration of imipenem in the range from 0.002 – 32 mcg/ml were used to determine the MIC of individual isolates from both group [7].

2.4.11. **Imipenem – EDTA combined disc synergy test – Carbapenemase phenotypic confirmatory test:** This experiment is used to detect the production of metallo-beta-lactamase (MBL) phenotypically. In this experiment, on a lawn culture of the test organism, two imipenem discs were spaced 20mm apart. One of the discs was then covered with 4 μ l of EDTA and the plate was incubated at 37⁰C for 24 hours. The inhibition zones of the discs with imipenem alone and imipenem-EDTA combined were measured after incubation. MBL positivity was defined as a 7mm increase in the inhibition zone of the disc containing imipenem-EDTA relative to the disc with imipenem alone [8].

2.5. Result:

2.5.1. Urine samples and statistical validation of each population:

A total of 126 urine samples from pregnant population and another 126 urine samples from non-pregnant population were obtained. The sample size for each group is statistically significant.

The sample size (n) is calculated according to the formula (From: <https://goodcalculators.com/sample-size-calculator/>):

$n = [z^2 \times p \times (1-p) / e^2] / [1 + (z^2 \times p \times (1-p) / (e^2 \times N))]$ where $z=1.96$ for a confidence level (α) of 95%, p = proportion (expressed as decimal), N =population size, e = margin of error

taking, $z=1.96$, $p=0.5$, $N=126$, $e=0.05$

$$n = [1.96^2 \times 0.5 \times (1-0.5) / 0.05^2] / [1 + (1.96^2 \times 0.5 \times (1-0.5) / (0.05^2 \times 126))]$$

$$n = 384.16 / 4.0489 = 94.88$$

$n \approx 95$ (The sample size (with finite population correction) is equal to 95)

2.5.2. Growth Positivity, Gram staining results, and Biochemical test results of the urine samples

Table 2.4A: Growth positivity, gram staining and biochemical test results collected from pregnant women

Sl. No.	Sample ID	Growth	Gram staining	IMViC Test				TSI	Presence of <i>Escherichia coli</i>
				Indole	MR	VP	Citrate		
1.	P001	+	-	+	+	-	-	yellow	+
2.	P002	-							-
3.	P003	+	-	-	-	+	+	yellow	-
4.	P004	-							-
5.	P005	+	-	+	+	-	-	yellow	+
6.	P006	+	-	+	+	-	-	yellow	+
7.	P007	+	-	+	+	-	-	yellow	+
8.	P008	+	-	+	+	-	-	yellow	+
9.	P009	-							-
10.	P010	-							-
11.	P011	+	-	+	+	-	-	yellow	+
12.	P012	+	-	+	+	-	-	yellow	+
13.	P013	-							-
14.	P014	-							-
15.	P015	-							-
16.	P016	+	-	-	-	+	+	yellow	-
17.	P017	+	+	-	-	-	-	red	-
18.	P018	-							-
19.	P019	-							-
20.	P020	+	-	+	+	-	-	yellow	+
21.	P021	-							-
22.	P022	-							-
23.	P023	-							-
24.	P024	-							-
25.	P025	+	-	+	+	-	-	yellow	+

26.	P026	+	-	-	-	+	+	yellow	-
27.	P027	-							-
28.	P028	-							-
29.	P029	-							-
30.	P030	+	-	+	+	-	-	yellow	+
31.	P031	+	-	+	+	-	-	yellow	+
32.	P032	-							-
33.	P033	+	-	+	+	-	-	yellow	+
34.	P034	-							-
35.	P035	+	-	+	+	-	-	yellow	+
36.	P036	+	-	+	+	-	-	yellow	+
37.	P037	-							-
38.	P038	-							-
39.	P039	-							-
40.	P040	+	-	+	+	-	-	yellow	+
41.	P041	-							-
42.	P042	-							-
43.	P043	+	-	+	+	-	-	yellow	+
44.	P044	+	-	+	+	-	-	yellow	+
45.	P045	-							-
46.	P046	-							-
47.	P047	+	+	-	-	-	-	red	-
48.	P048	-							-
49.	P049	+	-	+	+	-	-	yellow	+
50.	P050	+	-	+	+	-	-	yellow	+
51.	P051	-							-
52.	P052	-							-
53.	P053	-							-
54.	P054	+	-	+	+	-	-	yellow	+
55.	P055	+	-	+	+	-	-	yellow	+
56.	P056	-							-
57.	P057	-							-
58.	P058	+	-	-	-	+	+	yellow	-
59.	P059	+	-	-	-	+	+	yellow	-
60.	P060	+	+	-	-	-	-	red	-
61.	P061	-							-
62.	P062	-							-
63.	P063	-							-
64.	P064	-							-
65.	P065	+	-	+	+	-	-	yellow	+
66.	P066	-							-
67.	P067	-							-
68.	P068	-							-
69.	P069	+	-	+	+	-	-	yellow	+
70.	P070	+	-	+	+	-	-	yellow	+
71.	P071	-							-
72.	P072	-							-
73.	P073	-							-
74.	P074	+	-	+	+	-	-	yellow	+

75.	P075	-							-
76.	P076	+	-	+	+	-	-	yellow	+
77.	P077	-							-
78.	P078	+	-	+	+	-	-	yellow	+
79.	P079	-							-
80.	P080	-							-
81.	P081	-							-
82.	P082	-							-
83.	P083	+	-	+	+	-	-	yellow	+
84.	P084	-							-
85.	P085	-							-
86.	P086	-							-
87.	P087	+	-	+	+	-	-	yellow	+
88.	P088	-							-
89.	P089	-							-
90.	P090	-							-
91.	P091	+	-	+	+	-	-	yellow	+
92.	P092	-							-
93.	P093	-							-
94.	P094	+	+	-	-	-	-	red	-
95.	P095	+	-	-	+	-	-	red	-
96.	P096	+	-	-	-	+	+	yellow	-
97.	P097	+	-	-	-	+	+	yellow	-
98.	P098	-							-
99.	P099	-							-
100.	P100	+	-	-	+	-	-	red	-
101.	P101	-							-
102.	P102	+	-	-	+	-	-	red	-
103.	P103	-							-
104.	P104	-							-
105.	P105	-							-
106.	P106	-							-
107.	P107	-							-
108.	P108	+	-	+	+	-	-	yellow	+
109.	P109	+	-	+	+	-	-	yellow	+
110.	P110	+	-	+	+	-	-	yellow	+
111.	P111	-							-
112.	P112	-							-
113.	P113	+	-	+	+	-	-	yellow	+
114.	P114	+	-	+	+	-	-	yellow	+
115.	P115	-							-
116.	P116	-							-
117.	P117	-							-
118.	P118	-							-
119.	P119	-							-
120.	P120	-							-
121.	P121	-							-
122.	P122	-							-
123.	P123	-							-

124.	P124	+	-	+	+	-	-	yellow	+
125.	P125	-							-
126.	P126	-							-

2.4B: Growth positivity, gram staining and biochemical test results collected from non-pregnant women

Sl. No.	Sample ID	Growth	Gram staining	IMViC Test				TSI	Presence of <i>Escherichia coli</i>
				Indole	MR	VP	Citrate		
1.	NP001	-							-
2.	NP002	+	-	-	-	+	+	yellow	-
3.	NP003	+	-	-	+	-	-	red	-
4.	NP004	-							-
5.	NP005	-							-
6.	NP006	+	-	+	+	-	-	yellow	+
7.	NP007	-							-
8.	NP008	-							-
9.	NP009	+	-	-	-	+	+	yellow	-
10.	NP010	+	-	-	-	+	+	yellow	-
11.	NP011	-							-
12.	NP012	+	-	-	+	-	-	red	-
13.	NP013	+	-	-	+	-	-	red	-
14.	NP014	+	-	-	-	+	+	yellow	-
15.	NP015	-							-
16.	NP016	-							-
17.	NP017	-							-
18.	NP018	+	-	-	-	+	+	yellow	-
19.	NP019	-							-
20.	NP020	+	-	-	-	+	+	yellow	-
21.	NP021	+	-	-	-	+	+	yellow	-
22.	NP022	+	+	-	-	-	-	red	-
23.	NP023	-							-
24.	NP024	-							-
25.	NP025	-							-
26.	NP026	-							-
27.	NP027	+	-	-	-	+	+	yellow	-
28.	NP028	+	+	-	-	-	-	red	-
29.	NP029	-							-
30.	NP030	-							-
31.	NP031	-							-
32.	NP032	+	-	-	-	+	+	yellow	-
33.	NP033	+	-	-	-	+	+	yellow	-
34.	NP034	+	+	-	-	-	-	red	-
35.	NP035	-							-
36.	NP036	-							-
37.	NP037	-							-
38.	NP038	+	-	+	+	-	-	yellow	+
39.	NP039	-							-
40.	NP040	+	-	+	+	-	-	yellow	+

41.	NP041	-							-
42.	NP042	+	-	+	+	-	-	yellow	+
43.	NP043	-							-
44.	NP044	-							-
45.	NP045	-							-
46.	NP046	+	-	+	+	-	-	yellow	+
47.	NP047	+	-	+	+	-	-	yellow	+
48.	NP048	+	-	+	+	-	-	yellow	+
49.	NP049	+	-	+	+	-	-	yellow	+
50.	NP050	-							-
51.	NP051	+	-	+	+	-	-	yellow	+
52.	NP052	+	-	+	+	-	-	yellow	+
53.	NP053	-							-
54.	NP054	+	-	+	+	-	-	yellow	+
55.	NP055	-							-
56.	NP056	+	-	-	-	+	+	yellow	-
57.	NP057	-							-
58.	NP058	-							-
59.	NP059	-							-
60.	NP060	+	-	+	+	-	-	yellow	+
61.	NP061	+	-	+	+	-	-	yellow	+
62.	NP062	+	-	+	+	-	-	yellow	+
63.	NP063	-							-
64.	NP064	+	-	+	+	-	-	yellow	+
65.	NP065	+	-	+	+	-	-	yellow	+
66.	NP066	-							-
67.	NP067	-							-
68.	NP068	+	-	+	+	-	-	yellow	+
69.	NP069	+	-	+	+	-	-	yellow	+
70.	NP070	-							-
71.	NP071	-							-
72.	NP072	+	-	+	+	-	-	yellow	+
73.	NP073	+	-	+	+	-	-	yellow	+
74.	NP074	+	-	+	+	-	-	yellow	+
75.	NP075	+	-	+	+	-	-	yellow	+
76.	NP076	+	-	+	+	-	-	yellow	+
77.	NP077	-							-
78.	NP078	+	-	+	+	-	-	yellow	+
79.	NP079	-							-
80.	NP080	+	-	+	+	-	-	yellow	+
81.	NP081	-							-
82.	NP082	+	-	-	-	+	+	yellow	-
83.	NP083	+	-	-	-	+	+	yellow	-
84.	NP084	+	+	-	-	-	-	red	-
85.	NP085	-							-
86.	NP086	-							-
87.	NP087	-							-
88.	NP088	-							-
89.	NP089	+	-	-	+	-	-	red	-

90.	NP090	+	-	-	-	+	+	yellow	-
91.	NP091	-							-
92.	NP092	-							-
93.	NP093	+	-	+	+	-	-	yellow	+
94.	NP094	-							-
95.	NP095	-							-
96.	NP096	-							-
97.	NP097	-							-
98.	NP098	+	-	-	+	-	-	red	-
99.	NP099	-							-
100.	NP100	-							-
101.	NP101	-							-
102.	NP102	+	-	-	-	+	+	yellow	-
103.	NP103	-							-
104.	NP104	-							-
105.	NP105	+	-	+	+	-	-	yellow	+
106.	NP106	-							-
107.	NP107	+	-	+	+	-	-	yellow	+
108.	NP108	-							-
109.	NP109	-							-
110.	NP110	-							-
111.	NP111	+	-	-	-	+	+	yellow	-
112.	NP112	+	+	-	-	-	-	red	-
113.	NP113	-							-
114.	NP114	-							-
115.	NP115	-							-
116.	NP116	+	-	+	+	-	-	yellow	+
117.	NP117	+	-	+	+	-	-	yellow	+
118.	NP118	-							-
119.	NP119	+	-	+	+	-	-	yellow	+
120.	NP120	-							-
121.	NP121	+	-	+	+	-	-	yellow	+
122.	NP122	-							-
123.	NP123	-							-
124.	NP124	+	-	+	+	-	-	yellow	+
125.	NP125	-							-
126.	NP126	+	-	+	+	-	-	yellow	+

2.5.3. Sample highlights:

- From **126** Urine samples collected, **50 (39.68%)** were growth positive and uropathogenic *Escherichia coli* was detected in **36 (72%)** urine culture positive samples from pregnant population and was nomenclated as **UPECp** throughout the entire study
- **126** Urine samples, **60 (47.62%) growth positive** and uropathogenic *Escherichia coli* was detected in **34 (56.67%)** urine culture positive samples from non-pregnant population and was nomenclated as **UPECp** throughout the entire study

2.5.4. Demography of the UPEC isolates from both population:

Parameter	UPECp	UPECnp
Mean age (years)	24.19±4.09	33.76±8.48
range (years)	18 – 38	20 – 50
religion	Hindu 50%, Muslim 50%	Hindu 76%, Muslim 23%
Socio Economic Strata	lower 63.89%, lower-middle 33.33%, middle 2.78%	Lower 76.43%, Lower-Middle 5.88%, Middle 5.88%
Education	Literate 88.89%, Illiterate 11.1%	Literate 94.12%, Illiterate 5.88%

2.5.5. Antibiotic susceptibility pattern of UPECp and UPECnp isolates

Table 2.5A: Zone of inhibition observed against different antibiotics in UPECp isolates:

		AK	AMP	CAZ	CTX	CIP	NIT	COT	IPM	MRP	ETR
1.	P001	20	8	8	8	8	18	8	13	13	8
2.	P005	8	8	8	8	8	20	8	15	15	12.5
3.	P006	23	8	25	28	30	20	8	13	13	8
4.	P007	8	8	25	29	31	22	29	26	26	27
5.	P008	8	8	8	10	30	23	8	13	15	13
6.	P011	25	8	12	12	8	24	8	22	23	26
7.	P012	25	8	26	21	18	21	8	18	21	25
8.	P020	30	8	30	35	32	16	18	22	22	13
9.	P025	18	8	8	8	8	23	8	30	30	30
10.	P030	24	8	8	8	8	23	8	13	24	12
11.	P031	24	8	8	8	8	8	8	17.5	21	25
12.	P033	23	8	8	8	8	23	8	11	21	23
13.	P035	26	8	23	27	30	21	27	10	12	9
14.	P036	25	8	12	10	8	22	8	13	15	10
15.	P040	22	8	12	11	8	21	8	12	19	22
16.	P043	22	8	13	15	8	22	8	8	8	8
17.	P044	27	8	30	32	30	20	8	18	25	17
18.	P049	26	8	18	14	12	26	25	12	22	22
19.	P050	23	8	16	11	26	20	8	24	25	26
20.	P054	24	8	26	30	35	25	8	25	24	14
21.	P055	26	8	26	30	30	23	28	20	19	13
22.	P065	23	8	13	8	8	21.5	8	12	25	30
23.	P069	27.5	8	23	28	28	18	27	14	25	30
24.	P070	8	8	11	8	8	21	8	18	22.5	24
25.	P074	27	8	14	12	30	20	8	30	30	30
26.	P076	22	8	8	19	26	20	28	30	30	30
27.	P078	30	8	25	17	30	25	8	30	30	30
28.	P083	30	8	28	30	32	20	30	22	26	28
29.	P087	30	8	27	30	27	20	28	26	26	26
30.	P091	22	8	14	14	8	19	8	14	22	26
31.	P108	27	8	28	26	30	19	28	16	30	30
32.	P109	21	8	16	10	8	18	8	16	26	27

33.	P110	30	8	13	8	8	22	8	15	23	30
34.	P113	25	12	23	27	30	18	28	30	30	30
35.	P114	23	10	26	30	28	17	24	30	30	30
36.	P124	22	8	8	8	8	17	8	14	23	26

Table 2.5B: Zone of inhibition observed against different antibiotics in UPECnp isolates:

		AK	AMP	CAZ	CTX	CIP	NIT	COT	IPM	MRP	ETR
1.	NP006	21	14	19	24	28	18	27	16	22	25
2.	NP038	8	8	8	8	8	20	8	8	8	8
3.	NP040	8	8	16	16	11	20	8	15	26	27
4.	NP042	20	8	14	13	8	14	8	19	22	12
5.	NP046	8	8	8	8	8	20	8	12	11	9
6.	NP047	14	8	12	8	14	16	21	18	31	32
7.	NP048	20	8	26	8	25	25	16	11	11	9
8.	NP049	8	8	8	8	12	26	19	12	12	9
9.	NP051	18	8	18	8	20	23	22	8	8	8
10.	NP052	8	8	11	8	8	22	15	14	16	8
11.	NP054	21	8	30	8	21	27	21	15	29	33
12.	NP060	13	8	8	8	12	31	20	33	31	34
13.	NP061	28	8	30	30	32	23	28	8	8	8
14.	NP062	16	24	21	8	16	32	19	17	30	33
15.	NP064	25	8	17	8	16	30	19	13	13	8
16.	NP065	21	8	14	8	18	29	16	17	33	27
17.	NP068	22	16	25	8	30	30	21	30	30	30
18.	NP069	21	8	13	8	8	23	29	30	30	30
19.	NP072	8	8	8	8	8	21	8	31	37	33
20.	NP073	10	8	10	8	20	30	18	18	32	37
21.	NP074	11	8	12	8	11	10	16	14	27	28
22.	NP075	22	8	15	17	20	25	19	13	33	28
23.	NP076	15	8	8	8	10	18	12	11	24	31
24.	NP078	14	8	8	8	12	8	20	14	30	24
25.	NP080	11	8	8	8	13	26	18	12	24	8
26.	NP093	23	8	16.5	16	25	20	26	8	23	10
27.	NP105	21	8	8	8	8	8	8	44	32	16
28.	NP107	8	8	8	8	8	14.5	8	12	11	8
29.	NP116	25	8	20.5	25	30	18	31	11	11	8
30.	NP117	20	8	11	24	14	16	8	13	24.5	13
31.	NP119	22	8	15	8	8	22.5	18	15	39	12
32.	NP121	20	8	8	8	8	22	8	10	38	13
33.	NP124	8	8	8	8	8	19	8	19	22	25
34.	NP126	21	8	8	8	8	16	8	14	21	23

Table 2.6A: Susceptible and resistance pattern against different antibiotics in UPECp isolates:

		AK	AMP	CAZ	CTX	CIP	NIT	COT	IPM	MRP	ETR
1.	P001	S	R	R	R	R	S	R	R	R	R
2.	P005	R	R	R	R	R	S	R	R	R	R
3.	P006	S	R	S	S	S	S	R	R	R	R
4.	P007	S	R	S	S	S	S	S	S	S	S

5.	P008	R	R	R	R	S	S	R	R	R	R
6.	P011	S	R	R	R	R	S	R	S	S	S
7.	P012	S	R	S	R	R	S	R	R	R	S
8.	P020	S	R	S	S	S	R	S	S	R	R
9.	P025	S	R	R	R	R	S	R	S	S	S
10.	P030	S	R	R	R	R	S	R	R	S	R
11.	P031	S	R	R	R	R	R	R	R	R	S
12.	P033	S	R	R	R	R	S	R	R	R	S
13.	P035	S	R	S	S	S	S	S	R	R	R
14.	P036	S	R	R	R	R	S	R	R	R	R
15.	P040	S	R	R	R	R	S	R	R	R	S
16.	P043	S	R	R	R	R	S	R	R	R	R
17.	P044	S	R	S	S	S	S	R	R	S	R
18.	P049	S	R	S	R	R	S	S	R	S	S
19.	P050	S	R	R	R	S	S	R	S	S	S
20.	P054	S	R	S	S	S	S	R	S	S	R
21.	P055	S	R	S	S	S	S	S	R	R	R
22.	P065	S	R	R	R	R	S	R	R	S	S
23.	P069	S	R	S	S	S	S	S	R	S	S
24.	P070	R	R	R	R	R	S	R	R	S	S
25.	P074	S	R	R	R	S	S	R	S	S	S
26.	P076	S	R	R	R	S	S	S	S	S	S
27.	P078	S	R	S	R	S	S	R	S	S	S
28.	P083	S	R	S	S	S	S	S	S	S	S
29.	P087	S	R	S	S	S	S	S	S	S	S
30.	P091	S	R	R	R	R	S	R	R	S	S
31.	P108	S	R	S	S	S	S	S	R	S	S
32.	P109	S	R	R	R	R	S	R	R	S	S
33.	P110	S	R	R	R	R	S	R	R	S	S
34.	P113	S	R	S	S	S	S	S	S	S	S
35.	P114	S	R	S	S	S	S	S	S	S	S
36.	P124	S	R	R	R	R	S	R	R	S	S

Table 2.6B: Susceptible and resistance pattern against different antibiotics in UPECnp isolates:

		AK	AMP	CAZ	CTX	CIP	NIT	COT	IPM	MRP	ETR
1.	NP006	S	R	R	R	R	R	R	R	S	S
2.	NP038	S	R	R	R	R	R	R	R	R	R
3.	NP040	R	R	R	R	R	S	R	R	S	S
4.	NP042	R	R	R	R	R	R	R	R	S	R
5.	NP046	R	R	R	R	S	R	S	R	R	R
6.	NP047	R	R	R	R	R	S	R	R	S	S
7.	NP048	R	R	R	R	S	S	S	R	R	R
8.	NP049	R	R	R	R	R	S	R	R	R	R
9.	NP051	R	R	S	R	R	S	R	R	R	R
10.	NP052	R	R	S	R	R	S	S	R	R	R
11.	NP054	R	R	S	S	R	S	S	R	S	S
12.	NP060	S	R	R	R	S	S	R	S	S	S
13.	NP061	S	R	R	R	S	S	S	R	R	R

14.	NP062	S	R	R	R	R	S	R	R	S	S
15.	NP064	S	R	S	R	R	S	R	R	R	R
16.	NP065	S	R	S	R	R	S	R	R	S	S
17.	NP068	R	R	R	R	R	R	R	S	S	S
18.	NP069	S	R	R	R	R	S	S	S	S	S
19.	NP072	R	R	R	R	R	R	R	S	S	S
20.	NP073	S	R	R	R	R	S	S	R	S	S
21.	NP074	S	R	R	R	R	R	R	R	S	S
22.	NP075	S	R	R	R	R	S	R	R	S	S
23.	NP076	R	R	R	R	R	R	R	R	S	S
24.	NP078	R	R	R	R	R	R	R	R	S	S
25.	NP080	S	R	R	R	R	S	S	R	S	R
26.	NP093	S	R	R	R	R	S	R	R	S	R
27.	NP105	S	R	R	R	R	R	R	S	S	R
28.	NP107	R	R	R	R	R	R	R	R	R	R
29.	NP116	S	R	R	S	S	S	S	R	R	R
30.	NP117	S	R	R	R	R	S	R	R	S	R
31.	NP119	S	R	R	R	R	S	S	R	S	R
32.	NP121	S	R	R	R	R	S	R	R	S	R
33.	NP124	R	R	R	R	R	S	R	R	S	S
34.	NP126	S	R	R	R	R	S	S	R	S	S

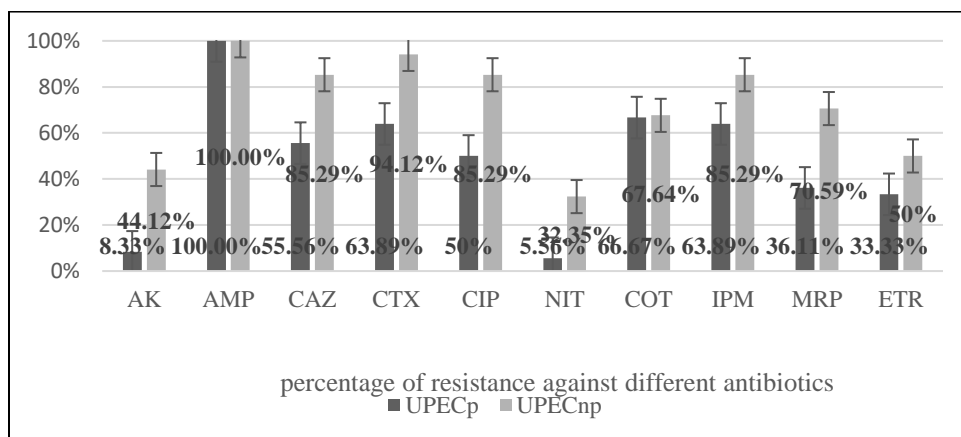


Figure 2.16: Resistance pattern against different antibiotics in UPECp and UPECnp isolates

Table 2.7. Correlation of antibiotic resistance pattern in UPECp and UPECnp isolates

UPECp										
	AK	AMP	CAZ	CTX	CIP	NIT	COT	IPM	MRP	ETR
AK	1									
AMP	^a	a								
CAZ	0.270	^a	1							
CTX	0.227	^a	.841**	1						

CIP	0.101	^a	.671**	.752**	1					
NIT	-0.073	^a	-0.027	-0.070	0.000	1				
COT	0.213	^a	.672**	.695**	.589**	-0.086	1			
IPM	0.227	^a	0.259	0.278	.520**	-0.070	0.327	1		
MRP	0.192	^a	0.091	0.084	0.173	0.323	0.164	0.445**	1	
ETR	0.213	^a	-0.079	-0.204	-0.118	0.086	0.125	0.286	0.573**	1
UPECnp										
	AK	AMP	CAZ	CTX	CIP	NIT	COT	IPM	MRP	ETR
AK	1									
AMP	^a	^a								
CAZ	-0.133	^a	1							
CTX	-0.030	^a	0.249	1						
CIP	0.034	^a	-0.172	0.249	1					
NIT	0.272	^a	0.287	0.173	0.110	1				
COT	0.108	^a	0.068	.361*	.423*	.344*	1			
IPM	0.034	^a	-0.172	-0.104	0.062	-0.245	-0.110	1		
MRP	0.206	^a	-0.279	0.113	-.461**	-0.032	-0.243	0.268	1	
ETR	-0.059	^a	-0.083	0.000	-0.249	-0.063	-0.189	0.249	.645**	1

** . Correlation is significant at the 0.01 level (2-tailed)

* . Correlation is significant at the 0.05 level (2-tailed)

^a . cannot be computed because at least one of the variables is constant

2.5.6. Key points of Antibiotic resistance pattern of UPECp and UPECnp isolates:

Antibiogram study of 36 UPECp and 34 UPECnp isolates revealed that,

- Overall, UPECnp isolates were more resistant to every group of antibiotics tested, when compared with UPECp isolates.
- Aminopenicillin group of drug Ampicillin (AMP) was completely ineffective and they exhibited a complete resistance (100%) against both group of isolates.
- Moreover, UPECp isolates also exhibited resistance against Sulfonamides (COT, 66.67%), 3rd generation cephalosporins (CTX, 63.89% and CAZ, 55.56%), and carbapenem (IPM, 63.89%). They were somewhat resistance against Fluoroquinolones (CIP, 50%).
- Aminoglycosides (AK, 8.33%) were mostly effective against these group followed by synthetic drug (NIT, 5.56%), and some other carbapenems (ETR 33.33%, MRP 36.11%).

- Additionally, UPECnp isolates displayed resistance against 3rd generation cephalosporins (CTX, 85.29% and CAZ 94.12%), carbapenems (IPM, 85.29%, MRP, 70.59%, and ETR 50%), sulfonamides (COT, 67.64%).
- Synthetic drug (NIT, 32.35%) were mostly effective against this group of isolates, followed by Aminoglycosides (AK, 44.12%).

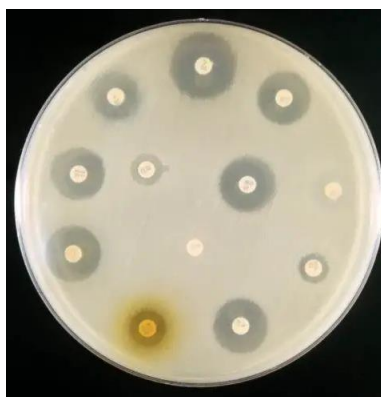


Figure 2.17: Representative picture of the antibiotic susceptibility test result

A significantly very high positive correlation between the resistance patterns of CAZ and CTX; high positive correlation between CIP and CAZ, CIP and CTX, COT and CAZ, COT and CTX; moderate positive correlation between COT and CIP, IPM and CIP, IPM and MRP, MRP and ETR was observed in UPECp population (Table 2.7). In UPECnp population, significant strong positive correlation between ETR and MRP; moderate positive correlation between COT and CIP; moderate negative correlation between MRP and CIP; weak negative correlation between COT and CTX, COT and NIT was observed (Table 2.7).

2.5.7. ESBL phenotype confirmatory test results:

Table 2.8: ESBL phenotype confirmatory test results of UPECp (left) and UPECnp (right) isolates.

Sl No.	Sample ID	CAZ	CAC	CTX	CEC	Conc.	Sl No.	Sample ID	CAZ	CAC	CTX	CEC	Conc.
1.	P001	8	8	8	8	BLIR	1.	NP006	8	30	8	30	E
2.	P005	8	8	8	8	BLIR	2.	NP038	8	8	8	10	BLIR
3.	P006					NE	3.	NP040	8	8	8	8	BLIR
4.	P007					NE	4.	NP042	16	23	8	22	E

5.	P008	8	8	8	8	BLIR	5.	NP046	12	20	8	13	E
6.	P011	15	22	8	21	E	6.	NP047	8	11	10	11	BLIR
7.	P012					NE	7.	NP048	8	8	8	8	BLIR
8.	P020					NE	8.	NP049	8	8	8	8	BLIR
9.	P025	8	8	8	8	BLIR	9.	NP051	12	20	8	20	E
10.	P030	17	20	8	24	E	10.	NP052	11	19	11	22	E
11.	P031	8	8	8	8	BLIR	11.	NP054	30	30	30	30	NE
12.	P033	8	8	8	8	BLIR	12.	NP060	8	24	12	30	E
13.	P035					NE	13.	NP061	8	24	10	22	E
14.	P036	12	18.5	10	22	E	14.	NP062	8	20	8	20	E
15.	P040	10	22	10	16	E	15.	NP064	20	28	15	24	E
16.	P043	16	21	10	24	E	16.	NP065	18	28	10	20	E
17.	P044	25	27	25	27	BLIR	17.	NP068	8	28	20	30	E
18.	P049	8	8	8	8	BLIR	18.	NP069	8	22	10	22	E
19.	P050	18	24	13	20.5	E	19.	NP072	8	8	8	8	BLIR
20.	P054					NE	20.	NP073	8	8	8	8	BLIR
21.	P055					NE	21.	NP074	8	18	10	15	E
22.	P065	12	20	8	13	E	22.	NP075	8	22	8	25	E
23.	P069					NE	23.	NP076	8	8	8	8	BLIR
24.	P070	8	16	8	13	E	24.	NP078	8	8	8	8	BLIR
25.	P074	13	19	12	22	E	25.	NP080	8	8	8	8	BLIR
26.	P076					NE	26.	NP093	8	14	8	15	E
27.	P078	27	30	17	23	E	27.	NP105	8	15	8	13	E
28.	P083					NE	28.	NP107	8	20	8	20	E
29.	P087					NE	29.	NP116	8	15	8	15	E
30.	P091	15	20	9	16	E	30.	NP117	8	13	8	15	E
31.	P108					NE	31.	NP119	8	20	8	20	E
32.	P109	14	22	8	13	E	32.	NP121	8	8	8	8	BLIR
33.	P110	17	25	8	18	E	33.	NP124	8	20	8	15	E
34.	P113					NE	34.	NP126	8	15	8	15	E
35.	P114					NE							
36.	P124	8	15	8	13	E							

E=ESBL (Extended Spectrum β -lactamase); BLIR = β -lactamase resistant inhibitor; NE=non-ESBL

ESBL phenotype confirmatory test revealed that,

- Out of 36 UPECp isolates, 22 (61.1%) isolates were resistant towards 3rd generation cephalosporins and, rest 14 (38.89%) isolates were susceptible and were termed as non-ESBL isolates.
- Out of 22 UPECp isolates were responsive towards β -lactamase inhibitors, and are Extended spectrum β -lactamase (ESBL) producers, whereas rest 8 isolates (36.36%) were non-responsive towards β -lactamase inhibitors and hence are termed as β -lactamase resistant inhibitors (BLIRs).

- Within 34 UPECnp isolates, 33 (97.06%) isolates were resistant towards 3rd generation cephalosporins and the remaining 1 (2.94%) was non-ESBL.
- In the group of 33 resistant isolates, 23 (69.7%) responsive towards β -lactamase inhibitors (ESBL) and rest 10 (30.3%) were non-responsive, i.e. BLIR.

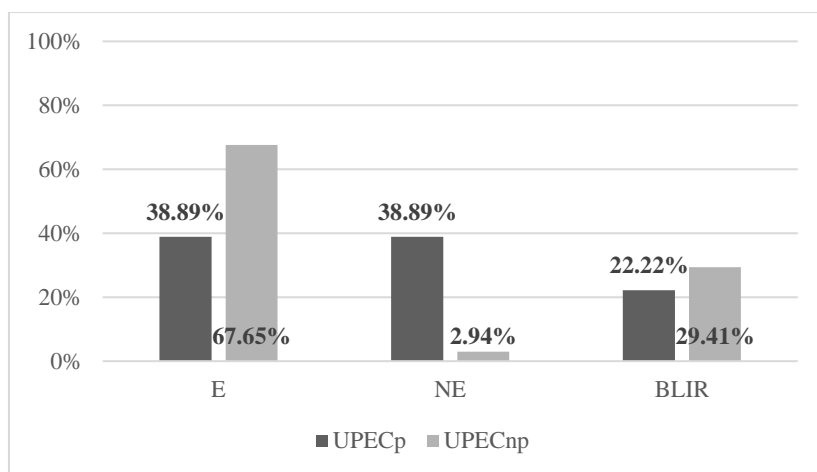


Figure 2.18: Distribution of ESBL, BLIR and non-ESBL in UPECp and UPECnp isolates

2.5.8. Carbapenemase phenotype confirmatory test results: Both populations of UPEC exhibited high resistance (UPECp 63.89%, $p < 0.001$ and UPECnp 85.29%, $p < 0.001$) against IPM, with MIC in the range from <4 to >16 $\mu\text{g}/\mu\text{l}$ in the UPECp group, whereas <3.5 to >32 $\mu\text{g}/\mu\text{l}$ in the UPECnp group. Combined disc test with IPM and IPM+EDTA indicated MBL-production in 21.73% (5/23, $p = 0.022$) UPECp and 55.17% (16/29, $p < 0.000$) UPECnp isolates respectively.

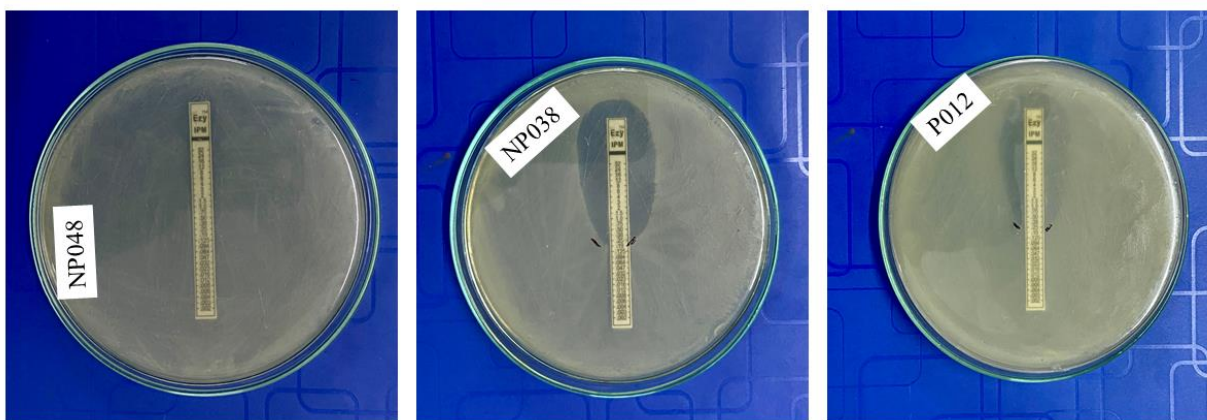


Figure 2.19: Representative picture of MIC by IPM MIC strips

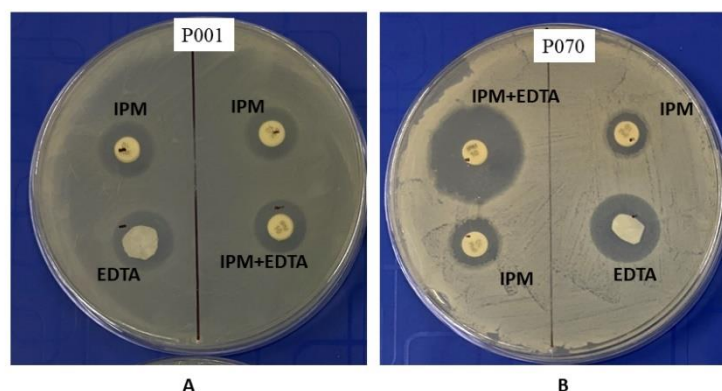


Figure 2.20: Representative picture of (A) MBL positive (B) MBL negative isolates

2.6. Discussion:

UTI caused by uropathogenic *E. coli* cause a frequent complication during pregnancy. Our study reported a high incidence of *E. coli* in the urine culture positive samples collected from pregnant women (72%), and non-pregnant women (56.67%), similar to different studies comprising of pregnant [9, 10] and non-pregnant [11, 12, 13] population. In recent times, emergence of multidrug resistance (MDR) *E. coli* isolates in pregnant population [14, 15, 16, 17] was documented, which turned into limited treatment options for the MDR infection. Additionally, very high frequency of MDR *E. coli* isolates were observed in non-pregnant population in different studies from all over the world [18, 19, 20]. This study indicated high incidence of ESBL and BLIR in pregnant and non-pregnant population. Additionally, this study also presented high incidence of carbapenemase production in both pregnant and non-pregnant population.

2.7. Reference:

1. Hadifar S, Moghoofei M, Nematollahi S, Ramazanzadeh R, Sedighi M, Salehi-Abargouei A, Miri A. Epidemiology of Multidrug Resistant Uropathogenic *Escherichia coli* in Iran: A Systematic Review and Meta-Analysis. 2017. Japanese Journal of Infectious Disease. 70(1): 19-25.
2. Subhashini N, Joby J, Latha A, Indira A. Access the prevalence of urinary tract infection among patients admitted in tertiary care hospital at Nellore. 2016. International Journal of Applied Research. 2(6): 865-866
3. Mukherjee M, Basu S, Mukherjee SK, Majumdar M. Multidrug-resistance and Extended Spectrum Beta-Lactamase production in Uropathogenic *E. coli* which were isolated from Hospitalized Patients in Kolkata, India.

4. Kamat US, Fereirra A, Amonkar D, Kulkarni MS. Epidemiology of the hospital acquired urinary tract infections in a medical college hospital in Goa. 2009. IJU. 25(1): 76
5. Poulou A, Evgenia G, Vrioni G, Koumaki V, Pittaras T, Pournaras S, Tsakris A. Modified CLSI Extended-Spectrum β -Lactamase (ESBL) Confirmatory Test for Phenotypic Detection of ESBLs among Enterobacteriaceae Producing Various β -Lactamase. 2014. JCM. 52(5)
6. Abdelmuktader A, Talal El Far A. Methods of ESBLs detection in Clinical Microbiology Lab. 2019. Virology & Immunology Journal. 3(4): 1-8.
7. Nisha KV, Veena SA, Rathika SD, Vijaya SM, Avinash SK. Antimicrobial susceptibility, risk factors and prevalence of bla cefotaximase, temoneira, and sulfhydryl variable genes among *Escherichia coli* in community-acquired pediatric urinary tract infection. 2017. Journal of Laboratory Physicians. 9(3): 156 – 162.
8. Vamsi KS, Moorthy SR, Murali TS, Hemilamma M, Reddy YRR, Reddy BRC, Kumar JS. Phenotypic methods for the detection of Metallo-beta-lactamase production by gram-negative bacterial isolates from hospitalized patients in a tertiary care hospital in India. 2021. Journal of Pure and Applied Microbiology. 15(4): 2019-2026.
9. Sekyere JO, Reta MA, and Fourie PB. Risk factors for, and molecular epidemiology and clinical outcomes of carbapenem- and polymyxin- resistant gram-negative bacterial infections in pregnant women, toddlers: a systematic review and meta-analysis. 2021. Annals of New York Academy of Sciences. 1502: 54 – 71.
10. Moradi Y, Eshrati B, Motevalian SA, Baradaran HR. A systemic review and meta-analysis on the prevalence of *Escherichia coli* and extended-spectrum β -lactamase-producing *Escherichia coli* in pregnant women. 2021. Archives of Gynecology and Obstetrics. 303: 363 – 379.
11. Yigit Y, Yazici V, Ayhan H, Gencer EG, Halhalli HC, Karakakayali O, Gunaydin YK. The analysis of *Escherichia coli* resistance in urine culture and in antibiograms as requested by emergency service. 2014. Turkish Journal of Emergency Medicine. 14(3): 121 – 124.
12. Grados MC, Thuissard IJ, Alós J-I. Stratification by demographic and clinical data of the antibiotic susceptibility of *Escherichia coli* from urinary tract infections of the community. 2018. Atención Primaria. 51(8): 494 – 498.
13. Alanazi MQ, Alqahtani FY, Aleanizy FS. An evaluation of *E. coli* in urinary tract infection in emergency department at KAMC in Riyadh, Saudi Arabia: retrospective study. 2018. Annals of Clinical Microbiology and Antimicrobials. 17: 3.
14. Mansouri F, Sheibani H, Javedani MM, Afsharian M. Extended-spectrum beta-lactamase (ESBL)-producing Enterobacteriaceae and urinary tract infections in pregnant/postpartum women: A systematic review and meta-analysis. 2019. International Journal of Clinical Practice. 73: e13422.
15. Chelkeba L, Fanta K, Mulugeta T, Melaku T. Bacterial profile and antimicrobial resistance pattern of common bacteria among pregnant women with bacteriuria in Ethiopia: a systemic review and meta-analysis. 2022. Archives of Gynecology and Obstetrics. 306: 663 – 686.

16. Milenkov M, Rasoanandrasana S, Rahajamanan LV, Rakotomalala RS, Razafindrakoto CA, Rafalimanana LV, Ravelomandranto E, Ravaoarisaina Z, Westeel E, Petitjean M, Mullaert J, Clermont O, Raskine L, Samison LH, Endtz H, Andremont A, Denamur E, Komurian-Pradel F, Armand-Lefevre L. Prevalence, Risk factors, and Genetic Characterization of Extended-spectrum Beta-Lactamase *Escherichia coli* isolated from healthy pregnant women in Madagascar. 2021. *Frontiers of Microbiology*. 12: 786146.
17. Elsariti HO, Elmeheishi FM, Elgrabulli FR. Detection of extended spectrum β -lactamase and AmpC gene in *Escherichia coli* isolated from pregnant women in Misurata City. 2021. *Journal of Humanitarian and Applied Sciences*. 12: 282 – 289.
18. Ramírez-Castillo FY, Moreno-Flores AC, Avelar-González FJ, Márquez-Díaz F, Harel J, Guerrero-Barrera AL. An evaluation of multidrug-resistant *Escherichia coli* isolates in urinary tract infections from Aguascalientes, Mexico: cross-sectional study. 2018. *Annals of Clinical Microbiology and Antimicrobials*. 17: 34.
19. Ku JH, Bruxvoort KJ, Salas SB, Varley CD, Casey JA, Raphael E, Robinson SC, Nachman KE, Lewin BJ, Contreras R, Wei RX, Pomichowski ME, Takhar HS, Tartof SY. Multidrug resistance of *Escherichia coli* from outpatient uncomplicated urinary tract infections in a large United States integrated healthcare Organization. 2023. *Open Forum Infectious Diseases*. 10(7): ofad287.
20. Madrazo M, Esparcia A, López-Cruz I, Alberola J, Piles L, Viana A, Eiros JM, Artero A. Clinical impact of multidrug-resistant bacteria in older hospitalized patients with community-acquired urinary tract infection. 2021. *BMC infectious Diseases*. 21, 1232.

Chapter 3: Characterization of MDR uropathogenic *Escherichia coli* isolates from pregnant and non-pregnant population according to acquired β -lactamase genes, mobile genetic elements and resistant plasmid replicon types

3.1. Background Study:

Antimicrobial resistance (AMR) in UPEC was caused by the acquisition of various resistance genes, most often extended-spectrum- β -lactamase (ESBL) variants such as *bla*_{TEM}, *bla*_{OXA}, and *bla*_{CTX-M} that conferred resistance to broad-spectrum penicillin, cephalosporins and monobactams [1, 2, 3]. Earlier studies also showed that the β -lactam resistant UPEC strains may be classified as ESBL or carbapenemase producers according to the enzyme-substrate [4]. The most often carbapenemases found in this pathogen were *bla*_{NDM} and *bla*_{OXA-48} [5]. The insertion elements, transposons and integrons that are crucial in the accumulation and transmission of the resistant determinants along with antibiotic resistant genes in a variety of pathogens, including UPEC, as well as the mobile genetic elements (MGEs), especially those encompassed plasmids of different incompatibility (Inc) groups, that encoded antibiotic resistant genes (ARGs), including β -lactam resistance [6, 7].

The presence and transmission of ESBL and carbapenemase in the UPEC isolated from non-pregnant population have been documented in numerous studies around the world [5, 8]. However, there are a few reports on the molecular determinants of β -lactam resistance and their dissemination in UPEC isolated from pregnant population both worldwide and nationwide.

3.2. Objectives:

- To identify the prevalence of major EBSL genes: *bla*_{CTX-M}, *bla*_{TEM}; major oxacillinase genes: *bla*_{OXA-I}, *bla*_{OXA-II}, *bla*_{OXA-III}; major carbapenemase genes: *bla*_{NDM}, *bla*_{OXA-48} in UPEC_p and UPEC_{np} populations
- To identify and classify mobile genetic elements acquired by UPEC_p and UPEC_{np} isolates
- To classify replicon types of resistant plasmids acquired by UPEC_p and UPEC_{np} isolates that harbored the antibiotic resistant determinants.

3.3. Materials:

3.3.1. Equipment:

Laminar Air Flow (BD Instrumentation) • Shaker-Incubator (ICT) • Autoclave • Spirit Lamp • Eppendorf Tubes (1.5ml and 2ml) (Tarsons) • Microtips (0.5-10 μ l, 2-20 μ l, 20-200 μ l, 200-2000 μ l) (Himedia) • Micropipettes ((0.5-10 μ l, 2-20 μ l, 20-200 μ l, 200-2000 μ l) (P'Fact, Microlit,

Biohit) • Cotton (Bengal Surgicals Limited) (Laxmi Healthcare Products (P) Ltd.) • Glass Culture Tubes (Touff, Borosil) • Test Tubes Racks (Tarsons) • Surgical Gloves (Pricare, Himedia) • Cryogenic Tubes 1.5ml (Tarsons) • Cooling Centrifuge (Remi) • Tabletop Centrifuge (Remi) • Weighing Machine (K Mitra) • Refrigerator (Godrej) • -20⁰C deep freezer (Cellfrost) • Thermal Cycler (Applied Biosystems) • Gel Documentation System (Bio-Rad, USA)

3.3.2. Reagents:

Luria Bertani (LB) media (SRL) • Mueller Hinton (MH) media (SRL) • Barium Chloride (Merck) • Sulphuric Acid (Merck) • 70% Ethanol (Bengal Chemical) • 95% Ethanol (Himedia) • 87% Glycerol (SRL) • Single Distilled Water (SDW) (Kemecos India Pvt. Ltd., Hospital Supply) • Double distilled water (Prepared from SDW in the distillation plant of department) • Agar Agar (HiMedia) • Antibiotic Discs (Himedia) for ESBL screening • 0.5 M EDTA (pH 8.0)

3.4. Experimental Procedures:

3.4.1. Isolation of bacterial plasmid:

Extra-chromosomal DNA or plasmids, can replicate on their own apart from the bacterial chromosome. They are typically circular, super-coiled covalently closed molecules. They contain genes that code for different functions (like antibiotic resistance) that may be advantageous to the cell but are not essential for the normal cellular activities. Plasmid DNA is utilized as a vector in recombinant DNA technology to transport any foreign DNA. In the host cell they can replicate, and possess phenotypic traits by which they can be detected.

Alkaline lysis was first described by Birnboim and Doly in 1979 and has, with a few modifications, been the preferred method for plasmid DNA extraction from bacteria ever since. It is probably one of the most generally useful techniques because it is a fast, reliable and relatively clean way to obtain DNA from cells. If necessary, DNA from an alkaline lysis prep can be further purified. Alkaline lysis depends on a unique property of plasmid DNA. It is able to rapidly anneal following denaturation. This is what allows the plasmid DNA to be separated from bacterial chromosome. The process is described here in step by step.

3.4.1.1. The protocol:

- 6ml of LB broth inoculated by 5µl of test organism & incubated in a shaker (>250 rpm) at 37°C
- 6ml of 18-24 hours culture is taken in centrifuge tube and centrifuged at 8000 rpm for 5 minutes
- Bacterial pellets are obtained by discarding the supernatant
- The pellet is resuspended in **100µl ice-cold solution I** (50mM glycerol, 10mM EDTA, 25mM Tris; pH 8, stored at 4°C) [Stock solution prepared: 10ml 500mM glucose, 2ml 500mM EDTA (pH 8), 2.5ml 1M Tris, 85.5ml DDH₂O & stored at 4°C]
- The resulting solution is vortexed to fully resuspend the bacteria [EDTA chelates the bivalent metals (mainly Ca²⁺ and Mg²⁺), removal of metals destabilizes the cell membrane, inhibits DNases. Glucose maintains osmolarity and prevents the buffer from lysing the cells].
- **200 µl solution II (freshly prepared)** is added to the suspension [20 µl 0.2 N NaOH, 100 µl 1% SDS stored at room temperature, 880 µl DDH₂O: prepared freshly]
- The suspension is mixed thoroughly by repeated gentle inversion [SDS creates pores in the cell membrane. NaOH loosen the cell wall and releases the plasmid DNA & shared cellular DNA. NaOH denatures the DNA. Cellular DNA becomes linearized & the strands are separated. Plasmid DNA is circular and remains topologically].
- **150 µl of ice-cold solution III** is added to the lysate. [3M Potassium Acetate (pH 6), Stock solution prepared: 60ml, 5M potassium acetate (49.07 gm potassium acetate in 100 ml water), 11.5 ml glycerol acetic acid (70%) & 28.5 ml water].
- The solution is mixed by repeated inversion. [Potassium Acetate allows circular DNA to renature, sheared cellular DNA remains denatured as single stranded DNA (ss DNA). Large ssDNA molecules are insoluble in high salt concentration & precipitated].
- The solution is **centrifuged at 10000 rpm for 20 minutes at 4°C** [mix volume 300 – 350 µl].
- The supernatant is **collected & transferred** to a fresh centrifuge tube. It is **centrifuged** again for at **10000 rpm for 10 minutes at 4°C**.
- Supernatant are **recovered and transferred** to a new centrifuge tube. **5 µl of RNase** is added to the supernatant to remove cellular DNA present in the supernatant and **incubated at 37°C for 1 hour** in the incubator.

- **1:1 Phenol: Chloroform (200 µl: 200 µl)** is added to each vial. It is centrifuged for **5 minutes at 10000 rpm at 4°C** (350 µl mix → 175 µl: 175 µl)
- **Supernatant** (aqueous layer) **collected and transferred** to each centrifuge tube.
- Equal volume of **chloroform (400 µl)** added to each tube.
- Centrifuged at **10000 rpm for 5 minutes at 4°C**.
- **Supernatant** was collected (**400 µl/ 350 µl**) & **1/10 V of sodium acetate** (40 µl/ 35 µl) and **2 V of absolute alcohol** (800 µl/ 700 µl) was added at incubated at -20°C over-night.
- On the next morning, it was centrifuged again at **10000 rpm for 30 minutes at 4°C**.
- **Supernatant is removed** and plasmid DNA pellets are obtained.
- The **pellet is washed in freshly prepared 70% Ethanol** (200 µl).
- Centrifuged at **10000 rpm for 10 minutes at 4°C**.
- Pellets are collected and air dried for ethanol to evaporate.
- Dried plasmid DNA is **dissolved in ~20 µl 1X TE buffer** (pH 7.0).
- Centrifuge tube containing dissolved **plasmid stored at 4°C overnight** to **resuspend the plasmid DNA completely** and **stored at -20°C** for future use.
- Plasmids were visualized in 0.8% Agarose gel electrophoresis.

3.4.2. Agarose gel electrophoresis: The gel casting tray was sealed at first with adhesive tapes or within gel caster whichever available, and then combs were fitted properly into the well notches. To wipe the tray and combs 70% ethanol was used. Conical flask was then filled with 0.8 to 1.5 gram of agarose (according to the required percentage) and 100 ml of 1X TAE buffer or 98 ml SDW and 2 ml of 50X TAE buffer whichever available. The solution was further microwaved for 1-2 minutes for complete melting of the agarose. After microwaving, when the gel was completely melted, it was recovered and 5 µl of EtBr (Ethidium Bromide) was added to the solution per 100 ml. The flask was immediately spun before pouring into the gel casting tray to eliminate bubbles and it was allowed to get solid for next 20-30 minutes. After the gel has been solidified, the adhesive tapes and combs were removed, and the gel was placed in electrophoresis tank. 1X TAE buffer was poured in electrophoresis chamber, thoroughly covering the gel. Once the gel is ready, 3 µl DNA was mixed with 1 µl gel loading dye and put into the wells. 1 µl of 1kb marker DNA was mixed with 1 µl of gel-loading dye and 4 µl of DDH₂O and the mixture was then loaded onto

the last well. The samples were then electrophoresed for 1 hour at 100 volts. The gel was then visualized under UV transilluminator and documented in a gel documentation system.

3.4.2.1. **Preparation of 50X TAE and 1X TAE buffer:**

To prepare 1000 ml of 50X TAE electrophoresis buffer, 242 grams Tris base was mixed in 750ml DDH₂O using magnetic stirrer. 57.1ml Glacial acetic acid and 100 ml of 0.5 M EDTA solution (pH 8.0) is added. The volume is adjusted to 1000 ml with additional DDH₂O. It was mixed properly and autoclaved. 1X TAE buffer was prepared using 49 parts of DD Water with 1 part of 50X TAE buffer. The pH of the final solution was checked to be at 8.0.

3.4.3. The Polymerase Chain Reaction: Polymerase Chain Reaction (PCR) is a powerful method for amplifying particular segments of DNA, distinct from cloning and propagation within the host cell. This procedure is carried out entirely biochemically, that is, in vitro.

3.4.3.1. Principle: In PCR, a single-stranded DNA template is used as a substrate for the enzyme DNA polymerase, which regulates the synthesis of DNA from deoxynucleotide substrates. When a tailor-made oligonucleotide is annealed to a longer template DNA, DNA polymerase adds nucleotides to the 3' end of the molecule. In this way, DNA polymerase can employ a synthetic oligonucleotide as a primer and extend its 3' end to create an extended stretch of double-stranded DNA if it is annealed to a single-stranded template that has a region that is complementary to the oligonucleotide.

3.4.3.2. **Procedure/Steps of PCR:**

- **Denaturation:** DNA template is heated to 95⁰C. This breaks the weak hydrogen bonds that hold DNA strands together in a helix, allowing the strands to separate creating ssDNA.
- **Annealing:** The mixture is cooled to anywhere from 50⁰C – 70⁰C. This allows primers to bind (anneal) to their complementary sequence in the template DNA.
- **Extension:** The reaction is then heated to 72⁰C, the optimal temperature for DNA polymerase to act. DNA polymerase extends the primers, adding nucleotides onto the primer in a sequential manner, using the target DNA as a template.

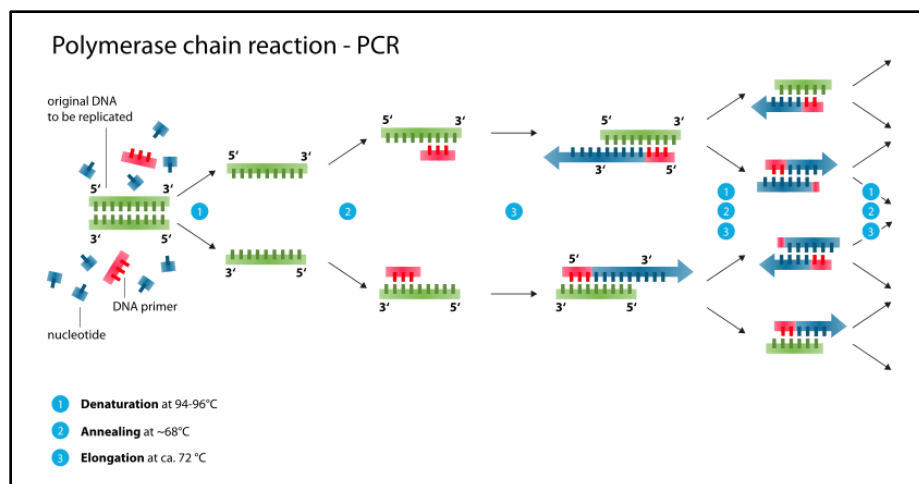


Figure 3.1: Polymerase chain reaction – An overview

Table 3.1: PCR reaction mixture:

Reagents	Volume
Template DNA	1 µl
Forward Primer (FP) (100pMol)	0.5 µl (2.5pmol)
Reverse Primer (RP) (100pMol)	0.5 µl (2.5pmol)
Buffer Stock 10X	2 µl (1X)
MgCl ₂ (50mM)	0.6 µl (1.5mM)
dNTPs (10mM)	0.2 µl (100 µM)
Taq Polymerase (5U/Reaction)	0.1 µl (0.025 U)
Double Distilled Water	14 µl
Total	20 µl

3.4.4. Oxacillinase genes: There are four main types of β -lactamases according to the most basic classification system, which is based on molecular structure [9]. Enzymes from classes A through C have a long history of being both chromosomally encoded and plasmid-mediated [10]. Class D β -lactamases have proven to be significantly more difficult to identify and, for the most part, were only found in gram negative bacteria as plasmid-encoded-lactamases. These early enzymes were essentially penicillinases, which, unlike the class A β -lactamases, could hydrolyze and confer resistance to oxacillin as well as penicillin, hence the name oxacillinases and the prefix ‘OXA’ [11].

The capacity to hydrolyze oxacillin allowed one small set of plasmid-encoded-lactamases in GNB to be distinguished from the more prevalent TEM enzymes, shown by Hedges et al. [12]. This

group of enzymes has a diverse substrate profile and was encoded by a significantly smaller number of plasmids than TEM. These β -lactamases shared similar characteristics with a plasmid (R1818) discovered by Datta and Kontomichalou [13] and later given the designation R46. Compared to the TEM lactamases, these enzymes displayed less selective activity against penicillin, but more active against methicillin and oxacillin [11]. They were also relatively less effective against 1st generation cephalosporins and are poorly inhibited by major class A β -lactamases inhibitors such as clavulanic acid.

Isoelectric points were initially used to differentiate closely related β -lactamases. Three different oxacillinases, designated OXA-1, OXA-2, and OXA-3, were identified by Sykes and Matthew [14]. The first two shared a trait with the majority of the individuals in this class in that chloride ions inhibited them. The first gene to be sequenced was *bla*_{OXA-2}, which was found on plasmid R46. The first *bla*_{OXA-1} gene to be sequenced was part of a transposon carried on plasmid RGN238. There was about 48% homology with the OXA-2- β -lactamase. The active-site serine at position 71 and the leucine at position 179, however, showed a large degree of conservation.

71	179
APD <u>S</u> TFKIALS	SLKISPEEQIQFLRK – OXA-1
SPAS <u>T</u> FKIPHT	SLAISAEQIAFLRK – OXA-2

Figure 3.2: The active-site serine at position 71 and position 179.

These were the first motifs that were identified in the OXA enzymes, and they have become an important characteristic in the examination of these enzymes. The location of the *bla*_{OXA-1} gene was in a Tn21- derived transposon, inserted between the *aad* gene encoding aminoglycoside resistance and its promoter. Interestingly, the rather dissimilar *bla*_{OXA-2} gene was found in exactly the same position, which suggests some strong evolution pressure not just for the presence of these genes in the bacterial cell but also for their carriage within this specific transposon.

3.4.4.1. Identification of oxacillinase genes: Oxacillinase genes, *bla*_{OXA-I}, *bla*_{OXA-II}, and *bla*_{OXA-III} were detected using gene-specific primers using PCR. Separate PCR reactions for each gene were carried using plasmid DNA as template. PCR assays were performed in 20 μ l reaction volume, containing 0.8 μ l (10ng) of plasmid DNA, 0.8 μ l of each primer, 2 μ l 10X buffer, 0.3 μ l dNTP, 0.6

μl MgCl₂, 0.1 μl Taq DNA polymerase (Invitrogen), and 14.6 μl of DDH₂O. The primers and conditions of *bla_{OXA-I}*, *bla_{OXA-II}* and *bla_{OXA-III}* were given Table 3.1. The primer sequences of the target genes are depicted in section 3.4.6.2. and primers are marked in green. Generated amplicons were separated by 1.5% agarose gel electrophoresis and visualized using Ethidium Bromide by Gel Documentation system (Bio-Rad, USA).

Table 3.2: Primer sequences for major oxacillinase, ESBL and carbapenemase genes identification used in this study.

SI No.	Gene names	Primers (5' → 3')	PCR conditions	No. of cycles	Amplicon size (bp)
1.	<i>bla_{OXA-I}</i>	FP: TTTCAAATGGGACGGMAAGCC RP: CCAACCCACCAWGCACAC	95°C – 30'' 52°C – 30'' 72°C – 1'	30	462
2.	<i>bla_{OXA-II}</i>	FP: CGCKGCVTCSACATTCAAG RP: ACCCAHCCBACCCACCAACC	95°C – 30'' 56°C – 30'' 72°C – 1'		450
3.	<i>bla_{OXA-III}</i>	FP: CACTTATGGCATTGATGCGGA RP: TGCTGTGAATCCTGCACCAG	95°C – 30'' 52°C – 30'' 72°C – 1'		434
4.	<i>bla_{TEM}</i>	FP: ATGAGTATTCAACATTTCCGTG RP: TTACCAATGCTTAATCAGTGAG	95°C – 30'' 52°C – 30'' 72°C – 1'		861
5.	<i>bla_{CTXM}</i>	FP: ATGYGCAGYACCAGTAAG RP: ATATCRTTGGTGGTGCCT			546
6.	<i>bla_{NDM}</i>	FP: GGTTTGGCGATCTGGTTTTCC RP: GATCGTGATGAGCCATTCCG	95°C – 30'' 52°C – 30'' 72°C – 1'		621
7.	<i>bla_{OXA-48}</i>	FP: CACGTATCGGAGCGCAGC RP: CTTGGCGCAGCCTAAACC	95°C – 30'' 55°C – 30'' 72°C – 30''		211

B=G+T+C, M=A+C, W=A+T, K=G+T, V=G+A+C, S=G+C, H=A+T+C, Y=C/T

3.4.4.2. Target genes for oxacillinase determination. Respective forward and Reverse primer sequences (5' → 3') are marked in green.

bla_{OXA-I}

>J02967.2:1609-2189 Plasmid RGN238 (from E.coli) transposon 2603 OXA-1 beta-lactamase and recombinase genes, complete cds, and streptomycin resistance gene, 5' end

CGGAAATAATAGATCAGAAAACCATATTCAAATGGGATAAAACCCCAAGGAATGGAGATCTGGAACAG
CAATCATACACCAAAGACGTGGATGCAATTTTCTGTTGTTTGGGTTTCGCAAGAAATAACCCAAAAAATT
GGATTAAATAAAATCAAGAATTATCTCAAAGATTTTGATTATGGAAATCAAGACTTCTCTGGAGATAAAG
AAAGAAACAACGGATTAACAGAAGCATGGCTCGAAAGTAGCTTAAAAATTTACCAGAAGAACAATTCA
ATTCTGCGTAAATTATTAATCACAATCTCCAGTTAAAACTCAGCCATAGAAAACACCATAGAGAAC
ATGTATCTACAAGATCTGGATAATAGTACAAAACCTGTATGGGAAAACCTGGTGCAGGATTCACAGCAAATA
GAACCTTACAAAACGGATGGTTTGAAGGGTTTATTATAAGCAAATCAGGACATAAATATGTTTTTGTGTC

CGCACTTACAGGAACTTGGGGTCGAATTTAACATCAAGCATAAAAGCCAAGAAAAATGCGATCACCATT
CTAAACACACTAAATTTATAA

bla_{OXA-II}

>M95287.4:2661-3283 Plasmid R46 class 1 integron In1 integrase, beta-lactamase, aminoglycoside adenylyltransferase and dihydropteroate synthase genes, complete cds

CGCCTGCATCGACATTCAAGATACCTCATACACTTTTTGCACTTGATGCAGGCGCTGTTTCGTGATGAGTTCAGATTTTCGATGGGACGGCGTTAACAGGGGCTTTCAGGCCACAATCAAGACCAAGATTTGCGATCAGCAATGCGGAATTCTACTGTTTGGGTGTATGAGCTATTTGCAAAGGAAATTGGTGATGACAAAGCTCGGCCTATTTGAAGAAAATCGACTATGGCAACGCCGATCCTTCGACAAGTAATGGCGATTACTGGATAGAAGCAGCCTTGCAATCTCGGCGCAGGAGCAAATTGCATTTCTCAGGAAGCTCTATCGTAACGAGCTGCCCTTTCGGGTAGAACATCAGCGCTTGGTCAAGGATCTCATGATTGTGGAAGCCGGTCGCAACTGGATACTGCGTGCAAAGACGGGCTGGGAAGGCCGTATGGGTTGGTGGGTAGGATGGGTGAGTGGCCGACTGGCTCCGTATTCTTCGCACTGAATATTGATACGCCAAACAGAATGGATGATCTTTTCAAGAGGGAGGCAATCGTGCGGGCAATCCTTCGCTCTATTGAAGCGTTACCGCCCAACCCGGCAGTCAACTCGGACGCTGCGCGATAA

bla_{OXA-III}

>KX171191.1 Escherichia coli strain ZR3 plasmid beta-lactamase (OXA) gene, partial cds

AGGAAGTGAAGGTTGTTTTTACTTTACGATGCATCCACAAACGCTGAAATTGCTCAATTCAATAAAGCAAGTGTGCAACGCAAATGGCACCAGATTCAACTTTCAAGATCGCATTATCACTTATGGCATTGATGCGGAAATAATAGATCAGAAAACCATATTCAAATGGGATAAAACCCCAAAGGAATGGAGATCTGGAACAGCAATCATAACACCAAAGACGTGGATGCAATTTCTGTTGTTTGGGTTTCGCAAGAAATAACCCAAAAAATTGGAATAATAAATCAAGAATTATCTCAAAGATTTTGATTATGGAAATCAAGACTTCTCTGGAGATAAAGAAAGAAACAACGGATTAACAGAAGCATGGCTCGAAAGTAGCTTAAAAATTTACCAGAAGAACAATTCATTCTGCGTAAAATTATTAATCACAATCTCCCAGTTAAAACTCAGCCATAGAAAACCATAGAGAACATGTATCTACAAGATCTGGATAATAGTACAAAACGTATGGGAAAACTGGTGCAGGATTCACAGCAATAGAACCTTACAAAACGGATGGTTTGAAGGGTTATTATAAGCAAATCAGGACATAA

3.4.5. Extended Spectrum Beta Lactamase (ESBL) genes: Plasmids which contain ESBL genes can be easily transferred between and within bacterial species. Some ESBL genes, like *bla_{TEM/SHV}*, are mutant derivatives of well-established plasmid-mediated β -lactamases, whereas other ESBL genes, like *bla_{CTX-M}*, are mobilized from ambient bacteria. Most ESBL gene reports from the 1990s focused on the *bla_{TEM/SHV}* types, which were connected to the hospital cross-infections. However, *bla_{CTX-M}* type genes have been primarily responsible for the current global surge. The epidemiology of ESBL genes is evolving quickly and *bla_{CTX-M}*- β -lactamase genotype distribution demonstrates distinct geographic variances. The most common drug resistance gene in humans in the US is now *bla_{CTX-M-15}*, which is frequently connected to the widely dispersed variant of *E. coli*, serotype O:25b, sequence type 131. Infections from people living in the community who have never been hospitalized are frequently caused by bacteria with ESBL genes, and these organisms can then be brought into hospitals [15]. These ESBL enzymes are capable of hydrolyzing extended-spectrum- β -lactam antibiotics such as penicillins, cephalosporins along with a

monobactam (aztreonam) but are inhibited by suicide inhibitors such as clavulanic acid, sulbactam and tazobactam. ESBLs are derived from genes for the narrow-spectrum β -lactamases by mutations that alter the amino acid configuration around the enzyme active site [16].

3.4.5.1. Identification of ESBL genes: ESBL genes, *bla_{TEM}*, and *bla_{CTX-M}* were detected using gene-specific primers using PCR. Multiplex PCR reactions was carried using plasmid DNA as template. PCR assays were performed in 20 μ l reaction volume, containing 0.8 μ l (10ng) of plasmid DNA, 0.8 μ l of each primer (for both genes), 2 μ l 10X buffer, 0.3 μ l dNTP, 0.6 μ l $MgCl_2$, 0.1 μ l Taq DNA polymerase (Invitrogen), and 13.0 μ l of DDH_2O . The primers and conditions of *bla_{TEM}*, and *bla_{CTX-M}* were given Table 3.2. The primer sequences of the target genes are depicted in section 3.4.5.2. and primers are marked in green. Generated amplicons were separated by 1.5% agarose gel electrophoresis and visualized using Ethidium Bromide by Gel Documentation system (Bio-Rad, USA).

3.4.5.2. Target genes for ESBL determination. Respective forward and Reverse primer sequences (5' \rightarrow 3') are marked in green.

bla_{TEM}

```
>KR872626.1 Escherichia coli plasmid beta-lactamase (blaTEM) gene, complete
cds
AAAATTCTTGAAGACGAAAGGGCCTCGTGATACGCCTATTTTTATAGGTTAATGTCATGATAATAATGGT
TTCTTAGACGTCAGGTGGCACTTTTCGGGGAAATGTGCGCGGAACCCCTATTTGTTTATTTTTCTAAATA
CATTCAAATATGTATCCGCTCATGAGACAATAACCCTGGTAAATGCTTCAATAATATTGAAAAAGGAAGA
GTATGAGTATTCAACATTTTCGTGTCGCCCTTATTCCCTTTTTTTCGGGCATTTTGCCTTCCTGTTTTTGC
TCACCCAGAAACGCTGGTGAAAGTAAAGATGCTGAAGATCAGTTGGGTGCACGAGTGGGTACATCGAA
CTGGATCTCAACAGCGGTAAGATCCTTGAGAGTTTTTCGCCCCGAAGAACGTTTTCCAATGATGAGCACTT
TTAAAGTTCTGCTATGTGGTGCGGTATTATCCCGTGTTGACGCCGGGCAAGAGCAACTCGGTCGCCGCAT
ACACTATTCTCAGAATGACTTGTTGAGTACTACCAGTCACAGAAAAGCATCTTACGGATGGCATGACA
GTAAGAGAATTATGCAGTGCTGCCATAACCATGAGTGATAACACTGCTGCCAACTTACTTCTGACAACGA
TCGGAGGACCGAAGGAGCTAACCGCTTTTTTGCACAACATGGGGGATCATGTAACCTCGCCTTGATCGTTG
GGAACCGGAGCTGAATGAAGCCATACCAAACGACGAGCGTGACACCACGATGCCTGCAGCAATGGCAACA
ACGTTGCGCAAATATTAACCTGGCGAACTACTTACTCTAGCTTCCCGGCAACAATTAATAGACTGGATGG
AGGCGGATAAAGTTGCAGGACCACTTCTGCGCTCGGCCCTTCCGGCTGGCTGGTTTATTGCTGATAAATC
TGGAGCCGGTGAGCGTGCGGTCTCGCGGTATCATTGCAGCACTGGGGCCAGATGGTAAGCCCTCCCGTATC
GTAGTTATCTACACGACGGGGAGTCAGGCAACTATGGATGAACGAAATAGACAGATCGCTGAGATAGGTG
CTCACTGATTAAGCATTGGTAA
```

bla_{CTX-M}

```
>AY156923.1 Escherichia coli plasmid beta-lactamase CTX-M-27 (blaCTX-M-27)
gene, complete cds
ATGGTGACAAAGAGAGTGCAACGGATGATGTTTCGGCGGCGGCGGCGTGTCATTCCGCTGCTGCTGGGCAGCG
CGCCGCTTTATGCGCAGACGAGTGCGGTGCAGCAAAAGCTGGCGGCGCTGGAGAAAAGCAGCGGAGGGCG
GCTGGGCGTCGCGCTCATCGATACCGCAGATAATACGCAGGTGCTTTATCGCGGTGATGAACGCTTTCCA
```

ATGTGCAGTACCAGTAAAGTTATGGCGGCCGCGGCGGTGCTTAAGCAGAGTGAAACGCAAAAGCAGCTGC
TTAATCAGCCTGTGCGAGATCAAGCCTGCCGATCTGGTTAACTACAATCCGATTGCCGAAAAACACGTCAA
CGGCACAATGACGCTGGCAGAACTGAGCGCGGCCGCGTTGCAGTACAGCGACAATACCGCCATGAACAAA
TTGATTGCCAGCTCGGTGGCCCGGGAGGCGTGACGGCTTTTGCCCGCGCGATCGGCGATGAGACGTTTC
GTCTGGATCGCACTGAACCTACGCTGAATACCGCCATTCCCGGCGACCCGAGAGACACCACCACGCCGCG
GGCGATGGCGCAGACGTTGCGTCAGCTTACGCTGGGTCATGCGCTGGGCGAAACCCAGCGGGCGCAGTTG
GTGACGTGGCTCAAAGGCAATACGACCGGCGCAGCCAGCATTGCGGCGCGCTTACCGACGTCGTGGACTG
TGGGTGATAAGACCGGCAGCGGCGGCTACGGCACCACCAATGATATGCGGTGATCTGGCCGCAGGGTCG
TGCGCCGCTGGTTCTGGTGACCTATTTTACCCAGCCGCAACAGAACGCAGAGAGCCGCCGCGATGTGCTG
GCTTCAGCGGCGAGAATCATCGCCGAAGGGCTGTAA

3.4.6. Carbapenemase genes: The development of carbapenem resistance in the Enterobacteriaceae is a serious concern since these medications are frequently the final line of effective therapy for the treatment of infections brought on by these bacteria. The carbapenems are inactivated by three different types of metallo- β -lactamases (MBLs), oxacillinases, and KPC types. The VIM and IMP types of MBL are the two most prevalent types of MBL identified in Enterobacteriaceae.

K. pneumoniae and *E. coli* collected from a Swedish patient who was hospitalized in New Delhi, India, have recently been identified as belonging to a new kind of MBL known as NDM-1. NDM-producing Enterobacteriaceae, primarily *K. pneumoniae* and *E. coli*, are common in India, Pakistan and the UK, according to a research by Kumaraswamy and colleagues [17]. NDM-producing enterobacteriaceae were have also recently been isolated from patients residing in the US, Netherlands, Australia, Canada, France and the Sultanate of Oman. Most of the patients received medical care while visiting the subcontinent of Pakistan, India and Bangladesh [18].

Carbapenemases belong to molecular class A, B and D β -lactamases, where classes A & D include the β -lactamases with serine at their active site while class B β -lactamases are metalloenzymes with zinc at their active site. OXA-48, a class D carbapenemase, is of major concern owing to its difficulty in detection and its association with treatment failure. Moreover, OXA-48-like enzyme variants are plasmid coded and hence associated with rapid dissemination in community settings. They were first isolated in Istanbul, Turkey, in 2001, from carbapenem resistant *K. pneumoniae*. The most common GNB that produce OXA-48-like enzymes are *E. coli*, *K. pneumoniae*, *E. cloacae*, *S. marcescens* etc. [19].

3.4.6.1. Identification of carbapenemase genes: carbapenemase genes, *bla*_{NDM-1}, and *bla*_{OXA-48} were detected using gene-specific primers using PCR. Multiplex PCR reactions was carried using

plasmid DNA as template. PCR assays were performed in 20 µl reaction volume, containing 0.8 µl (10ng) of plasmid DNA, 0.8 µl of each primer (for both genes), 2 µl 10X buffer, 0.3 µl dNTP, 0.6 µl MgCl₂, 0.1 µl Taq DNA polymerase (Invitrogen), and 13.0 µl of DDH₂O. The primers and conditions of *bla*_{NDM-1}, and *bla*_{OXA-48} were given Table 3.2. The primer sequences of the target genes are depicted in section 3.4.6.2. and primers are marked in green. Generated amplicons were separated by 1.5% agarose gel electrophoresis and visualized using Ethidium Bromide by Gel Documentation system (Bio-Rad, USA).

3.4.6.2. Target genes for carbapenemase determination. Respective forward and Reverse primer sequences (5' → 3') are marked in green.

*bla*_{NDM-1}

```
>MT809687.1 Klebsiella pneumoniae strain N83 NDM family beta-lactamase
(blaNDM) gene, partial cds
ATGCACCCGGTCGCGAAGCTGAGCACCGCATTAGCCGCTGCATTGATGCTGAGCGGGTGCATGCCCGGTG
AAATCCGCCCGACGATTGGCCAGCAAATGGAACTGGCGACCAACGGTTTGGCGATCTGGTTTTCCGCCA
GCTCGCACCGAATGTCTGGCAGCACACTTCCTATCTCGACATGCCGGGTTTCGGGGCAGTCGCTTCCAAC
GGTTTGATCGTCAGGGATGGCGGCCGCGTGCTGGTGGTCGATACCGCCTGGACCGATGACCAGACCGCCC
AGATCCTCAACTGGATCAAGCAGGAGATCAACCTGCCGGTCGCGCTGGCGGTGGTGACTCACGCGCATCA
GGACAAGATGGGCGGTATGGACGCGCTGCATGCGGCGGGGATTGCGACTTATGCCAATGCGTTGTGCAAC
CAGCTTGCCCCGCAAGAGGGGATGGTTGCGGCGCAACACAGCCTGACTTTCGCCGCCAATGGCTGGGTGCG
AACCAGCAACCGCGCCCAACTTTGGCCCGCTCAAGGTATTTTACCCCGCCCCGGCCACACCAGTGACAA
TATCACCGTTGGGATCGACGGCACCAGACATCGCTTTTGGTGGCTGCCTGATCAAGGACAGCAAGGCCAAG
TCGCTCGGCAATCTCGGTGATGCCGACACTGAGCACTACGCCGCGTCAGCGCGCGCGTTTGGTGCGGCGT
TCCCCAAGGCCAGCATGATCGTGATGAGCCATTCCGCCCCCGATAGCCGCGCGCGCAATCACTCATACGGC
C
```

*bla*_{OXA-48}

```
>NZ_CP034283.1:10853-11120 Klebsiella pneumoniae strain I72 plasmid
p72_LM_OXA48, complete sequence
TCACAATAAGTTACACGTATCGGAGCGCAGCCAGCGTATTGTCAAACAAGCCATGCTGACCGAAGCCAAT
GGTGACTATATTATTCGGGCTAAAACTGGATACTCGACTAGAATCGAACCTAAGATTGGCTGGTGGGTGCG
GTTGGGTTGAACTTGATGATAATGTGTGGTTTTTTGCGATGAATATGGATATGCCACATCGGATGGTTT
AGGGCTGCGCCAAGCCATCACAAAAGAAGTGCTCAAACAGGAAAAAATTATTCCCTAG
```

3.4.7. Mobile genetic elements (MGEs): Mobile genetic elements are moveable DNA segments, transferring among bacterial genomes. MGEs carry the so-called non-core genes and they have an important contribution to the plasticity of bacterial genomes. Plasmids, transposable elements, insertion sequences, gene cassettes, integrons, genomic islands, and bacteriophages are MGEs. Rearrangements, excision, and integration of the DNA fragments can be mechanisms behind the rapid evolution of *E. coli* strains and also the emerging pathogenic *E. coli* strains [20].

An integron is generally defined by the presence of an integrase gene (*intI*) and a proximal primary recombination site (*attI*). The amino acid sequences of IntI integrases have been used as a basis for dividing integrons into ‘classes’, with those carrying *intI* defined as ‘class1’, *intI2* as ‘class2’, *intI3* as ‘class3’ etc. *intI1*, *intI2* and *intI3* were first identified in association with mobile genetic elements and *intI4* and others with chromosomal integrons. IntI-catalysed recombination between *attI* and/or *attC* sites results in insertion or excision of cassettes. The class 1 integrase (IntI1) recognises three types of recombination site: *attI1*, *attC* and secondary sites. Binding domains and consensus sequences have been determined for these. The *attI1* site is a simple site which contains two inverted sequences that bind the integrase, and two additional integrase-binding sites known as strong (DR1) and weak (DR2) [21].

3.4.7.1. Class 1 integron: Integrons have been found in approximately 9% of the sequenced bacterial genomes, and class 1 integron platform is the most ubiquitous and has been the most commonly reported among clinical bacteria and remains the focus of numerous studies. Three types of recombination sites (*attI1*, *attC* and secondary sites) are able to recognize by *intI1*. Class 1 integron has been well established and documented in GNB, with its role in the distribution and spread of antimicrobial resistance also verified and identified [21].

3.4.7.2. Class 2 integron: Class 2 integron is commonly found to be associated with the Tn7 transposon family, carrying both of its recombination site *attI2* and promoter *Pc* found within such transposons. Its 3’ conserved segment contains 5 *tns* genes (*tnsA*, *tnsB*, *tnsC*, *tnsD* and *tnsE*) functioning in the movements of transposon, which mediates the mobility of class 2 integron via a preferential insertion into a unique site within bacterial chromosomes [21].

3.4.7.3. Insertion Sequence 5 (IS5): The genomes of *E. coli* strains contain variable numbers of insertion sequences (IS). These are mobile bacterial DNA elements that can transpose to many sites on the chromosome and their activity can result in various genetic rearrangements. One of the most common IS elements is the 1195bp IS5. IS5 can be localized to a number of conserved positions in the genome and the copy number can vary from 11 in the sequenced *E. coli* strain MG1655 to 23 in W3110. They are found inserted within genes, as well as in intergenic regions, and can have both enhancer and silencer functions [22].

3.4.7.4. Insertion Sequence 26 (IS26): IS26 family members are known to play a key role in the dissemination of antibiotic resistance genes. IS26 performs this in GNB. The first description of IS26 came in 1982 when the transfer of a transposon carrying the kanamycin-resistant gene (*aphA1a*) from Rts1 to phage P1 was reported. Tn2680 contained a 5kb insert flanked by 0.8 kb direct repeats that correspond to the IS, which was named IS26. While many ISs transpose by either a ‘cut-out-paste-in’ or a ‘copy-out-paste-in’ mechanism, IS26 uses a characteristic ‘replicative’ or ‘copy-in’ mechanism to exclusively form cointegrates rather than to move alone to a new location. [23].

3.4.7.5. Insertion Sequence ISE_{Cp1}: The insertion sequence ISE_{Cp1} appears to have been responsible for the capture and mobilization of a number of unrelated antibiotic resistance genes, including several of the bla_{CTX-M} groups encoding a family of extended-spectrum-β-lactamases that now appear dominant worldwide. ISE_{Cp1} is bounded by 14-bp inverted repeats, IR_L at the left-hand end with respect to the direction the transcription of the transposase gene and IR_R at the right-hand end [24].

3.4.7.6. Identification of MGE genes: MGE genes, *intI1*, *intI2*, IS5, IS26 and ISE_{Cp1} were detected using gene-specific primers using PCR. Separate PCR reactions was carried using plasmid DNA as template. PCR assays were performed in 20 µl reaction volume, containing 0.8 µl (10ng) of plasmid DNA, 0.8 µl of each primer (for both genes), 2 µl 10X buffer, 0.3 µl dNTP, 0.6 µl MgCl₂, 0.1 µl Taq DNA polymerase (Invitrogen), and 13.0 µl of DDH₂O. The primers and conditions of *intI1*, *intI2*, IS5, IS26 and ISE_{Cp1} were given Table 3.3. The primer sequences of the target genes are depicted in section 3.4.7.7. and primers are marked in green. Generated amplicons were separated by 1.5% agarose gel electrophoresis and visualized using Ethidium Bromide by Gel Documentation system (Bio-Rad, USA).

Table 3.3: Primer sequences for MGE identification used in this study.

Sl No.	Gene names	Primers (5' → 3')	PCR conditions	No. of cycles	Amplicon size (bp)
1.	<i>intI1</i>	FP: GGTCAAGGATCTGGATTTCG	95°C – 30'' 50°C – 30'' 72°C – 1'	30	482
		RP: ACATGCGTGTAATCATCGTC			
2.	<i>intI2</i>	FP: CACGGATATGCGACAAAAAG	95°C – 30'' 50°C – 1' 72°C – 1'		789
		RP: GTAGCAAACGAGTGACGAAATG			

3.	IS5	FP: CATGCTACGCATTCACTGC	95°C – 30'' 50°C – 30'' 72°C – 1'		686
		RP: GAACTGTCGCTTGATGATGC			
4.	IS26	FP: CGCTGGTACTGCAAATACGGC	95°C – 30'' 52°C – 30'' 72°C – 1'		587
		RP: GCTGAGGCCTGGCCTTTG			
5.	ISEcp1	FP: CTGCGGTCACTTCATTGGC	95°C – 30'' 50°C – 30'' 72°C – 1'		402
		RP: GATCATTTCCGCAGCACCG			

3.4.7.7. Target genes for Mobile genetic elements. Respective forward and Reverse primer sequences (5' → 3') are marked in green.

intI1:

>KC417377.1:c564-66 Escherichia coli In848 integron IntI1 (intI1), AacA4 (aacA4), VIM-1 (blaVIM-1), AadA1 (aadA1), CatB2 (catB2), and QacEdelta1 (qacEdelta1) genes, complete cds
TTGCAACTGCG **GGTCAAGGATCTGGATTTCG**ATCACGGCACGATCATCGTGCGGGAGGGCAAGGGCTCCA
AGGATCGGGCCTTGATGTTACCCGAGAGCTTGGCACCCAGCCTGCGCGAGCAGCTGTCGCGTGACGGGC
ATGGTGGCTGAAGGACCAGGCCGAGGGCCGAGCGGCGTTGCGCTTCCCGACGCCCTTGAGCGGAAGTAT
CCGCGCGCCGGGCATTCTGGCCGTGGTTCTGGGTTTTTGGCGAGCACACGCATTTCGACCGATCCACGGA
GCGGTGTCGTGCGTCGCCATCACATGTATGACCAGACCTTTCAGCGCGCCTTCAAACGTGCCGTAGAACA
AGCAGGCATCACGAAGCCCGCCACACCGCACACCCTCCGCCACTCGTTTCGCGACGGCCTTGCTCCGCAGC
GGTTACGACATTTCGAACCGTGCAGGATCTGCTCGGCCATTCCGACGTCTCTAC **GACGATGATTTACACGC**
ATGTGCTGA

intI2:

>EU780012.1:c1841-864 Escherichia coli strain 8157 class II integron, partial sequence, IntI2 (intI2), dihydrofolate reductase (dfrA14), and putative lipoprotein signal peptidase (lsp) genes, complete cds, and putative outer membrane lipoprotein (lip) pseudogene, complete sequence
ATGTCTAACAGTCCATTTTTAAATTCTATACG **CACGGATATGCGGCAAAAAG**GTTATGCGCTGAAAACTG
AAAAAATTACCTGCACTGGATTAAGCGTTTTATTCTGTTTACAAAAACGTCATCCTCAGACCATGGG
CAGTGAAGAGGTGAGGCTGTTTTTATCCAGCTTAGCAAACAGCAGACATGTAGCCATAAACACGCAGAAA
ATCGCTTTAAATGCCCTAGCTTTTTTGTACAACAGGTTTTTACAACAGCCGTTGGGCGATATTGATTATA
TCCCTGCAAGCAAGCCTAGACGGCTACCCTCTGTTATCTCTGCAAATGAAGTGCAACGCATTTTGCAGGT
TATGGATACTCGCAACCAAGTAATTTTTGCGCTGCTGTATGGTGCAGGTTTGCGCATTAATGAATGCTTG
CGTTTGGGGTTAAAGATTTTGATTTTGATAATGGCTGCATCACTGTGCATGACGGTAAGGGTGGGAAAA
GCAGAAACAGCCTACTGCCCACGCGCCTAATCCCAGTAATAAAACAACCTATTGAGCAAGCGCGGCTTAT
TCAGCAAGACGACAACCTACAAGGCGTAGGGCCATCGCTGCCTTTTGTCTTTAGATCGCAAATACCCTTCT
GCTTATCGACAAGCGGCGTGATGTTTGTCTTTCCCTCCAGCACGCTCTGCAACCACCCGTATAACGGCA
AATTATGCCGCCATCATCTGCATGACTCCGTTGCGCGAAAGGCATTGAAGGCAGCCGTACAAAAAGCAGG
CATCGTTAGCAAGCGTGTCACTTGTCTATA **CATTTGCTCACTCGTTTGCTAC**GCATCTATTACAAGCGGGG
CGTGATATTTCGCACTGTGCAAGAACTCTTAGGGCATACCGATGTTAAGACCACGCAAATCTATACGCATG
TGTTGGGTGAGCATTTTGCCGGCACCACCAGTCCTGCGGATGGACTGATGCTACTTATCAATCAGTAA

IS5:

>HQ680722.1:1800-2490 Escherichia coli strain CUMC-201 plasmid CMY-2 (blaCMY-2) gene, complete cds; disrupted insertion sequence ISEcp1, and insertion sequence IS5, complete sequence; and CMY-2 (blaCMY-2) gene, complete cds

AACCATGCTACGCATTCACTGCATGCAGCATTGGTACAACCTGAGCGATGGCGCGATGGAAGATGCTCTGTACGAAATCGCCTCCATGCGTCTGTTTGCCCGGTTATCCCTGGATAGCGCCTTGCCGGACCGCACCACCATCATGAATTTCCGCCACCTGCTGGAGCAGCATCAACTGGCCCCCAATTGTTCAAGACCATCAATCGCTGGCTGGCCGAAGCAGGCGTCATGATGACTCAAGGCACCTTGGTCGATGCCACCATCATTGAGGCACCCAGCTCGACCAAGAACAAGAGCAGCAACGCGATCCGGAGATGCATCAGACCAAGAAAGGCAATCAGTGGCACTTTGGCATGAAGGCCCACATTGGTGTGCGATGCCAAGAGTGGCCTGACCCACAGCCTGGTCACCACCGCGGCCAACGAGCATGACCTCAATCAGCTGGGTAATCTGCTGCATGGAGAGGAGCAATTTGTCTCAGCCGATGCCGGCTACCAAGGGGCGCCACAGCGCGAGGAGCTGGCCGAGGTGGATGTGGACTGGCTGATCGCCGAGCGCCCGGGCAAGGTAAGAACCTTGAAACAGCATCCACGCAAGAACAACGCGCCATCAACATCGAATACATGAAGCCAGCATCCGGGCCAGGTTGGAGCACCCATTTCCGCATCATCAAGCGACAGTTCCGGCTTC

IS26:

>MF175191.1:c9313-8609 Escherichia coli strain CDF8 plasmid pCDF8, complete sequence

ATGAACCCATTCAAAGGCCGGCATTTCAGCGTGACATCATTCTGTGGGCCGTACGCTGGTACTGCAAAATACGGCATCAGTTACCGTGAGCTGCAGGAGATGCTGGCTGAACGCGGAGTGAATGTCGATCACTCCACGATTTACCGCTGGGTTTACGCGTTATGCGCCTGAAATGGAAAAACGGCTGCGCTGGTACTGGCGTAACCCCTTCGATCTTTGCCCGTGGCACATGGATGAAACCTACGTGAAGGTCAATGGCCGCTGGGCGTATCTGTACCGGCCGTCGACAGCCGGGGCCGCACTGTGATTTTTATCTCTCCTCCCGTCGTAACAGCAAAGCTGCATACCGGTTTCTGGGTAAATCCTCAACAACGTGAAGAAGTGGCAGATCCCGCGATTCAACACGGATAAAGCGCCCGCTATGGTCGCGCGCTTGCTCTGCTCAAACGCGAAGGCCGGTGCCCGTCTGACGTTGAACACCGACAGATTAAGTACCGGAACAACGTGATTGAATGCGATCATGGCAAATGAAACGGATAATCGGCGCCACGCTGGGATTTAAATCCATGAAGACGGCTTACGCCACCATCAAAGGTATTGAGGTGATGCGTGCCTACGCAAAAGGCCAGGCCTCAGCATTTTATTATGGTGATCCCTGGGCGAAATGCGCCTGGTAAGCAGAGTTTTTTGAATGTAA

ISEcp1:

>KM377240.1:85334-85816 Escherichia coli strain HV295 plasmid pHV295, complete sequence

AATCATATAAAGACCATGCTCTGCGGTCACTTCATTGGCATTGATAAGTTAGAACGTCTAAAGCTACTTCAAAATGATCCCTCGTCAACGAGTTTGATATTTCCGTAAAAGAACCTGAAACAGTGTACGGTTTTCTAGGAACTTCAACTTCAAGACAACCCAAATGTTTAGAGACATTAATTTTAAAGTCTTTAAAAAAGTCTCACTAAAAGTAAATTGACATCCATTACGATTGATATTGATAGTAGTGTAATTAACGTAGAAGGTCATCAAGAAGGTGCGTCAAAAGGATATAATCCTAAGAACTGGGAAACCGATGCTACAATATCCAATTTGCATTTTGCGACGAATTAAGCATATGTTACCGGATTTGTAAGAAGTGGCAATACTTACACTGCAAAACGGTGCTGCGGAAATGATCAAGAAATTGTTGCTAACATCAAATCAGACGATTTAGAAATTTTATTTTCAATGGAT

3.4.8. Characterization of Resistant Plasmids: A formal scheme of plasmid classification is based on incompatibility (*Inc*) groups. The procedure for incompatibility grouping is based on the introduction, by conjugation or transformation, of a plasmid of an ‘unknown’ *Inc* group into a strain carrying a plasmid of a known *Inc* group. If the resident plasmid is eliminated in the progeny, the incoming plasmid is assigned to its same *Inc* group. Plasmid with the same *Inc* group cannot be propagated in the same cell line. *Inc* group identification has been frequently used to classify plasmids. The method has been an important tool to trace the diffusion of plasmids conferring antimicrobial resistance and also to follow the evolution and spread of emerging plasmids. In 1988 Couturier et al. developed a new method for the identification of the major replicons of plasmids circulating among the Enterobacteriaceae. The conjugation- and hybridization- based

methodologies cannot be easily applied to a large number of strains and their application has been limited by the laborious and time-consuming work required. A PCR-based detection of plasmids was previously devised on the basis of published sequences but it was limited to IncP, IncN, IncW and IncQ plasmids. The necessity of tracing plasmids conferring drug resistance prompted Carattoli et al. to develop an inc/rep PCR-based typing method [25].

To assess the incompatibility groups of resistance plasmids, PCR-based replicon typing (PBRT) was utilized using IncFrep, F1B, N, I1, A/C, H1, X, Y, L/M, W specific primer sets, as described in Carattoli et al. 2005 [25]. In-silico analysis was performed on Enterobacteriaceae family-annotated plasmids from Genbank BLAST (<https://blast.ncbi.nlm.nih.gov/>) to type transmissible resistance plasmids, based on genes involved in transmission from various replicon types. BlastN (<https://www.ncbi.nlm.nih.gov/nucleotide>) and ClustalW2 (<https://www.ebi.ac.uk/Tools/msa/clustalw2/>) were used to confirm the target genes.

3.4.8.1. Identification of PBRT genes: PBRT genes, I1, HI1, X, W, FII_s, N_{rep}, A/C, F_{rep}, F1B, L/M, and Y were detected using gene-specific primers using PCR. Separate PCR reactions was carried using plasmid DNA as template. PCR assays were performed in 20 µl reaction volume, containing 0.8 µl (10ng) of plasmid DNA, 0.8 µl of each primer (for both genes), 2 µl 10X buffer, 0.3 µl dNTP, 0.6 µl MgCl₂, 0.1 µl Taq DNA polymerase (Invitrogen), and 13.0 µl of DDH₂O. The primers and conditions of all PBRT genes were given Table 3.4. The primer sequences of the target genes are depicted in section 3.4.8.2. and primers are marked in green. Generated amplicons were separated by 1.5% agarose gel electrophoresis and visualized using Ethidium Bromide by Gel Documentation system (Bio-Rad, USA).

3.4.8.2. Target genes for PCR- based replicon typing. Respective forward and Reverse primer sequences (5' → 3') are marked in green.

I1

```
>M20413.1 Plasmid incI-1 minireplicon RNA
GATCGTTGTAATGCTTTTCAAATTAACGTAAAGCGGGTATATTTTCGGCTGTTATTAGCTGTGCAGAGGGT
GGCACTCTGTGGAGCAAAGCGGGCGAAAGCCGGACGGCAGAATGCGCCATAAGGCATTCAGGAGAGATGGC
ATGTACGGGCAGTAAGTCAGAAGACTGAAGATGTTCCGGAAGCCATAAAAGGAAAACCCCACTATCTTT
CTTACGAACCTGGCGGAACGACGAAAGATAGTGGGGGCCTCACAGAATACGGGTAAAGTATAATGAAACC
GTACCAGAGATTCAACCCTGTGCAGTGTATAAATACACGGCACAATCGCTCCGCCATAAGCGACAGCTTG
TGGCAGGTCTGAAGAATACTCCATATAACGCAGTACACTGGAGTCAGTTAGCACCCGAAGAGCAGATC
```

HI1

>AF250878.1:c24600-23900 *Salmonella typhi* R27 plasmid complete sequence
CGTTTTAAAGAGGTAATCCTGCCGGTCTTGAAGAGCAAGTACGACCTGATCATTATCGATACTCCACCAG
AAGATTCGCCAATCACATGGGCAGCGGATGAAGCTGCTGATGGCATTGTTGGT**TGCCGTTTCACCTCGTGA**
GTATGATTATGCCTCAACAACTGATTTTCATGTTGACGATCAGTGAGCGATTCAAACAATCGCCGAGCAAG
GGCGAAAATCTAAGCTGGTTCAAAGTGTGGCAGTGAATGTCGACGATAAGAGTCCCTATGAAAAGATTG
TCCTGGATAAACTGGTAAGGACAGTGCAGGAACCTCTTTATGTCTGCAAATATCAAAAACCTCAGAAGCGTT
TAAAGCCGCAGCTTCTAGGGGTAGAACCGTATTGGATATCAAAAAATCAGAAGAGCTCTGCTCTCCCAA
CAGCTTGATGTTGCCGAAGAATCCGTGATGGCGGTCTACCAGCAATTTATTAATGAGATTAAGAGTTTTT
CAGTGAAGCAAGGGGGTAATGTATGAGTGATGAGCAGCATATCGGGAACGACAAATCCCGTTATATTAA**T**
GCGCCTAAGCGTACTGAAGTAATCCATCGCTCCGGGCTTCAAGGCCTGAAAGGTCAGCCACGCCTGAAGA
AACTTTTTACATTACACAATGGGCGGAAGCTTGAGGCGGAACACATCATTGTTCCGGCGGAAAAGGTGGA
A

X

>Y00768.1:210-629 *E. coli* mini-plasmid R6K pir gene fragment with ts and
trcop mutations
GAGAGCTTAGTACGTGAAACATGAGAGCTTAGTACGTACTATCAACAGGTTGAACTGCTGATCTTCAGAT
CTAGCTTAAACAGGTGGCTTTTTTAATCATCTTTGCCAAGCATG**GCGCGGGTTTGGGGTAATAT**AGCGAC
TCATAAAAGCGTTAAACATGAGTGGATAGTACGTTGCTAAACATGAGATAAAAATTGACTCTCATGTTA
TTGGCGTTAAGATATACAGAATGATGAGGTTTTTTTATGAGACTCAAGGTCATGATGGACGTGAACAAAA
AAACGAAAATTTCGCCACCGAAACGAGCTAAATCACACCCTGGCTCAACTTCCTTTGCCCGCAAAGCGAGT
GATGTATAT**GGCGCTTGCTCCCATTGA**TAGCAAAGAACCTCTTGAACGAGGGCGAGTTTTTCAAATTAGG

W

>U12441.2:240-850 *Escherichia coli* plasmid R388 class 1 integron In3,
complete sequence
GTAACGGCCATCGGTGTGCATTCCGAGCCTTTGTAGAAATTCCGATTGCGACCGGCCAAGGTTCAACACG
GGGTCTTTTCGTTTCGCACGG**CCTCGGTGCATATCCAAGCAAG**CAAGGTGCGCGGCATAGAACCGTAGGGCA
GGCCGATGCTCGGCTTGCCCATGATCGACAAGGTGACGATGCCATTGGTGCGCTCAAAGTAGCTGGTCTT
GGGGTTCGGTGTGGGGCATGGTCGCTTGACACAAGGCAACGGGCCATGTAGCCGACTAAGCCAGCTTCGCGG
GCATCCTCCATTTTCGAGCGCGAGGCTCGTCTTGATGATCTCGTTGATACGATGGCCGGGGGCTTTGTTGT
TCTTAGGCATGTTGTTCCCTCCCCGGCATGGTGATGGTTGGTCTAGTGTTTGTGGGTTTGATGTTCCGGC
GTTTGATGAACAGGCGCAAGGTGTGAGGGCTGACGCCTAACAACCTCGGCTGCGCGACTTTGCGGCAAGCC
AAGGTTACGTATGCCTGTACTTCATCAATACGGCTGTCCAG**CTTCAAGGCGCTCGATTGCT**GCCCTTG
GGTCGCCCCGAGCGTCTTGCCGCGCTCTCTGGCGACTTGTAGCGCCTCGGTG

FIIs

>AE006471.2:1940-2340 *Salmonella enterica* subsp. *enterica* serovar Typhimurium
str. LT2 plasmid pSLT, complete sequence
GTTCACTCATTACCGACAGGTCAAAAATCCGAATCCGGAATTCACGCCGAGAGAAGGGAAAAAGACCCT**G**
CCGTTCTGTCTGTAAGCTGATGGCGAAAGCCGAAGGGTTCAGTCCCCTTTGATTTTTCCGTCCATGTGG
CGTTTCGTTTCGTTTCGCTGGGAAAGCGTACCGGATGCCGCTTTGCTGCGCCGTCGTGCCATCGATGCGCT
GCTTCAGGGGTTGTGCTTCCATTATGATCCACTGGCCAACCGTGTACAGAGATCCATCACCAATCTGGCT
ATAGAGTGCAGTCTGGCCACTGAGTCAAAAAGTGGTAATCTGTCCATCACCCGCGCCACACGGGCGCTGA
A**GTTTATGGCAGAGCTGGGGC**TGATTACCTACCAGACCGAGTACGATCCGC

N_{rep}

>NC_003292.1:31760-32452 *Salmonella enterica* subsp. *enterica* serovar
Typhimurium plasmid R46, complete sequence
CAAAAAGATAAAAGTTAAGCAGTCTAACGAGCTTA**CCGAAGCTGCTTACTACCTCTC**GCTAAAAGCAAAG

CGCGTTCTCTGGTTATGTCTTATGCAGACGTATTTACAGCTTCAGTAAGCGAAGATGATGATGAGATGG
CTGTACTCGGTGACTCTACTTTCAAAGTAAAGGTGGCTGACTATCAGCAAATTTTTTCAGGTAAGCCGTAA
CCAGGCTATCAAGGATGTTAAAGAAGGCGTGTGGAGTTAAGCCGTTCTGCGGTAATCTTTTACCCGAAA
GAAGGGAGTTTTGACTGCGTCGCGCGCCCTGGCTAACAGAGGCTGGCAGCCGATCAGCTCGTGGTATCT
GGGAAATCGAATTTAACCATAAACTCCTGCGGTACATTTACGGCCTGACGAACCAAGTTCAACCACTACTC
GCTCCGCGATTGTGGCAGTCTTCGAAATC**CACGGACGATCCGCCTTTATG**AAAGTCTTGCTCAATTCAAA
TCTTCAGGCTTATGGGTACTACTCATGCTTGGTTAAATGACCGTTTCCTTTTGCCGGAATCCCAACAGA
AGAACTTGGCAGAGTTGAAACGATCTTTCCTTGATCCTGCTCTCAAGCAGATAAATGAGAAAACACCTTT
ACTTGCTAAGTATAGTATTGATGATTGAGGAAAATTTCTGTTCTCAATAATTGATAAGCAAAA

A/C

>X73674.1:701-1300 E.coli RA1 plasmid DNA
AGCAACGGTAGCAGCGGGAGTTTTGACACTGCTG**GCGGCATGGACCACCAGC**TAGAAAGTATTAACGGAA
CAATCATGAGTAAGAGAACCAAAGACAAAGACCTGGAGAACTCGACGTTATCAAAGACTCACCGCAAAT
GAGCCTGTTTTGAGATCATTGAATCTCCGGCCAAGAAAGACGACTACTCCAACACAATCGAGATCTACGAT
GCGTTACCTAAGTACATTTGGGACCAAAGCGTGAGCAGCAAGACCTGTCCAACGCCGTAGTGACGCGAC
AATGCTCCATCAGAGGCCAGCAGTTACCGGTGAAGGTGAAACCAGCCATCATCGAGAAGGACGACGGCAG
AACCGTGCTGATCTACGCGGGGCGAGAGAGGAAATCCTTGAGGATGCTCTACGCAAGCTCGCAGTAAAC
GGGAAGGGCCATATCATAGAAGGCAAGGCTGGGGTCATGTTCACTCTGTACGAACTCCAGAAGGAGCTCT
CGAAGATG**GGGCACGGGTACAACCTGACAG**AGATCAAGGAGGCAATTCAGGTTTGTCTGGCGCAACACT
AGAATGTATCAGTGATGACGGAGAGGCATTCATCAGCTCC

F_{rep}B

>AY234375.1:1681-2030 Escherichia coli plasmid pRK100 RmoA (rmoA) gene,
complete cds; and RepFIIA replication region, complete sequence
AGCATGCTAGATTACTGATCGTTTTAAGGAATTTTGT**GGCTGGCCACGCCGTAAG**GTGGCAAGGAACTGGT
TCTGATGTGGATTTACAGGAGCCAGAAAAGCAAAACCCCGATAATCTTCTTCAACTTTGGCGAGTACGA
AAAGATTACCGGGGGCCACTTAAACCGTATAGCCAACAATTCAGCTATGCGGGGAGTATAGTTATATGCC
CGGAAAAGTTCAAGACTTCTTTCTGTGCTCGCTCCTTCTGCGCATTGTAAGTGCAGGATGGTGTGACTGA
TCTTCACCAAACGTATTACCGCCAGGTAAAGAACC**GAATCCGGTGTTCACCTCCCG**TGAAGGTGCCGGA

F1B

>M26308.1:2171-2940 IncF plasmid RepFIB replicon
CAGACTCAGTTGTAAATACAGGCTGCAGGTTTTTCTTCAGTCAGTT**AGCGGAGTTCTGACACACG**ATTT
TCTGTTTATTCTTTTACTGTCCACAGGCTGGAGGCTTTCTGGAAAACGAAAATTCAGACATCAAAAACT
GTTCCGGCAGGTGGATAAGTCGTCCGGTGAGCTGGTGACACTGACACCAACAATAACAACACCGTACAA
CCTGTGGCGCTGATGCGTCTGGGCGTTTTTGTACCGACCCTTAAATCACTGAAGAACAGTAAAAAATA
CACTGTCACGTACTGATGCCACGGAAGAGCTGACACGTCTTTCCTGGCCCGTGCTGAGGGATTGATAA
GGTTGAGATCACCGGCCCCCGCTGGATATGGATAACGATTTCAAGACCTGGGTGGGGATCATTATTCC
TTTGCCCGCCATAACGTGATTGGTGACAAAGTTGAACTGCCTTTTGTTGAGTTTGCAAACTGTGTGGTA
TACCTTCAAGCCAGTCATCCCGCAGGCTGCGTGAGCGCATCAGCCCTTCCCTGAAGCGCATTGCCGGTAC
CGTGATCTCGTTTTCCCGTACCGATGAGAAGCACACCCGGGAATACATCACCCATCTGGTACAATCAGCC
TACTACGATACTGAGCGGGATATTGTTCACTTACAGGCTGATCCCCGCTGTTTGAAGTGTACCACTTTG
ACAGAAAAGTCCTTCTCCAGCTTAAGGCGATT**AATGCCCTGAAGCGACGG**GAGTCCGCCAGGCACTCTA

L/M

>U27345.1:141-840 Klebsiella pneumoniae plasmid pMU407.1 RepC (repC), RepB
(repB) and replication initiation protein RepA (repA) genes, complete cds
TAGTCGTTTGTAGT**CGGAGGGCTTGTGAGCAG**AGTAGTTGAGCGGCAGGTGCATAAGAGTAACCTGGATA
AGCAGAAGGATTACAGGAATCGCATCAGAGATACTCATGACCAGCTAAATCTTTATCTGCCCCAAGATGC
AAAAAGAATGTTGATAGAGATCACAAAAGTAAAAAGCTCACTCAGGCGGAGGTTATTGAATTTCTTGTG
AAAAGTTATTACGACGGCTTAAATTTGACGATTCTGAAGAGTGAGGTTACTCTGTAAGTGCAGGATCGC

AGGTATTGCCCCGCTTAGAAACGCATGATATGTTAAGCGGCGTTTACATAACCTTACGGGGTTATTACAG
AATTTAGCACGGGAAGAGCGGCCCGGAGATGTTCCGCTTAGGAGTGGCAGGAGCCACAAAAAGTAAACC
CCCTGATCCTATTTTCAAGACTTTGGCCGGCTCGGAATAGAATCAGGGGGTGCAAACCTGCCCACTGGCAGA
AAGGATTATAGCAAATGCGTACCCTATTGCAATACAGCCCCGCCAATATGTGCAGGGGGCTGGTGAATCAA
AAGAATCCATACCTACAGCTTTCTGACATTGAGTCAGTAGAAGGTCTTTTCGCCGGAGTTTCATCTCCTGGC
TTGAAAGCCAGTCCCCTAAAGAATCGCCCCCTGCAGCTGCTTCTC**GATGAAGGCACCAAGCCCG**TGCGCAA

Y

>K02380.1:1045-1986 Enterobacteria phage P1 RepA (repA), ParA (parA), and ParB (parB) genes, complete cds; and unknown gene

ATTGAAAGTAAGGCAAAAGAACTAACAGTTAATTCAAA**CAACACTGTGCAGCCTGTAGC**GTTGATGCGCT
TGGGGGTATTTCGTGCCGAAGCCATCAAAGAGCAAAGGAGAAAGTAAAGAGATTGATGCCACCAAAGCGTT
TTCCCAGCTGGAGATAGCTAAAGCCGAGGGTTACGATGATATTAAATCACCAGGTCCTCGACTCGATATG
GATACTGATTTCAAACGTGGATCGGTGTCTACGCGTTACGCAAATACGGCTTGTCTCTCAAACACCA
TCCAGTTATCGTTTTCAGGAATTCGCTAAAGCCTGTGGTTTCCCTCAAACGTCTGGATGCGAAACTGCG
TTTAACCATTCATGAATCACTTGGACGCTTGCCTAACAAAGGGTATCGCTTTTAAGCGCGAAAGATGCT
AAAGGCGGCTATCAGACTGGTCTGCTGAAGGTCGGGCGTTTTGATGCTGACCTTGATCTGATAGAGCTGG
AGGCTGATTGCAAGTTGTGGGAGCTGTTCCAGCTTGATTATCGCGTTCTGTTGCAACACCACGCCTTGCG
TGCCCTTCCGAAGAAAGAAGCTGCACAAGCCATTTACACTTTTCATCGAAAGCCTTCCGCGAAGCCGTTG
CCGCTATCGTTTCGCGCAATCCGTGAGCGCCTGGCTTTGCAGTCAGCTGTTGGCGAGCAAAACCGTATCA
TTAAGAAAGCGATAGAACAGCTTAAACAATCGGCTATCTCGACTGTTCTATTGAGAAGAAAGGCCGGGA
AAGTTTTGTAATCGTCCATTCTCGCAATCCAAAGCTGAAACTCCCCGAATAAGTGTGTGCTGGAGGGAAA
CCGCATTAAAAAGATGTGTGCTGCCGGAAGGCTTGTCCAATTTCTGTT**TTTGATGTGCGCTGGAGGG**G
GACGCCCCCTCAGTTTGCCAGACTTTCCCTCC

Table 3.4: Primer sequences for PBRT identification used in this study.

Name	Primer Sequences (5'- 3')	Target Site	PCR condition (time)	No. of Cycles	Amplicon Size (bp)
I1	F- GCTGTGCAGAGGGTGGCAC	RNAI	95°C(30sec) 55°C(30sec) 72°C(30sec)	30	177
	R- CGTCGTTCCGCCAAGTTCGT				
HI1	F- TGCCGTTTCACCTCGTGAGTA	parA- parB	95°C(30sec) 50°C(30sec) 72°C(1min)		460
	R- TTACTTCAGTACGCTTAGGCGCA				
X	F- GCGCGGGTTTGGGGTAATAT	oriγ	95°C(30sec) 52°C(30sec) 72°C(1min)		263
	R- TCAATGGGAGCAAGCGCC				
W	F- CCTCGGTGCATATCCAAGCAAG	repA			452
	R- AGCAAATCGAGCGCCTTGAAG				
FII _s	F- GCCGTTCTGTCTGTAAGCTGATG	repA			302
	R- GCCCCAGCTCTGCCATAAAC				
Nrep	F- CCGAAGCTGCTTACTACCTCTC	repA	95°C(30sec) 55°C(30sec) 72°C(1min)		435
	R- CATAAAGGCGGATCGTCCGTG				
A/C	F- GCGGCATGGACCACCAGC	repA			487
	R- CTGTCAGGTTGTACCCGTGCCC				
F _{repB}	F- GGCTGGCCACGCCGTAAG	RNAI/ repA			301
	R- CGGGGAGTGAACACCGGATTC				
F1B	F- AGCGGAGTTCTGACACACG	repA	95°C(30sec) 50°C(1min) 72°C(1min)		703
	R- CCGTCGCTTCAGGGCATT				
L/M	F- CGGAGGGCTTGTGAGCAG	repA,B, C	95°C(30sec) 52°C(1min)		679
	R- CGGGCTTGGTGCCTTCATC				

Y	F- CAACACTGTGCAGCCTGTAGC	repA	72°C(1min)		871
	R- CCCTCCAGCGCACATCAAA				

3.5. Result:

3.5.1. Prevalence of aminopenicillinase, β -lactamase and carbapenemase resistance genes in UPECp and UPECnp isolates:

The presence of aminopenicillinase genes *bla*_{OXA-I}, *bla*_{OXA-II}, *bla*_{OXA-III}; β -lactamase genes *bla*_{TEM} and *bla*_{CTX-M}, and carbapenemase genes *bla*_{NDM} and *bla*_{OXA-48} have been reported in UPECp and UPECnp group of isolates.

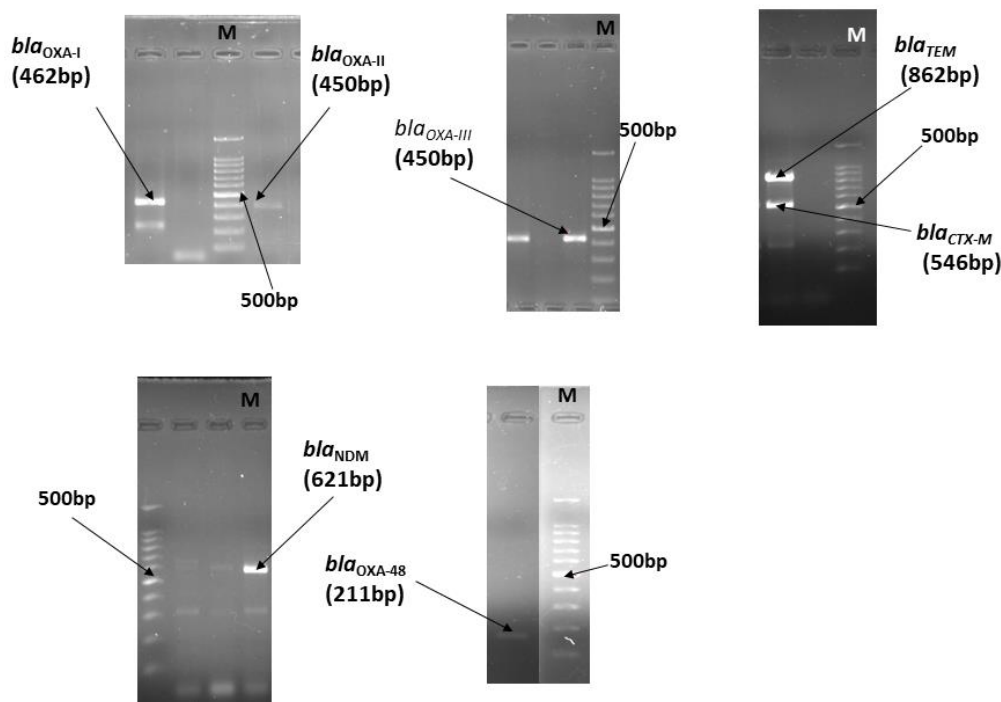


Figure 3.3: Representative pictures of aminopenicillinase (*bla*_{OXA-I}, *bla*_{OXA-II}, *bla*_{OXA-III}), ESBL (*bla*_{TEM}, *bla*_{CTX-M}) and carbapenemase (*bla*_{NDM}, *bla*_{OXA-48}) genes on agarose gel electrophoresis. M represents the DNA marker lane (100 bp DNA ladder).

- Co-occurrence of *bla*_{TEM}, *bla*_{CTX-M}, *bla*_{OXA-I}, *bla*_{OXA-II}, *bla*_{OXA-III}, *bla*_{NDM}, *bla*_{OXA-48} were observed in 17 out of 36 UPECp isolates along with the presence of *bla*_{OXA-I}, *bla*_{OXA-II} and *bla*_{TEM} only in 2,3 and 6 isolates respectively. Remaining 8 isolates resistant to at least 1 β -lactam antibiotic revealed absence of these respective β -lactamase encoding genes.

- In UPECp isolates, prevalence of *bla*_{TEM} gene was highest, i.e. in 22 (61.11%) isolates, followed by *bla*_{CTXM}, in 15 (41.67%) isolates. The prevalence of *bla*_{TEM} and *bla*_{CTXM} genes were statistically significant in this population. The presence of *bla*_{OXA-I}, *bla*_{OXA-II}, *bla*_{OXA-III}, *bla*_{NDM} and *bla*_{OXA-48} genes were observed in 6 (16.67%), 8 (22.22%), 5 (13.89%), 4 (11.11%) and 1 (2.78%) isolates respectively. *E. coli* isolates those harbored either *bla*_{TEM} alone ($p < 0.001$) or in combination with *bla*_{CTX-M} ($p < 0.001$) formed a distinct cluster (Cluster II) with respect to the distribution of the other β -lactamases (Cluster I). Additionally, two distinct clusters (A and B) with multiple sub-clusters were observed with respect to the absence of *bla*_{TEM} and its presence in combination with the other β -lactamases (Figure 3.4 a).
- Co-occurrence of *bla*_{TEM}, *bla*_{CTX-M}, *bla*_{OXA-I}, *bla*_{OXA-II}, *bla*_{OXA-III}, *bla*_{NDM}, *bla*_{OXA-48} were observed in 25 out of 34 UPECnp isolates along with the presence of *bla*_{CTX-M}, *bla*_{OXA-II}, *bla*_{OXA-III} and *bla*_{TEM} only in 1, 1, 2 and 5 isolates respectively. No isolates unlike UPECp had absence of aforementioned β -lactamase resistance genes.
- In UPECnp isolates also, presence of *bla*_{TEM} was highest, i.e. in 27 (79.41%), followed by *bla*_{OXA-III}, in 22 (64.71%) isolates. The prevalence of *bla*_{TEM} and *bla*_{OXA-III} genes were statistically significant in this population. The presence of *bla*_{CTX-M}, *bla*_{OXA-I}, *bla*_{OXA-II}, *bla*_{NDM} and *bla*_{OXA-48} genes were observed in 7 (20.59%), 13 (38.24%), 7 (20.59%), 9 (26.47%), and 0 (0%) isolates respectively. Prevalence of these genes were not significant in UPECnp population. *E. coli* isolates those harbored either *bla*_{TEM} alone ($p < 0.001$) or in combination with *bla*_{OXA-III} ($p < 0.001$) formed a distinct cluster (Cluster II) with respect to the distribution of the other β -lactamases (Cluster I). Additionally, three distinct clusters (A, B and C) with multiple sub-clusters were observed with respect to the presence and absence of *bla*_{TEM} and *bla*_{OXA-III} genes (Figure 3.4 b).

Table 3.5A: Prevalence of aminopenicillinase, β -lactamase and carbapenemase resistance genes in UPECp isolates

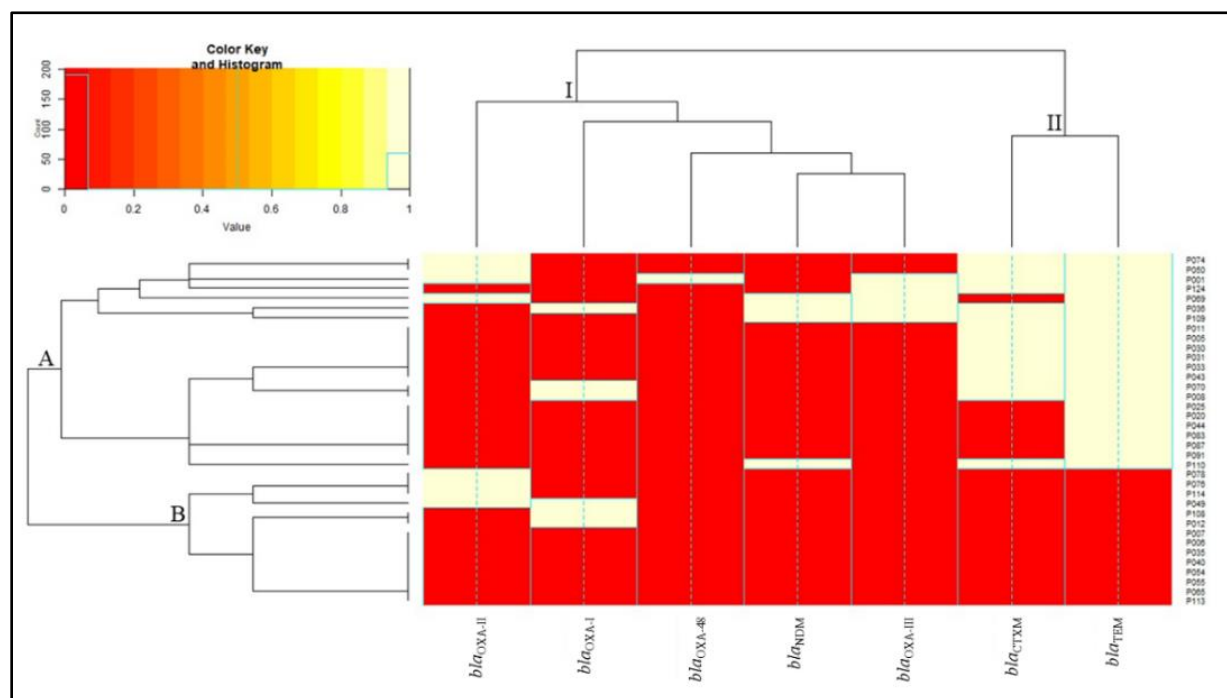
Sample ID	<i>bla</i> _{OXA-I}	<i>bla</i> _{OXA-II}	<i>bla</i> _{OXA-III}	<i>bla</i> _{TEM}	<i>bla</i> _{CTXM}	<i>bla</i> _{NDM}	<i>bla</i> _{OXA-48}
P001	-	+	+	+	+	-	+
P005	-	-	-	+	+	-	-
P006	-	-	-	-	-	-	-

P007	-	-	-	-	-	-	-
P008	+	-	-	+	+	-	-
P011	-	-	-	+	+	-	-
P012	+	-	-	-	-	-	-
P020	-	-	-	+	-	-	-
P025	-	-	-	+	-	-	-
P030	-	-	-	+	+	-	-
P031	-	-	-	+	+	-	-
P033	-	-	-	+	+	-	-
P035	-	-	-	-	-	-	-
P036	+	-	+	+	+	+	-
P040	-	-	-	-	-	-	-
P043	-	-	-	+	+	-	-
P044	-	-	-	+	-	-	-
P049	+	+	-	-	-	-	-
P050	-	+	-	+	+	-	-
P054	-	-	-	-	-	-	-
P055	-	-	-	-	-	-	-
P065	-	-	-	-	-	-	-
P069	-	+	+	+	-	+	-
P070	+	-	-	+	+	-	-
P074	-	+	-	+	+	-	-
P076	-	+	-	-	-	-	-
P078	-	+	-	-	-	-	-
P083	-	-	-	+	-	-	-
P087	-	-	-	+	-	-	-
P091	-	-	-	+	-	-	-
P108	+	-	-	-	-	-	-
P109	-	-	+	+	+	+	-
P110	-	-	-	+	-	+	-
P113	-	-	-	-	-	-	-
P114	-	+	-	-	-	-	-
P124	-	-	+	+	+	-	-

Table 3.5B: Prevalence of aminopenicillinase, β -lactamase and carbapenemase resistance genes in UPECnp isolates

Sample ID	<i>bla</i> _{OXA-I}	<i>bla</i> _{OXA-II}	<i>bla</i> _{OXA-III}	<i>bla</i> _{TEM}	<i>bla</i> _{CTXM}	<i>bla</i> _{NDM}	<i>bla</i> _{OXA-48}
NP006	+	-	+	-	-	+	-
NP038	-	-	-	+	-	-	-
NP040	+	-	-	+	-	+	-
NP042	-	+	-	-	-	-	-
NP046	+	-	+	+	-	-	-
NP047	-	-	-	+	-	-	-
NP048	-	-	-	+	-	-	-
NP049	+	-	+	+	-	-	-
NP051	-	-	+	+	-	-	-
NP052	-	-	+	+	-	-	-

NP054	-	-	+	+	-	-	-
NP060	+	-	+	+	+	-	-
NP061	+	-	+	-	-	-	-
NP062	+	-	+	+	+	-	-
NP064	-	-	-	+	-	+	-
NP065	+	-	+	-	-	+	-
NP068	+	-	+	+	-	-	-
NP069	-	-	-	-	+	-	-
NP072	-	-	-	+	+	-	-
NP073	+	-	+	+	-	-	-
NP074	+	-	+	+	+	-	-
NP075	-	-	-	+	-	-	-
NP076	-	-	+	+	-	-	-
NP078	+	+	-	+	-	-	-
NP080	-	-	-	+	-	+	-
NP093	-	+	+	+	-	-	-
NP105	-	+	+	+	+	-	-
NP107	-	-	+	+	-	-	-
NP116	-	+	+	+	-	-	-
NP117	-	+	+	+	-	+	-
NP119	-	+	+	+	-	+	-
NP121	-	-	+	-	-	-	-
NP124	+	-	-	+	+	+	-
NP126	-	-	+	-	-	+	-



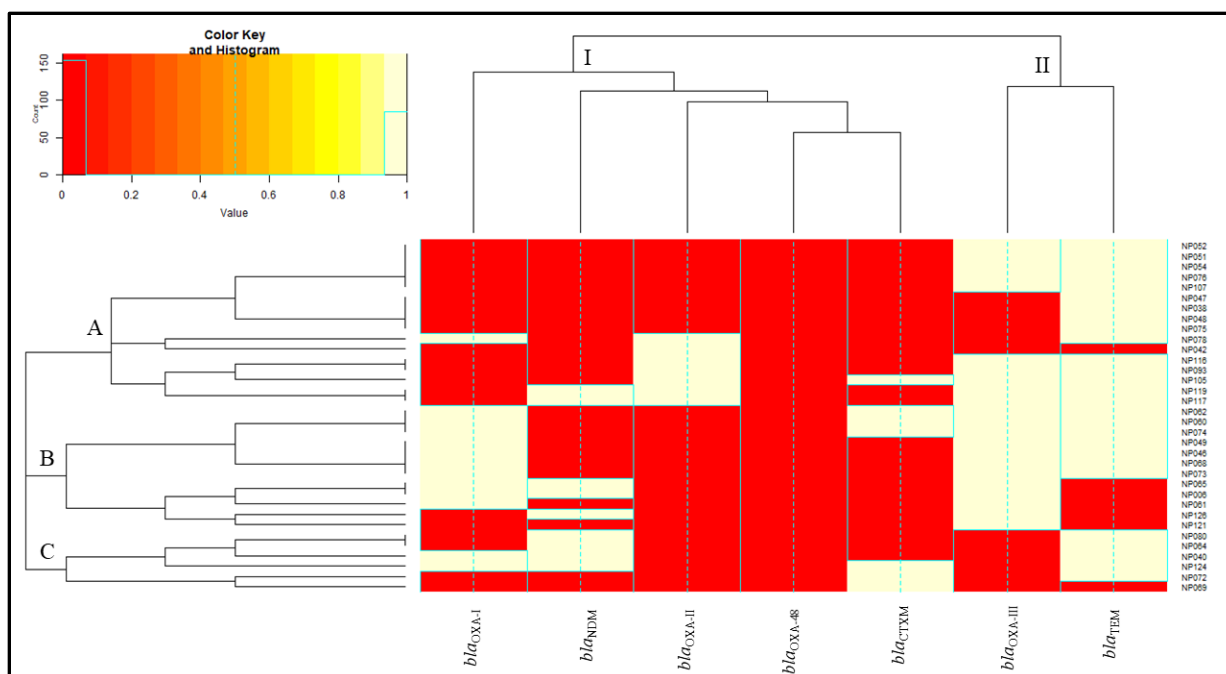


Figure 3.4: Heatmap representation of β -lactamase genes in the UPEC isolates collected from (a) pregnant women (b) non-pregnant women. The cluster analysis was based on presence and absence *bla*_{TEM}, *bla*_{CTXM}, *bla*_{OXA-I}, *bla*_{OXA-II}, *bla*_{OXA-III}, *bla*_{NDM}, *bla*_{OXA-48} either alone or in varied combinations. Numbers in right side indicates sample ID of each isolate. Color key represented the variation in colors from red to white, illustrating the absence of particular gene to its presence respectively.

3.5.2. Prevalence of mobile genetic elements in UPEC isolates

Table 3.6: Prevalence of mobile genetic elements in UPECp (left) and UPECnp (right) isolates:

Sample ID	intI1	intI2	IS5	IS26	ISEcp1	Sample ID	intI1	intI2	IS5	IS26	ISEcp1
P001	+	-	+	-	-	NP006	-	-	+	-	+
P005	-	+	+	-	+	NP038	+	-	+	-	-
P006	+	-	+	-	+	NP040	-	-	+	-	+
P007	-	-	-	-	-	NP042	-	-	-	-	-
P008	+	-	+	-	+	NP046	+	-	-	-	+
P011	+	-	-	-	+	NP047	-	+	-	-	-
P012	+	-	+	+	+	NP048	+	+	+	-	+
P020	+	+	+	-	+	NP049	-	-	+	-	+
P025	-	-	-	-	-	NP051	+	-	+	-	+
P030	-	-	-	-	+	NP052	+	-	+	-	+
P031	-	-	+	-	+	NP054	-	-	-	-	+
P033	+	-	-	-	-	NP060	+	-	-	-	-
P035	+	-	+	+	+	NP061	-	-	-	-	-

P036	+	+	-	-	+	NP062	+	-	-	-	-
P040	+	-	-	-	-	NP064	+	+	+	-	+
P043	+	-	-	-	+	NP065	-	+	-	-	+
P044	+	-	-	-	+	NP068	-	-	-	-	-
P049	+	-	-	-	+	NP069	-	-	-	-	-
P050	+	-	-	-	+	NP072	+	-	-	-	-
P054	+	-	-	-	-	NP073	+	-	+	-	-
P055	+	-	+	-	+	NP074	+	+	+	-	+
P065	-	-	-	-	-	NP075	-	+	+	-	+
P069	+	-	+	-	+	NP076	+	+	-	-	-
P070	+	-	-	-	+	NP078	+	-	+	-	-
P074	+	-	-	-	+	NP080	+	+	+	+	+
P076	-	+	-	-	-	NP093	+	+	-	-	+
P078	+	-	+	-	+	NP105	+	-	-	-	+
P083	+	-	+	-	+	NP107	-	+	+	-	+
P087	+	-	-	-	+	NP116	+	+	+	-	+
P091	+	-	-	-	-	NP117	-	+	+	-	+
P108	+	-	+	-	+	NP119	-	-	-	-	+
P109	+	-	-	-	+	NP121	+	-	-	-	-
P110	+	-	-	-	+	NP124	+	+	+	-	+
P113	+	-	-	-	+	NP126	-	-	-	-	+
P114	+	-	-	-	-						
P124	+	+	+	-	+						

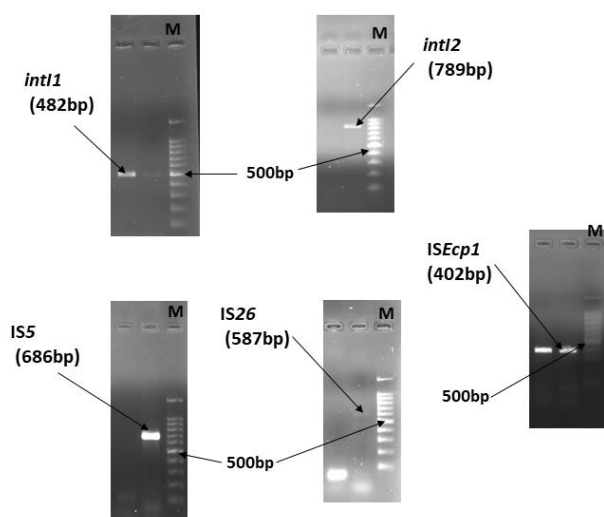


Figure 3.5: Representative picture of integrases (*intI1*, *intI2*) and insertion sequences (IS5, IS26 and *ISEcp1*) on Agarose Gel Electrophoresis. M represents the DNA marker lane (100 bp DNA ladder).

3.5.2.1. Distribution of mobile genetic element combinations in UPECp isolates:

In *bla*_{TEM} positive UPECp isolates, 9 different combination of MGEs were observed (Figure 3.6a), whereas in *bla*_{TEM} negative isolates, 5 different combinations of MGEs were observed (Figure 3.6b).

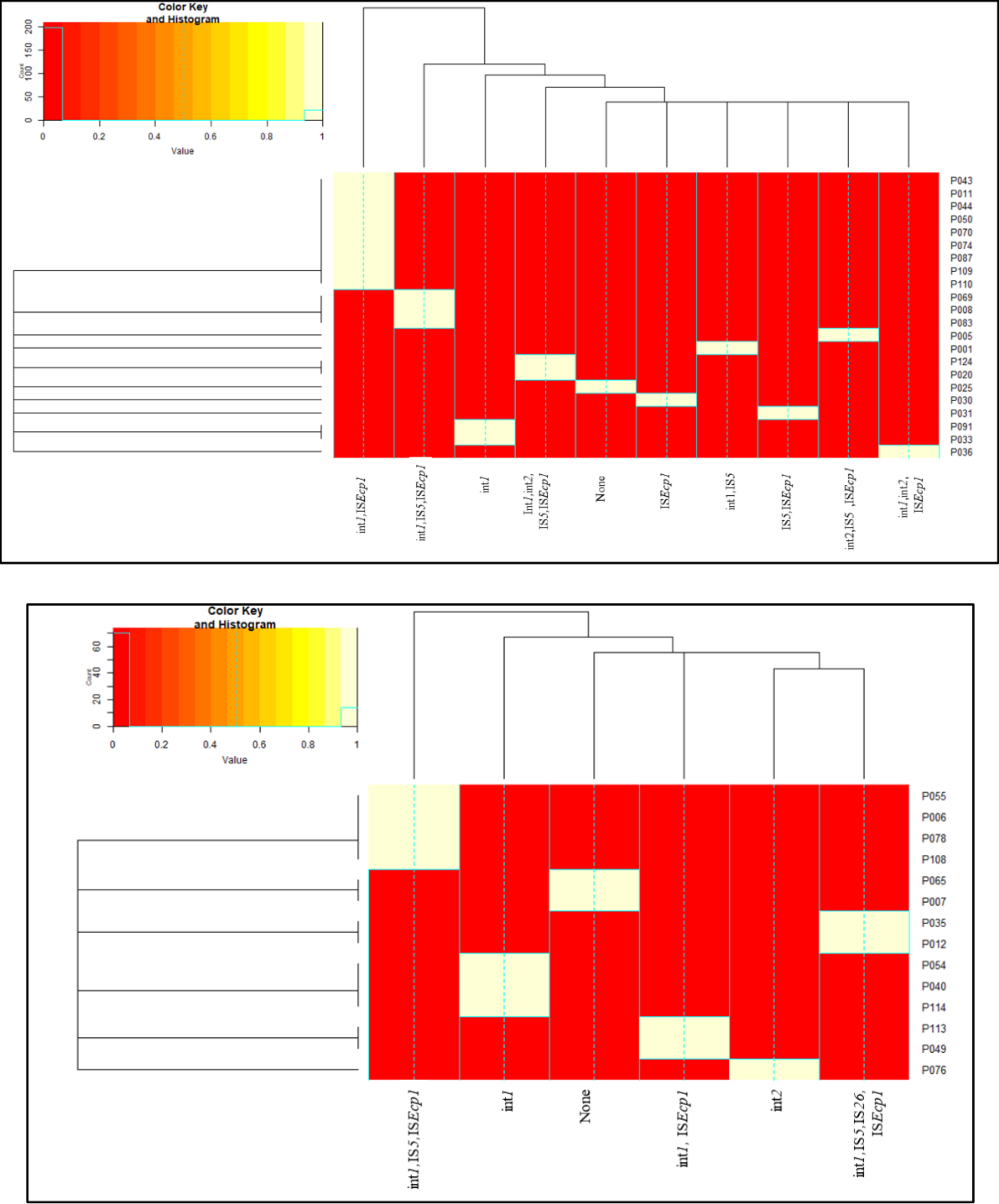
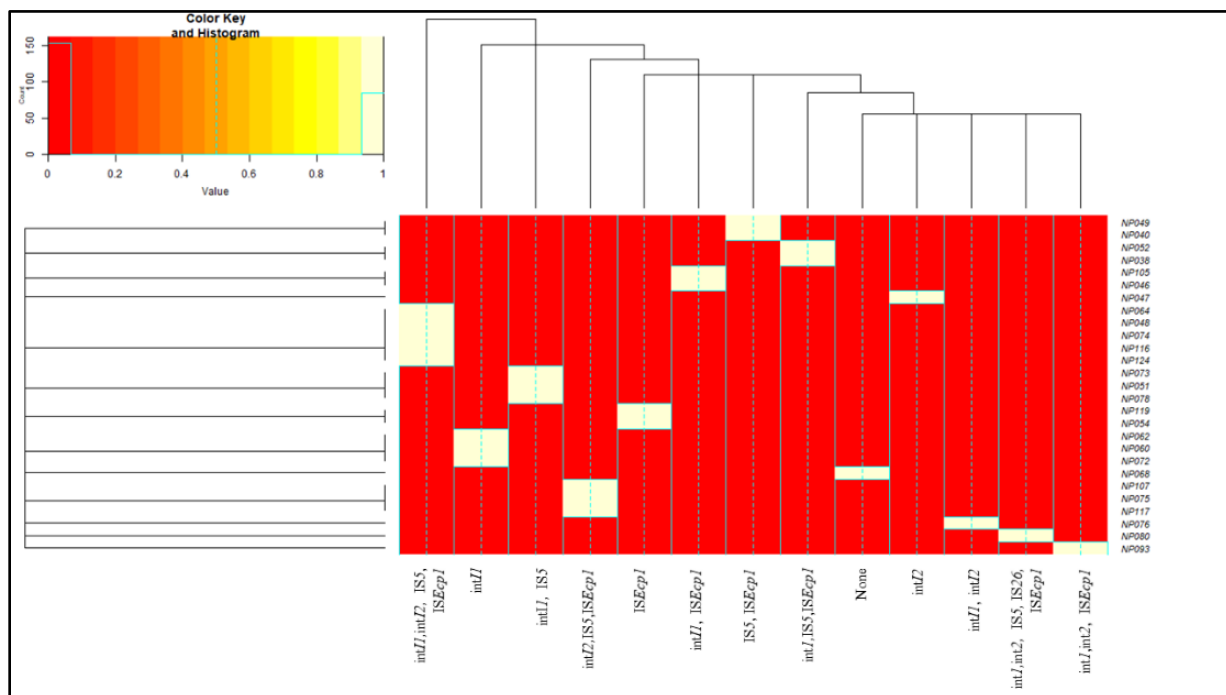


Figure 3.6: Heatmap representation of different combinations of MGEs; integrons (*intI1*, *intI2*) and insertion elements (*IS5*, *ISEcp1*, *IS26*) in *bla*_{TEM} positive (a) and *bla*_{TEM} negative (b) UPEC isolates collected from pregnant women. Numbers in right side indicates sample ID of each UPEC isolate. Color key represented the variation in colors from red to white, illustrating the absence of specific combination of MGEs to the presence of that particular combination respectively.

3.5.2.2. Distribution of mobile genetic element combinations in UPECnp isolates:

In *bla*_{TEM} positive UPECp isolates, 12 different combination of MGEs were observed (Figure 3.7a), whereas in *bla*_{TEM} negative isolates, 4 different combinations of MGEs were observed (Figure 3.7b).



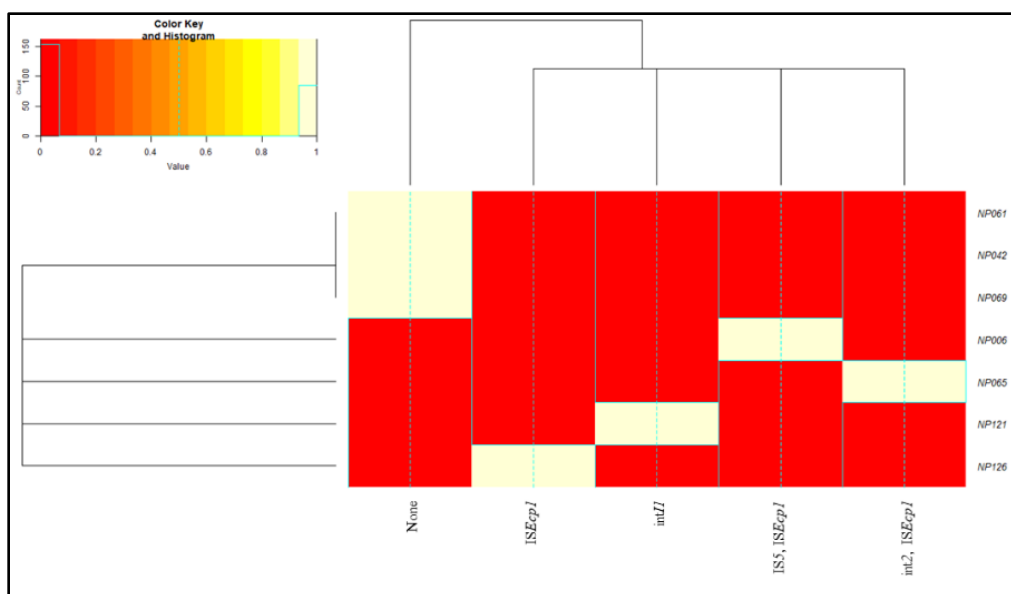


Figure 3.7: Heatmap representation of different combinations of MGEs; integrons (*intI1*, *intI2*) and insertion elements (*IS5*, *ISEcp1*, *IS26*) in *bla*_{TEM} positive (a) and *bla*_{TEM} negative (b) UPEC isolates collected from non-pregnant women. Numbers in right side indicates sample ID of each UPEC isolate. Color key represented the variation in colors from red to white, illustrating the absence of specific combination of MGEs to the presence of that particular combination respectively.

The distribution of the combination of MGEs in *bla*_{TEM} positive UPECp and UPECnp isolates were discreetly different. Similarly, discreet combination of MGEs were also observed in *bla*_{TEM} negative UPECp and UPECnp isolates.

3.5.3. Prevalence of plasmid-based replicon types in UPEC isolates

Table 3.7A: Prevalence of PBRTs in UPECp isolates

Sample ID	IncF _{repB}	IncN _{rep}	IncX	IncW	IncFII _s	IncA/C	IncL/M	IncY	IncI1	IncHI1	IncF1B
P001	+	-	-	-	-	-	-	-	+	-	+
P005	+	+	+	+	-	-	-	-	+	-	+
P006	+	-	-	+	-	+	-	+	+	-	-
P007	+	-	-	-	-	-	-	-	-	-	-
P008	+	-	+	-	+	-	+	-	+	-	+
P011	+	-	+	-	-	-	-	-	-	-	+

P012	+	-	+	-	+	-	+	-	-	-	+
P020	+	-	+	+	-	-	+	-	+	-	+
P025	+	-	+	-	-	-	-	-	-	-	+
P030	+	-	-	-	-	-	+	-	-	-	+
P031	+	-	+	-	-	+	+	-	-	-	+
P033	+	-	-	-	-	-	-	-	-	-	+
P035	+	-	-	-	+	-	-	-	-	+	+
P036	+	-	+	-	+	-	+	-	-	-	+
P040	+	-	-	-	-	-	-	-	-	-	+
P043	+	-	+	-	+	-	-	-	-	-	+
P044	+	-	+	-	-	-	-	-	-	-	+
P049	+	-	+	-	-	-	+	-	-	-	+
P050	+	-	+	-	-	-	-	-	-	-	-
P054	+	-	-	-	-	-	-	-	-	-	+
P055	+	-	+	-	-	-	-	-	-	-	+
P065	+	-	-	-	-	-	-	-	-	-	+
P069	+	-	+	-	-	+	-	-	+	-	+
P070	+	-	-	-	-	-	-	-	-	-	+
P074	+	-	-	-	-	-	-	-	-	-	+
P076	+	+	+	-	-	-	-	+	-	-	+
P078	+	-	+	-	-	-	-	-	+	-	-
P083	+	-	-	-	-	-	-	-	-	-	+
P087	+	-	+	-	-	-	-	-	+	-	+
P091	+	-	-	-	-	-	-	-	-	-	+
P108	+	-	-	-	-	-	-	+	-	-	+
P109	-	-	+	-	-	+	-	-	-	-	+
P110	+	-	+	-	-	+	-	-	-	-	+
P113	+	-	+	-	-	-	-	-	-	-	+
P114	+	-	+	-	-	-	-	-	-	-	-
P124	+	-	+	-	-	-	-	-	-	-	+

Table 3.7B: Prevalence of PBRTs in UPECnp isolates

Sample ID	IncF_{repB}	IncN_{rep}	IncX	IncW	IncFII_s	IncA/C	IncL/M	IncY	IncI1	IncHI1	IncF1B
NP006	+	-	+	-	-	-	+	-	-	-	+
NP038	+	-	+	+	-	+	+	+	-	-	+
NP040	+	-	+	-	-	-	+	+	-	-	+
NP042	+	-	-	-	-	-	-	-	-	-	+
NP046	+	-	-	-	-	-	-	-	+	-	+
NP047	+	-	+	-	-	-	+	+	-	-	-
NP048	+	+	+	-	+	-	+	-	+	-	+
NP049	+	+	+	-	+	+	+	-	+	-	-
NP051	+	-	+	-	+	-	-	+	+	-	+
NP052	+	-	+	-	-	-	+	+	+	-	+
NP054	+	-	+	-	+	-	+	+	+	-	+
NP060	+	-	-	-	+	-	-	-	+	-	+

NP061	+	-	-	+	-	-	+	-	-	-	+
NP062	+	-	+	-	+	-	-	-	-	-	+
NP064	+	-	+	-	+	-	+	+	+	-	+
NP065	+	-	+	-	+	+	+	-	-	-	+
NP068	+	-	-	-	-	-	-	-	-	-	+
NP069	+	-	-	-	-	-	-	-	-	-	+
NP072	+	-	+	-	+	+	-	-	-	-	+
NP073	+	+	+	-	+	+	-	+	+	-	+
NP074	+	+	+	+	+	-	+	-	+	-	+
NP075	-	+	+	+	+	-	+	-	+	-	-
NP076	+	+	+	-	+	-	-	-	+	-	+
NP078	+	+	+	-	+	+	+	-	-	-	+
NP080	+	+	+	-	+	-	+	+	+	-	+
NP093	+	+	+	-	-	-	+	+	+	-	+
NP105	+	+	+	-	-	-	-	-	+	-	+
NP107	+	+	+	-	+	+	+	-	+	-	+
NP116	+	+	+	-	-	+	+	-	+	-	+
NP117	+	+	+	-	+	-	+	+	+	-	+
NP119	+	+	+	-	+	+	+	+	+	-	+
NP121	+	+	+	-	+	-	-	+	+	-	+
NP124	+	+	+	-	+	+	+	+	+	-	+
NP126	+	+	+	-	+	-	+	+	+	-	+

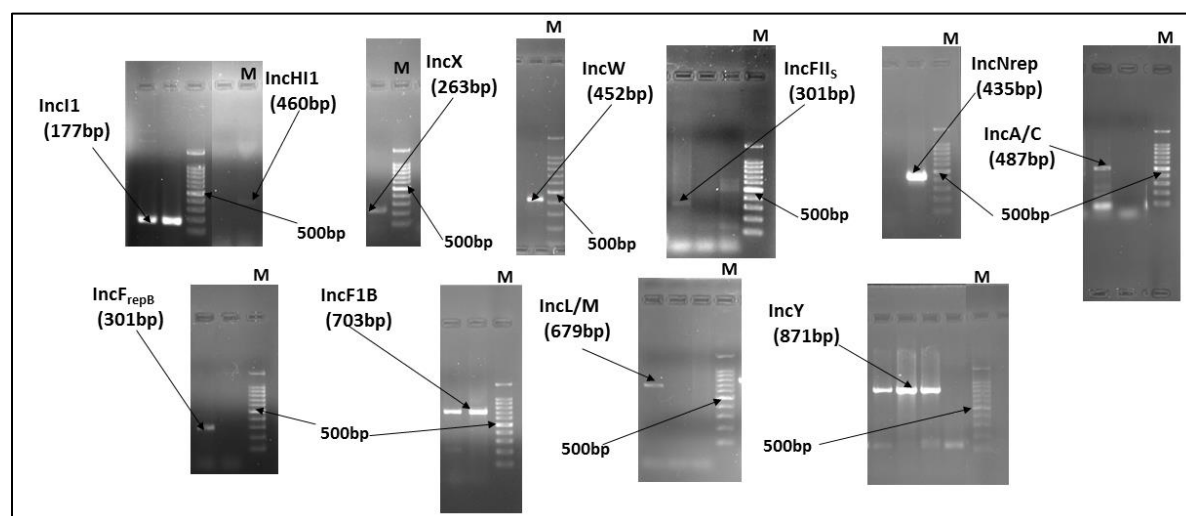


Figure 3.8: Representative picture of Plasmid Based Replicon Types run on Agarose Gel Electrophoresis. M represents the DNA marker lane (100bp DNA ladder).

3.5.3.1. Distribution of replicon type combinations in UPECp isolates:

In *bla*_{TEM} positive UPECp isolates, 15 different *Inc* types were observed (Figure 3.9a), whereas in *bla*_{TEM} negative isolates, 11 different *Inc* types were observed (Figure 3.9b).

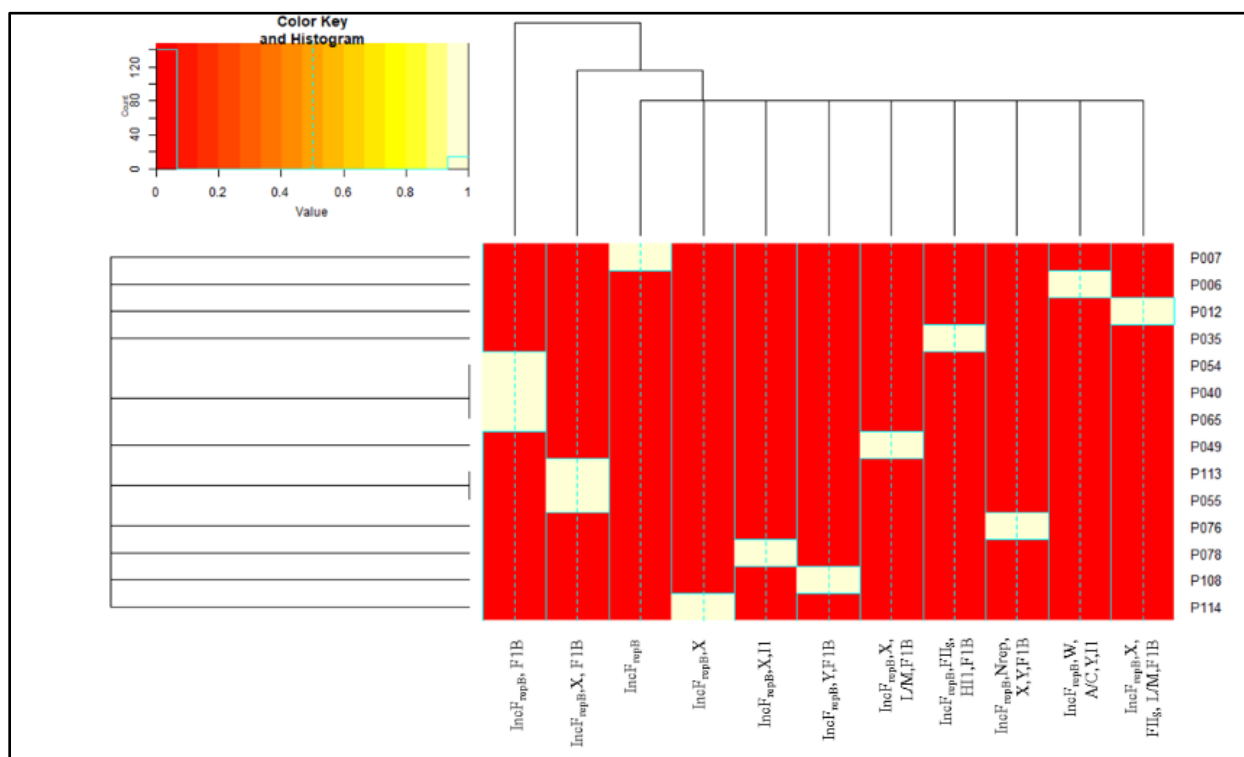
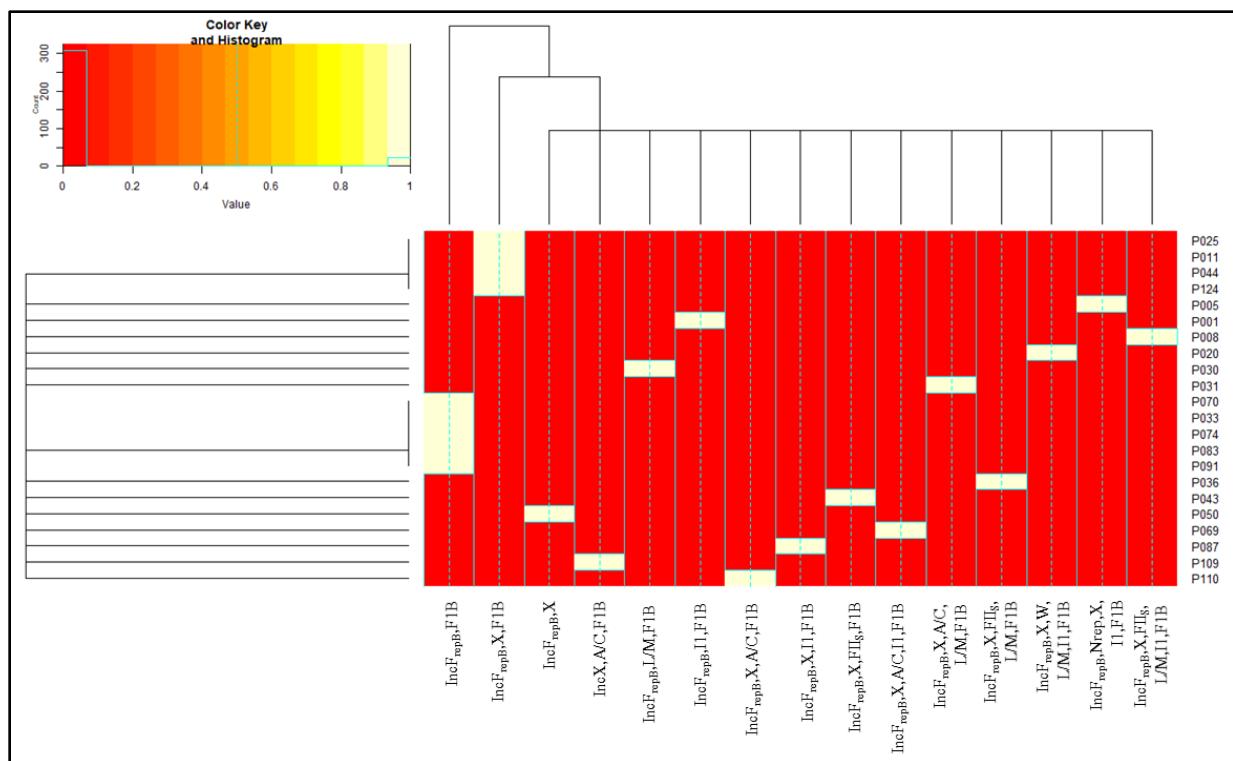
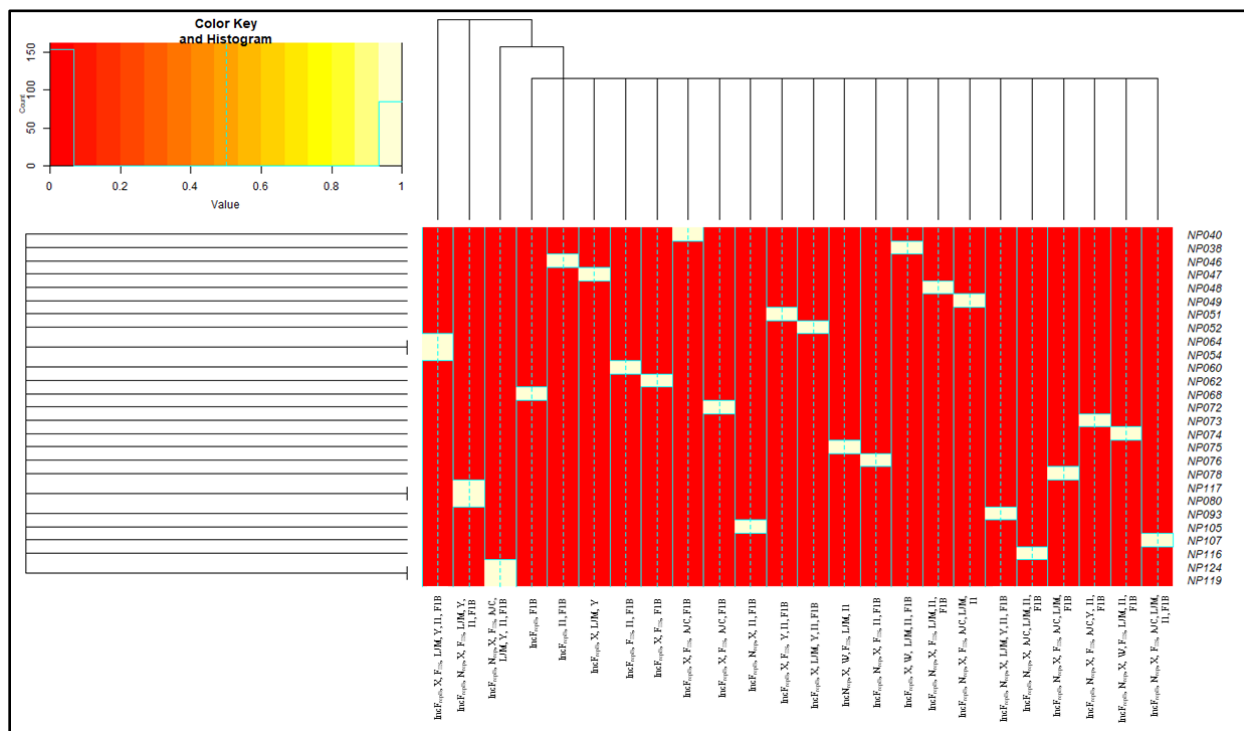


Figure 3.9: Heatmap representation of multiple-replicon plasmids in the *bla*_{TEM} positive (a) and *bla*_{TEM} negative (b) UPEC isolates collected from pregnant women. Numbers in right side

indicates sample ID of each UPEC isolate. Color key represented the variation in colors from red to white, illustrating the absence of specific combination of multiple-replicon plasmids to presence of that particular combination respectively.

3.5.3.2. Distribution of replicon type combinations in UPECnp isolates:

In *bla*_{TEM} positive UPECp isolates, 24 different *Inc* types were observed (Figure 3.10a), whereas in *bla*_{TEM} negative isolates, 06 different *Inc* types were observed (Figure 3.10b).



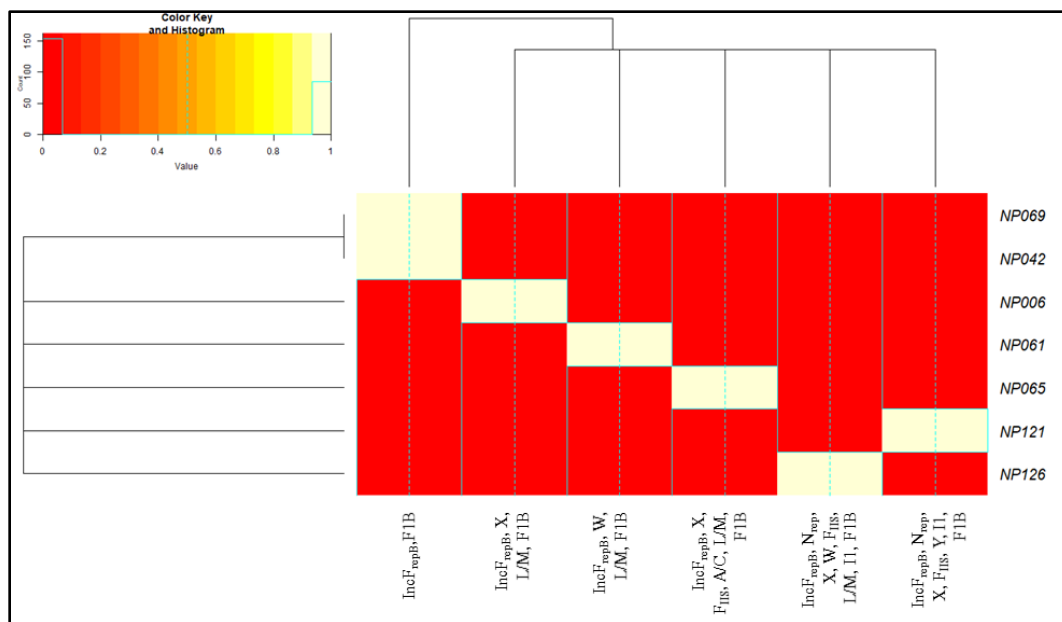


Figure 3.10: Heatmap representation of multiple-replicon plasmids in the *bla*_{TEM} positive (a) and *bla*_{TEM} negative (b) UPEC isolates collected from non-pregnant women. Numbers in right side indicates sample ID of each UPEC isolate. Color key represented the variation in colors from red to white, illustrating the absence of specific combination of multiple-replicon plasmids to presence of that particular combination respectively.

3.6. Discussion:

Additionally, akin to our study, moderate to high ESBL *E. coli* occurrences were also observed amongst pregnant women [26, 27, 28, 29, 30] and amongst non-pregnant women [31, 32, 33] from different parts of the world. The majority of documented cases of carbapenemase-producing Enterobacteriaceae (CPE), primarily *E. coli*, in mothers and newborns were caused by the bacteria being directly transferred from the mother to her child during birth. Therefore, mothers pose major risk factor for the transmission of CPE to the neonates [1, 34]. Additionally, carbapenemase producing *E. coli* also limits treatment in non-pregnant population [35, 36].

Similar to other recent studies worldwide [27, 28, 29, 37], co-occurrence of various β -lactamase genes (oxacillinase, ESBL, carbapenemases) was seen in our study with the highest incidence of *bla*_{TEM} gene (61%) amongst *E. coli* isolated from pregnant women. Additionally, high incidence of *bla*_{CTX-M} was observed in a few studies amongst pregnant women [30, 38]. Moreover, our study also indicated highest co-occurrence of *bla*_{TEM} and *bla*_{CTX-M} similar to a study from Lebanon [30].

In non-pregnant women, role of plasmid has been demonstrated in dissemination of antibiotic resistant genes (ARGs) either by integrating those plasmids into the chromosomal DNA, or by transmitting the DNA through conjugation [6, 39], but there was paucity of information regarding the incidence of MGEs and/or incidence of different *Inc* types of resistant plasmids in UPECs isolated from pregnant population. In our study, the IncF_{repB} was the most common replicon in both pregnant and non-pregnant population, that was found either solely or concomitantly in 35 of 36 (97.22%) UPECp and 33 of 34 (97.06%) UPECnp isolates, which was akin to a study from India with non-pregnant isolates [6], but unlike another study from Saudi with non-pregnant isolates [40], where IncFII was found as the most common replicon type. As far as we are aware, no study has ever worked with the replicon types of uropathogenic *E. coli* isolates from pregnant population. Following IncF_{repB}, IncF1B was second most predominant replicon types found solely or concurrently in 31 of 36 (86.11%) UPECp and 31 of 34 (91.18%) UPECnp isolates, this was similar to a study where IncF1B and IncB/O replicons were predominant in UPEC isolates from USA [41]. IncF1B followed by IncFII was mostly predominant in a study from Germany [42]. IncHII was least predominant in our pregnant population but it was absent in non-pregnant population. To best of our knowledge, no study previously identified MGEs of uropathogenic *E. coli* isolated from any pregnant population. IncW was least predominant in non-pregnant population (11.76%), which also was different from the study from Riyadh [40]. In both pregnant and non-pregnant isolates, type-1 integrons (85.29% and 55.88% respectively) and insertion sequence *ISEcp1* (72.22% and 58.82% respectively) was mostly predominant, which was different from a study of Spain [43] where IS26 was most prevalent. Class 1 integrons was prevalent in studies from Spain [43], China [44], Portugal [45], USA [46].

In our study, we identified the replicon types of resistant plasmids which harbored β -lactamase genes (*bla*_{OXA-I}, *bla*_{OXA-II}, *bla*_{OXA-III}, *bla*_{TEM}, *bla*_{CTX-M}, *bla*_{NDM}, *bla*_{OXA-48}) and associated mobile genetic elements (*int11*, *int12*, *ISEcp1*, IS5, IS26) to gain an insight into the acquisition and risk of dissemination of anti-microbial resistance mediated by these resistant determinants identified in UPECs collected from both pregnant and non-pregnant women. Our study demonstrated significant distribution of plasmids with multiple replicon types in both UPECp and UPECnp, similar to other studies which also demonstrated resistance plasmids with multiple replicon types in UPEC isolates from non-pregnant population [47, 48]. The spread of resistance genes might be facilitated by acquisition of multiple replicon plasmids, leading to the selection of the antibiotic-

resistant pathogen which is highly alarming in both populations. According to the statistically significant distribution of MGEs in *bla*_{TEM} negative isolates compared to *bla*_{TEM} positive ones in UPECp, a risk of horizontal transmission of resistant determinants from mother to the fetus or neonates after birth, is evident if not addressed with appropriate therapeutics.

3.7. Reference:

1. Sekyere JO, Reta MA, and Fourie PB. Risk factors for, and molecular epidemiology and clinical outcomes of carbapenem- and polymyxin- resistant gram-negative bacterial infections in pregnant women, toddlers: a systematic review and meta-analysis. 2021. Annals of New York Academy of Sciences. 1502: 54 – 71.
2. Alqasim A, Abu Jaffal A, Alyousef AA. Prevalence of Multidrug Resistant and Extended-spectrum- β -lactamase carriage of Clinical Uropathogenic *Escherichia coli* isolates in Riyadh, Saudi Arabia. 2018. International Journal of Microbiology. 1 – 9.
3. Malekzadegan Y, Khashei R, Ebrahim-Saraie HS, Jahanabadi Z. Distribution of virulence genes and their association with antimicrobial resistance among uropathogenic *Escherichia coli* isolates from Iranian patients. 2018. BMC Infectious Diseases. 18(1): 572.
4. Bush K, Jacoby GA. Updated functional classification of β -lactamases. 2010. Antimicrobial Agents and Chemotherapy. 54(3): 969 – 976.
5. Khajuria A, Praharaj AK, Kumar M, Grover N. Emergence of *Escherichia coli* producing NDM-1 and OXA-48 carbapenemases, in Urinary Isolates, at a Tertiary Care Centre at Central India. 2014. Journal of Clinical and Diagnostic Research. 8(6): DC01 – DC04.
6. Mukherjee SK, Mukherjee M. Characterization and bio-typing of multidrug resistance plasmids from uropathogenic *Escherichia coli* isolated from clinical setting. 2019. Frontiers in Microbiology. 10: 2913.
7. Vrancianu CO, Popa LI, Bleotu C, Chifiruc MC. Targeting plasmids to limit acquisition and transmission of antimicrobial resistance. 2020. Frontiers in Microbiology. 11: 761.
8. Ghosh B, Mukherjee M. Emergence of co-production of plasmid-mediated AmpC beta-lactamase and ESBL in cefoxitin – resistant uropathogenic *Escherichia coli*. 2016. European Journal of Clinical Microbiology and Infectious Diseases. 35(9): 1449 – 1454.
9. Ambler RP. The structure of beta-lactamases. 1980. Philosophical transactions of the Royal Society of London. Series B, Biological Sciences. 289 (1036): 321-31.
10. Gutkind GO, Conza JD, Power P, Radice M. β -lactamase mediated resistance: a biochemical, epidemiological and genetic overview. 2013. Current Pharmaceutical Design. 19(2): 164-208.
11. Evans BA, Amyes SGB. OXA β -Lactamases. 2014. Clinical Microbiology Reviews. 27(2): 241-263.

12. Hedges RW, Datta N, Kontomichalou P, Smith JT. Molecular specificities of R-factor-determined-beta-lactamases: correlation with plasmid compatibility. 1974. *Journal of Bacteriology*. 117(1): 56-62.
13. Datta N, Kontomichalou P. Penicillinase synthesis controlled by infectious R factors in Enterobacteriaceae. 1965. *Nature*. 208 (5007): 239-41.
14. Sykes RB, Matthew M. The beta-lactamases of gram-negative bacteria and their role in resistance to beta-lactam antibiotics. 1976. *The Journal of Antimicrobial Chemotherapy*. 2(2): 115-57.
15. Overdevest I, Rinsburger M, Eustace A, Xu L, Hawkey P, Heck M et al. Extended-Spectrum β -Lactamase genes of *Escherichia coli* in chicken meat and humans, the Netherlands. 2014. *Emerging Infectious Diseases*. 17(7): 1216 – 1222.
16. Bajpai T, Pandey M, Varma M, Bhatambare GS. Prevalence of TEM, SHV, and CTX-M Beta-Lactamase genes in the urinary isolates of a tertiary care hospital. 2017. *Avicenna Journal of Medicine*. 7(1): 12 – 16.
17. Kumarasamy KK, Toleman MA, Walsh TR, Bagaria J, Butt F, Balakrishnan R et al. Emergence of a new antibiotic resistance mechanism in India, Pakistan, and the UK: A molecular, biological and epidemiological study. 2010. *The Lancet: Infectious disease*. 10(9): 597-602.
18. Peirano G, Schreckenberger PC, Pitout JDD. Characteristics of NDM-1-Producing *Escherichia coli* isolates that belong to the successful and virulent clone ST 131. 2011. *Antimicrobial Agents and Chemotherapy*. 55(6): 2986 – 2988.
19. Gurung S, Kafle S, Dhungel B, Adhikari N, Shrestha UT, Adhikari B et al. Detection of OXA-48 gene in carbapenem-resistant *Escherichia coli* and *Klebsiella pneumoniae* from Urine samples. 2020. *Infection and Drug Resistance*. 13: 2311 – 2321.
20. Bozcal E. Insight into the mobilome of *Escherichia coli*. 2019. Intechopen. DOI: 10.5772/intechopen.82799.
21. Deng Y, Bao X, Lili J, Chen L, Liu J, Miao J et al. Resistance integrons: class 1, 2 and 3 integrons. 2015. *Annals of Clinical Microbiology and Antimicrobials*. 14:45.
22. Sawers RG. Transcript analysis of *Escherichia coli* K-12 insertion element IS5. 2005. *FEMS Microbiology Letters*. 244 (2): 397 – 401.
23. Harmer CJ, Hall RM. An analysis of the IS6/IS26 family of insertion sequences: is it a single family? 2019. *Microbial Genomics*. 5(9): e000291.
24. Zong Z, Patridge SR, Iredell JR. ISECp1-mediated transposition and homologous recombination can explain the context of bla_{CTX-M-62} linked to qnrB2. 2010. *Antimicrobial Agents and Chemotherapy*. 54(7): 3039 – 3042.
25. Carattoli A, Bertini A, Villa L, Falbo V, Hopkins KL, Threlfall EJ. Identification of plasmids by PCR-based replicon typing. 2005. *Journal of Microbiological Methods*. 63: 219–228.

26. Milenkov M, Rasoanandrasana S, Rahajamanan LV, Rakotomalala RS, Razafindrakoto CA, Rafalimanana LV, Ravelomandranto E, Ravaoarisaina Z, Westeel E, Petitjean M, Mullaert J, Clermont O, Raskine L, Samison LH, Endtz H, Andremont A, Denamur E, Komurian-Pradel F, Armand-Lefevre L. Prevalence, Risk factors, and Genetic Characterization of Extended-spectrum Beta-Lactamase *Escherichia coli* isolated from healthy pregnant women in Madagascar. 2021. *Frontiers of Microbiology*. 12: 786146.
27. Elsariti HO, Elmeheishi FM, Elgrabulli FR. Detection of extended spectrum β -lactamase and AmpC gene in *Escherichia coli* isolated from pregnant women in Misurata City. 2021. *Journal of Humanitarian and Applied Sciences*. 12: 282 – 289.
28. Adedze-Kpodo RK, Feglo PK, Agboli E, Asmah RH, Kwadzokpui PK. Genotypic characterization of extended-spectrum β -lactamase producing urinary isolates among pregnant women in Ho municipality, Ghana. 2022. *Heliyon*. 8: e12513.
29. Bello RH, Ibrahim YKE, Olayinka BO, Jimoh AAG, Afolabi-Balogun NB, Oni-Babatunde AO, Olabode HOK, David MS, Aliyu A, Olufadi-Ahmed HY. Molecular characterization of Extended spectrum beta-lactamase producing *Escherichia coli* isolated from pregnant women with urinary tract infections attending ante-natal clinics in Ilorin Metropolis. 2021. *Nigerian Journal of Pharmaceutical Research*. 17: 119 – 129.
30. Ghaddar N, Anastasiadis E, Halimeh R, Ghaddar A, Matar GM, Fayad AA, Sherri N, Dhar R, Alfouzan W, Yusef H, Elchaar M. Phenotypic and Genotypic Characterization of Extended-Spectrum Beta-Lactamases produced by *Escherichia coli* colonizing pregnant women. 2020. *Infectious Diseases in Obstetrics and Gynecology*. 4190306.
31. Belete MA. Bacterial profile and ESBL screening of urinary tract infection among asymptomatic and symptomatic pregnant women attending antenatal care of northeastern Ethiopia region. 2020. *Infection and Drug Resistance*. 13: 2579 – 2592.
32. Naushad VA, Purayil NK, Wilson GJ, Chandra P, Joseph P, Khalil Z, Zahid M, Kayakkool MK, Shaik N, Ayari B, Chalihadan S, Elmagboul EBI, Doiphode SH. Epidemiology of urinary tract infection in adults caused by extended-spectrum beta-lactamase (ESBL)-producing Enterobacteriaceae – a case-control study from Qatar. 2022. *IJID Regions*. 3: 278 – 286.
33. Jia P, Zhu Y, Li X, Kudinha T, Yang Y, Zhang G, Zhang J, Xu Y, Yang Q. High prevalence of extended-spectrum beta-lactamases in *Escherichia coli* strains collected from strictly defined community acquired urinary tract infections in adults in China: A multicenter prospective clinical microbiological and molecular study. 2021. *Frontiers in Microbiology*. 12: 663033.
34. Djuikoue CI, Djouela Djoulako PD, Same Njanjo HV, Kiyang CP, Djantou Biankeu FL, Guegang C, Tchouotou AS, Wouambo RK, Thumamo Pokam BD, Apalata T, Jeannot K. Phenotypic characterization and prevalence of carbapenemase-producing *Pseudomonas aeruginosa* isolates in six health facilities in Cameroon. 2023. *BioMed*. 3: 77 – 88.
35. Tian X, Zheng X, Sun Y, Fang R, Zhang S, Zhang X, Lin J, Cao J, Zhou T. Molecular mechanisms and epidemiology of carbapenem-resistant *Escherichia coli* isolated from Chinese patients during 2002 -2017. 2020. *Infection and Drug Resistance*. 13: 501 – 512.

36. Doi Y. Treatment options for carbapenem-resistant gram-negative bacterial infections. 2019. *Clinical Infectious Diseases*. 69: S565 – S575.
37. Adekunle OO, Idris OJ, Wahab AA, Adekanle AM. Antibiotic susceptibility and detection of resistance genes of *E. coli* among healthy pregnant women in designated hospitals around Osogbo, Osun State, Nigeria. 2022. *Journal of Applied Sciences and Environmental Management*. 26: 1151 – 1155.
38. Mohebi S, Hashemizade Z, Hadadi M, Kholdi S, Javadi K, Motamedifar M. Pathogenic features of urinary *Escherichia coli* strains causing asymptomatic bacteriuria during pregnancy. In review. *Research square*. 2020.
39. Rozwadowski M, Gawel D. Molecular factors and mechanisms driving multidrug resistance in uropathogenic *Escherichia coli* – An update. 2022. *Genes*. 13(8): 1397.
40. Alangirir A, Jaffal AA, Almutairi N, Abdullah AA. Plasmid replicon diversity of clinical uropathogenic *Escherichia coli* isolates from Riyadh, Saudi Arabia. 2022. *Journal of Pure and Applied Microbiology*. 16(1): 540 – 548.
41. Johnson TJ, Wannemuehler YM, Johnson SJ, Logue CM, White DG, Doetkott C, Nolan LK. Plasmid replicon Typing of commensal and pathogenic *Escherichia coli* isolates. 2007. *Applied and Environmental Microbiology*. 73(6): 1976 – 1983.
42. Basha JA, Kiel M, Görlich D, Schütte-Nütgen K, Witten A, Pavenstädt H, Kahl BC, Dorbindt U, Reuter S. Phenotypic and Genotypic characterization of *Escherichia coli* causing urinary tract infections in kidney-transplanted patients. 2019. *Journal of Clinical Medicine*. 8(7): 988.
43. Pérez-Etayo L, Berzosa M, González D, Vitas AI. Prevalence of integrons and insertion sequences in ESBL-producing *E. coli* isolated from different sources in Navarra, Spain. 2018. *International Journal of Environmental Research and Public Health*. 15 (10): 2308.
44. Deng Y, Bao X, Ji L, Chen L, Liu J, Miao J, Chen D, Bian H, Li Y, Yu G. Resistance integrons: Class 1, 2 and 3 integrons. 2015. *Annals of Clinical Microbiology and Antimicrobials*. 14:45.
45. Machado E, Coque TM, Cantón R, Sousa JC, Peixe L. Antibiotic resistance integrons and extended-spectrum β -lactamases among Enterobacteriaceae isolates recovered from Chickens and swine in Portugal. 2008. *Journal of Antimicrobial Chemotherapy*. 62: 296 – 302.
46. Solberg O, Ajiboye R, Riley L. Origin of class 1 and 2 integrons and gene cassettes in a population-based sample of uropathogenic *Escherichia coli*. 2006. *Journal of Clinical Microbiology*. 44: 1347 – 1351.
47. Ghosh A, Ghosh B, Mukherjee M. Epidemiologic and molecular characterization of β -lactamase-producing multidrug-resistant uropathogenic *Escherichia coli* isolated from asymptomatic hospitalized patients. 2022. *International Microbiology*. 25(1): 27 – 45.
48. Dwiyanto J, Hor JW, Reidpath D, Su TT, Lee SWH, Ayub Q, Mustapha FB, Lee SM, Foo SC, Chong CW, Rahman S. Pan-genome and resistome analysis of extended-spectrum β -lactamase-producing *Escherichia coli*: A multi-setting epidemiological surveillance study from Malaysia. 2021. *PLoS ONE*. 17(3): e0265142.

Chapter 4: Characterization of imipenem-resistant UPECp and UPECnp isolates according to phylogenetic background, virulence factor genes and clonal lineages

4.1. Background of the study: One of the most common medical complications during pregnancy, both globally and in the Indian subcontinent, was Urinary tract infection [1, 2]. The most frequent cause of which in both hospital and community settings is uropathogenic *E. coli*, with high morbidity and mortality. Additionally, recurrent UTI during pregnancy was also caused by UPEC [3]. Generally, UTI is often treated empirically, but due to risk concerns associated with pregnancy, an appropriate prescription policy was developed that included penicillin, extended-spectrum- β -lactams, and nitrofurantoin, all of which were safe to use during pregnancy. Though in non-pregnant populations, empiric treatment with several antibiotic groups led to a random selection of multidrug-resistant (MDR) pathogens.

Production of extended-spectrum- β -lactamases (ESBLs), which conferred resistance to broad-spectrum penicillins, cephalosporins, and monobactams, was one of the most prevalent resistance mechanisms. Carbapenems were chosen as treatment alternatives in severe infections brought on by ESBL-producing bacteria. However, alarming incidences of carbapenems (imipenem, meropenem, ertapenem, and doripenem) resistance in UPEC isolated from non-pregnant populations from various regions of the world were described in a number of recent studies [4, 5, 6, 7]. Additionally, to the aforementioned reports, highly alarming emergence of ertapenem and imipenem resistance was also reported in Enterobacteriaceae (*K. pneumoniae*, *E. coli*) isolated from pregnant women [8].

UPEC strains belonged to 8 phylogenetic groups (A, B1, B2, C, D, E, F, and Clade I) and had a variety of virulence factors (VFs). Some of the VFs were found on areas of the chromosome known as pathogenicity islands (PAIs), which aided their ability to successfully colonize the urinary tract and cause infection. Irrespective of their AMR pattern, phylogroup B2 strains were shown to be most virulent [9]. However, virulence-related gene exchange between phylogroups was made easier by horizontal gene transfer (HGT) mechanisms, which may have contributed to the formation of strains with high pathogenic potential. In comparison to susceptible UPEC isolates, resistant isolates demonstrated an increase or decrease in several VFs in response to specific antibiotics [10]. It was concerning that the carbapenem-resistant UPEC had higher levels of various VFs than the susceptible ones [11], as these bacteria were linked to high mortality due to limited therapeutics.

There has been widespread evidence of a strong correlation between UPEC ST131 and UTI [12, 13], particularly in India [14]. Due to their substantially increased virulence, fitness, and metabolic capacities, along with the acquisition of AMR genes, several other successful clonal lineages of different sequence types (ST), such as ST410, ST95, and ST10, have spread around the world, much like ST131. Worldwide reports of ST38, ST410, ST131, and ST648 being linked to carbapenem-resistant *E. coli* samples were also reported [2].

There have only been a few studies on the prevalence of carbapenem-resistance in clinical isolates of *E. coli* from India [15, 16, 17, 18] till now. To the best of our knowledge, there is no evidence on imipenem-resistance in *E. coli* isolated from urine samples of pregnant women with UTI, where judicious antibiotic treatment is absolutely necessary.

4.2. Objective of the study:

- To characterize the imipenem-resistance UPECp and UPECnp isolates according to the phylogenetic background, virulence characteristics, and clonal lineages.

4.3. Materials:

4.3.1. Equipment:

Laminar Air Flow (BD Instrumentation) • Shaker-Incubator (ICT) • Autoclave • Glass spreader • Spirit Lamp • Eppendorf Tubes (1.5ml and 2ml) (Tarsons) • Microtips (0.5-10 µl, 2-20 µl, 20-200 µl, 200-2000µl) (Himedia) • Micropipettes ((0.5-10 µl, 2-20 µl, 20-200 µl, 200-2000µl) (P'Fact, Microlit, Biohit) • Cotton (Bengal Surgicals Limited) (Laxmi Healthcare Products (P) Ltd.) • 90mm Glass Petri Dish (Borosil) • Glass Culture Tubes (Touff, Borosil) • Test Tubes Racks (Tarsons) • Surgical Gloves (Pricare, Himedia) • Cryogenic Tubes 1.5ml (Tarsons) • Cooling Centrifuge (Remi) • Tabletop Centrifuge (Remi) • Weighing Machine (K Mitra) • Refrigerator (Godrej) • -20°C deep freezer (Cellfrost) • Thermal Cycler (Applied Biosystems) • Horizontal gel electrophoresis apparatus (Genei) • Power Pack for running gel (Genei) • Electrophoresis Gel Documentation System (Bio-Rad, USA) •

4.3.2. Reagent:

Luria Bertani (LB) media (SRL) • Mueller Hinton (MH) media (SRL) • Barium Chloride (Merck) • Sulphuric Acid (Merck) • 70% Ethanol (Bengal Chemical) • 95% Ethanol (Himedia) • Single Distilled Water (SDW) (Kemecos India Pvt. Ltd., Hospital Supply) • Double distilled water (Prepared from SDW in the distillation plant of department) • Agar Agar (Himedia) • Antibiotic Discs (Himedia) • TE buffer (HiMedia) • Proteinase K (HiMedia) • RNase A (HiMedia) • Phenol (HiMedia) • Chloroform (Merck) • Sodium Acetate (Merck) • DNA diluent (HiMedia) • Gene-specific primers (GCC biotech India Pvt. Ltd.) • dNTP (Invitrogen) • Taq DNA polymerase and buffer (Invitrogen) • 50mM MgCl₂ (Invitrogen) • DNA ladders (HiMedia) • Tris Base (SRL chemicals India) • 6X gel loading buffer (HiMedia) • Agarose (HiMedia) • Ethidium Bromide (SRL chemicals India)

4.4. Experimental Procedure:

4.4.1. **Bacterial strains for this study:** 36 UPECp and 34 UPECnp strains isolated previously and mentioned in Chapter 2 were included in this study. Kirby Bauer reports of these strains were analyzed and imipenem resistant isolates were considered for this study.

4.4.2. **Isolation of bacterial genomic DNA:** Genomic DNA was isolated from all UPEC isolates using the protocol as described in Wright et al. 2017 [19] with some modifications. The modified protocol was described below.

- Cell pellet from 2 ml overnight culture at room temperature for 5000 rpm at 8 minutes.
- The supernatant is discarded.
- 200 µl of TE buffer is added to the pellet and to resuspend, pellet was vortexed. (TE buffer maintain alkaline environment which is the first step of this experiment, EDTA destabilizes the cell membrane).
- Resuspended pellet is centrifuged at 4⁰C for 2 minutes at 10000 rpm.
- The supernatant is discarded.
- 400 µl of TE was added to the pellet and was resuspended by vortex (The bacterial cell is lysed by catalyzing the hydrolysis of 1,4-β linkage between NAG-NAM).
- 10 µl of lysozyme (10 mg/ml) is added and hand vortexed (Genomic DNA is taken out into the solution).
- The solution is kept on ice for 30 minutes.

- 30 µl of 10% SDS, 3 µl Proteinase K (20mg/ml), 52 µl TE buffer and 5 µl RNaseA (10mg/ml) added in each tube.
- The tube is further incubated at 37°C for 1 hour.
- Phenol and chloroform are added after 1 hour in 1:1 ratio (200 µl:200 µl).
- The tube is centrifuged at 10000 rpm for 5 minutes at 4°C.
- The supernatant is collected in fresh tube.
- Equal volume of chloroform (200 µl) is added in the supernatant.
- The solution is centrifuged at 10000 rpm for 5 minutes at 4°C.
- The supernatant is collected again in a new centrifuge tube.
- 1/10th volume of sodium acetate (CH₃COONa) and 2 volume of absolute alcohol (700 µl) were added to each tube and incubated for overnight at -20°C.
- On the next day, the solution was centrifuged at 10000 rpm for 30 minutes at 4°C.
- It is washed again with 70% alcohol (200 µl), further vortexed, and kept at 4°C for 10 minutes.
- The solution is centrifuged at 10000 rpm for 10 minutes at 4°C.
- The supernatant is removed and the pellet is airdried.
- 50 µl 1X TE buffer is added to the air-dried pellet.
- It is then kept at 37°C for 30 minutes.
- The pellet is stored at 4°C for further use.

4.4.3. Isolation of total DNA: Total DNA was isolated using the boiling method as mentioned in Abdallah et al. 2011 [20] and modified a little. The protocol is as follows:

- 2 ml of overnight culture was taken in a centrifuge tube & centrifuged at 8000 rpm for 5 minutes at room temperature.
- In this way the bacteria were pelleted from broth by discarding the supernatant and resuspending the pellet in 100 µl DDH₂O and boiled at 100°C for 10 minutes.
- After heating, the tube containing the bacterial suspension was placed on ice for 5 minutes.
- The cellular debris were removed by centrifugation at 10000 rpm for 30 minutes at 4°C.
- The supernatant (about 100 µl/ 150 µl) was taken in a fresh centrifuge tube and to it equal volume of chloroform was added to wash it. The entire suspension was mixed by vortexing.

- After centrifuging at 10000 rpm for 5 minutes at 4°C. The supernatant was then transferred in a fresh tube (divided in two fresh tubes) and stored at -20°C.

4.4.4. Analysis of phylogenetic background: Since 2000, the Multi-locus sequence type (MLST) data for *E. coli* collected from various hosts and ecosystems has been expanding quickly. MLST information increased the efficiency with which the triplex PCR approach for phylo-group assignment could be validated. According to this validation studies, 80 – 85% of the phylo-group allocations are accurate. It did, however, show that a sizeable portion of bacteria with specific triplex genotypes (A₀, D₁, D₂) were assigned incorrectly. Phylo-group E, historically a tiny collection of unassigned strains with O157:H7 as its most well-known member, is now widely acknowledged. Phylo-group B2's sibling group, Phylo-group F, which includes of strains, is now also known to exist. A phylo-group C has recently been proposed for a collection of strains that are related to, but different from B1. Several novel lineages of *Escherichia* that are genetically distinct but phenotypically indistinguishable from *E. coli*. At least one of these cryptic lineages, *Escherichia* clade I, should also be considered a phylo-group of *E. coli* based on the extent of recombination detected between strains belonging to clade I and *E. coli*. Therefore, at present there are eight recognized phylo-groups of *E. coli*, with seven belonging to *E. coli sensu stricto* (A, B1, B2, C, D, E, F) and one corresponding to *Escherichia* clade I.

The decision was made to keep the same original gene targets of *chuA*, *yjaA*, and *TspE4.C2* and similar PCR product fragment sizes while creating improvements to the original triplex PCR method of Clermont and colleagues. These targets are well-known to the *E. coli* research community. To avoid polymorphisms in the nucleotide sequence used for primer annealing and to prevent amplification of *TspE4.C2* and *chuA* in strains belonging to cryptic clades I and III, IV and V respectively, the new genomic data were used to modify the *chuA*, *yjaA* and *TspE4.C2* primer sequences. A fourth gene target, *arpA* was added, turning the new technique into a quadruplex PCR. The insertion of *arpA* accomplishes two objectives. The quadruplex PCR is expected to produce at least one PCR product from all *E. coli* and clade I strains, therefore its incorporation serves as an internal control for DNA quality. Second, the presence of *arpA* allows strains from phylo-group E (*chuA*⁺, *yjaA*⁻, *TspE4.C2*⁻), which were previously mistaken for strains from phylo-group D, to be recognized. *arpA* is present in all strains of *E. coli*, with the exception of those from phylo-groups B2 and F. Along with, *Escherichia fergusonii* and *Escherichia albertii*,

cryptic clades II, III, and IV, and V also lack *arpA*. Two more allele-specific PCR primer pairs were created to identify isolates that belonged to phylo-groups C and E [21].

Quadruplex genotype				Phylo-group	Next step
<i>arpA</i> (400 bp)	<i>chuA</i> (288 bp)	<i>yjaA</i> (211 bp)	TspE4.C2 (152 bp)		
+	–	–	–	A	
+	–	–	+	B1	
–	+	–	–	F	
–	+	+	–	B2	
–	+	+	+	B2	
–	+	–	+	B2	
+	–	+	–	A or C	Could be confirmed by testing <i>ibeA</i> gene ^a
+	+	–	–	D or E	Screen using C-specific primers. If C+ then C, else A
+	+	–	–	D or E	Screen using E-specific primers. If E+ then E, else D
+	+	–	+	D or E	Screen using E-specific primers. If E+ then E, else D
+	+	+	–	E or clade I	Screen using E-specific primers. If E– then clade I, confirm using cryptic clade primers ^b
–	–	+	–	Clade I or II	Confirm using cryptic clade primers ^b
–	(476) ^c	–	–	Clade III, IV or V	Confirm using cryptic clade primers ^b
–	–	–	+	Unknown	Perform MLST
–	–	+	+	Unknown	Perform MLST
+	–	+	+	Unknown	Perform MLST
+	+	+	+	Unknown	Perform MLST
–	–	–	–	Unknown	Confirm <i>Escherichia</i> identification using <i>uidA</i> or <i>gadA/B</i> ^d , if positive screen using cryptic clade primers ^b and/or perform MLST

a. Gordon and colleagues (2008).
b. Clermont and colleagues (2011b).
c. The quadruplex PCR reaction will result in strains belonging to cryptic clade III, IV or V yielding a 476 bp PCR product. If this outcome eventuates then such strains should be screened using the cryptic clade detection primers (Clermont *et al.*, 2011b).
d. McDaniels and colleagues (1996).

Figure 4.1.: Quadruplex genotypes and steps required for assigning *E. coli* isolates to phylo-groups (Excerpted from Clermont et al., 2012) [21]

4.4.4.1. PCR protocol for phylogenetic analysis: The new quadruplex PCR assay described by Clermont et. al. [21] (Figure 4.1.) was used to assign the UPECs to one of the eight phylogenetic groups: A, B1, B2, C, D, E, F, and clade I. Each of the PCR assay was performed in 20 µl reaction volume containing 0.8 µl of total DNA as template, 0.8 µl of each primer (GCC Biotech, India), 2.0 µl 10X PCR buffer (Invitrogen, Thermo Fisher Scientific), 0.4 µl dNTP (Invitrogen, Thermo Fisher Scientific), 0.6 µl MgCl₂ (Invitrogen, Thermo Fisher Scientific), 0.1 µl of the Taq DNA polymerase (Invitrogen, Thermo Fisher Scientific), and 14.5 µl DDH₂O. Generated amplicons were separated by 1.5% agarose gel electrophoresis and visualized using EtBr by Gel documentation system (BioRad, USA). The primers and PCR conditions used for this study were shown Table 4.1.

Table 4.1. Primer sequences and PCR conditions for phylogenetic analysis used in this study.

Sl. No.	Genes	Primers (5' → 3')	PCR condition	No. of Cycles	Amplicon Size (bp)
1.	<i>chuA</i>	FP: GACGAACCAACGGTCAGGAT	95°C – 30"	30	279
		RP: TGCCGCCAGTACCAAAGACA	62°C – 30" 72°C – 30"		
2.	<i>yjaA</i>	FP: GCATGATGAAGGGAATCTCA			383

		RP: CCAGGACCGCACTATCACT	95°C – 30" 58°C – 30" 72°C – 30"		
3.	<i>TspE4.C2</i>	FP: CACTATTCGTAAGGTCATCCC RP: GTTTATCGCTGCGGGTCG	95°C – 30" 50°C – 30" 72°C – 30"		151
4.	<i>arpA</i>	FP: AACGCTATTCGCCAGCTTGC RP: TCTCCCCATACCGTACGCTA	95°C – 30" 50°C – 30" 72°C – 1'		400
5.	<i>arpA. gpE</i> (Gr. E)	FP: GATGCCATCTTGTCAAAATATGC RP: GAAAAGAAAAAGAATTTCCAAGA	95°C – 30" 53°C – 30" 72°C – 1'		301
6.	<i>trpA</i> (Gr. C)	FP: AGTTTTATGCCAGTGCGAG RP: TCTGCGCCGGTCACGCCC	95°C – 30" 58°C – 30" 72°C – 1'		219
7.	<i>trpA</i> (int. control)	FP: CGGCGATAAAGACATCTTCAC RP: GCAACGCGGCCTGGCGGAAG	95°C – 30" 60°C – 30" 72°C – 1'		489

4.4.4.2. Target genes for Phylogenetic analysis of *E. coli*. Respective forward and Reverse primer sequences (5' → 3') are marked in green.

chuA

>U67920.1:721-1020 Escherichia coli ChuA gene, complete cds
TCTGGATGGTACCGGACGAACCAACGGTCAGGATGTAAATATGCGTGGCTATGATCATCGCGGCGTGCTG
GTTCTTGTGCGATGGTGTTCGTCAGGGAACGGATACCGGACACCTGAATGGCACTTTTCTCGATCCGGCGC
TGATCAAGCGTGTGAGATTGTTTCGTGGACCTTCAGCATTACTGTATGGCAGTGGCGCGCTGGGTGGAGT
GATCTCCTACGATACGGTCGATGCAAAAGATTTATTGCAGGAAGGACAAAGCAGTGGTTTTCTGTGTCTTT
GGTACTGGCGGCAACGGGGGA

yjaA

>CP000243.1:4461421-4461840 Escherichia coli UTI89, complete genome
TTTTGCATATCAATTATTTGCATGATGAAGGGAATCTCATGTGTCAGTTCTGTATATCCAAATTCGTCGTAA
TCAAATTACTGTTTCGCGATCTTGAAAGCAAACGTGAAGTGTGAGGAGATGCTGCCTTCAGTAACCAGCGC
CTGTTAATCGCCAATTTCTTTGTTGCAGAAAAAGTTCTGCAAGATCTTGTTCTGCAACTCCACCCACGTT
CAACCTGGCATTCTTTTTTGGCAGCAAAACGTATGGATATTGTTGTGAGCGCGCTGGAAATGAATGAGGG
CGGTTTGTGACAGGTTGAGGAACGCATTCTTCATGAAGTGGTTCGAGGGGCAACGTTAATGAAATATCGC
CAGTTCACATCCATGCGCAATCAGTGGTACTCAGTGATAGTGGGTCTGGCAATGTTTAAGCAGAAAT

TspE4.C2

>CP000243.1:4358633-4358842 Escherichia coli UTI89, complete genome
AGTAATGTCGGGGCATTACGCGGTGACACTATTCGTAAGGTCATCCCTTCAAGTTCGATAGTCTGAATAT
CTACCCGCGTTTCTGTCTCACCCGCAAGGACAGCGCTGGCGATATAGCCCTCTCTGCGCTGCGTAATACT
TTGTTGGCGCGATGAGGGGCGACCCGCGAGCGATAAACCTCTTCGACTAACTCTGCAATTCCTTTTTCCAGT

arpA

>CU928163.2:4708538-4708954 Escherichia coli UMN026 chromosome, complete
genome
TACGGTAACGCTATTCGCCAGCTTGCCTGCTAACATTTTCCCTGGCGACATGCTGTTTTAAAACTTCG
GTGTACCCGTCACGGGCGTGTGGTGTTTTATGATTACGATGAAATTTGCTACATGACGGAAGTGAACCT
CCGCGACATCCCGCCGCGCGCTACCCGAGGACGAACCTTGCCAGCGAACCCTGGTACAGCGTCTCGCCG
GGCGATGTTTTCCCGGAAGAGTTTCGCCACTGGCTATGCGCTGACCCCGCATTTGGGCCACTCTTTGAAG
AGATGCACGCCGACCTGTTCCGCGCTGATTACTGGCGCGCGCTACAAAACCGTATCCGTGACGGGCATGT
GGAAGATGTTTATGCGTATCGGCGCAGGCAAAGATTAGCGTACGGTATGGGGAGATGCTTTTTTTGA

arpA. gpE

>CU928163.2:4710423-4710782 Escherichia coli UMN026 chromosome, complete genome

TGATGCCATCTTGTCAAAATATGC TTTTCATAACTAGCCCGAAATCACCGCAGGCAGCAACGCAACGCCCC
TCAGGACGGCTGGAAATCAACGCCAAAGTCTGGTTTTTGCATTTTTTGTGGAAGTGAGTGAGAAATTTTT
CAACTGAAGAGTAATCATCTTTATGAGGTTTGTAGTCAACATTCTGATAAATATCATTAAATATATTGTGC
AGCAATGTGTGCGCATACTATACGGTTTTTGGGGTCGCCCCGAAAATAACATTGACCATTAAAGTTTAAT
CTTGGAATTCTTTTTCTTTTC TATCTGATTTTAGATTTAATTTTTTGTGTTATCAAGAGCGTCTGAGCGTT
GAGGTAAAT

trpA. grpC

>CU928163.2:c1568785-1568479 Escherichia coli UMN026 chromosome, complete genome

AAGCACCCGACCATTCCCATCGGCCTTTTGTATGTATGCCAACCTGGTGTGTTAGCAAAGGCATTGATGAGT
TTTATGCCCAGTGCAGAGAAAGTCGGCGTCGATTTCGGTGCTGGTTGCCGATGTGCCAGTGGAAGAGTCCGC
TCCCTTCCGCCAGGCCGCGTTGCGTCATAATGTGCGACCTATCTTTATTTGCCGCCGAATGCCGACGAT
GATTTGCTGCGCCAGATAGCCTCCTACGGTCGTGGATACACCTATTTATTGTACGTGC GGGCGTGACCG
GCGCAGAAACCGCGCCGCGTTACCCC

trpA. internal control

>CU928163.2:c1569125-1568607 Escherichia coli UMN026 chromosome, complete genome

ACCTTTCCGGTCGCGGCGATAAAGACATCTTCAC CGTTCACGATATTTTGAAAGCACGAGGGGAAATCTG
ATGGAACGCTACGAATCTCTGTTTGCCAGTTGAAGGAGCGCAAAGAAGGCGCATTCGTTCCCTTTCGTCA
CGCTCGGTGATCCGGGCATTGAGCAGTCGCTGAAAATTATCGACACGCTAATTGAAGCCGGTGCTGACGC
GCTGGAGTTAGGTATCCCCTTCTCCGACCCACTGGCGGATGGCCCGACGATTCAAACGCCACACTGCGT
GCCTTTGCGGCAGGTGTGACCCCGGCACAGTGCTTTGAGATGCTGGCACTGATTCGCCAGAAGCACCCGA
CCATTCCCATCGGCCTTTTGTATGTATGCCAACCTGGTGTGTTAGCAAAGGCATTGATGAGTTTTATGCCCA
GTGCGAGAAAGTCGGCGTCGATTTCGGTGCTGGTTGCCGATGTGCCAGTGGAAGAGTCCGCTCC CTTCCGC
CAGGCCGCGTTGCGTCATAATGTGCGACC

4.4.5. Virulence factor genotyping: All imipenem-resistant UPECp and UPECnp were subjected to examine by individual PCR based assay for presence of the following twenty-one virulence factor genes: *fimH*, *papC*, *papEF*, *papGI*, *papGII*, *papGIII*, *sfaA*, *afaA*, *hlyA*, *iroN*, *chuA*, *kpsmtII*, *iha*, *iucD*, *cdtB*, *cnfI*, *vat*, *ibeA*, *flu*, *csgA*, and *usp*.

4.4.5.1. ***fimH***: briefly discussed in 1.8.1.1. in Chapter 1.

4.4.5.2. ***papC***: briefly discussed in 1.8.1.2. in Chapter 2.

4.4.5.3. ***papEF***: part of the *pap* operon. Located in upstream of *papG*. N-terminal extension of PapF is required to adapt the PapG adhesin to the tip of the fiber. The pilin body of PapF is required to efficiently initiate assembly of the remainder of the pilus, with the assistance of the N-terminal extension [22].

4.4.5.4. ***papGI***: Variant of PapG. PapG is a 35kDa protein located at the distal end of the fibrillum, is joined to the tip fibrillum via a specialized adaptor protein named PapF. The tip fibrillum is

joined to the fimbrial rod by specialized adaptor protein PapK. The fimbrial determinant responsible for Gal α (1 \rightarrow 4) Gal-specific binding mediated by P fimbriae is PapG [23].

4.4.5.5. ***papGII***: see section 4.4.5.4.

4.4.5.6. ***papGIII***: see section 4.4.5.4.

4.4.5.7. ***sfaA***: S fimbrial adhesins (Sfa) interact with α -sialyl-(2-3)- β -D-galactose-containing receptor molecules. They are associated with UTI strains and, to a larger extent, newborn meningitis with *E. coli* isolates. The genetic determinant coding for Sfa has been cloned from the chromosome of a uropathogenic *E. coli* O6 strain. Recently, the S adhesin molecule, a protein of 12 kDa, was isolated and characterized, and the sequence of the *sfaA* gene, coding for the S fimbrial protein subunit, was determined. The *sfa* determinants from different strains have high sequence homology [24].

4.4.5.8. ***afaA***: The *afa* gene clusters encode afimbrial adhesins (Afas) that are expressed by uropathogenic and diarrhea-associated *E. coli* strains. These gene clusters are responsible for the biosynthesis of the Afa adhesins belonging to the Afa/Dr family of adhesins and for the biosynthesis of invasins. The genetic organization of the 6.7-kb DNA fragment encoding Afa adhesin involved five genes, *afaA*, *afaE*, *afaD*, *afaB*, and *afaC*. These five genes have been localized and shown to belong the same transcription unit. The AfaB, AfaC, and AfaE gene products are required for mannose-resistant hemagglutination (MRHA) [25].

4.4.5.9. ***hlyA***: briefly discussed in 1.8.2.1. in Chapter 1.

4.4.5.10. ***iroN***: *iroN* gene was identified by virtue of having increased expression in human urine, ascites and blood. IroN expression was shown to be Fe regulated, and a homology search based out on peptide sequences suggested that IroN was a siderophore receptor. Molecular epidemiologic evidence from several studies has demonstrated an increased prevalence of *iroN* among UTI isolates relative to fecal isolates. Taken together, this evidence suggests that IroN functions as a siderophore receptor and is a virulence factor, at least for UTI [26].

4.4.5.11. ***chuA***: In *E. coli* O157:H7 the gene *chuA*, which codes for a 69-kDa outer membrane protein responsible for heme uptake, was identified. The gene is part of a larger locus, termed the heme transport locus, which appears to be widely distributed among pathogenic *E. coli* strains.

This locus contains eight ORFs and is located at 78.7 min of the *E. coli* K-12 chromosome. The ability to use heme and/or hemoglobin might be especially advantageous to pathogenic bacteria. These pathogens often secrete cytotoxins, which gain access to the intracellular heme reservoir besides initiating tissue invasion. Cytotoxin production coupled with the capability to utilize heme and/or hemoglobin could serve as an effective iron acquisition strategy during the progression of infection [27].

4.4.5.12. ***kpsMTII***: *kpsMTII* gene is part of K1 capsule gene cluster. K1 capsule was found to be essential for the formation of IBCs, a key stage in the pathogenesis of UTI. Following growth in urine, strain UTI89 exhibited phase variable K1 capsule expression with the un-encapsulated bacteria being the initial colonizers of the bladder cells. Group 2 capsule gene clusters are composed of three regions. Region 1 and region 3, are conserved among all group 2 capsule gene clusters and encode proteins for polysaccharide export. Region 2, is serotype-specific and encodes proteins for the synthesis of each particular polysaccharide and its precursors. Region 1 contains six genes (*kpsFEDUCS*) organized in a single transcript that generates 8.0-kb polycistronic mRNA, which is processed to yield 1.3-kb *kpsS* specific transcript by an unknown mechanism. Region 3 contains two genes (*kpsMT*) organized in a single transcriptional unit, encoding for the KpsMT ATP binding cassette transporter for the export of polysaccharide across the cytoplasmic membrane [28].

4.4.5.13. ***iha***: *iha* encodes the IrgA homologue adhesin (Iha), an outer membrane protein (OMP) first characterized in *E. coli* O157:H7, which confers adherence to nonadherent laboratory strains. Iha occurs frequently among UPEC strains. Its designation is derived from the similarity of Iha to IrgA. Iha represents a Fur-regulated catecholate siderophore receptor that, uniquely, exhibits an adherence-enhancing phenotype and is the first described urovirulence factor identified in a clonal group A strain [29].

4.4.5.14. ***iucD***: *iucD* gene is a component of the aerobactin operon, and was the most prevalent gene, mostly detected simultaneously with adhesins and NTEC toxin genes. The product of *iucD* is of special interest for two reasons. First, it catalyzes a unique type of enzymatic reaction which does not occur in animal tissues, namely, the N^6 – oxygenation of lysine. Secondly, *iucD* mediates the first step of aerobactin biosynthesis, and hence effective inhibitors of its activity may have therapeutic value [30].

4.4.5.15. ***cdtB***: briefly discussed in 1.8.2.4. in Chapter 1.

4.4.5.16. ***cnfI***: briefly discussed in 1.8.2.2. in Chapter 1.

4.4.5.17. ***vat***: Vacuolating autotransporter toxin (Vat) is a member of serine protease autotransporter proteins of Enterobacteriaceae (SPATEs) present in some UPEC strains. Vat has been identified in 20 -36% of UPEC is present in almost 68% of urosepsis isolates. Vat included cellular damage, vacuole formation, and urothelial barrier dysregulation of bladder epithelial cells [31].

4.4.5.18. ***ibeA***: The *ibeA* gene encodes a 50-kDA protein that participates in *E. coli* penetration in the microvascular endothelial cells of the human brain, allowing *E. coli* to cross the blood-brain barrier. This virulence factor has an important role in neonatal meningitis. IbeA may also be essential for the invasion of intestinal epithelial cells and macrophages. The *ibeA*-positive *E. coli* were detected among adherent-invasive *E. coli* isolates from pediatric Crohn's disease patients, bacteremic *E. coli* isolates that translocated from the gastrointestinal tract and avian pathogenic *E. coli* isolates. It has been reported that *E. coli* in the gut can flood into bile duct causing acute biliary tract infection, and *ibeA*-positive *E. coli* strains showed increased oxidative stress (H₂O₂) resistance and persistence in macrophage [32].

4.4.5.19. ***flu***: Many *E. coli* strains have the ability to autoaggregate, observed as characteristic flocculation and settling of cells from liquid cultures. This phenomenon was reported first by Diderichsen who also defined a locus, flu, mapping at 43 min on *E. coli* K-12. The flu locus appeared to control several surface properties. A number of strains exhibited two distinct but interconverting forms. Form 1 was characterized by large, flat, frizzy and irregular colonies and was able to aggregate in static liquid medium. The other form gave rise to smaller, glossy colonies and did not autoaggregate in static liquid medium [33].

4.4.5.20. ***csgA***: Curli formation involves a complex machinery that is encoded by the divergently transcribed *csgBA* and *csgDEFG* operon. Curli fibers consist of two subunits: CsgA, which constitutes the major portion of the fiber, and CsgB, the minor component. Both CsgA and CsgB are secreted proteins with similar molecular weights of ~13kDa, and their interaction triggers wild type curli formation in bacteria. The *csgA* gene product is a soluble, unstructured protein that

requires the presence of CsgB to assemble into fibers in vivo. In the absence of CsgB, CsgA is secreted from the cell as monomers, and no fibrils are formed [34].

4.4.5.21. **usp:** It has been established that *E. coli* uropathogenic-specific protein (Usp) is associated with *E. coli* strains that cause pyelonephritis, prostatitis, and bacteremia, as well as to their higher virulence and fitness. The Usp N-terminal region is similar to the Type VI protein secretion system component (Hcp like), while the Usp C-terminal region shares around 45% sequence identity with the *E. coli* bacteriocin colicin E7 which possess nuclease activity. It has been proposed that Usp boosts infectivity in the urinary system and functions as a bacteriocin against rival *E. coli* strains [35].

4.4.5.22. **Identification of virulence genes:** Virulence genes *fimH*, *papC*, *papEF*, *papGI*, *papGII*, *papGIII*, *sfaA*, *afaA*, *hlyA*, *iroN*, *chuA*, *kpsMTII*, *iha*, *iucD*, *cdtB*, *cnfI*, *vat*, *ibeA*, *flu*, *csgA*, and *usp* were detected using gene-specific primers using PCR. Separate PCR reactions for each genes were carried using plasmid DNA as template. PCR assays were performed in 20 µl reaction volume, containing 0.8 µl (10ng) of plasmid DNA, 0.8 µl of each primer, 2 µl 10X buffer, 0.3 µl dNTP, 0.6 µl MgCl₂, 0.1 µl Taq DNA polymerase (Invitrogen), and 14.6 µl of DDH₂O. The primers and conditions of genes were given table 4.2. The primer sequences of the target genes are depicted in section 4.4.5.23. and primers are marked in green. Generated amplicons were separated by 1.5% agarose gel electrophoresis and visualized using Ethidium Bromide by Gel Documentation system (Bio-Rad, USA).

Table 4.2. Primer sequences and PCR conditions for virulence gene analysis used in this study.

Sl. No.	Genes	Primers (5' → 3')	PCR condition	No. of Cycles	Amplicon Size (bp)		
1.	<i>fimH</i>	FP: TGCAGAACGGATAAGCCGTGG	95°C – 30'' 63°C – 30'' 72°C – 1'	30	506		
		RP: GCAGTCACCTGCCCTCCGGTA					
2.	<i>papC</i>	FP: GACGGCTGTACTGCAGGGTGTGGCG					328
		RP: ATATCCTTTCTGCAGGGATGCAATA					
3.	<i>papEF</i>	FP: GCAACAGCAACGCTGGTTGCATCAT	95°C – 30'' 55°C – 30'' 72°C – 1'		336		
		RP: AGAGAGAGCCACTCTTATACGGACA					
4.	<i>papGI</i>	FP: CAACCTGCTCTCAATCTTTACTC	95°C – 30'' 50°C – 30'' 72°C – 1'		692		
		RP: CATGGCTGGTTGTTCTTAAACAT					
5.	<i>papG II</i>	FP: GGAATGTGGTGATTACTCAAAGC					562
		RP: TCCACAGACTGTTCAAGAAGGAC					
6.	<i>papG III</i>	FP: CATGGCTGGTTGTTCTTAAACAT			421		

		RP: TCCAGAGACTGTGCAGAAGGAC			
7.	<i>sfaA</i>	FP: CGGAGAACTGGGTGCATCTTAC RP: CGGAGGAGTAATTACAAACCTG	95°C – 15'' 63°C – 15'' 72°C – 45''		407
8.	<i>afaA</i>	FP: GGCAGAGGGCCGGCAACA RP: CCCGTAACGCGCCAGCATC			559
9.	<i>hlyA</i>	FP: AACAAGGATAAGCACTGTTCTGG RP: ACCATATAAGCGGTCATTCCCGTCA	95°C – 30'' 60°C – 30'' 72°C – 1'30''		1177
10.	<i>iroN</i>	FP: AAGTCAAAGCAGGGGTTGCC RP: GACGCCGACATTAAGACGCAG	95°C – 15'' 66°C – 15'' 72°C – 2'		668
11.	<i>chuA</i>	FP: GACGAACCAACGGTCAGGAT RP: TGCCGCCAGTACCAAAGACA	95°C – 30'' 62°C – 30'' 72°C – 30''		279
12.	<i>KPS MTII</i>	FP: GCGCATTGTGCTGATACTG RP: CATCAGACGATAAGCATGAG	95°C – 30'' 55°C – 30'' 72°C – 1'		291
13.	<i>iha</i>	FP: TGGCGGAGGCTCTGAGAT RP: TTAAGCTCCCGCGGCTGA	95°C – 30'' 62°C – 1' 72°C – 1'		823
14.	<i>iucD</i>	FP: TACCGGATTGTCATATGCAGACCGT RP: AATATCTTCCTCCAGTCCGGAGAAG	95°C – 30'' 50°C – 30'' 72°C – 1'		602
15.	<i>cdtBU</i>	FP: GCAACCTGGAATTTGCAGG RP: GATCAGAGGCAATTTGCCCTC			706
16.	<i>cnfI</i>	FP: AAGATGGAGTTTCCTATGCAG RP: TCAGAGTCCTGCCCTCATTAT			498
17.	<i>vat</i>	FP: CAGCTTTGGTTCGCTCGTG RP: GATTCAGGGCGGTACTGGTC	95°C – 30'' 52°C – 30'' 72°C – 1'		353
18.	<i>ibeA</i>	FP: GTATTGCCGCAGCAATGAGTG RP: CATCAACGGCGGTAATGTGTAG	95°C – 30'' 50°C – 30'' 72°C – 1'		309
19.	<i>flu</i>	FP: ATGAAACGACATCTGAATAC RP: CTTATCATTAATGACGGTTC			516
20.	<i>csgA</i>	FP: GGTGTTGTTCCCTCAGTACG RP: TAGTACTGATGAGCGGTCG			395
21.	<i>usp</i>	FP: ATGCTACTGTTTCCGGGTAGTGTGT RP: CATCATGTAGTCGGGGCGTAACA	95°C – 30'' 62°C – 30'' 72°C – 1'30''		1021

4.4.5.23. Target genes for virulence factors determination. Respective forward and Reverse primer sequences (5' → 3') are marked in green.

fimH

>NC_007946.1:4913899-4914413 Escherichia coli UTI89, complete sequence
TTATAAT **TCGAGAACGGATAAGCCGTGG** CCGGTGGCGCTTTATTTGACGCCGGTGAGCAGTGCGGGGGA
GTGGCGATTAAAGCTGGCTCATTAATTGCCGTGCTTATTTTGCACAGACCAACAACATAACAGCGATG
ATTTCCAGTTTGTGTGGAATATTTACGCCAATAATGATGTGGTGGTGCCCACTGGCGGCTGCGATGTTTC
TGCTCGTGATGTCACCGTTACTCTGCCGGAACCTGTTTCAGTGCCGATTCTCTTACCGTTTATTGT
GCGAAAAGCCAAAACCTGGGGTATTACCTCTCCGGCACAACCGCAGATGCGGGCAACTCGATTTTACCA
ATACCGCGTCGTTTTACCCGCGCAGGGCGTCGGCGTACAGTTGACGCGCAACGGTACGATTATTCCAGC
GAATAACACGGTATCGTTAGGAGCAGTAGGGACTTCGGCGGTAAGTCTGGGATTAACGGCAAATTACGCA
CG **TACCGGAGGGCAGGTGACTGC**AG

papC

>X61239.1:4643-4980 E.coli papABCDEFGHJK genes for F13 P-pili proteins

ATGTCTGACGGCTGTACTGCAGGGTGTGGCGTTGGATTGTCAGCCTCAAGGTCTAAATATCTGGGGCGT
 GATAACGATTCTGCTTACCTGCGTATATCCGTGCCGCTGGGGACGGGGACAGCGAGCTACAGTGGCAGTA
 TGAGTAATGACCGTTATGTGAATATGGCCGGCTACACTGACACGTTCAATGACGGTCTGGACAGCTACAG
 CCTGAACGCCGGCCTTAACAGTGGCGGTGGACTGACATCGCAACGTCAGATTAATGCCTATTACAGTCAT
 CGTAGTCCGCTGGCAAATTTGTCCGCGAAATTATGTCATCCCTGCAGAAAGGATATACGT

papEF

>X61239.1:8016-8365 E.coli papABCDEFHIJK genes for F13 P-pili proteins
 CCTTTCTCTGCAACAGCAACGCTGGTTGCATCATATTTCGTAATAGTATCAACTAAAATACGTTAATTTTA
 TATCTCGTAAATAAAATGTTTTCTGTACCGCTCTCCGGAGGGGGAATGATTTCGTTTATCATTATTTATA
 TCGTTGCTTCTGACATCGGTGCTGTACTGGCTGATGTGCAGATTAACATCAGGGGGAATGTTTATATCC
 CCCCATGCACCATTAATAACGGGCAGAATATTGTTGTTGATTTTGGGAATATTAATCCTGAGCACGTGGA
 CAACTCACGTGGTGAAGTCACAAAACCATAAGCATATCTGTCCGTATAAGAGTGGCTCTCTCTGGATA

papGI

>M20146.1:c2159-1452 E.coli papE, papF, and papG genes, complete cds, isolate J96

TACAACCTGCTCTCAATCTTTACTGTTTTTGAGCCGGCTGTGTACCAGCGTAATATTTCTCACTCTGTT
 CAACCCCATCAAGAGATATTATCGAATCCCAGCCATTACCTAACCCAACCGAAAATTTATTATTATTGTA
 TATTGGTGGTGTATTTCTGAGCAGAGATATTTTACACTAAGTGTACATCGCAATAAATGAAAGCGTC
 TGACTTGCAATATTTCCGTTAGCAGCATCAATCACAATACTCCCATGGTCTATATTAAGTACTTGTGTTG
 ACGGCTGGCATCCCCAACATTATCGAATGATAACATCAATGTATTAGTGGCAGGTAGCTGCTTAATCTG
 ATCGTAAGGCATTTTATAATGATCCTGCCAGAGATCATAGTAATGGTGCTGTATTCCACGTATATATCTC
 ACAGGAAAATTATAATGTCCCTTGGGGAGATCTACTGGCAAAGAACCCTGAATACTAAATCATTAAATT
 TATTGTTCAACTGCTTCATATTTCCAGGATAGAAACATATACGGGCACCATTATTTGTCCATGTATCCCA
 TTCATAACCATTAAACAAAGAAGTAAAAATCTTTGTCATTTTCATTCTCCATAGACCAACCATATTTGCTC
 TGAACATCAAGAAATATATTAAACCCCTCATTAGTATAGACATGTTTAGGAACAACCATCCAGGCCAGAT
 ACTCCTGA

papGII

>M20181.1:1332-1910 E.coli papE, papF, and papG genes, complete cds, isolate IA2

GGGAGGGAATGTGGTGATTACTCAAAGGCCACAATTTATAACTTCGTGGCGCCCGGGCATTGCTACGGTA
 ACCTGGAATCAGTGTAATGGTCCTGAGTTCGCTGATGGCTCCTGGGCTTACTACAGGGAGTATATTGCGT
 GGGTAGTATTTCCCCAAAAGGTTATGACCCAAAATGGATATCCCTTATTTATTGAGGTTTCATAATAAAGG
 TAGCTGGAGTGAGGAGAATACTGGTGACAATGACAGCTATTTTTTTCTCAAGGGGTATAAGTGGGATGAG
 CGGGCCTTTGATGCAGGTAATTTGTGTGAGAAACCAGGAGAAACAACCTCGTCTGACTGAGAAATTTGACG
 ATATTATTTTTTAAAGTCGCCTTACCTGCAGATCTTCCTTTAGGGGATTATTCTGTTACAATTCATACAC
 TTCCGGCATAACAGCGTCATTTTCGCGAGTTACTTGGGGGCGCGTTTAAATCCCATAACAATGTGGCCAAA
 ACCCTCCCAAGAGAGAATGAAATGTTATTCTTATTTAAGAATATCGGCGGATGCCGTCCTTCTTGAACAG
 TCTGTGGAAATAAAGCATGG

papGIII

>AY212281.1:240-672 Escherichia coli strain APEC 14 PapGIII (papGIII) gene, complete cds

GTATTTTGATGGCTGGTTGTTCTTAAACGTTTTCCTATAATGGATATGATATATATCTTGAACCTTCAG
 TCCAGAGGAAGTTTTTCACTTGATGCAGAAGATAATGATAATTACTATCTTACCAAGGGATTTCATGGG
 ATGAAGCAAACACATCTGGACGGACATGTTTCAATATCGGAGAAAAAGAAGTCTGGCATGGTCATTTGG
 TGGTGTTACCCTGAACGCCAGATTTCTGTTGACCTTCCTGAGGGGGATTATACGTTTCCAGTTAAGTTC
 TTACGTGGCATTTCAGCATAATAATTATGATTATATTGGTGGACGCTACAAAATTCCTTCTCTCGTTAATGA
 AAACATTTCTTTTAAATGGTACATTGAATTTCTCAATTAAGAATACCGGAGTATGCCGTCCTTCTGCACA
 GTCTCTGGAATA

sfaA

>X16664.4:17980-18399 Escherichia coli encoding determinant sfa(I)
 ATCAGCCTCGGAGAAGTGGGTGCATCTTACCCGCGAGATATGAACTGCATATGCAGGCGAGGTATAA
 GGCCACACATTATCCCGTCGCCGGGGGAAAGGCAAATGGACAGGTATGGTTTTCTCTGACCTATCTGTAA
 CTGGCAGATATAATGCCATTTAATTAAGGCTGTTAATAACATGATGAAGCACATGCGTATATGGGCCGTT
 CTGGCATCATTTTTAGTCTTTTTTTATATTCCGCAGAGCTATGCCGGGGTTGCTCTGGGTGCCACCCGTG
 TGATTTACCCTGAAGGGCAAAAACAGGTACAACCTGGCGGTAACAAATAATGATGATAAAGTAGTTACCT

TATTCAGTCATGGATTGAAAATGCTGAAGGAAAAAAGGATGC CAGGTTTGTAATTACTCCTCCG TTATTT

afaA

>X76688.1:4586-5184 E.coli afaF, afaA, afaB, afaC, afaD, afaE-3, int and rep genes

AGT GGCAGAGGGGCCGGCAACA GGCTGAAGGGGGTTAACCCGACGCCGTTTTACATCAACCTGTCCACGCT
GACGGTGGGGGGTAAGGAAGTGAAGGAGCGTGAATATATTGCGCCGTTTTCTCCCGTGAATATCCGCTG
CCTGCGGGGCATCGGGTAAGGTTTCAAGTGAAGGTGATAACGGATTACGGCGGGACCAGTAAGCAGTTTGA
GGCAGAGCTGAAGGGTTGAATACATAAGGTGATAACAGGGTAAATGACGGGCTGACAGATGCGTGATACT
TCTTCAGGGCGGATGAGAACGGGGGTGACAGGGCTGGCGCTGGCTGTGATGGTGGCCTGTGTGATGTTTC
GTGCGGAGAGTGGTATTGCGCGCACCTACTCCTTTGATGCGGCCATGCTGAAAGGTGGCGGGAAGGGGGT
GGACCTGACCCTGTTTGAGGAAGGTGGGCAGTTACCCGGCATTATCCGGTTGACATTATCCTGAATGGT
TCCCGTGTGGATTACAGGAGATGGCCTTTACGCGGAGAGGGACGCGGAGGGCAGGCCTTATCTGAAGA
CCTGTCTGACCCGTGA GATGCTGGCGCGTTACGGG GTCA

hlyA

>CP009072.1:c1763809-1762631 Escherichia coli ATCC 25922, complete genome

GTT AACAACGATAAGCACTGTTCTGG CTTCACTATCTTCAGGTATTAGTGCTGCTGCAACGACATCTCTG
GTTGGTGCACCGGTAAGCGCGCTGGTAGGGGCTGTTACGGGGATAATTTACGGCATCCTTGAGGCTTCAA
AACAGGCAATGTTTGAACATGTCGCCAGTAAATGGCCGATGTTATTGCTGAATGGGAGAAAAAACACGG
CAAAAATTACTTTGAAAATGGATATGATGCCGCCATGCTGCATTTTTAGAAAGATAACTTTAAATATTA
TCTCAGTATAATAAAGAGTATTCTGTTGAAAGATCAGTCCTCATTACCCAGCAACATTGGGATACGCTGA
TAGGTGAGTTAGCGGTGTCACCAGAAATGGAGACAAAACACTCAGTGGTAAAAGTTATATTGACTATTA
TGAAGAAGGAAAACGTCTGGAGAAAAACCGGATGAATTCCAGAAGCAAGTCTTTGACCCATTGAAAGGA
AATATTGACCTTTCTGACAGCAATCTTCTACGTTATTGAAATTTGTTACGCCATTGTTAACTCCCGGTG
AGGAAATTCGTGAAAGGAGGCAGTCCGGAATATGAATATATTACCGAGTTATTAGTCAAGGGTGTGTA
TAAATGGACGGTGAAGGGGGTTTCAAGACAAGGGGTCTGTATATGATTACTCTAACCTGATTACAGCATGCA
TCAGTCGGTAATAACAGTATCGGGAAATTCGTATTGAGTCACACCTGGGAGACGGGGATGATAAGGTCT
TTTTATCTGCCGGCTCAGCCAATATCTACGCAGGTAAAGGACATGATGTTGTTTATTATGATAAAACAGA
CACCGGTTATCTGACCATTGATGGCACAAAAGCAACCGAAGCGGGTAATTACACGGTAACACGTGTACTT
GGTGGTGTGTTAAGATTTTACAGGAAGTTGTGAAGGAGCAGGAGGTTTCAAGTTGGAAAAAGAACTGAAA
AAACGCAATATCGGAGTTATGAATTCATCATATCAATGGTAAAAATTTAACAGAGACTGATAACTTATA
TTCCGTGGAAGAACTTATTGGGACCACGCGTCCGACAAGTTTTTTGGCAGTAAATTTACTGATATCTTC
CATGGCGCGGATGGTGTGATGACCATATAGAAGGAAA TGATGGGAATGACCGCTTATATGG

iroN

>CP028770.1:c3116290-3115616 Escherichia coli strain A4 chromosome, complete genome

TCA AAGTCAAAGCAGGGGTTGCC CGAACCTTTAAAGCCCCAACCTGTATCAATCCAGTGAAGGCTATCT
GCTCTACTCGAAAGGCAATGGCTGTCCAAAAGATATTACATCAGGCGGGTGCTACCTGATCGGTAATAAA
GATCTCGATCCGGAATCAGCGTCAATAAAGAAATTGGACTGGAGTTACCTGGGAAGATTACCACGCAA
GTGTGACCTACTTCCGCAATGATTACCAGAATAAGATCGTGGCCGGGGATAACGTTATCGGGCAAACCGC
TTCAGGCGCATATATCCTCAAGTGGCAGAATGGCGGGAAAGCTCTGGTGGACGGTATCGAAGCCAGTATG
TCTTTCCCGCTGGTGAAGATCGTCTGAACTGGAATACCAATGCCACATGGATGATCACTTCGGAGCAAA
AAGACACCGGTAATCCTCTGTGCGTCATCCGAAATATACTATCAATAACTCGCTTAAGTGGACCATCAC
CCAGGCGTTTTCTGCCAGCGTCAACTGGACGTTATATGGCAGACAAAACCGGCTACTCATGCGGAAACC
CGCAGTGAAGATACTGGCGGTCTGTGAGGTAAAGAGCTGGGCGCTTATTCACTGGTGGGACGAACTTCA
ATTACGATATTAATAAAAAAT CTGCGTCTTAATGTGCGCGTCAGTA

chuA

>U67920.1:721-1020 Escherichia coli ChuA gene, complete cds

TCTGGATGGTACCG GACGAACCAACGGTCAGGAT GTAAATATGCGTGGCTATGATCATCGCGGCGTGCTG
GTTCTTGTGCGATGGTGTTCGTGAGGGAACGGATACCGGACACCTGAATGGCACTTTTCTCGATCCGGCGC
TGATCAAGCGTGTGAGATTGTTGCTGGACCTTCAGCATTACTGTATGGCAGTGGCGCGCTGGGTGGAGT
GATCTCCTACGATACGGTCGATGCAAAAGATTTATTGCAGGAAGGACAAAGCAGTGGTTTTCTG TGTCTTT
GGTACTGGCGGCA CGGGGGA

kps MTII

>X53819.1:294-568 E. coli kpsM and kpsT genes involved in polysaccharide transport

TCTGCGCATTGCTGATACTGTTGGGCATTTTTGGTTACATTATGCACCGCACGATGCCAGACATCTCAT
TCCCGGTGTTTTTACTTAATGGCCTGATTCCCTTTTTTATCTTTAGCAGTATCAGCAATCGTTCTGTAGG
CGCTATTGAAGCGAACCAGGGGTTGTTTAATTATCGACCAGTAAACCCATCGATACGATCATTGCACGC
GCACTGCTTGAGACGCTGATTTACGTTGCTGTTTATATATTGCTCATGCTTATCGTCTGGATGGC

iha

>DQ211582.1:335-1180 Escherichia coli strain UCB34 Iha (iha) gene, complete cds

GATCTGGCGGAGGCTCTGAGATCAGTAGAGGGTGTGGATGTTGAAAGTGGTACGGGTAAAACCGGTGGGC
TGGAAATCAGCATCCGAGGAATGCCAGCCAGTTACACGCTGATACTGATTGATGGTGTTTCGTAGGGCGG
AAGCAGTGACGTGACTCCCAACGGTTTTTCTGCCATGAATACCGGGTTCATGCCCCCTCTGGCCGCCATT
GAGCGTATTGAGGTTATCAGGGGGCCGATGTCCACACTGTATGGCTCTGATGCGATGGGCGGTGTGGTGA
ATATCATTACCAGAAAGAATGCAGACAAATGGCTCTCTTCCGTCAATGCAGGGCTGAATCTGCAGGAAAG
CAACAAATGGGGTAACAGCAGCCAGTTTAATTTCTGGAGCAGTGGTCCCCTTGTGGATGATTCTGTGACG
CTGCAGGTACGCGGTAGCACACAACAGCGTCAGGGCTCATCGGTCACATCACTGAGCGATACAGCAGCCA
CGCGTATTCTTATCCACGGAGTCACAGAATTATAATCTTGGTGCACGTCTTGACTGGAAGGCGTCGGA
GCAGGATGTGCTCTGGTTTGATATGGATAACCCCGGCAGCGTTATGATAACCGGGATGGGCAACTGGGG
AGTCTGACGGGGGATATGACCGGACCCTGCGCTATGAGCGAAACAAAATTTTCAGCTGGCTATGATCATA
CTTTACCTTCGGAACATGGAATCGTATCTGAACTGGAACGAGACAGAAAATAAAGGTCGTGAGCTCGT
ACGCAGTGTACTGAAGCGGACAAATGGGGCTTGCCGGTCAGCCGCGGGAGCTTAAAGGAATCGAACCTT
ATCCTG

iucD

>CP009072.1:1721622-1722231 Escherichia coli ATCC 25922, complete genome

TGGTACCGGATTGTCTATATGCAGACCGTCTTTCTGAAAGATCTGGTCAGTGCAGTTGCACCTACAAATCC
CTACAGCTTTGTTAACTATCTGGTGAAGCACAAAAAGTTCTATCGCTTCCTTACAAGCAGACTACGTACA
GTATCCCGTGAAGAGTTTTCTGACTATCTCCGCTGGGCTGCTGAAGATATGAATAACCTGTATTTTCAGTC
ATACCGTTGAAAATATTGATTTTCGACAAAAAAGTCGATTGTTTCTGGTTCAGACCAGTCGGGGAGAATA
TTTTGCCCGCAATATCTGCCTTGGTACAGGAAAACAACCTTATTTACCACCCTGTGTGAAGCATGTGACA
CAATCCTGTTTCCATGCCAGTGAATGAATCTTCGTGGCCGGACCTGAGTGGAAAACGGATAACTGTGG
TTGGTGGAGGACAGAGTGGTGCAGACCTGTTCTTAATGCATTACGCGGGGAATGGGGAGAAGCGGCGGA
AATAAAGTGGGTCTCACGGCGTAATAATTTTAACGCACTGGATGAGGCTGCTTTTGCTGATGAGTATTTT
ACACCTGAATATATTTTCAGGCTTCTCCGGACTGAAGGAAGATATTCGCCA

cdtB

>NC_017628.1:c2106685-2105973 Escherichia coli IHE3034, complete sequence

AGTTGCAACCTGGAATTTGCAGGGTCAAATGCACCGACAGAAAATAAATGGAACACACATGTCCGACAA
CTTGTTACGGGAAGTGGTGTGTTGATATCCTGATGGTTCAGGAGGCAGGGGCAGTACCAGCTTCTGCAA
CGTTGACTGAGCGAGAATTTAGCACTCCCGGTATTCCGATGAATGAGTATATCTGGAATACCGGAACCAA
TAGTCGTCCACAGGAGTTGTTTATATATTTCTCACGTGTTGATGCATTTCGCTAACAGAGTAAATCTTGCG
ATTGTTTCAAACAGAAGAGCTGATGAGGTGATTGTATTACCTCCTCCAAGTGTGTATCACGACCGATCA
TCGGCATTAGAATTGGTAATGATGTTTTCTTCTCAACCCATGCATTGGCGAATCGAGGCGTGGATTTCAGG
AGCAATTGTAAATAGTGTGTTTTGAGTTCTTCAACAGACAAACGGATCCTATAAGACAGGCCGCTAACTGG
ATGATTGCAGGAGATTTTAACCGTTACACGGCTACACTATTTTCAACTCTTGAACCAGGGATTTCGTAATC
ATGTAAATATTATTGCTCCACCAGATCCAACGCAAGCCAGTGGTGGTGTCTTGATTATGCGGTAGTTGG
AAATTCAGTGAGCTTTGTACTTCTCTGTTGAGGGCCTCGTTGTTATTCGATTATTAAAGAGGGCAAATT
GCCTCTGATCACT

cnf1

>U42629.1:1644-2160 Escherichia coli cytotoxic necrotizing factor 1 (cnf1) gene, complete cds

AGTCGTCAGATGGAGTTTCCTATGCAGGAGTAAATTCTGTTCTACATGCAATAGAAAATGATGGTAATT
TTAATGAGTCTTACTTTCTGTATTCCAATAAGACACTTAGCAATAAAGATGTTTTTGATGCTATAGCTAT
TTCTGTTAAGAAACGCAGTTTCAGTGATGGTGATATCGTTATAAAATCAAACAGTGAAGCTCAACGAGAC

TATGCTCTGACTATACTCCAGACGATTTTATCAATGACCCCTATATTTGATATCGTAGTCCCGGAGGTAT
 CTGTTCCGCTTGGACTGGGGATTATTACTTCCAGTATGGGGATCAGTTTTGATCAACTGATTAATGGTGA
 TACTTATGAAGAACGTCGTTCTGCTATACCTGGTTTGGCGACAAATGCAGTATTGCTTGGTCTGTCTTTT
 GCAATTCCACTCTTGATTAGTAAGGCAGGAATAAACCAGGAGGTACTTAGCAGCGTTATAAATAATGAGG
 GCAGGACTCTGAATGAAACAAATATCG

vat

>MH899682.1:5378-5743 Escherichia coli strain QT598 YkgJ (ykgJ), YagU (yagU),
 Vat-vacuolating autotransporter toxin (vat), VatX (vatX), and hypothetical
 protein genes, complete cds; tRNA-Thr gene, complete sequence; and ProA
 (proA) and ProB (proB) genes, complete cds

GACGTTGACGTTTGGTTTCGCTCGTCTTAAAAGATACAGACTTTGGTCTGGGCCGCAATGCCACACTGAAC
 ACCACCATCCAGGCAGATAACTCCAGCGTCACGCTGGGCGACAGTCGGGTATTTATCGACAAAAAGATG
 GCCAGGGAACAGCATTTACCCTTGAAGAAGGCACATCTGTTGCAACTAAAGATGCAGATAAAAGCGTCTT
 CAACGGCACCGTCAACCTGGATAATCAGTCAGTGCTGAATATCAATGAGATATTCAATGGCGGAATACAG
 GCGAACAACAGTACCGTGAATATCTCCTCAGACAGTGCCGTTCTGGAGAACTCAACGCTGACCAGTACCG
 CCCTGAATCTGAACAA

ibeA

>AY248744.1:120-435 Escherichia coli strain BEN 2908 invasion protein IbeA
 (ibeA) gene, complete cds

TCGGGTATTGCGCGAGCAATGAGTGCCGCTCGTGAAGGCGCAGCTACTATGCTGATTGAACGTTTCGGTT
 GTTTTGGCGGAATGATGACAACGGCTGGCGTCGAGTCAATTGCCTGGTGGCGTCATGAAAATACGGTAGA
 GTCAGGTGGACTGGCACGCGAAATAGAAGAAACGGCAAAATCAATGGGGGCGTCCAGCCCTGAGCCGCAA
 TCGAATAGTCAGGCTATTAACGCCGAGCGTTTCAAACCTGGTTGCGGATGCAATGCTTGAACAGGCAGGTG
 TGCGCCGCGTACTACACATTACCGCCGTTGATGTTA

flu

>NC_000913.3:2071537-2072067 Escherichia coli str. K-12 substr. MG1655,
 complete genome

TGATGAAACGACATCTGAATACCTGCTACAGGCTGGTATGGAATCACATGACGGGCGCTTTTCGTGGTTGC
 CTCCGAAGTGGCCCGCGCACGGGTAAACGTGGCGGTGTGGCGGTTGCACTGTCTCTTGCCCGCAGTCACG
 TCACTCCCGGTGCTGGCTGCTGACATCGTTGTGCACCCGGGAGAAACCGTGAACGGCGGAACACTGGCAA
 ATCATGACAACCAGATTGTCTTCGGTACGACCAACGGAATGACCATCAGTACCGGGCTGGAGTATGGGCC
 GGATAACGAGGCCAATACCGGCGGGCAATGGGTACAGGATGGCGGAACAGCCAACAAAACGACTGTCACC
 AGTGGTGGTCTTCAGAGAGTGAACCCCGGTGGAAGTGTCTCAGACACGGTTATCAGTGCCGGAGGCGGAC
 AGAGCCTTCAGGGACGGGCTGTGAACACCAGCTGAATGGTGGCGAACAGTGGATGCATGAGGGGCGAT
 AGCCACAGGAACCGTCATTAATGATAAGGGCTGGCAGGTCTG

csgA

>EU554560.1:3679-4081 Escherichia coli strain H8824 CsgG (csgG), CsgF (csgF),
 CsgE (csgE), CsgD (csgD), CsgB (csgB), CsgA (csgA), and CsgC (csgC) genes,
 complete cds

GGCAGGTGTTGTTTCCTCAGTACGCGCGGTGGCGGTAACCACGGTGGTGGCGGTAATAACAGCGGCCCCG
 AATTCAGAGCTGAATATTTATCAGTACGGTGGTGGTAACCTCTGCACTTGCTCTGCAAGCTGATGCTCGTA
 ACTCTGATCTTACTATTACCCAGCATGGTGGTGGTAACGGTGCAGATGTTGGTCAGGGCTCAGATGACAG
 CTCAATCGATCTGACCCAACGTGGCTTTGGTAACAGCGCCACTCTTGATCAGTGGAACGGTAAAGACTCT
 CATATGACAGTTAAACAATTCGGTGGCGGCAACGGTGCAGCGTTGACCAGACTGCATCTAATTCCACCG
 TCAACGTAACCTAGGTTGGCTTTGGTAACAACGCGACCGCTCATCAGTACTAA

usp

>AB027193.1 Escherichia coli gene for Usp, complete cds

ATGCTACTGTTCCCGAGTAGTGTGTTGGCGACTCAAATATGGGGAAAATGGTCGCTCAGTGGCGTACTCA
 GTGCAACCCGCGGCTCTTACATCGGTGCGTTGGCATCTGCTTTGTATATTCCTCTGCGGGCGAGGGCAG
 TGCTCGCGTGCCCGGACGTGATGAGTTCTGGTATGAGGAAGAACTGCGGCAGAAAGCACTAGCAGGCAGT
 ACCGCCACCAACCCGGGTACGTTTTTCTGGGGAACCTGACATTCACGGCAAGCCTCAGGTGTATGGTGTTC
 ATACGGGTGAAGGTACGCCGTATGAAAACGTCCGCGTGGCGAACATGCAGTGGAACGAGCAGACGCAGCG

TTATGAATTTACCCCGCTCACGATGTCGATGGCCCCCTGATTACCTGGACGCCGAAAAATCCGGAACAT
 GGGGAATGTTCCGGGCCATACCGGTAACGACAGGCCGCCGCTGGATCAGCCCACCATTCTGGTGACGCCGA
 TTCCGGACGGCACCGATACCTATACCACGCCGCCATTCCCGGTTCTGATCCGAAAGAATTCAACGATTA
 TATTCTGGTTTTTCCGGCGGGATCCGGTATTAAGCCCATCTATGTTTACCTGAAGGAGGATCCGCGAAAG
 CTGCCTGGTGTGTGAACAGGGCGCGGCGTCCCGCTTTACCAGGAACCTCGCTGGCTGGATATGTCGGTAT
 CCAATAACGGCAACGGCGCACCAATCCCGGCGCATATTGCTGATAAATTGCGCGGACGGGAGTTTAAAC
 CTTTGATGAGTTTCGCGAGGCGCTGTGGCTGGAGGTGAGTAAAGACTCAGTGTTATTGGCGCAGTTTATA
 AAAAGTAATCAGAATAACGTTAGTCAAGGATATTCCCCCTATGTCCCTGAGGAGGGGTATTATTACGGAC
 CAAATGAGATAGTTAAGAAATTCCAGATACATCATGTAGTTGCTATAGAACATGGTGGTGGAGTGTATGA
 TATTGATAATTTAGGAT **TGTTACGCCCCGACTACATGATG** AAATTCACTACAGGAGATAA

4.4.6. Pathogenic Island (PAI) identification:

Pathogenicity-associated islands (PAIs) are particular regions on the bacterial chromosomes where virulence genes have accumulated. PAIs, and their associated virulence genes, have spread among bacterial populations by horizontal transfer. Several PAIs were previously identified in uropathogenic *E. coli* strains such as *E. coli* 536, *E. coli* J96, and *E. coli* CFT073. PAIs I to IV from strain 536 (I₅₃₆ to IV₅₃₆) encode a range of virulence factors, including P fimbriae, P-related fimbriae, α -hemolysin, S fimbriae, and the Yersiniabactin siderophore system. PAI I_{J96} and II_{J96} encode P fimbriae, P-related fimbriae, and α -hemolysin; PAI I_{CFT073} and II_{CFT073} encode P fimbriae, α -hemolysin, and aerobactin. *usp* is prevalent among strains causing urinary tract infections. It enhances infectivity in a mouse ascending UTI model displays homology with S-type pyocin, and may function as bacteriocin [36].

4.4.6.1. Identification of Pathogenic island markers by Multiplex PCR: All isolates were analyzed by two multiplex PCR based assay to detect the presence of eight most investigated PAIs in UPECs. The primers and the PCR conditions of all eight PAI markers utilized in this study was described in Table 4.3. Briefly, Multiplex PCR reaction A (PAI III₅₃₆, PAI IV₅₃₆, PAI II_{CFT073}) and Multiplex PCR reaction B (PAI I₅₃₆, PAI II₅₃₆, PAI I_{CFT073}, PAI I_{J96}, PAI II_{J96}) assays were performed in 20 μ l reaction volume containing 1 μ l of total DNA, 0.7 μ l of each primer, 2 μ l 10X buffer, 0.3 μ l dNTP, 0.6 μ l MgCl₂, 0.1 μ l Taq DNA polymerase (Invitrogen), and rest of DDH₂O. The primer sequences of the target genes are depicted in Table 4.3 and section 4.4.6.2., primers are marked in green. Generated amplicons were separated by 1.5% agarose gel electrophoresis and visualized using Ethidium Bromide by Gel documentation system (Bio-Rad, USA).

Table 4.3. Primer sequences and PCR conditions for Pathogenic island analysis used in this study.

Sl. No.	Genes	Primers (5' → 3')	PCR condition	No. of Cycles	Amplicon Size (bp)
1.	PAI I ₅₃₆	FP: TAATGCCGGAGATTCATTGTC RP: AGGATTTGTCTCAGGGCTTT	95°C – 30'' 50°C – 30'' 72°C – 2'	30	1800
2.	PAI II ₅₃₆	FP: CATGTCCAAAGCTCGAGCC RP: CTACGTCAGGCTGGCTTTG			1000
3.	PAI III ₅₃₆	FP: CGGGCATGCATCAATTATCTTTG RP: TGTGTAGATGCAGTCACTCCG	95°C – 30'' 50°C – 30'' 72°C – 1'		200
4.	PAI IV ₅₃₆	FP: AAGGATTCGCTGTTACCGGAC RP: TCGTCGGGCAGCGTTTCTTCT			300
5.	PAI I _{CFT073}	FP: GGACATCCTGTTACAGCGCGCA RP: TCGCCACCAATCACAGCGAAC	95°C – 30'' 50°C – 30'' 72°C – 2'		930
6.	PAI II _{CFT073}	FP: ATGGATGTTGTATCGCGC RP: ACGAGCATGTGGATCTGC			400
7.	PAI I _{J96}	FP: TCGTGCTCAGGTCCGGAATTT RP: TGGCATCCCACATTATGC	95°C – 30'' 50°C – 30'' 72°C – 2'		400
8.	PAI II _{J96}	FP: GGATCCATGAAAACATGGTTAATGG RP: GATATTTTGTGTCATTGGTTACC			2300

4.4.6.2. Target genes for PAI markers determination. Respective forward and Reverse primer sequences (5' → 3') are marked in green.

PAI I₅₃₆

>CP000243.1:4806146-4807955 Escherichia coli UTI89, complete genome
TAATGCCGGAGATTCATTGTCATTATTTAAACGTATGCTAATACTCTTTTGAGTCGCCGGATAAACAACA
CGGGTTCCCATGATAACTACACTACCCTGAACAACGTGCAGATACAGATAGAGTAAAAAAGCAGCACAA
ACCTTAGCATGGTATCTCCAGAAGAAAACAGGGCAGTATTTCTGCCCAGAAATACAAAAGAGTAAAAAG
TTTTTTATTCGTAGGCAATGGTATAATGGACCGTCGCTTTTACATCCCCTGCGGTAGATTGTCCTGTTGC
ATAATACTGGGCCATATAACGCAATGTGGCACTTCCATCAGATCCGATTGTCTCAGACTGGACATCTTGC
CCATTATCCGCTTCCCCCAAAGAATAGTTGAAGTTCCATTACTATTTAGCAACTGAATCTGTACATTAT
CCGCTTTAGTTGGAGTAGCAGTATTTTTTAAATTATGTGTAGCTAAGTCAATGTTACTTGAAGGCTCAAA
GTACGCTTTAACATTCTGAGCACTATTCATACCAGTTGCACAACCAAGTTAAACGAATGGCAAAGGGTGTC
AGCCCTGACGTAGCAGCATTGTCTTTTAGAGATGAAGTGGCAACAGTGGGTAAAGTTACTGCTAAGTCTT
TGTCGCTTGTATTAAGTGTGAGGTCTGAGCTACAACCTTTACCGGTAAACGTAATTGTTCCGTCATAGGC
CATAGCTGAACCAGCAAACACAGCAGAAACAAATGTAGCCAATGCTATAACTTTTATTTTCATAAAATGA
ATTCCTGTTTAATTCCAGTATTGATCATTTGTTTCAGCAATCATCCCCAACAAAACAATCATTTTCAAAAT
GTTTTTACCGATCGATAACCAGCGTATGATAGATTGCACCTATCATGATTGCTAAAACGATCGGGAAAAA
CGATCAAAAACCATATTTATTGTGTTGGTAATGACAAAAGATATGCTTTACCCTGAAATGAGCGACCTAT
TCATGAAAATATGTAGGTCTGTATTTGATTACTATCATTGCTATATTTCCACTATCCAATTTATATTTCA
TGATTAAAATATACCTTTTACACTATTATTTATTTGTTGCAGCTTGCCTGGCTTTATCTTATTCCGACT
ATTTTATGGTAGATACAGAATACAATTAATTAACCTTATTTAAAGATTTTATAAATACCATATTGGAGTT
GACCGATAGATACCTACTAACAAGAGCAATCACCACACCCCATGAGGTGGTTTAGGAATACAATCAATA
AACAACATCCATGCCCGCGCAGTACATACCTGTTTGCTATGATATCTGTTACGCTACGCTTGTCTAATTT
ACTGAAACTCAGCGTCTGTGACGGAGATTCGTGCGGGCCCTGATACAACAAGGGCAAGAAAACCCCG
AAATACAGATATTCTTATAAAAATGGATCATATTTCCATGTGCAAGTTCAGCTGGCATCGTCCAGAATGC
GTGTCCAAGAAATGAAGCAAGCACGGTATACAGGCACAGAATAATGCTCACTGGCCGGGTGAAAAACCA
AAAACAATCATTAATGCTCCAACGATTTGACAAAGGACCACTATTGCTGCAGTAATCGCCGGAAATATAA
GCCCCAAGAGAGGCCATTTTATCGATAGTGCCAGTGAATGATAGCAGCTTGGGAACGCCGGATATCATATA

AAGGCATGCCAGCATCAGACGGGCAAGGAGCAACAATGCCGACGTGTAATTTCCCATATTAAATACCTG
ATTTTATCCACTATCAATGCTCAGTCTCCTTGTCTGATAAAGCCCTGAGCCAAATCCT

PAI II₅₃₆

>CP000243.1:4840603-4841644 Escherichia coli UTI89, complete genome
CATGTCCAAAGCTCGAGCCTTTGTCTTATTTTAGCCATATATCTATGAATCCTTATTAGTACAATTTTC
TATGAGATGTAGCCCAATAGTCTAGCGAGTTCGCAAGGTACAGCATTGCCGATTTGCTTTGCCATTGAA
TTCAGCGAACCTTTAAAAACATAGCTTAAAGGAAATGTTTGTAATCTTGATGCTTCTCTTATGCTAATTG
CTCTATGTTGAGTGGGGTCAGGATGCCCAAAACGACCATTGGAGTAACTATTACATTTTCGTCGTAAGTGT
AGGCGCAGGCTTATCCCAACTCATTCTTCCATAAGTATCTGTGTGGCCATCATAATTTTTATGGCATTTA
TTAACTAACTCTTCTGGCCAATTTCTTCTATCCCCTCCTTCTGGAGTGTGCATAATTCTTTTAGGTTAA
GAGGGCTCAGTGTTCAGCCCTATGTAAAGGATCTTTGGGGTCGGTTTCTCCTGAACATAACTTTGTGAA
GTCCTGGATATAATCTCGTACAGTTTTGAATGGGATTTTATTTTACCATGGGTTATCTCTGGTAGGGTA
ACTTTACCTACTCGACTAGCTAAGAGCACGAGTCTTTTCTTCTTTGGGAATCCCATAGTTCTCAGCAT
TGGCTATAAAAGATATATAGTTATACTCTAACTCTTTAAGTAGCTTAATAAACTCCTGAAATGGGCCTTC
TTTTTCTTCATCAATTTTTTGCATTCCAGGAACATTTTCAAGCATAATATATTCAGGAAGAAGTTCTCTA
ATAAAACGATGAGTTTCATTTAGTAGATTTCTCCTTGAGTCGTCAGTATTTTATTTTATTCTGTTGCG
AAAATGGTTGACATGGTGCACATGCACTCAGTAACAAAGGCCGTTTAGCTTTAATATCAATGATGTCGGA
GATATCTTGAGGTTGATTTTCTAATATCATCTTGATGAATTTTGCATCAGGGAAATTAGCTTTAAAT
GTTTCTGATGCTTGTGGTCAATATCTAATCCAAGCTCGATATCAAAGCCAGCCTGACGTAG

PAI III₅₃₆

>X16664.4:17230-17391 Escherichia coli encoding determinant sfa(I)
CGGGCATGCATCAATTATCTTTGCAGGAAATGTTATTGCTACACACAATGATGTGCTGTCTCTACAGAAT
AGTGCTGCAGGTAGTGCAACAAATGTAGGTATTAGATATTGGATCATAACAGGTACTGCAGTTCAATTTG
ACGGAGTGACTGCATCTACACA

PAI IV₅₃₆

>CP000243.1:2079027-2079313 Escherichia coli UTI89, complete genome
CAGGATTGCGTGTACCGGACAAACCGCCACGCGGCTGATTACCAACAATTACGCGAGCGGCTCATAACAGG
AACTGAATTTAACGCCGCAGCAGTTACATGAAGAGAGCAACCTGATCCAGGCCGGCCTGGATTCCATAAG
ATTGATGAGATGGTTACACTGGTTTCGTAAAAATGGCTACCGCCTTACCCTTCGCGAGCTGTATGCCGCC
CCCACGCTGGCGGCATGGAACAGTTAATGCTCAGCCGGTCGCCGGAGAACGCGGAAGAAGAAACGCCGC
CCGACGA

PAI IC_{FT073}

>AE014075.1:c3254118-3253197 Escherichia coli CFT073, complete genome
GGACATCCTGTTACAGCGCGCAATTTCATGAAATTGAACGGTATCTGTATGCCACTTTTAAATATGAATTA
ATTTTAGAAGAAAACTATATCTCTCTATTTCGTACCAAAGTATTAATGGACTAATTATATATAACATTTA
TATGAGATAACCCACATGAAACAAAAGAAAGCCTGGAGTTTTTTTTCAGAGCCTGGGGAAGGCATTTATGT
ATCCCATTGCTCTGCTAAGTGTATGTGGCATGATGCTAGGGCTGGGAAGTGGTTTAGCCAGTGATGATAT
GGCAAAGTTAATTCCATTTCTGGCTATTCCAATAATTAAACCATACTTGATTTTCATTGTTAGTCTTGGT
TTGTTTGCCTTTGTTAATTTACCTGTATTGTTTGCATAGCGATTCCCTTAGGATTATTAAGATAAAG
AGGATAAAGCCTATGGTGCCTTTTCTGGCTTAATTGGTTTTATGGCGATGCATCTGGGAACGAACTTTTA
TCTTAAACAGCACGACTTATTGGTCGTTGCTGACCAATGTGACACATGGGCAAACCATCTTCTGGGG
ATCCAGTCCTACAATACCAGCGTGTGGGGGGAATGTTGCTGGGTTATTAGTCGCCAGCATGTATAAAA
AGATCGTTAATTTACGCATTCCTGAATCGTTAGGTTTTATAGCGGCCACGTCTGGTGCCTATCATTAC
ACTGATTGTGATGAGTGGATTTGGTCTGATCATTCCTTTTATCTGGCCGCCGTTTTTCAATCTTTTCATG
CTCATTGGACACTGGATTTCAACTTCCGGTCCTGTTGGTTATTTCTTCTATGCAGTTGCCGAACGCGTGA
CGATTCTTTTGGCTTAAACCATCTGGTGACGTGAGTTTCCGCTTTACGCCAATCGGCGTTTCGGCTGT
GATTGGTGGCGA

PAI II_{CFT073}

>AE014075.1:278768-279188 Escherichia coli CFT073, complete genome
ATGGATGTTGTATCGCGCGAAACGCGAAGACGCAATATGGTTACGCTGGTCGTCTTACACGATATCAATA
TCGCACTGCGGCATGCCGCCAGGTCATCATGCTGAAAGAGGGGAACTTATCGACAGCGGCGACCCGCA
AACGGTGATCCATGCAGAGAGCCTTGCGCAGGTATACGGCGTACGCGGGAGAGTTGAACGTTGTGCTCAG
GGAAGATCGATGGTGATAGTGGATGGTGCAATCGAAAAATAGTCGGATTAACGTGGTTGCTTCAGCCTCA
GGTAAAGATCAATAGGAAGTCTGTAATGCAACATATAGACCGCTTAATGTCATTAAAGCACTTGTGCTT
CTAGAAGATGAGCAGATTGTTGTTTTAACATCGCTGCGAACGATAACGCCTCGCAGATCCACATGCTCG

T

PAI I_{J96}

>M20146.1:1414-1874 *E.coli* papE, papF, and papG genes, complete cds, isolate J96

TCGTGCTCAGGTCGGAATTTGCGAGTGGAGTGTATTTTCAGGAGTATCTGGCCTGGATGGTTGTTCTTA
AACATGTCTATACTAATGAGGGGTTTAATATATTTCTTGATGTTTCAGAGCAAATATGGTTGGTCTATGGA
GAATGAAAATGACAAAGATTTTTACTTCTTTGTTAATGGTTATGAATGGGATACATGGACAAATAATGGT
GCCCCGTATATGTTTCTATCCTGGAAATATGAAGCAGTTGAACAATAAATTTAATGATTTAGTATTCAGGG
TTCTTTTGCCAGTAGATCTCCCCAAGGGACATTATAATTTTCTGTGAGATATATACGTGGAATACAGCA
CCATTACTATGATCTCTGGCAGGATCATTATAAAATGCCTTACGATCAGATTAAGCAGCTACCTGCCACT
AATACATTGATGTTATCATTCGA TAATGTTGGGGGATGCCA

PAI II_{J96}

>CP000243.1:c4822815-4820400 *Escherichia coli* UTI89, complete genome

AAGAATATGAAAACATGGTTAATGGGTTTCAGCGAGTTCCTGTTGCGCTATAAACTTGTCTGGAGTGAAA
CATGGAAAATCCGGAAGCAATTAGATACCTCCGTACGTGAAAAGGACGAAAATGAATTCCTACCCGCTCA
TCTGGAATTAATTGAAACGCCGGTATCCAGACGCCGCGTCTGGTTGCTTATTTTATTATGGGGTTTCTG
GTTATTGCTGTCAATTTTATCTGTTTTAGGTGAGGTGGAATTTGTTGCCACTGCAAATGGGAAATTAACAC
TAAGTGGGCGTAGCAAAGAAATTAACCTATTGAAAACCTCAATAGTTAAAGAAATTATCGTAAAAGAAGG
AGAGTCAGTCCGGAAGGGGATGTGTTATTAAAGCTTACAGCACTGGGAGCTGAAGCTGATACGTTAAAA
ACACAGTCATCACTGTTACAGACCAGGCTGGAACAACTCGGTATCAAATTCTGAGCAGGTCAATTGAAT
TAAATAAACTACCTGAAGCTTCTGATGAGCCTTATTTTCAGAATGTATCTGAAGAGGAAGTACT
GCGTTTTAACTTCTTTGATAAAAGAACAGTTTTCCACATGGCAAATCAGAAGTATCAAAAAGAACTGAAT
CTGGATAAGAAAAGAGCAGAGCGATTAACAATACTTGCCCGTATAAACCGTTATGAAAATTTATCGAGAG
TTGAAAAAAGCCGTCTGGATGATTTTCAGGAGTTTATTGCATAAACAGGCAATTGCAAACATGCTGTACT
TGAGCAGGAGAATAAATATGTGAGGCAGCAAATGAATTACGGGTTTATAAATCGCAACTGGAGCAAAT
GAGAGTGAGATATTGTCTGCAAAAGAAGAATATCAGCTTGTACGCAGCTTTTTAAAAATGAAATTTTAG
ACAAGCTAAGACAAACAACAGACAGCATTGAGTTATTAACCTCTGGAGTTAGAGAAAAATGAAGAGCGTCA
ACAGGCTTCAGTAATCAGGGCCCCCTGTTTCGGGAAAAGTTTCAGCAACTGAAGGTTTCATACTGAAGGTGGG
GTTGTTACAACAGCGGAAACACTGATGGTCATCGTTCCGGAAGATGACACGCTGGAGGTTACTGCTCTGG
TACAAAATAAAGATATTGGTTTTTATTAACGTCGGGCAGAATGCCATCATTAAGTGGAGGCCTTTTCCTTA
CACCCGATATGGTTATCTGGTGGGTAAGGTGAAAAATATAAATTTAGATGCAATAGAAGACCAGAACTG
GGACTCGTTTTTAAATGTCAATTGTTTCTGTTGAAGAGAATGATTTGTCAACCGGAATAAGCACATTCCAT
TAAGCTCGGGTATGGCTGTCACTGCAGAAATAAAGACTGGAATGCGAAGCGTAATCAGCTATCTTCTTAG
TCCTCTGGAAGAGTCTGTAACAGAAAGTTTACATGAGCGTTAAGTCTCAGAGCCGCGGTATCCGGCTCAT
ATCTTCTCCTGTGATGTGACTGCAGTGTGTTTGTGGCAAACAGTACTGACTATCCACTGGAATTCGGT
AGTCATTAACCTATGGCATTGATGTCCTTTATAACTGTCTTACAGGGCGTATAACACATCCCGCGACGGAA
GCTTATCACAGAGGAAGAGGTAAGCTTCAGAATGGAAGTATATGAGAAGACTGTGATTGTTTAAAAATA
CACAATCCGCTGTGAGGTGGAGTCAGGGGAGGTACTGGCCCGCAGAAGCGGAGAATGGTTGATGTATGAG
GCGAGTGTGACATTTTTTCATGAAAGTAAAACAGGTGATAACCTCCTTTGGTTAGGGGGATTACAGGTAT
TATTACAGAACAATGTTGTTTCTGGCTTGTTCTTTTTTTGCAACTGGAATAGCCTCTTTTAATATGGGGC
ACCCCGAAATACTGTATTTCTCAGCCATCAGTACAGCACTTTCTCCGTTCTTTGCCTGGTGTGTTGCGGTA
TCCTGATGAGGAGATTAATGAAGGTATATGGGGATATAATGCTGTTCTGTATGGCATAGCCTGTGGCATG
CTTGTCCTGTGTGCTCAGTCTCCGGAATTGCTGTACTTATTGTGCGAACACTGGAGATGCTCCTTTTAATGG
GGTTTCAGATAATACTTAACCTGCTGGCCGACCTGTCTGGTGTATGCCAGGTTTACCAGCTTTCTTTCAA
TGTGGAATATATTAATAGAAATCCAGTGGTTTTGCATACCGGGATGTTGTGTAGTGCAAAATTTATACTA
CAGGGATCGGAGTAGTGATGTTTAAGATTCATTAAATAGTTTTCAAAGACGCTTTGTATACGACATGATTG
CTAACCTCTCGCCAGTGATTAGGTATTCTGATAAGGTGTAGTAAAATATTAATCTTCACAGAGGAGTTA
AAAATATTATG GGTAAACCAATGGCAACAAAAATATC

4.4.7. Multilocus Sequence Typing (MLST):

All UPEC isolates were ascribed to Multilocus sequence types by the classical seven gene approach (Achtman MLST scheme) as described previously in a study [37]. The primer sequences

and protocols (PCR conditions) specified at the *E. coli* MLST website (<https://enterobase.readthedocs.io/en/latest/mlst/mlst-legacy-info-ecoli.html>), PCR was performed on *E. coli* genomic DNA using the seven housekeeping genes (*adk*, *fumC*, *gyrB*, *icd*, *mdh*, *purA* and *recA*) [37]. All the PCR amplifications were performed using a high fidelity Taq DNA polymerase (Invitrogen, “Platinum™ Taq DNA Polymerase High Fidelity”). The consensus region of the seven housekeeping genes used for sequence typing of a particular *E. coli* isolate had been depicted in section 4.4.7.1. using the allele template as *E. coli* strain MG1655. Moreover, the target MLST genes with original sequence, the consensus region (pink) and the respective primer (green) sequence in the case of the *E. coli* strain MG1655 were described and marked in 4.4.7.1.

The amplicons from our isolates were purified and sequenced by Bioserve Biotechnologies (India) Pvt. Ltd. (Hyderabad, India) using protocols as described by Wang et al. [38]. Allele numbers for the seven gene fragments of each *E. coli* isolate were acquired by comparing with corresponding alleles available at the *E. coli* MLST database (https://enterobase.warwick.ac.uk/species/ecoli/allele_st_search) [39]. Sequences of the seven genes were concatenated for each isolate using https://www.bioinformatics.org/sms2/combine_fasta.html and STs and CCs of each isolate was identified on the basis of the aforesaid concatenated sequence data (combining seven allelic profiles) using the *E. coli* MLST database (https://enterobase.warwick.ac.uk/species/ecoli/search_strains?query=st_search) [39].

4.4.7.1. Target genes for PAI markers determination. Respective forward and Reverse primer sequences (5' → 3') are marked in green and the consensus region was marked in pink

adk

```
>NC_000913.3:497171-497799 Escherichia coli str. K-12 substr. MG1655,
complete genome
CGCAATGCGTATCATTCTGCTTGGCGCTCCGGGCGCGGGGAAAGGGACTCAGGCTCAGTTCATCATGGAG
AAATATGGTATTCGCGAAATCTCCACTGGCGATATGCTGCGTGCTGCGGTCAAATCTGGCTCCGAGCTGG
GTAAACAAGCAAAAGACATTATGGATGCTGGCAAACCTGGTCACCGACGAACCTGGTGATCGCGCTGGTTAA
AGAGCGCATTGCTCAGGAAGACTGCCGTAATGGTTTCCTGTTGGACGGCTTCCCGCGTACCATTCCGCAG
GCAGACGCGATGAAAGAAGCGGGCATCAATGTTGATTACGTTCTGGAATTCGACGTACCGGACGAACCTGA
TCGTTGACCGTATCGTCGGTCGCCGCGTTTCATGCGCCGCTCGGTCGTGTTTATCACGTTAAATTCAATCC
GCCGAAAGTAGAAGGCAAAGACGACGTTACCGGTGAAGAACTGACTACCGTAAAGATGATCAGGAAGAG
ACCGTACGTAAACGTCTGGTTGAATACCATCAGATGACAGCACCGCTGATCGGCTACTACTCCAAAGAAG
CAGAAGCGGGTAATACCAAATACGCGAAAGTTGACGGCACCAAGCCGGTTGCTGAAGTTCGCGCTGATC
```

fumC

>NC_000913.3:c1686522-1685841 Escherichia coli str. K-12 substr. MG1655, complete genome

GGCGCACAACTCAACGC TCGCTGGAGCATTTCCGCATTTTCGACGGAGAAAATGCCACCTCACTGATTCTGCGCTGGCGCTAACCAAGCGTGCAGCGGCAAAAGTTAATGAAGATTTAGGCTTGTTGTCTGAAGAGAAAGCGAGCGCCATTTCGTAGGCGGCGGATGAAGTACTGGCAGGACAGCATGACGACGAATTCCTGGCTATCTGGCAGACCGGCTCCGGCACGCAAAGTAACATGAACATGAACGAAGTGCTGGCTAACCGGGCCAGTGAATTACTCGGCGGTGTGCGCGGGATGGAACGTAAAGTTCACCCTAACGACGACGTGAACAAAAGCCAAAGTTCCAACGATGTCTTTCCGACGGCGATGCACGTTGCGGCGCTGCTGGCGCTGCGCAAGCAACTCATTCTCAGCTTAAAACCTTGACACAGACACTGAATGAGAAATCCCGTGCTTTTGCCGATATCGTCAAAATTGGTGTACTCACTTGCAGGATGCCACGCCGTTAACGCTGGGGCAGGAGATTTCCGGCTGGGTAGCGATGCTCGAGCATAATCTCAAACATATCGAATACAGCCTGCCTCAGTAGCGGAACCTGGCTCTTGGCGGTACAGCGGTGGTACTGGACTAAATACCCATCCGGAGTATGC GCGTCGCGTAGCAGATGAAC

gyrB

>NC_000913.3:c3879930-3879236 Escherichia coli str. K-12 substr. MG1655, complete genome

CACGCCGATAACTCTGTCTCTGTACAGGATGACGGGCGCGGCATTCCGACCGGTATTACCCGGAAGAGGGCGTATCGGCGGCGGAAGTGATCATGACCGTTCTGCACGCAGGCGGTAAATTTGACGATAACTCCTATAAAGTGTCCGGCGGTCTGCACGGCGTTGGTGTTCGGTAGTAAACGCCCTGTCGCAAAACTGGAGCTGGTTATCCAGCGCGAGGGTAAAATTACCGTCAGATCTACGAACACGGTGTACCGCAGGCCCCGCTGGCGGTTACCGGCGAGACTGAAAAACCGGCACCATGGTGCCTTTCTGGCCCAGCCTCGAAACCTTCACCAATGTGACCGAGTTCGAATATGAAATTCTGGCGAAACGTCTGCGTGAGTTGTCGTTCTCAACTCCGGCGTTTCCATTGCTCTGCGCGACAAGCGCGACGGCAAAGAAGACCACTTCCACTATGAAGGCGGCATCAAGGCGTTTCGTTGAATATCTGAACAAGAACAACGCGGATCCACCCGAATATCTTCTACTTCTCCACTGAAAAAGACGGTATTGGCGCTCGAAGTGGCGTTGCAGTGGAACGATGGCTTCCAGGAAAACATCTACTGCTTTACCAACAACATTCCGCAGCGTGACGGCGGTACTCACCTGGCAGGCTTCCGTGCGGCGAT GACCCGTACCCTGAACGC

icd

>NC_000913.3:1195135-1195999 Escherichia coli str. K-12 substr. MG1655, complete genome

GTAGTTGTTCCGGCACAAAGGCAAGAAGATCACCTGCAAAACGGCAAACTCAACGTTTCTGAAAATCCGATTATCCCTTACATTGAAGGTGATGGAATCGGTGTAGATGTAACCCCAGCCATGCTGAAAGTGGTTCGACGCTGCAGTCGAGAAAGCCTATAAAGGCGAGCGTAAAATCTCCTGGATGGAAATTTACACCGGTGAAAAATCCACACAGGTTTATGGTCAGGACGTCTGGCTGCCTGCTGAAACTCTTGATCTGATTCTGTAATATCGCGTTGCCATTAAAGGTCCGCTGACCACTCCGGTTGGTGGCGGTATTGCTCTCTGAACGTTGCCCTGCGCCAGGAAGTGGATCTCTACATCTGCCTGCGTCCGGTACGTTACTATCAGGGCACTCCAAGCCCGGTTAAACACCCTGAACCTGACCGATATGGTTATCTTCCGTGAAAACCTCGGAAGACATTTATGCGGGTATCGAATGGAAGACACTCTGCCGCGGCGAGAAAGTGATTAATCTTCCGTGAGAGATGGGGGTGAAGAAAATTCGTTCCCGGAACATTGTGGTATTCGTTATTAAGCCGTGTTTCGGAAGAAGGCACCAACGCTCTGGTTCTGTCAGCGCATCGAATACGCAATTGCTAACGATCGTGACTCTGTGACTCTGGTGACAAAGGCAACATCATGAAGTTACCGAAGGAGCGTTTAAAGACTGGGGCTACCAGCTGGCGCGTGAAGAGTTTGGCGGTGAAGTATCGACGGTGGCCCGTGGCTGAAAGTTAAAAACCCGAACACTGGCAAAGAGATCGTCATTAAAGACGTGATTGCTGATGCAATTCCTG CAACAGATCCTGCTGCGTC

mdh

>NC_000913.3:c3384148-3383430 Escherichia coli str. K-12 substr. MG1655, complete genome

GGTGTGGCTGTGATCTGAGCCATATCCCTACTGCTGTGAAAATCAAAGGTTTTTCTGGTGAAGATGCGACTCCGGCGCTGGAAGGCGCAGATGTCGTTCTTATCTCTGCAGGCGTAGCGCGTAAACCGGGTATGGATCGTTCCGACCTGTTTAAACGTTAAACGCCGGCATCGTGA AAAACCTGGTACAGCAAGTTGCGAAAACCTGCCCGAAAGCGTGCAATTGGTATTATCACTAACCCGGTTAACACCACAGTTGCAATTGCTGCTGAAGTGTGAAAAAAGCCGGTGTTTATGACAAAAACAACTGTTCCGGCGTTACCACGCTGGATATCATTGTTCCAACACCTTTGTTGCGGAAGTGAAGGCAACAGCCAGGCGAAGTTGAAGTGCCGGTTATTGGCGGTCACTCTGGTGTTACCATCTGCCGCTGCTGTACAGGTTCTGGCGTTAGTTTTACCGAGCAGGAAGTGGCTGATCTGACCAAACGCATCCAGAACGCGGGTACTGAAGTGGTTGAAGCGAAGGCCGGTGGCGGGTCTGCAACCCTGTCTATGGGCCAGGCAGCTGCACGTTTTTGGTCTGTCTCTGGTTTCGTGCACTGCAGGGCGAACAAGGCGTTGTGGAATGTGCCTACGTTGAAGGCGACGGTCAGTACGCCCGTTTCTTCTCTCAACCGCTGCTGCTGGGTAAAAACG

GCGTGGAAGAGCGTAAATC

purA

>NC_000913.3:4404981-4405672 Escherichia coli str. K-12 substr. MG1655, complete genome

CTGCTGTCTGAAGCATGTCGCTGATCCTTGATTATCACGTTGCGCTGGATAACGCGCGTGAGAAAGCGCGTGGCGCGAAAGCGATCGGCACCACCGGTCGTGGTATCGGGCCTGCTTATGAAGATAAAGTAGCACGTCGCGGTCTGCGTGTTGGCGACCTTTTCGACAAAGAAACCTTCGCTGAAAACTGAAAGAAGTGATGGAATATCACAACTTCCAGTTGGTTAACTACTACAAAGCTGAAGCGGTTGATTACCAGAAAGTTCTGGATGATACGATGGCTGTTGCCGACATCCTGACTTCTATGGTGGTTGACGTTTCTGACCTGCTCGACCAGGCGCGTCAGCGTGGCGATTTTCGTCATGTTTGAAGGTGCGCAGGGTACGCTGCTGGATATCGACCACGGTACTTATCCGTACGTAACCTTCTTCCAACACCACTGCTGGTGGCGTGGCGACCGGTTCCGGCCTGGGCCCGCGTTATGTTGATTACGTTTCTGGGTATCCTCAAAGCTTACTCCACTCGTGTAGGTGCAGGTCCGTTCCCGACCGAACTGTTTGTGAAACTGGCGAGTTTCTCTGCAAGCAGGGTAACGAATTCCGGCGCAACTACGGGGCGTCGTCGTCGTACCGCTGGCTGGACACCGTTGCCGTTTCGTCGTGCGGTACAGCTGAACTCCCTGTCTGGCTTCTG

recA

>NC_000913.3:c2823515-2822852 Escherichia coli str. K-12 substr. MG1655, complete genome

GCGTGAAGGTAAACCTGTGCGTTTATCGATGCTGAACACGCGCTGGACCCAATCTACGCACGTAAACTGGCGTCGATATCGACAACCTGCTGTGCTCCAGCCGGACACCGGCGAGCAGGCACTGGAAATCTGTGACGCCCTGGCGCGTTCTGGCGCAGTAGACGTTATCGTCGTTGACTCCGTGGCGGCACTGACGCCGAAAGCGGAATCGAAGGCGAAATCGGCGACTCTCACATGGGCCTTGCGGCACGTATGATGAGCCAGGCGATGCGTAAGCTGGCGGGTAACCTGAAGCAGTCCAACACGCTGCTGATCTTCATCAACCAGATCCGTATGAAAATTGGTGTGATGTTTCGGTAACCCGGAACCACTACCGGTGGTAACGCGCTGAAATTCTACGCCTCTGTTCTGTCGATCCGTCGTATCGGCGCGGTGAAAGAGGGCGAAAACGTGGTGGGTAGCGAAACCCGCGTGAAAGTGGTGAAGAACAAAATCGCTGCGCCGTTTAAACAGGCTGAATTCCAGATCCTCTACGGCGAAGGTATCAACTTCTACGGCGAAGTGGTTGACCTGGGCGTAAAAGAGAAGCTGATCGAGAAAGCAGGCGCGTGGTACAGCTACAAAGGTGAGAAGATCGGTACGGGTAAAGCGAATGCG

Table 4.4. Primer sequences and PCR conditions for MLST analysis used in this study.

Sl. No.	Genes	Primers (5' → 3')	PCR condition	No. of Cycle s	Amplicon Size (bp)
1.	adk	FP: CGCAATGCGTATCATTCTGC	95°C – 30'' 50°C – 1' 72°C – 1'	30	629
		RP: GAGCTGCGCGAACTTCAG			
2.	fumC	FP: GGCGCACAAACTCAACGC	95°C – 30'' 55°C – 1' 72°C – 1'		682
		RP: GTTCATCTGCTACGCGACGC			
3.	gyrB	FP: CACGCCGATAACTCTGTCTC			695
		RP: GCGTTCAGAGTACGGGTC			
4.	icd	FP: GTAGTTGTTCCGGCACAAGG	95°C – 30'' 52°C – 1' 72°C – 1'		865
		RP: GACGCAGCAGGATCTGTTG			
5.	mdh	FP: GGTGTGGCTGTCGATCTG	95°C – 30'' 55°C – 1' 72°C – 1'		722
		RP: GATTTACGCTCTTCCACGCC			
6.	purA	FP: CTGCTGTCCGAAGCATGTC	95°C – 30'' 52°C – 1' 72°C – 1'		692
		RP: CAGAAGCCAGACAGGGAG			
7.	recA	FP: GCGCGAAGGTAAAACCTG			664
		RP: CGCATTCGCTTTACCCTG			

4.4.7.2. Determination of evolutionary relationships among different UPECs and their STs and CCs: The concatenated MLST sequence data of the 23 UPECp and 29 UPECnp isolates was aligned using Clustal Omega (<https://www.ebi.ac.uk/Tools/msa/clustalo/>) and their evolutionary history was inferred using the maximum likelihood method based on Tamura-Nei Model in Molecular Evolutionary Genetic Analysis (MEGA) version 11.0 [40].

4.4.8. Statistical analysis: Statistical analysis was performed using SPSS version 26.0 (SPSS Inc., Chicago, IL, USA) and the Prism Software Package (Graphpad Prism Version 8.0, GraphPad Software Inc., San Diego, CA, USA). To compare the categorical variables, the chi-square test, fisher exact test, and logistic regression tests were used. $P < 0.05$ was considered to be statistically significant.

4.5. Result:

4.5.1. Bacterial strains: This part of the study is initiated with highly resistant imipenem-resistant isolates. 23 imipenem-resistant UPECp isolates and 29 UPECnp isolates were chosen for this study.

4.5.2. Phylogenetic analysis of the Imipenem-resistance UPECp and UPECnp isolates: Discrete distribution of different phylogroups (A, B1, B2, C, D, E, F, Clade V and NPP) were observed amongst 23 and 29 imipenem-resistant UPECp and UPECnp isolates respectively (Table 4.5). Phylogroup E was predominantly distributed, followed by NPP in the two population. Phylogroup C and F were only observed in the former group with complete absence of isolates with phylogenetic background D in the latter (Table 4.6.).

Table 4.5. Quadruplex PCR amplification result for UPECp and UPECnp isolates

Sl No.	Sample ID	<i>arpA</i>	<i>chuA</i>	<i>yjaA</i>	<i>TspE4.C2</i>	<i>arpA. gpE</i>	conclusion
UPECp isolates							
1.	P001	-	+	-	-		F
2.	P005	+	+	-	+	+	E
3.	P006	+	+	+	+	+	NPP
4.	P008	-	+	-	+		B2
5.	P012	-	+	-	-		F
6.	P030	-	+	-	-		F
7.	P031	-	+	-	+		B2
8.	P033	+	+	-	-	+	E
9.	P035	-	-	-	-	-	Clade V

10.	P036	+	-	-	-		A
11.	P040	+	-	-	-		A
12.	P043	+	-	+	-		C
13.	P044	+	-	-	-		A
14.	P049	+	+	+	-	+	E
15.	P055	-	-	-	+	-	Unknown
16.	P065	+	+	+	+	+	NPP
17.	P069	-	-	-	+		Unknown
18.	P070	+	-	-	+		B1
19.	P091	+	-	+	+		Unknown
20.	P108	-	-	-	-		Clade V
21.	P109	+	+	-	+	+	E
22.	P110	+	+	-	+	+	E
23.	P124	+	+	+	+		NPP
UPECnp isolates							
1.	NP006	+	+	+	+		NPP
2.	NP038	+	+	-	-		E
3.	NP040	+	+	+	+		NPP
4.	NP042	-	-	-	-		Clade V
5.	NP046	+	+	+	+		NPP
6.	NP047	+	-	-	+		B1
7.	NP048	-	+	-	+		B2
8.	NP049	+	+	-	+	+	E
9.	NP051	+	+	-	+	+	E
10.	NP052	+	+	+	+	+	NPP
11.	NP054	+	+	-	+	-	D
12.	NP061	+	+	-	-	-	D
13.	NP062	+	+	+	+	+	NPP
14.	NP064	+	+	+	+	+	NPP
15.	NP065	+	+	-	+	+	E
16.	NP073	-	+	-	+	+	B2
17.	NP074	+	+	-	+	+	E
18.	NP075	+	+	-	+	+	E
19.	NP076	-	-	-	+	+	Unknown
20.	NP078	+	+	-	+	+	E
21.	NP080	+	+	-	+	+	E
22.	NP093	-	+	-	+	-	B2
23.	NP107	+	+	-	+	+	E
24.	NP116	-	-	-	+	+	Unknown
25.	NP117	-	+	+	+	-	B2
26.	NP119	-	+	-	+	-	B2
27.	NP121	+	+	+	+	-	NPP
28.	NP124	+	-	-	-	-	A
29.	NP126	-	+	-	+	+	B2

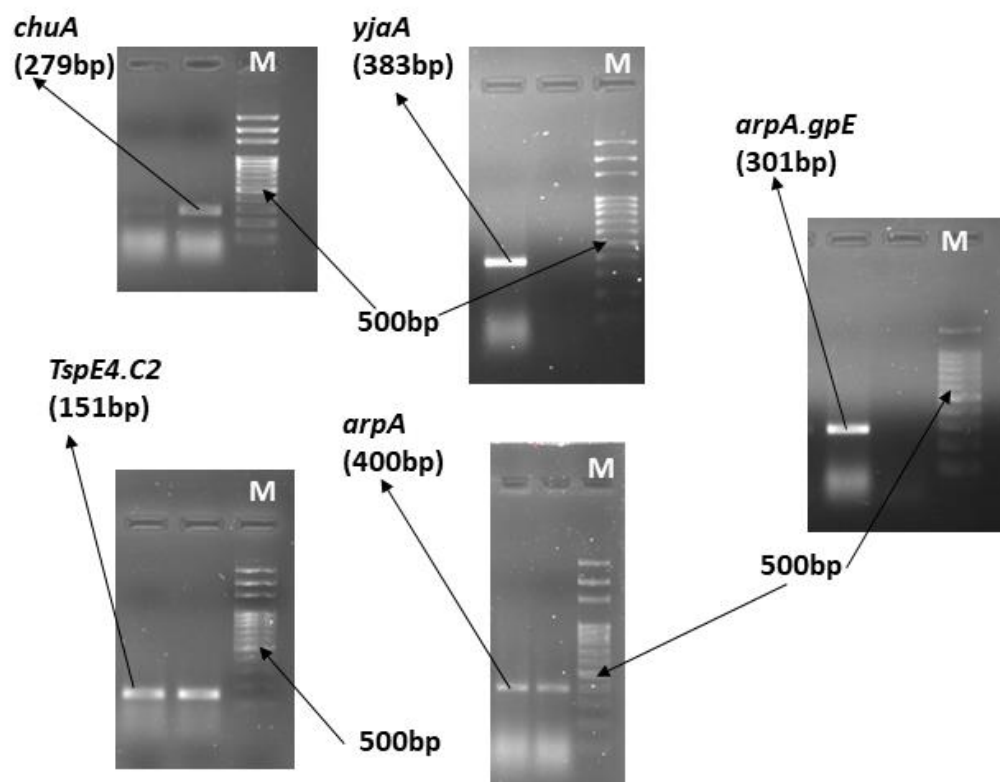


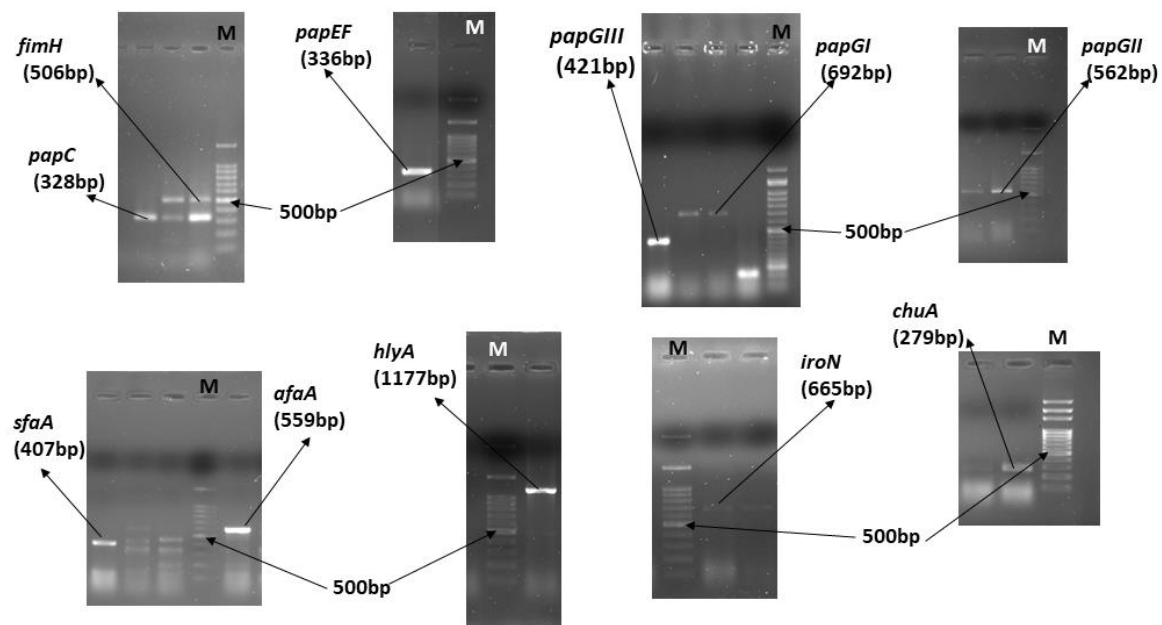
Figure 4.2: Representative pictures of the quadruplex genes *chuA*, *yjaA*, *TspE4.C2* and *arpA* genes, and *arpA.gpE* (for E-specific phylo-group). M represents the DNA marker lane (100 bp DNA ladder).

Table 4.6. Comparison between imipenem-resistant UPECp (n=23) and UPECnp (n=29) isolates with respect to their phylogenetic background and virulence score

	UPECp (n=23)	UPECnp (n=29)	Odds ratio ($\alpha=95\%$)	Fisher P
Phylogenetic Groups				
A	3 (13.04%)	1 (3.45%)	4.20 (0.41 – 43.37)	0.31
B1	1 (4.35%)	1 (3.45%)	1.27 (0.07 – 21.51)	1
B2	2 (8.70%)	6 (20.69%)	0.37 (0.07 – 2.011)	0.28
C	1 (4.35%)	0 (0.00%)	-	-
D	0 (0.00%)	2 (6.90%)	-	-
E	5 (21.74%)	9 (31.03%)	0.62 (0.17- 2.19)	0.54
F	3 (13.04%)	0 (0.00%)	-	-
Clade V	2 (8.70%)	1 (3.45%)	2.67 (0.23 – 31.41)	0.58
NPP	3 (8.70%)	7 (21.13%)	0.47 (0.11 – 2.08)	0.48
Unknown	3 (13.04%)	2 (6.90%)	2.03 (0.31 – 13.28)	0.64
Virulence Score, median (range)	8 (1-14)	9 (1-14)	0.82 (0.24 – 2.82)	1

4.5.3. Distribution of virulence factor genes (VFGs) in imipenem-resistant UPECp and UPECnp isolates: The presence and absence of twenty-one VFGs in 23 UPECp and 29 UPECnp isolates were depicted in Table 4.7. The prevalence and statistical significance of these VFGs in these two groups were depicted in Table 4.8.

Occurrence of twenty-one VFGs in the two populations studied indicated statistically significant ($P < .05$) incidence of *fimH*, *papC*, *papEF*, *papGII*, *hlyA*, *chuA*, *kps MTII*, *iucD*, *flu*, *csgA* in both population whereas prevalence of *iroN* in UPECp and *iha*, *cnf1* in UPECnp population were statistically significant amongst the respective batch of isolates. Overall prevalence of *fimH*, *papC*, *papGI*, *afaA*, *iroN*, *iucD*, *cdtB*, *ibeA*, and *csgA* genes were higher in UPECp isolates than in UPECnp isolates. On the contrary, prevalence of *papEF*, *papGII*, *papGIII*, *sfaA*, *hlyA*, *chuA*, *kps MTII*, *iha*, *cnf1*, *vat*, *flu*, *usp* genes were higher in UPECnp than in UPECp isolates (Table 4.7). Furthermore, difference in the occurrence of *chuA* between UPECp and UPECnp population were statistically significant ($P < .05$).



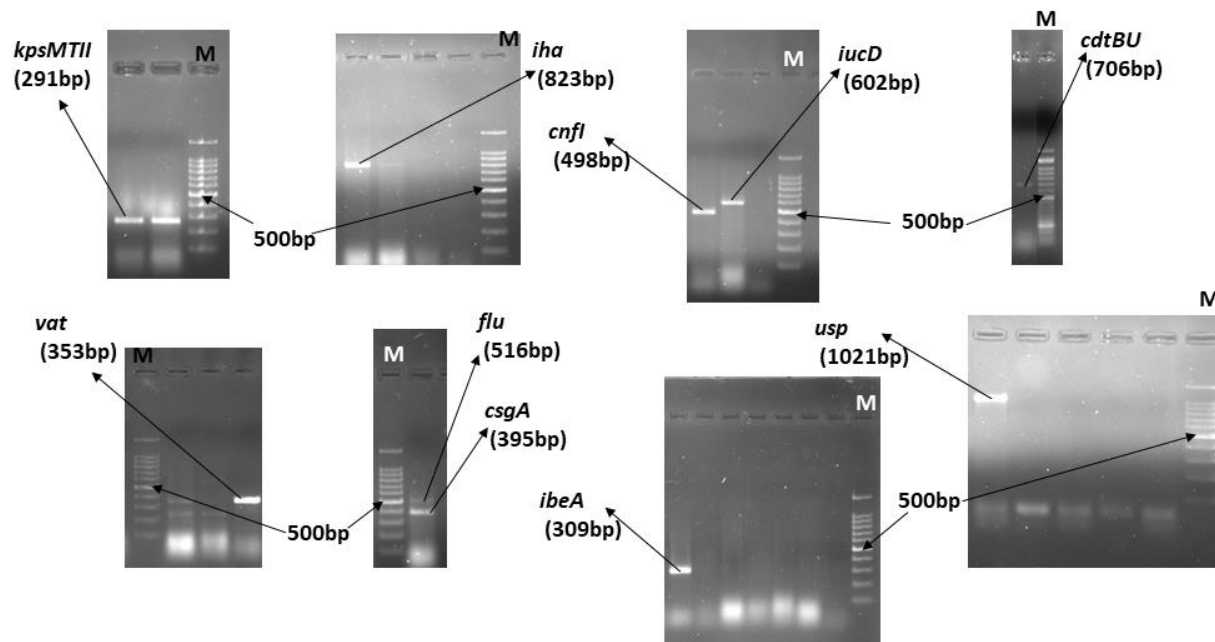


Figure 4.3: Representative picture of the adhesion genes (*fimH*, *papC*, *papEF*, *papGI*, *papGII*, *papGIII*, *sfaA*, *afaA*); toxin genes (*hlyA*, *iroN*, *chuA*, *ihfA*, *cnfI*, *iucD*, *cdtBU*, *vat*, *ibeA*, *usp*), capsule gene (*kpsMTII*), biofilm forming genes (*flu*, *csgA*) in agarose gel electrophoresis. M represents the DNA marker lane (100 bp DNA ladder).

Table 4.7. Results for virulence genes distribution in UPECp and UPECnp isolates.

	<i>fimH</i>	<i>papC</i>	<i>papEF</i>	<i>papGI</i>	<i>papGII</i>	<i>papGIII</i>	<i>sfaA</i>	<i>afaA</i>	<i>hlyA</i>	<i>iroN</i>	<i>chuA</i>	<i>kps MTII</i>	<i>ihfA</i>	<i>iucD</i>	<i>cdtBU</i>	<i>cnfI</i>	<i>vat</i>	<i>ibeA</i>	<i>flu</i>	<i>csgA</i>	<i>usp</i>
UPECp isolates																					
P001	+	-	+	-	-	-	-	-	-	+	+	+	-	+	-	-	+	+	-	-	-
P005	+	-	-	+	-	+	-	-	-	-	+	-	-	+	-	-	-	-	+	+	-
P006	+	+	+	-	-	+	+	-	+	+	+	+	-	+	-	+	+	+	-	+	-
P008	+	+	-	+	-	-	-	+	+	-	+	+	-	-	-	-	-	-	-	+	-
P012	+	+	+	-	+	-	-	+	+	+	+	+	+	+	-	-	-	-	+	+	-
P030	+	+	+	-	+	-	-	+	+	-	+	+	+	+	-	-	-	-	-	+	-
P031	+	+	-	-	+	-	-	+	-	-	+	-	-	+	-	-	-	-	+	+	-
P033	+	+	-	-	+	-	-	+	-	-	+	+	-	+	-	-	-	-	+	+	-
P035	+	+	-	-	+	-	-	-	+	+	-	-	-	-	-	-	-	-	-	-	-
P036	+	+	-	-	-	-	+	-	-	-	-	-	+	+	+	-	-	-	+	+	-
P040	+	-	-	-	-	-	-	-	-	+	-	-	-	+	-	-	-	-	+	+	-
P043	+	+	-	+	-	-	-	-	-	-	-	-	+	+	+	-	-	-	+	+	-
P044	-	-	-	-	-	-	-	-	-	-	-	-	+	-	-	-	-	-	-	-	-
P049	+	+	-	+	-	-	+	-	-	+	+	+	+	+	-	-	-	-	+	+	-
P055	+	-	-	-	-	-	+	-	-	-	-	-	-	+	-	-	-	-	-	-	-
P065	+	+	+	-	-	+	+	-	+	+	+	+	-	-	-	+	+	-	-	+	-
P069	+	+	+	-	+	-	-	-	+	+	-	-	-	+	+	-	-	-	-	-	-

P070	+	+	+	-	+	+	-	-	-	+	-	+	+	+	+	-	-	-	-	+	-
P091	+	+	+	-	-	-	-	-	-	+	-	-	-	+	+	-	-	-	+	+	-
P108	+	+	-	-	+	-	-	-	-	+	-	-	-	-	-	+	-	-	-	-	-
P109	-	+	+	-	+	-	-	+	+	+	+	+	-	+	-	-	-	-	+	+	-
P110	+	+	-	-	-	+	+	-	+	+	+	-	-	-	-	-	-	-	+	-	-
P124	+	+	+	-	+	+	+	-	+	+	+	-	+	+	-	-	-	-	+	+	-
UPECnp isolates																					
NP006	+	+	-	-	-	+	+	-	-	-	+	+	+	+	-	+	+	-	+	+	-
NP038	+	+	-	-	-	-	-	-	-	-	+	-	-	-	-	+	-	-	-	-	-
NP040	+	+	-	-	+	-	+	-	+	-	+	+	+	+	-	+	-	-	+	+	-
NP042	+	-	-	-	-	-	-	-	-	-	-	-	-	-	-	+	-	-	-	-	-
NP046	+	+	+	-	-	+	+	-	-	+	+	+	+	-	-	+	+	-	-	+	-
NP047	-	-	-	-	-	-	+	-	-	-	-	-	-	-	-	-	-	-	-	-	-
NP048	+	+	+	-	+	-	-	-	-	+	+	-	-	-	-	-	+	-	+	+	-
NP049	+	-	-	-	-	+	-	-	-	-	+	-	+	-	-	-	-	-	+	+	-
NP051	+	+	+	-	-	-	-	+	-	-	+	-	+	+	-	-	-	-	+	+	-
NP052	+	+	+	-	-	+	-	-	+	-	+	+	-	+	-	+	-	-	+	+	-
NP054	-	+	+	-	+	-	-	+	+	-	+	+	-	+	-	-	-	-	+	+	-
NP061	-	-	-	-	-	-	-	-	-	-	+	+	-	-	-	+	-	-	-	-	-
NP062	+	+	+	-	+	-	-	-	-	-	+	+	-	-	-	+	-	-	-	-	-
NP064	+	+	+	-	+	+	-	-	-	-	+	+	-	+	-	+	-	-	+	-	-
NP065	+	+	+	-	+	-	-	-	+	-	+	+	-	+	-	-	-	-	+	-	-
NP073	+	+	+	-	-	+	-	-	-	-	+	+	+	+	-	-	-	-	+	+	-
NP074	+	+	-	-	+	+	-	-	-	-	+	+	-	-	-	-	-	-	-	+	-
NP075	+	+	-	-	-	-	-	-	-	-	+	-	+	-	-	-	-	-	+	-	-
NP076	+	+	+	-	+	+	-	-	+	+	-	-	-	-	-	+	+	-	-	+	+
NP078	+	-	+	-	+	-	-	-	-	+	+	-	-	+	-	+	-	-	+	-	-
NP080	+	+	+	-	+	-	+	-	+	+	+	+	+	+	-	-	-	-	+	+	-
NP093	-	+	-	-	-	-	-	-	-	-	+	-	-	+	-	+	-	-	+	-	-
NP107	+	-	-	-	+	-	+	-	-	-	+	+	-	+	-	+	-	-	+	-	-
NP116	+	+	-	-	-	-	-	-	-	+	-	-	+	-	-	-	-	-	+	-	-
NP117	+	+	-	-	+	-	-	-	-	+	+	+	+	+	-	-	+	-	+	+	-
NP119	+	+	+	-	+	-	-	+	+	+	+	+	+	+	-	-	-	-	+	+	+
NP121	+	+	+	-	+	-	-	-	-	-	+	+	+	+	-	-	-	-	+	+	-
NP124	+	-	-	-	-	-	-	-	-	-	-	-	-	-	-	-	-	-	-	-	-
NP126	+	-	-	-	-	-	+	-	-	-	+	-	+	+	-	-	-	-	-	+	-

Table 4.8. Distribution of VFG's and PAIs in imipenem-resistant UPECp and UPECnp isolates

Genes	Imipenem-resistance				Odds ratio ($\alpha=95\%$)	P value (Fisher exact)
	UPECp isolates	P values	UPECnp isolates	P values		
Virulence factor genes (VFGs)						
<i>fimH</i>	21 (91.30%)	<0.05	25 (86.21%)	<0.05	1.68 (0.28 – 10.1)	0.68
<i>papC</i>	18 (78.26%)	<0.05	21 (72.41%)	<0.05	1.37 (0.38 – 4.95)	0.75
<i>chuA</i>	13 (56.52%)	<0.05	24 (82.76%)	<0.05	0.27 (0.08 – 0.96)	0.06
<i>iucD</i>	17 (73.91%)	<0.05	16 (55.17%)	<0.05	2.30 (0.71 – 7.52)	0.25
<i>csgA</i>	16 (69.57%)	<0.05	16 (55.17%)	<0.05	1.86 (0.59 – 5.87)	0.39
<i>flu</i>	12 (52.17%)	<0.05	19 (65.51%)	<0.05	0.57 (0.19 – 1.76)	0.4
<i>kpsmtII</i>	10 (43.48%)	<0.05	16 (55.17%)	<0.05	0.63 (0.21 – 1.88)	0.58
<i>papEF</i>	10 (43.48%)	<0.05	14 (48.28%)	<0.05	0.82 (0.27 – 2.48)	0.78
<i>papGII</i>	10 (43.48%)	<0.05	14 (48.28%)	<0.05	0.82 (0.27 – 2.48)	0.78
<i>hlyA</i>	10 (43.48%)	<0.05	13 (44.83%)	<0.05	0.95 (0.31 – 2.85)	1
<i>iroN</i>	14 (60.87%)	<0.05	9 (31.03%)	<0.05	3.46 (1.10 – 10.91)	0.05
<i>iha</i>	8 (34.78%)	<0.05	13 (44.83%)	<0.05	0.66 (0.21 – 2.03)	0.57
<i>sfaA</i>	7 (30.43%)	<0.05	9 (31.03%)	<0.05	0.97 (0.30 – 3.19)	1

<i>cnfI</i>	3 (13.04%)	0.083	13 (44.83%)	<0.05	0.18 (0.05 – 0.76)	0.02
<i>papGIII</i>	6 (26.09%)	<0.05	8 (27.59%)	<0.05	0.93 (0.27 – 3.19)	1
<i>afaA</i>	6 (26.09%)	<0.05	3 (10.34%)	0.083	3.06 (0.67 – 13.91)	0.16
<i>vat</i>	3 (13.04%)	0.083	5 (17.24%)	<0.05	0.72 (0.15 – 3.39)	1
<i>papGI</i>	4 (17.39%)	<0.05	0 (0.00%)	-	-	-
<i>cdtB</i>	4 (17.39%)	<0.05	0 (0.00%)	-	-	-
<i>ibeA</i>	2 (8.70%)	0.162	0 (0.00%)	-	-	-
<i>usp</i>	0 (0.00%)	-	2 (6.90%)	0.161	-	-
Pathogenic islands (PAIs)						
PAI III₅₃₆	1 (4.34%)	-	15 (51.72%)	<0.05	0.04 (0.005 – 0.36)	<0.052
PAI IV₅₃₆	19 (82.61%)	<0.05	26 (89.66%)	<0.05	0.55 (0.11 – 2.74)	0.69
PAI I_{CFT073}	2 (8.69%)	-	3 (10.34%)	-	0.83 (0.13 – 5.41)	1
PAI II_{CFT073}	0 (0.00%)	-	1 (3.44%)	-	-	-
PAI I_{J96}	1 (4.34%)	-	0 (0.00%)	-	-	-
PAI II_{J96}	2 (8.69%)	-	0 (0.00%)	-	-	-

4.5.4. Correlation between the VFGs in UPECp and UPECnp population: A significant correlation has been observed between *papC* and *hlyA* and between *papEF* and *hlyA* in both the population. All of the correlations were moderate, except between *papEF* and *hlyA* in UPECnp, which was weak. Additionally, significant moderate positive correlations have been observed between *papC* and *papGII*; *papEF* and *iroN*, *kps MTII*; *hlyA* and *chuA*; *chuA* and *kps MTII*; *iucD* and *flu*, *csgA*; *flu* and *csgA* in UPECp population (Figure 4.4a). Moreover, in UPECnp isolates, a significant weak positive correlation has been observed between *papC* and *kps MTII*, *csgA*; *hlyA* and *csgA*; and a significant moderate positive correlation have been observed between *papEF* and *papGII*; *papGII* and *kps MTII*; *chuA* and *kps MTII*; *chuA* and *iucD*, *flu*; *kps MTII* and *iucD*; *iha* and *csgA*; *iucD* and *flu* in UPECnp population (Figure 4.4b). Furthermore, A significant weak negative correlation have been observed between *iha* and *cnfI* in UPECnp isolates (Figure 4.4). Therefore, correlations between the VFGs in the two populations were very discrete.

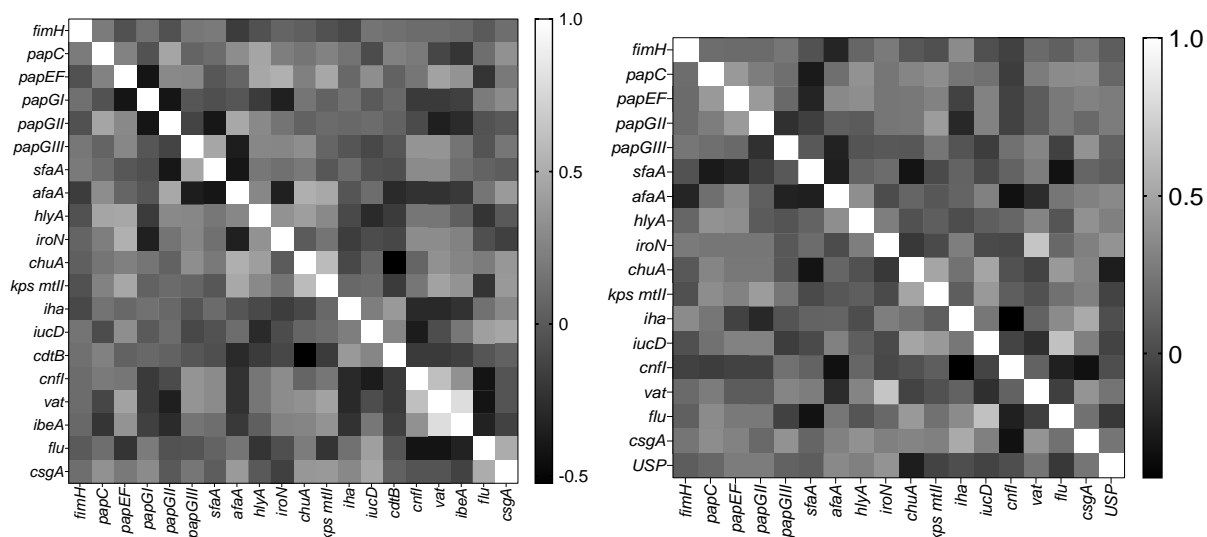


Figure 4.4. Statistical representations of the correlations between twenty-one VFGs among (a) UPECp isolates (left) and (b) UPECnp isolates (right). Correlations were individually computed among UPECp and UPECnps using GraphPad Prism 8 (Prism Software Package). Heat maps were generated on the correlation coefficient values represented by the color keys that ranged from (-) 0.5 (black) to (+)1 (white).

4.5.5. Distribution of pathogenic islands (PAIs) in imipenem-resistant UPECp and UPECnp isolates:

The presence and absence of different PAIs were addressed in Table 4.9. PAI IV₅₃₆ was most prevalent in both of isolates. The prevalence of PAI IV₅₃₆ was statistically significant in both group of isolates. Additionally, the prevalence of PAI III₅₃₆ was also statistically significant in UPECnp population. (Table 4.8).

Table 4.9. Results for pathogenic islands distribution in UPECp and UPECnp isolates.

	Multiplex PAI-A			Multiplex PAI-B				
	PAI III ₅₃₆	PAI IV ₅₃₆	PAI II _{CFT073}	PAI I ₅₃₆	PAI II ₅₃₆	PAI I _{CFT073}	PAI I _{J96}	PAI II _{J96}
UPECp isolates								
P001	-	+	-	-	-	-	-	-
P005	-	+	-	-	-	-	+	+
P006	+	+	-	-	-	-	-	-
P008	-	+	-	-	-	+	-	+
P012	-	+	-	-	-	+	-	-
P030	-	+	-	-	-	-	-	-
P031	-	+	-	-	-	-	-	-

P033	-	+	-	-	-	-	-	-
P035	-	-	-	-	-	-	-	-
P036	-	+	-	-	-	-	-	-
P040	-	+	-	-	-	-	-	-
P043	-	+	-	-	-	-	-	-
P044	-	+	-	-	-	-	-	-
P049	-	+	-	-	-	-	-	-
P055	-	+	-	-	-	-	-	-
P065	-	+	-	-	-	-	-	-
P069	-	+	-	-	-	-	-	-
P070	-	+	-	-	-	-	-	-
P121	-	+	-	-	-	-	-	-
P108	-	-	-	-	-	-	-	-
P109	-	+	-	-	-	-	-	-
P110	-	-	-	-	-	-	-	-
P124	-	-	-	-	-	-	-	-
UPECnp isolates								
NP006	+	+	-	-	-	-	-	-
NP038	+	+	-	-	-	-	-	-
NP040	-	+	-	-	-	-	-	-
NP042	+	+	-	-	-	-	-	-
NP046	+	+	-	-	-	-	-	-
NP047	-	-	-	-	-	-	-	-
NP048	-	+	-	-	-	-	-	-
NP049	-	+	-	-	-	-	-	-
NP051	-	+	-	-	-	-	-	-
NP052	-	+	-	-	-	-	-	-
NP054	-	+	-	-	-	-	-	-
NP061	+	+	-	-	-	-	-	-
NP062	+	+	-	-	-	-	-	-
NP064	+	+	-	-	-	-	-	-
NP065	-	+	-	-	-	-	-	-
NP073	+	+	+	-	-	+	-	-
NP074	-	+	-	-	-	-	-	-
NP075	-	+	-	-	-	-	-	-
NP076	+	-	-	-	-	-	-	-
NP078	+	+	-	-	-	-	-	-
NP080	+	+	-	-	-	-	-	-
NP093	+	+	-	-	-	-	-	-
NP107	+	+	-	-	-	-	-	-

NP116	+	+	-	-	-	-	-	-
NP117	+	+	-	-	-	-	-	-
NP119	-	+	-	-	-	+	-	-
NP121	-	+	-	-	-	+	-	-
NP124	-	-	-	-	-	-	-	-
NP126	-	+	-	-	-	-	-	-

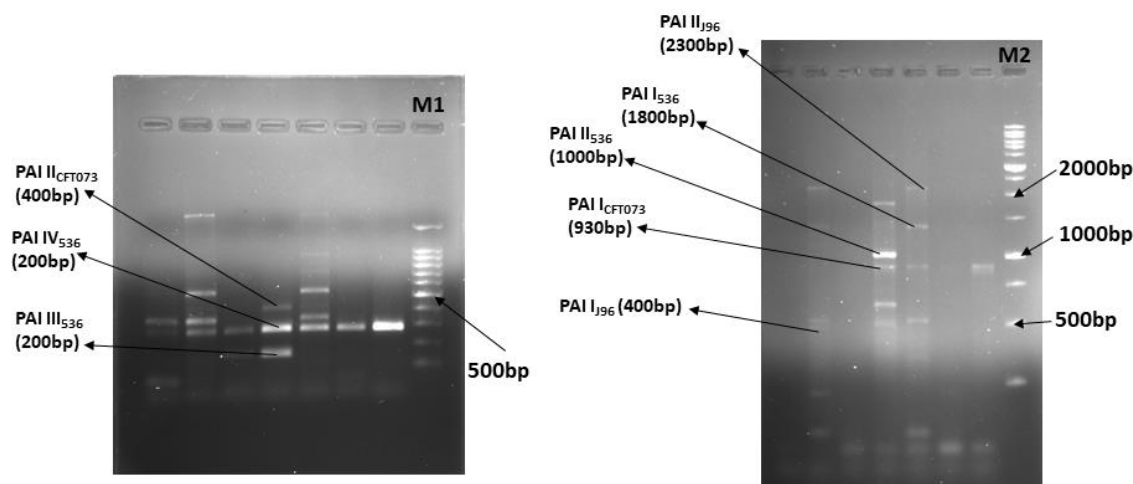


Figure 4.5: Representative pictures of PAI I₅₃₆, PAI II₅₃₆, PAI III₅₃₆, PAI IV₅₃₆, PAI I_{CFT073}, PAI II_{CFT073}, PAI I_{J96}, PAI II_{J96} markers on Agarose gel electrophoresis. M1 (100bp DNA ladder) and M2 (1kb DNA ladder) represents the DNA marker lane.

4.5.6. Correlation between PAIs in UPECp and UPECnp population: Apparently, no significant correlation could be drawn between UPECp and UPECnp isolates in these two populations.

4.5.7. Correlation between PAIs and VFGs in UPECp and UPECnp population: A statistically significant moderate positive correlation has been observed between PAI IV₅₃₆ and *iucD*, *csgA* in UPECp population. In UPECnp population, strong positive correlation has been observed between PAI IV₅₃₆ and *chuA*, low positive correlation has been observed between PAI IV₅₃₆ and *kps MTII* and moderate positive correlation has been observed between PAI IV₅₃₆ and *flu* gene. Additionally, a moderate negative correlation has been observed in between PAI III₅₃₆ and *cnfI* gene (Table 4.10).

Table 4.10. Correlation between statistically significant prevalent PAI genes alongwith VFGs of imipenem resistant UPECp and UPECnp isolates

		PAI IV ₅₃₆ P		PAI IV ₅₃₆ NP	PAI III ₅₃₆ NP
	<i>finHnp</i>	-0.142	<i>finHnp</i>	0.192	0.014
	<i>papCp</i>	-0.242	<i>papCnp</i>	0.297	0.021
	<i>papEFp</i>	0.171	<i>papEFnp</i>	0.102	-0.033
	<i>papGlp</i>	0.211	<i>papGlnp</i>	^a	^a
	<i>papGllp</i>	-0.292	<i>papGllnp</i>	0.102	-0.033
	<i>papGlllp</i>	-0.250	<i>papGlllnp</i>	-0.044	0.133
	<i>sfaAp</i>	-0.195	<i>sfaAnp</i>	-0.506**	0.051
	<i>afaAp</i>	0.273	<i>afaAnp</i>	0.115	-0.352
	<i>hlyAp</i>	-0.292	<i>hlyAnp</i>	0.079	-0.100
	<i>iroNp</i>	-0.368	<i>iroNnp</i>	-0.017	0.350
	<i>chuAp</i>	0.060	<i>chuAnp</i>	0.744**	-0.076
	<i>kpsmllp</i>	0.402	<i>kpsmllnp</i>	0.377*	0.100
	<i>ihap</i>	0.094	<i>ihannp</i>	0.306	-0.100
	<i>iucDp</i>	0.511*	<i>iucDnp</i>	0.77*	-0.038
	<i>cdtBp</i>	0.211	<i>cdtBnp</i>	^a	^a
	<i>cnflp</i>	-0.163	<i>cnflnp</i>	0.079	-0.593**
	<i>vatp</i>	0.178	<i>vatnp</i>	-0.145	0.258
	<i>ibeAp</i>	0.142	<i>ibeAnp</i>	^a	^a
	<i>flup</i>	0.020	<i>flunp</i>	0.468*	-0.120
	<i>csgAp</i>	0.444*	<i>csgAnp</i>	0.149	-0.316
	<i>uspp</i>	^a	<i>USPnp</i>	-0.354	-0.009

Table 4.11.

A: Virulence factor gene (VFG) scores, distribution of pathogenic islands, phylogenetic property, and resistance pattern against meropenem; MR, ertapenem; ETR of the imipenem-resistant UPECp (n=23) isolates

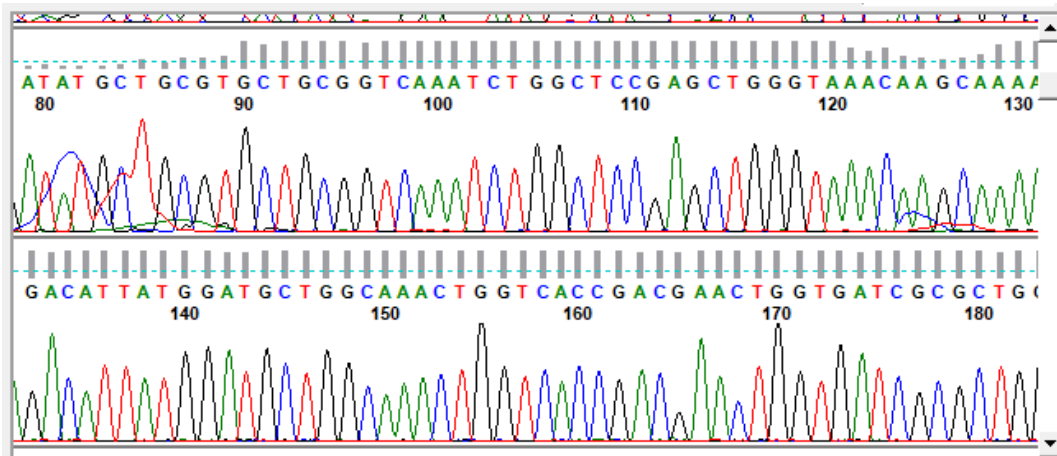
Sample ID	VFG score	PAI distribution	Phylogenic group	Resistance pattern
P001	8	PAI IV536	F	MR, ETR
P005	7	PAI IV536, PAI IJ96, PAI IJ96	E	MR, ETR
P006	14	PAI III536, PAI IV536	NPP	MR, ETR
P008	8	PAI IV536, PAI ICFT073, PAI IJ96	B2	MR, ETR
P012	13	PAI IV536, PAI ICFT073	F	MR
P030	11	PAI IV536	F	ETR
P031	8	PAI IV536	B2	MR
P033	9	PAI IV536	E	MR
P035	5	-	Clade V	MR, ETR
P036	8	PAI IV536	A	MR, ETR
P040	5	PAI IV536	A	MR
P043	8	PAI IV536	C	MR, ETR
P044	1	PAI IV536	A	ETR
P049	11	PAI IV536	E	-

P055	3	PAI IV536	Unknown	MR, ETR
P065	12	PAI IV536	NPP	-
P069	8	PAI IV536	Unknown	-
P070	11	PAI IV536	B1	-
P091	7	PAI IV536	Unknown	-
P108	5	-	Clade V	-
P109	11	PAI IV536	E	-
P110	8	-	E	-
P124	12	-	NPP	-

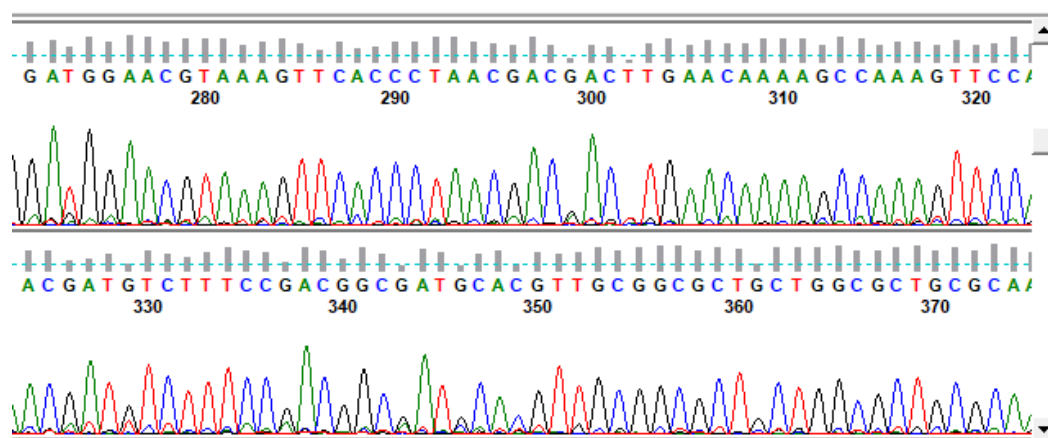
B: Virulence factor gene (VFG) scores, distribution of pathogenic islands, phylogenetic property, and resistance pattern against meropenem; MR, ertapenem; ETR of the imipenem-resistant UPECnp (n=29) isolates

Sample ID	VFG Score	PAI distribution	Phylogenic Groups	Resistance pattern
NP006	14	PAI III536, PAI IV536	NPP	-
NP038	5	PAI III536, PAI IV536	E	MR, ETR
NP040	12	PAI IV536	NPP	-
NP042	3	PAI III536, PAI IV536	Clade V	ETR
NP046	13	PAI III536, PAI IV536	NPP	MR, ETR
NP047	1	-	B1	-
NP048	10	PAI IV536	B2	MR, ETR
NP049	6	PAI IV536	E	MR, ETR
NP051	10	PAI IV536	E	MR, ETR
NP052	11	PAI IV536	NPP	MR, ETR
NP054	10	PAI IV536	D	-
NP061	3	PAI III536, PAI IV536	D	MR, ETR
NP062	7	PAI III536, PAI IV536	NPP	-
NP064	10	PAI III536, PAI IV536	NPP	MR, ETR
NP065	9	PAI IV536	E	-
NP073	10	PAI III536, PAI IV536, PAI IICFT073, PAI ICFT073	B2	-
NP074	7	PAI IV536	E	-
NP075	5	PAI IV536	E	-
NP076	12	PAI III536	Unknown	-
NP078	8	PAI III536, PAI IV536	E	-
NP080	13	PAI III536, PAI IV536	E	ETR
NP093	5	PAI III536, PAI IV536	B2	ETR
NP107	8	PAI III536, PAI IV536	E	MR, ETR
NP116	5	PAI IV536	Unknown	MR, ETR
NP117	11	PAI III536, PAI IV536	B2	ETR
NP119	14	PAI IV536, PAI ICFT073	B2	ETR
NP121	10	PAI IV536, PAI ICFT073	NPP	ETR
NP124	2	-	A	-
NP126	6	PAI IV536	B2	-

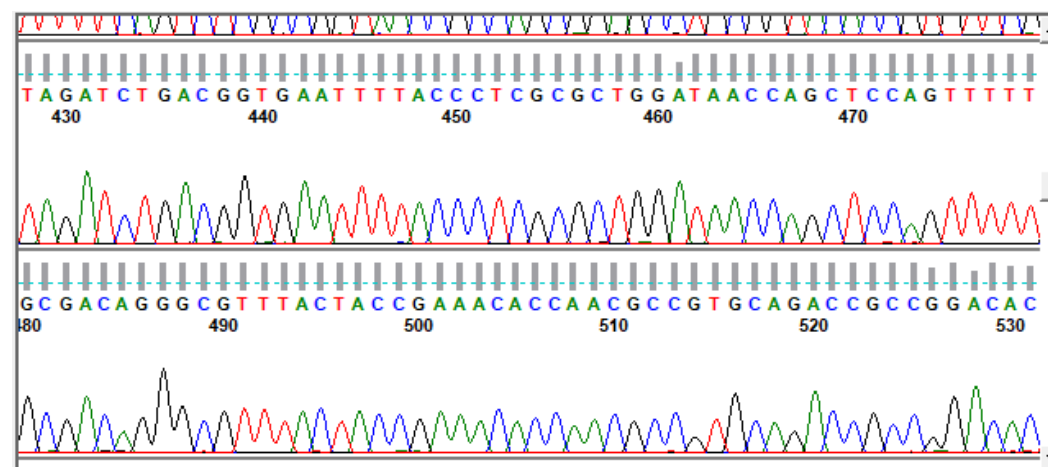
4.5.8. MLST analysis of UPECp and UPECnp isolates: Several alleles of the seven gene housekeeping genes were observed from the MLST analysis performed on the 52 (UPECp = 23, UPECnp = 29) imipenem-resistant UPEC isolates. One representative isolate from each population and its respective chromatogram (part of individual genes) of each of seven housekeeping genes indicating their respective alleles had been depicted below in Figure 4.6 and Figure 4.7. Number of alleles observed for each of the seven housekeeping genes were *adk* = 9 [UPECp = 2 (22.22%); UPECnp = 1 (11.11%); common = 6 (66.67%)], *fumC* = 11 [UPECp = 2 (18.18%); UPECnp = 4 (36.36%), common = 5 (45.45%)], *gyrB* = 14 [UPECp = 3 (21.42%), UPECnp = 2 (14.29%), common = 9 (64.29%)], *icd* = 16 [UPECp = 6 (37.5%), UPECnp = 5 (31.25%), common = 5 (31.25%)], *mdh* = 13 [UPECp = 3 (23.08%), UPECnp = 5 (38.46%), common = 5 (38.46%)], *purA* = 13 [UPECp = 4 (30.77%), UPECnp = 4 (30.77%), common = 5 (38.46%)], *recA* = 10 [UPECp = 1 (10%), UPECnp = 1 (10%), common = 8 (80%)]. Among UPECp, the alleles that most frequently occurred at each of the seven locus were *adk* 6 [n = 9], *fumC* 11 [n = 8], *gyrB* 4 [n = 8], *icd* 8 [n = 6], *mdh* 8 [n = 10], *purA* 8 [n = 6], *recA* 2 [n = 8]. However, most frequently occurring alleles among UPECnp isolates were *adk* 6 [n = 10], *fumC* 4 [n = 8], *gyrB* 47 [n = 7], *icd* 13 [n = 5], *mdh* 36 [n = 6], *purA* 28 [n = 6], *recA* 7 [n = 9] (Table 4.12).



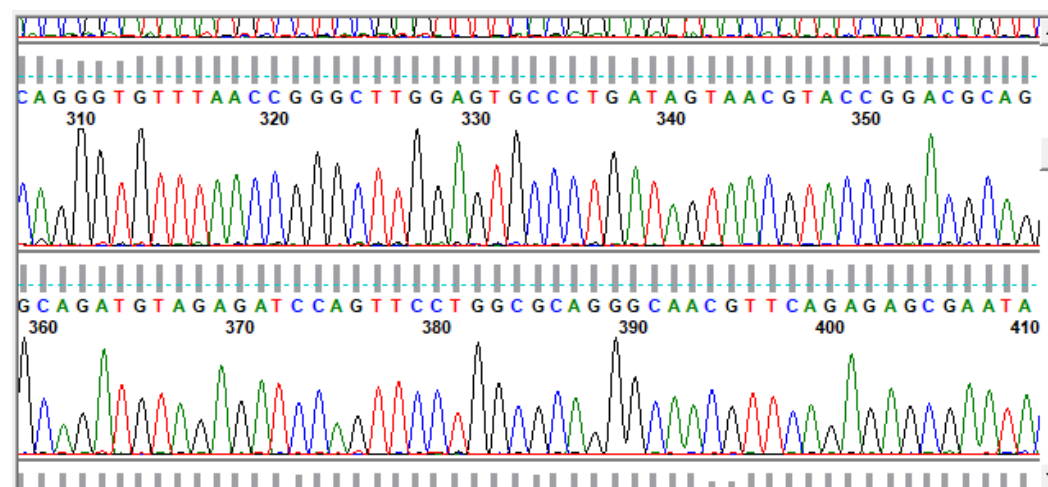
(a)



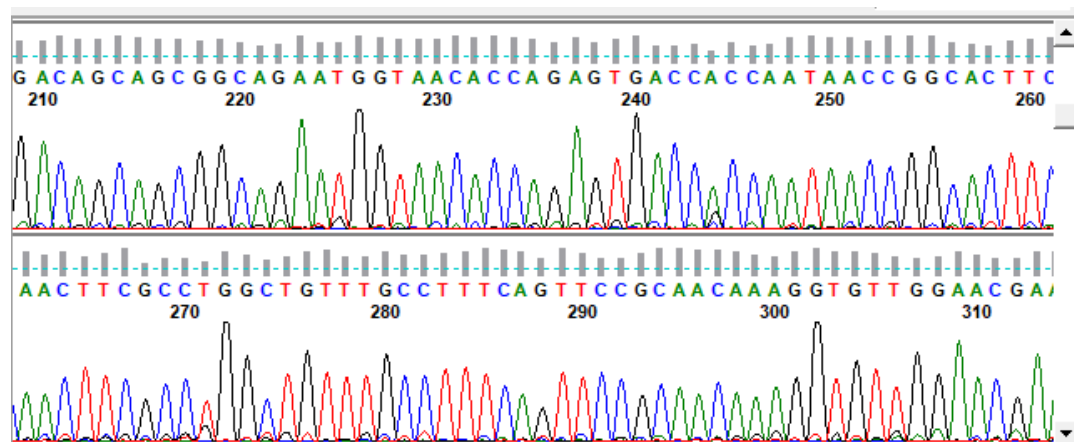
(b)



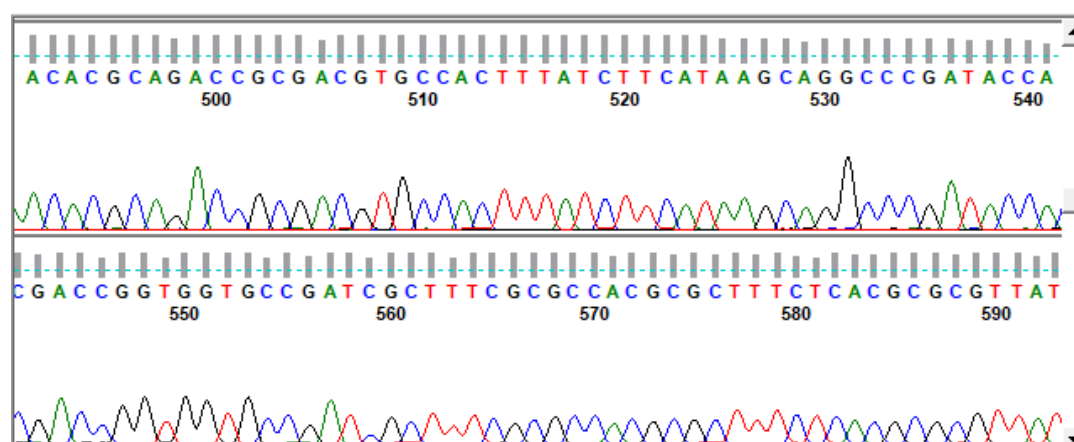
(c)



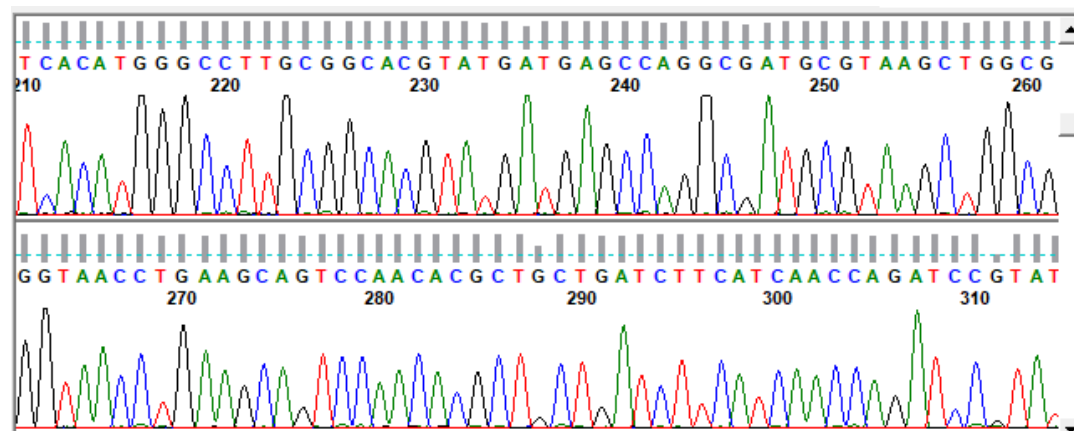
(d)



(e)

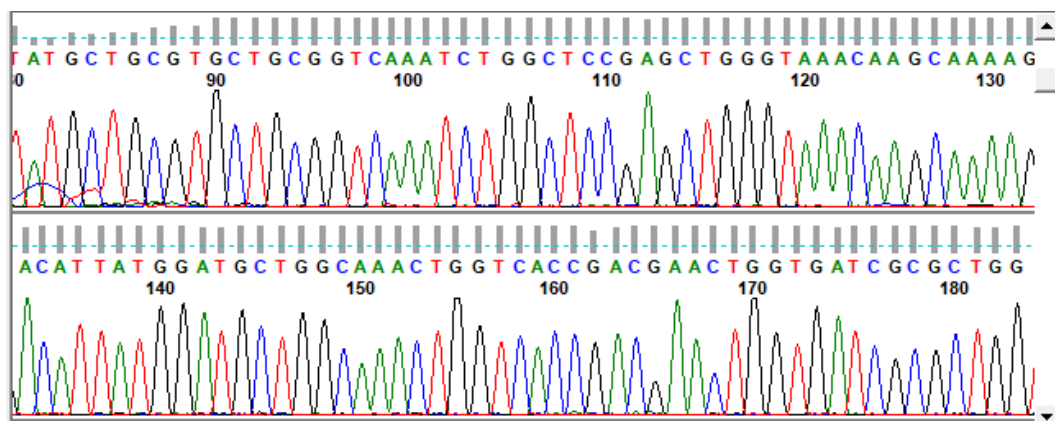


(f)

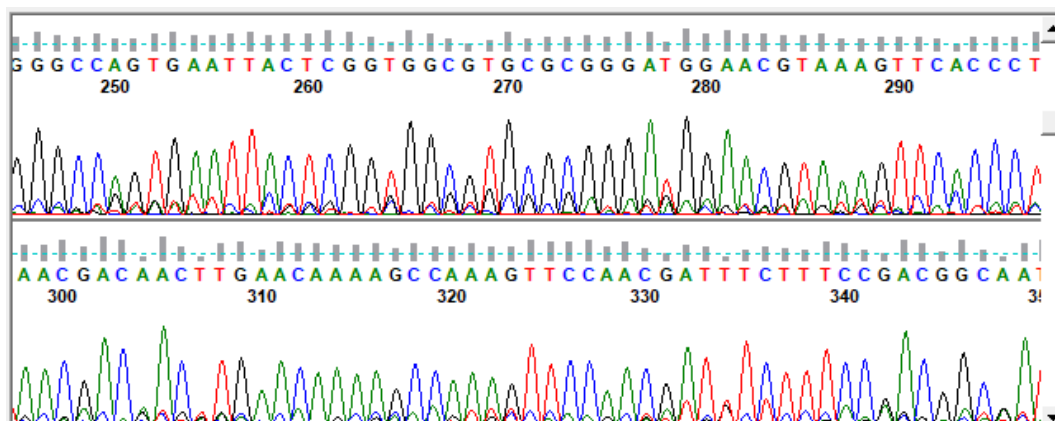


(g)

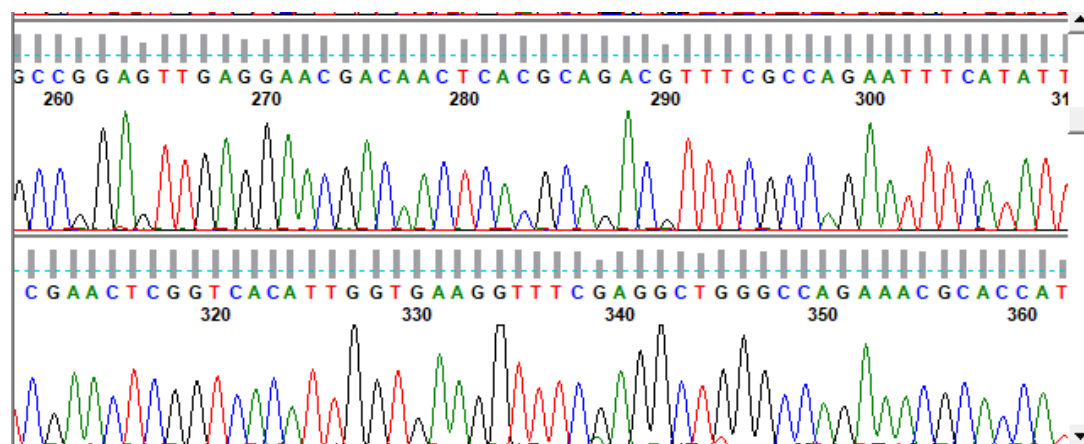
Figure 4.6: The representative chromatograms of seven different housekeeping genes obtained after sequencing of an isolate P033 (a) *adk* [(536bp), allele no. 10]; (b) *fumC* [(469bp), allele no. 11]; (c) *gyrB* [(460bp), allele no. 4], (d) *icd* [(518bp), allele no. 8], (e) *mdh* [(452bp), allele no. 8], (f) *purA* [(478bp), allele no. 13], (g) *recA* [(510bp), allele no. 2]. A part of the entire chromatogram of the respective genes had been depicted above. Allele numbers were obtained from MLST data analysis mentioned in ‘experimental procedure’ section.



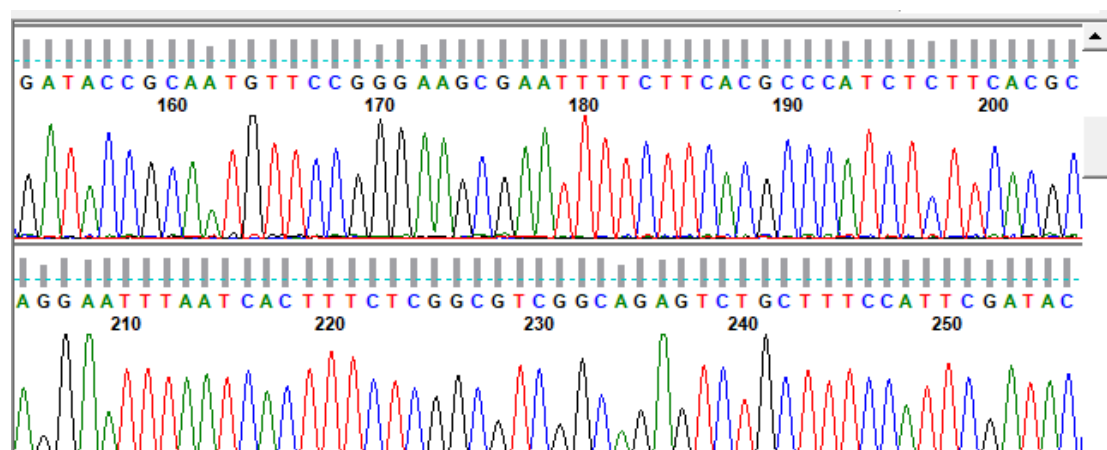
(a)



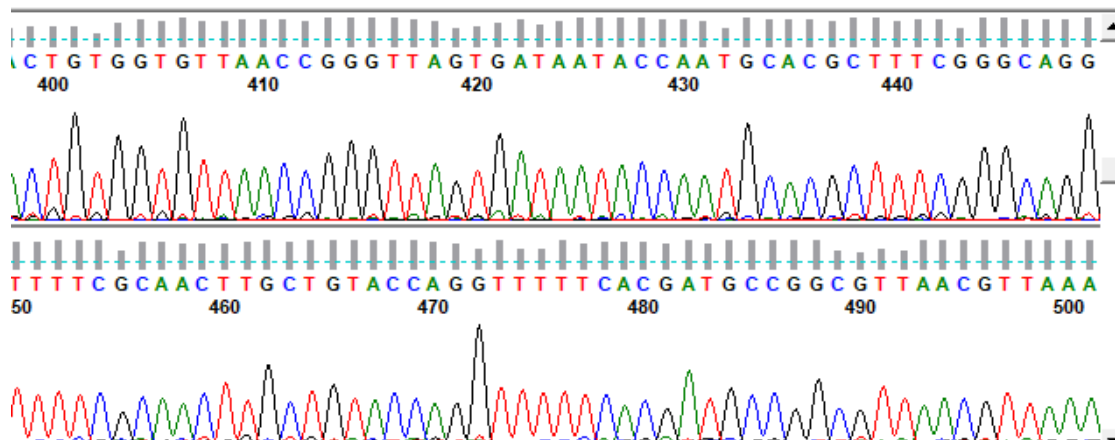
(b)



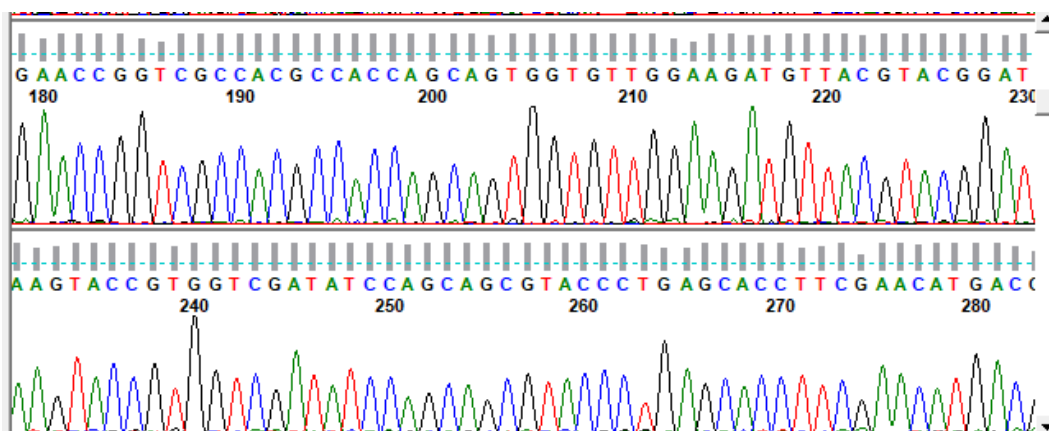
(c)



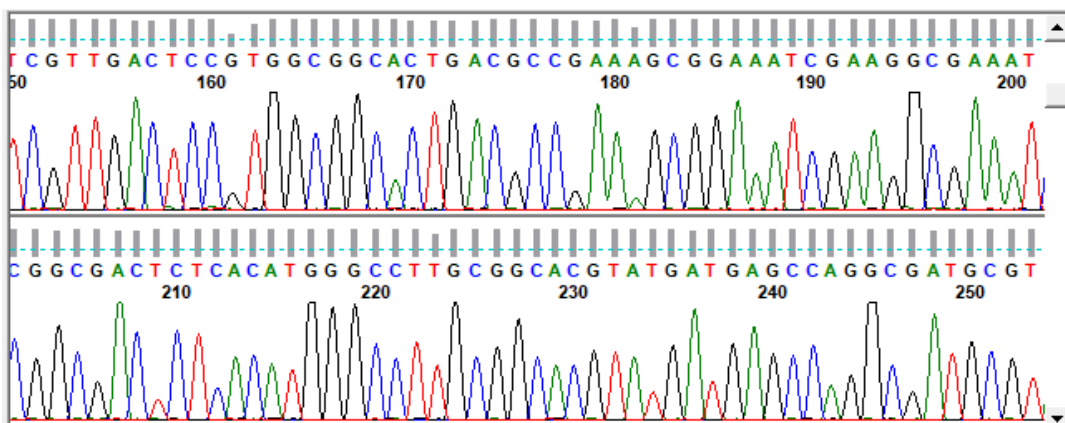
(d)



(e)



(f)



(g)

Figure 4.7: The representative chromatograms of seven different housekeeping genes obtained after sequencing of an isolate NP048 (a) *adk* [(536bp), allele no. 35]; (b) *fumC* [(469bp), allele no. 37]; (c) *gyrB* [(460bp), allele no. 29], (d) *icd* [(518bp), allele no. 25], (e) *mdh* [(452bp), allele no. 4], (f) *purA* [(478bp), allele no. 5], (g) *recA* [(510bp), allele no. 73]. A part of the entire chromatogram of the respective genes had been depicted above. Allele numbers were obtained from MLST data analysis mentioned in ‘experimental procedure’ section.

Table 4.12. Alleles of seven housekeeping genes in imipenem-resistant UPECp and UPECnp isolates along with their sequence types (ST) and clonal complexes (CC).

	<i>adk</i>	<i>fumC</i>	<i>gyrB</i>	<i>icd</i>	<i>mdh</i>	<i>purA</i>	<i>recA</i>	ST	CC
UPECp isolates									
P001	4	26	2	312	5	8	19	2659	38

P005	6	4	4	726	8	468	6	UD	UD
P006	10	99	1250	91	8	8	2	12953	UD
P008	6	4	15	103	24	8	7	441	UD
P012	35	37	29	25	4	5	73	405	405
P030	92	4	87	96	70	58	2	648	648
P031	100	37	29	25	4	5	73	1544	405
P033	10	11	4	8	8	13	2	167	10
P035	6	4	22	726	8	18	2	UD	UD
P036	6	30	32	16	974	8	7	UD	UD
P040	6	11	4	8	8	13	2	693	UD
P043	53	11	47	13	8	28	29	3145	131
P044	6	4	14	16	24	2	14	4162	155
P049	6	4	14	16	24	2	14	4162	155
P055	35	37	29	25	4	5	73	405	405
P065	13	13	22	1040	8	13	10	UD	UD
P069	10	11	4	8	8	13	2	167	10
P070	6	11	32	522	11	523	44	UD	UD
P091	10	11	4	8	822	13	73	UD	UD
P108	10	11	4	8	8	18	2	215	10
P109	92	4	4	16	11	8	7	UD	UD
P110	6	30	32	16	11	8	7	424	UD
P124	10	11	4	8	8	13	2	167	10
UPECnp isolates									
NP006	6	4	5	26	20	8	14	40	UD
NP038	13	14	19	36	23	11	10	127	UD
NP040	43	41	15	18	11	7	6	101	101
NP042	53	40	47	8	36	28	29	UD	UD
NP046	6	4	19	26	8	8	10	UD	UD
NP047	53	40	47	13	36	28	29	131	131
NP048	35	37	29	25	4	5	73	405	405
NP049	35	37	29	25	4	5	73	405	405
NP051	53	40	47	13	36	28	7	1195	131
NP052	6	4	12	1	20	18	7	410	23
NP054	53	40	47	13	36	28	7	1195	131
NP061	13	13	9	8	16	10	7	UD	UD
NP062	53	40	47	13	36	28	29	131	131
NP064	6	4	87	96	70	58	2	2112	648
NP065	4	26	2	25	5	5	19	38	38
NP073	53	40	47	13	36	28	7	1195	131
NP074	6	6	22	16	11	1	7	940	448
NP075	6	6	5	9	43	8	7	UD	UD
NP076	13	14	19	36	23	11	10	127	UD
NP078	43	41	15	18	11	7	6	101	101
NP080	6	4	12	1	20	18	7	410	23
NP093	92	4	87	96	70	58	2	648	648
NP107	43	41	15	18	11	7	6	101	101
NP116	43	41	10	18	11	7	6	UD	UD
NP117	6	11	4	8	8	18	139	UD	UD
NP119	92	4	87	96	70	58	2	648	648

NP121	53	40	47	13	36	28	29	131	131
NP124	6	11	4	8	8	18	139	UD	UD
NP126	6	4	12	1	20	18	7	410	23

To determine the clonal complex (CC) and sequence types (STs) in the UPECp and UPECnp isolates, MLST was used. Sequences were concatenated and aligned using ClustalW in MEGA 11. The maximum Likelihood method based on the Tamura-Nei model was used to infer the evolutionary history of the 52 UPEC (UPECp=23, UPECnp=29) isolates (Fig. 3.5). The isolates were assigned to 20 discrete STs and 9 different CCs. The most frequent ST assigned in 2 UPECp and 2 UPECnp (n=4, 7.69%) was ST405, followed by ST101, ST410, ST131, ST1195 in UPECnp (n=3 each, 5.77%) and ST167 in UPECp (n=3, 5.77%) respectively. The most frequent CC assigned in 6 UPECnp and 1 UPECp (n=7, 13.46%) was CC131, followed by CC405 in 3 UPECp and 2 UPECnp (n=5, 9.62%) and CC131 in 1 UPECp and 6 UPECnp isolates respectively. Moreover, 1 UPECp assigned to ST12953 and 1 UPECnp to ST648 carried a higher number of virulence-associated genes. Nonetheless, in accordance to the MLST database STs or CCs allocated to some isolates investigated in this study were found to be related to humans, companion animals, poultry, and/or to the environment although STs and CCs of several UPECp and UPECnp isolates remained undetermined (UD). Therefore, it might be inferred from this study that both UPECp and UPECnp isolates were widely distributed among multiple known STs and CCs (Figure 4.9).

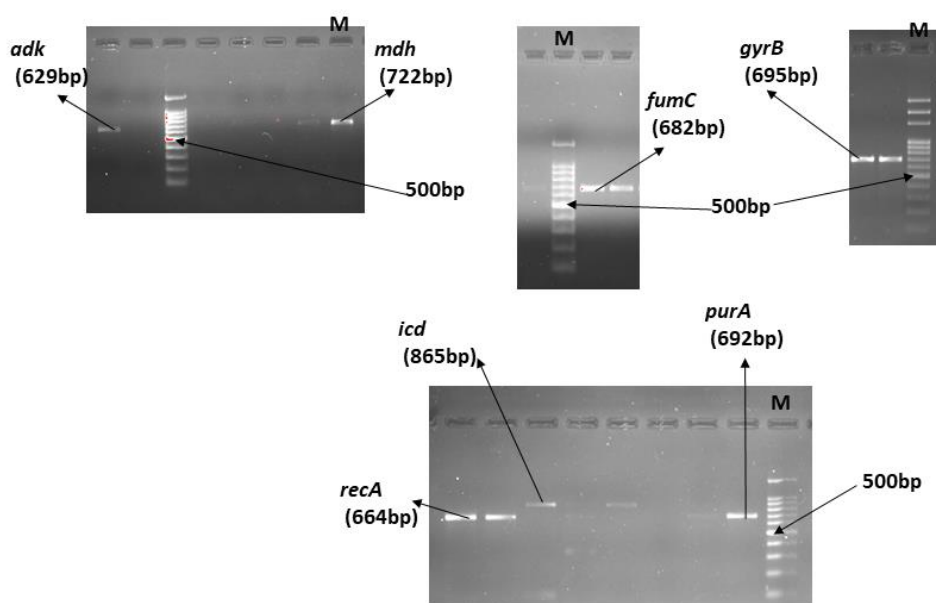


Figure 4.8: Representative pictures of *adk*, *fumC*, *gyrB*, *mdh*, *recA*, *purA*, *icd* control genes on Agarose gel electrophoresis. M represents the DNA marker lane (100 bp DNA ladder).

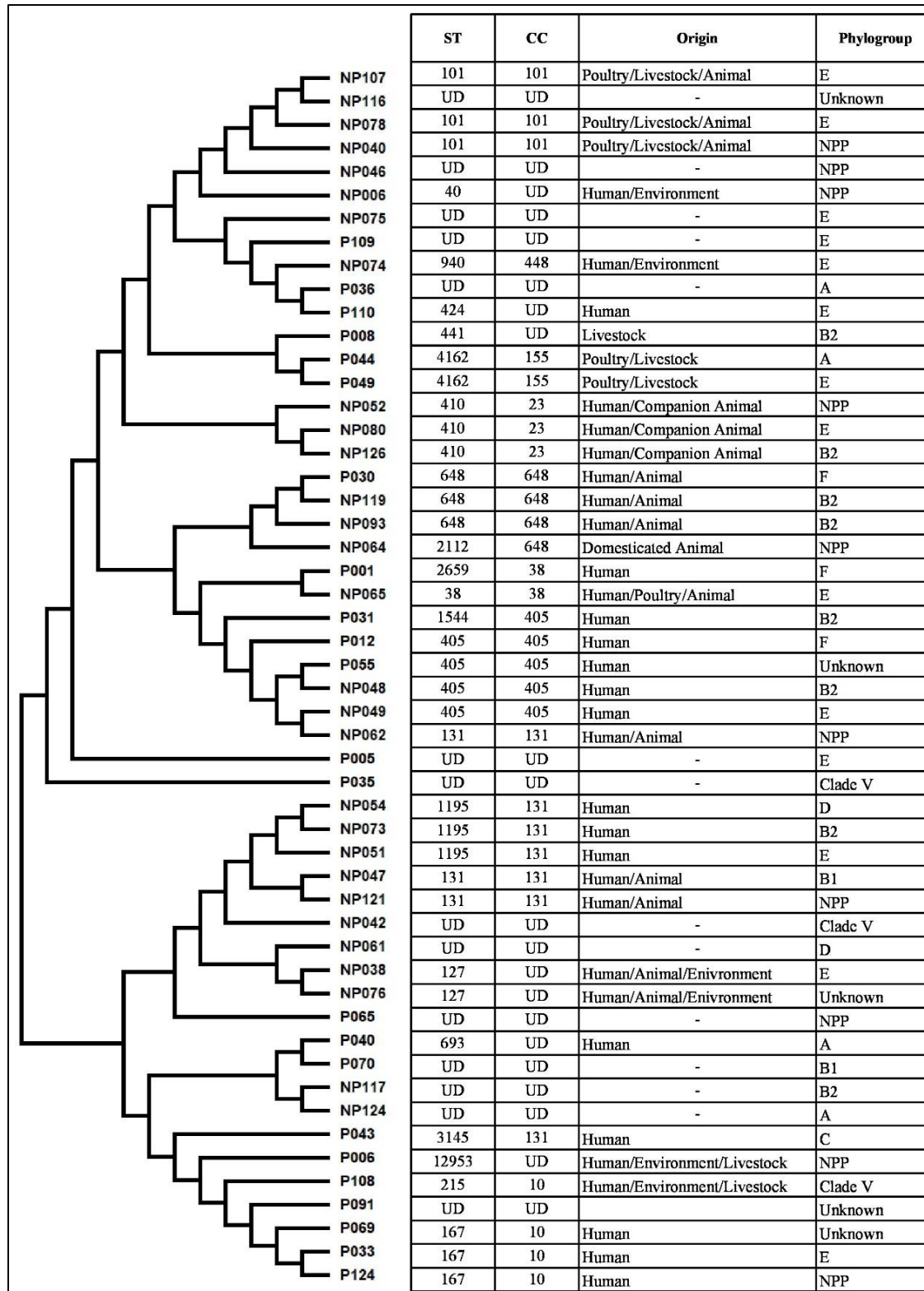


Figure 4.9: Maximum likelihood tree constructed using MEGA 11.0 based on the nucleotide sequence of seven housekeeping genes: *adhA*, *gyrB*, *fumC*, *icd*, *mdh*, *purA* and *recA*, and depicting inferred phylogeny of 52 UPEC. Sequence Types (ST), clonal complexes (CC), Origins, Phylogenetic Groups were displayed to the right of the dendrogram. (UD=Undetected)

4.6. Discussion:

Antibiotics can be used to treat UTIs, however, the growth of multidrug resistance isolates necessitates the introduction of proper prescription policies and limits on empirical treatment. Analyzing the antibiotic sensitivity pattern of uropathogenic *Escherichia coli* isolates is therefore absolutely necessary. According to several investigations, MDR *E. coli* was frequently found in samples taken from pregnant women who had UTIs (57% - 80%) [41]. Similar to previous studies, MDR *E. coli* was also found to be the most common pathogen isolated from non-pregnant women of all age groups [42]. Carbapenems were frequently used as treatment alternatives against the MDR pathogens. Our study indicated the efficacy of meropenem against UPECp and ertapenem against UPECnp. This finding is in exception with other study which demonstrated the efficacy of both meropenem and imipenem against UPECs from non-pregnant population [43]. Additionally, in our study moderate to high resistance against imipenem is observed in both UPECp (63.89%) and UPECnp (85.3%), similar to other studies with non-pregnant population from Iran and India [43, 44]. Nonetheless, our study showed that 34.62% of the *E. coli* isolates obtained from both pregnant and non-pregnant women exhibited resistance to all three carbapenems tested, which was significantly greater than studies reported from Iran and numerous Gulf countries [11, 45]. In addition, 74% of the total UPEC isolates in this study revealed resistance to at least one of the carbapenems tested, which was significantly higher than the results from other studies conducted throughout the world [43, 46, 47] and comparable to another study from India [44]. As a result, the worrisome rise in imipenem-resistant UPEC found in both pregnant and non-pregnant women pointed to improper amalgamated therapy used by patients and frequently treatment failure.

The phylogenetic history of the clinical UPEC isolates may be used to forecast their way of life. ExPEC, including UPEC, reported a prevalence of phylotypes B2 and D while enterohaemorrhagic *E. coli* (EHEC) strains were observed to be often distributed with phylogroups B1 and E. According to a study by Clermont et al. 2021 [48], phylotype E isolates were extremely diverse

and contained commensals, intra- and extra-intestinal pathogens, as well as pathogens from the environment. In comparison to the four major phylogroups (A, B1, B2, D), information on the epidemiology of the strains that belonged to the phylogroup E was limited. In our study, phylogroup E was detected as the predominant group among the imipenem-resistant UPECp (21.74%) and UPECnp (31.03%) isolates in contrary to other studies, which reported a very low incidence of this phylogroup in *E. coli* isolates from human [48]. Moreover, another study [49] reported that phylogroup E was monophyletic and emerged amid phylogroup D and phylogroup A/B1. Occurrence of ‘Novel Phylotype Properties’ i.e. ‘NPP’ in UPECnp isolates was found to be the second most common group. Contrary to several studies on isolates of *E. coli* that produce carbapenemase and reported a predominance of phylogroup B2 and C [11, 50, 51], UPECp isolates in our study showed equal distribution of isolates that belonged to the NPP group, phylogroup F, A, and unidentified phylogroup as the second most prevalent groups.

Similar to UPECnp isolates adhesion toxin production, and biofilm formation were the most frequent virulence factors in imipenem-resistant UPECp isolates. Type 1 fimbriae (*fimH*, $p < .05$, OR: 1.68), P fimbriae (*papC*, $p < .05$, OR: 1.37), salmochelin-siderophore receptor (*iroN*, $p < .05$, OR: 3.46), aerobactin (*iucD*, $p < .05$, OR: 2.30) and biofilm producing gene (*csgA*, $p < .05$, OR: 1.86), were predicted to be associated with UPECp isolates. All of the aforementioned genes except *csgA* were associated with adherence to the uroepithelial cells and facilitated invasion in addition to the establishment of intracellular bacterial communities (IBC) which assisted recurrent UTI, as well as helped the bacteria to successfully evade host immune defenses [52]. In the UPECp isolates, *csgA* was linked to the development of biofilms and may have contributed to antibiotic resistance [53].

A significant presence of other important virulence factors such as *papEF*, *papGII*, *hlyA*, *kps MTII* (43.48%); *flu* (52.17%); and *chuA* (56.52%) in UPECp and *iha*, *hlyA*, *cnfI* (44.83%); *papEF*, *papGII* (48.28%); *kps MTII* (55.17%); *flu* (65.51%) and *chuA* (82.76%) in UPECnp indicated higher pathogenic potential of UPECnp than UPECp isolates. The presence of pathogenicity islands, which were crucial in the spread of virulence in UPECs, indicated a high level of pathogenicity in both groups. As a result, the high virulence of PAI III₅₃₆ and PAI IV₅₃₆ in the UPECnp population also showed that they were significantly more prevalent than in the UPECp

population. Additionally, the mean virulence score ($p=1$) showed that there was no correlation between the distribution of virulence factor genes in the two populations.

This study found that imipenem-resistant UPEC from both pregnant and non-pregnant populations shared similar STs and CCs, indicating that they shared a comparable evolutionary history. Our study reported incidence of ST167 as the predominate ST in UPEC_p, in contrast to earlier studies that demonstrated the incidences of discrete STs namely; ST73, ST95, ST12, ST69, and ST10 in pregnant populations from France and Madagascar [54, 55]. This discrepancy may be explained by different geographic locations. Furthermore, a recent study from Germany [56] found that ST167, ST410, ST405, and ST361 predominated in clinical *E. coli* isolates resistant to carbapenem and extended-spectrum cephalosporin, which is similar to the findings of our study that ST405, ST648, and ST167 were frequently found in imipenem-resistant UPEC_p and UPEC_{np} isolates. A similar global prevalence of ST410, ST131, ST167, and ST405 was found in carbapenem-resistant *E. coli* in a recent study in Canada [57]. Along with an alarming incidence of strain ST405, many pandemic strains, including ST131, ST95, ST69, and ST73, related to carbapenem resistance in clinical *E. coli* isolates, were also identified from California [58]. Additionally, according to MLST results from our study, a large number of unknown STs (31.8%) and CCs (47.8%; UPEC_p, 34.5%; UPEC_{np}) were found in UPEC collected from both populations. This could be a result of improper use of carbapenem, which led to the development of resistance against this class of antibiotics. As the primary causative agent of UTI, UPEC is well established to increase the risk of UTI in pregnant women. Therefore, the treatment of maternal and fetal health is seriously threatened by drug resistant UPECs that are spread both in the community and in hospital settings.

4.7. References:

1. Matuszkiewicz-Rowińska J, Małyszko J, Wieliczko M. Urinary tract infections in pregnancy: old and new unresolved diagnostic and therapeutic problems. Archives of medical science. 2015. 11(1), 67–77.
2. Hossain M, Tabassum T, Rahman A et al. Genotype–phenotype correlation of β -lactamase-producing uropathogenic *Escherichia coli* (UPEC) strains from Bangladesh. 2020. Scientific Reports. 10, 14549.
3. Terlizzi ME, Gribaudo G, Maffei ME. UroPathogenic *Escherichia coli* (UPEC) Infections: Virulence Factors, Bladder Responses, Antibiotic, and Non-antibiotic Antimicrobial Strategies. 2017. Frontiers in microbiology, 8, 1566.

4. Abd El Ghany M, Sharaf H, Al-agamy MH, Shibl A, Hill-Cawthorne GA, Hong PY. Genomic characterization of NDM-1 and 5, and OXA-181 carbapenemases in uropathogenic *Escherichia coli* isolates from Riyadh, Saudi Arabia. 2018. PLoS One. 13(8):e0201613.
5. Shields RK, Zhou Y, Kanakamedala H, Cai B. Burden of illness in US hospitals due to carbapenem-resistant Gram-negative urinary tract infections in patients with or without bacteraemia. 2021. BMC Infectious Disease. 21:572.
6. Gurung S, Kafle S, Dhungel B, Adhikari N, Shrestha UT, Adhikari B et al. Detection of OXA-48 Gene in Carbapenem-Resistant *Escherichia coli* and *Klebsiella pneumoniae* from Urine Samples. 2022. Infection and Drug Resistance. 13: 2311-2321.
7. Adegoke AA, Ikott WE, Okoh AI. Carbapenem resistance associated with coluria among outpatient and hospitalised urology patients. 2022. New Microbes and New Infections. 48:101019.
8. Mairi A, Touati A, Bessai SA, Boutabtoub Y, Khelifi F, Sotto A, Lavigne JP, Pantel A. Carbapenemase-producing Enterobacteriaceae among pregnant women and newborns in Algeria: Prevalence, molecular characterization, maternal-neonatal transmission, and risk factors for carriage. 2018. American journal of infection control, 47(1), 105–108.
9. Rezaatofghi SE, Mirzarazi M, Salehi M. Virulence genes and phylogenetic groups of uropathogenic *Escherichia coli* isolates from patients with urinary tract infection and uninfected control subjects: a case-control study. 2021. BMC infectious diseases, 21(1), 361.
10. Cepas V, Soto SM. Relationship between Virulence and Resistance among Gram-Negative Bacteria. 2020. Antibiotics. 9, 719.
11. Jomehzadeh N, Jahangirimehr F, Chegeni SA. Virulence-associated genes ananalysis of carbapenemase-producing *Escherichia coli* isolates. Plos One. 2022. 17(5):e0266787.
12. Forde BM, Roberts LW, Phan MD. *et al.* Population dynamics of an *Escherichia coli* ST131 lineage during recurrent urinary tract infection. 2019. Nature Communications. 10, 3643.
13. Jafari A, Falahatkar S, Delpasand K, Sabati H, Ebrahim-Saraie HS. Emergence of *Escherichia coli* ST131 Causing Urinary Tract Infection in Western Asia: A Systematic Review and Meta-Analysis. 2020. Microbial Drug Resistance. 26 (11): 1357–1364.
14. Hussain A, Ewers C, Nandanwar N, Guenther S, Jadhav S, Wieler LH, Ahmed N. Multiresistant Uropathogenic *Escherichia coli* from a Region in India Where Urinary Tract Infections Are Endemic: Genotypic and Phenotypic Characteristics of Sequence Type 131 Isolates of the CTXM-15 Extended-Spectrum- β -Lactamase-Producing Lineage. 2012. Antimicrobial Agents and Chemotherapy. 56 (12): 6358 – 6365.
15. Sekar R, Srivani S, Amudhan M, Mythreyee M. Carbapenem resistance in a rural part of southern India: *Escherichia coli* versus *Klebsiella* spp. 2016. Indian Journal of Medical Research. 144(5): 781-783.
16. Jaggi N, Chatterjee N, Singh Vyoma, Giri SK, Dwivedi P, Panwar R, Sharma AP. Carbapenem resistance in *Escherichia coli* and *Klebsiella pneumoniae* among Indian and international patients in North India. 2019. Acta Microbiologica et Immunologica Hungarica. 1; 66(3): 367 - 376.

17. Srivastava P, Bisht D, Kumar A, Tripathi A. Prevalence of Carbapenem-Resistant *Escherichia coli* and *Klebsiella pneumoniae* in Rural Uttar Pradesh. 2022. Journal of Datta Meghe Institute of Medical Sciences University. 17(3): 584-588.
18. Chatterjee N, Nirwan PK, Srivastava S, Rati R, Sharma L, Sharma P, Dwivedi P, Jaggi N. Trends in carbapenem resistance in Pre-COVID and COVID times in a tertiary care hospital in North India. 2023. Annals of Clinical Microbiology and Antimicrobials. 22,1.
19. Wright MH, Adelskov J, Greene AC. Bacterial DNA extraction using individual enzymes and Phenol/Chloroform Separation. 2017. Journal of Microbiology & Biology Education. 18(2): 18.2.48.
20. Abdallah KS, Cao Y, Wei DJ. Epidemiologic investigation of extra-intestinal pathogenic *E. coli* (ExPEC) based on PCR phylogenetic group and *fimH* single nucleotide polymorphisms (SNPs) in China. 2011. International Journal of Molecular Epidemiology and Genetics. 2(4): 339–353.
21. Clermont O, Christenson JK, Denamur E, Gordon DM. The Clermont *Escherichia coli* phylo-typing method revisited: improvement of specificity and detection of new phylo-groups. 2013. Environmental Microbiology Reports. 5(1): 58–65.
22. Lee YM, Dodson KW, Hultgren SJ. Adaptor function of PapF depends on Donor Strand Exchange in P-Pilus Biogenesis of *Escherichia coli*. 2007. Journal of Bacteriology. 189(14): 5276–5283.
23. Tewari R, Ikeda T, Malaviya R, MacGregor JJ, Little JR, Hultgren SJ, Abraham SN. The PapG tip adhesin of P fimbriae protects *Escherichia coli* from Neutrophil Bactericidal Activity. 1994. Infection and Immunity. 62(12): 5296–5304.
24. Ott M, Hoschützky H, Jann K, VanDie I, Hacker J. Gene clusters for S fimbrial adhesin (sfa) and F1C fimbriae (foc) of *Escherichia coli*: comparative aspects of structure and function. 1988. Journal of Bacteriology. 170(9): 3983–3990.
25. Servin AL. Pathogenesis of Afa/Dr diffusely adhering *Escherichia coli*. 2005. Clinical Microbiology Reviews. 18(2): 264–292.
26. Russo TA, McFadden CD, MacDonald UCB, Beanan JM, Barnard TJ, Johnson JR. IroN functions as a siderophore receptor and is a urovirulence factor in an extraintestinal pathogenic isolate *Escherichia coli*. 2002. Infection and Immunity. 70(12): 7156–7160.
27. Nagy G, Dorbindt U, Kupfer M, Emody L, Karch H, Hacker J. Expression of hemin receptor molecule ChuA is influenced by RfaH in Uropathogenic *Escherichia coli* strain 536. 2001. Infection and Immunity. 69 (3): 1924–1928.
28. Aldawood E, Roberts IS. Regulation of *Escherichia coli* Group 2 capsule gene expression: A mini review and update. Frontiers in Microbiology. 2022. 13: 858767.
29. Johnson JR, Jelacic S, Schoening LM, Clabots C, Shaikh N, Mobley HLT, Tarr PI. The IrgA homologue adhesin Iha is an *Escherichia coli* virulence factor in murine urinary tract infection. 2005. Infection and Immunity. 73(2): 965–971.

30. Herrero M, De Lorenzo V, Neilands JB. Nucleotide sequence of the *iucD* gene of the pColV-k30 aerobactin operon and topology of its product studied with *phoA* and *lacZ* gene fusions. 1988. *Journal of Bacteriology*. 170 (1): 56–64.
31. Díaz JM, Dozois CM, Avelar-González FJ, Hernández-Cuellar E, Pokharel P, De Santiago AS, Guerrero-Barrera AL. The Vacuolating Autotransporter Toxin (Vat) of *Escherichia coli* causes cell cytoskeleton changes and produces non-lysosomal vacuole formation in bladder epithelial cells. 2020. *Frontiers in Cellular and Infection Microbiology*. 10:299.
32. Ikeda M, Kobayashi T, Fujimoto F, Okada Y, Higurashi Y, Tatsuno K, Okugawa S, Moriya K. The prevalence of the *iutA* and *ibeA* genes in *Escherichia coli* isolates from severe and non-severe patients with bacteremic acute biliary tract infection is significantly different. 2021. *Gut Pathogens*. 13 (32).
33. Hasman H, Chakraborty T, Klemm P. Antigen-43-mediated autoaggregation of *Escherichia coli* is blocked by Fimbriation. 1999. *Journal of Bacteriology*. 181(16): 4834 – 4841.
34. Shu Q, Crick SL, Pinkner JS, Ford B, Hultgren SJ, Frieden C. The *E. coli* CsgB nucleator of curli assembles to β -sheet oligomers that alter the CsgA fibrilization mechanism. 2012. *Proceedings of the National Academy of Sciences*. 109 (17): 6502-6507.
35. Črnigoj M, Podlesek Z, Budič M, Žgur-Bertok D. The *Escherichia coli* Uropathogenic-specific-protein-associated immunity protein 3 (Imu3) has nucleic acid binding activity. 2014. *BMC Microbiology*. 14, 16
36. Östblom A, Adlerberth I, Wold AE, Nowrouzian FL. Pathogenicity-island markers, virulence determinants *malX* and *usp*, and the capacity of *Escherichia coli* to persist in infants' commensal microbiotas. 2011. *Applied and Environmental Microbiology*. 77(7): 2303–2308.
37. Wirth T, Falush D, Lan R, Colles F, Mensa P, Wieler LH et al. Sex and Virulence in *Escherichia coli*: an evolutionary perspective. 2006. *Molecular Microbiology*. 60(5): 1136–1151.
38. Wang Y, Zhou J, Li X, Ma L, Cao X, Hu W et al. Genetic diversity, antimicrobial resistance and extended-spectrum- β -lactamase type of *Escherichia coli* isolates from chicken, dog, pig, and yak in Gansu and Qinghai Provinces, China. 2020. *Journal of Global Antimicrobial Resistance*. 22(9): 726–732.
39. Zheng B, Feng C, Xu H, Yu X, Guo L, Jiang X, Song X. Detection and characterization of ESBL-producing *Escherichia coli* expressing *mcr-1* from dairy cows in China. 2019. *Journal of Antimicrobial Chemotherapy*. 74(2): 321–325.
40. Liu X, Thungrat K, Boothe DM. Multilocus Sequence typing and virulence profiles in Uropathogenic *Escherichia coli* isolated from Cats in the United States. 2015. *PlosOne*. 10(11): e0143335.
41. Chelkeba L, Fanta K, Mulugeta T, Melaku T. Bacterial profile and antimicrobial resistance patterns of common bacteria among pregnant women with bacteriuria in Ethiopia: A systematic review and meta-analysis. 2022. *Archives of gynecology and obstetrics*. 306(3): 663–686.

42. Nobel FA, Akter S, Jebin RA, Sarker TC, Rahman M, Zamane et al. Prevalence of multidrug patterns of *Escherichia coli* from suspected urinary tract infection Mymensingh city, Bangladesh. 2021. Journal of Advanced Biotechnology and Experimental Therapeutics. 4(3): 256–264.
43. Sarahi JY, Hashemi A, Ardebili A, Davoudabadi S. Molecular characteristics of antibiotic-resistant *Escherichia coli* and *Klebsiella pneumoniae* strains isolated from hospitalized patients in Tehran, Iran. 2021. Annals of Clinical Microbiology and Antimicrobials. 20:32
44. Manohar P, Leptihn S, Lopes BS, Nachimuthu R. Dissemination of carbapenem resistance and plasmids encoding carbapenemases in gram-negative bacteria isolated in India. JAC Antimicrobial Resistance. 2021. 1(3).
45. Zowawi HM, Sartor AL, Balkhy HH, Walsh TR, Johani SMA, Aljindan RY et al. Molecular characterization of Carbapenemase-Producing *Escherichia coli* and *Klebsiella pneumoniae* in the Countries of the Gulf Cooperation Council: Dominance of OXA-48 and NDM producers. Antimicrobial Agents and Chemotherapy. 2014. 58(6): 3085 – 3090.
46. Matin FZ, Rezatofighi SE, Ardakani MR, Akhoond MR, Mahmoodi F. Virulence characterization and clonal analysis of uropathogenic *Escherichia coli* metallo-beta-lactamase-producing isolates. 2021. Annals of Clinical Microbiology and Antimicrobials. 20:50
47. Tian X, Zheng X, Sun Y, Fang R, Zhang S, Zhang X et al. Molecular Mechanisms and Epidemiology of Carbapenem-Resistant *Escherichia coli* isolated from Chinese patients during 2002–2017. 2020. Infection and Drug Resistance. 13:501 – 512.
48. Clermont O, Condamine B, Dion S, Gordon DM, Denamur E. The E phylogroup of *Escherichia coli* is highly diverse and mimics the whole *E. coli* species population structure. 2021. Environmental Microbiology. 23(11): 7139–7151.
49. Touchon M, Perrin A, de-Sousa AM, Vangchhia B, Burn S, O'Brien CL, Denamur E, Gordon D, Rocha EP. Phylogenetic background and habitat drive the genetic diversification of *Escherichia coli*. 2020. Plos Genetics. 16(6): e 1008866.
50. Ortega A, Sáez D, Bautista V, Fernández-Romero S, Lara N, Aracil B. et al. Carbapenemase-producing *Escherichia coli* is becoming more prevalent in Spain mainly because of the polyclonal dissemination of OXA-48. 2016. Journal of Antimicrobial Chemotherapy. 71: 2131–2138.
51. El-Shaer S, Abdel-Rhman SH, Barwa E, Hassan E. Genetic characterization of extended-spectrum-β-lactamase- and carbapenemase-producing *Escherichia coli* isolated from Egyptian hospitals and Environments. 2021. Plos One. 23;16:e0255219.
52. Flores-Mireles AL, Walker JN, Caparon M, Hultgren SJ. Urinary Tract Infections: epidemiology, mechanisms of infection and treatment options. 2015. Nature Reviews Microbiology. 13(5): 269 – 284.
53. Soto SM, Macro F, Guiral E, Vila J. Biofilm formation in Uropathogenic *Escherichia coli* Strains: Relationship with Urovirulence Factors and Antimicrobial Resistance. 2011. Intech. <https://doi.org/10.5772/24626>

54. Surgers L, Bleibtreu A, Burdet C, Clermont O, Laouénan C, Lefort A et al. *Escherichia coli* bacteremia in pregnant women is life-threatening for fetuses. 2014. Clinical Microbiology and Infection: The Official Publication of the European Society of clinical microbiology and infectious diseases 20 (12): O1035–O1041.
55. Milenkov M, Rasoanandrasana S, Rahajamanana LV, Rakotomalala RS, Razafindrakoto CA, Rafalimanana C. et al. Prevalence, Risk Factors, and Genetic Characterization of Extended-Spectrum Beta-Lactamase *Escherichia coli* isolated from Healthy Pregnant Women in Madagaskar. 2021. Frontiers in Microbiology. 12: 786146.
56. Hans JB, Pfenningwerth N, Neumann B, Pfeifer Y, Fischer MA, Einfeld J et al. Molecular surveillance reveals the emergence and dissemination of NDM-5-producing *Escherichia coli* high-risk clones in Germany, 2013 to 2019. 2023. Euro surveillance: bulletin Européen sur les maladies transmissibles = European communicable disease bulletin. 28(10): 2200509.
57. Pereino G, Chen L, Nobrega D, Finn TJ, Kreiswirth BN, DeVinney R, Pitout JDD. Genomic Epidemiology of Global Carbapenemase-producing *Escherichia coli*, 2015 – 2017. 2022. Emerging Infectious Diseases. 28(5), 924–931.
58. Slown S, Walas N, Amato HK, Llyod T, Varghese V, Bender M, Pandori M, Graham J. Clonal lineages and virulence factors of carbapenem resistant *E. coli* in Alameda County, California, 2017 – 2019. 2022. Antibiotic. 11, 1974.

Chapter 5: Host Cytokine Response upon Infection by different UPEC_p and UPEC_{np} isolates with discrete virulence profile *ex-vivo*

5.1 Background Study: Urinary tract infections (UTIs), both acute and recurrent, are a significant public health concern that significantly reduce the quality of life for patients. Various host defenses help keep the urinary system sterile in the normal state and prevent bacterial colonization and survival. In order to fend against bacterial infection, the host has many defense mechanisms built-in [1]. UTIs in pregnant women leads to a serious threat to the fetus, with frequent occurrence of premature birth, premature rupture of the membrane, maternal chorioamnionitis, and a fetus with low birth weight, developmental retardation or fetal necrosis [2, 3, 4]. Additionally, asymptomatic bacteriuria is frequently observed in pregnant women and can cause pyelonephritis in 20 -30% of cases if left untreated. In the non-pregnant population, UTIs can develop several complications, particularly in older women, and if left untreated, can be fatal. In both populations, uropathogenic *Escherichia coli* (UPEC) is responsible for 80–90 % of UTIs [3, 4]. Although, antibiotics are first treatment options for UTIs, their empiric administration has aided in the development of MDR and made clinical management of UTIs more challenging [5]. Early research from our lab demonstrated a high incidence of MDR in UPEC isolated from non-pregnant (92.5%) [6] and pregnant (59.1%) [7] women. Additionally, a recent study from a Mexican population identified 92.7% of the isolates from both pregnant and non-pregnant women were MDR [8].

The virulence factors (VFs) present in UPEC strains are many and include fimbrial (Type 1, P and S), afimbrial (Afa/Dr family), toxins (HlyA, Cnf1, autotransporter proteins), iron-acquisition systems, iron ion transport, and surface polysaccharides. VFs were discovered to be crucial in colonization and to enhance adherence to epithelial cells of the intestines, kidneys, and lower urinary tract [9, 10]. They triggered the host defense mechanisms even more, which led to inflammation and the exfoliation of bladder epithelial cells [1]. Epithelial cells in bladder and kidney after UPEC infection seem to be a major source of IL-6 and IL-8, which were essential in the development of local tissue damage. Moreover, the role of TNF- α , IFN- γ , IL-8 and IL-1 β in the clearance of UPEC were shown in various studies [11, 12, 13, 14, 15, 16, 17]. According to a study by Jung et al., [18] relationships between virulence factors and the evolutionary history of UPEC isolated from infants on TNF- α and IL-1 β expression further supported the idea that the cytokines play a role in UTI pathogenesis. Another in vitro study established the effect of different cytokines on the expression of virulence determinants in UPEC prototype strain CFT073 in the HTB-4 uroepithelial cell line [17]. Therefore, the development of infection was greatly influenced by the immunological responses of the host and the virulence determinants of the pathogens.

Although urine culture is the gold standard for detecting uropathogen [19], it is time-consuming, and without knowledge of the infection potential of the microbe, the only option is to administer empirical treatment. This has led to the rapid growth of MDR, which is quite concerning while treating UTIs, especially in the pregnant population. In order to evaluate the danger of empirical therapy in both populations, the antibiotic resistance pattern in UPEC isolates obtained from pregnant women was determined and compared with UPEC obtained from non-pregnant patients. Therefore, in depth understanding of the infection potential of the microbe and ability to trigger a host cytokine response is required to develop an effective therapeutic. Furthermore, in available references, no study related to the production of different cytokines upon infection with UPEC isolated the pregnant population was reported. Therefore, in this study HTB-4 uroepithelial cells were infected with clinical UPEC isolated in vitro, and the expression pattern of their virulence determinants and cytokines elicited in the host cells upon infection were determined. Correlations between the expression of varied cytokines and pathogenic determinants expressed in UPEC isolated from different hosts were ascertained, which might serve as noninvasive markers to formulate appropriate therapeutics before empirical therapy.

5.2 Objectives

- To determine the expression pattern of virulence determinants of UPECp and UPECnp isolates upon infection in uroepithelial cells (HTB-4).
- To determine the expression of cytokines of uroepithelial cells upon infection with UPECp and UPECnp isolates-
- To determine if there is any correlation between the virulence gene expression patterns in UPECp and UPECnp and the respective cytokines response in HTB-4 cells upon infection.

5.3 Materials

5.3.1. Equipment for *invitro* experiments:

Laminar Air Flow (B.D. Instrumentation) • Shaker Incubator (ICT) • Autoclave • Spectrophotometer (Bio-Rad, Model: SmartSpec™ Plus) • Hot Air Oven (Digitech Systems) • Cooling Centrifuge (Remi) • Refrigerator (Godrej) • Dry Bath (Remi) • Thermal Cycler (ABI instrument Private Ltd., Model: Veriti® Thermal Cycler) • Horizontal gel electrophoresis

apparatus (Genei) • Power Pack (Genei) • Gel Documentation System (Bio-Rad) • Inoculation Loop • Glass spreaders • Spirit Lamp • 100mm glass petri dish (Borosil) • 90mm plastic petri dish (Tarson) • Glass culture tubes (Touff, Borosil) • Test tube racks (Tarsons) • Micropipettes (0.5-10µl, 2-20µl, 20-200µl, 200-1000µl) (Corning, P'Fact, Microlit, Biohit) • Micro tips (0.5-10µl, 2-20µl, 20-200µl, 200-1000µl) (HiMedia) • Eppendorf Tubes (1.5ml, 2ml) (Tarsons) • Cotton (Bengal Surgicals Limited) (Lakshmi Healthcare Products (P) Ltd.) • Surgical Gloves (Pricare, HiMedia) • Wash Bottles (Tarsons)

5.3.2. Equipment for *ex vivo* experiments:

Laminar Air Flow Hood (Yorco Horizontal Laminar Flow) • CO₂ Incubator (Thermo Fisher Scientific) • Cooling Centrifuge (Remi) • Room Temperature Bench Top Centrifuge (Remi) • Refrigerator (Godrej) • Freezer (-20⁰C) (Celfrost) • Freezer (-80⁰C) (Remi UDFV90) • Aspiration pump (Thermo Fisher Scientific) • Pipette controller (Tarsons) • Cyro – storage container with boxes (HiMedia) • Haemocytometer (Sigma-Aldrich) • Water Bath (Borosil) • Light Microscope (Olympus) • Inverted Microscope (Dewinter) • pH meter (Hitech Lab India) • Spirit Lamps (UDS) • 10 ml syringes (Dispovan) • PVDF syringe-driven filters (0.22 micron) (HiMedia) • T25 cell culture flasks (Tarsons) • Cell culture bottles (Borosil) • 96 well and 24 well tissue cultures plates (HiMedia) • Sterile autoclavable 15ml and 50 ml centrifuge tubes (HiMedia) • Centrifuge tube holders (Tarsons) • Micropipettes (0.5-10µl, 2-20µl, 20-200µl, 100-1000µl) (Corning, Biohit) • Barrier Tips (0.5-10µl, 2-20µl, 20-200µl, 100-1000µl) (HiMedia) • Serological Pipettes (1.5ml, 2ml) (Tarsons) • Eppendorf Tubes (1.5ml, 2ml) (Tarsons) • Cotton (Bengal Surgical Limited, Lakshmi Healthcare Products (Pvt.) Ltd.) • Tissue paper (Hospital Store) • Nitrile Gloves (HiMedia) • Wash Bottles (Tarsons) • Applied Biosystems™ 7500 Plus Real-Time PCR (Applied Biosystems, Lithuania) • PowerUp™ SYBR™ Green Master Mix (Applied Biosystems, Lithuania)

5.3.3. Reagents:

Luria Bertani (LB) Media (SRL Chemicals India) • Bacteriological Agar / Agar Agar Type I (HiMedia) • McCoy's 5A medium (HiMedia) • Fetal Bovine Serum (FBS) (HiMedia) • Gentamicin Powder (HiMedia) • Trypsin (HiMedia) • Hank's balanced salt solution (HiMedia) • 1X Phosphate Buffer Solution (HiMedia) • 0.4% Trypan Blue Solution (HiMedia) • MTT Dye

(HiMedia) • Dulbecco's Phosphate Buffered Saline (DPBS) (HiMedia) • TRIzol (Takara) • Barium Chloride (Merck) • Sulfuric Acid (Merck) • 70% Ethanol (Bengal Chemical) • Isopropanol (Merck) • Phenol (Merck) • Chloroform (Merck) • 95% Ethanol (HiMedia) • Diethylpyrocarbonate (DEPC) water (HiMedia) • Molecular Biology Grade Nuclease free water (HiMedia) • Single Distilled Water (SDW) (Hospital supply) Double Distilled Water (DDW) (Laboratory distillation plant) • Gene-specific primers (GCC Biotech India Pvt. Ltd.) • dNTP (Invitrogen) • Taq DNA polymerase and Buffer (Invitrogen) • 50mM MgCl₂ (Invitrogen) • cDNA reverse transcription kit (Invitrogen) • DNA ladders (HiMedia) • 6X gel loading buffer (HiMedia) • Hydrogen Chloride (Hospital Supply) • Sodium Chloride (Hospital Supply) • Agarose (HiMedia) • Ethidium Bromide (SRL chemicals)

5.3.4. Preparation of reagents and compositions of solutions used:

- LB Broth: discussed briefly in section 2.3.3.1.
- LB Agar: discussed briefly in section 2.3.3.11.
- 1X TAE (Tris-Acetate EDTA) buffer: discussed briefly in section 3.4.4.1.
- MTT stock solution (5mg/ml): MTT stock solution (5mg/ml) was prepared by dissolving 50mg of MTT powder in 10 ml of DBPS at pH 7.4. This solution was filtered and sterilized through a 0.2-µm filter into a sterile and light-protected container. MTT solution was stored at -20⁰C until analysis or at 4⁰C for immediate use and was kept away from any light source (Light-sensitive)
- 1X PBS: In 800 ml distilled water, 8g of NaCl, 1.44g of Na₂HPO₄, 0.2g KCl, 0.24g KH₂PO₄ added, pH brought 7.2 or 7.4, further distilled water added to the volume upto 1 liter. Autoclaved.

5.4. Experimental Procedure:

5.4.1 Bacterial culture: For the present analysis, twenty-one (21) non-duplicate pregnant UPEC isolates (UPECp) from 126 hospitalized pregnant patients at their third trimester, and another Twenty-One (21) non-duplicate non-pregnant UPEC isolates (UPECnp) from 126 hospitalized non-pregnant patients were considered (discussed briefly section 2.5 of chapter 2).

5.4.2. **Antibiotic Susceptibility Test:** discussed briefly in section 2.4.8. in Chapter 2.

5.4.3. **Total DNA isolation:** Discussed briefly in section 3.4.3. in Chapter 3

5.4.4. **Virulence factor genotyping:** Total DNA template was used to detect the presence of six virulence genes (*fimH*, *papC*, *sfaA*, *afaA*, *hlyA*, *iroN*) using gene-specific primers (GCC Biotech, India) for all 22 UPECp and 22 UPECnp isolates. Virulence factors were discussed briefly in section 1.8.1.1, 1.8.1.2, 4.4.5.7, 4.4.5.8, 1.8.2.1, and 4.4.5.10 respectively.

5.4.4.1. **Identification of virulence genes:** The procedure for the detection of these six virulence genes were discussed briefly in section 4.4.5.22. Follow Table 4.2 for the primer sequences and PCR conditions. Follow 4.4.5.23. for primer sequences of the target genes.

5.4.5. **HTB-4 uroepithelial cells:**

- Product category: Human cells
- Organism: Homo sapiens
- Morphology: Epithelial
- Tissue: Urinary bladder
- Disease: Translational cell carcinoma
- Growth properties: Adherent
- Age: 81 years
- Ethnicity: White
- Gender: Female
- Karyotype: hypodiploidy to hypopentaploidy; stemline 86; 2 to 4 telocentrics, 3 to 4 minutes, hypotetraploid to hypertetraploid with abnormalities including dicentrics, breakes, pulverization, minutes and telocentric markers.

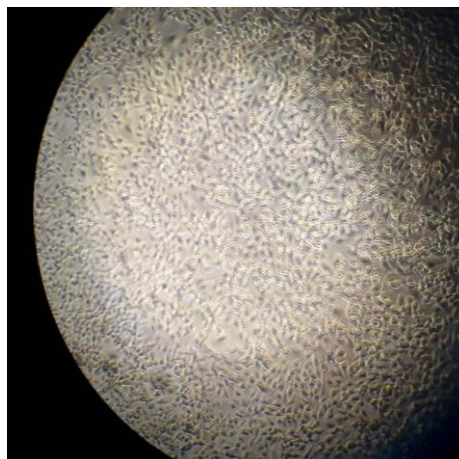


Figure 5.1. Representative photo of confluent monolayer T24 uroepithelial cells seen under inverted microscope at 20X magnification

- Generation time: 19 hours

5.4.6. Cell culture: The study used T24 cells (ATCC® HTB-4™) which is an uroepithelial cell line derived from the translational bladder carcinoma of an 81 years old Caucasian female patient in 1973. Rationale behind choosing this cell line was that this cell line reported to display similarity to the primary human bladder epithelial cells in several earlier studies conducted worldwide [20, 21]. HTB-4 cells were cultured using protocols as described elsewhere [21, 22] but with minor modifications. HTB-4 uroepithelial cells were grown and maintained in McCoy's 5A medium (HiMedia) supplemented with 10% v/v fetal bovine serum (FBS) (HiMedia) and gentamicin (0.05 mg/ml) (HiMedia) in T25 culture flasks (Tarsons). T25 flasks with cells were maintained at 37°C in an atmosphere with 5% CO₂ with constant humidity. Two or three days prior to the individual experiments, cells were removed from the cell culture flasks by Trypsin (0.05%, 10 min) treatment and were subsequently seeded into 24 well tissue culture plates (Tarsons) (Figure 5.2). They were grown for 24 to 72 hours to facilitate cell attachment and to obtain a confluent cell monolayer (Figure 5.1).

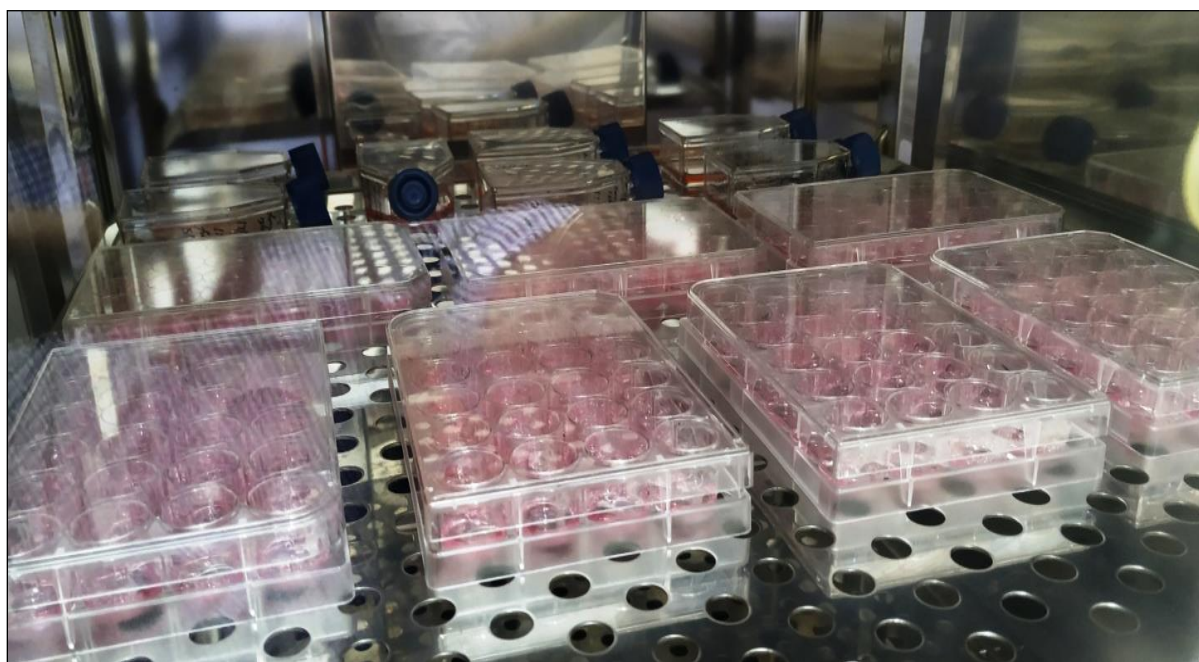


Figure 5.2. The representative picture for seeding of HTB-4 uroepithelial cells in 24-well tissue culture plate and T-25 flasks and maintaining them at 37°C in an atmosphere of 5% CO₂ with constant humidity.

5.4.7. Preparation of bacterial cells for infection: Each bacterial isolate was grown overnight in LB broth, further it was grown till log phase in LB broth. 10^7 CFU/ml of bacterial cells were pelleted at 8000 rpm for 5 minutes. Pellets were resuspended in 1X phosphate-buffered saline (PBS). 100 μ l of 1×10^7 cells were spread to each well of 24 wells tissue culture plates.

5.4.8. Adherence to HTB-4 uroepithelial cells: HTB-4 cells were purchased from National Center for Cell Science (Pune, India) and control strain ABU83972 (HM-50) was provided by BEI resources (ATCC, VA, USA). HTB-4 human bladder epithelial cells (3×10^5 cells) were seeded into each well of a 24-well plate, and cells were allowed to adhere overnight. The 10^7 CFU of bacteria were added and the plates were incubated at 37°C in 5% CO_2 (CO_2 incubator, Thermo Fisher Scientific, MA, USA) for 3 hours to allow for the adhesion of the bacteria. The HTB-4 infected cell monolayers were washed three times with PBS to remove nonadherent bacteria.

5.4.9. RNA extraction and cDNA generation from uroepithelial cells: Total RNA was extracted from the HTB-4 infected adherent monolayer cultures by TRIzol™ (Thermo Fisher Scientific, MA, USA) extraction as per the manufacturer's instructions. Briefly,

- Cells were scraped with 1500 μ l TRIzol™ reagent from the infected wells of the 24- well tissue culture plate.
- It was kept at room temperature for 5 minutes.
- 300 μ l chloroform was added to the scraped cells.
- The solution was vortexed for 5 minutes.
- It was again incubated for 5 minutes at room temperature.
- The solution was centrifuged at $13000 \times g$ for 15 minutes at 4°C .
- The aqueous phase was transferred into a 1.5ml fresh centrifuge tube.
- The aqueous phase was mixed with 750 μ l isopropanol (HiMedia, Mumbai, India).
- It was then incubated at room temperature for 10 minutes.
- The solution was centrifuged at $13000 \times g$ for 10 minutes at 4°C .
- The supernatant is removed.
- The RNA pellet was washed with 1ml 75% Ethanol prepared in DEPC water.
- The sample was mixed by vortexing.
- The sample was then centrifuged at 10500 rpm for 5 minutes.

- Supernatant is discarded, and pellet is air dried for 10 minutes.
- The RNA pellet is air dried in 30 μ l DEPC water, and kept at 60⁰C for 10 minutes.
- The Optical Density was measured at A₂₆₀ and A₂₈₀ by taking 1 μ l DEPC dissolved RNA in 999 μ l DDH₂O.
- To make DNA free RNA, 25 μ l RNA is to be taken, with 3 μ l DNase buffer and 0.1 μ l DNase enzyme and DEPC water 1.9 μ l.
- This solution is incubated at 37⁰C for 30 minutes.
- To the purified RNA, 1 μ l of EDTA is added and incubated at 65⁰C for 10 minutes.
- RNA concentration is calculated and 5ng of purified RNA is taken, Nuclease free water is added to make up the volume to 11 μ l and 1 μ l of hexamer is added. The solution is mixed by spinning and kept at 65⁰C for 5 minutes to remove the 2⁰ structure, then the mixture is kept in ice for 1 minute. Following, the mixture is spin down and kept in ice prior to use.
- With the 12 μ l purified RNA with hexamer, 4 μ l 5X reaction buffer, 1 μ l RNase inhibitor, 2 μ l 10mM dNTP mix and 1 μ l Reverse transcriptase enzyme is added.
- The cDNA preparation is run in thermocycler under following conditions: initial incubation at 25⁰C for 5 minutes, heating at 42⁰C for 60 minutes, and terminating the reaction by heating again at 70⁰C for 5 minutes.
- The prepared cDNA is stored at -20⁰C.

5.4.10. Quantitative Real Time PCR (qRT PCR) analysis: To determine the quantitative expression of six virulence genes (*fimH*, *papC*, *papGIII*, *sfaA*, *hlyA* and *iroN*) and ten cytokines genes (*IL-6*, *IL-8*, *TNF- α* , *IFN- γ* , *MCP-1*, *GCSF*, *IL-1 β* , *IL-17A*, *IL-5* and *TGF- β*), quantitative real-time PCR (qRT-PCR) assay were performed on the cDNA prepared from total RNA extracted from HTB-4 infected monolayer cultures using gene-specific primers. qRT-PCR was performed in an Applied Biosystem™7500 Fast Real-Time PCR system with PowerUp™ SYBR™ Green Master Mix (Applied Biosystems, Lithuania) using the following conditions: 10 min at 95⁰C, 40 cycles at 95⁰C for 30 sec, 55⁰C for 30 sec, and 72⁰C for 30 sec. The primers used in this study are listed in Table 5.1. To determine the fold change of different virulence genes and cytokine genes, the 2^{- $\Delta\Delta$ Ct} method was used [25]. Quantitative fold change analysis of each virulence gene (*fimH*, *papC*, *papGIII*, *sfaA*, *hlyA*, *iroN*) in the adherent UPEC is reported as fold change relative to their expression in adherent ABU83972. Moreover, the fold change analysis of each interleukin gene

(*IL-6*, *IL-8*, *TNF- α* , *IFN- γ* , *MCP-1*, *GCSF*, *IL-1 β* , *IL-17A*, *IL-5*, *TGF- β*) in the HTB-4 monolayer cell upon infection with the different UPECs, respectively, are reported as fold change relative to their expression upon infection with ABU83972. *16srRNA* and *GAPDH* expression were used for the normalization of the expression of the virulence genes and interleukin genes.

Table 5.1. Primer sequences for virulence genes and interleukins used in this study.

Sl. No.	Genes	Primers (5' \rightarrow 3')	Amplicon Size (bp)
qRT-PCR primer for Virulence genes			
1.	<i>fimH-RT</i>	FP: TGCAGAACGGATAAGCCGTGG RP: CACCACCACATCATTATTGGC	180
2.	<i>papC-RT</i>	FP: CAGCTACAGCCTGAACGCC RP: ATATCCTTTCTGCAGGGATGCAATA	133
3.	<i>papGIII-RT</i>	F: CATGGCTGGTTGTTCTTAAACAT R: GTCCAGATGTGTTTGCTTCATCCC	153
4.	<i>hlyA-RT</i>	F: CCGTGAAGAAGTATTGGGACCAC R: ACCATATAAGCGGTCATTCCCGTCA	128
5.	<i>iroN-RT</i>	F: CGTACTCATGCGGAAACCCGC R: GACGCCGACATTAAGACGCAG	129
6.	<i>sfaA-RT</i>	F: CCCTGAAGGGCAAAAACAGGTACA R: CGGAGGAGTAATTACAAACCTGGCA	127
7.	<i>16srRNA</i>	F: CCGCAAGGTTAAACTCAA R: CGACAGCCATGCAGCACC	169
qRT-PCR primer for Interleukin genes			
1.	<i>GAPDH-RT</i>	F: CAACAGCGACACCCACTC R: CATGTGGGCCATGAGGTC	136
2.	<i>IL-6 RT</i>	F: GTACATCCTCGACGGCATC R: GAATCCAGATTGGAAGCATCC	145
3.	<i>IL-8 RT</i>	F: GGTGCAGTTTTGCCAAGGAG R: GTTGGCGCAGTGTGGTCC	126
4.	<i>TNF-α RT</i>	F: CTGCCCTCCACCCATGTG R: CAGCTGGAAGACCCCTCCC	175
5.	<i>IFN-γ RT</i>	F: GAGGAAGAAGCGGGGAGTACTG R: GCTGAGTTGGGAGGAGAACACAC	152
6.	<i>MCP-1 RT</i>	F: GCAGAGGCTCGCGAGCTATAG R: CGGAGTTTGGGTTTGCTTGTCC	157
7.	<i>GCSF RT</i>	F: CTGCTGCTGTGGCACAGTG R: GGCACAGCTTGTAGGTGGC	178
8.	<i>IL-1β RT</i>	F: GTGCTCCTCCAGGACCTGG R: GGGAACCAGCATCTTCCTCAGC	142
9.	<i>IL-17A RT</i>	F: GGAATCTCCACCGCAATGAGGAC R: CGCAGGACCAGGATCTCTTGC	148
10.	<i>IL-5 RT</i>	F: GGTGAAAGAGACCTTGGCACTGC R: CTCTCCAGTGTGCCTATTCCCTG	141

11.	<i>TGF-β RT</i>	F: CAGCGACTCGCCAGAGTG	148
		R: CCCGTTGATGTCCACTTGCAG	

5.4.11. Target genes for VFG analysis of *E. coli* in qRT-PCR. Respective forward and Reverse primer sequences (5' → 3') are marked in green.

fimH

>NC_007946.1:4913899-4914413 Escherichia coli UTI89, complete sequence
TTATAATTCGAGAACGGATAAGCCGTGGCCGGTGGCGCTTTATTTGACGCCGGTGAGCAGTGCGGGGGGA
GTGGCGATTAAAGCTGGCTCATTAATTGCCGTGCTTATTTTGCACAGACCAACAATAACAGCGATG
ATTTCCAGTTTGTGTGGAATATTTACGCCAATAATGATGTGGTGGTGCCCACTGGCGGCTGCGATGTTTC
TGCTCGTGATGTCACCGTTACTCTGCCGGACTACCCTGGTTCAGTGCCGATTCTCTTACCGTTTATTGT
GCGAAAAGCCAAACCTGGGGTATTACCTCTCCGGCACAACCGCAGATGCGGGCAACTCGATTTTCACCA
ATACCGCGTCGTTTTACCCGCGCAGGGCGTCGGCGTACAGTTGACGCGCAACGGTACGATTATTCCAGC
GAATAACACGGTATCGTTAGGAGCAGTAGGGACTTCGGCGGTAAGTCTGGGATTAACGGCAAATTACGCA
CGTACCGGAGGGCAGGTGACTGCAG

papC

>X61239.1:4643-4980 E.coli papABCDEFGHJK genes for F13 P-pili proteins
ATGTCTGACGGCTGTACTGCAGGGTGTGGCGGTTGGATTGTCAGCCTCAAGGTCTAAATATCTGGGGCGT
GATAACGATTCTGCTTACCTGCGTATATCCGTGCCGCTGGGGACGGGGACAGCGAGCTACAGTGGCAGTA
TGAGTAATGACCGTTATGTGAATATGGCCGGCTACACTGACACGTTCAATGACGGTCTGGAACAGCTACAG
CCTGAACGCCGGCCTTAACAGTGGCGGTGGACTGACATCGCAACGTCAGATTAATGCCTATTACAGTCAT
CGTAGTCCGCTGGCAAATTTGTCCGCGAATATTGCATCCCTGCAGAAAGGATATACGT

papGIII:

>AY212281.1:240-672 Escherichia coli strain APEC 14 PapGIII (papGIII) gene, complete cds
GTATTTTGATGGCTGGTTGTTCTCTAAACGTGTTTCCTATAATGGATATGATATATATCTTGAACCTTCAG
TCCAGAGGAAGTTTTTCACTTGATGCAGAAGATAATGATAATTACTATCTTACCAAGGGATTTCATGGG
ATGAAGCAAACACATCTGGACGGACATGTTTCAATATCGGAGAAAAAAGAAGTCTGGCATGGTCATTTGG
TGGTGTACCCTGAACGCCAGATTTTCTGTTGACCTTCCTGAGGGGGATTATACGTTTCCAGTTAAGTTC
TTACGTGGCATTTCAGCATAATAATTATGATTATATTGGTGGACGCTACAAAATTCCTTCCTCGTTAATGA
AAACATTTCTTTTAAATGGTACATTGAATTTCTCAATTAAGAATACCGGAGTATGCCGTCCTTCTGCACA
GTCTCTGGAAATA

hlyA:

>CP009072.1:c1763809-1762628 Escherichia coli ATCC 25922, complete genome
GTTAACAACGATAAGCACTGTTCTGGCTTCAGTATCTTCAGGTATTAGTGCTGCTGCAACGACATCTCTG
GTTGGTGCACCGGTAAGCGCGCTGGTAGGGGCTGTTACGGGGATAATTTACGGCATCCTTGAGGCTTCAA
AACAGGCAATGTTTGAACATGTCGCCAGTAAAATGGCCGATGTTATTGCTGAATGGGAGAAAAAACACGG
CAAAAATTACTTTGAAAATGGATATGATGCCCGCCATGCTGCATTTTTAGAAAGATAACTTTAAAATATTA
TCTCAGTATAATAAAGAGTATTCTGTTGAAAGATCAGTCCTCATTACCCAGCAACATTGGGATACGCTGA
TAGGTGAGTTAGCGGGTGTACCCAGAAATGGAGACAAAACACTCAGTGGTAAAAGTTATATTGACTATTA
TGAAGAAGGAAAACGTCTGGAGAAAAAACCGGATGAATTCCAGAAGCAAGTCTTTGACCCATTGAAAGGA
AATATTGACCTTTCTGACAGCAAATCTTCTACGTTATTGAAATTTGTTACGCCATTGTTAACTCCCGGTG
AGGAAATTCGTGAAAGGAGGCAGTCCGGAATATGAATATATTACCGAGTTATTAGTCAAGGGTGTGTA
TAAATGGACGGTGAAGGGGGTTCAGGACAAGGGGTCTGTATATGATTACTCTAACCTGATTTCAGCATGCA
TCAGTCGGTAATAACAGTATCGGGAAATTCGTATTGAGTCACACCTGGGAGACGGGGATGATAAGGTCT
TTTTATCTGCCGGCTCAGCCAATATCTACGCAGGTAAAGGACATGATGTTGTTTATTATGATAAAACAGA
CACCGGTTATCTGACCATTGATGGCACAAAAGCAACCGAAGCGGGTAATTACACGGTAACACGTGTACTT
GGTGGTGTGTTAAGATTTTACAGGAAGTTGTGAAGGAGCAGGAGGTTTCAGTTGGAAAAAGAACTGAAA
AAACGCAATATCGGAGTTATGAATTCATCATATCAATGGTAAAAATTTAACAGAGACTGATAACTTATA

TTCCGTGGAAGAACTTATTGGGACCACGCGTGCCGACAAGTTTTTTGGCAGTAAATTTACTGATATCTTC
CATGGCGCGGATGGTGATGACCATATAGAAGGAAATGATGGGAATGACCGCTTATATGGTGA

iroN

>CP028770.1:c3116290-3115616 Escherichia coli strain A4 chromosome, complete genome

TCAAAGTCAAAGCAGGGGTTGCCCGAACCTTTAAAGCCCCAAACCTGTATCAATCCAGTGAAGGCTATCT
GCTCTACTCGAAAGGCAATGGCTGTCCAAAAGATATTACATCAGGCGGGTGCTACCTGATCGGTAATAAA
GATCTCGATCCGGAATCAGCGTCAATAAAGAAATTGGACTGGAGTTCACCTGGGAAGATTACCACGCAA
GTGTGACCTACTTCCGCAATGATTACCAGAATAAGATCGTGGCCGGGGATAACGTTATCGGGCAAACCGC
TTCAGGCGCATATATCCTCAAGTGGCAGAATGGCGGGAAAGCTCTGGTGGACGGTATCGAAGCCAGTATG
TCTTTCCCGCTGGTGAAAGATCGTCTGAACTGGAATACCAATGCCACATGGATGATCACTTCGGAGCAAA
AAGACACCGGTAATCCTCTGTCTGGTCACTCCGAAATATACTATCAATAACTCGCTTAACTGGACCATCAC
CCAGGCGTTTTCTGCCAGCGTCAACTGGACGTTATATGGCAGACAAAAACCGCGTACTCATGCGGAAACC
CGCAGTGAAGATACTGGCGGTCTGTCTAGGTAAAGAGCTGGGCGCTTATTCACTGGTGGGGACGAACCTCA
ATTACGATATTAATAAAAAATCTGCGTCTTAATGTCTGGCGTCAGTA

sfaA:

>X16664.4:17980-18399 Escherichia coli encoding determinant sfa(I)

ATCAGCCTCCGGAGAAGTGGGTGCATCTTACC CGCGGAGATATGAAACTGCATATGCAGGCGAGGTATAA
GGCCACACATTATCCCGTCGCGGGGGAAAGGC AAATGGACAGGTATGGTTTTCTCTGACCTATCTGTAA
CTGGCAGATATAATGCCATTTAATTAAGGCTGTTAATAACATGATGAAGCACATGCGTATATGGGCCGTT
CTGGCATCATTTTTTAGTCTTTTTTTTATATTCCGCAGAGCTATGCCGGGGTTGCTCTGGGTGCCACCCGTG
TGATTTTACCTGAAGGGCAAAAACAGGTACA ACTGGCGGTAACAAATAATGATGATAAAAGTAGTTACCT
TATTCAGTCATGGATTGAAAATGCTGAAGGAAAAAAGGATGC CAGGTTTGTAATTACTCCTCCGTTATTT

16srRNA

>Z83204.1:877-1050 E.coli 16S ribosomal RNA

ACGGCCGC AAGGTTAAACTCAAATGAATTGACGGGGGCCCCGACAAAGCGGTGGAGCATGTGGTTTAATT
CGATGCAACGCGAAGAACCTTACCTGGTCTTGACATCCACGGAAGTTTTTCAGAGATGAGAATGTGCCTTC
GGGAACCGTGAGACA GGTGCTGCATGGCTGTGCT

GAPDH

>NM_001256799.3:1035-1170 Homo sapiens glyceraldehyde-3-phosphate dehydrogenase (GAPDH), transcript variant 2, mRNA

CAACAGCGACACCCACTCTCCACCTTTGACGCTGGGGCTGGCATTGCCCTCAACGACCACTTTGTCAAG
CTCATTTTCTGGTATGACAACGAATTTGGCTACAGCAACAGGGTGGTG GACCTCATGGCCACATG

IL-6

>JQ250825.1:171-315 Homo sapiens interleukin 6 gene, complete cds

GTACATCCTCGACGGCATCTCAGCCCTGAGAAAGGAGACATGTAACAAGAGTAACATGTGTGAAAGCAGC
AAAGAGGCACTGGCAGAAAACAACCTGAACCTTCAAAGATGGCTGAAAAGATGGATGCTTCCAATCTG
GATTC

IL-8

>M28130.1:2463-2588 Human interleukin 8 (IL8) gene, complete cds

GGTGCAAGTTTGGCAAGGAGTGCTAAAGAACTTAGATGTCAAGTGCATAAAGACATACTCCAAACCTTTCC
ACCCCAAATTTATCAAAGAACTGAGAGTGATTGAGAGTGGACCACACTGCGCCAAC

TNF- α

>MH180383.1:2942-3116 Homo sapiens isolate RKL121_WG_new TNF-alpha (TNF-alpha) gene, promoter region and complete cds

CTGCCCCCTCCACCCATGTGCTCCTCACCCACACCATCAGCCGCATCGCCGTCTCCTACCAGACCAAGGTC
AACCTCCTCTCTGCCATCAAGAGCCCCTGCCAGAGGGAGACCCAGAGGGGGCTGAGGCCAAGCCCTGGT
ATGAGCCCATCTATCTGGGAGGGGTCTTCCAGCTG

IFN- γ

>J00219.1:2448-2599 Homo sapiens interferon-gamma (IFNG) gene, complete cds

GAGGAAGAAGCAGGGAGTACTGAGAAGCAGTTCTCTCATTGTCCCTTGCTCATATGATGGAAATTCTCTT
ACTTTGAATGAGAGGCTGTCTGTCTTAATGGAAAGAGCAGTGGGAGGAGCTGAGAAGATGTGTGTTCTCC
TCCCAACTCAGC

MCP-1

>S71513.1:188-344 monocyte chemoattractant protein-1 [human, mRNA, 739 nt]
GCAGAGGCTCGCGAGCTATAG AAGAATCACCAGCAGCAAGTGTCCCAAAGAAGCTGTGATCTTCAAGACC
ATTGTGGCCAAGGAGATCTGTGCTGACCCCAAGCAGAAGTGGGTTTCAGGATTCCATGGACCACCTGGACA
AGCAAACCCAAACTCCG

GCSF

>NM_000759.4:84-261 Homo sapiens colony stimulating factor 3 (CSF3),
transcript variant 1, mRNA
CTGCTGCTGTGGCAGAGTG CACTCTGGACAGTGCAGGAAGCCACCCCCCTGGGCCCTGCCAGCTCCCTGC
CCCAGAGCTTCCTGCTCAAGTGCTTAGAGCAAGTGAGGAAGATCCAGGGCGATGGCGCAGCGCTCCAGGA
GAAGCTGGTGAGTGAGTGTGCCACCTACAAGCTGTGCC

IL-1 β

>NM_000576.3:186-327 Homo sapiens interleukin 1 beta (IL1B), mRNA
GTGCTCCTTCCAGGACCTGG ACCTCTGCCCTCTGGATGGCGGCATCCAGCTACGAATCTCCGACCACCAC
TACAGCAAGGGCTTCAGGCAGGCCGCGTCAGTTGTTGTGGCCATGGACAAGCTGAGGAAGATGCTGGTTCC
CC

IL17A

>NM_002190.3:278-425 Homo sapiens interleukin 17A (IL17A), mRNA
GGAATCTCCACCGCAATGAGGAC CCTGAGAGATATCCCTCTGTGATCTGGGAGGCAAAGTGCCGCCACTT
GGGCTGCATCAACGCTGATGGGAACGTGGACTACCACATGAACTCTGTCCCCATCCA GCAAGAGATCCTG
GTCCTGCG

IL-5

>NM_000879.3:131-271 Homo sapiens interleukin 5 (IL5), mRNA
GGTGAAAGAGACCTTGGCACTGC TTTCTACTCATCGAACTCTGCTGATAGCCAATGAGACTCTGAGGATT
CCTGTTCTGTACATAAAAATCACCAACTGTGCACTGAAGAAATCTTT CAGGGAATAGGCACACTGGAGA
G

TGF- β

>M60316.1:528-694 Human transforming growth factor-beta (tgf-beta) mRNA,
complete cds
GGAATTCTTCCACCCACGCT ACCACCATCGAGAGTTCCGGTTTGATCTTTCCAAGATCCCAGAAGGGGAA
GCTGTACACGGCAGCCGAATTCCGGATCTACAAGGACTACATCCGGAACGCTTCGACAATGAGACGTTCC
GGATCA GCGTTTATCAGGTGCTCCAGG

5.4.12. Role of different interleukins in Urinary tract infection:

5.4.12.1. Interleukin – 6: Human IL-6 is made up of 212 amino acids, including a 28-amino-acid signal peptide, and its gene has been mapped to chromosome 7p21. Although the core protein is ~20kDa, glycosylation accounts for the size of 21-26 kDa of natural IL-6. IL-6 secretes rapidly by urothelial cells due to *Escherichia coli* exposure. Different studies implicate the urothelial IL-6 production by the elicitation of lipopolysaccharide (LPS) and P-fimbriae. In bladder uroepithelium, Toll-like receptor 4 (TLR4) is engaged by LPS, thereby triggering an intracellular signaling cascade leading to IL-6 secretion. Studies suggests that virulence correlates inversely with IL-6 production, such that low IL-6 confers a survival advantage for UPEC during cystitis. The IL-6 expression indicates the severity of clinical UTI. Children with pyelonephritis and renal

scarring have elevated urine and serum IL-6 levels compared to those with cystitis. An association between IL-6 production and severity has also been demonstrated in Animal models [26].

5.4.12.2. **Interleukin – 8:** Protein encoded by this gene is a member of the CXC chemokine family and is a major mediator of the inflammatory response. IL-8 is secreted by mononuclear macrophages, neutrophils, eosinophils, T-lymphocytes, epithelial cells, and fibroblasts. It functions as a chemotactic factor by guiding the neutrophils to the site of infection. Studies documented a rapid TLR4-dependent urine neutrophil response in the mouse model of UTI and the IL-8 family of chemokines (CXCL8) was shown to be activated during acute pyelonephritis in patients [27].

5.4.12.3. **Tumor Necrosis Factor – alpha (TNF- α):** This cytokine is mainly secreted by macrophages. It can bind to, and thus functions through its receptors TNFRSF1A/TNFR1 and TNFRSF1B/TNFR2. the cytokine is involved in the regulation of a wide spectrum of biological processes including cell proliferation, differentiation, apoptosis, lipid metabolism, and coagulation. Early studies demonstrated the cytokine production of bladder epithelial in response to UTI. It has been observed that the pro inflammatory cytokine TNF, rapidly and transiently expressed during the first days of infection and supports neutrophil recruitment and bacterial clearance in UTI [27].

5.4.12.4. **Interferon – gamma (IFN- γ):** This gene encodes a soluble cytokine that is a member of the type II interferon class. The encoded protein is secreted by cells of both the innate and adaptive immune systems. The active protein is a homodimer that binds to the interferon gamma receptor which triggers a cellular response to viral and microbial infections. IFN- γ modulates cytokine release by monocytes and macrophages and has been shown to reduce phagocytosis of different pathogens including *E. coli* [28]. Study demonstrated that within 4 hours of a UPEC infection in the kidney, an IFN- γ response is triggered in the spleen. This rapid infection-mediated inter-organ communication was found to be transmitted via nerve signaling. Bacterial expression of the toxin α -hemolysin directly and indirectly activated sensory neurons, which were identified in the basement membrane of renal tubules [29].

5.4.12.5. **Monocyte Chemoattractant protein (MCP-1):** MCP-1/CCL2 is one of the key chemokines that regulate migration and infiltration of monocytes/macrophages. Both CCL2 and its receptor CCR2 have been demonstrated to be induced and involved in various diseases [30].

Inflammatory cytokines, including MCP-1, play an important role in glomerular inflammation. It triggers migration and retention of monocytes and transformation of fibroblasts in the glomeruli. The urinary concentration of MCP-1 increases with increased activity of glomerular diseases. It is associated with flares of systemic lupus erythematosus and small vessel vasculitis. In diabetic nephropathy, increased urinary MCP-1 is associated with faster disease progression to kidney failure. However, the prognostic utility of urinary MCP-1 in primary proteinuric glomerulonephritis has not received much attention [31].

5.4.12.6. Granulocyte Colony Stimulating Factor (G-CSF): This cytokine controls the production, differentiation, and function of granulocytes. The gene for G-CSF is located on chromosome 17, locus q11.2-q12. G-CSF gene has 4 introns, and two different polypeptides are synthesized from the same gene by differential splicing of mRNA. A study demonstrated that, UPEC infection induces expression of several pro-inflammatory cytokines including G-CSF. G-CSF depletion resulted in a significant decrease in bladder-infiltrating neutrophils during infection. Yet, bacterial clearance in G-CSF-neutralized animals were significantly improved compared with control-treated animals. Elevated levels of several cytokines are able to activate macrophages accompanying G-CSF neutralization, including IL-1 β and MCP-1 [32].

5.4.12.7. Interleukin 1 beta (IL-1 β): Initially discovered as the major endogenous pyrogen, proinflammatory cytokine IL-1 β induces prostaglandin synthesis, neutrophil influx and activation, T-cell activation and cytokine production, B-cell activation, antibody production, and fibroblast proliferation and collagen production. It synergizes with IL-12 to induce IFN- γ synthesis from T-helper 1 cells. IL-1 β has also been known to be a fever-producing endogenous pyrogen that is detected early and throughout the inflammatory progression, which is also responsible for acute-phase reactions, as well as fever development. The evaluation of IL-1 β in urine specimen is both clinically workable and potentially beneficial in UTI, especially because of its role in systemic inflammation [33].

5.4.12.8. Interleukin 17A (IL-17A): IL-17A and IL-17F are highly proinflammatory, ‘single cytokines’ of effector T helper 17 (Th17) cells, a distinct lineage of CD4⁺ T helper cells of adaptive immune system that appears to play an important role in clearing pathogens not adequately handled by the Th1 or Th2 immune response [33]. Analysis of UPEC persistence and pyelonephritis in mice deficient in IL-17A revealed that UPEC CFT073 caused infection at a rate higher than the

multidrug resistant strain EC958. Il17a^{-/-} mice exhibited pyelonephritis with kidney bacterial burdens higher than those of wild-type mice. Synthesis of IL-17A in the bladder reflected a combination of $\gamma\delta$ -T and T_H 17 cell responses [34].

5.4.12.9. Interleukin 5 (IL-5): This cytokine that acts as a growth and differentiation factor for B cells and eosinophils. The cytokine plays a major role in the regulation of eosinophil formation, maturation, recruitment and survival. The increased production of this cytokine may be related to pathogenesis of eosinophil-dependent inflammatory diseases. This cytokine functions by binding to its receptor, which is a heterodimer, whose beta subunit is shared with the receptors for IL-3 and GM-CSF. A study suggested the presence of specific inflammatory cytokine (IL-5, IL-20 and IL-28A)-mediated association in bladder cancer development. Increasing IL-5 levels might be responsible for augmented development of bladder tumor cells and their inability to be recognized by inflammatory [36].

5.4.12.10. Transforming Growth Factor β (TGF- β): TGF- β protein initiates chemical signals that regulate a variety of cellular processes, including cell growth and division (proliferation), cell differentiation into different cell types with specific functions, cell motility, and regulated cell death. TGF- β also involved in the growth of blood vessels the development of muscle and body fat, the healing of wounds, immune system inflammation, and tumor prevention. It plays a crucial role in promoting extracellular matrix deposition and fibrosis leading to loss of functional renal tissue. Mouse kidney cells have been demonstrated to express increased mRNA of TGF- β during pyelonephritis, in vivo [37].

5.5. Results:

5.5.1. Bacterial isolates:

For this study, a total of 21 each out of 36 and 34 uropathogenic *Escherichia coli* isolates from pregnant population (UPECp) and non-pregnant population (UPECnp), respectively. A higher distribution of MDR was observed among UPECnp than UPECp isolates, when antibiotic resistant pattern was analyzed. A higher distribution of MDR was observed among UPECnp than UPECp isolates, when antibiotic resistance pattern was analyzed against the regimen of ten antibiotics.

A significant very strong positive correlation between CAZ and CTX, CIP and CTX, strong positive correlation between CIP and CAZ, COT and CAZ, COT and CTX, moderate positive correlation between COT and CIP, IPM and CIP and MRP and IPM was observed in the antibiotic resistance pattern between these 21 UPECp isolates. As for UPECnp isolates, strong positive correlation between ETR and MRP, moderate positive correlation between CAZ and CTX, COT and CIP and moderate negative correlation between MRP and CIP was observed (Table 5.2).

Table 5.2: Correlation of antibiotic resistance pattern in the UPECp(n=21) and UPECnp(n=21) isolates

UPECp										
	AK	AMP	CAZ	CTX	CIP	NIT	COT	IPM	MRP	ETR
AK	a									
AMP	a	a								
CAZ	a	a	1							
CTX	a	a	.816**	1						
CIP	a	a	.708**	.901**	1					
NIT	a	a	0.194	0.158	0.175	1				
COT	a	a	.730**	.671**	.589**	0.141	1			
IPM	a	a	0.204	0.357	.485**	0.158	0.224	1		
MRP	a	a	-0.091	0.000	0.062	0.354	0.167	.447*	1	
ETR	a	a	-0.194	-0.316	-0.252	-0.125	0.106	0.158	0.389	1
UPECnp										
	AK	AMP	CAZ	CTX	CIP	NIT	COT	IPM	MRP	ETR
AK	1									
AMP	a	a								
CAZ	-0.131	a	1							
CTX	-0.175	a	.461*	1						
CIP	-0.255	a	-0.157	-0.073	1					
NIT	-0.113	a	0.420	0.194	-0.047	1				
COT	-0.062	a	0.230	0.354	.513*	0.335	1			
IPM	0.080	a	-0.157	-0.073	-0.105	-0.375	-0.205	1		
MRP	0.139	a	-0.429	0.158	-.459*	-0.204	-0.224	0.229	1	
ETR	-0.037	a	-0.266	0.213	-0.340	-0.055	-0.241	-0.015	.742**	1

** . Correlation is significant at the 0.01 level (2-tailed)

* . Correlation is significant at the 0.05 level (2-tailed)

^a . cannot be computed because at least one of the variables is constant

5.5.2. Prevalence of virulence genes: The highest prevalence of *fimH* (UPECp 95.24%, UPECnp 90.48%) was observed in both groups followed by the prevalence of *papC* (UPECp 100%,

UPECnp 76.20%), presence of both of the genes were statistically significant ($P<0.001$). Moreover, in UPECp isolates the presence of *sfaA*, *hlyA*, and *iroN* and in UPECnp isolates the presence of *hlyA* and *papGIII* was statistically significant ($P<0.001$). The overall prevalence of virulence genes namely *fimH*, *papC*, *sfaA*, *hlyA* and *iroN* was greater in UPECp isolates than in UPECnp isolates, except for *papGIII*, whose distribution was higher in the UPECnp group than in the UPECp group (Figure 5.3).

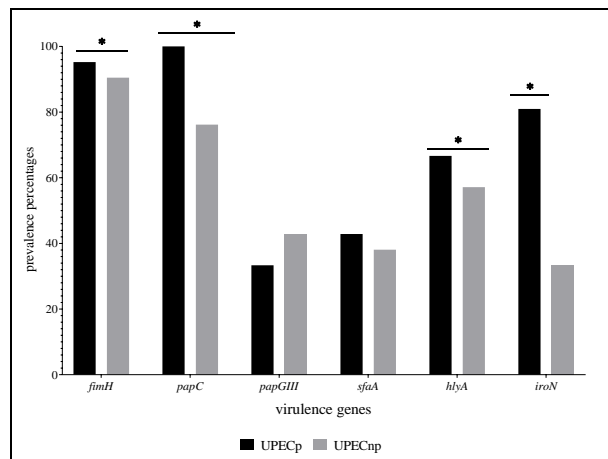


Figure 5.3. Prevalence of six virulence genes in uropathogenic *Escherichia coli* pregnant (n=21) and non-pregnant isolates (n=21).

5.5.3. Expression of virulence genes: In the UPECp and UPECnp isolates, a distinct pattern of relative expression of virulence genes (*fimH*, *papC*, *papGIII*, *sfaA*, *hlyA*, *iroN*) was observed 3 hours post-infection (hpi) in HTB-4 uroepithelial cells for their expression in the control strain ABU83972. An overall positive fold change of *fimH*, *hlyA*, *papGIII* and *sfaA* in 61.9%, 38.1%, 19.05% and 23.8%, and overall negative fold change of *papC* and *iroN* in 57.14% and 61.9% of UPECp isolates was observed (Figure 5.4A). The positive fold change of *fimH* ($p<0.001$) and negative fold change of *papC* ($p<0.001$) and *iroN* ($p<0.001$) in UPECp were statistically significant. An overall negative fold change of *fimH*, *papC*, *papGIII* and *iroN* in 61.9%, 52.4%, 28.57% and 28.57% and overall positive fold change of *sfaA* and *hlyA* in 23.80% and 42.86% of UPECnp isolates was observed (Figure 5.4B). The positive fold change in *hlyA* ($p<0.001$) and negative fold change in *fimH* ($p<0.001$) and *papC* ($p<0.001$) were statistically significant.

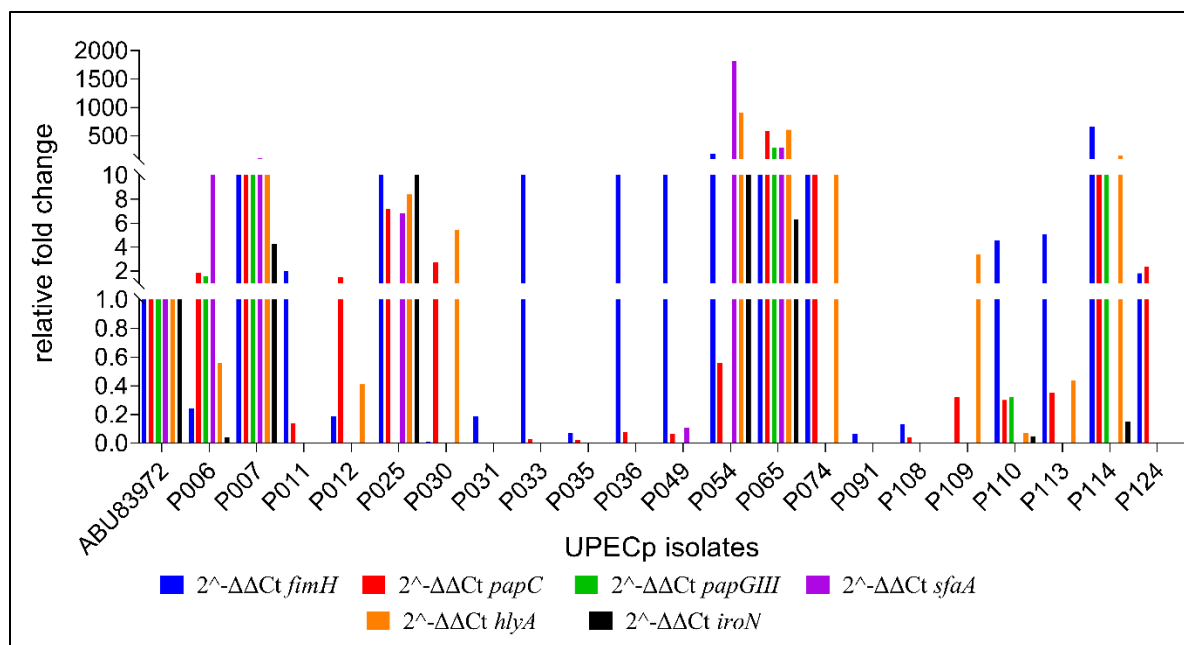


Figure 5.4A: Relative fold change of *fimH*, *papC*, *papGIII*, *sfaA*, *hlyA*, *iroN* genes in UPECp isolates

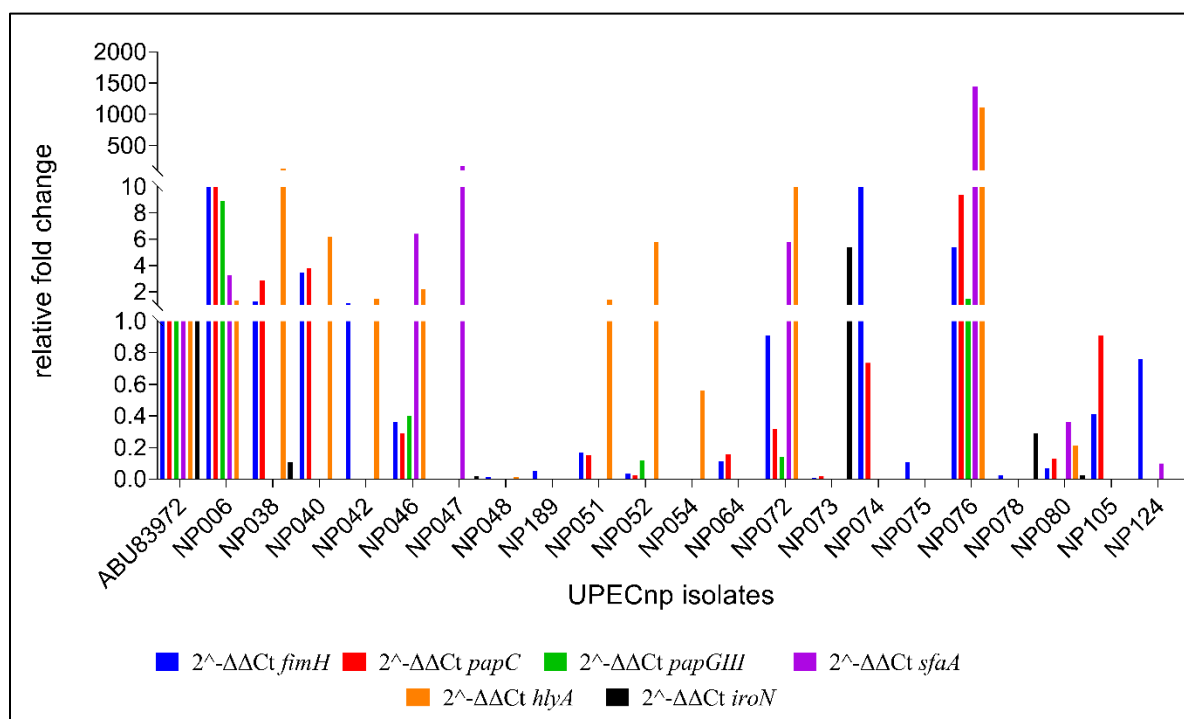


Figure 5.4B: Relative fold change of *fimH*, *papC*, *papGIII*, *sfaA*, *hlyA*, *iroN* genes in UPECnp isolates

5.5.4. Expression of cytokines: Infected HTB-4 cells showed a distinct pattern of relative fold expression of cytokines (*IL-6*, *IL-8*, *TNF- α* , *IFN- γ* , *MCP-1*, *GCSF*, *IL-1 β* , *IL-17A*, *IL-5*, and *TGF- β*) upon 3 hpi due to UPECp and UPECnp isolates, when compared with the expression of HTB-4 cells infected with ABU83972 cells. Overall enhanced relative fold expression of *IL-6*, *IL-8*, *IL-17A* and *IL-5* was observed in infected HTB-4 cells for 61.9%, 81%, 61.9%, and 71.4% of UPECp isolates, respectively and overall reduced relative fold expression of *TNF- α* , *IFN- γ* , *MCP-1*, *GCSF*, *IL-1 β* , and *TGF- β* was observed in HTB-4 cells infected with 81%, 95.2%, 76.2%, 95.2%, and 76.2% of UPECp isolates respectively, and their distribution was statistically significant ($p < 0.001$). Furthermore, an overall elevated relative fold expression of *TNF- α* , *IL-5*, and *TGF- β* were observed in HTB-4 cells infected with 52.4%, 76.2%, and 71.4% of UPECnp isolates respectively and overall reduced relative fold expression of *IL-6*, *IL-8*, *GCSF*, *IL-1 β* , and *IL-17A* were also observed in host cells infected with 76.2%, 76.2%, 66.7%, 85.7%, and 85.7% of UPECnp isolates respectively and in both of the cases, the distribution was also statistically significant ($p < 0.001$). Additionally, overall reduced relative fold expression of *IFN- γ* and *MCP-1* was observed in HTB-4 cells infected with all 21 (100%) UPECnp isolates, respectively, which was nonsignificant.

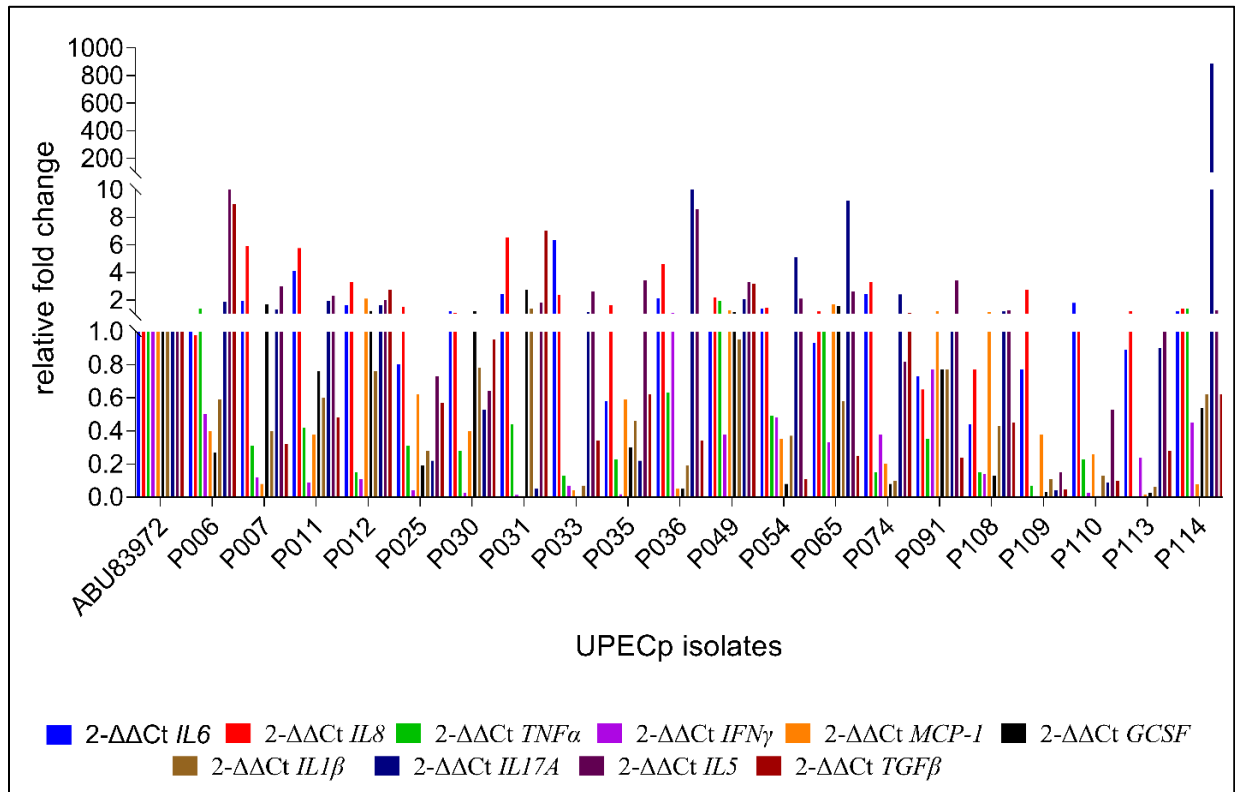


Figure 5.5A: Relative fold change of *IL-6*, *IL-8*, *TNF- α* , *IFN- γ* , *MCP-1*, *G-CSF*, *IL-1 β* , *IL17A*, *IL-5*, *TGF- β* of HTB-4 uroepithelial cells, due to infection by UPECp isolates.

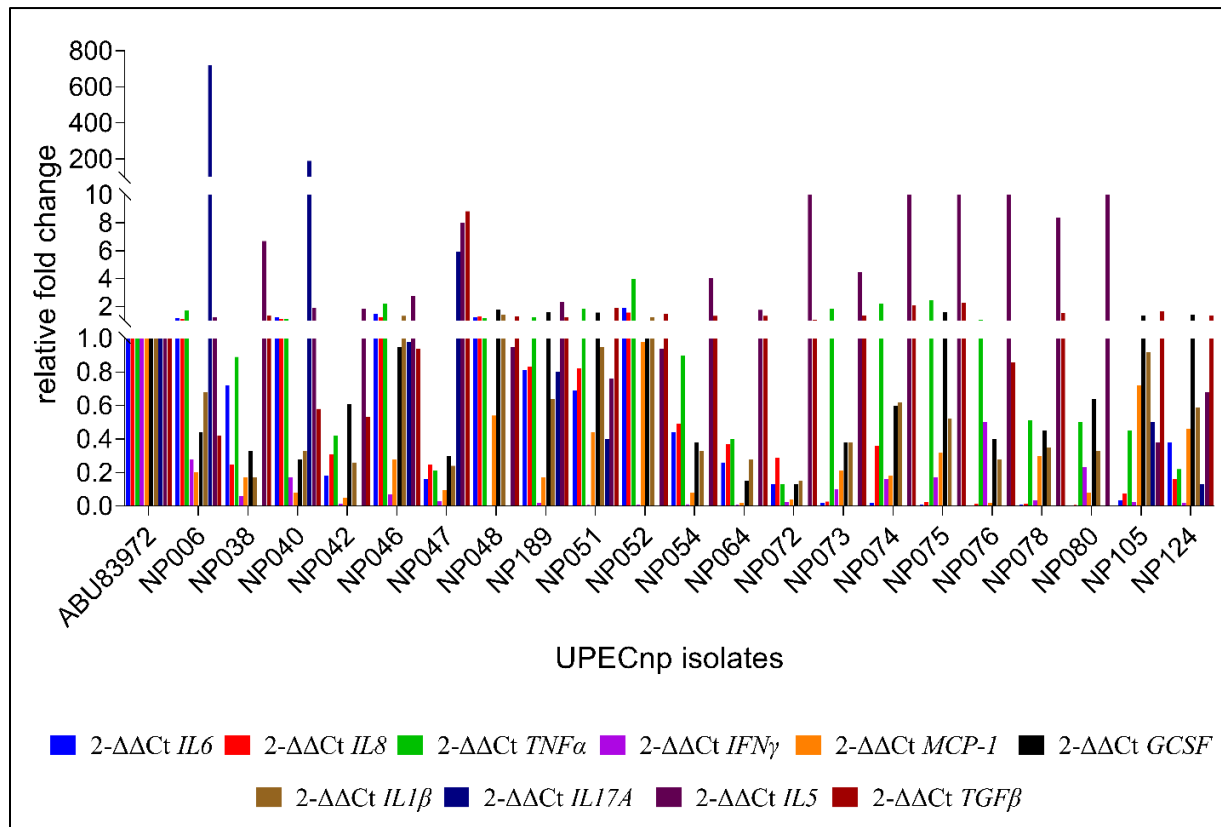


Figure 5.5B: Relative fold change of *IL-6*, *IL-8*, *TNF- α* , *IFN- γ* , *MCP-1*, *G-CSF*, *IL-1 β* , *IL17A*, *IL-5*, *TGF- β* of HTB-4 uroepithelial cells, due to infection by UPECnp isolates.

In UPECp isolates, significant moderate positive correlations were observed in between *fimH* and *IL-17A* and in between *fimH* and *IFN- γ* . Additionally, significant moderate negative correlations were observed in between *fimH* and *IL-1 β* (Table 5.3). Moreover, significant moderate negative correlations were observed in between *papC* and *G-CSF* and in between *hlyA* and *TGF- β* (Table 5.4).

Table 5.3: Correlation between expression of virulence genes and expression of cytokines in uropathogenic *Escherichia coli* pregnant isolates

UPECp											
	<i>fimH</i>	<i>IL-6</i>	<i>IL-8</i>	<i>TNF-α</i>	<i>IFN-γ</i>	<i>MCP-1</i>	<i>G-CSF</i>	<i>IL-1β</i>	<i>IL-17A</i>	<i>IL-5</i>	<i>TGF-β</i>
<i>fimH</i>	1										
<i>IL-6</i>	0.305	1									
<i>IL-8</i>	0.186	0.678 [†]	1								

<i>TNF-α</i>	0.182	0.200	0.048	1							
<i>IFN-γ</i>	0.402[‡]	0.109	-0.151	0.568	1						
<i>MCP-1</i>	-0.298	-0.452 [‡]	-0.354	0.197	0.022	1					
<i>GCSF</i>	-0.212	0.095	0.224	0.523 [†]	0.078	0.385 [‡]	1				
<i>IL-1β</i>	-0.396[‡]	0.090	0.040	0.640 [†]	0.172	0.436 [‡]	0.840 [†]	1			
<i>IL-17A</i>	0.475[‡]	0.348	0.147	0.612 [†]	0.821 [†]	0.103	0.210	0.213	1		
<i>IL-5</i>	0.186	0.143	0.114	0.586 [†]	0.590 [†]	0.188	0.348	0.374 [‡]	0.505 [†]	1	
<i>TGF-β</i>	-0.230	0.166	0.201	0.291	0.003	0.113	0.453 [‡]	0.513 [†]	0.125 [†]	0.192	1
<i>papC</i>	1										
<i>IL-6</i>	0.014	1									
<i>IL-8</i>	-0.049	0.678 [†]	1								
<i>TNF-α</i>	-0.020	0.200	0.048	1							
<i>IFN-γ</i>	0.160	0.109	-0.151	0.568 [†]	1						
<i>MCP-1</i>	0.016	-0.452 [‡]	-0.354	0.197	0.111	1					
<i>GCSF</i>	0.053	0.095	0.224	0.523 [†]	0.078	0.385 [‡]	1				
<i>IL-1β</i>	-0.243	0.090	0.040	0.640 [†]	0.172	0.436 [‡]	0.840 [†]	1			
<i>IL-17A</i>	0.279	0.348	0.147	0.612 [†]	0.812 [†]	0.103	0.210	0.213	1		
<i>IL-5</i>	-0.277	0.143	0.114	0.586 [†]	0.590 [†]	0.188	0.348	0.374 [‡]	0.505 [†]	1	
<i>TGF-β</i>	-0.084	0.166	0.201	0.291	0.003	0.113	0.453 [‡]	0.513 [†]	0.125	0.192	1
<i>iroN</i>	1										
<i>IL-6</i>	-0.088	1									
<i>IL-8</i>	0.004	0.678 [†]	1								
<i>TNF-α</i>	0.190	0.200	0.048	1							
<i>IFN-γ</i>	0.204	0.109	-0.151	0.568 [†]	1						
<i>MCP-1</i>	0.104	-0.452 [‡]	-0.354	0.197	0.111	1					
<i>GCSF</i>	0.126	0.095	0.224	0.523 [†]	0.078	0.385 [‡]	1				
<i>IL-1β</i>	-0.177	0.090	0.040	0.640 [†]	0.172	0.436 [‡]	0.840 [‡]	1			
<i>IL-17A</i>	0.279	0.348	0.147	0.612 [†]	0.821 [†]	0.103	0.210	0.213	1		
<i>IL-5</i>	0.012	0.143	0.114	0.586 [†]	0.590 [†]	0.188	0.348	0.374 [‡]	0.505 [†]	1	
<i>TGF-β</i>	-0.020	0.166	0.201	0.291	0.003	0.113	0.453 [‡]	0.513 [†]	0.125	0.192	1

[†]Correlation is significant at the 0.01 level (one-tailed)

[‡]Correlation is significant at the 0.05 level (one-tailed)

Table 5.4: Correlation between expression of virulence genes and expression of cytokines in uropathogenic *Escherichia coli* non-pregnant isolates

UPECnp	<i>fimH</i>	<i>IL-6</i>	<i>IL-8</i>	<i>TNF-α</i>	<i>GCSF</i>	<i>IL-1β</i>	<i>IL-17A</i>	<i>IL-5</i>	<i>TGF-β</i>
<i>fimH</i>	1								
<i>IL-6</i>	-0.011	1							
<i>IL-8</i>	-0.045	0.955 [‡]	1						
<i>TNF-α</i>	-0.006	0.302	0.282	1					
<i>GCSF</i>	-0.163	0.165	0.123	0.433 [‡]	1				
<i>IL-1β</i>	-0.124	0.449 [‡]	0.431 [‡]	0.661 [†]	0.762 [†]	1			
<i>IL-17A</i>	0.103	0.518 [†]	0.489 [‡]	0.044	0.175	0.395 [‡]	1		
<i>IL-5</i>	0.014	-0.637 [†]	-0.614 [†]	0.029	-0.329	-0.520 [†]	-0.474 [‡]	1	
<i>TGF-β</i>	-0.335	-0.189	-0.229	0.155	0.158	0.145	-0.112	0.015	1
<i>papC</i>	1								
<i>IL-6</i>	0.133	1							
<i>IL-8</i>	0.134	0.955 [†]	1						
<i>TNF-α</i>	0.096	0.302	0.282	1					
<i>GCSF</i>	-0.453[‡]	0.165	0.123	0.433 [‡]	1				
<i>IL-1β</i>	-0.086	0.449 [‡]	0.431 [‡]	0.661 [†]	0.762 [†]	1			
<i>IL-17A</i>	0.100	0.518 [†]	0.489 [‡]	0.044	0.175	0.395 [‡]	1		
<i>IL-5</i>	0.017	-0.637 [†]	-0.614 [†]	0.029	-0.329	-0.520 [†]	-0.474 [‡]	1	
<i>TGF-β</i>	-0.333	-0.189	-0.229	0.155	0.158	0.145	-0.112	0.015	1
<i>hlyA</i>	1								
<i>IL-6</i>	0.322	1							
<i>IL-8</i>	0.325	0.955 [†]	1						

<i>TNF-α</i>	0.064	0.302	0.282	1					
<i>GCSF</i>	-0.289	0.165	0.123	0.433 [†]	1				
<i>IL-1β</i>	-0.221	0.449 [‡]	0.431 [‡]	0.661 [†]	0.762 [†]	1			
<i>IL-17A</i>	-0.060	0.518 [†]	0.489 [‡]	0.044	0.175	0.395 [‡]	1		
<i>IL-5</i>	0.062	-0.637 [†]	-0.614 [†]	0.029	-0.329	-0.520 [†]	-0.474 [‡]	1	
<i>TGF-β</i>	-0.517[†]	-0.189	-0.229	0.155	0.158	0.145	-0.112	0.015	1

[†]Correlation is significant at the 0.01 level (one-tailed)

[‡]Correlation is significant at the 0.05 level (one-tailed)

5.6. Discussion

Multidrug resistance (MDR) creates a frequent complication in the treatment of UTIs worldwide. Additionally, due to pharmacokinetic and pharmacodynamic changes during pregnancy, the selection of antibiotics for treating UTIs in the pregnant population is constrained in comparison to the non-pregnant population. Numerous studies have documented the prevalence of MDR in the pregnant population, which makes choosing antibiotics even more difficult [8, 38, 39, 40, 41, 42, 43]. Additionally, as reported by other studies conducted globally [39, 40], MDR was found in all of the UPECnp isolates. Furthermore, this study revealed that the UPECp isolates had moderate to high resistance to AMP, CAZ, CIP and COT, whereas the UPECnp isolates had the highest resistance to AMP, CAZ, AK and CIP. This finding was alarming because there had been a significant drop in the number of specific medicines that may have ordinarily been used safely to treat UTIs in both populations. With the exception of sensitivity towards NIT, a study from Mexico observed a similar pattern of antibiotic resistance in *E. coli* isolates obtained from pregnant and non-pregnant women [8]. The study reported high resistance against NIT between both populations, unlike that reported in our study, which exhibited high susceptibility towards NIT in the pregnant populations, similar to other reports from Indian Subcontinent and Somaliland [38, 43]. Additionally, our study found high susceptibility to IPM, a member of carbapenem group of antibiotics, which is similar to a previous study that found the same with Meropenem, another carbapenem group of antibiotics [43]. Our study also found a statistically significant association between various antibiotics in co-resistant phenotypes.

According to the result, UPECp isolates with CAZ resistance also had resistance to CTX, CIP and COT and similarly, in the UPECnp isolates, resistance to AK and CIP was associated with resistance to IPM and COT or only IPM, respectively. The overall data being presented in our study, can be served as a rational indicator of antibiotic treatment and resistant patterns. To avoid further dissemination of MDR UPEC strains and/or to restrict co-selection mechanism this data might help in implementing a judicious prescription policy.

Virulence factors (VFs) are significant factors in bacterial pathogenicity. Bacterial and epithelial cell adhesion is a multifactorial and intricate process. The primary mechanism for colonization and the development of infection, which comprises numerous adhesins, iron-acquisition system proteins, and toxins, is thought to mediate the attachment to the uroepithelial cells. The first attachment to the epithelial cells is mediated by the tip adhesin, *fimH*. The *fimH* gene was shown to be widely distributed in both obtained from pregnant (95.24%) and non-pregnant (90.48%) women, according to our study. The prevalence of the *fimH* gene in the range of 86% - 100% in the clinically obtained UPEC isolates, which is directly associated to their pathogenic potential, has been found in other studies throughout the world [44, 45, 46, 47, 48, 49, 50, 51, 52]. Furthermore, studies from all over the world revealed that clinical UPEC isolates had a low-to-moderate prevalence of the *papC* gene, a component of the *pap*- operon, involved in upper UTI [44, 49, 51]. However, in our study, incidence of *papC* in UPECp isolates was 100%, compared to UPECnp isolates, which was 76.2%, comparable to another study, where *E. coli* was obtained from both pregnant and non-pregnant women [53]. It has also been reported that S-fimbria, the mannose-resistant adhesins encoded by *sfa*- operon of UPEC, controls the virulence of the organism. The main subunit of the S-fimbriae is encoded by *sfaA*. Similar to a study by Lee et al. [54] that found a low prevalence of *sfaS*, the tip adhesin of S-fimbriae when compared with the commensal UPEC, our study found a low incidence of *sfaA* in both UPEC pregnant and non-pregnant isolates. A couple of studies from various countries throughout the globe revealed [44, 47, 49, 51] and moderate-to-high incidences [45, 46, 55, 56] of *sfaA* in clinical UPEC isolates. The expression of hemolysin, a pore-forming toxin encoded by *hlyA*, was correlated with the severity of the UPEC infection and was related to the intracellular survival of UPEC [57]. The invasion of urothelial cells by UPEC was also documented to be mediated by siderophores. The siderophore outer membrane receptor that *iroN* encodes has been linked to the development of biofilms. Low-to-moderate occurrences of *hlyA* were found in UPEC isolates, according to studies from various parts of the world [44, 46, 49, 51, 52, 58, 59]. The increased prevalence of *hlyA* in UPECp (80.95%) compared to UPECnp (66.67%) isolates in our study was similar to a report from Iraq [53]. Different studies [46, 47, 59] revealed a moderate prevalence of *iroN* among UPEC isolates, which is consistent with the findings of our study in the UPECnp (33.33%) isolates. On the other, our study found that *iroN* was highly prevalent (80.95%) in UPECp isolates. It is noteworthy that, important YF genes *fimH*, *papC*, *hlyA*, and *iroN* were significantly found in UPECp isolates and

that this finding was concerning for the treatment of UTI, particularly in pregnant women from Kolkata, a city in Eastern India.

In order to create intracellular bacterial communities (IBC), UPEC invaded the superficial uroepithelial cells with the help of the expression of *fimH* gene. Within the first 1 to 3 hours of infection, this bacterial invasion may begin [60]. The severity of the infection was shown to be mirrored in the expression of virulence determinants in several studies [61, 62], with many VFs being expressed more frequently by symptomatic strains causing UTI than by bacterial strains producing ABU. DNA microarray analysis of *E. coli* 83972 ABU strain revealed downregulation of the hemolysin synthesis, activation and transportation genes, *hlyCABD*, which was also found to be downregulated to support its asymptomatic nature [61]. This was caused by a large deletion in the *fim* gene cluster with undetected signals for the *fimEAIC* genes. In our study, virulence gene expression of the significantly distributed VFs in the UPECp and UPECnp isolates upon 3 hpi in HTB-4 cells was explored to examine the adhesion, colonization and invading capacity of the UPEC isolates *in vitro*. The control strain was *E. coli* ABU strain 83972. Notably, there was discreet variance in the expression of major virulence genes upon 3 hpi even though their distribution was significant in the UPEC pregnant and non-pregnant isolates. An early attachment of the UPECnp isolates to the host cells may be the reason of an overall decreased relative fold change in *fimH* expression in UPECnp and an increased fold change in UPECp in the infected host cells at 3 hpi, suggesting an enhanced adherence and colonization potential of the former compared with UPECp isolates. Previous studies revealed that fimbrial or afimbrial adhesins that coupled to host cell receptors permitted adhesion, which was first stage of colonization before cellular invasion [63, 64]. FimH in type-1 fimbriae interacts to D-mannosylated uroplakin, promoting the colonization and growth of intracellular bacterial communities that resemble biofilms [64]. Additionally, higher adherence potential of the UPECnp isolates was correlated with the higher incidence of MDR in UPECnp isolates than in the UPECp isolates, a similar observation was drawn in a study by Shah et al. [65], which showed a positive correlation between high biofilm production, indicating high colonization capacity and MDR incidence in a batch of clinical UPEC isolates. Furthermore, the study on *E. coli* CFT073 found the expression of type-1 fimbriae coordinately affected the expression of P-fimbriae in an inverse manner, expressed one fimbria at a time during the coregulation of the fimbriae operon [66, 67], supported the reduced relative fold expression of *papC* in HTB-4 cells at 3 hpi with both batches of isolates in our study. Type 1

fimbriae were also highly upregulated in an in vivo DNA microarray analysis of *E. coli* CFT073, whereas other fimbrial genes like *pap*- and *foc/sfa* [66]. However, UPEC isolates showed an elevation of *papC* expression at 6 hpi in urothelial cells, thereby suggesting a late expression of *pap* genes [17]. The high invasion potential post-adhesion of UPECnp was demonstrated by a significant increase in the relative fold expression of *hlyA* [68]. The non-significant increase in the relative fold expression of *hlyA* in UPECp isolates, however, was most likely caused by late adherence followed by invasion at 3 hpi. The siderophores that UPEC expressed helped the bacteria survive and might continue to do so after successful adhesion and colonization. Our study found that both UPECp and UPECnp isolates lowered the relative fold expression of *iroN* at 3 hpi in HTB-4 cells, suggesting that the commencement of *iroN* expression may occur later in the course of the propagation of the infection.

Another crucial factor for determining the severity of the UTI is the monitoring of the basic inflammatory responses produced against the development of virulence determinants of UPEC within the infected host [60]. Innate immunity relies heavily on the different chemokines and cytokines, such as CXCL8, CCL2, interleukins (IL-6, IL-8, IL-17A, TNF- α , TGF- β and IFN- γ), GCSF, and MCP-1, for signaling. IL-6 may aid in the transition from a mostly neutrophilic to a predominantly monocyte response during infection. Additionally, circulating polymorphonuclear leukocytes may enter the bladder tissue and engulf UPEC in response to IL-8 and other chemotactic stimuli to treat the infection [69, 70]. The relative fold expression of *IL-6* and *IL-8* in our study was overall reduced in UPECnp-infected HTB-4 cells at 3 hpi, and it was higher in UPECp infection at 3 hpi compared to infection with ABU83972, suggesting that UPECnp had a higher potential for invasion than UPECp isolates. The result was in accordance with another study, where infection of HTB-4 uroepithelial cells with UPEC strains UTI89 or NU14 resulted in lower levels of IL-6 than infection with commensal or laboratory strain MG1655 [71]. According to another study, HTB-5 cells infected with CFT073 at 3 hpi and 5 hpi secreted considerably less IL-6 and IL-8 than uninfected cells [23]. Since *fimH* and *IL-8* expressions in UPECp infection were the only ones to show a statistically significant correlation, our study demonstrated that the effectiveness of colonization was related to *fimH*, *IL-6*, and *IL-8* expression at 3 hpi in HTB-4 cells in vitro. TNF- α is a powerful proinflammatory cytokine that is rapidly released in response to injury, illness, or exposure to lipopolysaccharide formed from bacteria [72]. It is one of the most common early mediators in inflamed tissue. In our work, a successful start to the infection was

demonstrated by an increased relative fold expression of *TNF- α* in HTB-4 cells with UPECnp at 3 hpi. On the other, the potential for the delayed adherence of the HTB-4 cells to the urothelial cells was substantiated by the reduced relative fold expression of *TNF- α* in UPECp-infected HTB-4 cells at 3 hpi. IFN- γ levels that are way high may make it difficult to get rid of bacteria, which would encourage bacterial infections [73]. Therefore, decreased adherence and invasion potential of the UPECp isolates to the HTB-4 cells at 3 hpi in our study may be due to a statistically significant reduced relative fold expression of *IFN- γ* in HTB-4 cells with UPECp isolates. Overall reduced relative fold expression of *IFN- γ* in our study was quite comparable to another one study that found no release of IFN- γ at 4 hpi in infected A498 renal epithelial cells [74]. Furthermore, the increased expression *fimH* was correlated ($p < 0.05$) with the elevated expression of *IFN- γ* in UPECp infected HTB-4 cells, indicating that *IFN- γ* was released slowly in uroepithelial cells. UPEC induces host inflammation by producing inflammatory cytokines like *IL-1 β* , which include hemolysin and cytotoxic necrotizing factors [18]. Contrary to the finding of Jung et al. [18], our study demonstrated an overall significant enhancement in the relative fold expression of *hlyA* in UPECnp isolates collected from infected HTB-4 cells at 3 hpi, with extremely low relative fold expression of *IL-1 β* in the HTB-4 cells. Brauner et al. [75] did note that detectable quantities of IL-1 β were present at 24 hpi, and that epithelial cell IL-1 β production increased gradually over time. Additionally, our study found a statistically significant correlation ($p < 0.05$) between increased expression of *fimH* in the isolates, and decreased expression of *IL-1 β* in the UPECp-infected HTB-4 cells, which suggested a bacterial strategy to evade the host defense system. IL-17A was released by $\gamma\delta$ T-cells during the innate immune response mice with acute UTI, and it was found to be involved in the management of both acute and chronic UPEC infections [76]. It caused suboptimal UPEC clearance and facilitated neutrophil recruitment to infected tissue. At 24 hpi, IL-6 was found to be an effective predictive marker for pyelonephritis because it encouraged IL-17 secretion from T-cells. In accordance with these observations, we also found that *IL-17A* expression was significantly higher in UPECp-infected HTB-4 cells 3 hpi compared to UPECnp-infected epithelial cells. Additionally, our finding on the degree of *IL-6* expression in HTB-4 cells infected with UPECp were in consistent with a study by Chamoun et al. [76]. Additionally, a statistical correlation ($p < 0.05$) between the increased expression of *fimH* in the isolates and the elevated expression of *IL-17A* in HTB-4 cells infected with UPECp isolates supported the idea that the bacteria thrived due to its successful attachment to the epithelial cells to establish infection at

3 hpi. Studies in the murine model have demonstrated that mice which had chronic bacteriuria had considerably increased levels of *IL-5* at 24 hpi [77, 78], which was inconsistent with the finding of our study of increased relative fold expression of *IL-5* at 3 hpi. It has been suggested that, MCP-1 and GCSF, as well as other proinflammatory cytokines, are involved in the clearance of bacteria [15, 16, 17]. Numerous studies have demonstrated increased MCP-1 and GCSF expression in humans and mice at various stages of UPEC infection [16, 76]. In our study, however, a decrease in the relative fold expression of inflammatory mediators in UPECnp-infected HTB-4 cells at 3 hpi supported the incidence of early invasion in UPECnp (i.e., a quick decrease in expression of both proteins within 3 hours). In contrast, the limited infection capability of UPECp may be the cause of the negative fold expression of *MCP-1* and *GCSF* in the UPECp-infected HTB-4 cells at 3 hpi, which may result in an increase in the expression level of the immunoregulators at a later stage of infection. Reduced *GCSF* expression in the HTB-4 cells was statistically correlated ($p < 0.05$) with reduced *papC* expression in the UPECnp isolates, suggesting an additional survival mechanism for the bacteria following the successful invasion of uroepithelial cells to outlast host clearance. *TGF- β* may reduce host inflammatory reactions to intestinal bacterial proteins, aiding in the stimulation of immunological tolerance. *TGF- β* upregulation in response to infection, gave it a protective function for the epithelial barrier against encroaching pathogens [79]. Bmp-4, a member of the *TGF- β* superfamily, had the lowest mRNA levels at 6 hpi in mice with UPEC isolates with high *fimH* expression [80, 81]. According to our study, the reduction in the relative fold expression in *TGF- β* with enhanced relative fold expression of *fimH* in UPECp isolates and the elevated relative fold expression in *TGF- β* with reduced relative fold expression of *fimH* in UPECnp isolates at 3 hpi supported the phenomenon of faster attachment of the UPECnp than UPECp isolates to the HTB-4 cells. In addition, this study found a statistically significant correlation ($p < 0.01$) between elevated *TGF- β* expression in HTB-4 cells following infection with UPECnp isolates that displayed elevated expression of *hlyA*. This finding further suggested that *TGF- β* expression induced a protective mechanism in the epithelial cells to counteract the cytotoxic function of *hlyA* expression in the UPECnp isolates.

5.7. Conclusions:

In our study, UPECnp isolates were more predominantly exhibited antibiotic resistance than UPECp isolates. Discreet expression pattern of the virulence determinants of the UPECp and

UPECnp isolates, along with their respective cytokine response elicited in HTB-4 cells upon 3 hours post infection were observed. This is first study of its kind, which compared the response of clinical UPEC isolates from different populations, with a special focus on pregnant population. Correlation were observed in between virulence determinant *fimH* and immunoregulatory cytokine *IFN- γ* , *IL-17A* and *IL-1 β* in UPECp isolates, and in between virulence determinants *papC* and *hlyA* to the immunoregulatory cytokine *GCSF* and *TGF- β* in UPECnp isolates. It is an absolute necessity to comprehend the severity of infection in a better way to administer appropriate therapeutics, and therefore we should need to understand the effect of the VFs namely *fimH*, *papC* and *hlyA* expression in the clinical UPEC isolates on both pro- and anti- inflammatory cytokines. Therefore, to cease empiric treatment and formulate a suitable prescription policy, cytokine profiling in addition to AMR analysis might be a great alternative choice. Furthermore, to predict the host-pathogen interactions in the treatment of UTI, intensive murine studies should be initiated.

5.8. References:

1. Bien J, Sokolova O, Bozko P. Role of uropathogenic *Escherichia coli* virulence factors in development of urinary tract infection and kidney damage. 2012. International Journal of Nephrology. 1-15.
2. Habak PJ, Griggs J. Urinary tract infection in pregnancy. 2022. In: StatPearls. StatPearls Publishing. FL USA
3. Konwar M, Gogtay NJ, Ravi R, Thatte UM, Bose D. Evaluation of efficacy and safety of Fosfomycin versus nitrofurantoin for the treatment of uncomplicated lower urinary tract infection in women – a systematic review and meta-analysis. 2022. Journal of Chemotherapy. 34(3), 139–148.
4. Czajkowski K, Broś-Konopielko M, Teliga-Czajkowska J. Urinary tract infection in women. 2021. Przegląd Menopauzalny. 20(1), 40 – 47.
5. Zhu H, Chen Y, Hang Y, Luo H, Fang X, Xiao Y et al. Impact of inappropriate empirical antibiotic treatment on clinical outcomes of urinary tract infections caused by *Escherichia coli*: a retrospective cohort study. 2021. Journal of Global Antimicrobial Resistance. 26(9): 148–153.
6. Basu S, Mukherjee SK, Hazra A, Mukherjee M. Molecular characterization of uropathogenic *Escherichia coli*: Nalidixic acid and ciprofloxacin resistance, virulent factors and phylogenetic background. 2013. Journal of Clinical and Diagnostic Research. 7(12): 2727–2731.
7. Mukherjee M, Koley S, Mukherjee SK, Basu S, Ghosh B, Chakraborty S. Phylogenetic background of *E. coli* isolated from asymptomatic pregnant women from Kolkata, India. 2015. Journal of infection in Developing Countries. 9(07): 720–724.

8. Ballesteros-Monrreal MG, Arenas-Hernández MM, Enciso-Martínez Y, Peña CFM, Rocha-Gracia RDC, Lozano-Zaraín P et al. Virulence and Resistance determinants of uropathogenic *Escherichia coli* strains isolated from pregnant and non-pregnant women from two states in Mexico. 2013. 13(1):295–310.
9. Aloob HMT, Ismail SSM, Ali AH. Molecular characterization of multi drug resistance *Escherichia coli* isolated among diabetes mellitus patients in Dongla State, Sudan. 2020. American Journal of Biomedical Science and Research. 9(5): 357–363.
10. Terlizzi ME, Gribaudo G, Maffei ME. uropathogenic *Escherichia coli* (UPEC) infections: virulence factors, bladder responses, antibiotic and non-antibiotic antimicrobial strategies. 2017. Frontiers in Microbiology. 8, 1566.
11. Spencer JD, Schwaderer AL, Becknell B, Watson J, Hains DS. The innate immune response during urinary tract infection and pyelonephritis. 2014. Pediatric Nephrology. 29(7), 1139–1149.
12. Nagamatsu K, Hannan TJ, Guest RL, Kostakioti M, Hadjifrangiskou M, Binkley J, Dodson K, Raivio TL, Hultgren SJ. Dysregulation of *Escherichia coli* α -hemolysin expression alters the course of acute and persistent urinary tract infection. 2015. Proceedings of the National Academy of Sciences of the United States of America. 112(8): E871–880.
13. Waldhuber A, Puthia M, Wieser A, Cirl C, Dürr S, Neumann-Pfeifer S et al. uropathogenic *Escherichia coli* strain CFT073 disrupts NLRP3 inflammasome activation. 2016. The Journal of Clinical Investigation. 126(7): 2425–2436.
14. Demirel I, Persson A, Brauner A, Särndahl E, Kruse R, Persson K. Activation of the NLRP3 inflammasome pathway by uropathogenic *Escherichia coli* is virulence factor-dependent and influences colonization of bladder epithelial cells. 2018. Frontiers in Cellular and Infection Microbiology. 14;8:81.
15. Ambite I, Puthia M, Nagy K, Cafaro C, Nadeem A, Butler DSC et al. Molecular basis of Acute Cystitis Reveals susceptible genes and immunotherapeutic targets. 2016. PlosPathogens. 12(10): e1005848.
16. Sundac L, Dando SJ, Sullivan MJ, Derrington P, Gerrard J, Ulet GC. Protein-based profiling of the immune response to uropathogenic *Escherichia coli* in adult patients immediately following hospital admission for acute cystitis. Pathogens and Disease. 74(6):ftw062.
17. Engelsöy U, Rangel I, Demirel I. Impact of Proinflammatory Cytokines on the Virulence of uropathogenic *Escherichia coli*. 2019. Frontiers in Microbiology. 10(5):1051.
18. Jung J-H, Hong HJ, Ghaderpour A, Cho JY, Baek B-S, Hur Y. Differential interleukin-1 β induction by uropathogenic *Escherichia coli* correlates with its phylotype and serum C-reactive protein levels in Korean infants. 2019. Scientific Reports. 9(1): 15654.
19. Chu CM, Lowder JL. Diagnosis and treatment of urinary tract infections across age groups. 2018. American Journal of Obstetrics and Gynecology. 219(1): 40–51.
20. Hilbert DW, Pascal KE, Libby EK, Mordechai E, Adelson ME, Trama JP. uropathogenic *Escherichia coli* dominantly suppress the innate immune response of the bladder epithelial cells

by a lipopolysaccharide- and Toll-like receptor 4- independent pathway. 2008. *Microbes and Infection*. 10(2): 114–121.

21. de Llano DG, Esteban-Fernández A, Sánchez-Patán F, Martínlvarez PJ, Moreno-Arribas MV, Bartolomé B. Anti-Adhesive activity of cranberry phenolic compounds and their microbial-derived metabolites against uropathogenic *Escherichia coli* in Epithelial cell cultures. 2015. *International Journal of Molecular Sciences*. 16(6): 12119–12130.

22. Geerlings SE, Meiland R, VanLith EC, Brouwer EC, Gaastra W, Hoepelman AI. Adherence of type 1-fimbriated *Escherichia coli* to uroepithelial cells: more in diabetic women than in control subjects. *Diabetes Care*. 25(8): 1405–1409.

23. Vega-Hernández R, Ochoa SA, Valle-Rios R, Jaimes-Ortega G, Arellano-Galindo J, Aparicio-Ozores G et al. Flagella, Type I fimbriae and curli of uropathogenic *Escherichia coli* promote the release of proinflammatory cytokines in a coculture systems. 2021. *Microorganisms*. 9(11): 2233.

24. Stork C, Kovács B, Rózsai B, Putze J, Kiel M, Dorn Á et al. Characterization of asymptomatic bacteriuria *Escherichia coli* isolates in search of alternative strains for efficient bacterial interference against Uropathogens. 2018. *Frontiers in Microbiology*. 9, 214.

25. Bandyopadhyay D, Mukherjee M. Reactive oxygen species and *uspA* overexpression: an alternative bacterial response toward selection and maintenance of multidrug resistance in clinical isolates of uropathogenic *E. coli*. 2020. *European Journal of Clinical Microbiology and Infectious Disease*. 39(9): 1753–1760.

26. Ching CB, Gupta S, Li B, Cortado H, Mayne N, Jackson AR, McHugh KM, Becknell B. Interleukin-6/Stat3 signaling has an essential role in the host antimicrobial response to urinary tract infection. *Kidney International*. 2018. 93(6): 1320 – 1329.

27. Ambite I, Butler D, Wan MLY, Rosenblad T, Tran TH, Ming CS, Svanborg C. Molecular determinants of disease severity in urinary tract infection. 2021. *Nature Reviews Urology*. 18(6): 468–486.

28. Schütze S, Kaufmann A, Bunkowski S, Ribes S, Nau R. Interferon-gamma impairs phagocytosis of *Escherichia coli* by primary murine peritoneal macrophages stimulated with LPS and differentially modulates proinflammatory cytokine release. 2021. *Cytokine X*. 3(3): 100057.

29. Steiner SE, Choong FX, Antypas H, Morado-Urbina CE, Schulz A, Farinotti AB et al. UPEC kidney infection triggers neuro-immune communication leading to modulation of local renal inflammation by splenic IFN γ . 2021. *Plos Pathogens*. 17(5): e1009553.

30. Deshmane SL, Kremlev S, Amini S, Sawaya BE. Monocyte chemoattractant protein-1 (MCP-1): An overview. 2010. *Journal of Interferon and Cytokine Research*. 29(6): 313 – 326.

31. Tofik R, Ohlsson S, Bakoush O. Urinary concentration of monocyte chemoattractant protein-1 in idiopathic glomerulonephritis: A long-term follow-up study. 2014. *PLoS One*. 9(1): e87857.

32. Ingersoll MA, Kline KA, Nielsen HV, Hultgren SJ. G-CSF induction in early uropathogenic *Escherichia coli* infection of the urinary tract modulates host immunity. 2008. *Cellular Microbiology*. 10(12): 2568 – 2578.

33. Gedikbaşı A, Şevketoğlu E, Karyağar S, Karyağar SS, Hatipoğlu SS, Yılmaz A. Urine interleukin-1 β can be used for early prediction of urinary tract infection in children. 2020. Journal of Child. 20(1): 1–6.
34. Goepfert A, Lehmann S, Wirth E, Rondeau JM. The human IL-17A/F heterodimer: A two faced cytokine with unique receptor recognition properties. 2017. Scientific Reports. 7(8): 8906.
35. Chamoun MN, Sullivan MJ, Goh GK, Acharya D, Ipe DS, Katupitiya L. et al. Restriction of chronic *Escherichia coli* urinary tract infection depends upon T cell-derived interleukin-17, a deficiency of which predisposes to flagella-driven bacterial persistence. 2020. FASEB journal. 34(11): 14572 – 14587.
36. Lee SJ, Lee EJ, Kim SK, Jeong P, Cho YH, Yun SJ, Kim S, Kim GY, Choi YH, Cha EJ, Kim WJ, Moon SK. Identification of Proinflammatory cytokines associated with muscle invasive bladder cancer: The roles of IL-5, IL-20 and IL-28A. 2012. PLoS One. 7(9): e40267.
37. Cotton SA, Gbadegesin RA, Williams S, Brenchley PEC, Webb NJA. Role of TGF- β 1 in renal parenchymal scarring following childhood urinary tract infection. 2002. Kidney International. 61(1): 61–67.
38. Bachchan KT, Ramanujan SS. Prevalence of multidrug resistant asymptomatic bacteriuria from pregnant and non-pregnant women in the Erode district. 2016. International Journal of Biochemistry and Biotechnology. 5(3): 665 – 669.
39. Paniagua-Contrearras GL, Monroy-Pérez E, Rodríguez-Moctezuma JR, Domínguez-Trejo P, Vaca-Paniagua F, Vaca S. Virulence factors, antibiotic resistance phenotypes and O-serogroups of *Escherichia coli* strains isolated from community-acquired urinary tract infection patients in Mexico. 2017. Journal of Microbiology, Immunology and Infection. 50(4): 478 – 485.
40. Ramírez-Castillo FY, Moreno-Flores AC, Avelar-González FJ, Márquez-Díaz F, Harel J, Gurrero-Barrera AL. An evaluation of multidrug-resistant *Escherichia coli* isolates in urinary tract infections from Aguascalientes, Mexico: cross-sectional study. 2018. Annals of Clinical Microbiology and Antimicrobials. 17(1), 34.
41. Abate D, Marami D, Letta S. Prevalence, antimicrobial susceptibility pattern, and associated factors of urinary tract infections among pregnant and non-pregnant women at public health facilities, Harar, Eastern Ethiopia: a comparative cross-sectional study. 2020. Canadian Journal of Infectious Disease and Medical Microbiology. 9356865.
42. Asmat U, Mumtaz Mz, Malik A. Rising prevalence of multidrug-resistant uropathogenic bacteria from urinary tract infections in pregnant women. 2021. Journal of Taibah University Medical Sciences. 16(1): 102 – 111.
43. Ali AH, Reda DY, Ormago MD. Prevalence and antimicrobial susceptibility pattern of urinary tract infection among pregnant women attending Hargeisa Group Hospital, Hargeisa, Somaliland. 2022. Scientific Reports. 12(1), 1419.

44. Yun KW, Kim HY, Park HK, Kim W, Lim IS. Virulence factors of uropathogenic *Escherichia coli* of urinary tract infections and asymptomatic bacteriuria in children. 2014. Journal of Microbiology, Immunology and Infection. 47(6): 455 – 461.
45. Rahdar M, Rashki A, Miri HR, Rashki Ghalehnoo M. Detection of pap, sfa, afa, foc and fim adhesin-encoding operons in uropathogenic *Escherichia coli* isolates collected from patients with urinary tract infection. 2015. Jundishapur Journal of Microbiology. 8(8): e22647.
46. Lee JH, Subharda B, Son Y-J, Kim DH, Park HS, Kim JM, Koo SH, Oh MH, Kim H-J, Choi CH. Phylogenetic group distributions, virulence factors and antimicrobial resistance properties of uropathogenic *Escherichia coli* strains isolated from patients with urinary tract infections in South Korea. 2016. Letters in Applied Microbiology. 62(1): 84 – 90.
47. Tabasi M. Genotypic characterization of virulence factors in *Escherichia coli* isolated from patients with acute cystitis, pyelonephritis and asymptomatic bacteriuria. 2016. Journal of Clinical and Diagnostic Research. 10(12), DC01 – DC07.
48. Munkhdelger Y, Gunregjav N, Dorjpurev A, Juniichiro N, Sarantuya J. Detection of virulence genes, phylogenetic group, and antibiotic resistance of uropathogenic *Escherichia coli* in Mongolia. 2017. Journal of infection in Developing Countries. 11(01): 51 – 57.
49. Ali I, Rafaque Z, Ahmed I, Tariq F, Graham SE, Salzman E, Foxman B, Dasti JI. Phylogeny, sequence-typing and virulence profile of uropathogenic *Escherichia coli* (UPEC) strains from Pakistan. 2019. BMC Infectious Diseases. 19(1): 620.
50. Cristea VC, Gheorghe I, Barbu IC, Popa LI, Ispas B, Grigore GA, Bucatari I, Popa GL, Angelescu M-C, Velican A, Marutescu L, Popa M, Chifiriuc MC, Popa IM. Snapshot of phylogenetic groups, virulence, and Resistance Markers in *Escherichia coli* uropathogenic strains isolated from outpatients with urinary tract infections in Bucharest, Romania. 2019. BioMed Research International. 5, 5712371.
51. Dadi BR, Abete T, Zhang L, Mihret A, Abebe W, Amogne W. Distribution of virulence genes and phylogenetics of uropathogenic *Escherichia coli* among urinary tract infection patients in Addis Ababa, Ethiopia. 2020. BMC Infectious Diseases. 20(1): 108.
52. Rezaatofigihi SE, Mirzarazi M, Salehi M. Virulence genes and phylogenetic groups of uropathogenic *Escherichia coli* isolates from patients with urinary tract infection and uninfected control subjects: a case-control study. 2021. BMC Infectious Diseases. 21(1), 361.
53. Al-Zubaidi SJJ. Prevalence of virulence factors genes of *Escherichia coli* isolated from pregnant and non-pregnant women with urinary tract infection in Diyala Iraq. 2020. Systematic Reviews in Pharmacy. 11(6): 1420 – 1427.
54. Lee S, Yu JK, Park K, Oh E-J, Kim S-Y, Park Y-J. Phylogenetic groups and virulence factors in pathogenic and commensal strains of *Escherichia coli* and their association with blaCTX-M. 2010. Annals of Clinical and Laboratory Science. 40(4): 361 – 367.

55. Tarchouna M, Ferjani A, Ben-Selma W, Boukadida J. Distribution of uropathogenic virulence genes in *Escherichia coli* isolated from patients with urinary tract infection. 2013. International Journal of Infectious Diseases. 17(6): e450 – e453.
56. Alabasi MS, Ghazal A, Sabry SA, Alasaly MM. Association of some virulence genes with antibiotic resistance among uropathogenic *Escherichia coli* isolated from urinary tract infection patients in Alexandria, Egypt: a hospital-based study. 2014. Journal of Global Antimicrobial Resistance. 2(2): 83 – 86.
57. Dhakal BK, Mulvey MA. The UPEC pore-forming toxin α -hemolysin triggers proteolysis of host proteins to disrupt cell adhesion, inflammatory, and survival pathways. 2012. Cell Host & Microbe. 11(1): 58 – 69.
58. Moeinizadeh H, Shaheli M. Frequency of hlyA, hlyB, hlyC and hlyD genes in uropathogenic *Escherichia coli* isolated from UTI patients in Shiraz. 2021. German Medical Science Hygiene and Infection Control. 16, Doc 25.
59. Karimian A, Momtaz H, Mahbobe Madani M. Detection of uropathogenic *Escherichia coli* virulence factors in patients with urinary tract infection in Iran. 2012. African Journal of Microbiology Research. 6(39): 6811 – 6816.
60. Reygaert WC. Innate immune response to urinary tract infections involving *Escherichia coli*. 2014. Journal of clinical and cellular immunology. 05(06).
61. Roos V, Ulett GC, Schembri MA, Klemm P. The asymptomatic bacteriuria *Escherichia coli* strains 83972 outcompetes uropathogenic *E. coli* strains in human urine. 2006. Infection and Immunity. 74(1): 615 – 624.
62. Hernández JG, Sundén F, Connolly J, Svanborg C, Wullt B. Correction: genetic control of the variable innate immune response to asymptomatic bacteriuria. 2012. PLOS One. 7(1).
63. Kalita A, Hu J, Torres AG. Recent advanced in adherence and invasion of pathogenic *Escherichia coli*. 2014. Current Opinion in Infectious Diseases. 27(5): 459 – 464.
64. Frömmel U, Lehmann W, Rödiger S, Böhm A, Nitschke J, Weinreich J, Groß J, Roggenbuck D, Zinke O, Ansorge H, Vogel S, Klemm P, Wex T, Schröder C, Wieler LH, Schierack P. Adhesion of human and animal *Escherichia coli* strains in association with their virulence-associated genes and phylogenetic origins. 2013. Applied and Environmental Microbiology. 79(19): 5814 – 5829.
65. Shah C, Baral R, Bartaula B, Shrestha LB. Virulence factors of uropathogenic *Escherichia coli* (UPEC) and correlation with antimicrobial resistance. 2019. BMC Microbiology. 19(1): 204.
66. Snyder JA, Haugen BJ, Buckles EL, Lockatell CV, Johnson DE, Donnenberg MS, Welch RA, Mobley HLT. Transcriptome of uropathogenic *Escherichia coli* during urinary tract infection. 2004. Infection and Immunity. 72 (11): 6373 – 6381.
67. Melican K, Sandoval RM, Kader A, Josefsson L, Tanner GA, Molitoris BA, Ritcher-Dahlfors A. uropathogenic *Escherichia coli* P and type 1 fimbriae act in synergy in a living host to facilitate renal colonization leading to nephron obstruction. 2011. PLoS Pathogens. 7(2), e1001298.

68. Flores-Mireles AL, Walker JN, Caparon M, Hultgren SJ. Urinary tract infections: epidemiology, mechanisms of infection and treatment options. 2015. *Nature Reviews Microbiology*. 13(5): 269 – 284.
69. Stocks CJ, Phan M-D, Achard MES, Nhu NTK, Condon ND, Gawthorne JA, Lo AW, Peters KM, McEvan AG, Kapetanovic R, Schembri MA, Sweet MJ. uropathogenic *Escherichia coli* employs both evasion and resistance to subvert innate immune-mediated zinc toxicity for dissemination. 2019. *Proceedings of The National Academy of Sciences, USA*. 116(13): 6341 – 6350.
70. Kim A, Ahn JH, Choi WS, Park HK, Kim S, Paick SH, Kim HG. What is the cause of Recurrent urinary tract infection? Contemporary microscopic concepts of pathophysiology. 2021. *International Neurourology Journal*. 25(3): 192 – 201.
71. Prasanphanich NS, Gregory EJ, Erickson JJ, Miller-Handley H, Kinder JM, Way SS. Preconceptual priming overrides susceptibility to *Escherichia coli* systemic infection during pregnancy. 2021. *mBio*. 12(1): e00002 – 00021.
72. Parameswaran N, Patial S. Tumor necrosis factor- α signaling in macrophages. 2010. *Critical Review in Eukaryotic gene expression*. 20(2): 87 – 103.
73. Schütze S, Kaufmann A, Bunkowski S, Ribes S, Nau R. Interferon-gamma impairs phagocytosis of *Escherichia coli* by primary murine peritoneal macrophages stimulated with LPS and differentially modulates proinflammatory cytokine release. 2021. *Cytokine: X*. 3(3): 100057.
74. Steiner SE, Choong FX, Antypas H, Morado-Urbina CE, Schulz A, Farinotti AB, Bas DB, Svensson CI, Richter-Dahlfors A. UPEC kidney infection triggers neuro-immune communication leading to modulation of local renal inflammation by splenic IFN γ . *PLoS Pathogens*. 17(5): e1009553.
75. Brauner A, Söderhäll M, Jacobson SH, Lundahl J, Andersson U, Andersson J. *Escherichia coli* induced expression of IL-1 α , IL-1 β , IL-6 and IL-8 in normal human renal tubular epithelial cells. 2001. *Clinical and Experimental Immunology*. 124(3): 423 – 428.
76. Chamoun MN, Sullivan MJ, Goh KGK, Acharya D, Ipe DS, Katupitiya L, Gosling D, Peters KM, Sweet MJ, Sester DP, Schembri MA, Ulett GC. Restriction of chronic *Escherichia coli* urinary tract infection depends upon T cell-derived interleukin-17, a deficiency of which predisposes to flagella-driven bacterial persistence. 2020. *Federation of American Societies for Experimental Biology Journal*. 34(11): 14572 – 14587.
77. O'Brien VP, Dorsey DA, Hannan TJ, Hultgren SJ. Host restriction of *Escherichia coli* recurrent urinary tract infection occurs in a bacterial strain-specific manner. 2018. *PLoS Pathogen*. 14(12), e1007457.
78. Gilbert NM, O'Brien VP, Waller C, Batourina E, Mendelsohn CL, Lewis AL. Gardnerella exposures alter bladder gene expression and augment uropathogenic *Escherichia coli* urinary tract infection in mice. 2022. *Frontiers in Cellular and Infection Microbiology*. 12: 909799.

79. Juang J, Yin H, Zhang C, Wang J. Effects of *E. coli* infection on the expressions of TGF- β /Smads signaling pathway in broiler intestine. 2020. Brazilian Journal of Poultry Science. 22(1).
80. Ljungberg JK, Kling JC, Tran TT, Blumenthal A. Functions of the WNT signaling network in shaping host response to infection. 2019. Frontiers in Immunology. 10, 2521.
81. Jafari NV, Rohn JL. The urothelium: A multi-faceted barrier against a harsh environment. 2022. Mucosal Immunology. 15: 1127 – 1142.

Chapter 6: *In-vivo* experiments and analysis of cytokines to stratify the UPEC pathogenesis in mice model of UTI

6.1. Background study:

One of the most frequent causes of urological and renal problems is urinary tract infections (UTIs). A particular strain of *Escherichia coli*, uropathogenic *Escherichia coli* (UPEC), was discovered to be the predominant etiologic agent in 80%-90% UTI cases. UTIs can be acute or recurrent, and as a result the quality of life for patients is significantly reduced. Additionally, it was discovered that 40%-50% of adult women would develop a UTI at least once in their lives, with many of them experiencing repeated infections [1]. Traditionally, antibiotics were the first line of defense against UTI, but in recent years, their empiric use has led to the establishment of multidrug-resistance (MDR) and challenging therapeutic management [2]. UPEC expressed many virulence factors (VFs) to employ various strategies to weaken and delay the initiation of the host response against the pathogen to establish the infection, even though various host defenses systems cooperate to combat bacterial colonization and survival in the urinary system [1, 3]. The uroepithelial cells of bladder and kidney were colonized and their adherence was improved by virulence factors [4, 5, 6].

In order to resist the bacterial infection, the attachment of UPEC to uroepithelial receptors caused the bladder epithelial cells to release an array of inflammatory substances, including antimicrobial peptides, the Tamm-Horsfall protein, the cytokines IL-6, TNF- α , IL-1 β , G-CSF, and IL-17, as well as several chemokines namely CXCL1, CXCL2, CXCL3, CXCL8, CCL4 to resist the bacterial infection [7]. The majority of early responders to infected bladders during the cellular infiltration were neutrophils [8]. Host response to UTI also included T-cells, antigen presenting macrophages, and dendritic cells [9]. The structural and functional integrity of the urinary tract were harmed by the subsequent inflammation. According to a study by Engelsöy et al., addition of various pro-inflammatory cytokines (TNF- α , IL-6, IL-8 and IFN- γ) controlled the proliferation of UPEC isolates *in vitro* [10]. Additionally, according to another study, G-CSF was involved in controlling the release of several cytokines (MCP-1, CCL-2 and IL-1 β) to manage the host immune response during UPEC infection [11]. An association between uropathogenicity expressed as bacterial load and inflammatory cytokine (TNF- α , IL-1 β , IL-6 and IL-8) mRNA expression in bladder and kidney tissues from infected mice was observed in a recent study in three strains namely, *P. mirabilis* ATCC29906, EAEC O42, and *P. mirabilis* RTX339 [12]. Additionally, a prior study from our lab demonstrated the varied virulence factors (*fimH*, *papC*, *hlyA*) linked to colonization

and invasion were significantly correlated to the mRNA expression of the pro- and anti-inflammatory cytokines IL-1 β , IL-17A, TGF- β and GCSF in HTB-4 uroepithelial cells upon 3 hours post infection with clinical UPEC isolates [13].

However, till date there are no studies on simultaneous expression of different pro- and anti-inflammatory cytokines associated to bacterial colonization upon infection with clinical UPEC isolates with varied distribution of virulent factor genes in mice urinary tract.

6.2. Objective of the study:

This study aimed to investigate: UPEC colonization together with concurrent expression of pro- and anti-inflammatory cytokines upon infection in mice with two different clinical UPEC isolates (*E. coli* P025 and *E. coli* NP105) that exhibited varied virulence characteristics.

6.3. Materials:

6.3.1. Equipment for *in-vitro* experiments:

Laminar Air Flow (B.D. Instrumentation) • Shaker Incubator (ICT) • Autoclave • Spectrophotometer (Bio-Rad, Model: SmartSpec™ Plus) • Hot Air Oven (Digitech Systems) • Cooling Centrifuge (Remi) • Refrigerator (Godrej) • Dry Bath (Remi) • Inoculation Loop • Glass spreaders • Spirit Lamp • 100mm glass petri dish (Borosil) • 90mm plastic petri dish (Tarson) • Glass culture tubes (Touff, Borosil) • Test tubes racks (Tarson) • Micropipettes (0.5-10 μ l, 2-20 μ l, 20-200 μ l, 200-1000 μ l) (Corning, P'Fact, Microlit, Biohit) • Micro tips (0.5-10 μ l, 2-20 μ l, 20-200 μ l, 200-1000 μ l) (HiMedia) • Eppendorf Tubes (1.5ml, 2ml) (Tarsons) • Cotton (Bengal Surgicals Limited) (Lakshmi Healthcare Products (P) Ltd.) • Surgical Gloves (Pricare, HiMedia) • Wash Bottles (Tarsons)

6.3.2. Equipment for *in-vivo* experiments:

Four weeks old, female, outbred BALB/C mice from the State Centre for Laboratory Animal Breeding (SCLAB) under West Bengal Livestock Development Corporation Limited (WBLDCL) • Mice Cage (Tarsons) • Cage Cover (Tarsons) • Feeding Bottle (Tarsons) • Filtered water for drinking (Aqua Guard) • Mice pellet feed (West Bengal Livestock Development Corporation Limited) • Haystack (Local Purchase) • Autoclave • Syringes (30 G hypodermic, Polymed Medical

Devices, Haryana, India) • Cold Centrifuge (Remi, India) • ELISA reader (Bio Rad, India) • Mouse IL-1 β ELISA kit (KinesisDX, USA) • Mouse IL-17A ELISA kit (KinesisDX, USA) • Mouse G-CSF ELISA kit (KinesisDX, USA) • Mouse TGF- β ELISA kit (KinesisDX, USA)

6.3.3. Reagents:

Xylocaine 2 % Jelly (Lignocaine Hydrochloride Gel IP) (Zydus Healthcare Limited) • Isoflurane (Raman & Weil Pvt. Ltd., Daman, India) • Chloroform (Merck) • 1X PBS

6.3.4. Preparation of reagents and compositions of solutions used:

- LB media: follow section 2.3.3.1
- 1X PBS: follow 5.3.4.

6.4. Experimental Procedure:

6.4.1. Procedures for *in vivo* experiment:

6.4.1.1. Preparation of bacterial inoculum:

- 2 ml of LB broth was inoculated from the selected frozen glycerol stock of uropathogenic *E. coli* isolates from both populations. It was grown at ~150rpm for 18–24 hours at 37°C.
- 100 μ l of overnight culture were sub-cultured into 10 ml of fresh LB broth and grown till log phase at ~150rpm for 1–2 hours at 37°C.
- The OD₆₀₀ of the log phase culture would be around 0.4 – 0.7.
- According to the OD₆₀₀ value the volume of culture equivalent to 2×10^7 colony-forming units (CFU) per ml culture have been taken into centrifuge tube and centrifuged at 10 minutes at 3000 \times g. The supernatant has been discarded and the pellet is resuspended with 100 μ l PBS to prepare 1×10^7 CFU per 50 μ l PBS.

6.4.1.2. Preparation of urinary catheters:

- Urinary catheters are arranged using a sterile laminar flow hood equipped with an UV lamp, and 70% ethanol would be sprayed in all working surfaces, gloves, and instruments.
- A length of polyethylene tubing (PE-10) has been cut with a sterile blade or scissors, and sufficient numbers of catheters being made.
- A sterile 30–ga \times ½ inch. needle is placed on a sterile 1ml tuberculin syringe.

- One end of the polyethylene tubing is picked up with forceps and by gentle sliding onto the needle up to the hub.
- The tubing is cut approximately ½ inch from the needle tip, and the catheter is removed from the syringe, and placed it in a sterile petri dish.
- The steps 2 – 5 were repeated as required. A minimum requirement of one catheter per cage of five mice to be infected (Figure 6.1).
- The catheters were UV-irradiated for at least 30 minutes to ensure sterility.
- The lid of the petri dish is replaced and secured and the catheters are stored for future use.

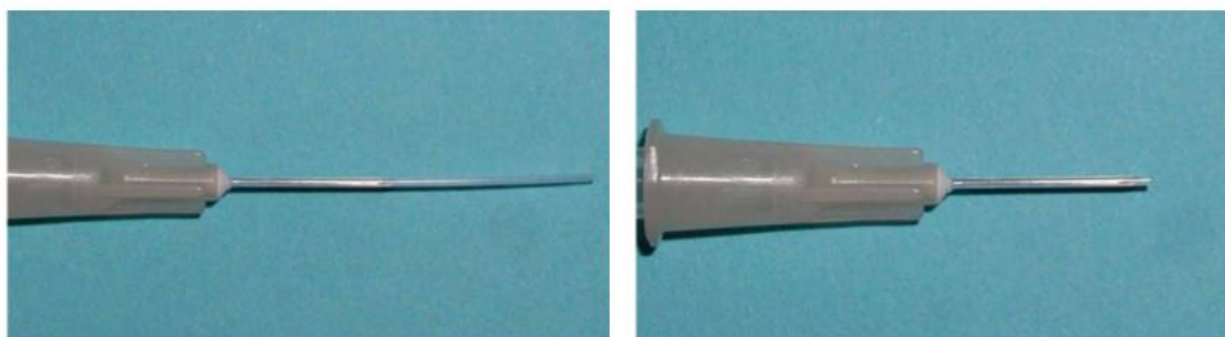


Figure 6.1: Urinary catheter. Urinary catheters are made out of polyethylene tubing on a 30-G hypodermic syringe. An unused catheter (a) (on the left) has extra tubing hanging off the end of the needle (b) (on the right) The extra tubing is cut off near the bevel of the needle prior to use.

6.4.1.3. Preparation of Mice prior to bacterial inoculation:

Four weeks old, female, outbred BALB/C mice were brought from the State Center for Laboratory Animal Breeding (SCLAB) under West Bengal Livestock Development Corporation Limited (WBLDCL), Kalyani, Nadia, West Bengal. The mice were housed individually in cages with sterile bedding made of haystack, had an ad libitum access of standard mice feed pellet diet from WBLDCL and filtered tap water and maintained in a noiseless room with a 12:12-h light/dark cycle (lights on at 7 am) at 25°C and relative humidity of 55% (Figure 6.2). The mice were kept in quarantine in Quarantine prior to taking them in the room specified for them in the Animal Facility of School of Tropical Medicine, Kolkata. The protocol for experiment on laboratory animals (**IAEC Ref No: STM/01/2023** dated **13.01.2023**) was approved by the Institutional Animal Ethics Committee, School of Tropical Medicine, Kolkata, under the regulation of The Committee for Purpose of Control and Supervision of Experiments of Animals (CPCSEA) at Animal Welfare Division, Ministry of Environment, Forest and Climate Change, New Delhi, India.



Figure 6.2: BALB/C mice in a cage kept in conditions and access of food mentioned in 6.4.1.3.

6.4.1.4. Intravesical inoculation of mice with bacteria [14]:

- The bacterial inoculum of the volume of 100 μ l have been drawn into a tuberculin syringe.
- The catheter is placed on syringe and the air is expelled.
- The catheter is trimmed using fine scissors, sterilized with 70% Ethanol or alcohol swabs, to 1–2 mm past the tip of the catheter needle.
- The syringe is set down, keeping the catheter tip in sterile lubricating jelly.
- Anesthesia is induced in mice with 2–3% isoflurane with the help of vaporizer.
- Once the effect of anesthesia was working on the mice, a mouse is removed and it was placed supine on the working surface (with the help of absorbent pad or piece of Styrofoam covered with a clean paper towel), keeping the tail directed toward the user. The anesthesia condition is maintained using a nose cone assembly connected to the vaporizer.
- The finger is placed on the caudal abdomen, the bladder is located, and pressure is applied in a gentle rostral/caudal motion to make the bladder empty of urine.
- The lubricated catheter tip is placed into the urethral opening, by keeping the catheter and syringe oriented perpendicular to the table.

- The catheter is advanced about 0.5 cm or till resistance encountered, and then the syringe is rotated caudally in an arc 90^0 so that the syringe remains parallel to the table and tail. The catheter can now pass freely into the urinary bladder through the pelvis.
- Once the catheter is advanced to the hub of the needle, the bladder is injected slowly with 50 μ l inoculum. The bladder expands slowly when the increment is delivered in 10 μ l increments over 10–15seconds.
- The syringe/catheter assembly is removed and kept aside with catheter tip in lubricating jelly (Figure 6.3).
- Mouse identification is recorded and inoculated mouse is kept back to its cage to recover.
- For each mouse, steps 6–12 is repeated, and catheter is changed according to the need. Catheters should be changed between strains, if different bacterial strains or mutants are part of a same experiment.



Figure 6.3: Catheterization process in the bladder of a BALB/C mice.

6.4.1.4. **Sera collection** [15]:

Infected mice groups at 5-, 7-, 9-, 12- and 15- days post infection (p.i.) would be euthanized with the help of chloroform, prior to blood sample collection via cardiac puncture. The p.i. days selected according to an established protocol [12]. Sampling was conducting at all time points under sterile conditions including the collection of bladders and kidneys (left and right lobules). Sera was extracted from the blood samples by centrifugation at 15000g \times 5minutes at -4^0C and stored at -80^0C [15].

6.4.1.5. **Tissue harvesting** [14]:

- Under the presence of anesthetics (Chloroform) the mice are euthanized by CO₂ asphyxiation or cervical dislocation.
- The mouse is placed on the back and the ventral abdomen is sprayed with 70% ethanol.

- The skin of the caudal ventral skin was pulled up using forceps. A small cut was made using blunt surgical scissors through the skin and peritoneum.
- Once the peritoneal cavity is entered, a V-shaped opening is made in the abdomen by cutting towards the ribs on either side of the body with the help of scissors.
- The flap is pulled forward towards the nose (rostrally) manually to bluntly make the opening larger.
- The bladders, kidneys and other tissues desired for downstream analyses (e.g. tissue homogenization for bacterial enumeration; fixation of tissues for imaging) were removed.
- One part of the bladder and kidney tissues were kept aside for histopathological examination, other part of the tissue was processed for homogenization.
- Once desired tissues have been harvested from the mice, animal carcasses have been disposed as biohazard waste according to the procedures established by CPCSEA.

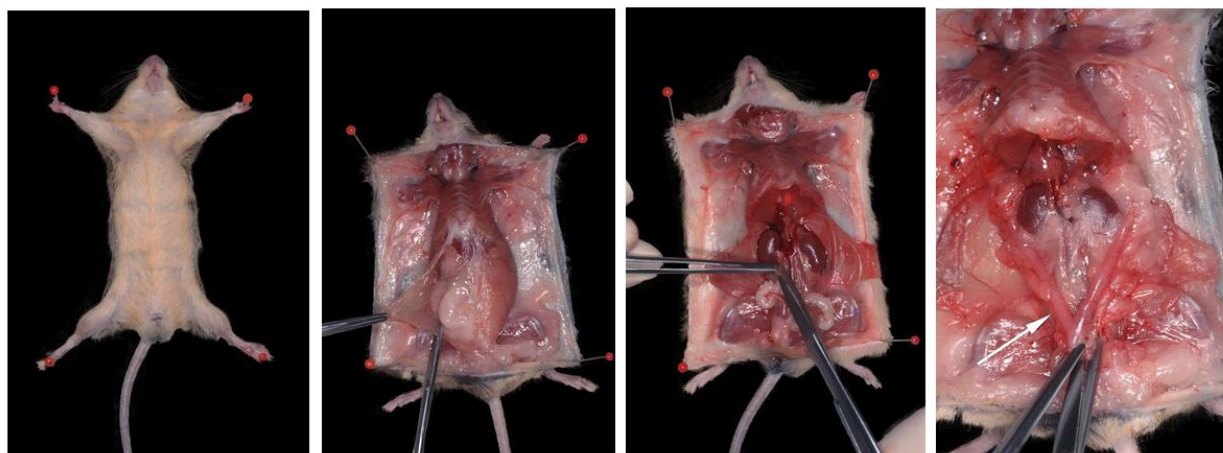


Figure 6.4: (From Left to Right) A. Position of the mice for autopsy B. Opening of the abdominal wall C. kidney and ureter extraction D. more detailed view for bladder removal

6.4.1.6. **Histological Examination** [16]:

- After the removal of part of bladder and kidney tissues, tissues were put in 10% neutral buffered formalin solution (NBF) in a 15-ml conical tube. In general, 5-ml of NBF is sufficient for a bladder and two kidneys from the same mouse.
- The tissues were fixed for at least 6 hours on benchtop at room temperature or overnight at 4°C.
- The tissues were rinsed three times in PBS.

- The bladder was bisected longitudinally and the two halves were placed in a tissue-embedding cassette.
- As kidneys are larger organs with complex architectures compared with the bladders, they were bisected longitudinally or cross-section of them is done into multiple slices. A kidney slice is placed in a tissue-embedding cassette.
- The tissues are stored in 70% ethanol (vol/vol in dH₂O) at 4⁰C. (Before embedding process, tissues can be stored for months at 4⁰C).
- The paraffin embedded tissues were cut into 5-µm sections.
- The slides were then stained with hematoxylin and eosin.
- Slides were then viewed under light microscope for physiological changes.

6.4.1.7. **Tissue Homogenization [16]:**

- Bladder tissue was placed in 1 ml 1X PBS in a 1.5 ml Eppendorf tube and homogenized using a hand-held micro pestle for about 2 minutes.
- An aliquot of homogenate was taken for bacterial enumeration.
- Remaining homogenate can be cleared by centrifugation at >12000×g for 5 minutes and the supernatants and cell pellets were separated and frozen at -80⁰C for cytokine analysis.

6.4.1.8. **Bacterial load estimation:**

According to infection protocol established for *E. coli* infection, organs were homogenized using sterile 1X PBS (pH 7.2) using a sterile micro pestle (Tarsons, India) manually. Tissue homogenates were serially diluted 10 times with sterile PBS and 100 µl of each dilution was plated on MacConkey agar. After an overnight incubation at 37⁰C, isolated colonies were counted to evaluate CFU/gm [12].

6.4.2. **RNA extraction and cDNA generation from infected tissue and kidney samples:**

- One-third part of the infected tissue from mice (bladder and kidney separately) were homogenized in 1500 µl TRIzolTM reagent with the help of handheld homogenizer.
- Kept at room temperature for 5 minutes.
- 300 µl chloroform was added to the scraped cells.
- Solution was vortexed vigorously for 15 seconds by hand and then incubated at room temperature for 3 minutes.

- The solution was centrifuged at $11600 \times g$ for 15 minutes at 4°C . The mixture was separated into lower red phenol chloroform phase, an interphase and colorless upper aqueous phase.
- Aqueous phase was transferred into a 1.5ml fresh centrifuge tube. 500 μl /1ml Trizol was added to it and pipetted up and down gently to precipitate RNA from aqueous phase. For better result, the solution was kept at -20°C overnight.
- On next day, the solution was centrifuged at $11600 \times g$ for 10 minutes at 4°C .
- The supernatant is discarded. RNA precipitate forms a translucent gel like pellet on side and bottom of the tube.
- The RNA is washed with 75% ice cold ethanol. 1 ml 75% ethanol was used per 1ml trizol.
- The solution was mixed properly by inversion, no vortex is required. Further, centrifugation is done at $10000 \times g$ for 10 minutes at 4°C .
- The supernatant is removed by pipetting. A quick spin centrifuge is required to collect any remaining 75% ethanol. The pellet is air-dried for 15 – 20 minutes. After a proper air-dry there would no visible ethanol. No over-drying is required.
- The pellet is resuspended in 50 μl nuclease free water by pipetting up & down and then incubating at 60°C for 10 minutes (if necessary, incubation should be done for 1 hour).
- 0.1 volume (5.6 μl) of DNase I buffer and 1 μl of DNase I enzyme (2 units) were added to RNA. A gentle mixing is done & then incubated at 37°C for 20 minutes.
- To the purified RNA, 1 μl of EDTA (DNase I inactivation reagent) is added and incubated at 65°C for 10 minutes.
- Optical density was measured at A_{260} and A_{280} by taking 1 μl DEPC dissolved RNA in 999 μl DDH_2O . RNA concentration is calculated and 5 ng of purified RNA is taken, nuclease free water is added to make up the volume to 11 μl and 1 μl of hexamer is added. The solution is mixed by spinning and kept at 65°C for 5 minutes to remove the 2° structure, then the mixture is kept in ice for 1 minute. Following, the mixture is spin down and kept in ice prior to use.
- With the 12 μl purified RNA with hexamer, 4 μl 5X reaction buffer, 1 μl RNase inhibitor, 2 μl 10mM dNTP mix and 1 μl Reverse transcriptase enzyme is added.
- The cDNA preparation is run in thermocycler under following conditions: initial incubation at 25°C for 5 minutes, heating at 42°C for 60 minutes, and terminating the reaction by heating again at 70°C for 5 minutes.

- Prepared cDNA is stored at -20°C.

6.4.3. Quantitative Real Time PCR (qRT-PCR) analysis: To determine the quantitative expression of adhesion genes (*fimH*, *papC*) and toxin genes (*hlyA*), qRT-PCR assay was performed on the cDNA prepared from total RNA extracted from bacteria infected tissues using gene-specific primers. qRT-PCR was performed in an Applied Biosystems™ 7500 Fast Real-Time PCR system with PowerUp™ SYBR™ Green Master Mix (Applied Biosystems, Lithuania) using the following conditions: 10 min at 95°C, 40 cycles at 95°C for 30 sec, 55°C for 30 sec, and 72°C for 30 sec. The primers used in this study are listed in Table 5.1. To determine the fold change of different virulence genes, the $2^{-\Delta\Delta C_t}$ method was used. Quantitative fold change analysis of each virulence genes in a specific p.i. day *in vivo*, was reported as fold change relative to their expression from previous p.i. days, keeping the expression of 5th day p.i. as 1.

6.4.4. Enzyme Linked Immuno-Sorbent Assay (ELISA): Concentration of cytokines namely IL-1 β , IL-17A, GCSF, TGF- β in mice sera and supernatant from bladder and kidney tissues were assayed using sandwich ELISA kits (Kinesis DX, USA), according to the manufacturers' protocol. All assays were run triplicate and results were represented as the mean value of the triplicate data. Results represented as pg/ml for serum and pg/ml in per mg of tissue for bladder and kidney tissues [15]. Standard curves were drawn in GraphPad Prism 8.0.2 and concentration of each cytokine was determined from their respective optical density values.

6.4.4.1. Mouse IL-1 β GENLISA™ ELISA:

6.4.4.1.1. Materials provided: Microtiter Coated Plate (12×8 wells) – 1no. • Recombinant Mouse IL-1 β Standard Lyophilized (1 μ g/ml) – 1vial • Mouse IL-1 β Biotin conjugated Detection Antibody Lyophilized (15 μ g/ml) – 1vial • Concentrated Streptavidin Horseradish Peroxidase – 1vial • 20X wash buffer – 25 ml • 1X assay diluent – 50 ml • TMB substrate – 12 ml • Stop Solution – 12 ml

6.4.4.1.2. Materials to be provided by the End-User: Microtiter plate reader able to measure absorbance at 450 nm • Adjustable pipettes and multichannel pipettor to measure volumes ranging from 25 μ l to 1000 μ l • Deionized (DI) water • Wash bottle or automated microplate washer • Graph paper or software for data analysis • Timer • Absorbent paper

6.4.4.1.3. Reagent Preparation:

- **Working Wash Buffer Solution:** To make 1X wash buffer, 5 ml of 20X Wash Buffer is added to 95 ml DI water. This is working solution.
- **1X assay diluent:** Ready to use.
- **Recombinant Mouse IL-1 β standard Lyophilized (110 ng/ml):** 40 μ l of 1X assay diluent is added to the vial. The concentration of reconstituted standard is 110 ng/ml. This is a single use vial. It should be used within 4 hours of reconstitution and should be discarded after use. 9.09 μ l of reconstituted standard (110 ng/ml) should be diluted with 990.91 μ l of 1X assay diluent to generate a 1000 pg/ml top standard.
- **Mouse IL-1 β Conjugates Detection Antibody Lyophilized (15 μ g/ml):** The lyophilized vial is reconstituted in 180 μ l 1X assay diluent to generate a 15 μ g/ml concentration. 83.33 μ l of detection antibody is added to 4916.67 μ l of 1X assay diluent to make final volume to 5 ml.
- **Concentrated Streptavidin-HRP (260 μ l):** 125 μ l of concentrated Streptavidin-HRP is added to 4875 μ l of 1X assay diluent to make a final volume to 5 ml.

6.4.4.1.4. Assay Procedure:

- All reagents were brought to room temperature prior to use. It is strongly recommended that all standards and samples should be run in duplicates. A standard curve is required for each assay.
- **Standards preparation:** The lyophilized vial is reconstituted with 40 μ l of 1X assay diluent to generate a 110 ng/ml standard concentration. Dilutions should be performed by using main stock solution as per the table below. Thus, the mouse IL-1 β standards concentrations are 1000pg/ml, 500pg/ml, 250pg/ml, 125pg/ml, 62.5pg/ml, 31.3pg/ml and 15.63pg/ml. 1X assay diluent serves as the zero standard (0 pg/ml).

Standard Concentrations	Standard No.	Dilution Particulars
110 ng/ml	Main stock	Original standard in the kit + 1X assay diluent 40 μ l
1000pg/ml	Standard No. 7	9.09 μ l main stock + 990.91 μ l 1X assay diluent
500pg/ml	Standard No. 6	500 μ l Standard No. 7 + 500 μ l 1X assay diluent

250pg/ml	Standard No. 5	500 µl Standard No. 6 + 500 µl 1X assay diluent
125pg/ml	Standard No. 4	500 µl Standard No. 5 + 500 µl 1X assay diluent
62.5pg/ml	Standard No. 3	500 µl Standard No. 4 + 500 µl 1X assay diluent
31.3pg/ml	Standard No. 2	500 µl Standard No. 3 + 500 µl 1X assay diluent
15.63pg/ml	Standard No. 1	500 µl Standard No. 2 + 500 µl 1X assay diluent
0pg/ml	Standard No. 0	500 µl 1X assay diluent

- 100 µl/ well of standards and samples were added to the plate, the plate was sealed and incubated for 2 hours at room temperature (18 – 25°C).
- The solution was aspirated and plate was washed 4 times with 1X wash buffer. The residual buffer was blotted by firmly tapping the plate upside down on absorbent paper. Any liquid from the bottom outside of the microtiter wells were wiped off as any residue can interfere in the reading step. All the washes should be performed similarly.
- 100 µl of detection antibody solution is added to each well, plate is sealed and incubated for 1 hour at room temperature (18 – 25°C).
- The plate was further washed 4 times with 1X wash buffer as in Step 4.
- 100 µl of diluted streptavidin – HRP solution is added to each well, plate was sealed and incubated for 30 minutes at room temperature.
- The plate was washed with 4 times with 1X wash buffer as in Step 4.
- 100 µl of TMB substrate solution is added to wells and incubated in the dark for 15 minutes at room temperature (18 – 25°C). Positive wells should turn bluish in color. It is not necessary to seal the plate during this step.
- The reaction is stopped by adding 100 µl of stop solution to each well. Positive wells should turn from blue to yellow.
- The absorbance is read at 450 nm within 30 minutes of stopping reaction.

6.4.4.2. Mouse Interleukin 17A (IL-17A) GENLISA™ ELISA:

6.4.2.2.1. **Materials provided:** Anti-Mouse IL-17A Antibody Coated Microtiter Plate (12×8 wells) – 1no. • Mouse IL-17A Standard (Concentrated, Lyophilized, 160ng/ml) – 1vial • Biotinylated IL-17A Antibody (Concentrated, Lyophilized, 3 µg/ml) – 1 vial • Streptavidin: HRP

conjugate – 1 vial • Streptavidin: HRP diluent – 12 ml • 1X assay diluent – 50 ml • 20X wash buffer – 25 ml • TMB substrate – 12 ml • Stop Solution – 12 ml

6.4.4.4.2. **Materials to be provided by the End-User:** same as 6.4.4.1.2.

6.4.2.4.3. **Reagent Preparation (all reagent should be diluted immediately prior to use):**

- All reagents need to be brought to room temperature prior to use.
- 25 ml of 20X wash buffer should be diluted in 475 ml of DI water.
- Standards preparation: The standard is reconstituted in 30 µl 1X assay diluent to get standard concentration of 160 ng/ml. 2.5 µl of reconstituted standard (160 ng/ml) added with 997.5 µl of 1X assay diluent to generate 400 pg/ml standard. The standards were prepared by serially diluting the standard stock solution as per the below table.

Standard Concentrations	Standard No.	Dilution Particulars
160 ng/ml	Original standard	Original standard in the kit + 30 µl 1X assay diluent
400 pg/ml	Standard No. 5	2.5 µl reconstituted standard + 997.5 µl 1X assay diluent
200 pg/ml	Standard No. 4	500 µl Standard No. 5 + 500 µl 1X assay diluent
100 pg/ml	Standard No. 3	500 µl Standard No. 4 + 500 µl 1X assay diluent
500 pg/ml	Standard No. 2	500 µl Standard No. 3 + 500 µl 1X assay diluent
25 pg/ml	Standard No. 1	500 µl Standard No. 2 + 500 µl 1X assay diluent
0 pg/ml	Standard No. 0	500 µl 1X assay diluent

6.4.2.4.4. **Assay Procedure:**

- It is strongly recommended that all standards and samples need to be run in duplicates or triplicates. A standard curve is required for each assay.
- 100 µl of prepared standard/samples were added to respective wells.
- The plate is covered with a sealer and incubated for 120 minutes at room temperature.
- The solution is aspirated and the plate is washed for 4 times with diluted 1X wash buffer and the residual buffer is blotted by firmly tapping the plate upside down on absorbent

paper. Any liquid from the bottom outside of microtiter wells should be wiped off as any residue can interfere in the reading step.

- 100 µl of prepared biotinylated detection antibody is added to respective wells.
- The plate is covered with a sealer to incubate at room temperature for 2 hours.
- The solution is aspirated and the plate is washed for 4 times with diluted 1X wash buffer and the residual buffer is blotted by firmly tapping the plate upside down on absorbent paper. Any liquid from the bottom outside of microtiter wells should be wiped off as any residue can interfere in the reading step.
- 100 µl streptavidin: HRP conjugate solution is added to respective wells and incubated at room temperature for 30 minutes.
- The solution is aspirated and the plate is washed for 4 times with diluted 1X wash buffer and the residual buffer is blotted by firmly tapping the plate upside down on absorbent paper. Any liquid from the bottom outside of microtiter wells should be wiped off as any residue can interfere in the reading step.
- 100 µl of TMB substrate is pipetted to each well.
- The plate is incubated at room temperature for 30 minutes. No shaking is expected as it may result in higher backgrounds and worse precision. Positive wells should turn bluish in color.
- 100 µl of Stop solution is pipetted to all wells. The wells should turn from blue to yellow in color.
- The absorbance is read at 450nm with a microplate reader with 10 – 15 minutes after addition of the stop solution.

6.4.4.3. Mouse Transforming Growth Factor β (TGF- β) GENLISA™ ELISA:

6.4.4.3.1. Materials provided:

Mouse TGF- β Antibody Coated Microtiter Plate (8×12 wells) – 1no. • Mouse TGF- β Standard (concentrated 2400 pg/ml) – 0.5 ml • Biotinylated TGF- β antibody – 1 ml • Streptavidin: HRP conjugate – 6 ml • Standard diluent – 3 ml • 1X sample diluent – 12 ml • 20X wash buffer – 25 ml • TMB substrate – 12 ml • Stop Solution – 12 ml

6.4.4.3.2. Materials to be provided by the End-User: same as 6.4.4.1.2

6.4.4.3.3. Reagent preparation:

- All reagents would be brought to room temperature prior to use.
- 25 ml 20X wash buffer would be diluted in 475 ml DI water to make 1X wash buffer.
- Standards preparation: 120 µl of original standard (2400 pg/ml) was diluted with 120 µl of standard diluent to generate a 1200 pg/ml standard stock solution. The standard is kept for 15 minutes with gentle agitation before making further dilutions. The standards were prepared by serially diluting the standard stock solution as per the below table.

Standard Concentrations	Standard No.	Dilution Particulars
2400 pg/ml	Original standard	Original standard in the kit
1200 pg/ml	Standard No. 5	120 µl original standard + 120 µl 1X assay diluent
600 pg/ml	Standard No. 4	120 µl Standard No. 5 + 120 µl 1X assay diluent
300 pg/ml	Standard No. 3	120 µl Standard No. 4 + 120 µl 1X assay diluent
150 pg/ml	Standard No. 2	120 µl Standard No. 3 + 120 µl 1X assay diluent
75 pg/ml	Standard No. 1	120 µl Standard No. 2 + 120 µl 1X assay diluent
0 pg/ml	Standard No. 0	120 µl 1X assay diluent

6.4.4.1.4. Assay Procedure:

- It is strongly recommended that all standards and samples need to be run in duplicates. A standard curve is required for each assay.
- 50 µl standard diluent is added to respective blank wells.
- 50 µl prepared standard is added to respective standard wells.
- 40 µl samples were added to respective samples wells.
- 10 µl biotinylated TGF-β antibody were pipetted to respective sample wells. (Note: No need to add biotinylated TGF-β antibody into standard wells and blank wells. Standards

provided in the kit are pre-offered as a complex of the standard and the biotin antibody for ease-of-use.)

- 50 µl streptavidin: HRP conjugate were pipetted to all wells and mixed.
- The plate is covered with a sealer and incubated for 60 minutes at 37°C.
- The solution is aspirated and washed 4 times with 1X wash buffer and residual buffer is blotted firmly tapping the plate upside down on absorbent paper. Any extra liquid on the bottom outside of the microtiter wells were wiped off as any residue can interfere in the reading step.
- 100 µl TMB substrate were pipetted to all wells.
- The plate was incubated at 37°C for 10 minutes. No shaking is needed as it may result in higher backgrounds and worse precision. Positive wells should turn bluish in color.
- 100 µl of stop solution is pipetted to all wells. The wells should turn blue to yellow in color.
- The absorbance is read at 450 nm with a microplate within 10 – 15 minutes after addition of stop solution.

6.4.4.4. Mouse Granulocyte Colony Stimulating Factor (G-CSF) GENLISA™ ELISA:

6.4.4.4.1. Materials Provided: Mouse G-CSF Antibody Coated Microtiter Plate (8×12 wells) – 1no. • Standard, Mouse G-CSF (concentrated, 1600 pg/ml) – 0.5 ml • Biotinylated G-CSF antibody – 1ml • Streptavidin: HRP conjugate – 6 ml • Standard Diluent – 3 ml • 1X Sample Diluent – 12 ml • 20X wash buffer – 25 ml • TMB substrate – 12 ml • Stop solution – 12 ml

6.4.4.4.2. Materials to be provided by the End-User: same as 6.4.4.1.2.

6.4.4.4.3. Reagent Preparation (all reagents should be diluted immediately prior to use):

- All the reagents should be brought to room temperature prior to use.
- 25 ml wash buffer is added in 475 ml of DI water to make 1X wash buffer.
- Standard Preparation: 120 µl of original standard (1600 pg/ml) is diluted with 120 µl of standard diluent to generate an 800 pg/ml standard stock solution. The standard is kept for 15 minutes with gentle agitation before making further dilutions. The standards are prepared by serially diluting the standard stock solution as per the below table.

Standard Concentrations	Standard No.	Dilution Particulars
1600 pg/ml	Original standard	Original standard in the kit
800 pg/ml	Standard No. 5	120 µl original standard + 120 µl 1X assay diluent
400 pg/ml	Standard No. 4	120 µl Standard No. 5 + 120 µl 1X assay diluent
200 pg/ml	Standard No. 3	120 µl Standard No. 4 + 120 µl 1X assay diluent
100 pg/ml	Standard No. 2	120 µl Standard No. 3 + 120 µl 1X assay diluent
50 pg/ml	Standard No. 1	120 µl Standard No. 2 + 120 µl 1X assay diluent
0 pg/ml	Standard No. 0	120 µl 1X assay diluent

6.4.4.4.4. Assay Procedure:

- It is strongly recommended that all standards and samples to be run in duplicates. A standard curve is required for each assay.
- 50 µl of standard diluent is added to respective blank wells.
- 50 µl of prepared standards is added to respective standard wells.
- 40 µl of samples were added to respective sample wells.
- 10 µl of biotinylated G-CSF Antibody is pipetted to respective sample wells. (Note: No need to add Biotinylated G-CSF antibody to standard wells and blank wells. The standards provided in the kit are pre-offered as a complex of the standard and the biotin antibody for ease-of-use.
- 50 µl streptavidin: HRP conjugate were pipetted to all wells and mixed.
- The plate was covered with a sealer and incubated for 60 minutes at 37°C.
- After aspiration of the solution, the plate was washed 4 times with diluted 1X wash buffer and residual buffer was blotted by firmly tapping the plate upside down on absorbent paper. Any extra liquid from the bottom outside of the microtiter wells were wiped off as any residue can interfere in the reading step.
- 100 µl TMB substrate was pipetted to all wells.

- The plate was incubated at 37°C for 10 minutes. No shaking is needed as it may result in higher backgrounds and worse precision. Positive wells should turn bluish in color.
- 100 µl of stop solution is pipetted to all wells. The wells should turn from blue to yellow in color.
- The absorbance is read at 450 nm with a microplate within 10 – 15 minutes after addition of stop solution.

6.4.5. Statistical Analysis: Graphs were drawn using GraphPad Prism version 8.0.2 (GraphPad Software, CA, USA). Statistical analyses were also performed in GraphPad Prism. A two-way ANOVA using Tukey's multiple tests were performed to compare differences between the bacterial colonization, relative gene expression and cytokine levels in the respective tissues and sera samples. The difference was statistically significant at $p \leq 0.05$ [12].

6.5. Results:

6.5.1. Bacterial isolates and virulence score: The clinical UPEC isolate *E. coli* P025 and *E. coli* NP105 exhibited incidence of varied virulence factor genes, that resulted in a virulence score of 10 and 13 respectively. The virulence profiles and their phylogenetic background were mentioned in Table 6.1. To investigate their infection potential in vivo, bacterial colonization in bladder and kidney tissues of infected mice were monitored.

Table 6.1. Distribution of virulence factor genes (VFGs) and phylogenetic background in *Escherichia coli* P025 and *Escherichia coli* NP105.

Bacterial Isolates	Phylogenetic Background	Virulence Profiles
P025	B2	<i>fimH, papC, papEF, papGII, sfaA, hlyA, iroN, chuA, kpsMTII, iha, iucD, vat, csgA</i>
NP105	D	<i>fimH, papC, papEF, iroN, chuA, kpsMTII, iha, iucD, flu, csgA</i>

6.5.2. Bacterial colonization in bladder and kidney: The evaluation of the bladder samples infected with *E. coli* P025 with a virulence score of 13 exhibited comparatively high bacterial colonization at the 7th and 9th day p.i. in comparison with other p.i. days. In contrary, the evaluation of the kidney samples infected with *E. coli* P025 showed highest bacterial load at 7th day p.i. with a drastic reduction at 9th day p.i. from day 7. However, evaluation of both bladder and kidney

samples infected with *E. coli* NP105 isolates with a virulence score 10 showed highest bacterial load at 9th day p.i. when compared with the bacterial load from 7th day p.i. Nonetheless, the difference in the bacterial counts in the bladder tissue was significantly different on 7th and 9th day from 5th day in *E. coli* P025 infection group ($p=0.0051$ and $p<0.0001$ respectively) and it was significantly different on 9th day from 7th day in *E. coli* NP105 infection group ($p=0.0025$). Moreover, the difference in bacterial counts in the kidney tissues was significantly different on 7th day from 5th day in *E. coli* P025 infection group ($p<0.0001$) and it was significantly different on 9th day from 7th day in *E. coli* NP105 infection group ($p=0.0023$) (Figure 6.5).

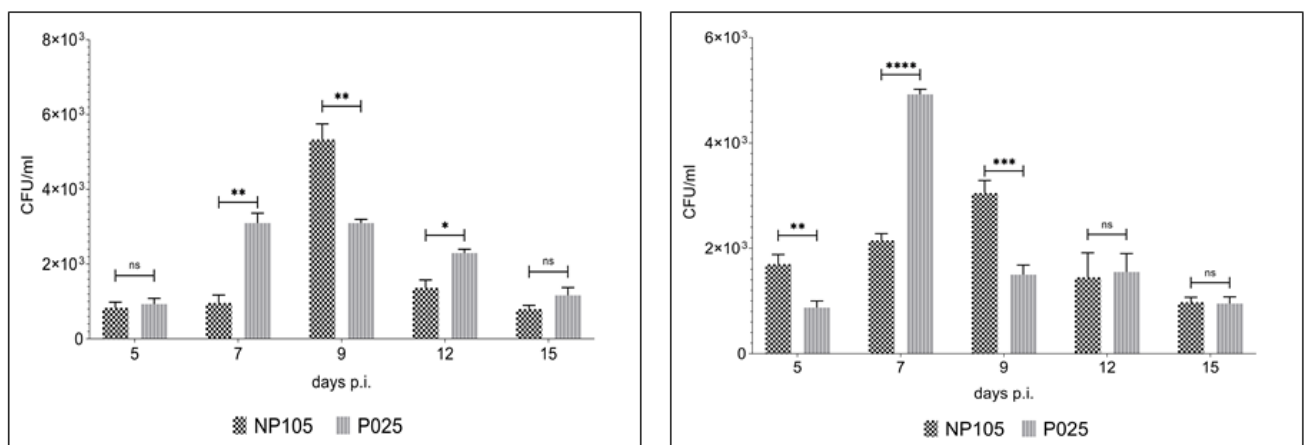


Figure 6.5: Bacterial colonization (CFU/ml) in (A) bladder (left) and (B) kidney (right) of mice infected with *E. coli* NP105 ☒ and *E. coli* P025 ■ and were euthanized on days 5, 7, 9, 12 and 15 p.i. Data were represented as the means \pm standard deviations (SD). * $p<0.05$, ** $p<0.01$, *** $p<0.001$ and **** $p<0.0001$ above the bars indicated differences among the infected groups.

6.5.3. Histopathology of bladder and kidney: Histological examinations performed on 7th and 9th day p.i. in bladder and kidney tissues from mice infected with *E. coli* P025 and *E. coli* NP105 respectively showed prominent morphological changes that indicated alteration of the normal architecture compared with uninfected bladder and kidney tissues. The tissues of the kidney presented swelling and enlargement of renal tubules and the tissues of bladder presented tissue deformation and the presence of erythrocytes at respective days of p.i. (Figure 6.6)

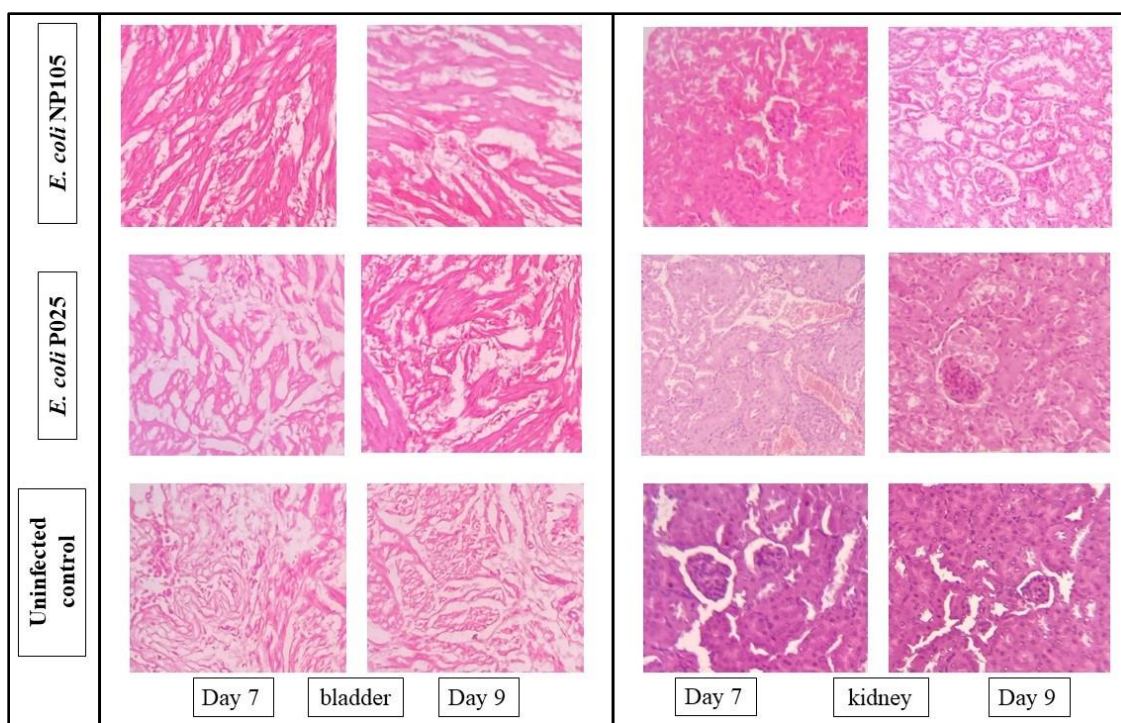


Figure 6.6: Histopathology of bladder and kidney samples of mice infected with *E. coli* P025 and *E. coli* NP105 on day 7th and day 9th p.i. Microscopic images were apprehended at 40X magnification.

6.5.4. Expression of bacterial virulence genes *fimH*, *papC*, *hlyA* in vivo: Expression of bacterial adhesin genes; *fimH* and *papC* in the bladder and kidney tissues infected with *E. coli* P025 and *E. coli* NP105 at different days of p.i. was monitored. A discrete pattern of expression of the adhesin genes was observed. Highest expression of *fimH* was observed in both bladder and kidney tissues on 7th day p.i. in *E. coli* P025 infection group of mice, and on 9th day p.i. in *E. coli* NP105 infection group of mice. The difference in expression of *fimH* was only significant in both bladder ($p \leq 0.05$) and kidney ($p \leq 0.05$) tissues of *E. coli* NP105 infection group of mice from the previous p.i. day, whereas the difference is not significant in both kidney ($p \geq 0.05$) and bladder ($p \geq 0.05$) tissues of *E. coli* P025 infection group of mice from the previous p.i. day (Figure 6.7A, 7B). Highest expression of *papC* was observed in both bladder and kidney tissues on 7th day p.i. in *E. coli* P025 infection group of mice only. The expression of *papC* decreased gradually from 5th day p.i. till 15th day p.i. in both bladder and kidney tissues of *E. coli* NP105 infection group of mice. The difference in expression of *papC* on 7th day p.i. was significant in both bladder ($p \leq 0.05$) and kidney ($p \leq 0.05$) tissues from its previous infection day p.i. (Figure 6.8A, 8B). On the other, the difference in

expression of *papC* was not significant from its previous infection day p.i. in both bladder ($p \geq 0.05$) and kidney ($p \geq 0.05$) tissues.

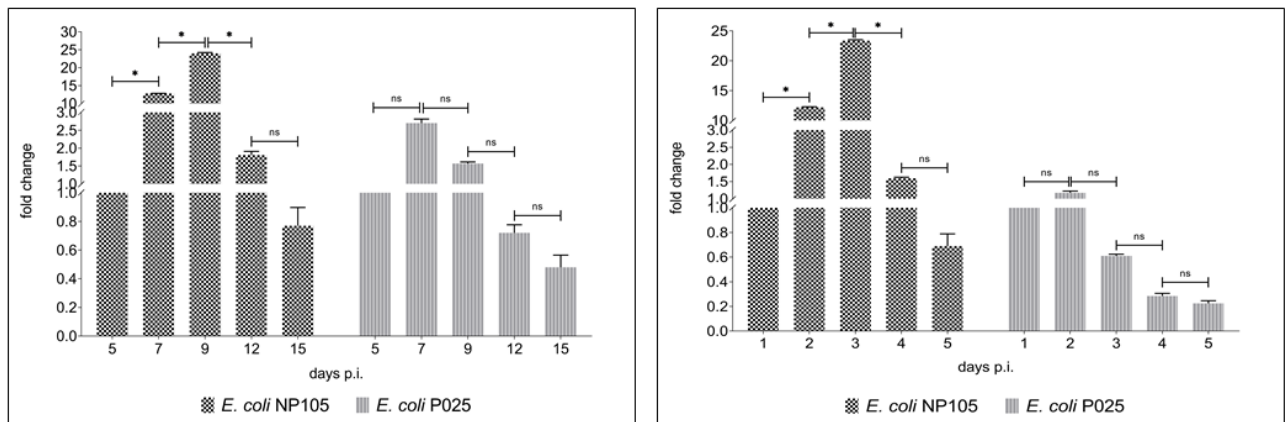


Figure 6.7: Relative expression of *fimH* in (A) bladder and (B) kidney of *E. coli* NP 105 ▨ and *E. coli* P025 ■ and euthanized on days 5, 7, 9, 12 and 15 p.i. Data were presented as the means \pm SD. * $p < 0.05$ above the bars indicate differences in fold expression between the infected groups. Non-significant differences are represented as 'ns'.

Additionally, pattern of expression of *hlyA* was distinctly different from the expression pattern of adhesins in both bladder and kidney tissues infected with *E. coli* P025 at different days of p.i. A gradual increase in the expression of *hlyA* was observed with the progression of the infection from 5th day p.i. to 15th day p.i. in both bladder and kidney tissues respectively and the difference from in expression in particular p.i. day from its previous p.i. day in both bladder ($p \leq 0.05$) and kidney ($p \leq 0.05$) tissues (Figure 6.9A, 9B).

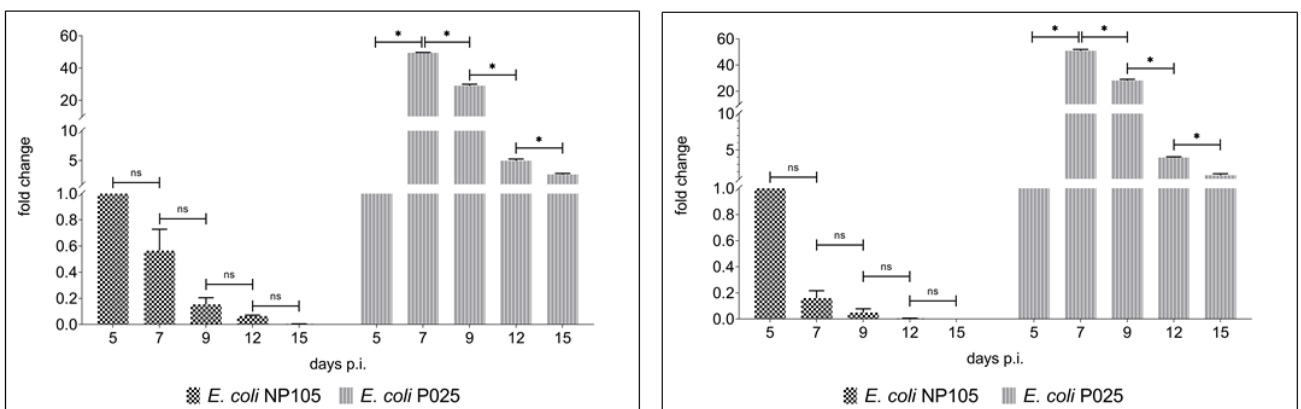


Figure 6.8: Relative expression of *papC* in bladder(A) and kidney(B) tissues of mice infected with *E. coli* NP 105 ☒ and *E. coli* P025 ■ and euthanized on days 5, 7, 9, 12, 15 p.i. Data are presented as the means \pm SD. * $p < 0.05$ above the bars indicate differences in fold expression between the infected groups. Non-significant are represented as ‘ns’.

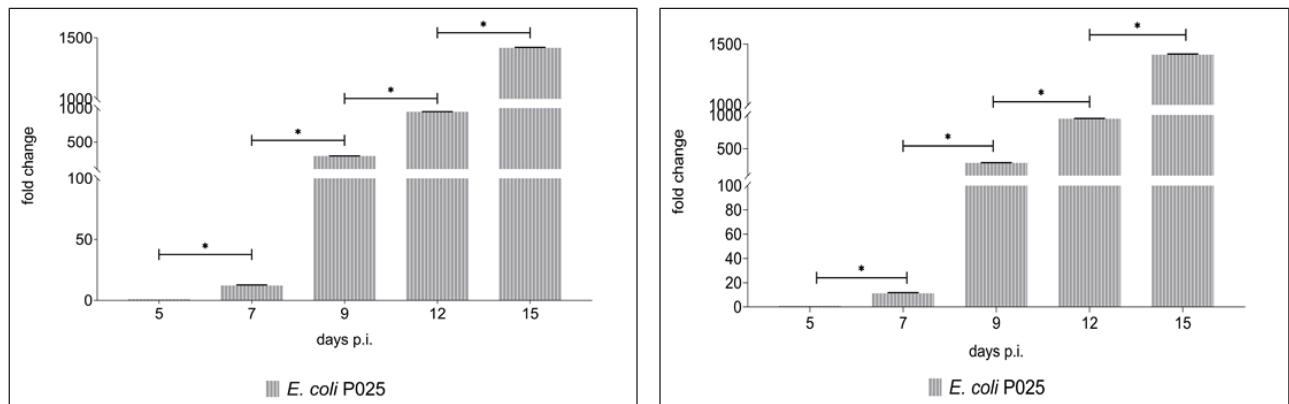


Figure 6.9: Relative expression of *hlyA* in bladder (A) and kidney (B) of *E. coli* P025 ■ and euthanized on days 5, 7, 9, 12 and 15 p.i. Data are represented as the means \pm SD. * $p < 0.05$ above the columns indicate significant differences compared with the uninfected group and p values above the bars indicate differences among the infected groups.

6.5.5. Cytokine concentrations:

Proinflammatory cytokines IL-1 β and IL17A concentrations were estimated in both bladder and kidney tissues from mice infected with *E. coli* P025 and *E. coli* NP105 isolates respectively. Highest concentration of IL-1 β was observed at 9th day p.i. in both bladder and kidney tissues from mice infected with *E. coli* NP105 which exhibited highest bacterial count and the increase in concentration in the bladder ($p \leq 0.05$) and kidney ($p \leq 0.05$) tissues from uninfected mice was statistically significant. Similar results were obtained in the level of IL-1 β in the serum collected from mice infected with *E. coli* NP105 at 9 days p.i. compared to the untreated mice ($p \leq 0.05$). In contrary mice infected with *E. coli* P025 at 7th day p.i., which exhibited highest bacterial load, similar concentration of IL-1 β in kidney tissues ($p \geq 0.05$) and minor enhancement in its concentration in bladder tissues ($p \geq 0.05$) than from the concentration of IL-1 β in respected tissues from uninfected mice was observed. However, the level of IL-1 β in sera sample obtained from infected mice was similar to the increase in its level in bladder tissues from sera collected from *E.*

coli P025 infected mice than uninfected control at 7th day p.i., although this observation was not statistically significant ($p \geq 0.05$) compared to uninfected control (Figure 6.10 A, B, C).

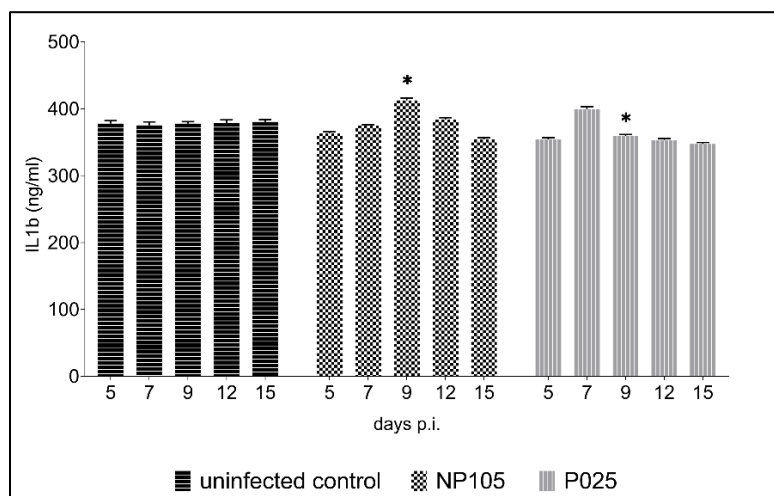
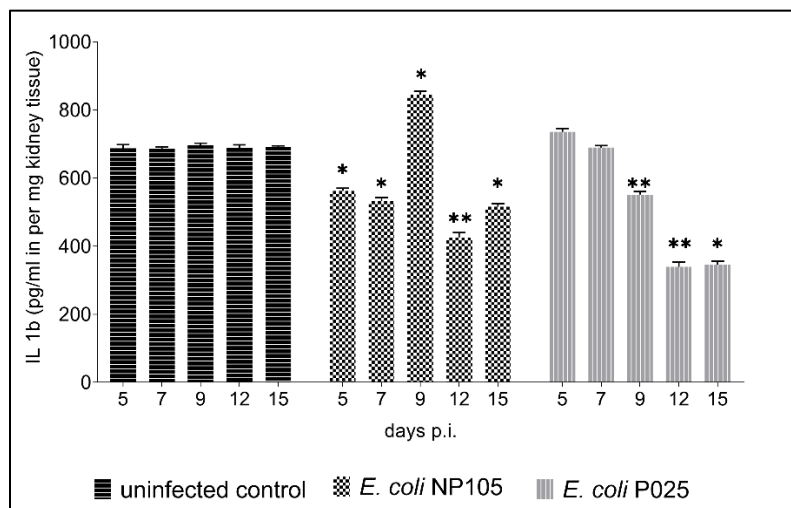
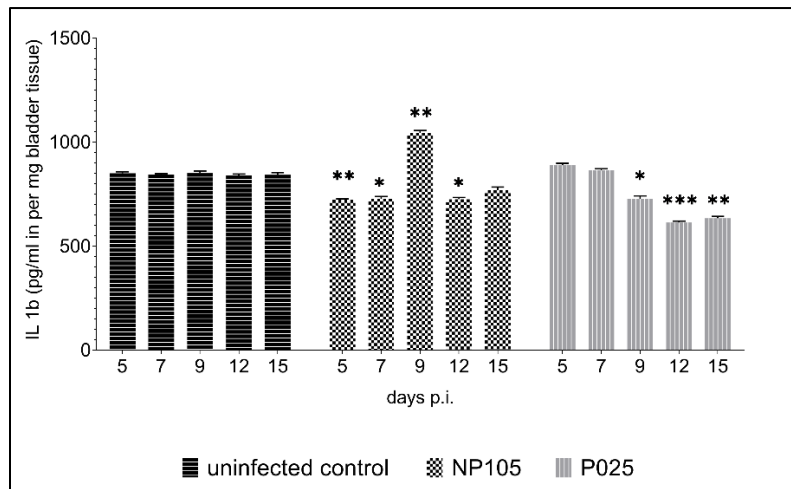
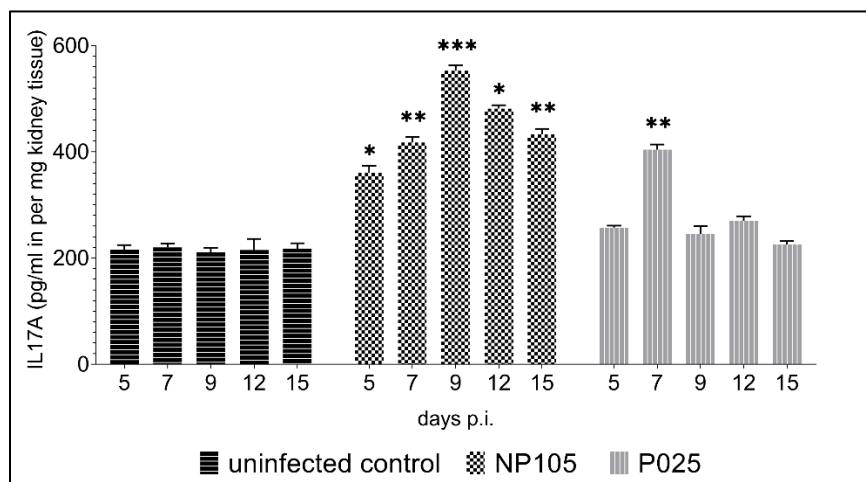
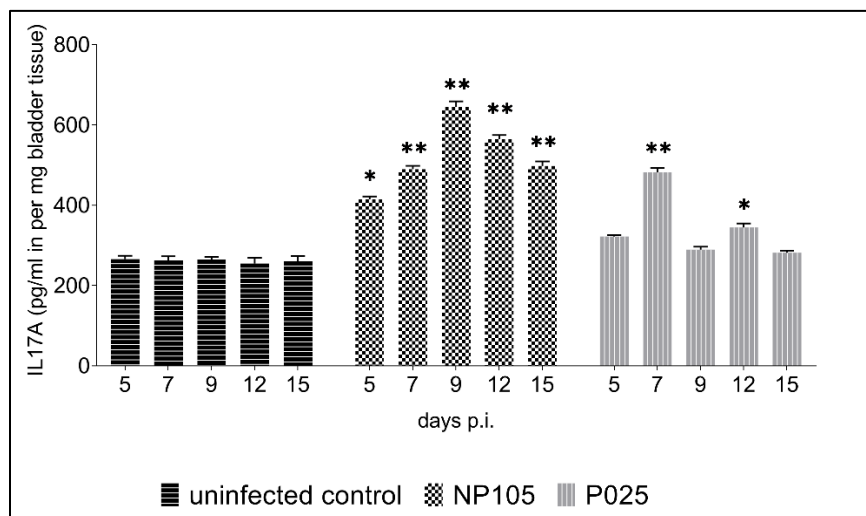


Figure 6.10: IL-1 β levels in bladder (A), kidney (B) and serum (C) from mice that were uninfected or infected with *E. coli* NP105 and *E. coli* P025 and euthanized on days 5, 7, 9, 12 and 15 p.i. Data are represented as the means \pm SD. * $p < 0.05$, ** $p < 0.01$, and *** $p < 0.001$ indicate significant differences compared with the uninfected group.

A sharp rise in the concentration of IL17A in both bladder ($p \leq 0.05$) and kidney ($p \leq 0.05$) tissues of mice infected with *E. coli* P025 and *E. coli* NP105 at 7th day and 9th day p.i. respectively from tissues collected from uninfected control mice was observed, which was statistically significant. Moreover, the enhancement in the IL-17A level in the bladder and kidney tissues was also reflected in the statistically significant increase in the level of cytokine in sera samples collected from mice infected with *E. coli* P025 ($p \leq 0.05$) and *E. coli* NP105 ($p \leq 0.05$) respectively (Figure 6.11 A, B, C).



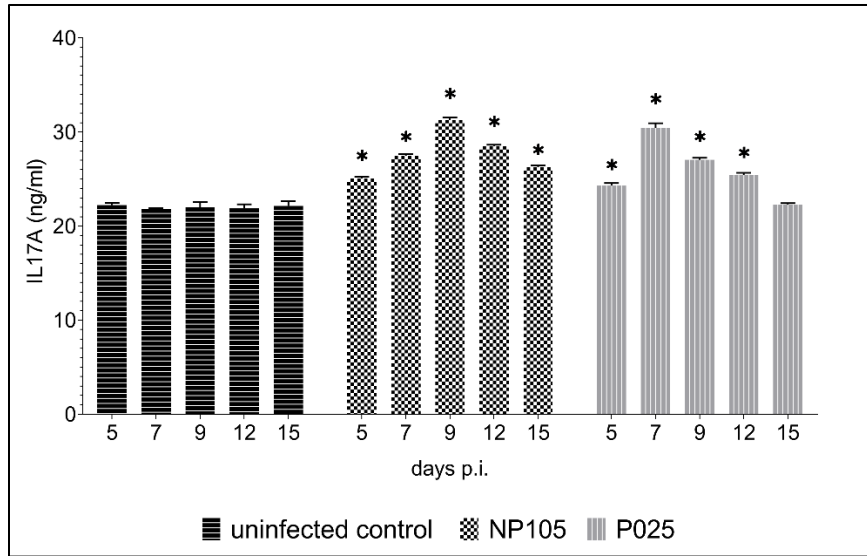


Figure 6.11: IL-17A levels in bladder (A), kidney (B) and serum (C) from mice that were uninfected or infected with *E. coli* NP105 and *E. coli* P025 and euthanized on days 5, 7, 9, 12, and 15 p.i. Data are represented as the means \pm SD. * $p < 0.05$, ** $p < 0.01$, and *** $p < 0.001$ indicate significant differences compared with the uninfected group.

Concentrations of the anti-inflammatory cytokine GCSF in the bladder and kidney tissues isolated from mice infected with *E. coli* P025 and *E. coli* NP105 exhibited discrete patterns during the days of p.i. At 7th day p.i. in both bladder (≤ 0.05) and kidney (≤ 0.05) of mice infected with *E. coli* P025, a statistically significant increase in the concentration of GCSF was observed compared to the uninfected control. In contrast, a statistically significant decrease in the concentration of GCSF was observed in both bladder (≤ 0.05) and kidney (≤ 0.05) tissues at 9th day p.i. in mice infected with *E. coli* NP105 in comparison to the uninfected control. However, the level of the cytokine in sera collected from both *E. coli* P025 (≤ 0.05) and *E. coli* NP105 (≤ 0.05) infected mice was significantly lower compared to the sera collected from the uninfected group (6.12 A, B, C).

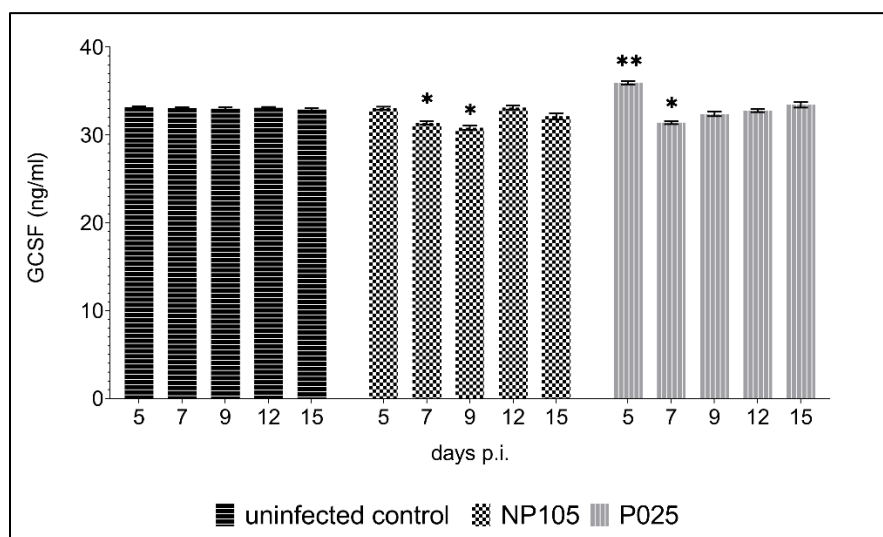
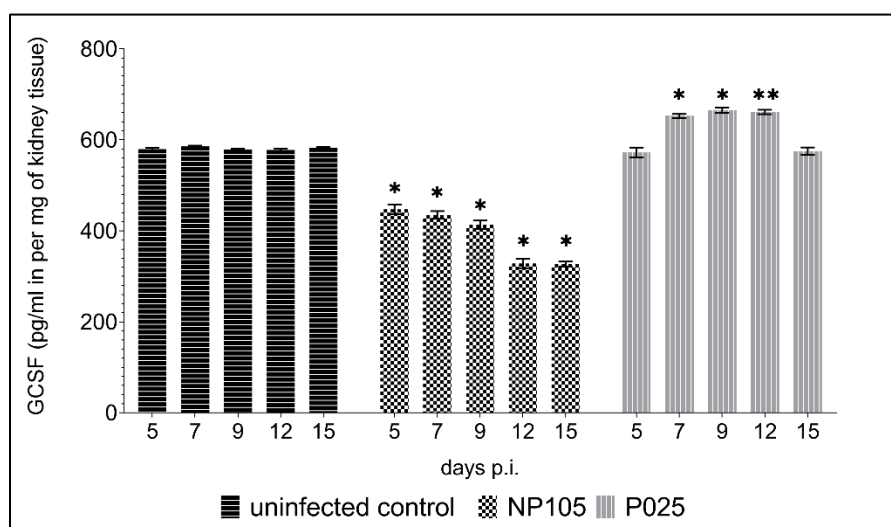
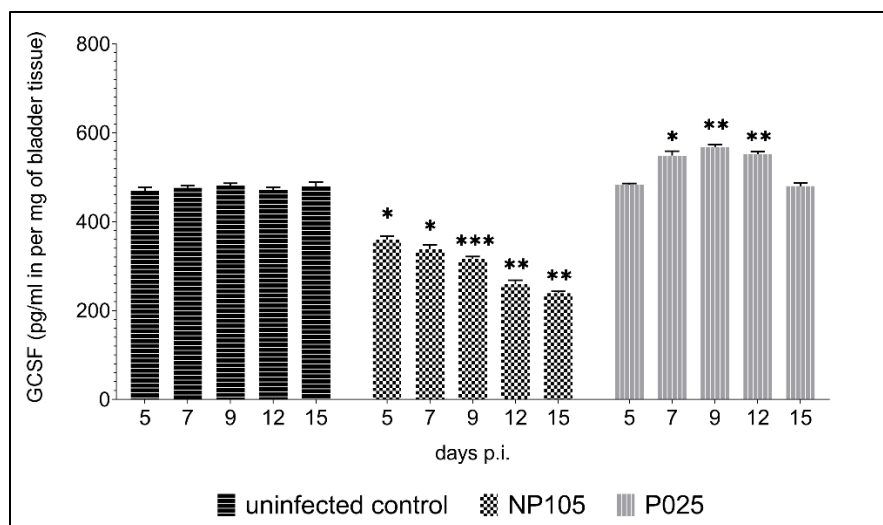
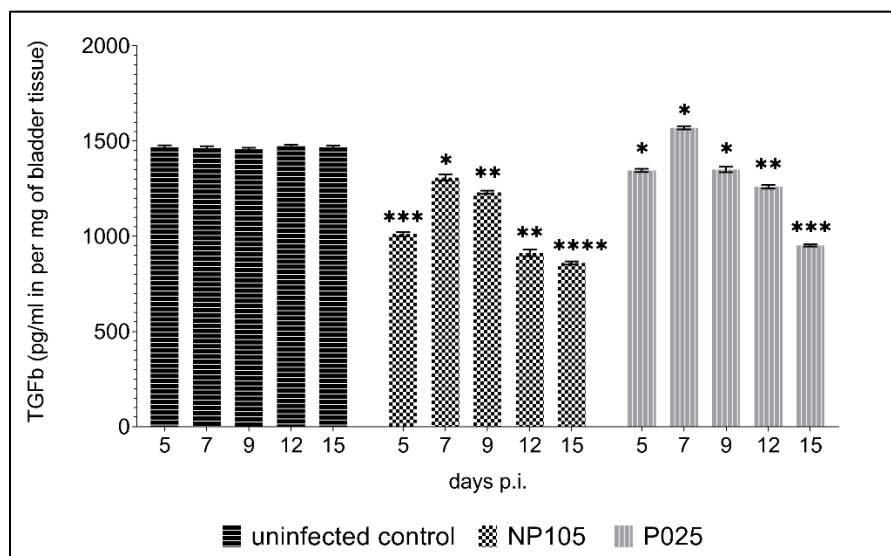


Figure 6.12: GCSF levels in bladder (A), kidney (B) and serum (C) from mice that were uninfected or infected with *E. coli* NP105 and *E. coli* P025 and euthanized on days 5, 7, 9, 12, and 15 p.i. Data are represented as the means \pm SD. * $p < 0.05$, ** $p < 0.01$, and *** $p < 0.001$ indicate significant differences compared with the uninfected group.

Concentration of the anti-inflammatory cytokine TGF- β in the bladder (≤ 0.05) and kidney (≤ 0.05) tissues similar to the levels of GCSF, i.e. increase in concentration at 7th day p.i. in mice infected with *E. coli* P025 than uninfected control. Moreover, bladder (≤ 0.05) and kidney (≤ 0.05) tissues from mice infected with *E. coli* NP105 at 9th day p.i. also showed similar statistically significant level of difference than uninfected control. Furthermore, the level of TGF- β in sera samples at 7th day and 9th day p.i. from *E. coli* P025 (≤ 0.05) and *E. coli* NP105 (≤ 0.05) infected mice was significantly reduced than their level in the control sera collected from uninfected mice (Figure 6.13 A, B, C).



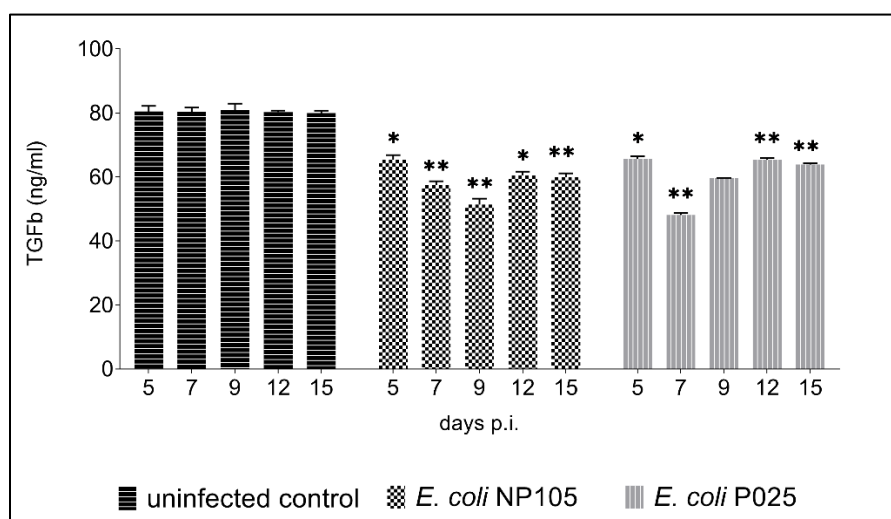
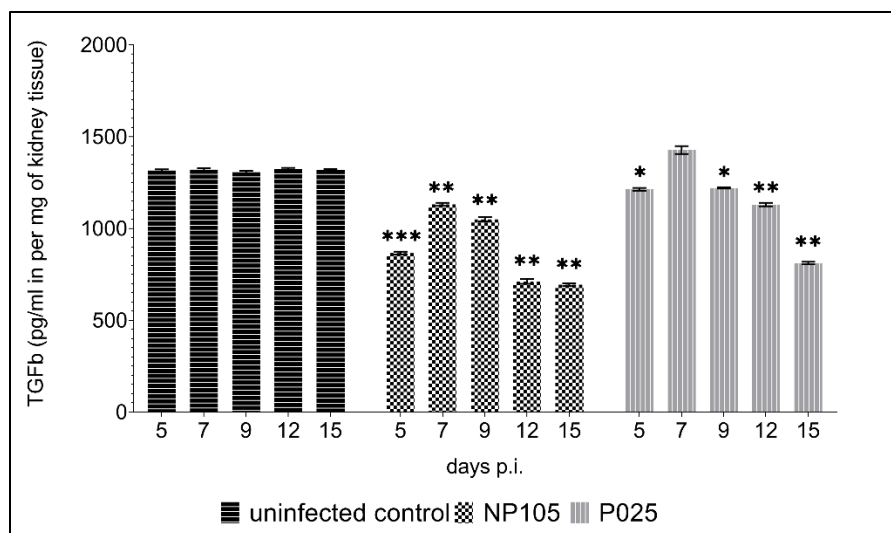


Figure 6.13: TGF- β levels in bladder (A), kidney (B) and serum (C) from mice that were uninfected or infected with *E. coli* NP105 and *E. coli* P025 and euthanized on days 5, 7, 9, 12, and 15 p.i. Data are represented as the means \pm SD. * $p < 0.05$, ** $p < 0.01$, and *** $p < 0.001$ indicate significant differences compared with the uninfected group.

6.6. Discussion:

The goal of this study was to characterize the cytokine response associated with various clinical isolates that expressed common adhesion factors, such as *fimH*, *papC* which are primarily involved in the attachment to host uroepithelial cells, and toxin genes such as *hlyA*, which are involved in host invasion, at the specific post infection days with the highest bacterial colonization in mice

model of UTI. The bacterial load in the bladder and kidney tissues of infected mice, followed by the histopathological alternations noticed as a result of infection, were used to describe the infection potential of the isolates. The pathogenic potential of *E. coli* strains was determined by their virulence attributes, but host factors are also equally important for invasion, colonization, and the progression of infection [3, 17, 18, 19]. Our previous study showed that cytokine expression profiles were correlated with the expression of virulence genes in UPEC that was isolated from two discrete population upon infection in HTB-4 uroepithelial cells [13]. Furthermore, it was shown that the tip adhesins *papC* of the P-fimbriae adhesin family and *fimH* of the type I fimbriae play crucial roles in adhering to bladder and kidney epithelial tissues [5, 20, 21]. Furthermore, it was discovered that *hlyA* actively participates in the process of cellular invasion [22]. In the current investigation, two clinical isolates of *E. coli* P025 and *E. coli* NP105, which displayed distinct virulence characteristics, showed a distinct pattern of expression of *fimH* and *papC*, which led to variations in bacterial colonization in the bladder and kidney tissues from infected mice. The expression of *fimH* of *E. coli* NP105 and *papC* of *E. coli* P025 was highest on 9th day and 7th day p.i. respectively along with a significant increase and decrease in *fimH* and *papC* expression in both the bladder and kidney from 7th to 9th day p.i. The difference in expression pattern of the respective virulence genes in bladder and kidney tissues may be attributed to the normal ecological processes that outline the bacterial community. Resource competition, bacterial growth, and bacterial mortality due to immune-mediated processes are possible additional factors that may regulate the production of the respective adhesins [23]

Proinflammatory cytokines and chemokines such as IL-8, CCL2, CCL5, TNF- α , IFN- γ , IFN- β , IL-1 β , IL-6, IL-10 and IL-17A are produced by macrophages and uroepithelial cells during UTIs, luring neutrophils to the site of infection and controls antibacterial defenses in an orchestrated way [24]. Additionally, an in vitro investigation revealed that the pro-inflammatory cytokines IL-1 β , IL-6, IL-8 and IFN- γ had concentration-dependent impacts on the development of the UPEC prototype strain CFT073 alone or in combination [10]. Additionally, it was discovered that secondary lymphoid tissue cells, of which T-cells were the primary sources, upregulated the IL-17A in response to UPEC antigens [7]. Serum from the *E. coli* NP105 infected mice in this investigation displayed the highest level of IL-1 β at the 9th day p.i., which also displayed the highest bacterial colonization. In contrast, mice infected with *E. coli* P025 showed a substantially different pattern in both tissues and serum. This difference in IL-1 β expression may be due to the

difference in phylogenetic background of the two *E. coli* isolates in accordance to a recent study which showed that the levels of IL-1 β , TNF- α and IL-6 in sera collected from mice infected with *E. coli* of different phylogroups was distinctly different [25]. In contrary to the variations in IL-1 β levels, the highest levels of IL-17A were seen in both tissue and sera from mice that had been exposed to *E. coli* NP105 and *E. coli* P025 at 9th and 7th day p.i. respectively which was consistent with the bacterial colonization on the respective p.i. days. The elevated IL-17A levels and greater bacterial (UPEC) loads in the infected bladder tissues were significantly positively correlated in an earlier investigation, which supports this conclusion [26].

In this study, the levels of G-CSF and TGF- β in the bladder, kidney and sera of mice infected with *E. coli* NP105 were significantly lower than those from tissues and sera of uninfected controls, at the 9th day p.i., where bacterial colonization was at its peak. Reduced neutrophil recruitment into the bladder tissues during UTI leads to less bacterial clearance because of G-CSF depletion [11]. TGF- β has been found to act as an anti-inflammatory cytokine and it adversely modulate renal inflammation in chronic kidney disease [27]. Another earlier study also supported the anti-inflammatory function of TGF- β in UTI found that its levels were lower in babies with acute pyelonephritis (APN) compared to controls [28]. Additionally, TGF- β level was found to increase in severe mucosal inflammation associated with a lower degree of bacterial colonization reported in *H. pylori* infection [29]. In contrast, bladder and kidney samples of mice infected with *E. coli* P025 showed considerably higher G-CSF and TGF- β levels on 7th day p.i., when bacterial colonization at its peak, compared to the corresponding tissue samples collected from uninfected control mice. It is also possible to relate this variation in G-CSF and TGF- β levels in the bladder and kidney tissues of mice infected with *E. coli* NP105 and *E. coli* P025 respectively to their distinct phylogenetic background [25]. However, G-CSF and TGF- β serum levels in the *E. coli* P025 infected mice group were considerably lower than those in the *E. coli* NP105 infected group.

Emergence of antimicrobial resistance (AMR) in UPEC forced a revision of the prescription policy for the treatment of UTIs. Strategies to understand the pathogenic nature of the UPEC strains might facilitate to design appropriate therapeutics. Although urine culture has been the gold standard for UTI detection and antibiogram profiling was used to select appropriate antibiotics for treatment, the process is laborious and time taking and sometimes may be ineffective for critically ill patients and pregnant women, especially in the third trimester of pregnancy, as many antibiotics may cause

a variety of complications [30, 31]. Furthermore, these techniques are insufficient to reveal the infection potential of any specific *E. coli* strain.

In the current study, two clinical UPEC isolates with distinctly different virulence factor acquisition showed a different pattern of bacterial colonization in the bladder and kidney tissues of infected mice. This study also has shown that the populations of mice infected with the respective UPEC isolates had varied IL-1 β levels in the serum collected on the p.i. day of highest colonization. The levels of other cytokines examined, such IL-17A, TGF- β , and G-CSF were comparable in the sera samples from the two groups of infected mice. As a result, the virulence potential of the UPEC isolates was correlated with the expression of IL-1 β , which was further reflected in the bacterial burden in the bladder and kidney tissues of the infected mice groups as well as in the sera. The results of this study therefore suggested that IL-1 β may have contribution to stratify UPEC-UTI pathogenicity.

6.7. References:

1. Bien J, Solokova O, Bozko P. Role of uropathogenic *Escherichia coli* Virulence Factors in Development of Urinary Tract Infection and Kidney Damage. 2012. International Journal of Nephrology. 1 – 15.
2. Zhu H, Chen Y, Hang Y, Luo H, Fang Y, Xiao Y, Cao X, Zou S, Hu X, Hu L, Zhong Q. Impact of inappropriate empirical antibiotic treatment on clinical outcomes of urinary tract infections caused by *Escherichia coli*: a retrospective cohort study. 2021. Journal of Global Antimicrobial Resistance. 26(9): 148 – 153.
3. Sarowska J, Futoma-Koloch B, Jama-Kmiecik A, Frej-Madrzak M, Ksiazczyk M, Bugla-Ploskonska G, Choroszy-Krol I. Virulence factors, prevalence and potential transmission of extraintestinal pathogenic *Escherichia coli* isolated from different sources: recent reports. 2019. Gut Pathogen 11:10.
4. Terlizzi ME, Gribaudo G, Maffei ME. uropathogenic *Escherichia coli* (UPEC) infections: virulence factors, bladder responses, antibiotic and non-antibiotic antimicrobial strategies. 2017. Frontiers in Microbiology. 8, 1566.
5. Schwartz DJ, Kalas V, Pinkner JS, Chen SL, Spaulding CN, Dodson KW, Hultgren SJ. Positively selected FimH residues enhance virulence during urinary tract infection by altering FimH conformation. 2013. Proceedings of National Academy of Sciences United States of America. 110: 15530 – 15537.

6. Ghazvini H, Taheri K, Edalati E, Sedighi M. Virulence factors and antimicrobial resistance in uropathogenic *Escherichia coli* strains from cystitis and pyelonephritis. 2019. Turkish Journal of Medical Sciences. 49(1): 361 – 367.
7. Sivick KE, Schaller MA, Smith SN, Mobley HLT. The innate immune response to uropathogenic *Escherichia coli* involves IL-17A in a murine model of Urinary Tract Infection. 2010. The Journal of Immunology. 184 (4): 2065 – 2075.
8. Abraham SN, Miao Y. The nature of immune responses to urinary tract infections. 2015. Nature Reviews Immunology. 15(10): 655 – 663.
9. Ortega Martell JA. Immunology of urinary tract infections. 2020. GMS Infectious Diseases. 8:Doc21. <https://doi.org/10.3205/ID000065>.
10. Engelsöy U, Rangel I, Demirel I. Impact of proinflammatory cytokines on the virulence of uropathogenic *Escherichia coli*. 2019. Frontiers in Microbiology. 10:1051.
11. Ingersoll MA, Kline KA, Nielsen HV, Hultgren SJ. G-CSF induction early in uropathogenic *Escherichia coli* infection of the urinary tract modulates host immunity. 2008. Cellular Microbiology. 10(12): 2568 – 2578.
12. Melendez-Avalos A, Sainz-Espuñes T, Castrillón-Rivera L, Mendoza-Pérez F, Palma-Ramos A, Castañeda-Sánchez JI, Drago-Serrano EM. Analysis of inflammatory cytokine expression in the urinary tract of BALB/C mice infected with *Proteus* (P.) *mirabilis* and enteroaggregative *Escherichia* (E.) *coli* (EAEC) strains. 2020. Folia Microbiologica. 65(1): 133 – 142.
13. Koley S, Mukherjee M. Cytokine profile in HTB-4 cells with respect to fimH, papC and hlyA expression in uropathogenic *Escherichia coli* invasion. 2023. Future Microbiology. 18(8): 489 – 503.
14. Hannan TJ, Hunstad DA. A murine model for *Escherichia coli* urinary tract infection. 2016. Bacterial Persistence. 133: 159 – 175. Edited by: Michiels J, Fauvart M., Springer New York, Methods Molecular Biology series.
15. Hannan TJ, Mysorekar IU, Hung CS, Isaacson-Schmid ML, Hultgren SJ. Early severe inflammatory responses to uropathogenic *E. coli* predispose to chronic and recurrent urinary tract infection. 2010. PLoS Pathogen. E1001042.
16. Hung CS, Dodson KW, Hultgren SJ. A murine model of urinary tract infection. 2009. Nature Protocols. 4(8): 1230 – 1243.
17. Schroeder M, Brooks B, Brooks A. The complex relationship between virulence and antibiotic resistance. 2017. Genes. 8: 39.

18. Cepas V, Soto SM. Relationship between virulence and resistance among gram-negative bacteria. 2020. *Antibiotics*. 9: 719.
19. Tseng CC, Lin WH, Wu AB, Wang MC, Teng CH, Wu JJ. *Escherichia coli* FimH adhesins act synergistically with PapGII adhesins for enhancing establishment and maintenance of kidney infection. 2022. *Journal of Microbiology, Immunology and Infection*. 55: 44 – 50.
20. Lane MC, Mobley HLT. Role of P-fimbrial-mediated adherence in pyelonephritis and persistence of uropathogenic *Escherichia coli* (UPEC) in the mammalian kidney. 2007. *Kidney International*. 72: 19 – 25.
21. Feenstra T, Thøgersen MS, Wieser E, Peschel A, Ball MJ, Brandes R, Satchell SC, Stockner T, Aarestrup FM, Rees AJ, Kain R. Adhesion of *Escherichia coli* under flow conditions reveal potential novel effects of FimH mutations. 2017. *European Journal of Clinical Microbiology and Infectious Disease*. 36: 467 – 478.
22. Wang C, Li Q, Lv J, Sun X, Cao Y, Yu K, Miao C, Zhang ZS, Yao Z, Wang Q. Alpha-hemolysin of uropathogenic *Escherichia coli* induces GM-CSF mediated acute kidney injury. 2020. *Mucosal Immunology*. 13: 22 – 33.
23. Walters MS, Lane MC, Vigil PD, Smith SN, Walk ST, Mobley HLT. Kinetics of uropathogenic *Escherichia coli* metapopulation movement during urinary tract infection. 2012. *mBio*. E00303-11.
24. Armbruster CE, Smith SN, Mody L, Mobley HLT. Urine cytokine and chemokine levels predict urinary tract infection severity independent of uropathogen, urine bacterial burden, host genetics, and host age. 2018. *Infection and Immunity*. 86: e00327-18.
25. Chang Y, Li X, Ding L, Yang C, Pan Z, Han N, Cui Y, Zhi F, Yang R, Gao H, Bi Y. Genetic and functional differences of *Escherichia coli* strains from Colorectal cancer mucosal tissues. 2022. *Engineering*. 16: 210 – 219.
26. Chamoun MN, Sullivan MJ, Goh KGK, Acharya D, Ipe DS, Katupitiya L, Gosling D, Peters KM, Sweet MJ, Sester DP, Schembri MA, Ulett GC. Restriction of chronic *Escherichia coli* urinary tract infection depends upon T-cell derived interleukin-17, a deficiency of which predisposes to flagella-driven bacterial persistence. 2020. *The FASEB Journal*. 34: 14572 – 14587.
27. Gu YY, Liu XS, Huang XR, Yu XQ, Lan HY. Diverse role of TGF- β in kidney disease. 2020. *Frontiers in Cellular and Developmental Biology*. 8: 123.
28. Krzemień G, Szmigielska A, Turczyn A, Pańczyk-Tomaszewska M. Urine interleukin-6, interleukin-8 and transforming growth factor β 1 in infants with urinary tract infection and asymptomatic bacteriuria. 2016. *Central European Journal of Immunology*. 3: 260–267.

29. Owyang SY, Zhang M, El-Zaatari M, Eaton KA, Bishu S, Hou G, Grasberger H, Kao JH. Dendritic cell-derived TGF- β mediates the induction of mucosal regulatory T-cell response to *Helicobacter* infection essential for maintenance of immune tolerance in mice. 2020. *Helicobacter*. 25: e12763.
30. Loh K, Sivalingam N, Urinary tract infections in pregnancy. 2007. *Malaysian Family Physician*. 2: 54–57.
31. Esme M, Topeli A, Yavuz BB, Akova M. Infections in the Elderly Critically-Ill Patients. 2019. *Frontiers in Medicine*. 6: 118.

Conclusions from the study:

Urinary tract infection is one of the most frequently encountered bacterial infectious diseases observed in clinical practices, with considerable morbidity rates and high healthcare expenses for treatment. The high morbidity rates in human, along with its comorbidities such as hypertension, chronic renal failures, chronic pyelonephritis and rapidly emerging antibiotic resistance, have made UTIs an important global public health concern, especially in hospitals. UTIs related to pregnancy can carry a significant risk to the developing foetus and are often linked to early membrane rupture, low birth weight, developmental retardation, premature birth and fetal necrosis. Untreated UTIs can have catastrophic implications for non-pregnant individuals, particularly in older women. Uropathogenic *Escherichia coli* (UPEC) is responsible for most of the UTIs in both populations.

This is the first study that identified the significant prevalence of ESBL resistance genes, PAI markers (PAI IV₅₃₆, PAI III₅₃₆), MGEs (*intI1*, *intI2*, *ISEcp1*, IS5, IS26), replicon types (IncF_{repB}, IncF1B), phylogenetic groups along with Novel Phylotype properties (NPP), virulence factors with the predominance of MDR and ESBL and carbapenemase production among UPECs isolated from hospitalized pregnant and non-pregnant population. This study exhibited the fact that rapid use of newer and potent antibiotics in the last decades might have facilitated the selection of novel β -lactamase resistance and carbapenemase resistance not only in non-pregnant population, but also transmitted in pregnant population, that had further developed complications in health care management. This study for the first time attempted to introduce a new approach to determine the phylogroups in pregnant population also. This study also displayed the clonal heterogeneity and predominance of ST167 in UPEC_p and ST405 in UPEC_{np} population.

The gold standard for diagnosing UTIs in humans is urine culture. However, this laborious procedure takes a long time and often results in the empirical prescription of antibiotics, which in turn causes MDR to emerge and makes clinical UTI management more challenging. Hence, to develop an effective prescription policy, an in-depth knowledge of the infection potential of the microbe and ability to trigger a host-cytokine response is required, which cannot be solved by AMR and urine culture. To address this challenge, this study for the first time attempted and successfully established a correlation between *fimH* and immunoregulatory cytokine *IFN- γ* , *IL-17A* and *IL-1 β* in UPEC_p isolates, and in between *papC* and *hlyA* to *GCSF* and *TGF- β* in

UPECnp isolates when infected with HTB-4 uroepithelial cells at 3 hours post infection. These findings were further extended to *in-vivo* analysis for the first time in mice model with two randomly chosen clinical isolates from two populations and a correlation could be drawn between virulence potential and serum and tissue IL-1 β levels and was further reflected in the bacterial burden in the bladder and kidney tissues of the infected mice groups. Therefore, this study concludes with the suggestion of a detailed cytokine in addition to antibiotic resistance analysis in the treatment of UTI, to cease the empiric treatment and formulate a proper prescription policy for the clinicians.

Contributions from this study:

- This study would contribute greatly in the benefit of the society by playing a vital role in the field of medical science and technology. Amongst the most significant discoveries of this century are antibiotics and it often takes ten to fifteen years and costs more than US\$2 billion, before a new medication can be found on the pharmacy shelf. Unfortunately, the majority of common infections around the world are becoming more resistant to drugs due to empiric use and natural selection. One of the most common bacterial diseases in humans, UTIs affect millions of people globally. UTI, which often starts as bladder infections, progresses throughout the body and cause renal failure or systemic dissemination, depending on the type of bacteria. The most common Enterobacteriaceae family member and key etiological agent responsible for UTIs is *Escherichia coli*.
- This study provided an insight on the molecular characterization of the MDR uropathogen by displaying high occurrence of several virulence genes, MGEs, replicon types, which is the need of this area. A strong association between widespread usage of antibiotics, dissemination and emergence of antimicrobial resistance is thus indicated.
- MLST, MEGA analysis displayed a high degree of genetic heterogeneity among the pregnant and non-pregnant UPEC isolates circulating in Kolkata, an eastern region of a resource-poor country like India, which provided an insight into their evolutionary origin.
- Urine culture and AMR analysis though till date are considered as the Gold Standard to detect the UTI, but does not reflect the pathogenic potential of the microbe. This study provided an insight into the interaction between a host and a microbe both *ex-vivo* and *in-vivo*. This study found several correlations between the pathogenic potential of the microbe and the expression of several immunoregulatory cytokines in an *ex-vivo* model by utilizing HTB-4 uroepithelial cells and in an *in-vivo* model by utilizing BALB/C mice. This study establishes the need of cytokine profiling in addition to urine culture and AMR analysis to get a proper insight into the pathogenic potential of the invading microbe. The findings from cytokine analysis will help clinicians to cease empiric treatment and formulate a suitable prescription policy.

List of Publications:

A. Research and Review Articles

- Ghosh A, Bandyopadhyay D, **Koley S**, Mukherjee M. Uropathogenic *Escherichia coli* in India—an Overview on Recent Research Advancements and Trends. *Appl Biochem Biotechnol.* 2021;193(7):2267-2296. doi:[10.1007/s12010-021-03521-z](https://doi.org/10.1007/s12010-021-03521-z) (equal contribution as author).
- **Koley S**, Mukherjee M, Halder P, Bose A, Lahre D, Mukhopadhyay S, Mallik S. Clinico-microbiological Profile of Urinary Tract Infection with Special Reference to Uropathogenic *E. coli*: Antibiotic Susceptibility Pattern, Phylogenetic Background and Virulent Factor Distribution from West Bengal India. *J Indian Med Assoc.* 2022; 120(10): 48 – 53.
- **Koley S**, Bose A, Mallik S, Halder P, Mukherjee M. COVID-19 Infection and Acute Kidney Injury in Paediatric Population: A Systematic Review and Meta-Analysis. *Int J Res Rev.* 2022;9(11):7-20. doi:[10.52403/ijrr.20221102](https://doi.org/10.52403/ijrr.20221102)
- **Koley S**, Mukherjee M. Cytokine profile in HTB-4 cells with respect to *fimH*, *papC* and *hlyA* expression in uropathogenic *Escherichia coli* invasion. *Future Microbiology.* 2023;18(8):489-503. doi:[10.2217/fmb-2022-0240](https://doi.org/10.2217/fmb-2022-0240)
- **Koley S**, Bose A, Mukherjee M. Acute Kidney Injury in Adults due to COVID-19 infection: A systematic review and meta-analysis. *Journal of Survey in Fisheries Sciences.*2023;10(1S): 6421 – 6431.
- **Koley S**, Ghosh A, Mukherjee M. Occurrence of imipenem-resistant Uropathogenic *Escherichia coli* in pregnant women: An insight into their virulence profile and clonal structure. Under final review in *Current Microbiology* (Springer Nature Switzerland AG. E-ISSN: 1432-0991)
- **Koley S**, Mukherjee M. Incidence of β -lactam resistance genes and related mobile genetic elements in Uropathogenic *Escherichia coli* from pregnant women: A study from eastern region of India. (under review)
- **Koley S**, Mukherjee M. Comprehensive analysis of multiple cytokines to stratify Uropathogenic *Escherichia coli* pathogenesis in mice model of urinary tract infection. (under review).

C. Book Chapters

- **Koley S**, Mukherjee M. Genetic Basis of Biofilm Formation and Spread of Nosocomial Infections. In: Nag M, Lahiri D, eds. *Analytical Methodologies for Biofilm Research*. Springer Protocols Handbooks. Springer US; 2021:269-298. doi:[10.1007/978-1-0716-1378-8_12](https://doi.org/10.1007/978-1-0716-1378-8_12)
- **Koley S**, Bose A, Mukherjee M. Quorum Sensing in Gram-Negative Bacteria. In: *Natural Products*. 1st ed. CRC Press; 2023:25-61. doi:[10.1201/9781003300557-3](https://doi.org/10.1201/9781003300557-3) (would be published on December 1, 2023)

Seminars and Workshops presented/attended:

Seminars:

- **Oral presentation** at the **International Conference (6th India Biodiversity Meet, 2019)**, held at Agricultural and Ecological Research Unit, Indian Statistical Institute, Kolkata. **Koley S** and Mukherjee M. (2019). Prophages: An Alternative Therapy for Recurrent Urinary Tract Infection.
- **Oral Presentation** at the **International Conference on Biotechnology and Biological Sciences (Biospectrum 2020)** held at the Department of Biotechnology, University of Engineering and Management, Kolkata, in association with Indian Ecological Society; Microbiologist society, India; Smart Society, USA. **Koley S**, Ghosh A, Bandyopadhyay D, Mukherjee M (2020). Uropathogenic *Escherichia coli* in India – an Overview on Recent Research Advancement and Trends.
- **Oral presentation** at the **International Conference on Technological Innovations in Agriculture, Life Sciences, and Food & Nutrition – ICALF 2023** held at Swami Vivekananda University (SVU) Barrackpore campus. Koley S, Bose A, Mukherjee M (2023). Acute Kidney Injury in Adults due to COVID-19 infection: A systematic review and meta-analysis.
- Participated in **CME7 on Tropical and Infectious Diseases** organized by **Society of Tropical Medicine and Infectious Diseases in India**, held on 11th June, 2017.
- Participated in **CME9 on Tropical and Infectious Diseases** organized by **Society of Tropical Medicine and Infectious Diseases in India**, held on 18th August, 2019.

Workshop:

- Participated in the “**Workshop and hands on training on Biomedical Techniques**” organized by **Department of Biochemistry and Medical Biotechnology, School of Tropical Medicine, Kolkata** from 13th to 15th February, 2017.



Uropathogenic *Escherichia coli* in India—an Overview on Recent Research Advancements and Trends

Arunita Ghosh¹ · Debojyoty Bandyopadhyay¹ · Snehashis Koley¹ ·
Mandira Mukherjee¹

Received: 28 October 2020 / Accepted: 27 January 2021 / Published online: 17 February 2021
© The Author(s), under exclusive licence to Springer Science+Business Media, LLC part of Springer Nature 2021

Abstract

Urinary tract infection (UTI), a prevalent disease in India, also ranks among the most common infections in developing countries. The rapid emergence of antibiotic-resistant uropathogenic *Escherichia coli* (UPECs), the leading etiologic agent of UTI, in the last few years, led to an upsurge in the health care cost. This caused a considerable economic burden, especially in low-middle income country, India. This review aimed to provide an explicit overview of the recent advancements in *E. coli*-mediated UTI in India by incorporation of valuable information from the works published in PubMed and Google Scholar in the last six years (2015 to August, 2020). The literature survey demonstrated UPECs as the most predominant uropathogen in India, especially among females, causing both asymptomatic bacteriuria (ABU) and symptomatic UTI. An overall increasing national trend in resistance to penicillins, cephalosporins, aminoglycosides, fluoroquinolones, and sulfonamides was perceived irrespective of ABU and symptomatic UPECs during the aforementioned study period. High incidences of multidrug resistance, extended-spectrum β -lactamases, metallo β -lactamases, and AmpCs in UPECs were reported. Notable information on the pathogenic profiles, phylogroups, pathogenicity islands, and evidence of pathoadaptive FimH mutations was described. Alternative therapeutics and potential drug targets against UPECs were also reconnoitered. Therefore, the nationwide widespread occurrences of highly virulent MDR UPEC together with the limited availability of therapeutics highlighted the urgent need for promotion and invention of alternative therapeutics, search for which had already been started. Moreover, investigation of several mechanisms of UPEC infection and the search for potential drug targets might help to design newer therapeutics.

Keywords Uropathogenic *Escherichia coli* · Urinary tract infection, multidrug resistance · Alternative therapeutics · India

Arunita Ghosh, Debojyoty Bandyopadhyay, and Snehashis Koley contributed equally to this review.

✉ Mandira Mukherjee
mandira_71@yahoo.com

Extended author information available on the last page of the article

Introduction

Escherichia coli (*E. coli*) was the most common cause of all forms of urinary tract infections (UTIs) that included symptomatic infections as well as asymptomatic bacteriuria (ABU), over the last few years in India [1–4]. UTIs, caused by uropathogenic *E. coli* (UPECs), although more prevalent in women mainly due to their anatomy (shorter urethra), were found to be a significant cause of hospital visits for people of all ages and both genders [3, 5].

Multidrug-resistant variants of UPECs with either inherited or transmissible resistance were on the rise for the last few years in India [4, 6, 7]. Moreover, infections caused by the aforementioned resistant UPEC strains were the leading cause of mortality in India as well as in the rest of the world [8–12]. India had witnessed a dramatic increase in resistance to several groups of antibiotics like penicillins, cephalosporins, aminoglycosides, quinolones/fluoroquinolones, and sulphonamides in the last decade [2, 3, 9, 13]. However, the patterns of antibiotic resistance with respect to one or more antibiotics of the same or different groups showed considerable intra [2, 14–16] and inter-regional difference [1–3, 17].

Incidence of extended-spectrum β -lactamase (ESBL) [4, 6, 7, 17–19], metallo β -lactamase (MBL) [4, 20], and AmpC producers [4] among MDR UPECs had also been on the rise in the last few years. The increasing trend of MBL and AmpC producers among MDR variants of UPECs in a resource-poor country India was highly alarming as, in addition to other groups of antibiotics, MBL and AmpC producers were also found to be resistant to carbapenems and/or β -lactamase inhibitors, unlike the ESBL producers. Thus, infections caused by these MDR UPECs are increasingly becoming very difficult to treat and this might lead to a therapeutic dead-end in the future. Earlier reports [9, 14] stated that several factors are responsible for the dissemination of antimicrobial resistance genes in UPECs and among them, the plasmid-mediated transfer is the most important mechanism for the horizontal transfer of multidrug resistance.

Several studies conducted in the recent past suggested that colonization of UPECs in the human urinary bladder for the establishment of UTI is mediated by the usage of several virulence factors like adhesins (type 1 fimbriae, P fimbriae, and S fimbriae), flagellin, lipopolysaccharides, and secreted virulence factors (α -hemolysin, cytotoxic necrotizing factor, secreted auto-transporter toxin) [2, 7, 11, 12]. Moreover, Miryala et al. [19] and Rubini et al. [11] stated that the type I pili adhesion is an important event in the pathogenesis of UPECs that also helps in biofilm formation which is considered a universal and the most effectual strategy adopted by UPECs for survival [7]. Likewise, earlier reports [1, 21–24] also advocated the fact that biofilm production in UPECs promotes bladder colonization, thereby leading to an increase in the rate of UTIs, and such infections might be difficult to treat as they display MDR. Furthermore, earlier studies also characterized asymptomatic [2, 25] and symptomatic [2] UPECs, with their phylogenetic background and distribution of pathogenicity islands (PAIs).

India saw the emergence of MDR UPEC strains, an increase in ESBL-, MBL-, and AmpC-producing UPEC strains and a high incidence of UPEC biofilm formers in the last few years. This shifted the attention of clinicians and researchers to several alternative therapeutic options [3, 10, 11, 21, 24, 26–28], which might help to cope with the upcoming therapeutic limitations and combat the spread of MDR UPECs. Therefore, this review aimed to provide an overview of recent advancements in UPEC-mediated UTI, in a resource-poor country like India.

Evidence Acquisition and Synthesis

An extensive literature hunt was performed using the electronic databases, PubMed and Google Scholar from 2015 to 2020 (last 6 years), using the following keywords: uropathogenic *Escherichia coli* and India in association with urinary tract infections in humans, multidrug resistance, pathogenicity, and therapeutics. Database search for articles of the year 2020 was restricted until the month of August. Articles written in English were considered in this review. Preprints were not considered in this review. Statistical significance of the data collected was analyzed using Prism software package (GraphPad Prism version 9) [29] and also further validated using SPSS version 21.0 (SPSS Inc., Chicago, IL, USA) [2, 30]. The correlation coefficient [29, 30] was determined to find the degree of association between different states (variables) of India with respect to the incidence of urine culture–positive symptomatic *E. coli* and their resistance against different antibiotics. Heat maps were constructed from the correlation matrices using the GraphPad Prism version 9 (GraphPad Software, La Jolla California USA) [29]. However, correlation coefficient values < 0.2 were found to be statistically insignificant according to SPSS version 21.0 software package. Moreover, values < 0.2 are considered a negligible or poor correlation [31]. Therefore, correlation coefficient values < 0.2 were not considered when ascertaining the highest and lowest correlations.

Incidence of *Escherichia coli* in Urine Culture–Positive Samples Isolated from Individuals with Symptomatic UTI or ABU

Escherichia coli (*E. coli*) is one of the most prevalent pathogen liable for more than 80% of all urinary tract infections (UTIs) and can cause both asymptomatic bacteriuria (ABU) and symptomatic UTI [2]. Results from the literature search also revealed that *E. coli* was one of the predominant uropathogen of this era responsible for symptomatic UTI in people residing in different states of India (Table 1).

Moreover, a statistically significant positive correlation that ranged from low to very high with p values ≤ 0.05 was observed in the incidence of urine culture–positive symptomatic *E. coli* among 14 different states during the time period (2015–2020). Two different Indian states and/or union territories between which the highest correlation with respect to the incidence of symptomatic UPECs was observed were Bihar (2015) [BH' 15]; Kerala (2017) [KL' 17], Andhra Pradesh (2016) [AP' 16]; Tamil Nadu (2019—1st) [TN' 19 (1)], Madhya Pradesh (2017) [MP' 17]; West Bengal (2018—1st) [WB' 18 (1)], Delhi (2017) [DL' 17]; Tamil Nadu (2019—2nd) [TN' 19 (2)], Kerala (2018) [KL' 18]; West Bengal (2019—3rd) [WB' 19 (3)], Maharashtra (2019) [MH' 19]; Chandigarh (2019) [CG' 19], West Bengal (2019—2nd) [WB' 19 (2)]; Telangana (2020) [TL' 20], Uttar Pradesh (2019) [UP' 19]; Delhi (2019) [DL' 19], Himachal Pradesh (2019) [HP' 19]; Delhi (2017) [DL' 17] and Tamil Nadu (2019—2nd); and Bihar (2015) respectively. Furthermore, three different Indian states and/or union territories among which the highest correlation was observed were Odisha (2016) [OD' 16]; Uttar Pradesh (2019) [UP' 19]; Delhi (2019) [DL' 19], West Bengal (2016) [WB' 16]; Kerala (2018) [KL' 18]; West Bengal (2019—3rd) [WB' 19 (3)], Kerala (2017) [KL' 17]; Bihar (2015) [BH' 15]; West Bengal (2018—1st) WB' 18 (1)], West Bengal (2018—1st) [WB' 18 (1)]; Madhya Pradesh (2017) [MP' 17], West Bengal (2018—2nd) [WB' 18 (2)]; West Bengal (2019—2nd) [WB' 19 (2)]; Telangana (2020) [TL' 20], Haryana (2018) [HR' 18]; Maharashtra (2019) [MH' 19]; Chandigarh (2019) [CG' 19] and West Bengal (2019—1st) [WB' 19 (1)];

Table 1 Incidence of *Escherichia coli* in urine culture–positive isolates obtained from urinary tract infected patients from different Indian states during the years 2015–2020

Sl. no.	<i>E. coli</i> (%)	Union territory/state of report	Reference
1	50	Bihar	[32]
2	26.3	Andhra Pradesh	[37]
3	21.37	Odisha	[36]
4	39.9	West Bengal	[13]
5	45.4	Manipur	[34]
6	48.9	Kerala	[35]
7	56.22	New Delhi	[44]
8	67.5	West Bengal	[42]
9	46.15	West Bengal	[52]
10	37.45	Kerala	[45]
11	76.60	Haryana	[43]
12	32.26	West Bengal	[2]
13	75	Maharashtra	[3]
14	70.1	West Bengal	[14]
15	22.01	Uttar Pradesh	[41]
16	74.95	Chandigarh	[8]
17	21.5	New Delhi	[48]
18	25.93	Tamil Nadu	[15]
19	59.8	Himachal Pradesh	[19]
20	38	West Bengal	[9]
21	54.29	Tamil Nadu	[16]
22	69.9	Telangana	[17]

Kerala (2018) [KL' 18]; and West Bengal (2019—3rd) [WB' 19 (3)] respectively. However, 10 (Bihar (2015) [BH' 15], Delhi (2017) [DL' 17], West Bengal (2018—2nd) [WB' 18 (2)], Haryana (2018) [HR' 18], Maharashtra (2019) [MH' 19], West Bengal (2019—2nd) [WB' 19(2)], Chandigarh (2019) [CG' 19], Himachal Pradesh (2019) [HP' 19], Tamil Nadu (2019—2nd) [TN' 19 (2)], and Telangana (2020) [TL' 20]) and 12 (Andhra Pradesh (2016) [AP' 16], Odisha (2016) [OD' 16], West Bengal (2016) [WB' 16], Madhya Pradesh (2017) [MH' 17], Kerala (2017) [KL' 17], West Bengal (2018—1st) [WB' 18 (1)], Kerala (2018) [KL' 18], West Bengal (2019—1st) [WB' 19 (1)], Uttar Pradesh (2019) [UP' 19], Delhi (2019) [DL' 19], Tamil Nadu (2019—1st) [TN' 19 (1)], and West Bengal (2019—3rd) [WB' 19 (3)]) different states and/or union territories were found to show their lowest correlation with Odisha (2016) [OD' 16] and Haryana (2018) [HR' 18] respectively (Fig. 1).

Furthermore, a remarkable incidence of *E. coli* was also reported in urine culture–positive samples isolated from the asymptomatic individuals besides the symptomatic ones [2, 25]

Age-Sex Parameter in Relation to UPECs

Reports from several Indian states like Haryana, Bihar, Jharkhand, West Bengal, Kerala, Tamil Nadu [2, 7, 15, 16, 20, 23, 32], and Karnataka [1] indicated a higher prevalence of female and male respectively among patients affected with *E. coli*–mediated symptomatic UTI. However, a study [2] from West Bengal conducted on asymptomatic UPECs proclaimed equal incidence of male and female individuals.

Moreover, Mittal et al. [22] and Karigoudar et al. [1] revealed that the maximum age group affected by symptomatic UPECs among both male and female patients was 21–30 years. However, Ghosh et al. [2] indicated the mean age as 48.2 years (range 7–82 years) among the

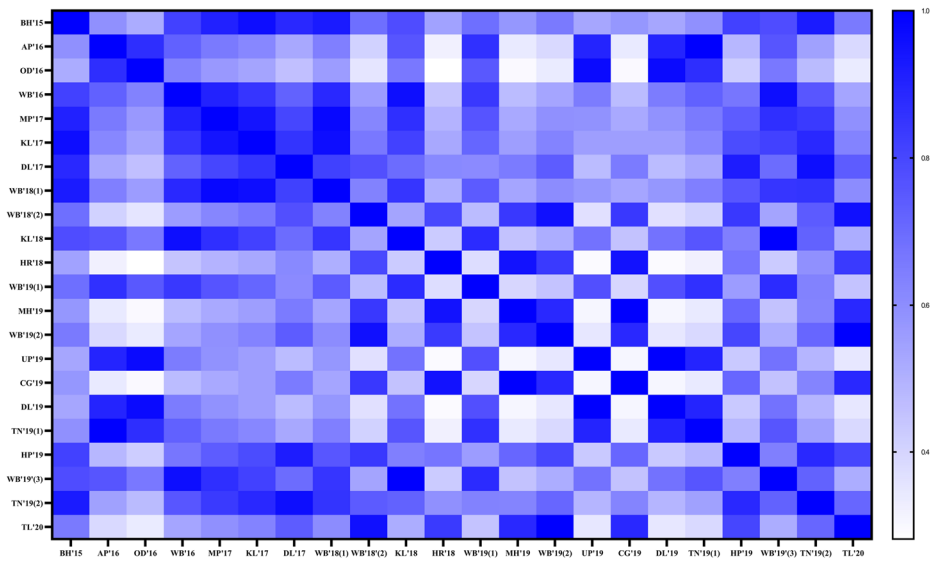


Fig. 1 Statistical significance of the incidence of symptomatic UPEC in the different Indian states was analyzed by GraphPad Prism version 9 (Prism software package). Heat maps were generated on the correlation coefficient values represented by the color keys that ranged from zero (white) to 1 (deep blue)

hospitalized individuals affected by symptomatic UPECs. Nonetheless, a study [32] found the mean age of their population as 33.1 years, though the mean age of the male and female population was 43.3 and 31.1 years respectively. Nevertheless, another study [15] conducted on symptomatic UPECs reported a higher prevalence of females and males in the age group 21–30 and 31–40 years respectively. Withal, Muraleetharan et al. [16] showed a higher prevalence of symptomatic UPECs above 35 years of age among both the affected males and females. Furthermore, studies by Mukherjee et al. [25] and Ghosh et al. [2] from West Bengal showed the mean age as 25.14 years (18–38 years) and 44.8 (22–82 years) respectively among individuals with ABU *E. coli*.

UPECs in Pregnant Females

A study from West Bengal [25] reported a remarkable incidence of *E. coli* in urine culture-positive samples isolated from the asymptomatic pregnant females

UPECs' Drug Resistance Pattern Nationwide

Antibiotic resistance in UPECs and the dissemination of the MDR UPECs is presently a global public health problem [5]. Moreover, the increasing frequency of MDR UPECs, especially in a developing country like India in the last few years, resulted in the increase in the cost of treatment and hospitalization. The literature search indicated resistance of UPECs to different groups of antibiotics.

Resistance to β -Lactam Antibiotics

At present, resistance of symptomatic UPECs to penicillin, aminopenicillin, and **antipseudomonal penicillin** groups of antibiotics is immensely high, especially to aminopenicillins (ampicillin and amoxicillin) and **antipseudomonal penicillin like** carbenicillin [1, 3, 15, 23, 24, 33–35]. Moreover, a study by Pullanhi et al. [7], during a period of 1 year, indicated a very high level of resistance of UPECs to aminopenicillin (amoxicillin) and **antipseudomonal penicillin** (piperacillin), even when used in combination with clavulanic acid (β -lactam inhibitors).

Moreover, literature search revealed that resistance to cephalosporins, especially to first and third generations, was moderate to [33, 36] extremely high among symptomatic UPECs [1, 2, 4, 9, 13, 16, 37–40]. Furthermore, studies by Mukherjee et al. [25] and Ghosh et al. [2] reported moderate and extremely high resistance, respectively, of asymptomatic UPECs to third-generation cephalosporins. However, Kammili et al. [17] and Vasudevan et al. [24] reported moderate resistance to second- and third-generation cephalosporins (cefuroxime and cefotaxime). A study [6] showed a significant increase in cephalosporin resistance of symptomatic UPECs from 51 to 58% over a period of 5 years (2013–2017). High resistance of symptomatic UPECs to cephalosporins was observed even when used in combination with β -lactam inhibitors [1, 23].

Presently, resistance of both asymptomatic [2, 25] and symptomatic UPECs [1–4, 7, 16, 33, 34, 39–41] to carbapenems (imipenem and/or meropenem) is quite low. Moreover, Kammili et al. [17] stated that none of the UPECs tested were resistant to meropenem. However, other studies [23, 42] showed much higher resistance against imipenem and meropenem in their population. Withal, a report by Prasada et al. [6] revealed an increasing trend in carbapenem resistance in symptomatic UPECs from 0 to 5.9% over a period of 5 years (2013–2017).

UPECs as ESBL Producers

β -Lactam antibiotics are one of the most commonly used antibiotics for the treatment of *E. coli*-mediated UTI. *E. coli* has developed a particular resistance mechanism for inactivation of the β -lactam groups of antibiotics by the production of ESBL enzymes. ESBL-producing *E. coli* have been known to be capable of hydrolyzing all penicillins, cephalosporins (first to third generations), mainly oxyimino cephalosporins, and monobactams. However, ESBLs are inhibited by β -lactamase inhibitors such as tazobactam, sulbactam, and clavulanic acid. However, over the past 6 years, low [37], moderate [6, 7, 19], and high incidence [4, 17, 43] of ESBL producers among the symptomatic UPECs was found from Andhra Pradesh; Karnataka, Kerala, and Himachal Pradesh; and Pondicherry and Telangana respectively. Moreover, a report by Prasada et al. [6] from Karnataka indicated an increase in the rate of ESBL production from 45.2 to 59.6% during the years 2013–2017.

Resistance to β -Lactam- β -Lactamase Inhibitors

Low to a high level of resistance to β -lactamase inhibitors like tazobactam, sulbactam, and clavulanic acid was observed among symptomatic UPECs [1, 6, 23, 34, 40]. Diversity in symptomatic UPECs' response to two different β -lactamase inhibitors was reported by

Karigoudar et al. [1] that showed very high and moderately low resistance against clavulanic acid and sulbactam respectively when used in combination with amoxicillin and piperacillin. However, Kammili et al. [17] reported similitude in UPECs' response to different β -lactamase inhibitors. The aforementioned study showed an extremely low level of resistance to both the β -lactamase inhibitors: clavulanic acid and tazobactam when used in combination with amoxicillin and piperacillin respectively. Moreover, Prasada et al. [6] specified an increasing (9.4 to 23%) trend in resistance to β -lactamase inhibitors over the 5 years duration. Furthermore, the same study revealed an overall increase (5.6 to 9.04%) and a decrease (33 to 31%) in resistance to sulbactam when used in combination with cefoperazone and ampicillin respectively over the aforementioned period; however, the trends were inconsistent.

UPECs as MBL Producers

MBL-producing *E. coli* are known to hydrolyze a broad range of β -lactam antibiotics that includes penicillins, cephalosporins, carbapenems, cephamycins, and even certain β -lactamase inhibitors (clavulanate, tazobactam, and sulbactam). However, they are found to be sensitive to aztreonam (monobactam). Over the last 6 years, low incidence of MBL producers was observed among symptomatic MDR UPECs in Haryana and Pondicherry [4, 20].

UPECs as AmpC Producers

E. coli AmpC producers are known to be capable of hydrolyzing penicillins, broad and extended-spectrum cephalosporins (first to third-generation), cephamycins, and β -lactamase inhibitors, but are found to be sensitive to fourth-generation cephalosporins and carbapenems. Moderate incidence of AmpC producers among symptomatic MDR UPECs has been reported in four (Haryana, West Bengal, Jharkhand, Pondicherry) different states or union territories of India, over the last 6 years [2, 4, 20, 23].

Co-production of ESBL, MBL, and AmpC in UPECs

Low to very high incidence of AmpC and ESBL co-production was observed in two different studies conducted in two different states (Haryana, West Bengal) [13, 20]. Moreover, a study Gopichand et al. [4] performed on samples collected over a period of 1 year (2016–2017) from Pondicherry revealed the incidence of co-production of ESBL, MBL, or AmpC among MDR UPECs.

Resistance to Other Cell Wall Synthesis Inhibitors

A high level of resistance to different cell wall inhibitors like fosfomycin, vancomycin, and bacitracin was observed among symptomatic UPECs [8, 15]. Moreover, Kaza et al. [8] revealed the prevalence of polymyxin like colistin (an antibiotic regarded as the last resort for MDR gram-negative bacteria) resistance (3.52%) among MDR UPECs. However, Singh et al. [23] found 100% sensitivity against colistin. Nonetheless, [4, 22] reported the incidence

of 100% fosfomycin sensitivity among highly MDR (UPECs), which included ESBL, carbapenemase, and/or AmpC producers.

Resistance to Aminoglycosides and Tetracyclines

Varied pattern of resistance of symptomatic UPECs to different aminoglycosides was observed since the last 6 years. Several studies reported a very low level of resistance to aminoglycosides: amikacin, kanamycin tobramycin, or streptomycin [7, 15–17, 24, 32–34, 44]. Moderate to a moderately high level of resistance of symptomatic UPECs against amikacin, gentamicin, kanamycin, or neomycin was also reported by various other studies [1–3, 13, 36–38, 45]. However, Gopichand et al. [4] indicated a low and very high level of resistance to two (amikacin and gentamicin respectively) different antibiotics of the aminoglycoside class. A report by Prasada et al. [6] indicated a decreasing (8.8 to 6.5%) trend in resistance to aminoglycoside netilmicin from 2013 to 2017. However, the same study reported an overall increase in gentamicin resistance from 31 to 34% over a period of 5 years. Studies conducted [2, 25] on asymptomatic UPECs reported low and moderate to moderately high level of resistance, respectively, to different antibiotics of the aminoglycoside group.

Kaza et al. [8] proclaimed susceptibility of UPECs towards tetracycline. However, a study by Gnanasekaran et al. [15] revealed an extremely high level of resistance of UPECs to tetracyclines.

Resistance to Macrolides and Chloramphenicol

A high level of resistance to macrolide (erythromycin) was reported in the recent past [15]. However, another study [3] indicated a low level of resistance to chloramphenicol.

Resistance to Quinolones/Fluoroquinolones

Resistance to first-generation quinolones/fluoroquinolones had been very high for the last few years among symptomatic UPECs [1, 15, 17, 24, 37, 41] except a study by Muraleetharan et al. [16] that reported moderate resistance against nalidixic acid, a first-generation quinolone. However, the resistance of asymptomatic [2, 25] and symptomatic [1, 2, 4, 13, 15, 23, 24, 32–34, 37, 38, 40, 41] UPECs to second-generation fluoroquinolones, i.e., ciprofloxacin, levofloxacin, and norfloxacin, was found to be very high for the last 6 years. Though a study by Wabale et al. [33] found a very low level of resistance against ciprofloxacin in their population, another report [6] stated a statistically significant rise (48 to 64%) in resistance to second-generation fluoroquinolone, i.e., norfloxacin, over a period of 5 years (2013–2017).

Resistance to Sulfonamides

Varied level of resistance of asymptomatic and symptomatic UPECs to sulfonamides like trimethoprim, cotrimoxazole, and trimethoprim/sulfamethoxazole had been observed for the last 6 years. Several studies reported low [24], moderate [1, 17, 36, 37], and high incidence [2,

3, 8, 13, 15, 23, 25, 32, 33, 38] of sulfonamide-resistant symptomatic UPECs. Moreover, Ghosh et al. [2] also reported a high incidence of sulfonamide-resistant asymptomatic UPECs. Furthermore, two studies [6, 44] reported a rising trend (35.5 to 63.3% and 52 to 59%) in resistance to cotrimoxazole during the time period of 2009–2014 and 2013–2017 respectively.

Resistance to Nitrofurans

Resistance to nitrofurans group of drugs like nitrofurantoin (synthetic drug) was found to be very low since 2015 among both asymptomatic [2, 25] and symptomatic [1, 2, 4, 7, 13, 17, 32, 37, 41] UPECs, except a study by Wabale et al. [33] that reported incidence of moderate nitrofurantoin resistance in symptomatic UPECs. Another study [15] reported 100% sensitivity of the tested symptomatic UPECs. However, Prasada et al. (2019) [6] reported an overall rise (12.8 to 13.3%) in resistance to nitrofurantoin from 2013 to 2017.

Multidrug Resistance in UPECs

Low [7, 8, 32], moderate [17, 33, 36], and very high [2, 16, 22–24, 41] levels of MDR were observed among the symptomatic UPECs from various union territories or states of India like Chandigarh, Kerala, Telangana, West Bengal, and Tamil Nadu respectively. Moreover, moderate [25] and extremely high [2] levels of MDR among asymptomatic UPECs were reported especially from Kolkata, West Bengal.

Trends in UPECs' Antibiotic Resistance Nationwide

India was broadly divided into six zones mainly North, South, East, West, Central, and Northeast zone. Antibiotic resistance trends of asymptomatic and symptomatic UPECs over the last 6 years in different regions/states of India were illustrated in Fig. 2a and b respectively.

A rise in resistance of asymptomatic UPECs to third-generation cephalosporins (cefotaxime and ceftazidime), aminoglycoside (amikacin), second-generation fluoroquinolone (ciprofloxacin), and sulfonamide (cotrimoxazole) in two reports from the eastern state, West Bengal, after a period of 4 years was observed. Moreover, both studies indicated a high level of resistance against cotrimoxazole (sulfonamide) and least resistance against amikacin (aminoglycoside) and nitrofurantoin (nitrofuran) respectively (Fig. 2a). However, during the present study period (2015–2020), there were no data on the resistance pattern of the asymptomatic *E. coli* collected from urine culture-positive isolates from the other parts of the Indian sub-continent.

Current trends in resistance to different groups of antibiotics among symptomatic UPEC were quite similar to their asymptomatic counterparts. Reports from different states of Northern, North Eastern, Eastern, and/or Southern India showed moderately high to very high level of aminopenicillin (ampicillin, amoxicillin) resistance over the last 6 years (2015–2020). One hundred percent resistance against ampicillin was reported from Tamil Nadu (Southern India) consecutively in 2019 and 2020. Moreover, very recently, two different states of southern India, i.e., Kerala and Tamil Nadu, reported a very high (80% and 100%) incidence of resistance respectively against piperacillin and carbenicillin of the antipseudomonal class (Fig. 2b).

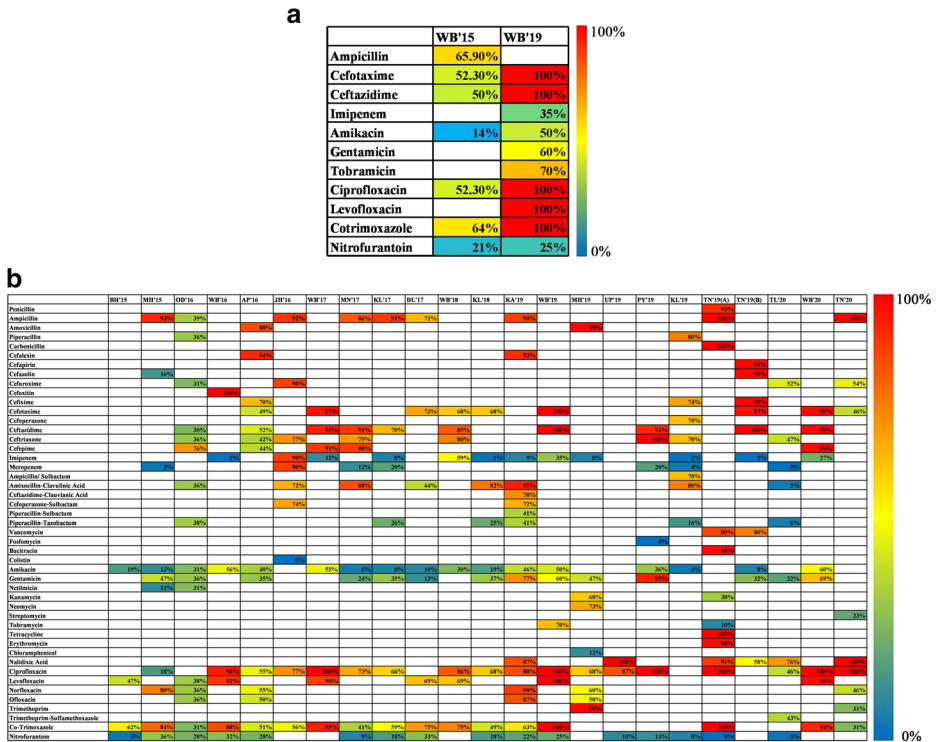


Fig. 2 Reports on percentage of resistance among **a** asymptomatic *E. coli* obtained from urine culture-positive isolates to different antibiotics in West Bengal in 2015 (WB'15), and in 2019 (WB'19), and **b** percentage of resistance among symptomatic uropathogenic *E. coli* to different antibiotics in various Indian states during the years 2015–2020 respectively. Color key represents the variation in colors from red to blue illustrating the percentage of resistance from 100 to zero

Furthermore, late reports from southern India (Karnataka and Tamil Nadu) showed very high (93 to 99%) first-generation cephalosporin resistance especially against cefalexin, cefazolin, and cefapirin with the highest being from Tamil Nadu, but moderate cefuroxime (second generation of cephalosporin) resistance from states of Telangana and Tamil Nadu. However, two reports from two different (Odisha and Jharkhand) states of eastern India in 2016 reported completely different (lowest and highest respectively) levels of cefuroxime resistance. Ninety-three percent cefoxitin resistance was reported only from West Bengal (2016). Resistance to third-generation cephalosporins, especially cefixime, cefotaxime, ceftazidime, and ceftriaxone, was reported to be from low to moderate ranges in the north-eastern, eastern, and southern regions of India between the years 2015–2016. However, a rising trend in third-generation cephalosporins (cefixime, cefotaxime, cefoperazone, ceftazidime, and ceftriaxone) resistance was noticed from the year 2017 to 2020 in almost all regions of India which included the states of West Bengal, Manipur, Delhi, Pondicherry, Kerala, Karnataka, and Tamil Nadu. Nonetheless, lately, Telangana and Tamil Nadu, parts of southern India, reported moderate resistance against ceftriaxone and cefotaxime (third-generation cephalosporins) respectively. One hundred percent resistance against cefotaxime and ceftazidime (third-generation cephalosporins) was reported from West Bengal and Tamil

Nadu in 2019. Cefepime (fourth-generation cephalosporin) resistance was found to be quite high (76 to 98.70%) over the last 5 (2016–2020) years in different states of India, except a report from Andhra Pradesh (2016) that stated moderately low (44%) incidence of cefepime resistance. However, the highest resistance was reported recently from West Bengal (Fig. 2b).

Presently, in carbapenem (meropenem and imipenem) resistance in symptomatic UPECs in different regions (northern, eastern, western, southern) of India, although found to be low, a rising trend from 2016 to 2019 could be noticed especially from the eastern state of India, West Bengal. However, moderately high and exceptionally high level of resistance to carbapenem (meropenem and/or imipenem) was reported from eastern Indian state West Bengal (2018) and Jharkhand (2016) respectively. Lately, a report from Telangana, a south Indian state, proclaimed 0% resistance against meropenem (Fig. 2b).

Resistance to one or more of the β -lactam- β -lactamase inhibitor combinations like ampicillin/sulbactam, amoxicillin/clavulanic acid, ceftazidime/clavulanic acid, and cefoperazone/sulbactam was reported to be high or very high in various Indian states like Jharkhand, Manipur, Kerala, and Karnataka that belonged to eastern, north-eastern, and southern parts of India. Moreover, the highest resistance to three β -lactam- β -lactamase inhibitor combinations amoxicillin/clavulanic acid, ceftazidime/clavulanic acid, and cefoperazone/sulbactam was reported from Manipur, 2017, and Karnataka in 2019. However, resistance against piperacillin/tazobactam was consistently reported to be quite low especially during the years 2016–2020, in Odisha, Kerala, Karnataka, and Telangana but the least resistance to β -lactam- β -lactamase inhibitor combination (amoxicillin/clavulanic acid) was reported in the recent past from Telangana. Moreover, the national trend in resistance to β -lactamase inhibitors when used in combination with penicillins or cephalosporins over the last 6 years was found to be inconsistent (Fig. 2b).

High resistance against vancomycin and bacitracin (cell wall inhibitors other than β -lactam) was reported from the south Indian state of Tamil Nadu lately. However, reports from an Eastern (Jharkhand) and Southern part (Pondicherry) of India stated 100% sensitivity to cell wall inhibitors colistin and fosfomycin respectively (Fig. 2b).

Resistance to one or more of the several antibiotics of aminoglycoside group like amikacin, gentamicin, neomycin, netilmicin, kanamycin, tobramycin, and streptomycin was found to range from low to very high over the last 6 years. The trend in amikacin resistance was found to be low to moderate in various regions of India that included states and union territories like Bihar, West Bengal, Maharashtra, Odisha, Andhra Pradesh, Manipur, Kerala, Delhi, Karnataka, Pondicherry, Telangana, and Tamil Nadu. However, recently, very low (4%) amikacin resistance was reported from the south Indian state of Kerala, which was in contrary to the report from the eastern Indian state of West Bengal that reported moderately high (60.25%) resistance of symptomatic UPECs against amikacin. An almost similar pattern of resistance against gentamicin was observed from most of the aforementioned states of India, but of late, a report from Pondicherry showed extremely high resistance against gentamicin. Resistance to one/more aminoglycoside (amikacin, gentamicin, kanamycin, tobramycin, streptomycin) class of antibiotics was reported to be low in the south Indian states of Kerala, Tamil Nadu, and Telangana (Fig. 2b).

An extremely high level of resistance of symptomatic UPECs to tetracycline and erythromycin (macrolide) was reported from the south Indian state of Tamil Nadu. However, a report from the western region of India (Maharashtra) indicated immensely low chloramphenicol resistance (Fig. 2b).

Resistance against nalidixic acid (first-generation quinolones) was very high except for a report from Tamil Nadu (southern India) that reported moderate nalidixic resistance lately. One hundred percent resistance against nalidixic acid was reported from the north Indian state of Uttar Pradesh and the south Indian state of Tamil Nadu (Fig. 2b).

Reports from the eastern, northern, and southern regions of India covering states like West Bengal, Karnataka, Uttar Pradesh, and Pondicherry stated very high resistance to second-generation fluoroquinolones, especially against ciprofloxacin and levofloxacin, over the last 5 years (2016–2020). However, moderate ciprofloxacin resistance was reported from Telangana (Southern region of India). However, reports from most of the aforesaid Indian states showed comparatively lower resistance to two other second-generation fluoroquinolones (norfloxacin or ofloxacin) (Fig. 2b).

Resistance against cotrimoxazole (sulfonamide) was found to have an increasing trend from 2015 to 2020; however, the trend was inconsistent. One hundred percent resistance against cotrimoxazole was reported recently from the eastern Indian state of West Bengal and the south Indian state of Tamil Nadu. However, surprisingly, another recent report from Tamil Nadu stated a low incidence of cotrimoxazole resistance among symptomatic UPECs (Fig. 2b).

Resistance against nitrofurantoin (nitrofurane) was found to be very low in almost all parts of India. However, in the recent past, a report from Tamil Nadu (South India) proclaimed 0% resistance against nitrofurantoin. Notably, recent reports especially those published in and after 2019 showed a decrease in nitrofurantoin resistance (Fig. 2b).

Moreover, a statistically significant positive correlation that ranged from low to very high with p values ≤ 0.05 was observed in the incidence of resistance of symptomatic UPECs against 20 (ampicillin, cefuroxime, cefixime, cefotaxime, ceftazidime, ceftriaxone, cefepime, imipenem, meropenem, amoxicillin-clavulanic acid, piperacillin-tazobactam, amikacin, gentamicin, nalidixic acid, ciprofloxacin, levofloxacin, norfloxacin, ofloxacin, co-trimoxazole, nitrofurantoin) different antibiotics over a period of 5 (2015–2020) years. However, the highest and the lowest correlation with respect to resistance against ampicillin was observed between the states of Jharkhand (2016), Manipur (2017) and Maharashtra (2015), and Odisha (2016) respectively (Fig. 3a). Furthermore, in case of resistance against second-generation cefuroxime, the highest correlation was observed between Telangana (2020) and Tamil Nadu (2020) and the lowest between Odisha (2016) and Jharkhand (2016) respectively (Fig. 3b). However, a statistically significant (p values ≤ 0.05) positive correlation with a correlation coefficient of 0.91 was perceived in the incidence of resistance against cefixime (third-generation cephalosporin) only between Andhra Pradesh (2016) and Kerala (2019) (Fig. 3c). Nevertheless, West Bengal (2017), Tamil Nadu (2019—second) and West Bengal (2018), and Kerala (2018) showed the strongest correlation with respect to the resistance against cefotaxime, another third-generation cephalosporin. Moreover, West Bengal (2017), West Bengal (2018), Kerala (2018), and Tamil Nadu (2019—second) was found to have the weakest correlation with West Bengal (2018), Kerala (2018) and West Bengal (2017), Tamil Nadu (2019—second) and West Bengal (2017), Tamil Nadu (2019—second) and West Bengal (2018), and Kerala (2018) respectively (Fig. 3d). However, with respect to another third-generation cephalosporin, ceftazidime, the highest and lowest correlation was perceived between Manipur (2017), Pondicherry (2019) and Odisha (2016), and Manipur (2017) respectively (Fig. 3e). To boot, resistance against another third-generation cephalosporin, ceftriaxone, in Jharkhand (2016), Manipur (2017) and Odisha (2016), and West Bengal (2018) respectively was found to be most strongly and weakly correlated (Fig. 3f). Withal, with respect to resistance against cefepime (fourth-generation cephalosporin), the highest and

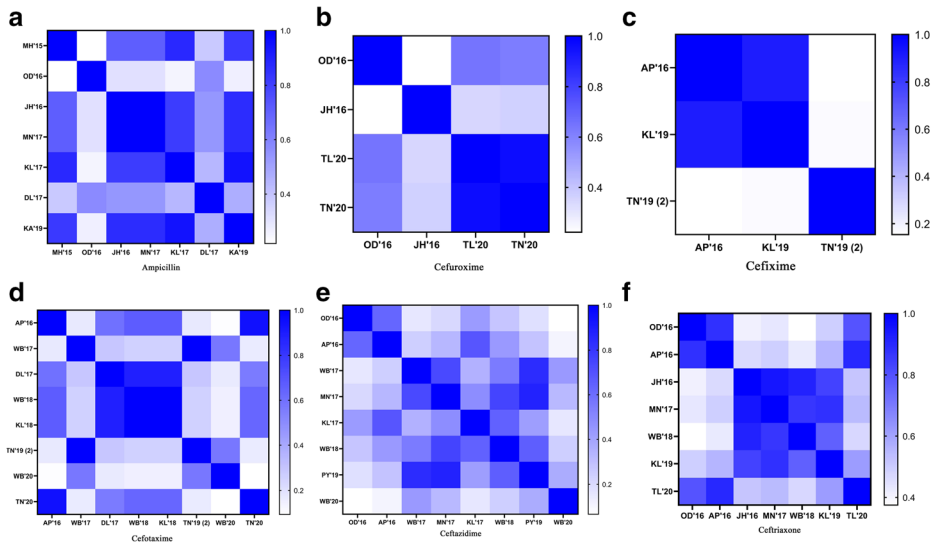


Fig. 3 Statistical significance of the incidence of resistance of symptomatic UPECs against 20 different antibiotics (a–t) in the various Indian states was analyzed by GraphPad Prism version 9 (Prism software package). Heat maps were generated on the correlation coefficient values represented by the color keys that ranged from zero (white) to 1 (deep blue)

lowest correlation was observed between West Bengal (2017), Manipur (2017) and Andhra Pradesh (2016), and West Bengal (2017) respectively (Fig. 3g). Moreover, West Bengal

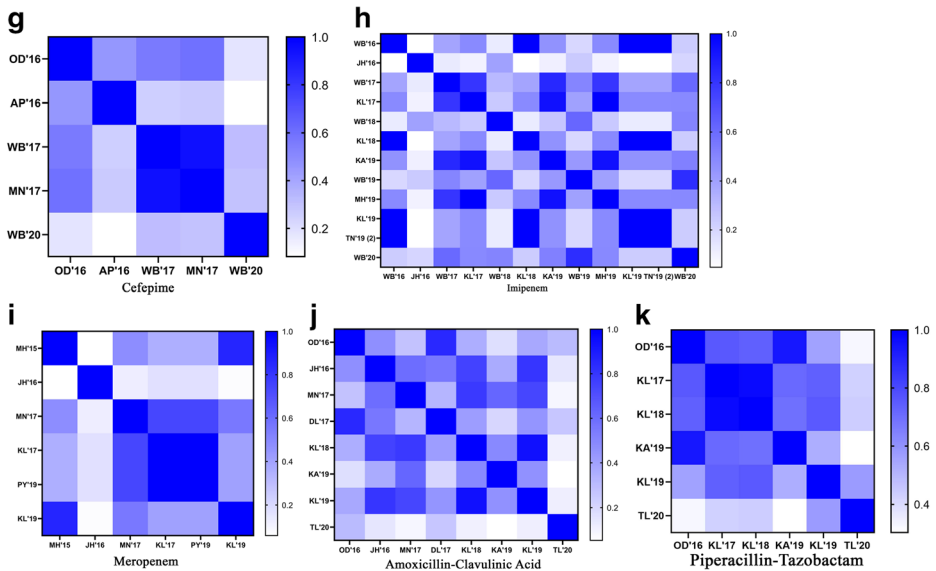


Fig. 3 continued.

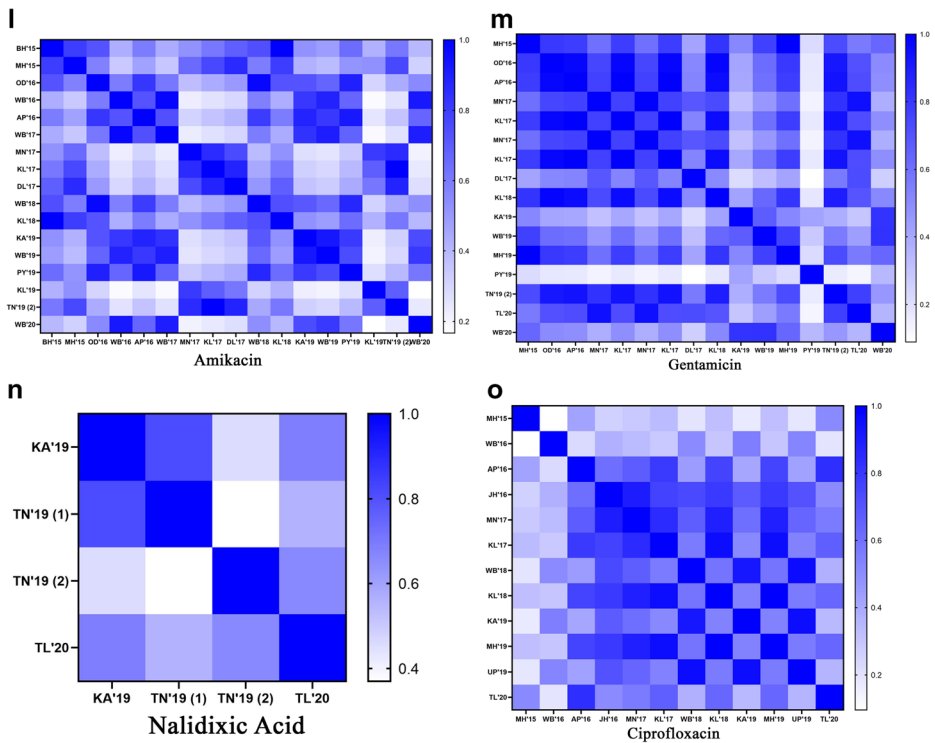


Fig. 3 continued.

(2016), Kerala (2018), Kerala (2019), Tamil Nadu (2019—second) and Kerala (2017), and Maharashtra (2019) respectively showed the highest correlation with respect to resistance against a carbapenem group of antibiotic: imipenem. However, lowest correlation was observed between Jharkhand (2016) and West Bengal (2020) (Fig. 3h). Moreover, the highest and lowest correlation with respect to resistance meropenem from carbapenem group was observed between Kerala (2017), Pondicherry (2019) and Maharashtra (2015), Kerala (2017), and Pondicherry (2019) respectively (Fig. 3i). Furthermore, in case of resistance against amoxicillin/clavulanic acid (Fig. 3j) and piperacillin/tazobactam (Fig. 3k) (β -lactam- β -lactamase inhibitor), the highest correlation was observed between Kerala (2018), Kerala (2019) and Kerala (2017), and Kerala (2018) and lowest between Delhi (2017), Karnataka (2019) and Karnataka (2019), and Telengana (2020) respectively. Bihar (2015) and Kerala (2017) were found to show the strongest correlation with Kerala (2018) and Tamil Nadu (2019—second) respectively with respect to resistance against an aminoglycoside group of antibiotic: amikacin. Notwithstanding, the lowest correlation was perceived between West Bengal (2019) and Kerala (2019) (Fig. 3l). In addition, Maharashtra (2015) and Andhra Pradesh (2016) displayed the strongest correlation with Maharashtra (2019) and Kerala (2017) respectively with respect to the resistance against gentamicin (aminoglycoside). However, the weakest correlation against gentamicin was perceived between Delhi (2017) and

Karnataka (2019) (Fig. 3m). Moreover, the highest and lowest correlation with respect to resistance against first-generation quinolone, nalidixic acid, was observed between the states of Karnataka (2019), Tamil Nadu (2019—first) and Tamil Nadu (2019—first), and Tamil Nadu (2019—second) respectively (Fig. 3n). Furthermore, in case of resistance against ciprofloxacin, a second-generation quinolone, the highest correlation was observed between Kerala (2018) and Maharashtra (2019) and lowest between West Bengal (2016) and Andhra Pradesh (2016) respectively (Fig. 3o). However, the strongest and weakest correlation in the incidence of resistance against two other second-generation fluoroquinolone, i.e., ofloxacin (Fig. 3p) and norfloxacin (Fig. 3q), was found between the states Andhra Pradesh (2016) and Maharashtra (2019) and Odisha (2016) and Karnataka (2019) respectively. Moreover, the highest and lowest correlation with respect to resistance against levofloxacin (second-generation quinolone) was observed between the states or union territories of Delhi (2017), West Bengal (2018) and Odisha (2016), and West Bengal (2016) respectively (Fig. 3r). Odisha (2016) and Manipur (2017) showed the highest and lowest correlation in the incidence of resistance against cotrimoxazole (sulfonamide) with Tamil Nadu (2020) and West Bengal (2020) respectively (Fig. 3s). Moreover, Bihar (2015) and Odisha (2016) and Kerala (2017) showed the strongest correlation with Tamil Nadu (2020), Andhra Pradesh (2016), and Kerala (2018) respectively with respect to the resistance against nitrofurantoin from the nitrofuran group (a synthetic drug). However, Maharashtra (2015) showed the lowest correlation both with Bihar (2015) and Telangana (2020) respectively (Fig. 3t).

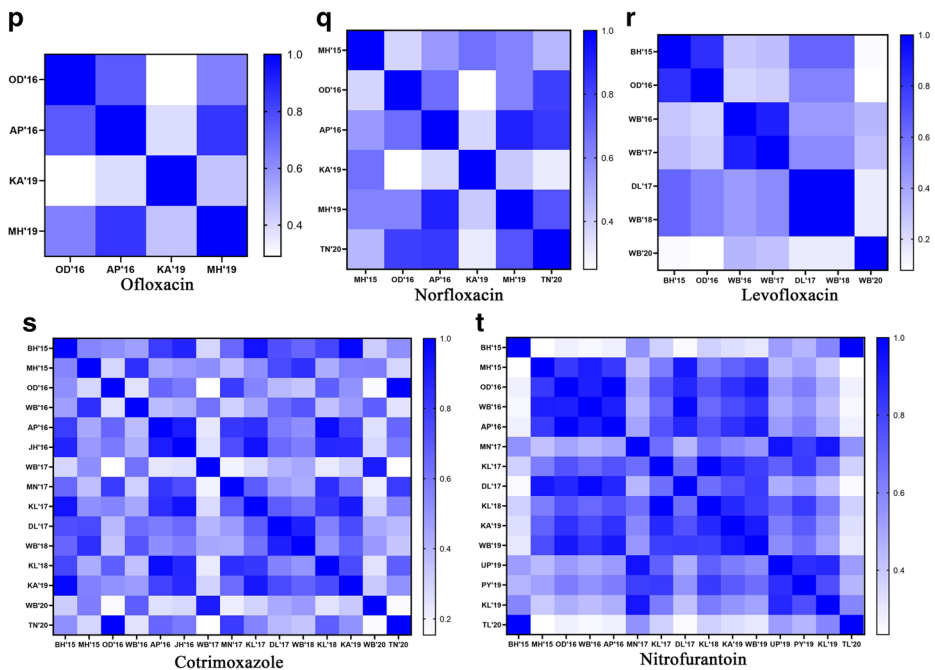


Fig. 3 continued.

Distribution of Plasmid-Mediated Antibiotic Resistance Genes in UPECs

Distribution of ESBL and AmpC Genes

UPEC isolates that exhibited AmpC phenotypes were reported to harbor *bla*_{CMY-2} and *bla*_{DHA-1} genes either alone or in combination. However, isolates that showed co-production of AmpC and ESBL were found to harbor *bla*_{CMY-2} and *bla*_{DHA-1} genes in combination with *bla*_{TEM} and *bla*_{CTX-M} genes [13]. Among the phenotypically confirmed ESBL *E. coli* isolates, the most common ESBL gene was *TEM* followed by *SHV* and *CTX-M*. Co-occurrence of *TEM*, *SHV*, and *CTX-M* was reported from Odisha [46]. However, Kammili et al. [17] from Telangana reported that among the phenotypically confirmed ESBL *E. coli* isolates, the most common ESBL gene was *TEM-1* followed by *CTX-M-15* and *SHV-38*. Moreover, the co-occurrence of *CTX-M-15* and *TEM-1* and *TEM-1*+*SHV-38* genes was also observed among the isolated UPECs.

Distribution of PMQR Genes

Among the phenotypically confirmed quinolone-resistant ESBL *E. coli*, the most common gene identified was *qnrS* followed by *aac* (6')-Ib-cr [17]. Moreover, other studies [9, 14, 42] from Kolkata, West Bengal, reported a high prevalence of *aac*(6')-Ib-cr alone and also in combination with *qnrB* and *qnrB* with *oqxB*.

Dissemination of Antibiotic Resistance Genes

A study by Ghosh et al. [13] reported a high incidence of AmpC-ESBL co-production among the p-AmpC-producing isolates. *bla*_{AmpC} and ESBL genes were harbored on transmissible plasmids which were successfully transmitted by conjugation. The transconjugants showed resistance to cephalosporins, fluoroquinolones, amikacin, and co-trimoxazole, which validated the rapid propagation of the different plasmid-mediated resistance genes along with the *bla*_{AmpC} genes. The predominance of IncF-type plasmid replicons Frep (65%), F1B (87%), followed by IncI (26%), IncH1 (8.7%), and IncN (4%) plasmids was found, harboring *bla*_{CMY-2}, *bla*_{TEM}, and *bla*_{DHA-1} genes. It was also found that plasmids carrying *bla*_{CMY-2} and *bla*_{DHA-1} genes were variants of IncF replicon family followed by IncF in combination with incI1, IncH1, and IncN, signifying a selection in plasmids, which contributed to the spread of AmpC beta-lactamases in combination with other ESBL genes. Moreover, an *in vitro* study conducted by [14] from Kolkata, West Bengal, reported efficacious transmission of PMQR genes, *aac*(6')-Ib-cr, *qnrA*, *qnrB*, *qnrS*, and *oqxB*, to susceptible *E. coli* J53Azide-resistant strain from ciprofloxacin-resistant UPECs in presence of high selection pressure of ciprofloxacin that generated transconjugants which further displayed varied MIC levels towards the drug with acquired mutations, Ser83Leu and Asp87Asn in the quinolone-resistant determining regions (QRDR) of *gyrA* gene (*E. coli* DNA gyrase subunit A). Moreover, another study [9] from Kolkata, West Bengal, revealed the successful transmission of the β -lactamase genes (*bla*_{TEM}, *bla*_{CTX-M}, *bla*_{OXA}) and the PMQR genes (*aac*(60)Ib-cr, *oqxAB*, *qnrB*) respectively in various combinations to the *E. coli* J53AziR recipients strain from all the tested UPECs against ceftazidime/ciprofloxacin selection. Furthermore, [9] proclaimed the predominance of *traF* irrespective of drug selection which indicated that F-type conjugation system was responsible for the transmission of the resistant plasmids resulting in the expeditious dissemination of antibiotic resistance in the isolated UPEC.

UPECs' Alternative Response Towards Survival

A study performed by Bandyopadhyay et al. [38] Kolkata, West Bengal, reported the incidence of the generation of reactive oxygen species (ROS) in response to the sub-inhibitory concentration of certain bactericidal antibiotics (ceftazidime, gentamicin, and ciprofloxacin) in the highly MDR UPECs that conveyed a protective function towards cell lethality, thereby suggesting an alternative mechanism of selection of the drug-resistant UPECs. Moreover, the study also portrayed the fact that the production of ROS assisted in the survival of the MDR UPECs by alteration in the transcription profile of different genes encoding the bacterial protective proteins, thereby affecting the core cellular functions. Additionally, a statistically significant correlation between *uspA* over-expression and ROS production at the sub-inhibitory dosage of ceftazidime, gentamicin, and ciprofloxacin among MDR UPECs was reported, also suggesting an alternative mechanism of selection of the drug-resistant UPECs.

UPEC Phenotypic Characterization

Evidence of hemolytic activity, hemagglutination activity, slime activity, β -lactamase activity, and biofilm formation capacity in UPECs.

Hemolytic Activity, Slime Activity, β -Lactamase Activity, Hemagglutination Activity by UPECs

Moderate incidence of hemolysin production was detected in studies conducted from two different states (Kerala, Tamil Nadu) of India on tested UPECs [7, 15, 16]. Gnanasekaran et al. [15] also reported the notable incidence of slime and β -lactamase activity in the tested UPECs. A remarkable incidence of mannose-resistant hemagglutination (MHRA) was observed in a study conducted from Haryana, Jharkhand, and Kerala [7, 22, 23].

UPECs as Biofilm Producers

The biofilm formation capacity ranged from a weak to very high level among the studied symptomatic UPECs from five different Indian states (Haryana, Jharkhand, Karnataka, Kerala, and Tamil Nadu) [1, 7, 22–24, 39]. Biofilm formation in UPECs was reported to be facilitated by type I fimbriae, especially the adhesion mediated by the FimH [21, 23]. Biofilm-producing UPECs were found to be more resistant to multiple groups of antibiotics as compared to the non-biofilm producers [1, 39] which was contrary to the report by Pullanhi et al. [7] that indicated similar antibiotic susceptibility pattern among both biofilm-producing and non-biofilm-producing *E. coli*. Moreover, a study by Vasudevan et al. [24] indicated high incidence of strong biofilm formers among the highly MDR UPECs.

Phylogenetic Background, Pathogenic Islands Distribution, and Genetic Makeup of UPECs

India, a country of diversity in geography, culture, religion, climate, race, and language, also exhibits diversity in phylogenetic background, distribution of pathogenic island (PAI) markers, and virulence characteristics of UPECs [2].

UPEC Phylotypes

Studies [25, 40] from Kolkata stated significant incidence of phylogroups B2, B1, and B2, D among the asymptomatic and symptomatic MDR UPECs respectively when analyzed by triplex PCR-based phylogenetic assay. However, another study from Kolkata by Ghosh et al. [2] demonstrated a significant incidence of asymptomatic and symptomatic MDR UPECs that could not be assigned to any of the eight known phylogroups (unknown phylogroup) when analyzed by quadruplex PCR-based phylogenetic assay.

Distribution of PAIs in UPECs

A study from Kolkata [2], West Bengal, reported a significant predominance of PAI IV536 and PAI I CFT073 among both asymptomatic and symptomatic UPECs.

Virulence Characteristics of UPECs

Moderate to a high incidence of several virulence factor genes including the fimbrial and afimbrial adhesins, and toxins was reported from two different Indian states (West Bengal and Tamil Nadu) in case of symptomatic [2, 19] and only from the state West Bengal in case of asymptomatic UPECs respectively [2].

Incidence of Mutation/Polymorphisms of Chromosomal Genes in UPECs

FimH Mutations

A study [2], from Kolkata, West Bengal, proclaimed the incidence of several synonymous and nonsynonymous mutations (NSMs) in the lectin and pilin domain of FimH of both asymptomatic and symptomatic UPECs, some of which were pathoadaptive. A very high prevalence of hot spot mutation V27A was observed among both the asymptomatic and symptomatic UPECs.

gyrA Mutations

A high incidence of *gyrA* mutations was observed among the studied UPECs from Kolkata, West Bengal [14].

Understanding Mechanisms for UPEC-Mediated UTI in Human

Role of Osmoregulatory Protein Pair in Transcription Regulation

A report by Narayan et al. [47] from Tamil Nadu stated that in all the pathogenic bacteria including UPECs, osmolarity alterations signal successful invasion in a mammalian host apart from temperature. UPECs were found to experience striking changes in external osmolarity that range from ~0 Osm in the soil to 1 Osm (~0.5 M ionic strength) upon infection. Moreover, Narayan et al. [47] reported that at high ionic strength (a condition generally observed after a successful invasion), Cnu (a member of the Hha-family of proteins), and H-NS (a transcription repressor) in 1:1 combination preferentially formed a complex with very weak affinity, thereby causing the expression of virulent genes. However, at low ionic strength, Cnu affinity for H-NS was found to increase and that also resulted in subsequent repression of virulence genes. Therefore, the study [47] showed that Cnu could act as a perfect molecular sensor of solvent ionic strength. Furthermore, the aforementioned study also depicted that the order-disorder transitions in H-NS could act synergistically with molecular swelling of Cnu, thereby giving way to a salt-driven switch in binding cooperativity.

Role of Inflammasomes and Their Components in UPEC-Mediated UTI

Verma et al. [48] from New Delhi stated that the inflammatory regulators (NLRP3, NAIP, NLRC4, ASC, and CASPASE-1) were upregulated at both mRNA and protein levels in the UPEC-infected UTI patients. Moreover, pro-inflammatory cytokines like IL-6, IL-8, IFN- γ , TNF- α , and MCP-1 were also found to be upregulated in the patients' group. However, no significant difference was perceived in the expression of AIM2 and CASPASE-4 genes at both mRNA and protein levels. Additionally, the involvement of NLRC4 inflammasome in UPEC-infected UTI was also observed. Moreover, Verma et al. [12] also reported that active α -hemolysin (HlyA) could induce the formation of the NLRP3 inflammasome by initiating deubiquitination of NLRP3-dependent potassium efflux, whereas the inactive form proHlyA was unable to do so, which suggested that the UPEC α -hemolysin's pore-forming property is an essentiality for initiation of pro-inflammatory response. Furthermore, Verma et al. [12] also displayed that disturbance in potassium homeostasis as a result of HlyA stimulation led to mitochondrial dysfunction which was followed by an acute inflammatory response that ensued in cell death. Previously, Verma et al. [49] demonstrated the most simple but perfect way for the production of active and inactive recombinant α -hemolysin for the aforementioned kind of functional studies.

Role of YadV in Pilus Biogenesis

A study [50] from New Delhi showed that the monomeric form of YadV, the chaperone component of the CU pathway of Yad pili, is the preferred state for its interaction with pilus subunits. Moreover, it was observed that the closed conformation for the proline lock was an important structural element for chaperone–pilus subunit interaction and the closed state of the proline lock was found to be energetically unstable. Therefore, the aforementioned report demonstrated that the monomeric YadV with its closed proline lock might act as an intermediate state to support suitable access to pilus subunits and also pilus biogenesis.

Alternative Therapeutic Strategies Against UPECs

The ineptitude of conventional antibiotics against UPECs demanded newer therapeutic interventions. The literature search yielded several reports that indicated various newer alternative therapeutic options that might help to combat the spread of UPECs.

Phage Therapy

Bacteriophages are viruses that are capable of infecting and killing bacteria without affecting humans. Phage therapy uses bacteriophages for the treatment of bacterial infections. A study [27] from the state of Maharashtra reported very high lytic activity of *Escherichia* virus myPSH2311 against UPECs which were found to be resistant to last-resort antibiotics like meropenem and colistin.

Sulfur Nanoparticles

Sulfur nanoparticles are widely used antimicrobial agents. A study by Paralikar et al. [3] from Maharashtra displayed the antibacterial potential of sulfur nanoparticles (SNPs) alone and in combination with antibiotics such as amoxicillin, norfloxacin, and trimethoprim against UPECs. Maximum zone of inhibition was observed when SNPs were used in combination with amoxicillin. Moreover, the aforementioned study also revealed a decrease in zeta potential when UPECs were exposed to SNPs that indicated an alteration in their surface potential owing to membrane damage.

1-Amino-4-Hydroxyanthraquinone (Disperse Red 15 or DR15)

A study [21] from Tamil Nadu stated that DR15, a natural product often found in wastewaters when derivatised into *N*-(4-hydroxy-9, 10-dioxo-9, 10-dihydroanthracen-1-yl) undec-10-enamide and self-assembled with linseed oil, could be used to inhibit biofilm formation in UPECs which could potentially help to reduce catheter-acquired UTI incidents and their subsequent healthcare costs.

Antimicrobial Peptides

Antimicrobial peptides (AMPs) are small proteins known to have effective antibacterial, antifungal, and antiviral activity. A report by Biswas et al. [26] from Telangana had shown that 2 mg/kg dose of recombinant Defensin 21 (DEFB21) when administered with 50 µg gentamycin for 3 days in UPEC-infected rats significantly decreased the bacterial load in the caput and cauda epididymis and testis of infected rats. A study [28] from Tamil Nadu declared that a synthetic analog of the membranolytic AMPs of the tritrypticin family significantly lowered solvation energy in the *E. coli* membrane, thereby showing higher antibacterial activity against *E. coli*, which might be used as alternative solutions for the treatment of *E. coli*-mediated UTI.

Lectins

Lectins are proteins that are found in fungi, bacteria, and viruses. The exclusive feature of lectin to recognize and bind specific carbohydrate structures makes it relevant for use in

targeted drug delivery. A study conducted from Tamil Nadu [10] revealed that the interaction between silver nanoparticles (AgNPs) and *Buteamonosperma* seed lectin (BMSL) formed efficient surface-functionalized AgNPs with exemplary antibiofilm competency against UPEC. The aforementioned study also displayed that BMSL–AgNP conjugate affected the integrity of the bacterial outer membrane and generated an imbalance in the antioxidant defense which induced cell death.

Chitosan

Chitosan is a linear polysaccharide (derived from chitin shells of shrimp and other crustaceans with an alkaline substance such as sodium hydroxide) composed of randomly distributed β -(1 \rightarrow 4)-linked D-glucosamine (deacetylated unit) and N-acetyl-D-glucosamine. Another study [11] from Tamil Nadu displayed the fact that commercial chitosan (CC) and extracted chitosan (EC) showed a high inhibitory percentage of 60–75% and 80–85% respectively on young biofilm and were also found to disrupt biofilm formation. Moreover, hemolysis assay exhibited a high inhibition potential of 79% against EC. Both the chitosan presented remarkable activity in suppression of the phenotypic virulence factors like swarming motility, mediated by type I pili, and were also found to repress cellulose production in UPEC. EC also downregulated the virulent genes responsible for the invasion in UPECs.

Type A Procyanidin

Type A procyanidin (TAP) are members of the proanthocyanidin class of flavonoids. A report from Tamil Nadu by [24] showed that TAP caused 70% inhibition in biofilm formation of MDR UPECs. The study also reported that at pH 5.8, TAP alone and in combination with nitrofurantoin downregulated the major fimbrial adhesins of UPEC, thereby affecting their ability to invade the host uroepithelial cells.

Potential Drug Targets to Combat Drug-Resistant UPECs

FimH

A study from Uttar Pradesh indicated successful repression of the fimH gene, a major virulent factor in UPEC infection by the CRISPRi technique that might be implemented in vivo to prevent UTI [51]. A computational screening was performed by Miryala et al. [21] from Tamil Nadu for identifying potential inhibitors against the FimH-mediated UPEC adhesion. The compounds, 1-amino-4-hydroxyanthraquinone (Disperse Red 15 or DR15) and 4-(4'-chloro-4-biphenyl)sulfonylamino benzoic acid (CB1), could enfeeble adhesion and biofilm formation without impeding the planktonic growth.

β -Lactamase

A study [52] from West Bengal identified a potent inhibitor-resistant TEM (IRT) β -lactamase inhibitor (naringenin triacetate) that was reported to hinder the growth of UPECs effectively in vitro and thus might act as a therapeutic alternative to the classical β -lactams and β -lactam– β -lactamase inhibitor combinations.

Discussion

In this review, an overview of the recent articles (from 2015) that dealt with the main and current developments and progress in the field of UPEC research that were published was presented. This included the national trends in incidence of UPEC-mediated UTIs, their age and gender-wise distribution, antibiotic resistance patterns, distribution of resistance genes, phenotypic characters, phylogenetic background, distribution of PAIs, and infection mechanisms. Moreover, the current alternative therapeutic strategies to fight against UPECs and their potential drug targets were also reviewed.

The literature search indicated that in the last 6 years, *E. coli* was the most predominant uropathogen causing symptomatic UTI in people residing in different (eastern, western, northern, southern) regions of India especially in the states and union territories like Bihar, West Bengal, Maharashtra, Haryana, Himachal Pradesh, Tamil Nadu, Telangana, New Delhi, and Chandigarh respectively. Moreover, the incidence of urine culture-positive symptomatic *E. coli* among different (northern, eastern, and southern) regions of India during the time period (2015–2020) was found to be statistically correlated (Fig. 1). However, the prevalence of UPEC-mediated symptomatic UTI was comparatively lower in the states like Manipur, Uttar Pradesh, and Kerala. The highest incidence of UPEC-mediated UTI was reported from the north Indian state, Haryana, in the year 2018 (Table 1). Moreover, although in West Bengal, Tamil Nadu, and New Delhi the main causative agent of UTI was UPECs, the disparity in the percentage of UPEC-mediated UTI in the same or different years was also observed (Table 1). However, a striking incidence of UPECs in asymptomatic individuals was only reported from the eastern region, West Bengal [2, 25]. This indicated that in current times, highest predominance of UPECs in both ABU and symptomatic UTI poses a public health concern in West Bengal which is in the eastern region of India where a major population lies below the poverty level.

Moreover, the literature study also displayed a higher prevalence of UPEC infections among the female population from various regions (northern, eastern, southern) covering states of Haryana, Bihar, Jharkhand, West Bengal, Kerala, and Tamil Nadu as compared to the males [2, 7, 15, 16, 20, 23, 32] except a report from a southern state, Karnataka [1], that indicated the predominance of the males. The maximum age group affected with UPEC-mediated UTI from various Indian states was found to be 21–40 years in case of both male and female populations with asymptomatic or symptomatic infections [1, 2, 15, 16, 20]. However, the prevalence of UPECs was also observed in pediatric and geriatric populations that consisted of both asymptomatic and symptomatic patients, especially from the eastern region, West Bengal [2].

Recent reports indicated an overall increasing trend in drug resistance in both asymptomatic (Fig. 2a) and symptomatic (Fig. 2b) UPECs to several groups of antibiotics like penicillins, cephalosporins, aminoglycosides, quinolones/ fluoroquinolones, and sulphonamides in various parts of India covering several Indian states over the last 6 years (2015–2020). Two different (2015 and 2019) reports from an eastern region of India, West Bengal, displayed a striking rise in resistance of asymptomatic UPECs to third-generation cephalosporins (cefotaxime and ceftazidime), aminoglycoside (amikacin), second-generation fluoroquinolone (ciprofloxacin), and sulfonamide (cotrimoxazole) after a period of 4 years (Fig. 2a). Although the two aforesaid studies were conducted on separate patient populations, the rising trend of resistance in these groups of antibiotics, especially among asymptomatic UPECs, was highly alarming and also indicated the rise in unprescribed usage of antibiotics in recent times. Later of the two reports stated the least resistance against nitrofurantoin (nitrofurantoin) (Fig. 2a) which betokened the

need to use it as a first-line antibacterial agent. Moreover, further studies also must be initiated to explore the antibiotic susceptibility pattern of asymptomatic *E. coli* obtained from urine culture-positive isolates from the different regions of the Indian sub-continent to cease the unprecedented use of antibiotics across the country.

National trends in resistance among symptomatic UPECs to various groups of antibiotics were quite similar to the asymptomatic ones. Moreover, a varied level of statistically significant positive correlation in the incidence of resistance against different antibiotics that belonged to various groups like aminopenicillin, cephalosporin, carbapenem, β -lactam- β -lactamase inhibitors, aminoglycosides, quinolone/ fluoroquinolones, sulfonamides, and nitro-furan among various Indian states over a period of 5 (2015–2020) years was observed (Fig. 3a–t). High incidence of penicillin resistance in different states of Northern, North Eastern, Eastern, and/or Southern India over the last 6 years (2015–2020) along with a rising trend from 2015 to 2020 (Fig. 2b) indicated that overuse of this group of antibiotics in last few years had rendered them ineffective.

Reports from different regions of India (northern, north-eastern, eastern, and southern) revealed a very high level of resistance to first–fourth-generation cephalosporins. Likewise, an overall rising trend in resistance to third (cefixime, cefotaxime, cefoperazone, ceftazidime, and ceftriaxone)- and fourth (cefepime)-generation cephalosporins in the aforementioned regions of India was noticed from 2017 to 2020 (Fig. 2b). This indicated to the ineffectiveness of first- and second-generation cephalosporins in the last decade due to which usage of third- and fourth-generation cephalosporins increased rapidly. Moreover, among all these four generation cephalosporins, the least resistance was observed against ceftriaxone from various Indian states (Fig. 2b) which suggested that ceftriaxone might be the last resort antibiotic of the third-generation cephalosporin group. However, the highest incidence of cefepime (fourth-generation cephalosporin) resistance recently among symptomatic UPECs (Fig. 2b) was exceedingly disquieting especially, when it was from one of the poorest Indian state, West Bengal.

Low incidence of resistance to carbapenems like imipenem and meropenem in symptomatic UPECs in different regions (northern, eastern, western, and southern) of India (Fig. 2b) indicated that these antibiotics can be the drugs of choice for treatment of symptomatic patients resistant to other classes of antibiotics. However, a rising trend in carbapenem resistance from 2016 to 2019 especially in an eastern state West Bengal (Fig. 2b) was highly alarming as indicated extra usage of these drugs in recent times.

Among the β -lactam- β -lactamase inhibitor combinations, resistance against piperacillin/tazobactam was consistently reported to be quite low especially during the years 2016–2020, in eastern (Odisha) and southern (Kerala, Karnataka, and Telangana) regions (Fig. 2b), thereby suggestive of the fact that aforementioned combination can be a suitable way to treat infections caused by ESBL-producing symptomatic UPECs. Moreover, the inconsistent increase in resistance to β -lactam- β -lactamase inhibitors combination from 2015 to 2020 (Fig. 2b) might be due to the diverse sample population with great disparity in age, sex, and environmental factors.

A recent report from the southern (Pondicherry) part of India that stated 100% sensitivity to fosfomycin (Fig. 2b), a cell wall inhibitor, lighted a glimmer of hope as this might turn out as a treatment option for patients resistant to other groups of antibiotics in future.

West Bengal (eastern India) recently reported moderately high (60.25%) resistance of symptomatic UPECs against amikacin unlike other reports from different regions that stated comparatively lower incidence of amikacin resistance. Moreover, a recent report from southern India (Pondicherry) showed extremely high resistance against gentamicin unlike the other states (Fig. 2b). This suggested the increase in the use of amikacin and gentamicin respectively

in recent years in these two states particularly. However, of late, resistance to aminoglycoside was reported to be low in the south Indian states of Kerala, Tamil Nadu, and Telangana (Fig. 2b) which implied to the controlled use of this antibiotic group in the recent past.

A very high incidence of tetracycline and erythromycin (macrolide) resistance among symptomatic UPECs was reported from the south Indian state of Tamil Nadu recently (Fig. 2b). This pointed out the fact that resistance to the aforementioned protein synthesis inhibitors also started rapidly in south India. However, a report from the western (Maharashtra) region (Fig. 2b) indicated immensely low chloramphenicol resistance which might be a ray of hope for future researchers and clinicians.

This literature survey showed that usage of nalidixic acid (first-generation quinolone) for treatment of UPEC-mediated symptomatic UTIs was not very common from 2015 to 2018. However, right from 2019, prevalence of nalidixic acid resistance was quite evident in the northern and southern parts of India (Fig. 2b). Moreover, reports from different regions, (northern, eastern, and southern) covering various Indian states demonstrated very high resistance to second-generation fluoroquinolones, especially against ciprofloxacin and levofloxacin, over the last 5 years (2016–2020) (Fig. 2b). This suggested that excessive use of nalidixic acid, the first synthetic quinolone antibiotic in the first few years of the past decade, had rendered them ineffective in the last few years, thereby causing a decline in their usage. However, the present scenario of resistance against nalidixic further affirmed the persistent futile nature of this drug. Furthermore, current evidence of the emergence of ciprofloxacin- and levofloxacin (second-generation fluoroquinolones)-resistant UPECs along with a somewhat rising trend in different parts of India is highly appalling as it limits the choice of antibiotics to a great extent.

Present trend in cotrimoxazole (sulphonamide) resistance was found to be very high from almost all regions of India with the highest (100%) being from the eastern Indian state of West Bengal and the south Indian state of Tamil Nadu. However, strangely another recent report from Tamil Nadu stated low (31%) incidence of cotrimoxazole resistance among symptomatic UPECs (Fig. 2b). The aforementioned reports suggested even the use of sulfonamides became rampant in recent years and thus the empiric usage of these drugs should be restricted in the future. However, numerous reports from various regions of India indicated nil or very low resistance against nitrofurantoin (nitrofurantoin), and strikingly recent reports, especially those published on and after 2019, implied a decrease in nitrofurantoin resistance which indicated the need for wise and proper prescription usage of this drug as this remained as the most effective oral agent for the treatment of symptomatic UPEC infections.

Extremely high incidence of MDR symptomatic UPECs [2, 16, 20, 23, 24, 42] was reported from the northern, eastern, and southern regions of India. This indicated the inappropriate antibacterial treatment and uncontrolled use of antibiotics nationwide that contributed to the emergence of MDR in UPECs. Moreover, a report from Kolkata, West Bengal, that stated exceedingly high [2] levels of MDR among asymptomatic UPECs was highly alarming and this furthermore justified the need to surcease dissemination of antibiotic resistance by immediate implementation of proper prescription policies in one of the poorest Indian states.

National trends of moderate to the high incidence of ESBL [4, 6, 7, 17, 19], MBL [4, 20], and/or AmpC [4, 13, 20, 23] producers among symptomatic UPECs from different regions (northern, eastern, and southern) of India were really alarming. Moreover, the incidence of co-production of ESBL, MBL, or AmpC among MDR UPECs was also reported in the recent past from southern India (Pondicherry) [4]. This incidence is highly worrisome as it poses a serious threat to the health care setting of a resource-poor country as India by limiting the

therapeutic options since unlike ESBL producers, MBL and AmpC producers were also found to be resistant to carbapenems and β -lactam inhibitors. Withal, the presence of ESBL [17], AmpC [13], and/or PMQR [9, 14, 17, 42] genes among the phenotypically confirmed symptomatic UPECs from southern and eastern India further pointed out to the dreadful implications of inappropriate clinical management in the aforementioned areas that led to the spread of these plasmid-mediated resistance genes through horizontal gene transfer.

A very recent report [38] from the eastern region (West Bengal) of India threw the spotlight on an alternative strategy that might be adopted by symptomatic MDR UPECs for their survival when exposed to sub-inhibitory concentration of different bactericidal antibiotics and this was really daunting as this might cause treatment failures in the future.

Moreover, the notable incidence of hemolytic activity [7, 15, 16]/slime activity [15]/ β -lactamase activity [15]/hemagglutination activity [7, 20, 23] by symptomatic UPECs was reported from northern, eastern, and southern regions of India in the last few years. Furthermore, a high incidence of several virulence factors genes (fimbrial, afimbrial adhesins, and toxins) was also reported from eastern and southern India [2, 16] in case of asymptomatic and/or symptomatic UPECs. These reports highlighted the high adherence and colonization potential of the circulated UPECs in India irrespective of their asymptomatic and symptomatic nature.

Weak to high biofilm formation capacity was recognized in various UPEC isolates in different parts of India (northern, north-eastern, and southern) [1, 7, 20, 23, 24, 39]. Moreover, incidences of PAI markers and pathoadaptive FimH mutations were reported from eastern India in both asymptomatic and symptomatic UPECs. To boot, a recent report from eastern India stated a very high incidence of asymptomatic and symptomatic UPECs that belonged to undesigned and/or pathogenic phylogroups [2]. The aforementioned reports drew attention to the enhanced virulence potential, survival, and fitness capacity of UPECs currently prevalent in various regions of India.

In the last few years, India had perceived the emergence of highly virulent MDR and mutated β -lactamase-producing UPEC strains due to indiscriminate use of unprescribed antibiotics, which further led to limitations in therapeutic options, thereby threatening the current health care setting, especially of a developing country, like India. Moreover, high-dosage administration of antibiotics was found to cause several adverse effects on humans [10]. It is therefore of urgent necessity to develop alternative therapeutic strategies to fight against these virulent MDR microbes. Very recently, several researchers especially from western [3, 27] and south Indian state [10, 11, 21, 24, 28] of Maharashtra and Tamil Nadu displayed the usage of several alternative therapeutics which might have preached the way to cope with the upcoming therapeutic challenges and combat the spread of MDR UPECs.

In the recent past, especially during 2019–2020, several mechanisms by which UPECs mediate UTI in the host [12, 47, 49, 50] and potential drug target against UPECs mediated UTI [21] were explored by several researchers from the northern, eastern, and southern regions of India. The exploration of various mechanisms of UPEC infections and the search for potential drug targets might turn to be a boon in the future, as this might help to design new therapeutics.

Last but not the least, this literature survey attempted to bring to the forefront the current trends and advancements in UPEC-mediated UTI in a resource-poor country like India by incorporating relevant information from most of the published reports (PubMed, Google Scholar); however, this could lack some available information. Nevertheless, reports included in this review successfully provided a well-defined overview of present developments of UPECs in India, which was further lucidly represented by a graphical model (Fig. 4).

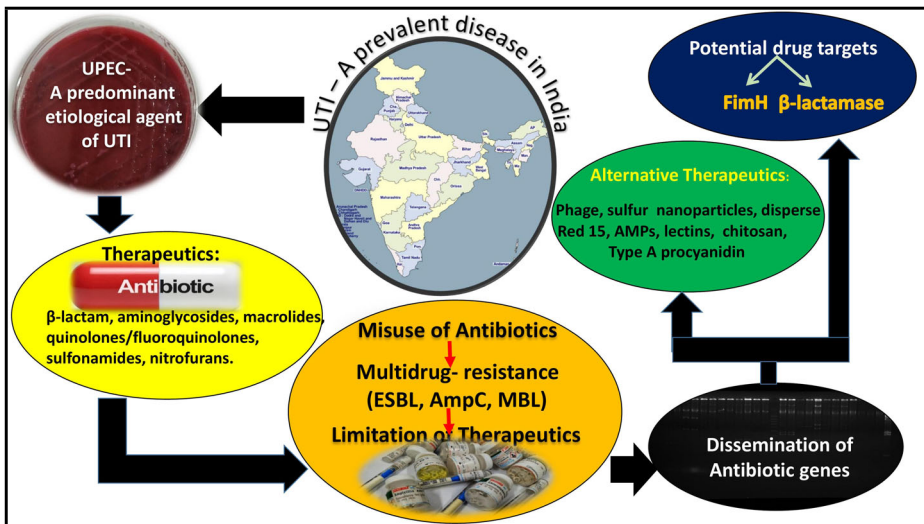


Fig. 4 Graphical model on present developments of UPECs in India

Conclusion

The present review based on the recent developments in UPECs, the most predominant uropathogen in India, threw the spotlight on the nationwide expeditious emergence and dissemination of antibiotic-resistant UPEC strains that included ESBL, MBL, and AmpC producers, in the last few years. Moreover, the incidence of symptomatic UPECs and their resistance against different groups of antibiotics was found to be statistically correlated at a significance level of ≤ 0.05 among various Indian states that covered different regions of India. This pointed out the atrocious implications of improper clinical management, thereby causing a significant rise in health care expenses and the consequent economic burden in a resource-poor country like India. Moreover, this review also displayed the high adherence and colonization potential of the circulated MDR UPECs currently prevalent in India. The present Indian scenario of limited availability of therapeutic options for treatment of UPEC-mediated UTI but the prevalence of the highly virulent MDR UPEC strains might have instigated several researchers, especially from southern India in the search of alternative therapeutic strategies to cope with the imminent therapeutic challenges and encounter the spread of virulent MDR UPECs. Furthermore, exploration of several mechanisms of UPEC infections and the quest for potential drug targets might aid in UPEC research in the future with successful novel therapeutic interventions.

Acknowledgements The authors would like to express their sincere gratitude to Prof (Dr.) Pratip Kumar Kundu, Director, Calcutta School of Tropical Medicine, Kolkata West Bengal, India, for his kind support and cooperation.

Materials Availability Not applicable

Author Contribution A. Ghosh, D. Bandyopadhyay, and S. Koley contributed equally in the data collection, compilation, and writing of this manuscript. M. Mukherjee participated in the preparation and correction of the manuscript.

Funding The study was supported by grants received from the Science and Engineering Research Board (SERB), Department of Science and Technology, Government of India, (Grant No. EMR/2016/001670 dated 22.08.17); Department of Higher Education, Science and Technology and Biotechnology, Government of West Bengal, India (Grant No. 62 (Sanc.)/BT/P/Budget/RD-60/2017 dated 12.03.2018); and the INSPIRE fellowship grant from Department of Science and Technology, New Delhi, Government of India, No.-DST/INSPIRE Fellowship/2016/ IF160069 (2016-2019).

Data Availability Not applicable

Declarations

Ethical Approval Not applicable

Consent to Participate Not applicable

Consent to Publish Not applicable

Competing Interests The authors declare no competing interests.

References

- Karigoudar, R. M., Karigoudar, M. H., Wavare, S. M., & Mangalgi, S. S. (2019). Detection of biofilm among uropathogenic *Escherichia coli* and its correlation with antibiotic resistance pattern. *Journal of Laboratory Physicians*, 11 [01], 017-022.
- Ghosh, A., & Mukherjee, M. (2019). Incidence of multidrug resistance, pathogenicity island markers, and pathoadaptive FimH mutations in uropathogenic *Escherichia coli* isolated from asymptomatic hospitalized patients. *Folia Microbiologica*, 64(4), 587-600.
- Paralikar, P., Ingle, A.P., Tiwari, V., Golinska, P., Dahm, H., & Rai, M. (2019). Evaluation of antibacterial efficacy of sulfur nanoparticles alone and in combination with antibiotics against multidrug-resistant uropathogenic bacteria. *Journal of Environmental Science and Health, Part A*, 54[5], 381-390.
- Gopichand, P., Agarwal, G., Natarajan, M., Mandal, J., Deepanjali, S., Parameswaran, S., & Dorairajan, L.N. (2019). In vitro effect of fosfomycin on multi-drug resistant gram-negative bacteria causing urinary tract infections. *Infection and Drug Resistance*, Volume 12, 2005-2013.
- Malik, S., Sidhu, P.K., Rana, J.S., & Nehra, K. (2019). Managing urinary tract infections through phage therapy: a novel approach. *Folia Microbiologica*, 65[2], 217-231.
- Prasada, S., Bhat, A., Bhat, S., Shenoy Mulki, S., & Tulasidas, S. (2019). Changing antibiotic susceptibility pattern in uropathogenic *Escherichia coli* over a period of 5 years in a tertiary care center. *Infection and Drug Resistance*, Volume 12, 1439-1443.
- Pullanhi, U., Khan, S., Vinod, V., Mohan, K., & Kumar, A. (2019). Outcome of acute urinary tract infections caused by uropathogenic *Escherichia coli* with phenotypically demonstrable virulence factors. *Annals of African Medicine*, 18[3], 138.
- Kaza, P., Mahindroo, J., Veeraraghavan, B., Mavuduru, R. S., Mohan, B., & Taneja, N. (2019). Evaluation of risk factors for colistin resistance among uropathogenic isolates of *Escherichia coli* and *Klebsiella pneumoniae*: a case-control study. *Journal of Medical Microbiology*, 68[6], 837-847.
- Mukherjee, S. K., & Mukherjee, M. (2019). Characterization and bio-typing of multidrug resistance plasmids from uropathogenic *Escherichia coli* isolated from clinical setting. *Frontiers in Microbiology*, 10.
- Bala Subramanian, S., Senthilnathan, R., Arunachalam, J., & Anbazhagan, V. (2019). Revealing the significance of the glycan binding property of *Butea monosperma* seed lectin for enhancing the antibiofilm activity of silver nanoparticles against uropathogenic *Escherichia coli*. *Bioconjugate Chemistry*, 31[1], 139-148.
- Rubini, D., Varthan, P. V., Jayasankari, S., Vedahari, B. N., & Nithyanand, P. (2020). Suppressing the phenotypic virulence factors of uropathogenic *Escherichia coli* using marine polysaccharide. *Microbial Pathogenesis*, 141, 103973.

12. Verma, V., Kumar, P., Gupta, S., Yadav, S., Dhanda, R.S., Thorlacius, H., & Yadav, M. (2020). α -Hemolysin of uropathogenic *E. coli* regulates NLRP3 inflammasome activation and mitochondrial dysfunction in THP-1 macrophages. *Scientific Reports*, 10[1]. doi:10.1038/s41598-020-69501-1
13. Ghosh, B., & Mukherjee, M. (2016). Emergence of co-production of plasmid-mediated AmpC beta-lactamase and ESBL in cefoxitin-resistant uropathogenic *Escherichia coli*. *European Journal of Clinical Microbiology & Infectious Diseases*, 35(9), 1449-1454.
14. Basu, S., & Mukherjee, M. (2019). Conjugal transfer of PMQR from uropathogenic *E.coli* under high ciprofloxacin selection pressure generates *gyrA* mutation. *Microbial Pathogenesis*, 132, 26-29.
15. Gnanasekaran, A., Manikandan, P., Poongothai, P., Senthilkumar, P.K. (2019). In vitro screening of multidrug resistance uropathogenic *Escherichia coli* from the urban area of Namakkal district. *Journal of Applied Pharmaceutical Science*, 9(9), 84-91.
16. Muraleetharan, M., Viswanathan, T., (2019). Genotyping and molecular characterization of extended-spectrum beta-lactamases-producing uropathogenic *Escherichia coli* in and around Coimbatore district, Tamil Nadu, India. *Urological Science* ; 30: 244
17. Kammili, N., Rani, M., Styczynski, A., Latha, M., Pavuluri, P. R., Reddy, V., & Alsan, M. (2020). Plasmid-mediated antibiotic resistance among uropathogens in primigravid women—Hyderabad, India. *Plos One*, 15(5). doi:10.1371/journal.pone.0232710
18. Siddaramappa, S., Pulella, K., Thimmappa, B., Devkota, R., Bajaj, R., Manivannan, B., . . . Pradeep, B. E. (2018). Characterization of blaCTX-M sequences of Indian origin and thirteen uropathogenic *Escherichia coli* isolates resistant to multiple antibiotics. *BMC Research Notes*, 11(1).
19. Mehreshi, P., Faujdar, S.S., Kumar, S., Solanki, S., Sharma, A. (2019) Antibiotic susceptibility profile of uropathogens in rural population of Himachal Pradesh, India: where we are heading? *Biomedical & Biotechnology Research Journal*, 3:171-5
20. Mittal, S., Sharma, M., & Chaudhary, U. (2015 a). Biofilm and multidrug resistance in uropathogenic *Escherichia coli*. *Pathogens and Global Health*, 109(1), 26-29.
21. Miryala, S., Makala, H., Yadavali, S. P., Venkatasubramanian, U., Subbaiah, N., & Srinandan, C. (2020). Disperse red 15 (DR15) impedes biofilm formation of uropathogenic *Escherichia coli*. *Microbial Pathogenesis*, 138, 103772.
22. Mittal, S., Sharma, M., & Chaudhary, U. (2015b). Fosfomycin use in multi drug resistant uropathogenic *Escherichia coli*. *Infectious Disorders - Drug Targets*, 15(3), 196-201.
23. Singh, S. K., Seema, K., & Gupta, M. (2016). Detection of Amp C β -lactamase and adherence factors in uropathogenic *Escherichia coli* isolated from aged patients. *Microbial Pathogenesis*, 100, 293-298
24. Vasudevan, S., Selvan, G. T., Bhaskaran, S., Hari, N., & Solomon, A. P. (2020). Reciprocal cooperation of type A procyandin and nitrofurantoin against multi-drug resistant (MDR) UPEC: a pH-dependent study. *Frontiers in Cellular and Infection Microbiology*, 10.
25. Mukherjee, M., Koley, S., Mukherjee, S. K., Basu, S., Ghosh, B., & Chakraborty, S. (2015). Phylogenetic background of *E. coli* isolated from asymptomatic pregnant women from Kolkata, India. *The Journal of Infection in Developing Countries*, 9(07), 720-724.
26. Biswas, B., Bhushan, S., Rajesh, A., Suraj, S. K., Lu, Y., Meinhardt, A., & Yenugu, S. (2015). Uropathogenic *Escherichia coli* (UPEC) induced antimicrobial gene expression in the male reproductive tract of rat: evaluation of the potential of Defensin 21 to limit infection. *Andrology*, 3(2), 368-375.
27. Manohar, P., Tamhankar, A. J., Lundborg, C. S., & Nachimuthu, R. (2019). Therapeutic characterization and efficacy of bacteriophage cocktails infecting *Escherichia coli*, *Klebsiella pneumoniae*, and *Enterobacter* species. *Frontiers in Microbiology*, 10.
28. Shruti, S. R., & Rajasekaran, R. (2020). Identification of therapeutic peptide scaffold from tritryptic family for urinary tract infections using in silico techniques. *Journal of Biomolecular Structure and Dynamics*, 38(15), 4407-4417
29. Parra, G.I., Squires, R. B., Karangwa, C.K., Johnson, J.A., Lepore, C J , Sosnovtsev, S.V., & Green, K.Y. (2017). Static and evolving norovirus genotypes: implications for epidemiology and immunity. *PLOS Pathog*.2017 Jan 19; 13(1):e1006136.
30. Yadav, S. (2018). Correlation analysis in biological studies. *J Pract Cardiovasc Sci*, 4:116-21.
31. Akoglu, H.(2018). User's guide to correlation coefficients. *Turk J Emerg Med*, 7; 18(3):91-93.
32. Bhattacharyya, S., Sarfraz, A., Ansari, M.A.A., Jaiswal, N., (2015). Characterization and antibiogram of Uropathogenic *Escherichia coli* from a tertiary care hospital in Eastern India. *Int J Curr Microbiol App Sci*, 4(2): 701-705
33. Wabale, V.R., Bharadwaj, R.S., Joshi, A.A., Chowdhary, A.S. (2015). Serotypes, Hemolysin production and drug resistance among uropathogenic *Escherichia coli* at a tertiary care hospital in Mumbai. *International Journal of Current Research* 7(07), 18596-18600

34. Yadav, M., Khumanthem, S.V., Kshtrimayum, M.D. (2017). Antibiotic resistance trends of Uropathogenic *Escherichia coli* isolated from inpatients in a tertiary care hospital in north East India. *International Journal of Recent Scientific Research*, 8(7), 18496-18500
35. Sukumaran, T.S., Mohan A.K. (2017). Antimicrobial resistance among uropathogenic bacteria in Rural Kerala, India. *Int.J.Curr.Microbiol.App.Sci*, 6(9): 2287-2296
36. Mishra, M. P., Sarangi, R., & Padhy, R. N. (2016). Prevalence of multidrug resistant uropathogenic bacteria in pediatric patients of a tertiary care hospital in eastern India. *Journal of Infection and Public Health*, 9(3), 308-314.
37. Tadepalli, S., Prudhivi, S., Myneni, R.B., Rao, S. (2016). Biofilm formation in uropathogenic *Escherichia coli* isolates and its association with extended betalactamase production and drug resistance. *Saudi Journal of Pathology and Microbiology*, 1(Iss-2), 60-64.
38. Bandyopadhyay, D., & Mukherjee, M., (2020). Reactive oxygen species and uspA overexpression: an alternative bacterial response toward selection and maintenance of multidrug resistance in clinical isolates of uropathogenic *E. coli*. *European Journal of Clinical Microbiology & Infectious Diseases*, 39(9), 1753-1760
39. Vysakh, A., Midhun, S. J., Jayesh, K., Jyothis, M., & Latha, M. (2018). Studies on biofilm formation and virulence factors associated with uropathogenic *Escherichia coli* isolated from patient with acute pyelonephritis. *Pathophysiology*, 25(4), 381-387.
40. Bandyopadhyay D, Mukherjee M. (2017). Distribution of class D-oxacillinases amongst third generation cephalosporin resistant nosocomial *Escherichia coli* isolates, their phylogenetic background and clonal analysis *International Journal of Current Research*. 9(10) 59099-59106
41. Singh, B. R. (2019). Quinolones and fluoroquinolones are useless to counter uropathogenic *Escherichia coli* infections (Letter). *Infection and Drug Resistance*, Volume 12, 2161-2162.
42. Basu, S., & Mukherjee, M. (2018). Incidence and risk of co-transmission of plasmid-mediated quinolone resistance and extended-spectrum β -lactamase genes in fluoroquinolone-resistant uropathogenic *Escherichia coli*: a first study from Kolkata, India. *Journal of Global Antimicrobial Resistance*, 14, 217-223.
43. Das, B., Mittal, N., Goswami, R., Adhana, D., & Rathore, N. (2018). Prevalence of multidrug resistance (MDR) and extended spectrum beta-lactamases (ESBLs) among uropathogenic *Escherichia coli* isolates from female patients in a tertiary care hospital in North India. *International Journal of Reproduction, Contraception, Obstetrics and Gynecology*, 7(12), 5031
44. Patwardhan, V., Kumar, D., Goel, V., & Singh, S. (2017). Changing prevalence and antibiotic drug resistance pattern of pathogens seen in community-acquired pediatric urinary tract infections at a tertiary care hospital of North India. *Journal of Laboratory Physicians*, 9(04), 264-268.
45. Thattai, S.J., & Santhosh, S. (2018). Prevalence of UTI in different age groups in a tertiary care hospital and their Antibioigram. *International Journal of Contemporary Medical Research*, 5(1), 2454-7379.
46. Jena, J., Sahoo, R. K., Debata, N. K., & Subudhi, E. (2017). Prevalence of TEM, SHV, and CTX-M genes of extended-spectrum β -lactamase-producing *Escherichia coli* strains isolated from urinary tract infections in adults. *3 Biotech*, 7(4).
47. Narayan, A., Gopi, S., Fushman, D., & Naganathan, A. N. (2019). A binding cooperativity switch driven by synergistic structural swelling of an osmo-regulatory protein pair. *Nature Communications*, 10(1).
48. Verma, V., Gupta, S., Kumar, P., Yadav, S., Dhanda, R.S., Gaiind, R., Arora, R., Frimodt-Møller, N., & Yadav, M. (2019b). Involvement of NLRP3 and NLRC4 inflammasome in uropathogenic *E. coli* mediated urinary tract infections. *Frontiers in Microbiology*, 10. .
49. Verma, V., Gupta, S., Kumar, P., Rawat, A., Singh Dhanda, R., & Yadav, M. (2019a). Efficient production of endotoxin depleted bioactive α -hemolysin of uropathogenic *Escherichia coli*. *Preparative Biochemistry and Biotechnology*, 49[6], 616-622.
50. Pandey, N. K., Verma, G., Kushwaha, G. S., Suar, M., & Bhavesh, N. S. (2020). Crystal structure of the usher chaperone YadV reveals a monomer with the proline lock in closed conformation suggestive of an intermediate state. *FEBS Letters*, 594(18), 3057-3066.
51. Zuberi, A., Ahmad, N., & Khan, A. U. (2017). CRISPRi induced suppression of fimbriae gene (fimH) of a uropathogenic *Escherichia coli*: an approach to inhibit microbial biofilms. *Frontiers in Immunology*, 8. doi: 10.3389/fimmu.2017.01552
52. Mukherjee, S., Mandal, R., Das, S., & Mukherjee, M. (2018). Effect of non- β -lactams on stable variants of inhibitor-resistant TEM β -lactamase in uropathogenic *Escherichia coli*: implication for alternative therapy. *Journal of Applied Microbiology*, 124(3), 667-681.

Affiliations

Arunita Ghosh¹ • Debojyoty Bandyopadhyay¹ • Snehashis Koley¹ • Mandira Mukherjee¹

¹ Department of Biochemistry and Medical Biotechnology, School of Tropical Medicine, 108, C.R. Avenue, Kolkata 700073, India

Original Article

Clinico-microbiological Profile of Urinary Tract Infection with Special Reference to Uropathogenic *E coli* : Antibiotic susceptibility Pattern, Phylogenetic Background and Virulent Factor Distribution from West Bengal, India

Snehashis Koley¹, Mandira Mukherjee², Prantiki Halder³, Ambar Bose⁴, Dushyant Lahre⁵, Sumi Mukhopadhyay⁶, Sudeshna Mallik⁷

Background and Objectives : Routine surveillance and monitoring studies pose a constant need to update clinicians on prevalent pathogens and rational and empirical treatment in Urinary Tract Infection (UTI). *Escherichia coli* (*E coli*) is the most commonly isolated uropathogen globally. Extended-Spectrum β -Lactamase (ESBL) production and β -Lactamase Inhibitor Resistance (BLIR) among these pathogens together with their uro-virulence determinants further complicate treatment approaches. This study investigated the clinico-microbiological pattern of UTI and determined the antibiotic sensitivity pattern, the phylogenetic background, and virulence determinants of *E coli*, the most commonly isolated uropathogen.

Methods : Uropathogens isolated by urine culture from community and hospitalized patients were biochemically speciated. Antibiotic susceptibility was tested by Kirby-bauer disk diffusion method. Phylogenetic background and virulence determinants of *E coli* isolates were identified by PCR. SPSS 16.0 was used for statistical interpretation.

Results : 45% of the urine samples showed growth positivity. 44% amongst them were *E coli*. All isolates were multidrug-resistant. 50% and 40% were ESBL producers and BLIR respectively. Former showed highest resistance to quinolone, fluoroquinolones, cotrimoxazole, and latter were resistant against all drugs tested except nitrofurantoin. Significant correlation existed between the β -lactams, quinolone, fluoroquinolones, cotrimoxazole ($p \leq 0.05$) resistance pattern. BLIR and ESBL *E coli* recorded highest prevalence of pathogenic phylogroup B2 and D respectively. Varied prevalence of fimbrial (fimH, papC, papEF, papG, GII) and toxin genes (iroN, hlyA, cnfI, iucD, cdtBU) in ESBL, BLIR and non-ESBL isolates were observed. Their distribution was statistically significant ($p=0.05$).

Interpretation and Conclusions : Nitrofurantoin is the drug of choice in empirical treatment of uncomplicated UTI. Aggressive and consistent investigation and health education are highly recommended for effective clinical management in UTI.

[J Indian Med Assoc 2022; 120(10): 48-53]

Key words : Antibiotic resistance, Phylogenetic background, Virulence factor, Uropathogenic *E coli*, Urinary Tract Infection.

Urinary Tract Infections (UTIs) pose a major public health issue globally. In everyday practice, at least for the first 72 hours, treating UTI is empirical. The known risk factors associated with UTI primarily constitute recent hospitalization, history of urinary instrumentation or Urological surgery, Neurogenic infections, Prostate cancer, benign hyperplasia of the prostate and bladder. Additionally, other potential

Editor's Comment :

- ESBL producing *E coli* being the most frequent isolate from complicated and uncomplicated UTI, correct choice of antibiotics in empirical treatment is very important.
- Nitrofurantoin is a good option for treating uncomplicated UTI and BL-BLI for complicated cases. Further decision could be taken after getting the urine CS (Culture & Sensitivity) report in hand.

Department of Biochemistry and Medical Biotechnology, School of Tropical Medicine, Kolkata 700073

¹M Tech, Research Scholar

²PhD, Associate Professor

³MD, Assistant Professor, Department of Tropical Medicine

⁴MSc, Research Scholar

⁵MD, Senior Resident, Department of Tropical Medicine

⁶PhD, Research Associate, Department of Laboratory Medicine

⁷MD, Associate Professor, Department of Tropical Medicine

and Correspondence Author

Received on : 01/07/2022

Accepted on : 23/07/2022

dangers include diabetes, HIV, and immuno-suppressive therapies.

Escherichia coli, *Klebsiella pneumoniae*, *Proteus mirabilis*, *Enterococcus faecalis*, and *Staphylococcus saprophyticus* were frequently identified micro organisms in UTI¹. 80-90% of all UTIs were caused by *E coli* designated as uropathogenic *E coli* (UPEC) to differentiate the pathogenic species from their commensal types in the intestinal flora. UPEC strains cause 75-95% of uncomplicated and 40-50% of

complicated UTIs².

Earlier, extended-spectrum cephalosporins (ceftriaxone, ceftazidime, cefotaxime,) contributed to the UTI treatment arsenal³. Unfortunately, the advent of Extended-Spectrum Lactamases (ESBLs) in *E coli* rendered resistance to these antibiotics to complicate treatment options^{4,5}. The genes encoding ESBLs were frequently harbored on plasmids with genes encoding resistance to aminoglycosides and sulphonamides. Moreover rampant use of quinolones, fluoroquinolones, aminoglycosides and sulphonamides in UTI also resulted in the selection and dissemination of multidrug-resistant bacteria⁶. Many *Enterobacteriaceae spp.* reported mutations that exhibited high quinolone and fluoroquinolone resistance. Therefore advent of multidrug resistance complicated UTI therapy and posed a serious health risk⁷.

UPEC exhibits varied Virulence Factors (VFs) to establish UTI. Essential VFs were broadly classified into two categories; cell surface and secretory types. Adhesins encoded by type I fimbriae and *pap* operon assisted in adhesion to host cell surface, an important event in the establishment of infection. Toxins and siderophores supported bacterial colonization and helped in persistence against host defense mechanism. Reports revealed that Horizontal Gene Transfer (HGT) enabled the evolution of UPEC from non-pathogenic strains by the acquisition of different VFs⁸. Moreover, studies on the phylogenetic background of pathogenic UPEC isolates indicated an incidence of phylotypes that belonged to commensal *E coli* strains⁹.

Appropriate clinical management in UTI demands information on UTI incidence concerning Gender, Age, Socio-economic status, Clinical symptoms, associated risk factors in the propagation of the illness, and characteristics of causative microorganisms and antibiotic exposures. This study was undertaken to investigate the clinico-microbiological aspects of UTI from Kolkata City in Eastern India with an insight into the antibiotic susceptibility pattern and uro-virulence determinants among *E coli*, the most commonly isolated uropathogen to administer appropriate therapeutics according to the severity of infection.

MATERIALS AND METHODS

Sample Collection and Bacteriology :

A total of 100 urine samples were collected from outdoor patients of the School of Tropical Medicine Kolkata and patients admitted to Carmichael Hospital of Tropical Disease, Kolkata, with clinical features of UTI. The case history and the clinical investigation data were collected from the hospital records. Urine culture positivity was tested for 24-48 hours. Samples that yielded significant monomicrobial growth ($>10^5$ cfu/ml)

were subjected to gram staining and biochemical analysis¹⁰. The study protocol was approved by the Institutional Ethics Committee.

Antibiotic Susceptibility and Extended-Spectrum β -Lactamase Production :

Kirby-bauer disk diffusion assay was conducted using antibiotics: Ampicillin(AMP; 10mcg), Cefalexin (CN;30mcg), Ceftriaxone(CTR;30mcg), Ceftazidime (CAZ;30mcg), Cefotaxime(CTX;30mcg), Cefoxitin (CX;30mcg), Nalidixic acid(NA;5mcg), Ciprofloxacin (CIP;5mcg), Levofloxacin(LE;5mcg), Amikacin (AK;10mcg), Gentamicin(GEN;10mcg), Tobramycin (TOB;10mcg), Chloramphenicol (C;30mcg), Cotrimoxazole (COT;25mcg), Nitrofurantoin (NIF;300mcg), Meropenem (MR;10mcg). Isolates resistant to CAZ, CTR and/or CTX were subjected to ESBL confirmatory test¹¹.

Bacterial total DNA isolation, Phylogenetic Background and Virulence gene determination :

Total DNA was released from whole bacterial cells using the boiling method. The phylogenetic background and virulence factors (*fimH*, *papC*, *papEF*, *papGI*, *GII*, *GII*, *iroN*, *hlyA*, *cnfI*, *iucD*, *cdtBU*) were identified by PCR using gene-specific primers on the total DNA as template¹².

Statistical Analysis :

Data were analyzed by One-way ANOVA, the Bonferroni test and Pearson's correlation coefficient for two-tailed bivariate correlation using SPSS 16.0 software¹³. A $p < 0.05$ was considered to be statistically significant.

RESULTS

45 out of 100 urine samples showed significant microbial growth after 24 hours of culture. The remaining samples were culture-negative even after 48-hour incubation. Samples collected from females (60%) revealed higher culture positivity rate than males (40%). Moreover highest (51.1%) culture positivity was reported in community-acquired uncomplicated UTI cases. The occurrence of UTI was mostly reported in the elderly population (>60 years, 28.88%), followed by age group; 41-50 years(26.66%) and 51-60 years (20%). 62.22% of the culture-positive patients belonged to a low socio-economic class with 64.44% without any addiction history towards alcohol or tobacco, 86.66% reported fever, 55.55% dysuria, 51.11% urinary frequency, 31.11% burning micturition, 26.67% suprapubic/flank pain and 6.66% reported urgency. 62.22% had a normal total WBC count (4000-11000), followed by 24.45% having raised WBC count (>10000). A very few patients (13.33%) reported a raised serum urea (>40 mg/dl) and serum creatinine

level(>1.2mg/dl). 33.33%, 8.89%, and 51.11% patients reported albuminuria, glycosuria, and pyuria respectively. 86.6% had associated one or more risk factors including diabetes mellitus (73.33%), history of recent hospitalization (26.66%), antibiotic intake (20%), urinary catheterization (13.33%), benign prostatic hyperplasia (11.1%), immunocompromised state (6.66%), renal stone (4.44%), and history of past UTI(4.44%).

The biochemically speciated pathogens were; *Escherichia coli* (20; 44.4%), *Pseudomonas aeruginosa* (11;24.4%), *Enterobacter spp.*(6;13.3%), *Klebsiella pneumoniae* (5;11.1%), *Staphylococcus aureus* (1;2.2%), *Staphylococcus epidermidis* (1;2.2%) and *Enterococcus spp.*(1;2.2%). The highest prevalence of *E. coli* (31%) in community-acquired uncomplicated UTI cases and *P. aeruginosa*(11%) and *K. pneumoniae* (8.8%) in hospital-acquired uncomplicated UTI cases were observed. Moreover comparable incidence of *E. coli* (4.4%, 2.2%), *P. aeruginosa* (4.4%, 2.2%) and *Enterobacter spp.* (4.4%, 4.4%) were reported from the community and hospital-acquired complicated UTI cases respectively. *E. coli* isolates were further characterized for antibiotic sensitivity and the occurrence of virulence determinants.

E. coli isolates revealed high resistance to β -lactams; AMP (95%), CN (80%), CX (90%), CAZ (90%), CTR (85%), CTX (85%), quinolone; NA (85%), fluoroquinolones; CIP (80%), LE(80%) and trimethoprim-sulfamethoxazole; COT (80%). The highest sensitivity was observed against NIF(75%) followed by AK (65%), TOB (65%), GEN (60%), C(50%), and MR(55%) respectively (Fig 1). Overall 14 discrete patterns of resistance were observed among the 20 isolates against the 16 antibiotics tested (Table 1). Furthermore, a significant correlation in the antibiotic resistance pattern was observed amongst the different antibiotics for CTR, NIF and MR respectively (Table 2).

Two out of the 20 *E. coli* isolates were sensitive to all three third-generation cephalosporins (3-GC; CTR, CAZ, CTX) however the remaining 18 isolates were resistant to either one/all 3-GCs. ESBL confirmatory test revealed that 10 out of 18 were ESBL producers and 8 were BLIR. A discrete difference in the antibiotic resistance pattern was observed amongst the ESBL and BLIR isolates to the 16 antibiotics tested (Figs 2A,B).

The overall predominance of the pathogenic phylogroup D followed by pathogenic phylogroup B2 and non-pathogenic or commensal phylogroup B1 was observed among ESBL isolates. However, the BLIR

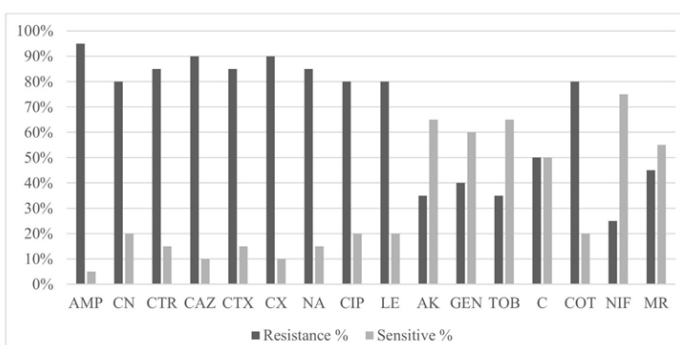


Fig 1 — Drug resistance among the uropathogenic *E. coli* isolates (n=20) against various antibiotics. AMP; ampicillin (10 μ g), CN; cefalexin (30 μ g), CTR; ceftriaxone (30 μ g), CAZ; Ceftazidime (30 μ g), CTX; Cefotaxime (30 μ g), CX; Cefoxitin (30 μ g), NA; Nalidixic acid (30 μ g), CIP; Ciprofloxacin (5 μ g), LE; Levofloxacin (5 μ g), AK; Amikacin (10 μ g), GEN; Gentamicin (10 μ g), TOB; Tobramycin (10 μ g), COT; Cotrimoxazole (25 μ g), NIF; Nitrofurantoin (300 μ g), MR; Meropenem (10 μ g). All assays were done in triplicate with each pathogenic isolate.

isolates primarily belonged to phylogroup B2 followed by B1 and D. Moreover the 2 non-ESBL isolates belonged to phylogroup B2 and B1 respectively (Fig 3).

Distribution of virulence gene *fimH* (adhesin gene) from the type I fimbriae operon, *papGI*, *papGIII* from pap-operon and toxin gene *cdtBU* were higher in BLIR isolates compared to their incidence in ESBL producers. Furthermore, the distribution of other pap-operon genes *papC*, *papEF*, and *papGII* was higher in ESBL isolates in comparison to BLIR isolates. However, the distribution of the toxin genes, *iroN*, *cnf1*, *iucD* were comparable. Additionally, it was observed that the pap-operon genes *papC*, *papEF*, *papGII*, and toxin genes *iroN*, *hlyA*, *cdtBU* were absent among non-ESBL producers. (Fig 4). The overall gene frequency of the virulence genes was statistically significant ($p=0.05$) among the non-ESBL, BLIR, ESBL isolates (Fig 4).

Table 1 — Resistance pattern of the <i>E. coli</i> isolates (n=20)	
Resistance Pattern	No of isolates
AMP, CAZ, CTX, NA, CIP, COT	1
AMP, CN, CTR, CAZ, CTX, CX, NA, CIP, COT	1
AMP, CN, CTR, CAZ, CTX, CX,	1
AMP, CN, CTR, CAZ, CTX, CX, NA, CIP, LE, AK, GEN, TOB, C, COT, MR	5
AMP, CN, CTR, CAZ, CTX, CX, NA, CIP, LE, C, COT, NIF	2
AMP, CX	1
AMP, CN, CTR, CAZ, CTX, CX, NA, CIP, LE, C, COT, NIF, MR	1
AMP, CN, CTR, CAZ, CTX, CX, NA, CIP, LE, AK, GEN, TOB, COT, NIF, MR	1
AMP, CN, CTR, CAZ, CTX, CX, NA, CIP, LE	1
AMP, CN, CTR, CAZ, CX, NA, CIP, LE, COT, NIF, MR	1
AMP, CN, CTR, CAZ, CTX, CX, NA, CIP, LE, C, COT	1
AMP, CTR, CAZ, CTX, CX, NA, CIP, LE, GEN, C, COT	1
AMP, CN, CTR, CAZ, CTX, CX, NA, CIP, LE, AK, GEN, TOB, COT, MR	1
AMP, CN, CTR, CAZ, CTX, CX, NA, CIP, LE, COT	1

Table 2 — Correlation of antibiotic resistance pattern in the uropathogenic *E. coli* isolates (n=20)

		AMP	CN	CTR	CAZ	CTX	CX	NA	CIP	L	AK	GEN	TOB	C	COT	NIF	MR
C T R	Pearson correlation	.546*	.840**	1	.793**	.608**	.793**	.608**	.608**	.840**	.308	.343	.308	.420	.490*	.243	.343
	Sig. (2-tailed)	.013	.000	-	.000	.004	.000	.004	.004	.000	.186	.139	.186	.065	.028	.303	.139
	Sum of squares & cross products	.850	2.400	2.550	1.700	1.550	1.700	1.550	1.550	2.400	1.050	1.200	1.050	1.500	1.400	.750	1.200
	Covariance	.045	.126	.134	.089	.082	.089	.082	.082	.126	.055	.063	.055	.079	.074	.039	.063
	N	20	20	20	20	20	20	20	20	20	20	20	20	20	20	20	20
N I F	Pearson correlation	.132	.289	.243	.192	-.081	.192	.243	.243	.289	-.182	-.236	-.182	.115	.289	1	.000
	Sig. (2-tailed)	.578	.217	.303	.416	.735	.416	.303	.303	.217	.444	.317	.444	.628	.217	-	1.000
	Sum of squares & cross products	.250	1.000	.750	.500	-.250	.500	.750	.750	1.00	-.750	-1.00	-.750	.500	1.000	3.750	.000
	Covariance	.013	.053	.039	.026	-.013	.026	.039	.039	.053	-.039	-.053	-.039	.026	.053	.197	.000
	N	20	20	20	20	20	20	20	20	20	20	20	20	20	20	20	20
M R	Pearson correlation	.187	.408	.343	.272	.057	.272	.343	.343	.408	.685**	.583**	.685**	.408	.408	.000	1
	Sig. (2-tailed)	.429	.074	.139	.246	.811	.246	.139	.139	.074	.001	.007	.007	.074	.074	1.000	
	Sum of squares & cross products	.400	1.600	1.200	.800	.200	.800	1.200	1.200	1.600	3.200	2.800	2.800	2.000	1.600	.000	4.800
	Covariance	.021	.084	.063	.042	.011	.042	.063	.063	.084	.168	.147	.147	.105	.084	.000	.253
	N	20	20	20	20	20	20	20	20	20	20	20	20	20	20	20	20

*Correlation is significant at the 0.05 level (2-tailed) ;

**Correlation is significant at the 0.01 level (2-tailed)

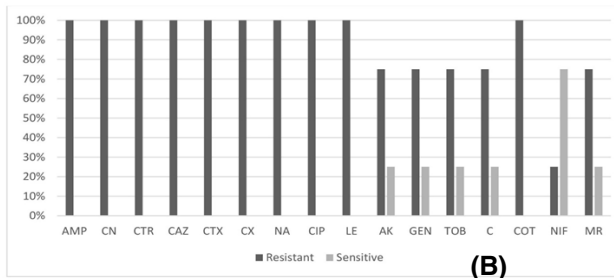
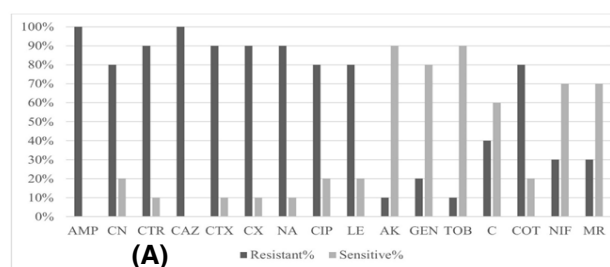
DISCUSSION

Community- or healthcare-acquired UTIs is clinically divided into complicated or uncomplicated and this classification determines the selection of antibiotics for treatment. Empirical therapy accentuated the emergence of antibiotic resistance, especially in uncomplicated UTI. This study documented information on the various aspects associated with UTI from Kolkata, an Eastern region in India.

Studies from different parts of India revealed a varied urine culture positivity rate ranging from 9.7-53.82%¹⁴⁻²¹. Our study reported an overall high culture positivity rate (51.1%) among community-acquired uncomplicated UTI cases in hospitalized patients with a higher prevalence among females (60%) than males (40%). The latter observation was consistent with findings from other studies^{15,18,20}. Highest occurrence of UTI was reported among the elderly population^{14,15,17} which was very similar to the observation stated in this study which consisted of a mean age group of 51.95 years that reflected the association between age and complicity in UTI.

Fever and dysuria were the most common clinical manifestations among the urine culture-positive patients in our study in concurrence to observations from other studies^{14,22}. Moreover several studies reported increased frequency to urinate as the commonest symptom in acute uncomplicated UTI patients^{14,23}. A similar symptomatology was also observed in our study although the symptoms were not always strong enough to conclude about the predictability of UTI.

Diabetes Mellitus (DM) affects the genitourinary system and frequently causes diabetic nephropathy. It also affects the immune system and enhances the chances of acquiring infection of the urinary tract. In our study, DM posed the most common risk factor associated with UTI (73.33%), very similar to the findings registered in another study¹⁴. Our study also indicated that clinical manifestations and associated risk factors may not always rightly predict the occurrence of UTI, reaffirming the fact that urine culture is the only confirmatory test to diagnose complicated and uncomplicated UTI.

Fig 2 – Antibiogram pattern amongst (A) ESBL and (B) BLIR *E. coli* isolates

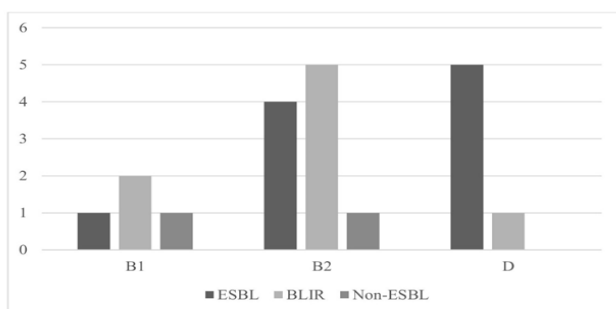


Fig 3 — Phylogenetic background of the ESBL, BLIR, non-ESBL *E. coli* isolates

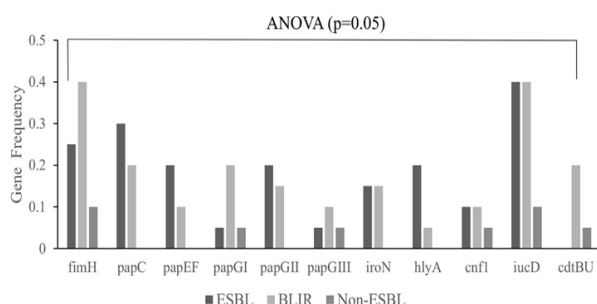


Fig 4 — Distribution of virulence genes among the ESBL, BLIR, non-ESBL *E. coli* isolates

Gram-negative bacilli constituted 93.4% of the uropathogens isolated in this study. Our study also demonstrated that *E. coli* was the leading uropathogen being responsible for UTI (44.4%) in Kolkata an Eastern region in India which was in concurrence with reports from other studies^{15,17,18,20}. However on the contrary several reports also revealed *S. aureus*, *P. aeruginosa* and *Klebsiella spp.* to be the most predominant uropathogen detected respectively^{19,24,25}.

The choice of antimicrobials for the treatment of UTI is often based on local resistance profiles of the uropathogen. The increasing pattern of resistance is emerging as a universal threat. In this study, the antibiotic susceptibility was conducted on the most frequent isolate *E. coli*. The highest resistance was documented against the 3-GC (CTR, CAZ, CTX) as well as the second generation of fluoroquinolones (CIP, LE) and COT. The highest sensitivity was seen against NIF as well as the aminoglycosides (AK, GEN, TOB). This result was very similar to previous studies conducted in the different States of India^{15,17,18}.

A significant correlation in the resistance pattern against CTR and CAZ, CTX, CX, CIP, LE, COT and MR and AK, GEN, TOB respectively further delineated the fact that resistance to the cephalosporin (CTR, CX, CAZ, CTX) group of the drug was accompanied by the fluoroquinolone (CIP, LE) group and COT and resistance against aminoglycosides (AK, GEN, TOB) was accompanied by MR respectively. Therefore our

study suggested that NIF should be an ideal choice for this population. However orally acceptable NIF formulation has drawbacks and was often not advised for severe upper UTI or individuals with systemic involvement and in such cases, aminoglycosides were the best choice. Therefore routine monitoring and intricate analysis of drug sensitivity patterns among uropathogens pose an absolute necessity to develop proper prescription policies. Our study also successfully detected the ESBL producers (50%) among *E. coli* isolates resistant to third-generation cephalosporins (CTR, CAZ, CTX) which was much higher than that reported from other studies¹⁴. Incidence of BLIR was also observed in 40% of the *E. coli* isolates. The ESBL and the BLIR isolates were highly resistant towards the fluoroquinolones in consistent with an Indian study²⁶. Our study also indicated that the BLIR isolates were more difficult to treat as they revealed resistance to all drugs tested except NIF. In this study AK, GEN, TOB was found to be effective against the ESBL producers together with NIF, MR and C. Siddaramappa, *et al*²⁶ in his study stated that at least 70% of UTI-associated ESBL-producing *E. coli* isolates could be sensitive to chloramphenicol and it may be an appropriate choice to treat the ESBL producers.

UPEC strains that routinely cause infections have been shown to belong to pathogenic phylogroups B2 and D²⁷. In our study, 50% of the ESBL producers belonged to phylogroup D followed by B2 (40%) which was in agreement with another previous Indian study²⁸. Moreover, for the first time, our study also showed that 62.5% of the BLIR isolates belonged to phylogenetic group B2 followed by B1 (25%) which was distinctly different from the phylogenetic background of the ESBL producers isolated in this study. Furthermore, our study also revealed a varied prevalence of virulence genes (*fimH*, *papC*, *papEF*, *papGII*, *hlyA*, *iroN*, *cnf1*, *iucD*, *cdtBU*) across the ESBL and BLIR isolates with the absence of some other virulence genes; *papC*, *papEF*, *papGII*, *iroN*, *hlyA*, *cdtBU* among the non-ESBL isolates very similar to another study that showed a high incidence of multiple virulence genes among the multidrug-resistant ESBL *E. coli*²⁸. An earlier study reported that the presence of *papC*, *cnf1* and *hlyA* in UPEC isolates played an important role in recurrent infections of the urinary tract²⁷. Therefore the incidence of *papC* (50%), *cnf1* (25%) and *hlyA* (25%) in *E. coli* isolated in this study indicated their possibility to cause recurrent infection.

Our study had some limitations. This work relied on very few UPEC isolates from a single hospital. Studies using many isolates from hospitals from different parts of West Bengal could provide broader

insights into the clinico-microbiological aspects of UTI from this Region in India. Future studies of such kind may be very useful to design appropriate clinical management strategies.

CONCLUSION

Therefore in the present study, we wanted to highlight the importance of investigating the clinico-microbial aspects of UTI together with intricate analysis on the antibiotic sensitivity pattern and distribution of uropathogen *E. coli*. Moreover increasing resistance against 3GCs together with the presence of β -lactamase inhibitor resistance indicated that Cephalosporins, as well as their inhibitor combination drugs, must not be recommended in treating UTI. However, nitrofurantoin can be started as an empiric antibiotic, which can later be altered according to the drug susceptibility pattern of the uropathogen.

Conflict of interest : The authors declare that they have no conflict of interest.

REFERENCES

1. Bien J, Sokolova O, Bozko P — Role of Uropathogenic *Escherichia coli* Virulence Factors in Development of Urinary Tract Infection and Kidney Damage. *Int J Nephrol* 2012; 2012: 681473. doi: 10.1155/2012/681473. Epub 2012 Mar 8.
2. Tan CW, Chlebicki MP — Urinary tract infections in adults. *Singapore Med J* 2016; **57**(9): 485-90.
3. Bush K — The impact of beta-lactamases on the development of novel antimicrobial agents. *Curr Opin Investig Drugs* 2002; **3**(9): 1284-90.
4. Rupp ME, Fey PD — Extended spectrum beta-lactamase (ESBL)-producing Enterobacteriaceae: considerations for diagnosis, prevention and drug treatment. *Drugs* 2003; **63**(4): 353-65.
5. Shah AA, Hasan F, Ahmed S, Hameed A — Extended-spectrum beta-lactamases (ESBLs): characterization, epidemiology and detection. *Crit Rev Microbiol* 2004; **30**(1): 25-32.
6. Bader MS, Loeb M, Brooks AA — An update on the management of urinary tract infections in the era of antimicrobial resistance. *Postgrad Med* 2017; **129**(2): 242-58.
7. Vellinga A, Cormican M, Hanahoe B — Antimicrobial management and appropriateness of treatment of urinary tract infection in general practice in Ireland. *BMC Fam Pract* 2011; 108(12).
8. Tarchouna M, Ferjani A, Ben-Selma W, Boukadida J — Distribution of uropathogenic virulence genes in *Escherichia coli* isolated from patients with urinary tract infection. *Int J Infect Dis* 2013; **17**(6): e450-3.
9. Mukherjee M, Koley S, Mukherjee S, Basu S, Ghosh B, Chakraborty S — Phylogenetic background of *E. coli* isolated from asymptomatic pregnant women from Kolkata, India. *J Infect Dev Ctries* 2015; **9**(7): 720-4.
10. Mukherjee M, Basu S, Majumdar M — Detection of bla_{TEM} and bla_{CTX-M} genes by multiplex polymerase chain reaction amongst Uropathogenic *Escherichia coli* strains isolated from hospitalized patients in Kolkata, India. *Int J Biosci* 2011; **1**(6): 64-9.
11. Mukherjee M, Basu S, Mukherjee SK, Majumder M — Multidrug-Resistance and Extended Spectrum Beta-Lactamase Production in Uropathogenic *E. coli* which were Isolated from Hospitalized Patients in Kolkata, India. *J Clin Diagn Res* 2013; **7**(3): 449-53.
12. Basu S, Mukherjee SK, Hazra A, Mukherjee M — Molecular Characterization of Uropathogenic *Escherichia coli*: Nalidixic Acid and Ciprofloxacin Resistance, Virulent Factors and Phylogenetic Background. *J Clin Diagn Res* 2013; **7**(12): 2727-31.
13. Liu Y, Huang H, Gao R and Liu Y — Dynamic Phenotypes and Molecular Mechanisms to Understand the Pathogenesis of Diabetic Nephropathy in Two Widely Used Animal Models of Type 2 Diabetes Mellitus. *Front Cell Dev Biol* 2020; **8**: 172.
14. Eshwarappa M, Dosegowda R, Aprameya IV, Khan MW, Kumar PS, Kempegowda P — Clinico-microbiological profile of urinary tract infection in south India. *Indian J Nephrol* 2011; **21**(1): 30-6.
15. Sood S, Gupta R — Antibiotic resistance pattern of community acquired uropathogens at a tertiary care hospital in jaipur, rajasthan. *Indian J Community Med*. 2012; **37**(1): 39-44.
16. Akram M, Shahid M, Khan AU — Etiology and antibiotic resistance patterns of community-acquired urinary tract infections in J N M C Hospital Aligarh, India. *Ann Clin Microbiol Antimicrob* 2007; **6**: 4.
17. Dash M, Padhi S, Mohanty I, Panda P, Parida B — Antimicrobial resistance in pathogens causing urinary tract infections in a rural community of Odisha, India. *J Family Community Med*. 2013; **20**(1): 20-6.
18. Sahay S — Prevalence of Urinary Tract Infection and the Antibiotic Sensitivity Pattern of the Most Common Uropathogen from a Tertiary Care Hospital of Jamshedpur. *Int J Med Res Prof* 2020; **6**(1): 51-3.
19. Ghosh S, Bandyopadhyay, Lahiri A, Adhya S, Bhattacharjee A — Pattern of antibiotic sensitivity in clinically suspected cases of urinary tract infections: An observation from a tertiary care hospital in west Bengal. *J Med Sci Clin Res* 2017; **5**(8).
20. Mehta M, Bhardwaj S, Sharma J — Screening of Urinary Isolates for the Prevalence and Antimicrobial Susceptibility of Enterobacteria other than *Escherichia coli*. *International Journal of Life Science and Pharma Research* 2013; **3**(1): 100-4.
21. Prakash D, Saxena RS — Distribution and antimicrobial susceptibility pattern of bacterial pathogens causing urinary tract infection in urban community of Meerut city, India. *ISRN Microbiol* 2013; **2013**: 749629.
22. McNulty CA, Richards J, Livermore DM, Little P, Charlett A, Freeman E, *et al* — Clinical relevance of laboratory-reported antibiotic resistance in acute uncomplicated urinary tract infection in primary care. *J Antimicrob Chemother* 2006; **58**(5): 1000-8.
23. Little P, Merriman R, Turner S, Rumsby K, Warner G, Lowes JA, *et al* — Presentation, pattern, and natural course of severe symptoms, and role of antibiotics and antibiotic resistance among patients presenting with suspected uncomplicated urinary tract infection in primary care: observational study. *BMJ* 2010; **340**: b5633.
24. Ehinmidu JO, Bolaji RO, Adegboye EEA — Isolation and antibiotic susceptibility profile of *Neisseria gonorrhoeae* isolated from urine samples in Zaria, northern Nigeria. *Journal of Phytomedicine and Therapeutics* 2003; **8**-11: 20-4.
25. Aboderin OA, Abdu AR, Odetoyn BW, Lamikanra A — Antimicrobial resistance in *Escherichia coli* strains from urinary tract infections. *J Natl Med Assoc* 2009; **101**(12): 1268-73.
26. Siddaramappa S, Pullela K, Thimmappa B, Devkota R, Bajaj R, Manivannan B, *et al* — Characterization of bla_{CTX-M} sequences of Indian origin and thirteen uropathogenic *Escherichia coli* isolates resistant to multiple antibiotics. *BMC Res Notes* 2018; **11**(1): 630.
27. Chakraborty A, Adhikari P, Shenoy S, Saralaya V — Molecular characterisation of uropathogenic *Escherichia coli* isolates at a tertiary care hospital in South India. *Indian J Med Microbiol* 2017; **35**(2): 305-10.
28. Padmavathy K, Padma K, Rajasekaran S — Multidrug Resistant CTX-M-Producing *Escherichia coli*: A Growing Threat among HIV Patients in India. *J Pathog* 2016; **2016**: 4152704.

COVID-19 Infection and Acute Kidney Injury in Paediatric Population: A Systematic Review and Meta-Analysis

Snehashis Koley¹, Ambar Bose¹, Sudeshna Mallik², Prantiki Halder²,
Mandira Mukherjee¹

¹Department of Biochemistry and Medical Biotechnology, School of Tropical Medicine,
Kolkata, West Bengal, India

²Department of Tropical Medicine, School of Tropical Medicine, Kolkata, West Bengal, India

Corresponding Author: Mandira Mukherjee

DOI: <https://doi.org/10.52403/ijrr.20221102>

ABSTRACT

Background: Acute Kidney Injury (AKI) posed a dreaded health complication in COVID-19 infection in paediatrics. In this review we systematically documented evidence on AKI incidence and associated death in COVID-19 infection among paediatric populations to aid healthcare workers towards appropriate clinical management.

Methods: Documentation on AKI incidence and associated death in COVID-19 infection worldwide in paediatrics in PubMed and medRxiv databases during December, 2019-June 19, 2021 was included in this study. Guidelines laid by Preferred Reporting Items for Systematic Reviews and Meta-analysis (PRISMA) were followed which facilitated clarity and transparency in the reporting.

Result: 23 out of 1976 total articles were eligible with mean age of 8.6 years. Database of Abstract of Reviews of Effects (DARE) tool was used for quality assessment. Studies on AKI incidence (19), mortality (19) and AKI related mortality (10) respectively were included for meta-analysis. An estimated AKI incidence of 28.8% with overall death of 2.3% and AKI related death of 5.2% were reported. Overall pooled AKI incidence in the paediatric population was statistically significant.

Conclusion: Therefore, aggressive investigation of COVID-19 infection associated with AKI in paediatrics posed a necessity for efficient health-care management.

Keywords: Acute kidney injury; Box plot; COVID-19; Forest plot; Meta-analysis

INTRODUCTION

The coronavirus outbreak is a fast-emerging pandemic, empowering immense stress on community healthcare management globally. The etiologic agent identified as a novel coronavirus; SARS-CoV-2 caused acute respiratory illness described as Coronavirus Disease 2019 (COVID-19). In January 2020, COVID-19 was declared a global health emergency of international concern by the World Health Organization (WHO).⁽¹⁾ COVID-19 infection was reported in more than a 272.6 million people of all ages with a mortality of 5.33 million worldwide as on December 16, 2021 (John Hopkins University Coronavirus Tracker). Our knowledge about the pathophysiology, diagnosis, management, and post-infection complications of COVID-19 infection has developed substantially over the past two and half years however several

areas are yet to be explored to combat the evolving pandemic effectively.⁽²⁾

Coronaviruses (CoVs) (known as *Coronaviridae* and belonging to the order *Nidovirales*) are a group of highly diverse, enveloped, positive-sense, and single-stranded RNA viruses of zoonotic origin. These groups of viruses can be subdivided into four different classes: *Alphacoronavirus*, *Betacoronavirus*, *Gammacoronavirus*, and *Deltacoronavirus*.⁽³⁾ Some variants are HCoV-OC43, HCoV-229E, HCoV-NL63, and HCoV-HKU1, which generally cause mild respiratory illnesses like the common cold.^(4,5) Intricate studies were conducted to understand the infection strategy of these viruses. The SARS-CoV2 virus required an angiotensin-converting enzyme (ACE-2) to infect the host. ACE-2 was found to be expressed in various organs including the kidney, in addition to alveolar cells in the lungs, the latter being the primary site of injury by the virus as it reached the lungs after entry through the nose or mouth.^(6,7) Dipeptidyl peptidase 4 (DPP-4), a type II transmembrane ectopeptidase was found to act as the receptor for the MERS-CoV virus.⁽⁸⁾ DPP-4 was found to be principally expressed in type I and II cells, alveolar macrophages, vascular endothelia, and pleural mesothelial and hence showed signs of lower respiratory tract-associated illness.⁽⁹⁾ Moreover, DPP-4 similar to ACE-2 was also found to be expressed in different tissues including the renal tubular cells. Furthermore, in both SARS and MERS infections, viral RNA has been found in kidney tissue and urine.⁽¹⁰⁾

Patients infected by nCoV-19 were categorized into three types, mild, severe, and critical, according to the severity of the symptoms. Serious patients report dyspnea, respiratory frequency ≥ 30 /minute, blood oxygen saturation $\leq 93\%$, partial pressure of arterial oxygen to fraction of inspired oxygen

ratio less than 300, and/or lung infiltrates greater than 50% within 24 to 48 hours.⁽⁴⁾

Primarily thought to be immune to the deleterious effect of COVID-19, children were susceptible to the virus. Most of the cases of COVID-19 in children are mild diseases like other viral infections. Nonetheless, there is a high probability that it can be fatal in children with underlying chronic diseases of the heart, liver, and kidney, children suffering from malnutrition, and children with immune deficiency. The Centers for Disease Control and Prevention published a case definition for Multisystem Inflammatory Syndrome in Children (MIS-C) associated with recent COVID-19 infection in May 2020 along with a public health recommendation. Children showed symptoms resembling those of Kawasaki Disease including toxic shock syndrome, macrophage activation syndrome, secondary hemophagocytic lymphohistiocytosis, and multisystem organ involvement, including AKI.⁽¹¹⁾ An independent risk factor for mortality in patients with acute respiratory distress syndrome was the development of AKI irrespective of their age. High intrathoracic pressures in ventilated children can cause low cardiac output, resulting in inadequate renal perfusion. Subsequent gas exchange abnormalities that resulted in hypoxemia, hypercarbia, and systemic acidosis might affect renal vascular resistance, which might change renal perfusion pressures and cause AKI.⁽²⁾ Moreover, studies found the deleterious effect of AKI on patient outcomes like mortality, length of stay (LOS) and duration of ventilation (PICU LOS and Length of Ventilation [LOV] were almost twice as long in patients with severe AKI compared to those with no AKI, which has a significant effect in the case of COVID-19 pandemic where ICU resources may be scarce.⁽¹²⁾ However, recent emerging evidence shows that AKI is prevalent in COVID-19 patients and that

SARS-CoV-2 specifically invades the kidneys⁽¹³⁾ and more than 20% of the deceased patients are affected by chronic kidney disease.⁽¹⁴⁾ Since there exist little early data on the incidence of AKI in paediatrics with COVID-19 infection, the rates, outcomes, and clinical characteristics was not conclusively elucidated which results in difficulty in paediatric health management issues. Worldwide COVID-19 vaccination among adults and children between 12-18 years has effectively aided the present clinical management of the viral infection. However, the paediatric population below 12 years has remained vulnerable to COVID-19 disease severity.

This systemic review and meta-analysis aimed to account for the important summary of published reports on AKI incidence, mortality, and mortality due to AKI in the course of COVID-19 infection in the paediatric population across the world.

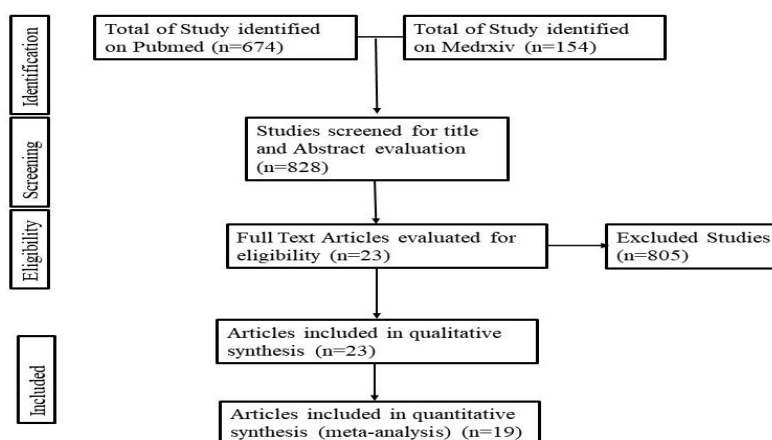
METHODOLOGY

Review of literature

This study conducted a comprehensive search of scientific publications using the keywords

“COVID-19”, “Coronavirus”, “SARS-CoV-2”, “Kidney injury”, “Paediatric”, “MIS-C” in the ‘Pubmed’ and ‘medRxiv’ electronic database spanned from December 2019 to June 19, 2021. The Preferred Reporting Items for Systematic Reviews and Meta-Analyses “PRISMA” checklist (Figure 1) used to compose the systematic review.⁽¹⁵⁾ Inclusion criterion included different studies (original research articles on relevant experimental and observational research, case studies, and reports) in paediatric (age <18 years) populations on the incidence of COVID-19 with AKI and reported mortality as an outcome of interest. The data were retrieved from the studies relevant to zone and country, duration, the mean age of the patients, total population included, AKI incidence, MIS-C incidence and diagnosis associated with kidney involvement in COVID-19 infection. Publications that included systemic review and meta-analysis on COVID-19 in paediatrics with incidence of AKI and publications not in English language excluded from the study.

Figure 1. - PRISMA Flowchart for the different stages of the systematic review on acute kidney injury in COVID-19 infection



Quality Assessment

The quality assessment on the included publications was evaluated using the Database of Abstract of Reviews of Effects (DARE)

tool.⁽¹⁶⁾ The study quality had five questions: (i) were exclusion/inclusion criteria reported; (ii) was the search adequate; (iii) were the included studies synthesized; (iv) was the

quality of the included studies assessed and (v) are sufficient details about the individual included studies presented. Publications that met at least four out of five criteria were included for meta-analysis. Two reviewers with a third reviewer to settle in case of dispute performed the quality assessment process.

Statistical analysis

The statistical analysis was performed using Open Meta-Analyst software (for Windows 10 version; Brown University, Providence, USA).⁽¹⁷⁾ Random effects models and the Dersimonian-Laird method used to examine the pooled estimate of the incidence of AKI, mortality and AKI associated mortality in COVID-19 infected paediatric populations. All outcomes evaluated at their 95 % confidence interval (CI). The outcome from each study along with the combined estimated outcomes with 95% confidence interval (CI) represented by Forest plots. The extent of statistical heterogeneity among different study groups was assessed by I^2 values, where $I^2 > 75\%$ indicated high statistical heterogeneity. The mean, median values with the interquartile ranges (IQR) were calculated. Funnel Plots were drawn using QI-Macros add-ins in Microsoft Excel 2016 to graphically assess publication bias in each study. Box plots drawn using Microsoft Excel

2016 and were used to visualize the distribution of the data for each parameter (Student's T-test was applied to calculate the statistical significance. A P-value ≤ 0.05 used to consider statistically significant). The data obtained through independent-sample Student's T-test for AKI incidence and mortality used to infer the difference and a P-value ≤ 0.05 was used to consider the statistical significance.

RESULTS

Study details and selection criteria

The database search yielded 23 reports that included outcomes of interest in the COVID-19 infected paediatric population. (Figure 2). Out of the 23 studies, 3 were retrospective studies, 6 included case reports, 1 each of retrospective cohort, observational and prospective study and 1 cross-section analysis (Table 1). Most of the studies were reported from the USA (10) followed by UK (3), China (2), France (2), Italy (2), Chile (1), Luxembourg (1), Russia (1), Saudi Arabia (1) and India (1) (Figure 2). The mean age of the study population was 8.6 years. 19 out of the 23 studies reported sufficient data on the incidence of AKI according to Kidney Disease: Improving Global Outcomes (KDIGO) criteria in the COVID-19 infected patients.

Figure 2. - Reports on incidence of AKI from adult and paediatric patients in COVID-19 infection across the globe

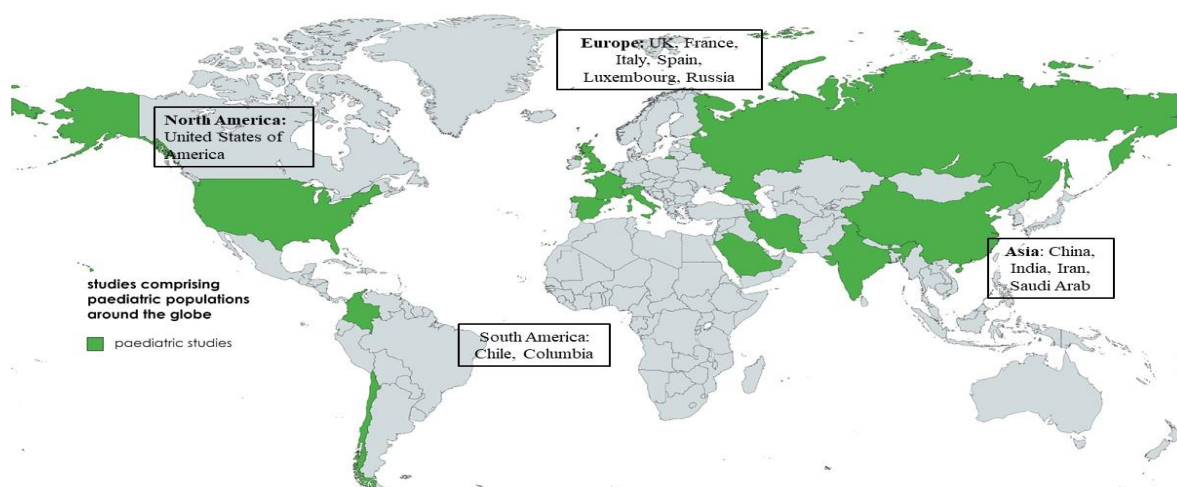


Table 1. Details on the pediatric population with COVID-19 infection

Article Name	Zone and Country	Time of Study	Type	Mean age (years)	Population	AKI reported and stages	MIS-C incidence	Diagnosis
González-Dambras et al. (2020) ⁽¹⁸⁾	Chile, Colombia, Italy, Spain, United States	Dec 2019 – April 23, 2020	Retrospective Multicenter Study	4.0	17	3 (18%)	NA	13 out 17 high CRP on admission
Dufort et al. (2020) ⁽¹⁹⁾	New York, USA	March 1, 2020 - May 10, 2020	Multicenter Retrospective Study	0-20	99	10 (10%)	Y	Kawasaki's disease, toxic shock syndrome, or myocarditis
Lee et al. (2020) ⁽²⁰⁾	Boston, USA	March 17, 2020 – June 6, 2020	Retrospective Study	9.0	28	6 (21%)	Y	High CRP in 93%. complete or incomplete KD, and coronary abnormalities were found
Whittaker et al. (2020) ⁽²¹⁾	England	March 23, 2020 - May 16, 2020	Uncontrolled Multicenter case series Study	9.0	45	11 (24%)	Y	myocardial dysfunction. High CRP, neutrophilia, and ferritin. Troponin concentrations 68%
Capone et al. (2020) ⁽²²⁾	New York, USA	April 17, 2020 - May 13, 2020	Retrospective study	8.6	33	23 (70%)	Y	72% developed myocardial dysfunction. Complete KD 64%, High CRP
Wang et al. (2020) ⁽²³⁾	Wuhan, China	January 24, 2020 - March 20, 2020	Retrospective study	13 months, 10 months, 8 years	238	3 (1.3%)	NA	high CRP, IL-6, BUN and creatinine
Samies et al. (2020) ⁽²⁴⁾	Alabama, USA	May, 2020	Case Study	16	1	Not reported	NA	High BUN, creatinine, Aminotransferase and aspartate aminotransferase and creatine kinase
Qiu L et al. (2020) ⁽²⁵⁾	China	January 25, 2020 - March 16, 2020	Case Study	8 months	1	Not reported	NA	lymphocytes, white blood cells, CD3+, CD4+, CD8+ T cells and fibrinogen were below the normal range.
Niño-Taravilla et al. (2020) ⁽²⁶⁾	Chile	May 11, 2020 - May 28, 2020	Case Study	8	1	Not reported	Y	Multi-organ dysfunction with acute kidney failure, metabolic acidosis, hyponatremia, slight increase in creatinine, lactate and hypoalbuminemia.
Mamishi et al. (2020) ⁽²⁷⁾	Iran	March 7, 2020 - June 23, 2020	Retrospective study	7.0	45	13 (29%)	Y	Kawasaki-like disease (69%), while toxic shock-like and sepsis-like diseases 11%
Grimaud M et al. (2020) ⁽²⁸⁾	France	April 15-27, 2020	Retrospective study	10 (2.9–15)	20	14 (70%)	NA	High CRP and procalcitonin
Oberweis et al. (2020) ⁽²⁹⁾	Luxembourg	NS	Case report	8	1	Not reported	NA	Rapid increase in CRP, IL-6, ferritin, C-reactive protein, leukopenia with

								lymphopenia thrombocytopenia, renal function impairment serum creatinine, hepatic cytolysis
Toubiana et al. (2020) ⁽³⁰⁾	Paris, France	April 27, 2020 - May 15, 2020	Prospective Study	7.9 (3.7-16.6)	21	11 (52%)	NA	Lymphopenia in 81%, transient kidney failure in 52 %
Shahbaznejad L et al. (2020) ⁽³¹⁾	Sari, Iran	March 28,2020 - June 24, 2020	Case study	5.37 ± 3.9	10	3 (30%)	Y	High level of CRP, Lymphopenia, hypoalbuminemia
Godfred-Cato et al. (2020) ⁽³²⁾	District of Columbia and New York, USA	March 2020- July 2020	Retrospective study	8 (2 weeks to 20 years)	570	Distribution of these AKI incidences in class I (37.9%) and class II (16.6%) stages of MIS-C patients	Y	Shock, cardiac dysfunction, gastrointestinal symptoms, significantly elevated markers of inflammation and cardiac damage
Dionne et al. (2020) ⁽³³⁾	Boston, USA	March 1, 2020- May 30, 2020	Retrospective cohort study	9.7 (2.7–15.0)	25	2 (8%)	Y	Hypotension (44%) and acute renal failure (8%), elevated values for C-reactive protein,interleukin 6
Derespina et al. (2020) ⁽³⁴⁾	New York, USA	March 14, 2020 - May 2, 2020	Retrospective study	15 (1 month – 21 years)	70	9 (12.5%)	Y	Elevated CRP, creatinine.
Stewart et al. (2020) ⁽³⁵⁾	London, UK	Till March 25,2020	Retrospective study	0- 16 years	52	15 (29%)	Y	Higher creatinine in 46%, Effected with AKI
Bjornstad et al. (2020) ⁽³⁶⁾	United States, Western Europe, Eastern Europe/Russia	April 15, 2020 - May 20, 2020	Cross-sectional analysis	Age 1 month to 18 years; Median range 11	106	47 (44%) AKI stage-1, 47%, stage 2 – 23%, stage 3 – 30%	NA	High prevalence of AKI in critically ill children
Deep A et al. (2020) ⁽¹²⁾	United Kingdom	March 14, 2020, to May 20, 2020	Observational study	11.0 (7-14)	116	48 (41.4%)	Y	27% patients diagnosed to develop severe AKI
Kari et al. (2021) ⁽³⁷⁾	Jeddah, Kingdom of Saudi Arabia	March 1, 2020 – Mid-July 2020	Retrospective multicentre study	54.6 (30.0 – 79.3) for AKI, 74.7 (61.1 -88.3) for non-AKI	89	19 (21%) AKI Stage 1: (58%), Stage 2: (31.5%), Stage 3: (10.5%)	NA	Baseline creatinine, estimated glomerular filtration rate (eGFR), highest creatinine.
Chopra et al. (2021) ⁽³⁸⁾	New Delhi, India	March 1, 2020 – November 30, 2020	Retrospective study	6 (1.04 – 10)	105	24 (22.8%) AKI Stage 1: (33.3%), Stage 2: (29.2%), and Stage 3:(37.5).	NA	Elevated AKI, fever (73.3%) vomiting (37.1%). Diarrhea (11.4%)
Basalely et al. (2021) ⁽¹¹⁾	New York, USA	March 9, 2020 – August 13, 2020	Retrospective multicentre study	8.2 (1.5 – 13.8)	97	8 (8.2%) AKI; AKI Stage I: (75%), Stage and 3: each (12.5%)	Y	Elevated AKI

Data Analysis

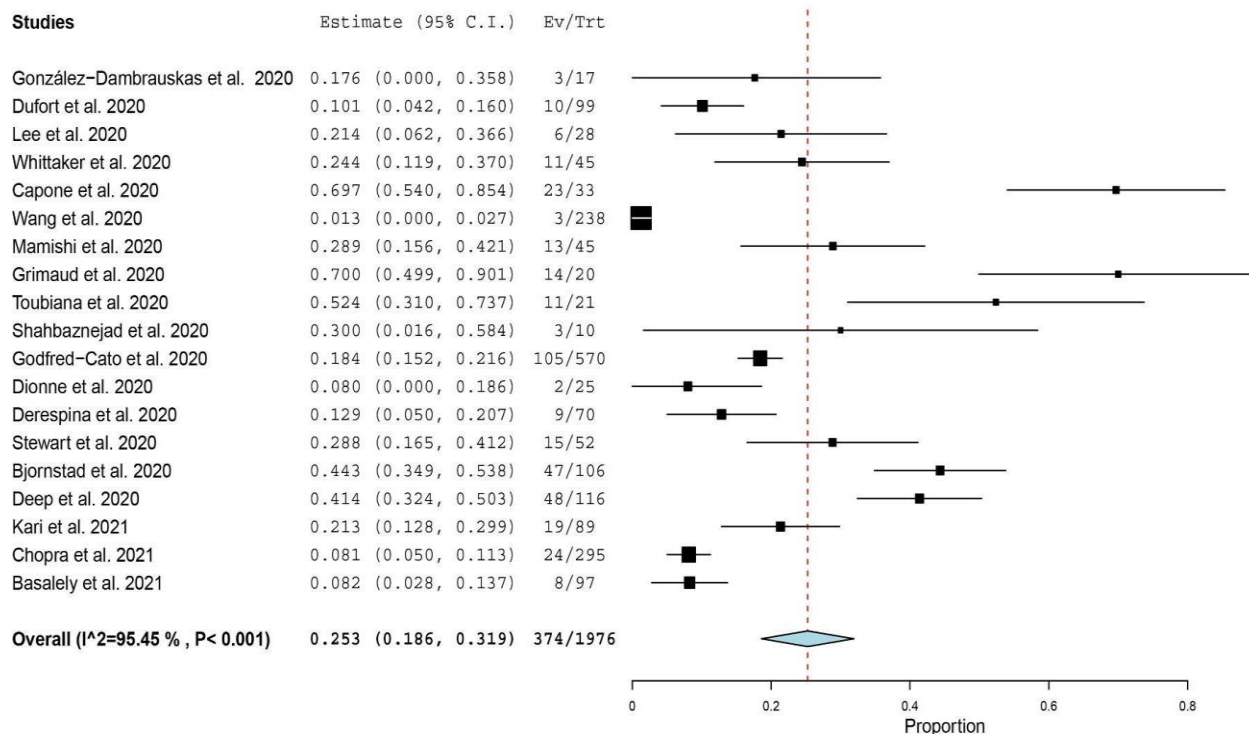
The overall sample across the 19 different studies on paediatric population with AKI was 1976; however, the incidence estimated from the individual studies included a total sample size ranging from 10-570. Meta-analysis conducted on the 19 different studies demonstrated 25.3% (18.6-31.9%) [$I^2 = 95.35\%$, $P < 0.001$] pooled (95% CI) AKI incidence in the COVID-19 infected paediatric population (Figure 3A, 3B) with considerable heterogeneity.

Our analysis revealed a very low overall mortality rate among the 19 studies analyzed. The estimated pooled mortality value (95% CI) of 2.3% (1.2 – 3.3%) [$I^2 = 61.49$, $P < 0.001$] was evident in an overall sample size of 1976 (ranging from 10-570) (Figure 3C, 3D) with substantial heterogeneity. Mortality due to AKI was reported in 10 out of 19 different studies with overall sample size $n = 215$,

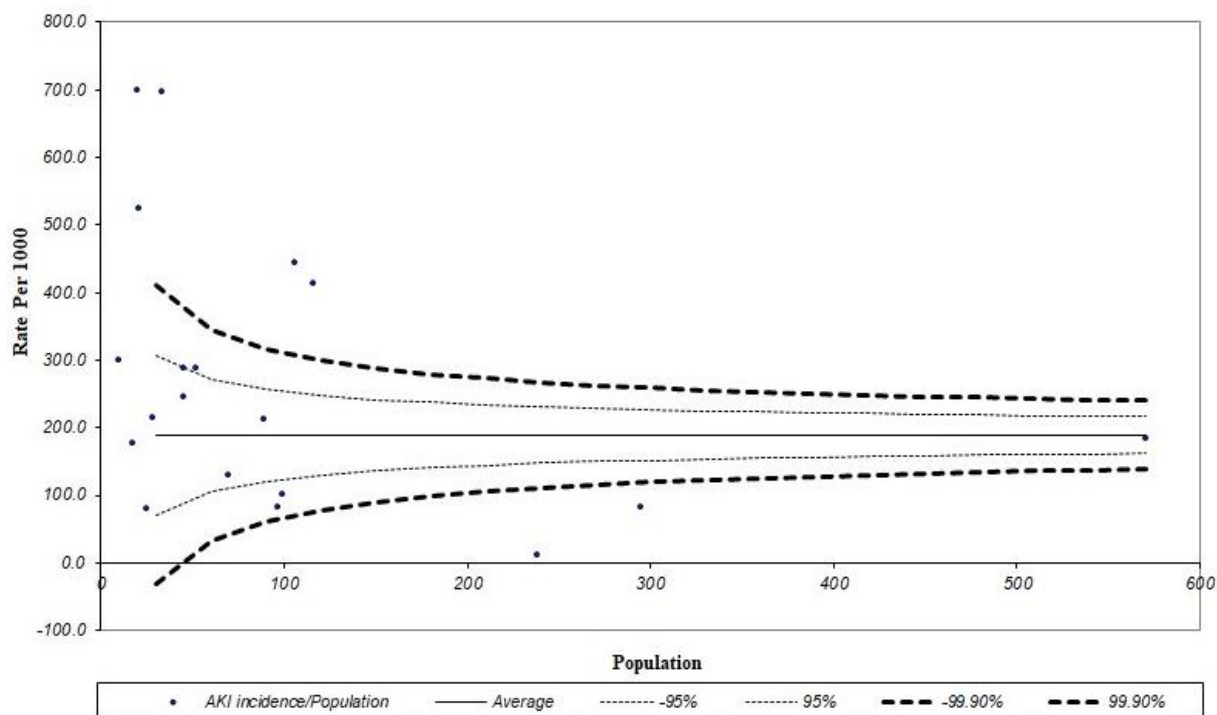
however, the incidence from the individual studies included a total sample size ranging from 6-48. Our analysis on estimated mortality rate due to AKI showed a higher pooled mortality (95% CI) of 5.2% (1.4 – 9.0%) [$I^2 = 42.51\%$, $P = 0.074$, $n = 10$] in the overall sample size of 215 (ranging from 6 – 48) (Figure 3E, 3F) with moderate heterogeneity.

Figure 3. - Forest Plot of the meta-analysis (A, C, E) and Funnel Plot (B, D, F) for AKI incidence, overall mortality, and AKI-related death respectively in COVID-19 infection in paediatrics across different studies. The lower diamond in the Forest Plot represents the pooled estimate. 'Ev' indicates the event sizes. 'Trt' indicates the total number of COVID-19 positive patients screened (A, C) and the total number of COVID-19 positive patients screened with AKI only (E) in this population

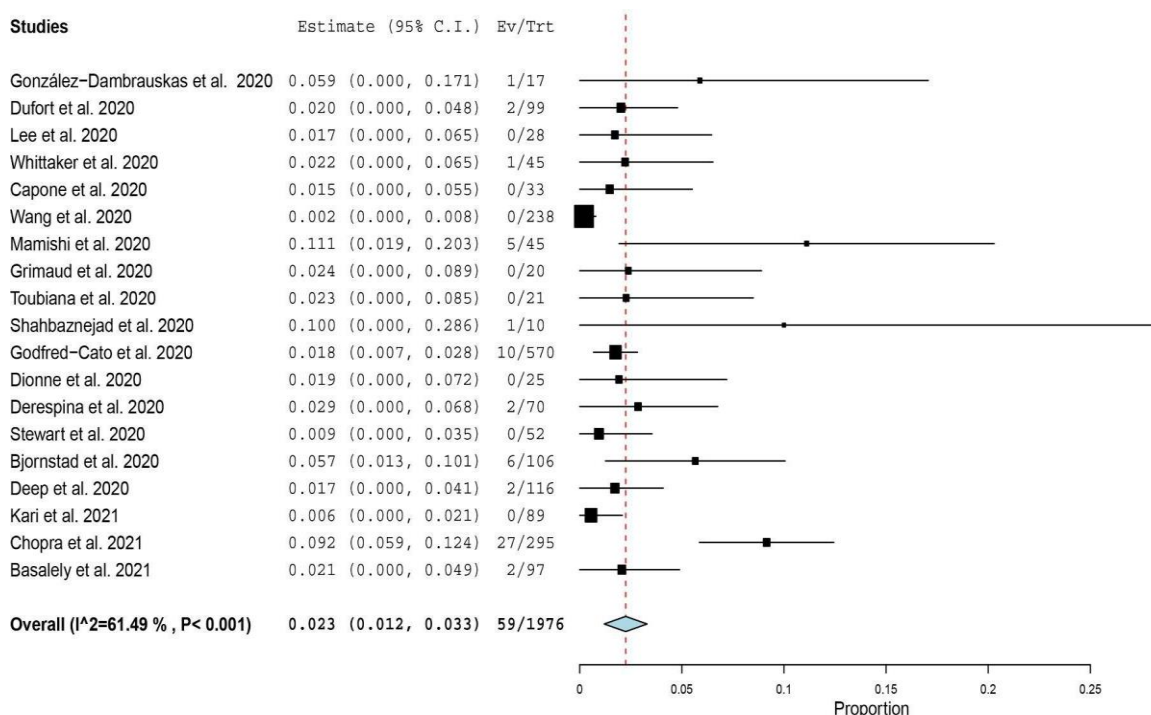
A



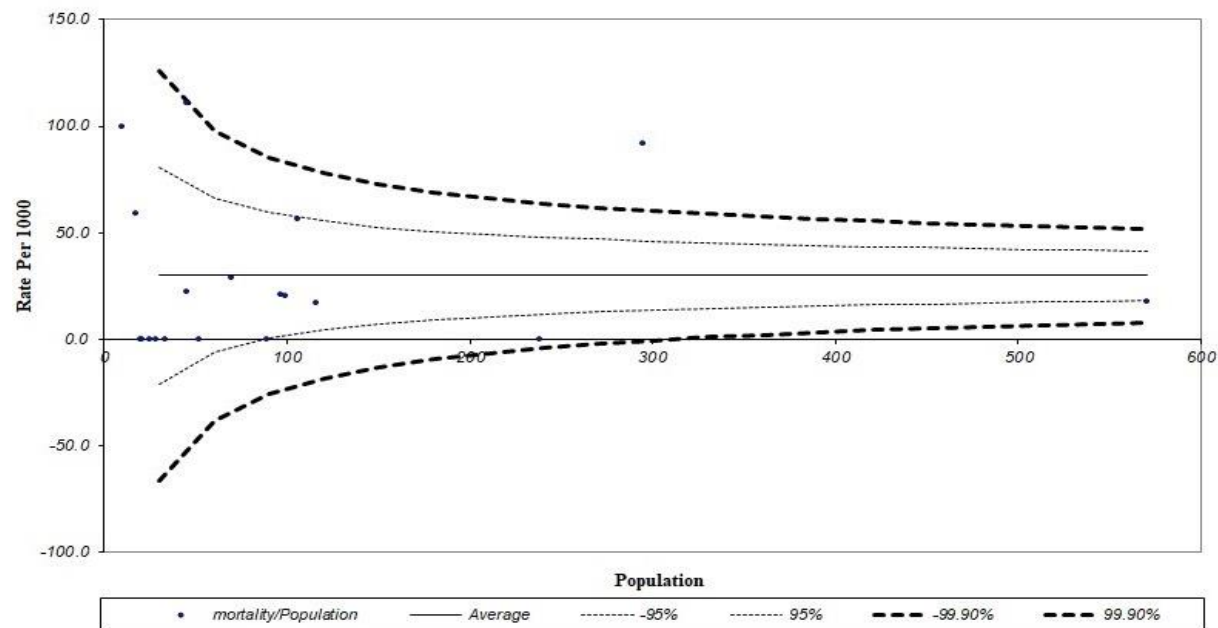
B



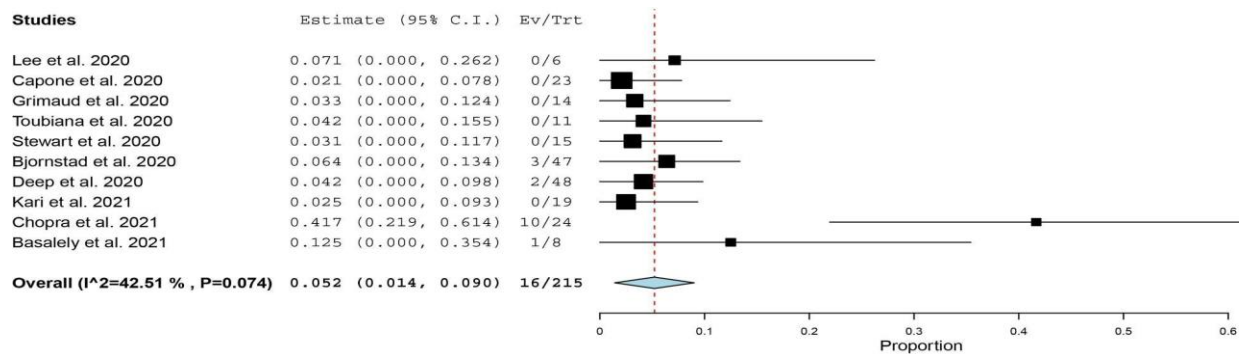
C



D



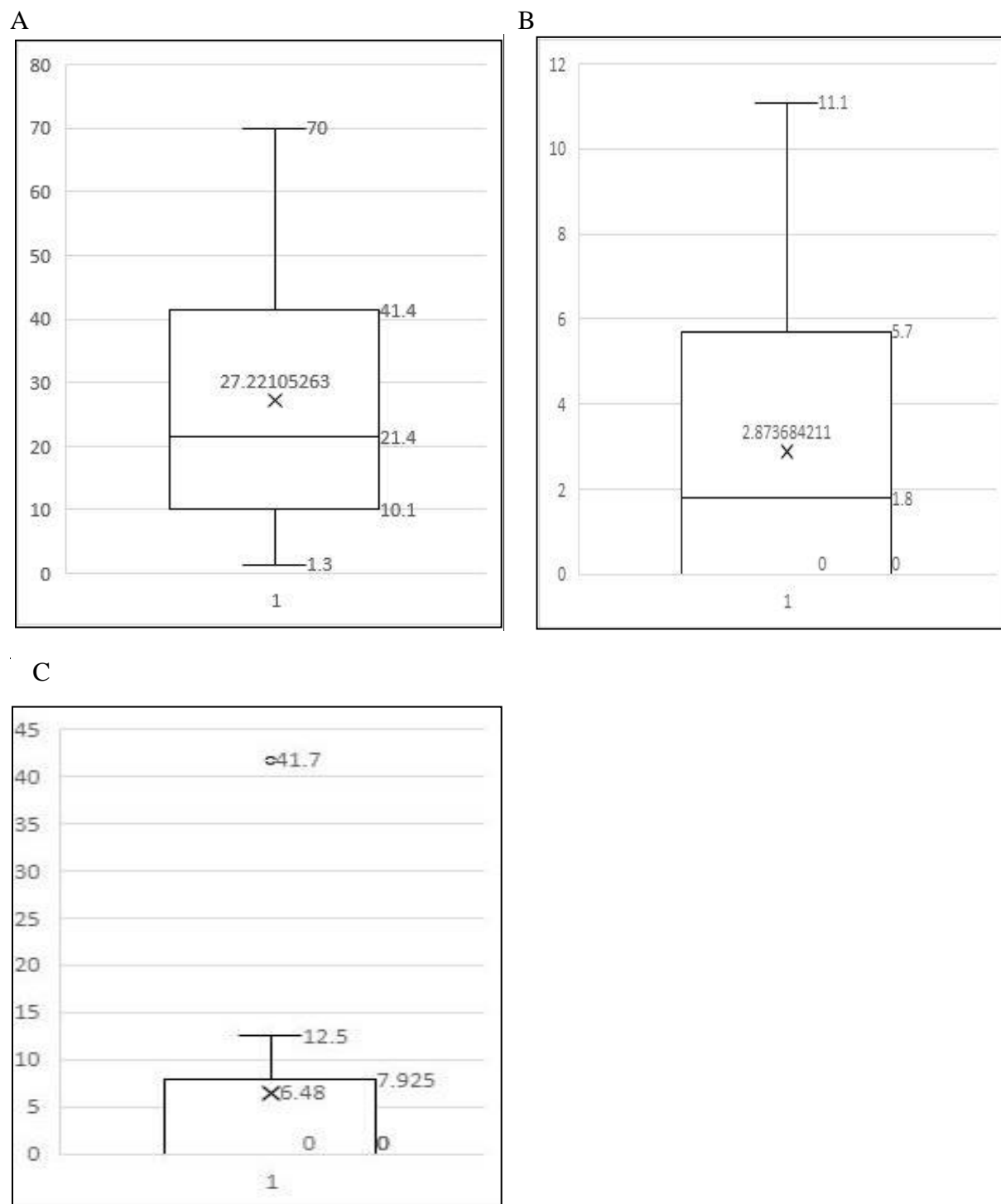
E



F

Box plots represented the median (IQR) AKI incidence estimate [21.4% (10.1 – 41.4%), $P < 0.10$], overall estimated death [1.8% (0 – 5.7%), $0.001 < P$] and estimated death due to AKI [0% (0 – 7.295%) $0.001 < P$] in the COVID-19 infected paediatric population (Figure 4A, 4B, 4C).

Figure 4.– Box plot distribution of AKI incidence, overall mortality, and AKI-related death in COVID-19 infection in the paediatrics (A, B, C) respectively from different studies. The circular dots represent the outliers.



DISCUSSION

There were several reports on significant incidence of AKI associated with morbidity and mortality in adults with COVID-19 infection across the globe, which aided clinicians to formulate appropriate health-care guidelines.⁽³⁹⁾ Reports on AKI prevalence in paediatrics with COVID-19 with related morbidity and mortality were infrequent. In this systemic review and meta-analysis we accumulated the findings of relevant individual reports on AKI, mortality and mortality rates due to AKI in COVID-19 infection in the paediatric population and presented balanced important summary of findings with due consideration of any error in the evidence. More precise estimate of the effect size, which enhanced simplification of the results from the individual studies, presented.

A wide variance of incidence of AKI in critically ill COVID-19 infected paediatric patients was estimated; 70.0% (49.9 – 90.1%) in a population of 20 from a study in the France⁽²⁸⁾ to as low as 1.3% (0.0– 2.7%) in a population of 238 from a study in Wuhan, China.⁽²³⁾ Meta-analysis on reports from 14 different paediatric population (n=1247) by Raina et al.⁽²⁾ revealed 30.51% (21.84 – 39.94%) pooled prevalence of AKI associated with COVID-19 infection which was higher compared to our study; 25.3% (18.6 – 31.9%) in the COVID-19 infected paediatric population (n=1976). Additionally, they reported a higher median (IQR) incidence of 26.6% (17.8–43.6%) among their paediatric patients associated with AKI, in comparison to the estimated incidence obtained from this study 21.4% (10.1 – 41.4%).

Among the paediatric population, AKI incidence and mortality rate revealed high statistical heterogeneity, although mortality estimated due to AKI retained a very low value. Therefore, AKI may complicate COVID-19 clinical management and framing of appropriate guidelines is necessary to address effective clinical management.

At present, COVID vaccination to eligible kids and teenagers is an absolute necessity. A vaccine that lowers COVID transmission in this age group might restrict transmission from kids and teens to older adults. Such a strategy will help to diminish hospital admission especially with COVID-19 infection and avoid complications in children with co-morbid conditions and will help to control the health-care management in resource limiting countries like India.

The main limitation in this study was the insufficient sample size among the paediatric population especially on mortality rate due to AKI. Moreover, as to date, there is paucity of literature on COVID-19 and AKI incidence from different parts of the world in the aforementioned population, which further limits the study globally. Nonetheless, in our meta-analysis for AKI mortality in COVID-19 paediatric populations, only studies with a sample size >5 was included to eliminate the outcome of studies with small sample sizes.

CONCLUSION

Our study provided important insights of AKI in paediatric population with COVID-19 which will aid clinicians in better preparedness towards health-care management. AKI incidence in COVID-19 infection was statistically significant which is alarming in view of this ongoing fourth wave COVID-19 pandemic era.

Acknowledgement: None

Conflict of Interests: All authors declare that there is no conflict of interest.

Funding sources: None.

REFERENCE


1. Puliatti S, Eissa A, Eissa R, Amato M, Mazzone E, Dell'Oglio P, et al. COVID-19 and urology: a comprehensive review of the literature. *BJU Int.* 2020;125(6):E7–14.
2. Raina R, Chakraborty R, Mawby I, Agarwal N, Sethi S, Forbes M. Critical analysis of acute kidney injury in paediatric COVID-19 patients in the intensive care unit. *PediatrNephrol.* 2021;36(9):2627–38.
3. Zumla A, Chan JFW, Azhar EI, Hui DSC, Yuen KY. Coronaviruses-drug discovery and therapeutic options. *Nat Rev Drug Discov.* 2016;15(5):327–47.
4. He F, Deng Y, Li W. Coronavirus disease 2019: What we know? *J Med Virol.* 2020; 92(7):719–25.
5. Payus AO, Liew Sat Lin C, Mohd Noh M, Jeffree MS, Ali RA. SARS-CoV-2 infection of the nervous system: A review of the literature on neurological involvement in novel coronavirus disease (COVID-19). *Bosn J of Basic Med Sci.* 2020; 20(3):283–292.
6. Li W, Moore MJ, Vasilieva N, Sui J, Wong SK, Berne MA, et al. Angiotensin-converting enzyme 2 is a functional receptor for the SARS coronavirus. *Nature.* 2003; 426(6965): 450–4.
7. Alebrahim-Dehkordi E, Reyhanian A, Saberianpour S, Hasanpour-Dehkordi A. Acute kidney injury in COVID-19; a review on current knowledge. *J Nephropathol.* 2020;9(4):e31–e31.
8. Wang Q, Wong G, Lu G, Yan J, Gao GF. MERS-CoV spike protein: Targets for vaccines and therapeutics. *Antiviral Research.* 2016;133:165–77.
9. Meyerholz DK, Lambertz AM, McCray PB. Dipeptidyl Peptidase 4 Distribution in the Human Respiratory Tract. *The American Journal of Pathology.* 2016;186(1):78–86.
10. Naicker S, Yang CW, Hwang SJ, Liu BC, Chen JH, Jha V. The Novel Coronavirus 2019 epidemic and kidneys. *Kidney International.* 2020;97(5):824–8.
11. Basalely A, Gurusinghe S, Schneider J, Shah SS, Siegel LB, Pollack G, et al. Acute kidney injury in paediatric patients hospitalized with acute COVID-19 and multisystem inflammatory syndrome in children associated with COVID-19. *Kidney International.* 2021;100(1):138–45.
12. Deep A, Upadhyay G, du Pré P, Lillie J, Pan D, Mudalige N, et al. Acute Kidney Injury in Paediatric Inflammatory Multisystem Syndrome Temporally Associated With Severe Acute Respiratory Syndrome Coronavirus-2 Pandemic: Experience From PICUs Across United Kingdom. *Critical Care Medicine.* 2020;48(12):1809–18.
13. Gagliardi I, Patella G, Michael A, Serra R, Provenzano M, Andreucci M. COVID-19 and the Kidney: From Epidemiology to Clinical Practice. *JCM.* 2020;9(8):2506.
14. Boraschi P. COVID-19 Pulmonary Involvement: Is Really an Interstitial Pneumonia? *Academic Radiology.* 2020; 27(6):900.
15. Moher D, Liberati A, Tetzlaff J, Altman DG, The PRISMA Group. Preferred Reporting Items for Systematic Reviews and Meta-Analyses: The PRISMA Statement. *PLoS Med.* 2009;6(7):e1000097.
16. Tran L, Tam DNH, Elshafay A, Dang T, Hirayama K, Huy NT. Quality assessment tools used in systematic reviews of in vitro studies: A systematic review. *BMC Med Res Methodol.* 2021;21(1):101.
17. OpenMeta[Analyst] -- CEBM @ Brown. <http://www.cebm.brown.edu/openmeta/>. Published 2021. Accessed July 10, 2021.
18. González-Damrauskas S, Vázquez-Hoyos P, Camporesi A, Díaz-Rubio F, Piñeres-Olave BE, Fernández-Sarmiento J, et al. Paediatric Critical Care and COVID-19. *Paediatrics.* 2020;146(3):e20201766.
19. Dufort EM, Koumans EH, Chow EJ, Rosenthal EM, Muse A, Rowlands J, et al. Multisystem Inflammatory Syndrome in Children in New York State. *N Engl J Med.* 2020;383(4):347–58.
20. Lee PY, Day-Lewis M, Henderson LA, Friedman KG, Lo J, Roberts JE, et al. Distinct clinical and immunological features of SARS-CoV-2-induced multisystem inflammatory syndrome in children. *Journal of Clinical Investigation.* 2020;130(11):5942–50.

21. Whittaker E, Bamford A, Kenny J, Kaforou M, Jones CE, Shah P, et al. Clinical Characteristics of 58 Children With a Paediatric Inflammatory Multisystem Syndrome Temporally Associated With SARS-CoV-2. *JAMA*. 2020;324(3):259.
22. Capone CA, Subramony A, Sweberg T, Schneider J, Shah S, Rubin L, et al. Characteristics, Cardiac Involvement, and Outcomes of Multisystem Inflammatory Syndrome of Childhood Associated with severe acute respiratory syndrome coronavirus 2 Infection. *The Journal of Paediatrics*. 2020;224:141–5.
23. Wang X, Chen X, Tang F, Luo W, Fang J, Qi C, et al. Be aware of acute kidney injury in critically ill children with COVID-19. *PediatrNephrol*. 2021;36(1):163–9.
24. Samies NL, Pinninti S, James SH. Rhabdomyolysis and Acute Renal Failure in an Adolescent With Coronavirus Disease 2019. *Journal of the Paediatric Infectious Diseases Society*. 2020;9(4):507–9.
25. Qiu L, Jiao R, Zhang A, Chen X, Ning Q, Fang F, et al. A Case of Critically Ill Infant of Coronavirus Disease 2019 With Persistent Reduction of T Lymphocytes. *Paediatric Infectious Disease Journal*. 2020;39(7):e87–90.
26. Niño-Taravilla C, Espinosa-Vielma YP, Otaola-Arca H, Poli-Harlowe C, Tapia LI, Ortiz-Fritz P. Paediatric Inflammatory Multisystem Syndrome Temporally Associated with SARS-CoV-2 Treated with Tocilizumab. *Paediatric Reports*. 2020;12(3):142–8.
27. Mamishi S, Movahedi Z, Mohammadi M, Ziaee V, Khodabandeh M, Abdolsalehi MR, et al. Multisystem inflammatory syndrome associated with SARS-CoV-2 infection in 45 children: a first report from Iran. *Epidemiol Infect*. 2020;148:e196.
28. Grimaud M, Starck J, Levy M, Marais C, Chareyre J, Khraiche D, et al. Acute myocarditis and multisystem inflammatory emerging disease following SARS-CoV-2 infection in critically ill children. *Ann Intensive Care*. 2020;10(1):69.
29. Oberweis ML, Codreanu A, Boehm W, Olivier D, Pierron C, Tsobo C, et al. Paediatric Life-Threatening Coronavirus Disease 2019 With Myocarditis. *Paediatric Infectious Disease Journal*. 2020;39(7):e147–9.
30. Toubiana J, Poirault C, Corsia A, Bajolle F, Fourgeaud J, Angoulvant F, et al. Kawasaki-like multisystem inflammatory syndrome in children during the covid-19 pandemic in Paris, France: prospective observational study. *BMJ*. 2020;3:m2094.
31. Shahbaznejad L, Navaeifar MR, Abbaskhanian A, Hosseinzadeh F, Rahimzadeh G, Rezai MS. Clinical characteristics of 10 children with a paediatric inflammatory multisystem syndrome associated with COVID-19 in Iran. *BMC Pediatr*. 2020;20(1):513.
32. Godfred-Cato S, Bryant B, Leung J, Oster ME, Conklin L, Abrams J, et al. COVID-19–Associated Multisystem Inflammatory Syndrome in Children — United States, March–July 2020. *MMWR Morb Mortal Wkly Rep*. 2020;69(32):1074–80.
33. Dionne A, Mah DY, Son MBF, Lee PY, Henderson L, Baker AL, et al. Atrioventricular Block in Children With Multisystem Inflammatory Syndrome. *Paediatrics*. 2020;146(5):e2020009704.
34. Derespina KR, Kaushik S, Plichta A, Conway EE, Bercow A, Choi J, et al. Clinical Manifestations and Outcomes of Critically Ill Children and Adolescents with Coronavirus Disease 2019 in New York City. *The Journal of Paediatrics*. 2020;226:55–63.e2.
35. Stewart DJ, Hartley JC, Johnson M, Marks SD, du Pré P, Stojanovic J. Renal dysfunction in hospitalised children with COVID-19. *The Lancet Child & Adolescent Health*. 2020;4(8):e28–9.
36. Bjornstad EC, Krallman KA, Askenazi D, Zappitelli M, Goldstein SL, Basu RK, et al. Preliminary Assessment of Acute Kidney Injury in Critically Ill Children Associated with SARS-CoV-2 Infection: A Multicenter Cross-Sectional Analysis. *CJASN*. 2021;16(3):446–8.
37. Kari JA, Shalaby MA, Albanna AS, Alahmadi TS, Alherbish A, Alhasan KA. Acute kidney injury in children with COVID-19: a retrospective study. *BMC Nephrol*. 2021;22(1):202.

38. Chopra S, Saha A, Kumar V, Thakur A, Pemde H, Kapoor D, et al. Acute Kidney Injury in Hospitalized Children with COVID19. *Journal of Tropical Paediatrics*. 2021; 17;67(2): fmab037.
39. Hansrivijit P, Qian C, Boonpheng B, Thongprayoon C, Vallabhajosyula S, Cheungpasitporn W, et al. Incidence of acute kidney injury and its association with mortality in patients with COVID-19: a meta-analysis. *J Investig Med*. 2020;68(7):1261–70.

How to cite this article: Snehashis Koley, Ambar Bose, Sudeshna Mallik et.al. COVID-19 infection and acute kidney injury in paediatric population: a systematic review and meta-analysis. *International Journal of Research and Review*. 2022; 9(11): 7-20.
DOI: <https://doi.org/10.52403/ijrr.20221102>

Cytokine profile in HTB-4 cells with respect to *fimH*, *papC* and *hlyA* expression in uropathogenic *Escherichia coli* invasion

Snehashis Koley¹  & Mandira Mukherjee^{*1} ¹Department of Biochemistry & Medical Biotechnology, School of Tropical Medicine, Kolkata, 700073, India*Author for correspondence: Tel.: +91 943 394 8556; mandira_71@yahoo.com

Background: In this study, uropathogenic *Escherichia coli* (UPEC) from pregnant and nonpregnant patients were characterized with respect to antimicrobial resistance (AMR) and expression of their virulence factors and cytokines elicited upon infection in urothelial (HTB-4) cells *in vitro* to frame proper therapeutics. **Methods:** Antibiotic sensitivity and adherence to HTB-4 cells were tested and PCR and real-time PCR were performed. **Results:** UPEC from nonpregnant patients showed the most resistance with a significant correlation between the expression of *hlyA* and *TGF- β* and *papC* and *GCSF*. The expression of *fimH* and *IFN- γ* , *fimH* and *IL-1 β* , and *fimH* and *IL-17A*, respectively, were significantly correlated in UPEC from pregnant patients. **Conclusion:** Cytokine expression profiles were correlated with the expression of virulence genes in UPEC that was isolated from different populations, and should be accounted for along with AMR analysis.

First draft submitted: 21 October 2022; Accepted for publication: 24 March 2023; Published online: 8 June 2023

Keywords: antimicrobial resistance • host–pathogen interaction • interleukin regulation • UPEC

Urinary tract infections (UTIs), both acute and recurrent, pose widespread public health issues leading to a significant reduction in the quality of life for patients. The urinary system is normally sterile, with a variety of host defenses to prevent bacterial colonization and survival. Primarily, there are several built-in host defense mechanisms that resist bacterial infection [1]. UTIs in pregnant women pose a serious threat to the fetus, with frequent occurrence of premature birth, premature rupture of the membrane, maternal chorioamnionitis and a fetus with low birth weight, developmental retardation or fetal necrosis [2–4]. Moreover, asymptomatic bacteriuria is commonly observed in pregnant women and, if untreated, 20–30% of cases may lead to pyelonephritis. UTIs in the nonpregnant population also lead to the development of several complications, especially in older women and, if undetected, may be fatal. About 80–90% of UTIs are caused by uropathogenic *Escherichia coli* (UPEC) in both populations [3,4]. Antibiotics are usually the first treatment option for UTIs, however, their administration has contributed to the emergence of multidrug resistance (MDR) and has complicated the clinical management of UTIs [5]. Early studies from the current authors' laboratory indicate a high incidence of MDR in UPEC isolated from nonpregnant (92.5%) [6] and pregnant (59.1%) women [7]. A recent study from Mexico revealed that 92.7% of isolates from pregnant and nonpregnant women were MDR [8].

UPEC strains have a large number of virulence factors (VFs) including fimbrial (type 1, P and S), afimbrial (Afa/Dr family), toxins (α -hemolysin [HlyA], cytotoxic necrotizing factor 1 [CNF1], autotransporter proteins), iron-acquisition systems, iron ion transport and surface polysaccharides. VFs facilitated adherence to epithelial cells of the intestines, kidneys or lower urinary tract and were also found to play an important role in colonization [9,10]. They further activated host defense systems and resulted in the exfoliation of bladder epithelial cells and inflammation [1]. After infection with UPEC, epithelial cells in the bladder and kidney appear to be a key source of IL-6 and IL-8, which played crucial roles in the development of local tissue damage. Moreover, several reports also showed the role of TNF- α , IFN- γ , IL-8 and IL-1 β in the clearance of UPEC [11–17]. A study by Jung *et al.* [18] revealed relationships between virulence determinants and the phylogenetic background of UPEC isolated from infants on TNF- α and IL- β expression that further suggested the function of the cytokines in UTI pathogenesis. Another

in vitro study established the effect of different cytokines on the expression of virulence determinants in UPEC prototype strain CFT073 in the HTB-4 uroepithelial cell line [17]. Therefore, the immune responses of the host and the virulence determinants of the pathogen were major factors in the establishment of infection.

Although urine culture is the gold standard for the detection of the uropathogen [19], it is time consuming, and the administration of empirical treatment is the only choice without knowledge of the infection potential of the microbe. This has caused the rapid emergence of MDR, which is highly alarming in the treatment of UTIs, especially in the pregnant population. In this study, the antibiotic resistance pattern in UPEC isolates collected from pregnant women was ascertained and compared with UPEC collected from nonpregnant patients to assess the risk of empirical therapy in both populations. Accordingly, to formulate appropriate therapy, intricate knowledge of the infection potential of the microbe and its capacity to elicit host cytokine response is a necessity. Additionally, in available references, no study related to the production of different cytokines upon infection with UPEC isolated from the pregnant population was reported. Therefore, in this study, HTB-4 uroepithelial cells were infected with clinical UPEC isolated *in vitro*, and the expression pattern of their virulence determinants and cytokines elicited in the host cells upon infection were determined. Correlations between the expression of varied cytokines and pathogenic determinants expressed in UPEC isolated from different hosts were ascertained, which might serve as noninvasive markers to formulate appropriate therapeutics before empirical therapy.

Methods

Bacterial strains

A total of 110 urine samples each were isolated from pregnant and nonpregnant women admitted to the Medical College and Hospital and Carmichael Hospital of Tropical Diseases, Kolkata, India. *E. coli* was identified biochemically, cultured and archived in the Department of Biochemistry and Medical Biotechnology, School of Tropical Medicine, Kolkata, India, as described by Basu *et al.* [6]. The study protocol was approved by the institutional ethics committee (ref. no. CREC-STM/2020-AG-13).

Antibiotic susceptibility test

The Kirby–Bauer disc diffusion method was used to determine the susceptibility of the isolates to various antibiotics, including amikacin (AK; 10 µg), ampicillin (AMP; 10 µg), ceftazidime (CAZ; 30 µg), cefotaxime (CTX; 30 µg), ciprofloxacin (CIP; 5 µg), nitrofurantoin (NIT; 300 µg), cotrimoxazole (trimethoprim/sulfamethoxazole; COT; 1.25/23.75 µg) and imipenem (IPM; 10 µg; HiMedia, Mumbai, India) following Clinical Laboratory Standard Institute standards [20] to determine the zone of inhibition. *E. coli* ATCC 25922 was used as a control. An isolate that was resistant to at least three different antibiotic classes was classified as MDR.

Determination of virulence genes

Total bacterial DNA was extracted from a single colony of each UPEC isolate grown on Luria-Bertani (LB) (HiMedia, Mumbai, India) agar plates. Briefly, a bacterial suspension was prepared in 100 µl of sterile water. After 10 min incubation at 100 °C, it was subjected to centrifugation at 8000× *g* for 10 min. The supernatant was further purified using chloroform (HiMedia, Mumbai, India) and used as a DNA template to detect the presence of six virulence genes (*fimH*, *papC*, *sfaA*, *afaA*, *hlyA*, *iroN*) using gene-specific primers (GCC Biotech, Kolkata, India) [6].

Adherence to HTB-4 uroepithelial cells

HTB-4 cells were purchased from the National Center for Cell Science (Pune, India) and control strain ABU83972 (HM-50) was provided by BEI resources (ATCC, VA, USA). HTB-4 human bladder epithelial cells (3×10^5) were seeded into each well of a 24-well plate, and cells were allowed to adhere overnight. The 10^7 CFU of bacteria (grown overnight in LB, further grown until log phase in LB and resuspended in 1X phosphate-buffered saline [PBS]) were added and the plates were incubated at 37 °C in 5% CO₂ (CO₂ incubator, Thermo Fisher Scientific, MA, USA) for 3 h to allow for the adhesion of the bacteria. The HTB-4 infected cell monolayers were washed three times with PBS to remove nonadherent bacteria [21,22].

RNA extraction

Total RNA was extracted from the HTB-4 infected adherent monolayer cultures by TRIzol™ (Thermo Fisher Scientific, MA, USA) extraction as per the manufacturer's instructions. Briefly, cells were scraped with 1500 µl TRIzol™

reagent combined with 300 µl chloroform. After centrifugation at $13,000\times g$ for 15 min, the aqueous phase was recovered and mixed with 750 µl isopropanol (HiMedia, Mumbai, India). For quantification, the supernatant was removed and the RNA precipitate was dissolved in deionized water (HiMedia, Mumbai, India). The quantity of purified RNA was determined by measuring the absorbance at OD₂₆₀ (Spectrophotometer, Bio-Rad, CA, USA). Then, cDNA was generated from total RNA using a Thermo Scientific RevertAid™ First Strand cDNA synthesis kit (Thermo Fisher Scientific Baltics UAB, Vilnius, Lithuania) following the manufacturer's instructions. Each cDNA pool was stored at -20 °C until further real-time PCR (Applied Biosystems, MA, USA) [23,24].

Real-time PCR analysis

To determine the quantitative expression of six virulence genes (*fimH*, *papC*, *papGIII*, *sfaA*, *hlyA* and *iroN*) and ten cytokines genes (*IL-6*, *IL-8*, *TNF-α*, *IFN-γ*, *MCP-1*, *GCSF*, *IL-1β*, *IL-17A*, *IL-5* and *TGF-β*), quantitative real-time PCR (qRT-PCR) assay were performed on the cDNA prepared from total RNA extracted from T-24 infected monolayer cultures using gene-specific primers. qRT-PCR was performed in an Applied Biosystems™ 7500 Fast Real-Time PCR system with PowerUp™ SYBR™ Green Master Mix (Applied Biosystems, Lithuania) using the following conditions: 10 min at 95 °C, 40 cycles for 30 s, 55 °C for 30 s and 72 °C for 30 s. The primers used in this study are listed in Table 1. To determine the fold change of different virulence genes and cytokine genes, the $2^{-\Delta\Delta C_t}$ method was used [25]. Quantitative fold change analysis of each virulence gene (*fimH*, *papC*, *papGIII*, *sfaA*, *hlyA*, *iroN*) in the adherent UPEC is reported as fold change relative to their expression in adherent ABU83972. Moreover, the fold change analysis of each interleukin gene (*IL-6*, *IL-8*, *TNF-α*, *IFN-γ*, *MCP-1*, *GCSF*, *IL-1β*, *IL-17A*, *IL-5*, *TGF-β*) in the HTB-4 monolayer cell upon infection with the different UPECs, respectively, are reported as fold change relative to their expression upon infection with ABU83972. *16srRNA* and *GAPDH* expression were used for the normalization of the expression of the virulence genes and interleukin genes.

Statistical analysis

Statistical analyses were performed using IBM® SPSS® statistics version 25.0 (IBM, NY, USA). A one-sample *t*-test was performed to identify the statistical significance of the prevalence of virulence gene and nonparametric bivariate correlations were performed to determine the associations between antibiotics and between expression of virulence genes and cytokines; *p*-values <0.05 were considered statistically significant [26]. Graphs were drawn using GraphPad Prism version 8.0.2 (GraphPad Software, CA, USA) [27].

Results

Bacterial isolates & antibiotic susceptibility

A total of 110 urine samples each from pregnant and nonpregnant women were screened for the presence of bacteriuria. Significant monomicrobial growth of *E. coli* was detected in 36 of 40 (90.0%) and 30 of 35 (85.7%) culture-positive urine samples from pregnant and nonpregnant women, respectively. A total of 21 each out of 36 and 32 *E. coli* isolates from pregnant women (UPECp) and nonpregnant women (UPECnp), respectively, were randomly selected for this study. The antibiotic resistance pattern of 21 UPECp showed the highest resistance against AMP (90.48%) and moderate resistance against COT (71.43%) and CTX (61.90%). However, the 21 UPECnp isolates showed high resistance against AMP (100%), CTX (95.24%), CIP (90.48%) and CAZ (80.95%). Similar to the UPECp isolates, UPECnp isolates also exhibited moderate resistance to COT (71.43%). Antibiotic resistance pattern analysis against the regimen of eight antibiotics showed a higher distribution of MDR among UPECnp than UPECp isolates. Resistance against all eight antibiotics was observed in UPECnp compared with UPECp, where resistance against six antibiotics was observed (Table 2). Nevertheless, a significant positive correlation in the antibiotic resistance pattern between CAZ/CTX and CIP and COT, and between AK and IPM and CIP and COT in UPECp and UPECnp, respectively, were observed. A significant negative correlation was also observed between AMP and AK and IPM and CIP in UPECp and UPECnp, respectively (Table 3).

Prevalence of virulence genes

The highest prevalence of *fimH* and *papC* genes was observed in both groups of isolates and their presence was statistically significant (*p* < 0.001). Moreover, the presence of *sfaA*, *hlyA* and *iroN* in UPECp isolates and *hlyA* and *papGIII* in UPECnp isolates was also statistically significant (*p* < 0.001). The overall prevalence of virulence genes (*fimH*, *papC*, *sfaA*, *hlyA* and *iroN*) was greater in UPECp isolates than in UPECnp isolates, except for *papGIII*, whose distribution was higher in the latter than the former (Figure 1).

Table 1. Primers used in this study.

Genes	Primer sequences (5'–3')	Amplicon size (bp)	Ref.
Real-time PCR primers for virulence genes			
<i>fimH</i> RT	F: TGCAGAACGGATAAGCCGTGG R: CACCACCACATCATTATTGGC	180	[6] This study
<i>papC</i> RT	F: CAGCTACAGCCTGAACGCC R: ATATCCTTTCTGCAGGGATGCAATA	133	[6] This study
<i>papGIII</i> RT	F: CATGGCTGGTTGCTTCTTAACAT R: GTCCAGATGTGTTGCTTCATCCC	153	[6] This study
<i>hlyA</i> RT	F: CCGTGAAGAACTATTGGGACCAC R: ACCATATAAGCGGTATTCCCGTCA	128	[6] This study
<i>iroN</i> RT	F: CGTACTCATGCGGAACCCGC R: GACGCCGACATTAGACGCAG	129	[6] This study
<i>sfaA</i> RT	F: CCCTGAAGGGCAAAAACAGGTACA R: CGGAGGAGTAATTACAAACCTGGCA	127	[6] This study
<i>16srRNA</i> RT	F: CCGCAAGGTTAAAACTCAA R: CGACAGCCATGCAGCACC	169	This study
Real-time PCR primers for interleukin genes			
<i>GAPDH</i> RT	F: CAACAGCGACCCCACTC R: CATGTGGGCCATGAGGTC	136	This study
<i>IL6</i> RT	F: GTACATCTCGACGGCATC R: GAATCCAGATTGGAAGCATCC	145	
<i>IL8</i> RT	F: GGTGCAGTTTGGCCAAGGAG R: GTTGGCGCAGTGTGTGCC	126	
<i>TNFα</i> RT	F: CTGCCCTCCACCCATGTG R: CAGCTGGAAGACCCCTCCC	175	
<i>IFNγ</i> RT	F: GAGGAAGAAGCGGGAGTACTG R: GCTGAGTTGGGAGGAGAACACAC	152	
<i>MCP1</i> RT	F: GCAGAGGCTCGCGAGCTATAG R: CGGAGTTTGGGTTTGCTTGCC	157	
<i>GCSF</i> RT	F: CTGCTGCTGTGGCACAGTG R: GGCACAGCTTGTAGGTGGC	152	
<i>IL1β</i> RT	F: GTGCTCCTCCAGGACCTGG R: GGGAAACGACATCTTCTCAGC	142	
<i>IL17A</i> RT	F: GGAATCTCCACCGCAATGAGGAC R: CGCAGGACCAAGGATCTCTTGC	148	
<i>IL5</i> RT	F: GGTGAAGAGACCTTGGCACTGC R: CTCTCCAGTGTGCCTATTCCCTG	141	
<i>TGFβ</i> RT	F: CAGCGACTCGCCAGAGTG R: CCCGTTGATGTCCACTTGCA	148	

Expression of virulence genes

A discrete pattern of relative expression of virulence genes (*fimH*, *papC*, *papGIII*, *sfaA*, *hlyA* and *iroN*) in the UPECp and UPECnp isolates was observed 3 h post-infection (hpi) in HTB-4 uroepithelial cells for their expression in the control strain ABU83972. An overall positive relative fold change of *fimH*, *hlyA*, *papGIII* and *sfaA* in 61.9%, 38.1%, 19.05% and 23.8%, and an overall negative relative fold change of *papC* and *iroN* in 57.14% and 61.9% of UPECp isolates was observed. The positive fold change of *fimH* ($p < 0.001$) and negative fold change of *papC* ($p < 0.001$) and *iroN* ($p < 0.001$) in UPECp were statistically significant. Alternatively, negative fold changes of *hlyA* and *sfaA* in 42.86% and 23.81% were prevalent in UPECnp isolates. The positive fold change in *hlyA* ($p < 0.001$) and negative fold change in *fimH* ($p < 0.001$) and *papC* ($p < 0.001$) were statistically significant.

Table 2. Antibiotic resistance patterns of uropathogenic *Escherichia coli* pregnant; P (n = 21) and nonpregnant; EC (n = 21) isolates.

Uropathogenic <i>E. coli</i> isolates		Antibiotic resistance
UPECp	P25, P33	AMP, CAZ, CTX, CIP, COT, IPM
	P31	AMP, CAZ, CTX, CIP, NF, COT
	P11, P30, P36, P65, P121, P139, P154	AMP, CAZ, CTX, CIP, COT
	P140	AK, CAZ, CTX, CIP, COT
	P74	AMP, CAZ, CTX, COT
	P12	AMP, CIP, COT
	P49	AMP, CTX, COT
	P6, P54	AMP, COT
	P35, P138, P143, P144	AMP
	P7	–
UPECnp	EC182, EC212	AK, AMP, CAZ, CTX, CIP, NF, COT, IPM
	EC189, EC266	AK, AMP, CAZ, CTX, CIP, COT, IPM
	EC216, EC218	AK, AMP, CAZ, CTX, CIP, NF, COT
	EC146, EC178, EC214, EC215	AMP, CAZ, CTX, CIP, NF, COT
	EC180, EC187	AK, AMP, CAZ, CTX, CIP, COT
	EC186	AK, AMP, CAZ, CTX, NF, IPM
	EC188	AK, AMP, CAZ, CTX, IPM
	EC191	AK, AMP, CTX, CIP, COT
	EC215	AMP, CAZ, CTX, CIP, COT
	EC213, EC220	AMP, CAZ, CTX, CIP
	EC204	AMP, CTX, CIP, COT
	EC192	AK, AMP, CTX, CIP
	EC194	AK, AMP, CIP

Table 3. Correlations of antibiotic resistance patterns in uropathogenic *Escherichia coli* pregnant (n = 21) and nonpregnant (n = 21) isolates.

UPECp	AK	AMP	CAZ	CTX	CIP	NF	COT	IPM
AK	1							
AMP	-0.689[†]	1						
CAZ	0.194	0.047	1					
CTX	0.175	0.080	0.906[†]	1				
CIP	0.175	0.080	0.708[†]	0.798[†]	1			
NF	-0.050	0.073	0.194	0.175	0.175	1		
COT	0.141	0.154	0.730[†]	0.589[†]	0.589[†]	0.141	1	
IPM	-0.073	0.105	0.281	0.255	0.255	-0.073	0.205	1
UPECnp								
AK	1							
AMP	§	§						
CAZ	-0.131	§	1					
CTX	-0.175	§	0.461[‡]	1				
CIP	-0.255	§	-0.157	0.073	1			
NF	-0.113	§	0.420	0.194	-0.047	1		
COT	-0.062	§	0.230	0.354	0.513[‡]	0.335	1	
IPM	0.496[‡]	§	0.307	0.141	-0.513[‡]	0.091	-0.067	1

[†]Correlation is significant at the 0.01 level (two-tailed).[‡]Correlation is significant at the 0.05 level (two-tailed).[§]Cannot be computed because at least one of the variables is constant.

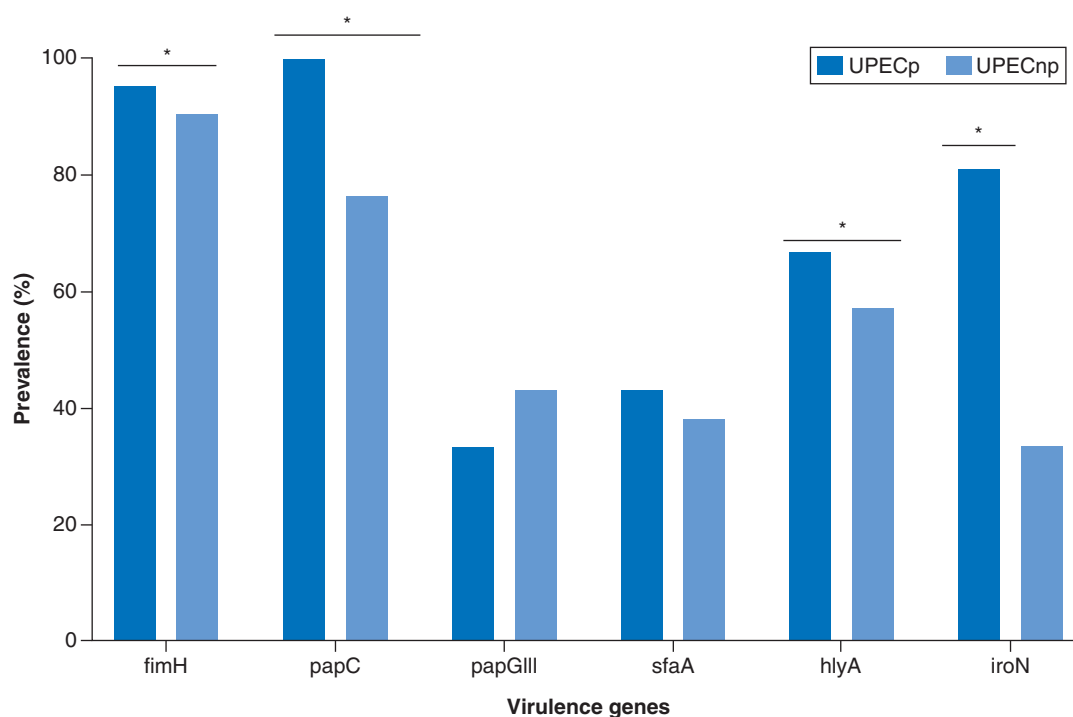


Figure 1. Prevalence of six virulence genes in uropathogenic *Escherichia coli* pregnant (n = 21) and nonpregnant isolates (n = 21).

Cytokine expression in infected HTB-4 cells

Infected HTB-4 cells exhibited a distinct pattern of relative fold expression of cytokines (*IL-6*, *IL-8*, *TNF- α* , *IFN- γ* , *MCP-1*, *GCSF*, *IL-1 β* , *IL-17A*, *IL-5* and *TGF- β*) upon 3 hpi in UPECp and UPECnp isolates. Enhanced relative fold expression of *IL-6*, *IL-8*, *IL-17A* and *IL-5* was observed in infected HTB-4 cells for 61.9%, 81%, 61.9% and 71.4% of UPECp isolates, respectively, and their distribution in the population was statistically significant ($p < 0.001$). Furthermore, elevated relative fold expression of *TNF- α* , *IL-5* and *TGF- β* were observed in host cells infected with 52.4%, 76.2% and 71.4% UPECnp isolates, respectively, with a statistically significant ($p < 0.001$) distribution. On the contrary, reduced relative fold expression of *TNF- α* , *IFN- γ* , *MCP-1*, *GCSF*, *IL-1 β* and *TGF- β* were observed in host cells infected with 81%, 95.2%, 76.2%, 71.4%, 95.2% and 76.2% of UPECp isolates, respectively, and their distribution was statistically significant ($p < 0.001$). Moreover, reduced relative fold expression of *IL-6*, *IL-8*, *GCSF*, *IL-1 β* and *IL-17A* were also observed in host cells infected with 76.2%, 76.2%, 66.7%, 85.7% and 85.7% of UPECnp isolates, respectively, and the distribution was also statistically significant ($p < 0.001$). Additionally, reduced relative fold expression of *IFN- γ* and *MCP-1* was observed in the HTB-4 cells infected with 21 (100%) UPECnp isolates, respectively, which was nonsignificant. Significant positive correlations between UPECp *fimH* and *IL-17A* and UPECp *fimH* and *IFN- γ* and significant negative correlations between UPECp *fimH* and *IL-1 β* , UPECnp *papC* and *GCSF* and UPECnp *hlyA* and *TGF- β* were observed (Tables 4 & 5).

Discussion

MDR poses a common complication in UTI treatment globally. Moreover, the choice of antibiotics to treat UTIs in the pregnant population is limited compared with the nonpregnant population due to pharmacokinetic and pharmacodynamic changes during pregnancy. Several studies have reported the incidence of MDR among the pregnant population, which further challenges the selection of antibiotics [8,28–33]. *E. coli* was reported as the most prevalent etiologic agent in UTIs in both populations [8]. In this study, 66.7% of the UPECp isolates were MDR, very similar to studies from Pakistan [32] and the Republic of Somaliland [33]. Additionally, MDR was observed in all the UPECnp isolates, as reported by several studies globally [29,30]. Furthermore, this study showed moderate-to-high resistance against AMP, CAZ, CTX, CIP and COT in the UPECp isolates, and the highest resistance to AMP, CAZ, CTX, AK and CIP in the UPECnp isolates. This observation was alarming, as there was

Table 4. Correlations between expression of virulence genes and expression of cytokines in uropathogenic *Escherichia coli* pregnant isolates.

UPECp											
	<i>fimH</i>	<i>IL-6</i>	<i>IL-8</i>	<i>TNF-α</i>	<i>IFN-γ</i>	<i>MCP-1</i>	<i>GCSF</i>	<i>IL-1β</i>	<i>IL-17A</i>	<i>IL-5</i>	<i>TGF-β</i>
<i>fimH</i>	1										
<i>IL-6</i>	0.305	1									
<i>IL-8</i>	0.186	0.678 [†]	1								
<i>TNF-α</i>	0.182	0.200	0.048	1							
<i>IFN-γ</i>	0.402[‡]	0.109	-0.151	0.568 [†]	1						
<i>MCP-1</i>	-0.298	-0.452 [‡]	-0.354	0.197	0.111	1					
<i>GCSF</i>	-0.212	0.095	0.224	0.523 [†]	0.078	0.385 [‡]	1				
<i>IL-1β</i>	-0.396[‡]	0.090	0.040	0.640 [†]	0.172	0.436 [‡]	0.840 [†]	1			
<i>IL-17A</i>	0.475[‡]	0.348	0.147	0.612 [†]	0.821 [†]	0.103	0.210	0.213	1		
<i>IL-5</i>	0.186	0.143	0.114	0.586 [†]	0.590 [†]	0.188	0.348	0.374 [‡]	0.505 [†]	1	
<i>TGF-β</i>	-0.230	0.166	0.201	0.291	0.003	0.113	0.453 [‡]	0.513 [†]	0.125	0.192	1
	<i>papC</i>	<i>IL-6</i>	<i>IL-8</i>	<i>TNF-α</i>	<i>IFN-γ</i>	<i>MCP-1</i>	<i>GCSF</i>	<i>IL-1β</i>	<i>IL-17A</i>	<i>IL-5</i>	<i>TGF-β</i>
<i>papC</i>	1										
<i>IL-6</i>	0.014	1									
<i>IL-8</i>	-0.049	0.678 [†]	1								
<i>TNF-α</i>	-0.020	0.200	0.048	1							
<i>IFN-γ</i>	0.160	0.109	-0.151	0.568 [†]	1						
<i>MCP-1</i>	0.016	-0.452 [‡]	-0.354	0.197	0.111	1					
<i>GCSF</i>	0.053	0.095	0.224	0.523 [†]	0.078	0.385 [‡]	1				
<i>IL-1β</i>	-0.243	0.090	0.040	0.640 [†]	0.172	0.436 [‡]	0.840 [†]	1			
<i>IL-17A</i>	0.279	0.348	0.147	0.612 [†]	0.821 [†]	0.103	0.210	0.213	1		
<i>IL-5</i>	-0.277	0.143	0.114	0.586 [†]	0.590 [†]	0.188	0.348	0.374 [‡]	0.505 [†]	1	
<i>TGF-β</i>	-0.084	0.166	0.201	0.291	0.003	0.113	0.453 [‡]	0.513 [†]	0.125	0.192	1
	<i>iroN</i>	<i>IL-6</i>	<i>IL-8</i>	<i>TNF-α</i>	<i>IFN-γ</i>	<i>MCP-1</i>	<i>GCSF</i>	<i>IL-1β</i>	<i>IL-17A</i>	<i>IL-5</i>	<i>TGF-β</i>
<i>iroN</i>	1										
<i>IL-6</i>	-0.088	1									
<i>IL-8</i>	0.004	0.678 [†]	1								
<i>TNF-α</i>	0.190	0.200	0.048	1							
<i>IFN-γ</i>	0.204	0.109	-0.151	0.568 [†]	1						
<i>MCP-1</i>	0.104	-0.452 [‡]	-0.354	0.197	0.111	1					
<i>GCSF</i>	0.126	0.095	0.224	0.523 [†]	0.078	0.385 [†]	1				
<i>IL-1β</i>	-0.177	0.090	0.040	0.640 [†]	0.172	0.436 [‡]	0.840 [‡]	1			
<i>IL-17A</i>	0.279	0.348	0.147	0.612 [†]	0.821 [†]	0.103	0.210	0.213	1		
<i>IL-5</i>	0.012	0.143	0.114	0.586 [†]	0.590 [†]	0.188	0.348	0.374 [‡]	0.505 [†]	1	
<i>TGF-β</i>	-0.020	0.166	0.201	0.291	0.003	0.113	0.453 [‡]	0.513 [†]	0.125	0.192	1

† Correlation is significant at the 0.01 level (one-tailed).

‡ Correlation is significant at the 0.05 level (one-tailed).

a substantial reduction in the number of selected antibiotics that might otherwise be safely used in UTI treatment in both populations. A study from Mexico reported a similar antibiotic resistance pattern in the *E. coli* isolates collected from nonpregnant women and pregnant women with an exception in sensitivity to NIT [8]. The study reported high resistance against nitrofurantoin between both populations, unlike that reported in this study, which showed high susceptibility against the antibiotic in the pregnant population, similar to other published reports from the Indian subcontinent and Somaliland [28,33]. Furthermore, in this study, high susceptibility was observed against IPM, a carbapenem group of antibiotics, similar to another study that reported a similar observation using meropenem, another carbapenem group of antibiotics [33].

This study also revealed a statistically significant correlation among the different antibiotics in co-resistant phenotypes. The analysis revealed that resistance to CAZ was correlated with resistance to CTX, CIP and COT

Table 5. Correlation between the expression of virulence genes and expression of cytokines in uropathogenic *Escherichia coli* nonpregnant isolates.

UPECnp									
	<i>fimH</i>	<i>IL-6</i>	<i>IL-8</i>	<i>TNF-α</i>	<i>GCSF</i>	<i>IL-1β</i>	<i>IL-17A</i>	<i>IL-5</i>	<i>TGF-β</i>
<i>fimH</i>	1								
<i>IL-6</i>	-0.011	1							
<i>IL-8</i>	-0.045	0.955 [‡]	1						
<i>TNF-α</i>	-0.006	0.302	0.282	1					
<i>GCSF</i>	-0.163	0.165	0.123	0.433 [‡]	1				
<i>IL-1β</i>	-0.124	0.449 [‡]	0.431 [‡]	0.661 [†]	0.762 [†]	1			
<i>IL-17A</i>	0.103	0.518 [†]	0.489 [‡]	0.044	0.175	0.395 [‡]	1		
<i>IL-5</i>	0.014	-0.637 [†]	-0.614 [†]	0.029	-0.329	-0.520 [†]	-0.474 [‡]	1	
<i>TGF-β</i>	-0.335	-0.189	-0.229	0.155	0.158	0.145	-0.112	0.015	1
	<i>papC</i>	<i>IL-6</i>	<i>IL-8</i>	<i>TNF-α</i>	<i>GCSF</i>	<i>IL-1β</i>	<i>IL-17A</i>	<i>IL-5</i>	<i>TGF-β</i>
<i>papC</i>	1								
<i>IL-6</i>	0.133	1							
<i>IL-8</i>	0.134	0.955 [†]	1						
<i>TNF-α</i>	0.096	0.302	0.282	1					
<i>GCSF</i>	-0.453 [‡]	0.165	0.123	0.433 [‡]	1				
<i>IL-1β</i>	-0.086	0.449 [‡]	0.431 [‡]	0.661 [†]	0.762 [†]	1			
<i>IL-17A</i>	0.100	0.518 [†]	0.489 [‡]	0.044	0.175	0.395 [‡]	1		
<i>IL-5</i>	0.017	-0.637 [†]	-0.614 [†]	0.029	-0.329	-0.520 [†]	-0.474 [‡]	1	
<i>TGF-β</i>	-0.333	-0.189	-0.229	0.155	0.158	0.145	-0.112	0.015	1
	<i>hlyA</i>	<i>IL-6</i>	<i>IL-8</i>	<i>TNF-α</i>	<i>GCSF</i>	<i>IL-1β</i>	<i>IL-17A</i>	<i>IL-5</i>	<i>TGF-β</i>
<i>hlyA</i>	1								
<i>IL-6</i>	0.322	1							
<i>IL-8</i>	0.325	0.955 [†]	1						
<i>TNF-α</i>	0.064	0.302	0.282	1					
<i>GCSF</i>	-0.289	0.165	0.123	0.433 [†]	1				
<i>IL-1β</i>	-0.221	0.449 [‡]	0.431 [‡]	0.661 [†]	0.762 [†]	1			
<i>IL-17A</i>	-0.060	0.518 [†]	0.489 [‡]	0.044	0.175	0.395 [‡]	1		
<i>IL-5</i>	0.062	-0.637 [†]	-0.614 [†]	0.029	-0.329	-0.520 [†]	-0.474 [‡]	1	
<i>TGF-β</i>	-0.517 [†]	-0.189	-0.229	0.155	0.158	0.145	-0.112	0.015	1

†Correlation is significant at the 0.01 level (one-tailed).

‡Correlation is significant at the 0.05 level (one-tailed).

in UPECp isolates. Similarly, resistance to AK and CIP was correlated with resistance to IPM and COT and only IPM, respectively, in the UPECnp isolates. Therefore, the overall data in the present study served as a rational indicator of antibiotic treatment and resistance patterns that might help to implement a judicious prescription policy to avoid dissemination and further emergence of MDR UPEC strains or restrict the coselection mechanism.

Important determinants of bacterial pathogenesis include VFs. The attachment of bacteria and epithelial cells is a multifactorial and complex phenomenon. Adherence to uroepithelial cells is considered the prime cause for colonization and establishment of infection that includes several adhesins, iron acquisition system proteins and toxins. FimH, the tip adhesin mediates the initial attachment of the bacteria to the epithelial cells. The current study revealed a predominant distribution of the *fimH* gene in both UPEC isolates collected from pregnant (95.24%) and nonpregnant (90.48%) women. Several reports across the world have also revealed a predominant distribution of the *fimH* gene in the range of 86–100% among clinically isolated UPEC isolates, which is directly related to their pathogenic potential [34–42]. Furthermore, worldwide reports indicated a low-to-moderate prevalence of the *papC* gene, a member of the *pap* operon, involved in upper UTI among clinical UPEC isolates [34,39,41]. However, in this study, the incidence of *papC* was 100% in UPECp isolates compared with 76.2% in UPECnp isolates, similar to another study conducted on *E. coli* isolated from pregnant and nonpregnant women [43]. S fimbria, the mannose-resistant adhesins, encoded by *sfa*-operon of UPEC, was also reported to control UPEC virulence. *sfaA*

encodes the major subunit of the S fimbriae. The current study indicated a low incidence of *sfhA* in both UPECp and UPECnp isolates, similar to a study by Lee *et al.* [44] that indicated a low prevalence of *sfhS*, the tip adhesin of S fimbriae compared with commensal UPEC. Several other studies from different parts of the world indicated a low incidence [34,37,39,41] and moderate-to-high incidence [35,36,45,46] of *sfhA* in clinical UPEC isolates.

Hemolysin, a pore-forming toxin encoded by *hlyA*, was related to the intracellular survival of the UPEC, and its expression was correlated with the severity of the UPEC infection [47]. Urothelial cell invasion by UPEC was also found to be mediated by siderophores. *iroN* encoded a siderophore outer membrane receptor that was reported to be associated with biofilm formation. Studies from varied regions across the globe reported low-to-moderate incidences of *hlyA* among UPEC isolates [34,36,39,41,42,48,49]. In this study, higher occurrence of *hlyA* in UPECp (80.95%) compared with UPECnp (66.67%) isolates resembled a study from Iraq [43]. Moderate incidence of *iroN* among UPEC isolates was reported in different studies [36,37,49] similar to the results obtained in this study in the UPECnp (33.33%) isolates. However, on the contrary, this study reported a high (80.95%) occurrence of *iroN* in UPECp isolates. Therefore, it is noteworthy that the incidence of major VF genes, *fimH*, *papC*, *hlyA* and *iroN*, in UPECp isolates was statistically significant and was worrisome for the management of UTI, especially in pregnant women from Kolkata, a city in the eastern part of India.

The expression of the *fimH* gene facilitated UPEC invasion of the superficial uroepithelial cells to generate intracellular bacterial communities. This bacterial invasion could initiate as early as the first 1–3 h of infection [50]. Several studies showed that the expression of virulence determinants reflected the severity of infection, with many VFs being expressed at a higher frequency by symptomatic strains causing UTI than by strains causing ABU [51,52]. DNA microarray analysis of the *E. coli* 83972 ABU strain showed downregulation of *fimBDFGH* genes due to a large deletion in the *fim* gene cluster with undetected signals for *fimEAIC* genes, and the hemolysin synthesis, activation and transportation genes, *hlyCABD*, which were also found to be downregulated to support its asymptomatic nature [51]. In this study, to explore the adherence, colonization and invading potential of the UPEC isolates *in vitro*, virulence gene expression of the significantly distributed VFs in the UPECnp and UPECp isolates upon 3 hpi in HTB4 cells was investigated. ABU strain *E. coli* 83972 was used as the control. It was noteworthy that, although the distribution of the major virulent genes was significant in the UPECp and UPECnp isolates, there was discrete variation in their expression upon 3 hpi. An overall reduced relative fold change in *fimH* expression in UPECnp and an increased fold change in UPECp in the infected host cells at 3 hpi might be due to an early attachment of the former to the host cells, which suggests an enhanced adherence and colonization potential of UPECnp compared with UPECp isolates. Earlier studies revealed that fimbrial or afimbrial adhesins that bound to host cell receptors enabled adhesion, which was the first stage of colonization that preceded cellular invasion [53,54]. FimH in type-1-fimbriae binds to D-mannosylated uroplakin, which promotes colonization and development of intracellular bacterial communities, which are similar to biofilms [53]. Additionally, a higher incidence of MDR in UPECnp isolates than in UPECp isolates corroborated the higher adherence potential of the former, similar to a study by Shah *et al.* [55] that showed a positive correlation between high biofilm production indicating high colonization capacity and MDR incidence in a batch of clinical UPEC isolates. Furthermore, reduced relative fold expression of *papC* in HTB4 cells at 3 hpi with both batches of isolates supported by a study conducted on *E. coli* CFT073, where the expression of type 1 fimbriae coordinately affected the expression of P fimbriae in an inverse manner, expressed one fimbriae at a time during the coregulation of the fimbriae operon [56,57]. DNA microarray analysis of *E. coli* CFT073 *in vivo* also showed high upregulation of type 1 fimbriae along with downregulation of other fimbrial genes like *pap* and *foc/sfa* [56]. Nonetheless, an upregulation of *papC* expression was reported in UPEC isolates at 6 hpi in urothelial cells, which also indicated a late expression of *pap* genes [17]. A significant increase in the relative fold expression of *hlyA* in UPECnp indicated their high invasion potential post-adhesion [58]. However, a nonsignificant increase in the relative fold expression of *hlyA* in UPECp isolates was probably attributed to late adherence followed by invasion at 3 hpi. The siderophores expressed by UPEC assisted bacterial survival and might be expressed after successful adherence and colonization. In this study, reduced relative fold expression of *iroN* at 3 hpi in HTB4 cells upon infection with both UPECp and UPECnp isolates indicated that the initiation of expression of *iroN* might be a later event in the propagation of infection.

Basic inflammatory responses generated against the expression of virulence determinants of UPEC within the infected host also pose essential criteria for the assessment of the severity of a UTI [50]. The various chemokines and cytokines, such as CXCL8, CCL2, interleukins (IL-6, IL-8, IL17A, IL-5, TNF- α , TGF- β and IFN- γ), GCSF and MCP-1 were used to a great extent for signaling in innate immunity. During infection, IL-6 might facilitate the conversion from a neutrophilic to a mostly monocyte response. Additionally, in response to IL-8 and other

chemotactic stimuli, circulating polymorphonuclear leukocytes might penetrate the bladder tissue and engulf UPEC to overcome the infection [59,60]. An overall reduced relative fold expression of *IL-6* and *IL-8* at 3 hpi in UPECnp-infected HTB-4 cells and an increase in their relative fold expression in UPECp infection, respectively, at 3 hpi compared with infection with ABU83972 indicated that the invading potential of UPECnp was higher than the UPECp isolates. This finding was consistent with another study that reported UPEC strains UTI89 or NU14 induced reduced *IL-6* compared with commensal or laboratory strain MG1655 when infected in HTB-4 uroepithelial cells [61]. An additional study also reported that *IL-6* and *IL-8* secretion were significantly lower in HTB-5 cells infected with CFT073 at 3 hpi and 5 hpi compared with uninfected cells [21]. Therefore, the current study showed that the efficiency of colonization was related to *fimH*, *IL-6* and *IL-8* expression at 3 hpi in HTB-4 cells *in vitro*, although a statistically significant correlation was only observed in *fimH* and *IL-8* expressions in UPECp infection. *TNF- α* is a potent proinflammatory cytokine, which is one of the most prevalent early mediators in inflamed tissue and is promptly released following trauma, infection or exposure to bacterial-derived lipopolysaccharide (LPS) [62]. In this study, at 3 hpi, an enhanced relative fold expression of *TNF- α* in HTB-4 cells with UPECnp indicated a successful initiation of infection. On the contrary, the reduced relative fold expression of *TNF- α* in HTB-4 cells infected with UPECp at 3 hpi supported their slow adherence potential to the urothelial cells. Elevated levels of *IFN- γ* might lead to low bacterial clearance and hence promote bacterial infections [63]. Therefore, a statistically significant reduced relative fold expression of *IFN- γ* in HTB-4 cells with UPECp isolates at 3 hpi might be the cause of low adherence and invading potential of the UPECp isolates to the HTB-4 cells at 3 hpi. Overall, a reductive relative fold expression of *IFN- γ* in this study was very similar to another study that reported a lack of *IFN- γ* release in infected A498 renal epithelial cells at 4 hpi [64]. Furthermore, reduced expression of *IFN- γ* in UPECp-infected HTB-4 cells was correlated ($p < 0.05$) with the elevated expression of *fimH*, suggesting its late release in uroepithelial cells. UPEC causes host inflammation by different VFs, including hemolysin and cytotoxic necrotizing factors, by inducing inflammatory cytokines such as *IL-1 β* [18]. However, this study showed an overall significant enhancement of relative fold expression of *blyA* in UPECnp isolates collected from infected HTB-4 cells at 3 hpi, with very low relative fold expression of *IL-1 β* in the HTB-4 cells, which was contrary to the study by Jung *et al.* [18]. Nonetheless, Brauner *et al.* [65] reported that the frequency of *IL-1 β* production by epithelial cells increased gradually over time and detectable levels were observed at 24 hpi. Additionally, in this study, reduced expression of *IL-1 β* in the UPECp-infected HTB-4 cells was statistically correlated ($p < 0.05$) with elevated expression of *fimH* in the isolates, which suggested a bacterial mechanism to overcome the host defense system. In acute UTI in mice, *IL-17A* was released from $\gamma\delta$ T-cells during the innate immune response and was implicated in the control of acute and chronic UPEC infections [66]. It enhanced neutrophil migration to infected tissue and resulted in suboptimal clearance of UPEC. *IL-6* promoted the release of *IL-17* from $\gamma\delta$ T-cells and was identified as an efficient prognostic marker for pyelonephritis at 24 hpi. Consistent with these studies, we also found a significant enhancement in the relative fold expression of *IL-17A* in UPECp-infected HTB-4 cells 3 hpi compared with UPECnp-infected epithelial cells. Moreover, the level of *IL-6* expression in this study in HTB-4 cells infected with UPECp was also consistent with the study by Chamoun *et al.* [66]. Furthermore, elevated expression of *IL-17A* in HTB-4 cells infected with UPECp isolates was statistically correlated ($p < 0.05$) with elevated expression of *fimH* in the isolates, which further supported the fact that the bacteria thrived by its efficient attachment to the epithelial cells to establish infection at 3 hpi. Studies in the murine model have shown that mice that developed persistent bacteriuria had significantly enhanced levels of *IL-5* at 24 hpi [67,68], which was consistent with this study showing enhanced relative fold expression of *IL-5* at 3 hpi. MCP-1 and GCSF along with other proinflammatory cytokines were reported to be involved in bacterial clearance [15–17]. Several studies have shown elevated expression of MCP-1 and GCSF in humans and mice at varied time points in UPEC infection [16,66]. However, in this study, reduction in relative fold expression of inflammatory mediators in UPECnp-infected HTB-4 cells at 3 hpi advocated the incidence of early invasion in UPECnp (i.e., rapid reduction in expression of both proteins within 3 h). Conversely, the negative fold expression of *MCP-1* and *GCSF* in UPECp-infected HTB-4 cells at 3 hpi might be due to the low infection potential of UPECp, which may lead to a rise in the expression level of the immunoregulators at a later stage of infection. In the UPECnp isolates, reduced expression of *papC* was statistically correlated ($p < 0.05$) with the reduced expression of *GCSF* in HTB-4 cells, which also suggested an alternative survival mechanism in the bacteria after the successful invasion of uroepithelial cells to prevail over host clearance. Host inflammatory responses against intestinal bacterial proteins might be suppressed by *TGF- β* , which helped in the stimulation of immune tolerance. Upregulation of *TGF- β* upon infection imparted a protective role in the epithelial barrier function against invading pathogens [69]. Mice infected with UPEC isolates that exhibited high

fimH expression showed the lowest mRNA levels of Bmp-4, a member of the TGF- β superfamily, at 6 hpi [70,71]. In this study, the reduction in the relative fold expression in TGF- β with enhanced relative fold expression of *fimH* in UPECp isolates and the elevated relative fold expression in TGF- β with reduced relative fold expression of *fimH* in UPECnp isolates at 3 hpi supported the phenomenon of faster attachment of the UPECnp than UPECp isolates to the HTB-4 cells. Moreover, this study also revealed a statistical correlation ($p < 0.01$) between elevated expression of TGF- β in HTB-4 cells upon infection with UPECnp isolates that exhibited elevated expression of *hlyA*, which further indicated that TGF- β expression induced a protective mechanism to the epithelial cells to combat the cytotoxic function of *hlyA* expression in the UPECnp isolates.

Conclusion

In this study, antimicrobial resistance was more predominant among UPECnp than UPECp isolates. The expression pattern of the virulence determinants of the UPECp and UPECnp isolates with respective cytokine response elicited in HTB-4 cells upon 3 hpi *in vitro* was discrete. This is the first study of its kind to compare clinical UPEC isolates collected from different populations, especially from pregnant patients. Correlation between virulence determinants, *fimH* expressed in UPECp and *papC* and *hlyA* expressed in UPECnp isolates during infection, to the immunoregulatory cytokines, *IFN- γ* , *IL-17A* and *IL-1 β* in the former, and *GCSF* and TGF- β in the latter, were observed, respectively. Therefore, understanding the effect of the VFs, *fimH*, *papC* and *hlyA* expression in the clinical UPEC isolates on both the pro and anti-inflammatory cytokines poses an absolute necessity to better comprehend the severity of infection to administer appropriate therapeutics. Hence, cytokine profiling in addition to AMR analysis might be an alternative to cease empiric treatment and formulate a suitable prescription policy for effective therapeutics. Intensive murine studies must be initiated to validate the same to envisage host–pathogen interactions in the treatment of UTI.

Summary points

- Antibiotic resistance patterns of uropathogenic *Escherichia coli* isolated from nonpregnant (UPECnp) and pregnant (UPECp) populations, their infection potential and capacity to elicit host cytokine responses were investigated.
- Overall, the incidence of multidrug resistance was higher in UPECnp isolates than in UPECp isolates.
- The highest resistance was observed against ampicillin in both populations (100% and 90.48%), followed by cefotaxime, ciprofloxacin and ceftazidime in UPECnp and cotrimoxazole and cefotaxime in UPECp.
- A significant correlation was observed in the resistance patterns between amikacin and imipenem and between ciprofloxacin and cotrimoxazole in UPECnp and between ceftazidime/cefotaxime and ciprofloxacin and cotrimoxazole in UPECp.
- Relative expression of different virulence genes (*fimH*, *papC*, *papGIII*, *sfaA*, *hlyA*, *iroN*) indicated significant positive fold change of *hlyA* and significant negative fold change of *fimH* and *papC* in UPECnp.
- A positive fold change of *fimH* and negative fold change of *papC* and *iroN* were statistically significant in UPECp upon 3 h postinfection in HTB-4 cells.
- UPECnp-infected HTB-4 cells exhibited elevated relative fold expression of *TNF- α* , *IL-5* and TGF- β , with relatively reduced fold expression of *IL-6*, *IL-8*, *GCSF*, *IL-1 β* and *IL-17A*.
- Comparatively high expression of *IL-6*, *IL-8*, *IL-17A* and *IL-5* with relatively low expression of *TNF- α* , *IFN- γ* , *MCP-1*, *GCSF*, *IL-1 β* and TGF- β in HTB-4 cells upon UPECp infection were observed.
- Significant positive correlation patterns in UPECp between *fimH* and *IL-17A* and in UPECp between *fimH* and *IFN- γ* and significant negative correlation patterns in UPECp between *fimH* and *IL-1 β* , in UPECnp between *papC* and *GCSF* and in UPECnp between *hlyA* and TGF- β were observed.
- Cytokine profiling of infected hosts in addition to antibiotic resistance pattern analysis of the uropathogenic *Escherichia coli* isolates might pave the way toward suitable guidelines for appropriate therapeutics and cease empiric treatment.

Author contributions

S Koley and M Mukherjee proposed the concepts of the study and design. Data acquisition was done by S Koley. Data analysis and drafting and revision of the manuscript were done by S Koley and M Mukherjee.

Acknowledgments

The authors would like to express their sincere gratitude to the Director, Calcutta School of Tropical Medicine, Kolkata, and West Bengal, India for his kind support and cooperation.

Financial & competing interests disclosure

The authors have no relevant affiliations or financial involvement with any organization or entity with a financial interest in or financial conflict with the subject matter or materials discussed in the manuscript. This includes employment, consultancies, honoraria, stock ownership or options, expert testimony, grants or patents received or pending, or royalties.

No writing assistance was utilized in the production of this manuscript.

Ethical conduct of research

The study protocol was approved by the Institutional Ethics Committee (IEC ref. no. CREC-STM/2020-AG-13).

References

Papers of special note have been highlighted as: ● of interest; ●● of considerable interest

1. Bien J, Sokolova O, Bozko P. Role of uropathogenic *Escherichia coli* virulence factors in development of urinary tract infection and kidney damage. *Intl J. Nephrol.* 2012, 1–15 (2012).
2. Habak PJ, Griggs J. Urinary tract infection in pregnancy. In: *StatPearls*. StatPearls Publishing, FL, USA (2022).
3. Konwar M, Gogtay NJ, Ravi R, Thatte UM, Bose D. Evaluation of efficacy and safety of fosfomycin versus nitrofurantoin for the treatment of uncomplicated lower urinary tract infection (UTI) in women—a systematic review and meta-analysis. *J. Chemother.* 34(3), 139–148 (2022).
4. Czajkowski K, Broś-Konopielko M, Teliga-Czajkowska J. Urinary tract infection in women. *PM* 20(1), 40–47 (2021).
5. Zhu H, Chen Y, Hang Y *et al.* Impact of inappropriate empirical antibiotic treatment on clinical outcomes of urinary tract infections caused by *Escherichia coli*: a retrospective cohort study. *J. Glob. Antimicrob. Resist.* 26, 148–153 (2021).
6. Basu S, Mukherjee SK, Hazra A, Mukherjee M. Molecular characterization of uropathogenic *Escherichia coli*: nalidixic acid and ciprofloxacin resistance, virulent factors and phylogenetic background. *JCDR* 7(12), 2727–2731 (2013).
7. Mukherjee M, Koley S, Mukherjee SK, Basu S, Ghosh B, Chakraborty S. Phylogenetic background of *E. coli* isolated from asymptomatic pregnant women from Kolkata, India. *J. Infect. Dev. Ctries* 9(07), 720–724 (2015).
8. Ballesteros-Monreal MG, Arenas-Hernández MM, Enciso-Martínez Y *et al.* Virulence and resistance determinants of uropathogenic *Escherichia coli* strains isolated from pregnant and non-pregnant women from two states in Mexico. *IDR* 13, 295–310 (2020).
- **Discrete virulence gene distribution was reported in this study from pregnant and nonpregnant populations.**
9. M Taha Aloo H. Molecular characterization of multi drug resistance *Escherichia coli* isolated among diabetes mellitus patients in Dongla State, Sudan. *AJBSR* 9(5), 357–363 (2020).
10. Terlizzi ME, Gribaudo G, Maffei ME. Uropathogenic *Escherichia coli* (UPEC) infections: virulence factors, bladder responses, antibiotic, and non-antibiotic antimicrobial strategies. *Front. Microbiol.* 8, 1566 (2017).
11. Spencer JD, Schwaderer AL, Becknell B, Watson J, Hains DS. The innate immune response during urinary tract infection and pyelonephritis. *Pediatr. Nephrol.* 29(7), 1139–1149 (2014).
12. Nagamatsu K, Hannan TJ, Guest RL *et al.* Dysregulation of *Escherichia coli* α -hemolysin expression alters the course of acute and persistent urinary tract infection. *Proc. Natl Acad. Sci. USA* 112(8), E871–E880 (2015).
13. Waldhuber A, Puthia M, Wieser A *et al.* Uropathogenic *Escherichia coli* strain CFT073 disrupts NLRP3 inflammasome activation. *J. Clin. Invest.* 126(7), 2425–2436 (2016).
14. Demirel I, Persson A, Brauner A, Särndahl E, Kruse R, Persson K. Activation of the NLRP3 inflammasome pathway by uropathogenic *Escherichia coli* is virulence factor-dependent and influences colonization of bladder epithelial cells. *Front. Cell. Infect. Microbiol.* 8, 81 (2018).
15. Ambite I, Puthia M, Nagy K *et al.* Molecular basis of acute cystitis reveals susceptibility genes and immunotherapeutic targets. *PLOS Pathog.* 12(10), e1005848 (2016).
16. Sundac L, Dando SJ, Sullivan MJ, Derrington P, Gerrard J, Ulett GC. Protein-based profiling of the immune response to uropathogenic *Escherichia coli* in adult patients immediately following hospital admission for acute cystitis. *Pathog. Dis.* 74(6), fw062 (2016).
17. Engelsöy U, Rangel I, Demirel I. Impact of proinflammatory cytokines on the virulence of uropathogenic *Escherichia coli*. *Front. Microbiol.* 10, 1051 (2019).
- **This study investigated the impact of proinflammatory cytokines (TNF- α , IL-1 β , IL-6, IL-8 and IFN- γ) on the virulence of uropathogenic *Escherichia coli* (UPEC) prototype strain CFT073.**
18. Jung J-H, Hong HJ, Ghaderpour A *et al.* Differential interleukin-1 β induction by uropathogenic *Escherichia coli* correlates with its phylotype and serum C-reactive protein levels in Korean infants. *Sci. Rep.* 9(1), doi:10.1038/s41598-019-52070-3 (2019).
- **This study revealed that IL1 β production in infected hosts was dependent on hemolysin and cytotoxic necrotizing factors of the invading UPEC.**
19. Chu CM, Lowder JL. Diagnosis and treatment of urinary tract infections across age groups. *Am. J. Obstet. Gynecol.* 219(1), 40–51 (2018).

20. Clinical and Laboratory Standards Institute. *Performance Standards for Antimicrobial Susceptibility Testing*. (30th edition). CLSI supplement M100, PA USA (2020).
21. Vega-Hernández R, Ochoa SA, Valle-Rios R *et al*. Flagella, Type I fimbriae and curli of uropathogenic *Escherichia coli* promote the release of proinflammatory cytokines in a coculture system. *Microorganisms* 9(11), 2233 (2021).
22. Stork C, Kovács B, Rózsai B *et al*. Characterization of asymptomatic bacteriuria *Escherichia coli* isolates in search of alternative strains for efficient bacterial interference against uropathogens. *Front. Microbiol.* 9, 214 (2018).
23. Ho C-H, Fan C-K, Yu H-J *et al*. Testosterone suppresses uropathogenic *Escherichia coli* invasion and colonization within prostate cells and inhibits inflammatory responses through JAK/STAT-1 signaling pathway. *PLOS ONE* 12(6), e0180244 (2017).
24. Monroy-Pérez E, Cerón AB, García Cortés LR *et al*. Virulence gene transcription, phylogroups, and antibiotic resistance of cervico-vaginal pathogenic *E. coli* in Mexico. *PLOS ONE* 15(6), e0234730 (2020).
25. Bandyopadhyay D, Mukherjee M. Reactive oxygen species and *uspA* overexpression: an alternative bacterial response toward selection and maintenance of multidrug resistance in clinical isolates of uropathogenic *E. coli*. *Eur. J. Clin. Microbiol. Infect. Dis.* 39(9), 1753–1760 (2020).
26. Yadav S. Correlation analysis in biological studies. *J. Pract. Cardiovasc. Sci.* 4(2), 116 (2018).
27. Ghosh A, Bandyopadhyay D, Koley S, Mukherjee M. Uropathogenic *Escherichia coli* in India – an overview on recent research advancements and trends. *Appl. Biochem. Biotechnol.* 193(7), 2267–2296 (2021).
28. Bachchan KT, Ramanujan SS. Prevalence of multidrug resistant asymptomatic bacteriuria from pregnant and non-pregnant women in the Erode district. *Int. J. Biochem. Biotechnol.* 5(3), 665–669 (2016).
29. Paniagua-Contreras GL, Monroy-Pérez E, Rodríguez-Moctezuma JR, Domínguez-Trejo P, Vaca-Paniagua F, Vaca S. Virulence factors, antibiotic resistance phenotypes and O-serogroups of *Escherichia coli* strains isolated from community-acquired urinary tract infection patients in Mexico. *J. Microbiol. Immunol. Infect.* 50(4), 478–485 (2017).
30. Ramírez-Castillo FY, Moreno-Flores AC, Avelar-González FJ, Márquez-Díaz F, Harel J, Guerrero-Barrera AL. An evaluation of multidrug-resistant *Escherichia coli* isolates in urinary tract infections from Aguascalientes, Mexico: cross-sectional study. *Ann. Clin. Microbiol. Antimicrob.* 17(1), 34 (2018).
31. Abate D, Marami D, Letta S. Prevalence, antimicrobial susceptibility pattern, and associated factors of urinary tract infections among pregnant and nonpregnant women at public health facilities, Harar, Eastern Ethiopia: a comparative cross-sectional study. *Can. J. Infect. Dis. Med. Microbiol.* 2020, 9356865 (2020).
32. Asmat U, Mumtaz MZ, Malik A. Rising prevalence of multidrug-resistant uropathogenic bacteria from urinary tract infections in pregnant women. *J. Taibah Univ. Med. Sci.* 16(1), 102–111 (2021).
33. Ali AH, Reda DY, Ormago MD. Prevalence and antimicrobial susceptibility pattern of urinary tract infection among pregnant women attending Hargeisa Group Hospital, Hargeisa, Somaliland. *Sci. Rep.* 12(1), 1419 (2022).
34. Yun KW, Kim HY, Park HK, Kim W, Lim IS. Virulence factors of uropathogenic *Escherichia coli* of urinary tract infections and asymptomatic bacteriuria in children. *J. Microbiol. Immunol. Infect.* 47(6), 455–461 (2014).
35. Rahdar M, Rashki A, Miri HR, Rashki Ghalehnoo M. Detection of *pap*, *sfa*, *afa*, *foc*, and *fim* adhesin-encoding operons in uropathogenic *Escherichia coli* isolates collected from patients with urinary tract infection. *Jundishapur J. Microbiol.* 8 (8), e22647 (2015).
36. Lee JH, Subhadra B, Son Y-J *et al*. Phylogenetic group distributions, virulence factors and antimicrobial resistance properties of uropathogenic *Escherichia coli* strains isolated from patients with urinary tract infections in South Korea. *Lett. Appl. Microbiol.* 62(1), 84–90 (2016).
37. Tabasi M. Genotypic characterization of virulence factors in *Escherichia coli* isolated from patients with acute cystitis, pyelonephritis and asymptomatic bacteriuria. *JCDR* 10(12), DC01–DC07 (2016).
38. Munkhdelger Y, Gunregjav N, Dorjpurev A, Juniichiro N, Sarantuya J. Detection of virulence genes, phylogenetic group and antibiotic resistance of uropathogenic *Escherichia coli* in Mongolia. *J. Infect. Dev. Ctries* 11(01), 51–57 (2017).
39. Ali I, Rafaque Z, Ahmed I *et al*. Phylogeny, sequence-typing and virulence profile of uropathogenic *Escherichia coli* (UPEC) strains from Pakistan. *BMC Infect. Dis.* 19(1), 620 (2019).
40. Cristea VC, Gheorghe I, Czobor Barbu I *et al*. Snapshot of phylogenetic groups, virulence, and resistance markers in *Escherichia coli* uropathogenic strains isolated from outpatients with urinary tract infections in Bucharest, Romania. *BioMed Res. Intl* 2019, 5712371 (2019).
41. Dadi BR, Abebe T, Zhang L, Mihret A, Abebe W, Amogne W. Distribution of virulence genes and phylogenetics of uropathogenic *Escherichia coli* among urinary tract infection patients in Addis Ababa, Ethiopia. *BMC Infect. Dis.* 20(1), 108 (2020).
42. Rezaatfighi SE, Mirzarazi M, Salehi M. Virulence genes and phylogenetic groups of uropathogenic *Escherichia coli* isolates from patients with urinary tract infection and uninfected control subjects: a case-control study. *BMC Infect. Dis.* 21(1), 361 (2021).
43. Al-Zubaidi SJJ. Prevalence of virulence factors genes of *Escherichia coli* isolated from pregnant and non-pregnant women with urinary tract infection in Diyala Iraq. *Syst. Rev. Pharm.* 11(6), 1420–1427 (2020).

44. Lee S, Yu JK, Park K, Oh E-J, Kim S-Y, Park Y-J. Phylogenetic groups and virulence factors in pathogenic and commensal strains of *Escherichia coli* and their association with blaCTX-M. *Ann. Clin. Lab. Sci.* 40(4), 361–367 (2010).
45. Tarchouna M, Ferjani A, Ben-Selma W, Boukadida J. Distribution of uropathogenic virulence genes in *Escherichia coli* isolated from patients with urinary tract infection. *Intl J. Infect. Dis.* 17(6), e450–e453 (2013).
46. Alabsi MS, Ghazal A, Sabry SA, Alasaly MM. Association of some virulence genes with antibiotic resistance among uropathogenic *Escherichia coli* isolated from urinary tract infection patients in Alexandria, Egypt: a hospital-based study. *J. Glob. Antimicrob. Resist.* 2(2), 83–86 (2014).
47. Dhakal BK, Mulvey MA. The UPEC pore-forming toxin α -hemolysin triggers proteolysis of host proteins to disrupt cell adhesion, inflammatory, and survival pathways. *Cell Host Microbe* 11(1), 58–69 (2012).
- **This study showed that HlyA-induced proteolysis of host proteins likely allow UPEC to suppress inflammatory responses in the host.**
48. Moeiniazadeh H, Shaheli M. Frequency of hlyA, hlyB, hlyC and hlyD genes in uropathogenic *Escherichia coli* isolated from UTI patients in Shiraz. *GMS Hyg. Infect. Control* 16, Doc25 (2021).
49. Karimian A, Momtaz H, MahbobeMadani M. Detection of uropathogenic *Escherichia coli* virulence factors in patients with urinary tract infection in Iran. *Afr. J. Microbiol. Res.* 6(39), 6811–6816 (2012).
50. Reygaert WC. Innate immune response to urinary tract infections involving *Escherichia coli*. *J. Clin. Cell Immunol.* 05(06), doi:10.4172/2155-9899.1000280 (2014).
51. Roos V, Ulett GC, Schembri MA, Klemm P. The asymptomatic bacteriuria *Escherichia coli* strain 83972 outcompetes uropathogenic *E. coli* strains in human urine. *Infect. Immun.* 74(1), 615–624 (2006).
52. Hernández JG, Sundén F, Connolly J, Svanborg C, Wullt B. Correction: genetic control of the variable innate immune response to asymptomatic bacteriuria. *PLOS ONE* 7(1), doi:10.1371/annotation/ab823a8e-01b1-48b8-8b2a-0993d805fc50 (2012).
53. Kalita A, Hu J, Torres AG. Recent advances in adherence and invasion of pathogenic *Escherichia coli*. *Curr. Opin. Infect. Dis.* 27(5), 459–464 (2014).
54. Frömmel U, Lehmann W, Rödiger S *et al.* Adhesion of human and animal *Escherichia coli* strains in association with their virulence-associated genes and phylogenetic origins. *Appl. Environ. Microbiol.* 79(19), 5814–5829 (2013).
55. Shah C, Baral R, Bartaula B, Shrestha LB. Virulence factors of uropathogenic *Escherichia coli* (UPEC) and correlation with antimicrobial resistance. *BMC Microbiol.* 19(1), 204 (2019).
- **This study established a significant association between virulence factors of UPEC and their antimicrobial resistance pattern. The highest resistance toward ampicillin, cotrimoxazole and norfloxacin was also reported.**
56. Snyder JA, Haugen BJ, Buckles EL *et al.* Transcriptome of uropathogenic *Escherichia coli* during urinary tract infection. *Infect. Immun.* 72(11), 6373–6381 (2004).
- **In this study, transcriptomic analysis of *Escherichia coli* prototype strain CFT073 isolated from infected CBA/J mice was reported.**
57. Melican K, Sandoval RM, Kader A *et al.* Uropathogenic *Escherichia coli* P and Type 1 fimbriae act in synergy in a living host to facilitate renal colonization leading to nephron obstruction. *PLoS Pathog.* 7(2), e1001298 (2011).
58. Flores-Mireles AL, Walker JN, Caparon M, Hultgren SJ. Urinary tract infections: epidemiology, mechanisms of infection and treatment options. *Nat. Rev. Microbiol.* 13(5), 269–284 (2015).
59. Stocks CJ, Phan M-D, Achard MES *et al.* Uropathogenic *Escherichia coli* employs both evasion and resistance to subvert innate immune-mediated zinc toxicity for dissemination. *Proc. Natl Acad. Sci. USA* 116(13), 6341–6350 (2019).
60. Kim A, Ahn JH, Choi WS *et al.* What is the cause of recurrent urinary tract infection? Contemporary microscopic concepts of pathophysiology. *Int. Neurol.* 25(3), 192–201 (2021).
61. Prasanphanich NS, Gregory EJ, Erickson JJ, Miller-Handley H, Kinder JM, Way SS. Preconceptual priming overrides susceptibility to *Escherichia coli* systemic infection during pregnancy. *mBio* 12(1), e00002–00021 (2021).
62. Parameswaran N, Patial S. Tumor necrosis factor- α signaling in macrophages. *Crit. Rev. Eukar. Gene Expr.* 20(2), 87–103 (2010).
63. Schütze S, Kaufmann A, Bunkowski S, Ribes S, Nau R. Interferon-gamma impairs phagocytosis of *Escherichia coli* by primary murine peritoneal macrophages stimulated with LPS and differentially modulates proinflammatory cytokine release. *Cytokine X* 3(3), doi:10.1016/j.cytok.2021.100057 (2021).
- **This study concluded that elevated levels of IFN- γ might lead to reduced bacterial clearance in aged individuals.**
64. Steiner SE, Choong FX, Antypas H *et al.* UPEC kidney infection triggers neuro-immune communication leading to modulation of local renal inflammation by splenic IFN γ . *PLoS Pathog.* 17(5), e1009553 (2021).
65. Brauner A, Söderhäll M, Jacobson SH, Lundahl J, Andersson U, Andersson J. *Escherichia coli*-induced expression of IL-1 α IL-1 β IL-6 and IL-8 in normal human renal tubular epithelial cells. *Clin. Exp. Immunol.* 124(3), 423–428 (2001).
66. Chamoun MN, Sullivan MJ, Goh KGK *et al.* Restriction of chronic *Escherichia coli* urinary tract infection depends upon T cell-derived interleukin-17, a deficiency of which predisposes to flagella-driven bacterial persistence. *FASEB J.* 34(11), 14572–14587 (2020).

●● This study showed that deficiency in production of IL-17A contributed to bacterial persistence.

67. O'Brien VP, Dorsey DA, Hannan TJ, Hultgren SJ. Host restriction of *Escherichia coli* recurrent urinary tract infection occurs in a bacterial strain-specific manner. *PLoS Pathog.* 14(12), e1007457 (2018).
68. Gilbert NM, O'Brien VP, Waller C, Batourina E, Mendelsohn CL, Lewis AL. Gardnerella exposures alter bladder gene expression and augment uropathogenic *Escherichia coli* urinary tract infection in mice. *Front. Cell. Infect. Microbiol.* 12, doi:10.3389/fcimb.2022.909799 (2022).
69. Juang J, Yin H, Zhang C, Wang J. Effects of *E. coli* infection on the expressions of TGF- β /Smads signaling pathway in broiler intestine. *Braz. J. Poult. Sci.* 22(1), doi:10.1590/1806-9061-2019-1101 (2020).
70. Ljungberg JK, Kling JC, Tran TT, Blumenthal A. Functions of the WNT signaling network in shaping host responses to infection. *Front. Immunol.* 10, 2521 (2019).
71. Jafari NV, Rohn JL. The urothelium: a multi-faceted barrier against a harsh environment. *Mucosal Immunol.* 15, 1127–1142 (2022).

Acute Kidney Injury in Adults due to COVID-19 infection: A Systematic Review and Meta-Analysis

Snehashis Koley¹, Ambar Bose², Mandira Mukherjee³

Senior Research Fellow, Department of Biochemistry and Medical Biotechnology, School of Tropical Medicine, Kolkata

Junior Research Fellow, Department of Biochemistry and Medical Biotechnology, School of Tropical Medicine, Kolkata

Associate Professor and HOD, Department of Biochemistry and Medical Biotechnology, School of Tropical Medicine

Abstract:

Background: In COVID-19 infection, Acute Kidney Injury (AKI) poses a severe complication. To help clinicians to implement effective clinical therapy, we systematically documented evidence on AKI incidence and associated death in COVID-19 infection among adult populations. **Methods:** For the systematic review and meta-analysis Guidelines laid by Preferred Reporting Items for Systematic Reviews and Meta-analysis (PRISMA) were followed. Studies were searched from Pubmed and MedRxiv databases published between December 2019 - June 19, 2021. **Results:** 55 out of 3175 total articles were identified as eligible for the qualitative review with 32 reports on adults (n=169560); mean age 65.34 years. Studies on AKI incidence, mortality, and AKI-related mortality in COVID-19-infected adults were included in the meta-analysis. Estimated AKI incidence in adults was 16.4% ([95%CI, 12.8 – 20.0%], $I^2 = 99.39\%$, $P < 0.001$). Moreover, overall death 34.8% ([95%CI, 21.3- 48.3%], $I^2 = 99.88\%$, $P < 0.001$) and AKI-related death 68.4% ([95%CI, 55.9–81.0%], $I^2 = 99.2\%$, $P < 0.001$) among adults revealed high statistical heterogeneity. **Conclusion:** AKI-related mortality was significantly high in COVID-19-infected adults. Therefore, AKI is common in COVID-19 infection and clinical management must be accordingly formulated.

Keywords: Acute kidney injury, Box plot, COVID-19, Forest plot, Meta-analysis

Introduction:

The Coronavirus disease 2019 (COVID-19) outbreak posed a pandemic that rapidly spread and generated tremendous pressure on healthcare management worldwide. The novel coronavirus SARS-CoV-2 (nCoV-19), was identified as the causative agent that produced acute respiratory illness. Coronaviruses (CoVs) belonged to the family of RNA viruses of zoonotic origin, enveloped, positive-sense, single-stranded with a wide range of genetic characteristics. These virus families are typed as α -, β -, γ -, δ - coronavirus (Zumla et al., 2016).

The World Health Organization (WHO) classified COVID-19 as a global health emergency of international concern in January 2020 (Puliatti, 2020). As of February 16, 2023, COVID-19 infection had been documented in more than 673 million people of all ages, with a mortality rate of 6.8 million (John Hopkins University Coronavirus tracker). In the past 2.5 years, we have made significant progress in our understanding of the pathophysiology, diagnosis, treatment, and post-infection complications of COVID-19 infection; however, there are hitherto several unexplored post-infection complications that demand investigation towards effective clinical management (Raina et al., 2021).

nCoV-19 infected patients were divided into three groups based on the severity of their symptoms: mild, severe, and critical. Pneumonia or non-pneumonia was documented in mild individuals. Over 80% of adult nCoV-19 infected patients had mild symptoms or were asymptomatic, according to reports. However, in a tiny subset of the population, the virus caused severe respiratory illness with multi-organ failure and fatal effects. During 24 to 48 hours, serious patients experienced dyspnea, respiratory frequency less than 30/minute, blood oxygen saturation below 93%, partial pressure of arterial oxygen to fraction of inspired oxygen ratio below 300, and/or lung infiltrates above 50%. (He et al., 2020). Co-morbid illnesses among elderly adults posed a significant risk of the development of complicated conditions. Acute kidney injury (AKI) symptoms were frequently documented in critically sick patients and caused significant morbidity and death (Peerapornratana et al., 2019), although, primarily least attention was given to the incidence of AKI in the nCoV-19 infected patients, and kidney involvement was viewed as minor clinical condition (Wang et al., 2020). However, subsequent reports indicated AKI as one of the most common complications in COVID-19 patients as SARS-CoV-2 especially invaded the kidneys, and more than 20% of the deceased patients had chronic kidney disease (Gagliardi et al., 2020). Therefore, careful monitoring of kidney function during the long-term effects of SARS-CoV-2 infection posed an absolute necessity. This meta-analysis and systemic review were conducted on documented evidence of AKI incidence and related mortality during COVID-19 infection from numerous publications around the globe.

Methodology:

Review of literature

Using the keywords "COVID-19," "Coronavirus," "SARS-CoV-2," and "Kidney damage," this study conducted a thorough search of scholarly articles in the electronic databases "Pubmed" and "Medrxiv" from December 2019 to June 19, 2021. The systematic review was created using the Preferred Reporting Items for Systematic Reviews and Meta-Analyses "PRISMA" criteria (Figure 1). (Moher et al., 2009). The inclusion criteria included various studies on the incidence of COVID-19 with AKI and reported mortality as an outcome of interest in adult (age >24 years) populations (original research articles on pertinent experimental and observational research, case studies, and reports). We gathered information from research related to the zone and country, time, mean patient age, clinical symptoms, lab findings, and pathological findings connected to kidney involvement in COVID-19 infection. For inclusion and eligibility, the authors separately reviewed the retrieved papers. Also, this investigation omitted scientific literature that incorporated systemic reviews and meta-analyses on COVID-19 with the incidence of AKI.

Quality Assessment

The Database of Abstract of Reviews of Effects (DARE) tool was used to assess the quality of the included papers. (Tran et al., 2021) The study's five questions were as follows: (i) Exclusion and inclusion criteria were disclosed, (ii) the search was sufficient, (iii) the included studies were synthesized, (iv) the included studies' quality was evaluated, and (v) there was enough information provided about each included study. For the meta-analysis, publications that matched at least four of the five criteria were considered. The quality assessment process was carried out by two reviewers, with a third reviewer acting as a referee in case of disagreement.

Statistical Analysis

Open Meta-Analyst software (for Windows 10 version; Brown University, Providence, USA) was used to conduct the statistical analysis (OpenMeta [Analyst], 2021). The pooled estimate of AKI incidence in COVID-19-infected adult populations, as well as the pooled estimate of mortality and AKI-associated mortality, were examined using random effects models and the Dersimonian-Laird technique, respectively. Each result was assessed within its 95% confidence interval (CI). Forest plots were used to display the results from each research as well as the total estimated results with a 95% confidence interval (CI). I^2 values, which indicate strong statistical heterogeneity when $I^2 > 75\%$, were used to measure the degree of statistical heterogeneity between various research groups. To graphically assess publication bias in each study Funnel Plots were drawn using QI-Macros add-ins in Microsoft Excel 2016. Box plots were created using Microsoft Excel 2016 and used to visualize the distribution of the data belonging to the adult population for each parameter. The mean and median values with the interquartile ranges (IQR) were also calculated. A P-value of ≤ 0.05 was used to determine the statistical significance of the difference between the AKI incidence and death statistics acquired using an independent-sample Student's T-test.

Results:

Study details and selection criteria

The database search on the COVID-19-infected population yielded a total of 32 reports on the adult population, shown in Table 1. Of these studies, 11 were retrospective studies, 8 were case studies, 4 were retrospective cohort, 4 were retrospective observational, 2 were observational, 1 each was Retrospective investigation, consecutive cohort, observational cohort, cohort, prospective and cross-section analysis.

Among the 32 studies on COVID-19 infection in the adult population, 17 reports were from China, 6 from the USA, 2 from Germany, and 1 each from France, Argentina, Italy, the UK, Turkey, and India respectively. The mean age of the COVID-19 patients was 65.34 years. Furthermore, it was observed that out of the 32 reports, 26 reports documented sufficient data on the incidence of AKI according to Kidney Disease: Improving Global Outcomes (KDIGO) criteria in the COVID-19 infected population.

Data Analysis

The overall sample size of COVID-19-infected adult patients considered across the 26 available studies with AKI was 169560, with the incidence estimated from individual studies that included a total sample size ranging from 5-154170. Meta-analysis was conducted to demonstrate AKI incidence in COVID-19 infection. The results obtained revealed that the pooled (95% CI) AKI incidence in COVID-19 positive

adult population was 16.4% (12.8 – 20.0%) [$I^2 = 99.39\%$, $P < 0.001$] (Figure 2a).

13 out of the 26 different studies on AKI COVID-19 adult patients with an overall sample size of 163877 (ranging from 52-154170) and with individual event sizes ≥ 17 revealed sufficient data on AKI and non-AKI related mortality. Our analysis of the 13 different studies related to AKI COVID-19 infection revealed a pooled mortality (95% CI) of 34.8 % (21.3 – 48.3%) [$I^2 = 99.83\%$, $P < 0.001$] (Figure 2b), however, the mortality rate due to AKI among the 13 different studies estimated a much higher pooled mortality (95% CI) of 68.4% (55.9 – 81.0%) [$I^2 = 99.2\%$, $P < 0.001$] with an overall sample size of 19563 (ranging from 15-16773) and with individual event sizes ≥ 12 (Figure 2c).

Further analysis of distributions and differences in AKI incidence, overall mortality, and mortality due to AKI in COVID-19 infection among adult populations was visualized by the box plots (Figure 3). The median (IQR) AKI incidence, death in COVID-19, and death related to AKI in COVID-19 infected adults were 19% (8.5 – 28.575%) (Figure 3a); 24.5% (17.8 – 46.85%) (Figure 3b) and 75% (40.45 – 96.5%) (Figure 3c) respectively.

Discussion:

Several reports on the substantial prevalence of AKI linked to morbidity and mortality in adults with COVID-19 infection were published globally, which helped clinicians create useful healthcare recommendations. We gathered the results of pertinent individual reports on AKI, mortality, and mortality rates due to AKI in COVID-19 infection in adults for this systemic review and meta-analysis, and we presented a reasonable and important summary of the results while taking into account any inconsistencies in the evidence. A more accurate estimate of the effect size was offered, which improved the simplicity of the findings from the various documented research.

In this study a wide variance of incidence of AKI in critically ill COVID-19-infected adult patients was estimated; at 31.7% (30.5 – 33%) in a population of 5216 from a study in the United States (Bowe et al., 2021) to as low as 0.5% (0.01 – 1.0%) in a population of 1099 from a study in Wuhan, China (Guan et al., 2020). Moreover, an incidence of AKI of 57.1% (20.5 – 93.8) - 20.0% (0.0 – 55.1) was also observed in studies that reported a low sample size (Lescure et al., 2020; Banerjee et al., 2020). Our meta-analysis of 26 different studies showed a pooled AKI incidence (95% CI) of 16.4% (12.8 – 20.0%) in the COVID-19-infected adult population (n=169560) that was significantly high compared to studies by Chan et al., 2021 on reports from 12 different adult population (n=3266) which revealed 7.58% (3.30 – 13.54%) pooled prevalence of AKI associated with COVID-19 infection, Kunutsor, and Laukkanen., 2020 revealed a pooled prevalence of AKI (95% CI) as 11.0 % (7.4 – 15.1%) in a population of n=13019 and a study by Hansrivijit et al., 2020 on the pooled incidence of AKI of 8.4% (6.0 – 11.7%) in a population of n=5497. Furthermore, the range of mean age of the COVID-19-infected adult population in this study was observed to be much higher (65.8±14.2-44.0 years) than in the population studied by Chan et al., 2021 (47.4 years). Therefore, age poses a risk factor in AKI-related COVID-19 infection among the adult population.

In our meta-analysis, the observation regarding pooled mortality and AKI-related pooled mortality established 2.6 times increased risk of mortality associated with AKI in the COVID-19-infected adult population. A study by Hansrivijit et al., 2020 revealed that pooled incidence of AKI in COVID-19 (95% CI) was 10.1% (6.0- 16.4%) with pooled mortality (95% CI) of 26.8% (16.9 - 39.7%) from 8 studies with sufficient data on AKI COVID- 19 infected population. However, the study also revealed a pooled mortality of 18.7 % (13.2 – 25.8%) in a population (n=26) of an overall sample size of 5497. Moreover, the pooled mortality for AKI COVID-19 estimated in our analysis was very high in comparison to that estimated by Hansrivijit et al., 2020. Therefore, this analysis indicated that AKI poses a risk factor for mortal consequences in COVID-19 infection.

The meta-analysis data obtained from this study established that AKI incidence and associated mortality in COVID-19 infection in adults was statistically significant with high statistical heterogeneity. Although most of the number studies on the adult population (sample size= 41 - 701) were reported from China the highest number of adults considered in the population, were from Germany (sample size = 154170; 91%).

Conclusion:

Insights from our investigation into AKI in the adult population in COVID-19 infection will help physicians to formulate appropriate guidelines for improved healthcare

management. Considering the present COVID-19 era, the statistically substantial AKI incidence and death in COVID-19 infection pose a severe global health apprehension.

Author contributions: SK, AB and MM contributed to the conception and design of the systematic review and meta-analysis. SK, AB contributed to the initial electronic literature search, study eligibility assessment, data extraction and analysis, interpretation and drafted the manuscript. MM critically revised the manuscript. All authors approved the final version of the manuscript.

Conflict of Interest: The authors declare that they have no conflict of interest

Acknowledgment: The authors would like to express their sincere gratitude to Director, Calcutta School of Tropical Medicine, Kolkata West Bengal, India for his kind support and cooperation.

References:

- Alberici, F., Delbarba, E., Manenti, C., Econimo, L., Valerio, F., Pola, A., Maffei, C., Possenti, S., Zambetti, N., Moscato, M., Venturini, M., Affatato, S., Gaggiotti, M., Bossini, N., & Scolari, F. (2020). A single center observational study of the clinical characteristics and short-term outcome of 20 kidney transplant patients admitted for SARS-CoV2 pneumonia. *Kidney International*, 97(6), 1083–1088. <https://doi.org/10.1016/j.kint.2020.04.002>
- Arentz, M., Yim, E., Klaff, L., Lokhandwala, S., Riedo, F. X., Chong, M., & Lee, M. (2020). Characteristics and Outcomes of 21 Critically Ill Patients With COVID-19 in Washington State. *JAMA*, 323(16), 1612. <https://doi.org/10.1001/jama.2020.4326>
- Banerjee, D., Popoola, J., Shah, S., Ster, I. C., Quan, V., & Phanish, M. (2020). COVID-19 infection in kidney transplant recipients. *Kidney International*, 97(6), 1076–1082. <https://doi.org/10.1016/j.kint.2020.03.018>
- Bowe, B., Cai, M., Xie, Y., Gibson, A. K., Maddukuri, G., & Al-Aly, Z. (2021). Acute Kidney Injury in a National Cohort of Hospitalized US Veterans with COVID-19. *Clinical Journal of the American Society of Nephrology*, 16(1), 14–25. <https://doi.org/10.2215/CJN.09610620>
- Cao, J., Tu, W.-J., Cheng, W., Yu, L., Liu, Y.-K., Hu, X., & Liu, Q. (2020). Clinical Features and Short-term Outcomes of 102 Patients with Coronavirus Disease 2019 in Wuhan, China. *Clinical Infectious Diseases*, 71(15), 748–755. <https://doi.org/10.1093/cid/ciaa243>
- Chan, V. W.-S., Chiu, P. K.-F., Yee, C.-H., Yuan, Y., Ng, C.-F., & Teoh, J. Y.-C. (2021). A systematic review on COVID-19: Urological manifestations, viral RNA detection and special considerations in urological conditions. *World Journal of Urology*, 39(9), 3127–3138. <https://doi.org/10.1007/s00345-020-03246-4>
- Chen, T., Wu, D., Chen, H., Yan, W., Yang, D., Chen, G., Ma, K.,

- Xu, D., Yu, H., Wang, H., Wang, T., Guo, W., Chen, J., Ding, C., Zhang, X., Huang, J., Han, M., Li, S., Luo, X., ... Ning, Q. (2020). Clinical characteristics of 113 deceased patients with coronavirus disease 2019: Retrospective study. *BMJ*, m1091. <https://doi.org/10.1136/bmj.m1091>
- Cheng, Y., Luo, R., Wang, K., Zhang, M., Wang, Z., Dong, L., Li, J., Yao, Y., Ge, S., & Xu, G. (2020). Kidney disease is associated with in-hospital death of patients with COVID-19. *Kidney International*, 97(5), 829–838. <https://doi.org/10.1016/j.kint.2020.03.005>
- Dellepiane, S., Vaid, A., Jaladanki, S. K., Paranjpe, I., Coca, S., Fayad, Z. A., Charney, A. W., Bottinger, E. P., He, J. C., Glicksberg, B. S., Chan, L., & Nadkarni, G. (2021). *Temporal Trends in COVID-19 associated AKI from March to December 2020 in New York City* [Preprint]. Nephrology. <https://doi.org/10.1101/2021.01.18.21249414>
- Deng, Y., Liu, W., Liu, K., Fang, Y.-Y., Shang, J., Zhou, L., Wang, K., Leng, F., Wei, S., Chen, L., & Liu, H.-G. (2020). Clinical characteristics of fatal and recovered cases of coronavirus disease 2019 in Wuhan, China: A retrospective study. *Chinese Medical Journal*, 133(11), 1261–1267. <https://doi.org/10.1097/CM9.0000000000000824>
- Du, Y., Tu, L., Zhu, P., Mu, M., Wang, R., Yang, P., Wang, X., Hu, C., Ping, R., Hu, P., Li, T., Cao, F., Chang, C., Hu, Q., Jin, Y., & Xu, G. (2020). Clinical Features of 85 Fatal Cases of COVID-19 from Wuhan. A Retrospective Observational Study. *American Journal of Respiratory and Critical Care Medicine*, 201(11), 1372–1379. <https://doi.org/10.1164/rccm.202003-0543OC>
- Fernández, P., Saad, E. J., Douthat, A., Marucco, F. A., Heredia, M. C., Barra, A. T., Bonazzi, S. T. R., Zlotogora, M., Barovero, M. A. C., Villada, S., Maldonado, J. P., Caeiro, J. P., Albertini, R. A., De La Fuente, J., & Douthat, W. G. (2021). *Acute kidney injury in hospitalized patients due to COVID-19* [Preprint]. Nephrology. <https://doi.org/10.1101/2021.05.31.21257656>
- Gagliardi, I., Patella, G., Michael, A., Serra, R., Provenzano, M., & Andreucci, M. (2020). COVID-19 and the Kidney: From Epidemiology to Clinical Practice. *Journal of Clinical Medicine*, 9(8), 2506. <https://doi.org/10.3390/jcm9082506>
- Guan, W., Ni, Z., Hu, Y., Liang, W., Ou, C., He, J., Liu, L., Shan, H., Lei, C., Hui, D. S. C., Du, B., Li, L., Zeng, G., Yuen, K.-Y., Chen, R., Tang, C., Wang, T., Chen, P., Xiang, J., ... Zhong, N. (2020). Clinical Characteristics of Coronavirus Disease 2019 in China. *New England Journal of Medicine*, 382(18), 1708–1720. <https://doi.org/10.1056/NEJMoa2002032>
- Guo, T., Fan, Y., Chen, M., Wu, X., Zhang, L., He, T., Wang, H., Wan, J., Wang, X., & Lu, Z. (2020). Cardiovascular Implications of Fatal Outcomes of Patients With Coronavirus Disease 2019 (COVID-19). *JAMA Cardiology*, 5(7), 811. <https://doi.org/10.1001/jamacardio.2020.1017>
- Hansrivijit, P., Qian, C., Boonpheng, B., Thongprayoon, C., Vallabhajosyula, S., Cheungpasitporn, W., & Ghahramani, N. (2020). Incidence of acute kidney injury and its association with mortality in patients with COVID-19: A meta-analysis. *Journal of Investigative Medicine*, 68(7), 1261–1270. <https://doi.org/10.1136/jim-2020-001407>
- He, F., Deng, Y., & Li, W. (2020). Coronavirus disease 2019: What we know? *Journal of Medical Virology*, 92(7), 719–725. <https://doi.org/10.1002/jmv.25766>
- Huang, C., Wang, Y., Li, X., Ren, L., Zhao, J., Hu, Y., Zhang, L., Fan, G., Xu, J., Gu, X., Cheng, Z., Yu, T., Xia, J., Wei, Y., Wu, W., Xie, X., Yin, W., Li, H., Liu, M., ... Cao, B. (2020). Clinical features of patients infected with 2019 novel coronavirus in Wuhan, China. *The Lancet*, 395(10223), 497–506. [https://doi.org/10.1016/S0140-6736\(20\)30183-5](https://doi.org/10.1016/S0140-6736(20)30183-5)
- Karabulut, I., Cinislioglu, A. E., Cinislioglu, N., Yilmazel, F. K., Utlu, M., Alay, H., Celik, E. C., & Adanur, S. (2020). The Effect of the Presence of Lower Urinary System Symptoms on the Prognosis of COVID-19: Preliminary Results of a Prospective Study. *Urologia Internationalis*, 104(11–12), 853–858. <https://doi.org/10.1159/000510761>
- Khalili, S., Sabaghian, T., Sedaghat, M., Soroureddin, Z., Askari, E., & Khalili, N. (2021). Prevalence, Risk Factors and Outcomes Associated with Acute Kidney Injury in Patients Hospitalized for COVID-19: A Comparative Study between Diabetic and Nondiabetic Patients. *Journal of Diabetes Research*, 2021, 1–9. <https://doi.org/10.1155/2021/6666086>
- Kunutsor, S. K., & Laukkanen, J. A. (2020). Renal complications in COVID-19: A systematic review and meta-analysis. *Annals of Medicine*, 52(7), 345–353. <https://doi.org/10.1080/07853890.2020.1790643>
- Lescure, F.-X., Bouadma, L., Nguyen, D., Parisey, M., Wicky, P.-H., Behlil, S., Gaymard, A., Bouscambert-Duchamp, M., Donati, F., Le Hingrat, Q., Enouf, V., Houhou-Fidouh, N., Valette, M., Mailles, A., Lucet, J.-C., Mentre, F., Duval, X., Descamps, D., Malvy, D., ... Yazdanpanah, Y. (2020). Clinical and virological data of the first cases of COVID-19 in Europe: A case series. *The Lancet Infectious Diseases*, 20(6), 697–706. [https://doi.org/10.1016/S1473-3099\(20\)30200-0](https://doi.org/10.1016/S1473-3099(20)30200-0)
- Li, Z., Wu, M., Yao, J., Guo, J., Liao, X., Song, S., Li, J., Duan, G., Zhou, Y., Wu, X., Zhou, Z., Wang, T., Hu, M., Chen, X., Fu, Y., Lei, C., Dong, H., Xu, C., Hu, Y., ... Yan, J. (2020). *Caution on Kidney Dysfunctions of COVID-19 Patients* [Preprint]. Infectious Diseases (except HIV/AIDS). <https://doi.org/10.1101/2020.02.08.20021212>
- Ling, Y., Xu, S.-B., Lin, Y.-X., Tian, D., Zhu, Z.-Q., Dai, F.-H., Wu, F., Song, Z.-G., Huang, W., Chen, J., Hu, B.-J., Wang, S., Mao, E.-Q., Zhu, L., Zhang, W.-H., & Lu, H.-Z. (2020). Persistence and clearance of viral RNA in 2019 novel coronavirus disease rehabilitation patients. *Chinese Medical Journal*, 133(9), 1039–1043. <https://doi.org/10.1097/CM9.0000000000000774>
- Moher, D., Liberati, A., Tetzlaff, J., Altman, D. G., & The PRISMA Group. (2009). Preferred Reporting Items for Systematic Reviews and Meta-Analyses: The PRISMA Statement. *PLoS Medicine*, 6(7), e1000097. <https://doi.org/10.1371/journal.pmed.1000097>

- Moledina, D. G., Simonov, M., Yamamoto, Y., Alausa, J., Arora, T., Biswas, A., Cantley, L. G., Ghazi, L., Greenberg, J. H., Hinchcliff, M., Huang, C., Mansour, S. G., Martin, M., Peixoto, A., chulz, W., Subair, L., Testani, J. M., Ugwuowo, U., Young, P., & Wilson, F. P. (2021). The Association of COVID-19 With Acute Kidney Injury Independent of Severity of Illness: A Multicenter Cohort Study. *American Journal of Kidney Diseases*, 77(4), 490–499.e1. <https://doi.org/10.1053/j.ajkd.2020.12.007>
- Mumm, J.-N., Osterman, A., Ruzicka, M., Stihl, C., Vilsmaier, T., Munker, D., Khatamzas, E., Giessen-Jung, C., Stief, C., Staehler, M., & Rodler, S. (2020). Urinary Frequency as a Possibly Overlooked Symptom in COVID-19 Patients: Does SARS-CoV-2 Cause Viral Cystitis? *European Urology*, 78(4), 624–628. <https://doi.org/10.1016/j.eururo.2020.05.013>
- Puliatti, S., Eissa, A., Eissa, R., Amato, M., Mazzone, E., Dell'Oglio, P., Sighinolfi, M. C., Zoeir, A., Micali, S., Bianchi, G., Patel, V., Wiklund, P., Coelho, R. F., Bernhard, J.-C., Dasgupta, P., Mottrie, A., & Rocco, B. (2020). COVID-19 and urology: A comprehensive review of the literature. *BJU International*, 125(6), E7–E14. <https://doi.org/10.1111/bju.15071>
- Peerapornratana, S., Manrique-Caballero, C. L., Gómez, H., & Kellum, J. A. (2019). Acute kidney injury from sepsis: Current concepts, epidemiology, pathophysiology, prevention and treatment. *Kidney International*, 96(5), 1083–1099. <https://doi.org/10.1016/j.kint.2019.05.026>
- Raina, R., Chakraborty, R., Mawby, I., Agarwal, N., Sethi, S., & Forbes, M. (2021). Critical analysis of acute kidney injury in pediatric COVID-19 patients in the intensive care unit. *Pediatric Nephrology*, 36(9), 2627–2638. <https://doi.org/10.1007/s00467-021-05084-x>
- Richardson, S., Hirsch, J. S., Narasimhan, M., Crawford, J. M., McGinn, T., Davidson, K. W., and the Northwell COVID-19 Research Consortium, Barnaby, D. P., Becker, L. B., Chelico, J. D., Cohen, S. L., Cockingham, J., Coppa, K., Diefenbach, M. A., Dominello, A. J., Duer-Hefele, J., Falzon, L., Gitlin, J., Hajizadeh, N., ... Zanos, T. P. (2020). Presenting Characteristics, Comorbidities, and Outcomes Among 5700 Patients Hospitalized With COVID-19 in the New York City Area. *JAMA*, 323(20), 2052. <https://doi.org/10.1001/jama.2020.6775>
- Ruan, Q., Yang, K., Wang, W., Jiang, L., & Song, J. (2020). Clinical predictors of mortality due to COVID-19 based on an analysis of data of 150 patients from Wuhan, China. *Intensive Care Medicine*, 46(5), 846–848. <https://doi.org/10.1007/s00134-020-05991-x>
- Shi, S., Qin, M., Shen, B., Cai, Y., Liu, T., Yang, F., Gong, W., Liu, X., Liang, J., Zhao, Q., Huang, H., Yang, B., & Huang, C. (2020). Association of Cardiac Injury With Mortality in Hospitalized Patients With COVID-19 in Wuhan, China. *JAMA Cardiology*, 5(7), 802. <https://doi.org/10.1001/jamacardio.2020.0950>
- Sundaram, S., Soni, M., & Annigeri, R. (2021). Urine abnormalities predict acute kidney injury in COVID-19 patients: An analysis of 110 cases in Chennai, South India. *Diabetes & Metabolic Syndrome: Clinical Research & Reviews*, 15(1), 187–191. <https://doi.org/10.1016/j.dsx.2020.12.021>
- Tran, L., Tam, D. N. H., Elshafay, A., Dang, T., Hirayama, K., & Huy, N. T. (2021). Quality assessment tools used in systematic reviews of in vitro studies: A systematic review. *BMC Medical Research Methodology*, 21(1), 101. <https://doi.org/10.1186/s12874-021-01295-w>
- Walendy, V., Girndt, M., & Greinert, D. (2021). *COVID-19 and acute kidney injury in German hospitals 2020* [Preprint]. Nephrology. <https://doi.org/10.1101/2021.04.30.21256331>
- Wang, D., Hu, B., Hu, C., Zhu, F., Liu, X., Zhang, J., Wang, B., Xiang, H., Cheng, Z., Xiong, Y., Zhao, Y., Li, Y., Wang, X., & Peng, Z. (2020). Clinical Characteristics of 138 Hospitalized Patients With 2019 Novel Coronavirus-Infected Pneumonia in Wuhan, China. *JAMA*, 323(11), 1061. <https://doi.org/10.1001/jama.2020.1585>
- Wang, L., Li, X., Chen, H., Yan, S., Li, D., Li, Y., & Gong, Z. (2020). Coronavirus Disease 19 Infection Does Not Result in Acute Kidney Injury: An Analysis of 116 Hospitalized Patients from Wuhan, China. *American Journal of Nephrology*, 51(5), 343–348. <https://doi.org/10.1159/000507471>
- Yang, X., Yu, Y., Xu, J., Shu, H., Xia, J., Liu, H., Wu, Y., Zhang, L., Yu, Z., Fang, M., Yu, T., Wang, Y., Pan, S., Zou, X., Yuan, S., & Shang, Y. (2020). Clinical course and outcomes of critically ill patients with SARS-CoV-2 pneumonia in Wuhan, China: A single-centered, retrospective, observational study. *The Lancet Respiratory Medicine*, 8(5), 475–481. [https://doi.org/10.1016/S2213-2600\(20\)30079-5](https://doi.org/10.1016/S2213-2600(20)30079-5)
- Zhang, G., Hu, C., Luo, L., Fang, F., Chen, Y., Li, J., Peng, Z., & Pan, H. (2020). Clinical features and short-term outcomes of 221 patients with COVID-19 in Wuhan, China. *Journal of Clinical Virology*, 127, 104364. <https://doi.org/10.1016/j.jcv.2020.104364>
- Zhou, F., Yu, T., Du, R., Fan, G., Liu, Y., Liu, Z., Xiang, J., Wang, Y., Song, B., Gu, X., Guan, L., Wei, Y., Li, H., Wu, X., Xu, J., Tu, S., Zhang, Y., Chen, H., & Cao, B. (2020). Clinical course and risk factors for mortality of adult inpatients with COVID-19 in Wuhan, China: A retrospective cohort study. *The Lancet*, 395(10229), 1054–1062. [https://doi.org/10.1016/S0140-6736\(20\)30566-3](https://doi.org/10.1016/S0140-6736(20)30566-3)
- Zumla, A., Chan, J. F. W., Azhar, E. I., Hui, D. S. C., & Yuen, K.-Y. (2016). Coronaviruses—Drug discovery and therapeutic options. *Nature Reviews Drug Discovery*, 15(5), 327–347. <https://doi.org/10.1038/nrd.2015.37>

Table 1: Details on adult population with COVID-19 infection

ArticleName	Zone and Country	Time of Study	Type	Mean Age (years)	Population	Male(%)	AKI reported	Diagnosis
Huang et al. (2020)	Wuhan, China	Dec 16, 2019 – Jan 2, 2020	Retrospective study	49.0	41	73	3 (7%)	Diabetes Mellitus (DM), hypertension and cardiovascular diseases. High bilirubin and creatinine in ICU patients
Yang et al. (2020)	Wuhan, China	Dec 24, 2019 – Jan 26, 2020	Retrospective Observational Study	59.7	52	67	15 (29%)	ARDS, Cardiac Injury, Hyperglycaemia, high creatinine, bilirubin, haemoglobin in non-survivors
Guan et al. (2020)	China	Dec 11, 2019 – Jan 29, 2020	Retrospective cohort study	47.0	1099	58	6 (0.5%)	DM, Hypertension, Chronic Heart Disease. High CRP, procalcitonin in severe patients
Zhou et al. (2020)	Wuhan, China	Dec 29, 2019 – Jan 31, 2020	Retrospective cohort study	56.0	191	62	28 (15%)	High DM and hypertension. Creatinine, troponin, creatine kinase, IL6 in non-survivor group
Li et al. (2020)	China	Jan 6 – Feb 21, 2020	Retrospective observational study	57.0	193	49	55 (28%)	Cardiovascular and cerebrovascular diseases, High creatinine, BUN, uric acid in severe group
Cheng Yet al. (2020)	Wuhan, China	Jan 28 – Feb 11, 2020	Consecutive cohort study	63.0	701	52.4	36 (5.1%)	High procalcitonin, creatinine kinase BUN in elevated baseline serum creatinine group. Higher prevalence of hypertension, DM, CKD
Wang et al. (2020)	Wuhan, China	Jan 14 – Feb 13, 2020	Retrospective study	54.0	116	57.8	-	Hypertension and DM as comorbidities. BUN and serum creatinine level mildly increased in infected patients
Ling et al. (2020)	Shanghai, China	Jan 20 – Feb 10, 2020	Retrospective study	44.0	66	42.4	-	High CRP, ESR, PCT levels during admission
Wang Det al. (2020)	Wuhan, PRC	January 1-28, 2020	Single-center case study	56.0	138	54.3	5 (3.6%)	Hypertension, Cardiovascular disease, DM higher in ICU groups. Creatinine, BUN, PCT, higher in the same.
Ruan et al. (2020)	Wuhan, China	January 2020	Retrospective Multicenter study	57.7	150	68.0	23 (15.3%)	High Hypertension, cardiovascular disease in fatal group. Creatine, BUN, CRP, IL6 high in fatal group
Chen et al. (2020)	Wuhan, China	Jan 13 – Feb 12, 2020	Case study	62.0	274	62.0	29 (11%)	Hypertension, DM, Cardiovascular disease high in death group. Higher CRP, PCT, BUN, ferritin, creatinine in death group
Du et al. (2020)	Wuhan, China	Jan 9 – Feb 15, 2020	Retrospective Observational study	65.8	85	72.9	30 (35%)	Hypertension, DM, coronary heart disease high. Increased BUN, creatine kinase, PCT, CRP
Cao et al. (2020)	Wuhan, China	Jan 3 – Feb 1, 2020	Observational cohort study	54.0	102	52.0	20 (19.6%)	Hypertension, DM, CKD in non-survivor group. High PCT, ALT, BUN, CRP, troponin in non-survivor group
Zhang et al. (2020)	Wuhan, China	Jan 2 – Feb 10, 2020	Retrospective single-center study	55.0	221	48.9	10 (4.5%)	Hypertension, DM in severe group. PCT, creatine kinase, ALT, BUN, CRP, troponin in severe group
Shi et al. (2020)	Wuhan, China	January 20 - February 10, 2020	Cohort Study	64	416	49.3	8 (1.9%)	Hypertension, DM, CKD, cerebrovascular disease high in cardiac injury.
Guo et al. (2020)	Wuhan, China	January 23, 2020 – February 23, 2020	Retrospective single-center observational case series	58.5	187	48.7	18 (9.6%)	Hypertension, CHD, DM, COPD, CKD in high TnT group than normal
Lescure et al. (2020)	Paris, France	January 24-29, 2020	Case study	47	5	60.0	1 (20%)	First confirmed case of COVID-19 in Europe. Most aged patient was severely ill, suffered from AKI, liver failure and shock
Deng et al. (2020)	Wuhan, China	Jan 1 – Feb 21, 2020	Retrospective investigation	54.0	225	55.1	20 (8.9%)	Creatinine, CRP, ALT, AST level high in death group. Hypertension, DM in death group

Acute Kidney Injury in Adults due to COVID-19 infection: A Systematic Review and Meta-Analysis

Khalili et al. (2021)	Iran	February–May 2020	Retrospective cohort study	65.7	254	55.9	58 (22.8%)	29.3% death in AKI patients. In recovered cases, 77% in stage 1 AKI, whereas in death cases 60% were in Stage 3 AKI
Bowe et al. (2021)	USA	February 1 – July 23, 2020	Retrospective cohort study	70	5216	94	1655 (31.7%)	58%, 13% and 16% in AKI stage 1, 2, 3. Mortality rate were higher than non-AKI and increased according to stages
Walendy et al. (2021)	Germany	February 1–December 31, 2020	Retrospective case study	-	154170	51.8	16773	32%, 27.4% and 40% in AKI stage 1, 2 and 3. ICU admission rate higher in stage 3 patients
Arentz et al. (2020)	Washington, USA	February 20 – March 5, 2020	Case series	70	21	52	4 (19%)	COPD, CKD, DM, KD observed. Troponin, Creatinine, ALP level higher in patients
Alberici et al. (2020)	Brescia, Italy	February 20, – March 24, 2020	Single-center observational study	59	20	80	6 (30%)	All were kidney transplant recipient and 6 of them had grown AKI
Fernandez et al. (2021)	Córdoba, Argentina	February – October 2020	Retrospective case study	63	448	63.6	85 (19%)	50.6%, 20%, 29.4% in stage 1, 2 and 3. 18 out 25 in stage 3 require renal replacement therapy
Banerjee et al. (2020)	South London, UK	March 2020	Case study	54	7	57.14	4 (57%)	1 out 4 patient developing AKI, succumbed to death. Hypertension in 4 out of 7
Moledina et al. (2021)	Connecticut, USA	March 10 – August 31, 2020	Retrospective study	65.6	2600	50.8	796 (30.6%)	COPD, HT, DM high prevalence. 19.5%, 5.9% and 5.2% in stage 1, 2 and 3. 29.6% death in AKI patients
Mumm et al. (2020)	Munich, Germany	March – April, 2020	Case study	62.0	7	100	-	Urinary sepsis as initial symptoms with fever, shivering, urgency and increased urinary frequency.
Richardson et al. (2020)	New York, USA	March– April, 2020	Multicenter case series	63.0	2634	60.3	523 (19.8%)	Frequency of AKI is higher in death group. High CRP, PCT, Ferritin observed
Dellepiane et al. (2021)	New York City, USA	March 2020 – December 2020	Retrospective case study	-	-	-	-	AKI incidence consistent (>40%) in March to May, 2020 followed by reduction (21.8%) in June and stable through December, 2020 (17.4%)
Karabulut et al. (2020)	Erzurum, Turkey	April 1, 2020 – May 15, 2020	Retrospective case study	44.8	68	92.6	-	Longer hospital stays, frequent ICU, higher mortality rate in severe I-PSS score group in COVID-19 positive cases
Sundaram et al. (2020)	Chennai, India	April 2020 – July 2020	Retrospective Study	61.2	110	70	31 (28.2%)	Hematuria, proteinuria, pyuria was high in non-survivor group.

Figure 1: PRISMA Flowchart for the different stages of the systemic review on acute kidney injury in COVID-19 infection

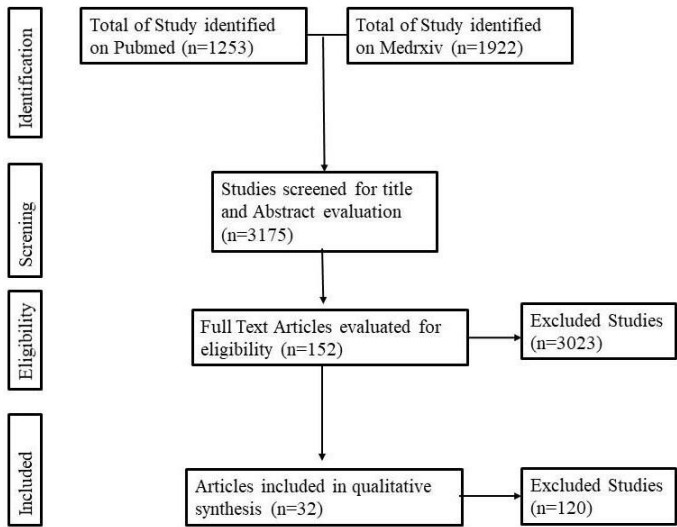
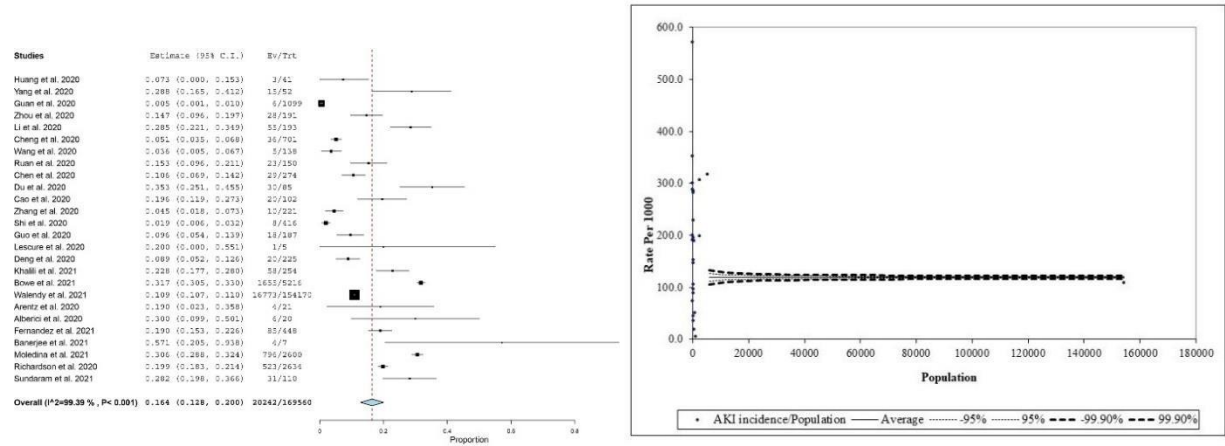


Figure 2: Forest Plot of the meta-analysis (A, C, E) and Funnel Plot (B, D, F) for AKI incidence, overall mortality, and AKI-related death respectively in COVID-19 infection in adults across different studies. The lower diamond in the Forest Plot represents the pooled estimate. ‘Ev’ indicates

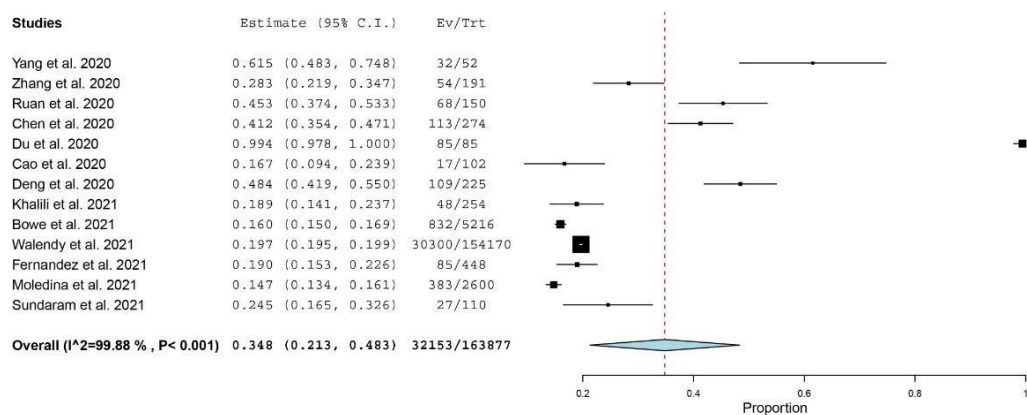
the event sizes. ‘Trt’ indicates the total number of COVID-19 positive patients screened (A, C) and the total number of COVID-19 positive patients screened with AKI only (E) in this population

A and B

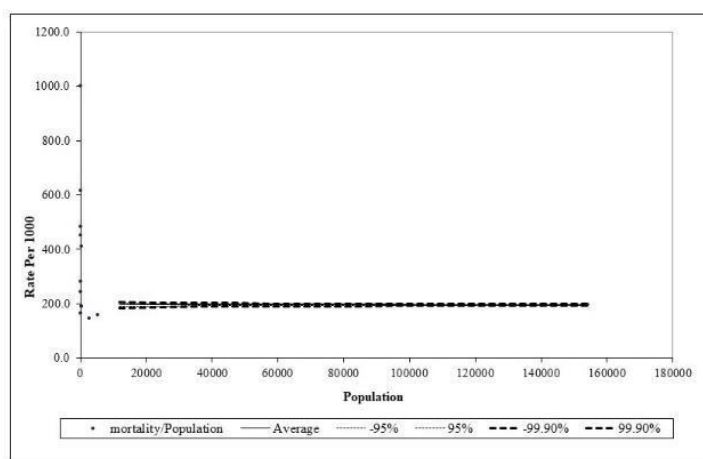


C.

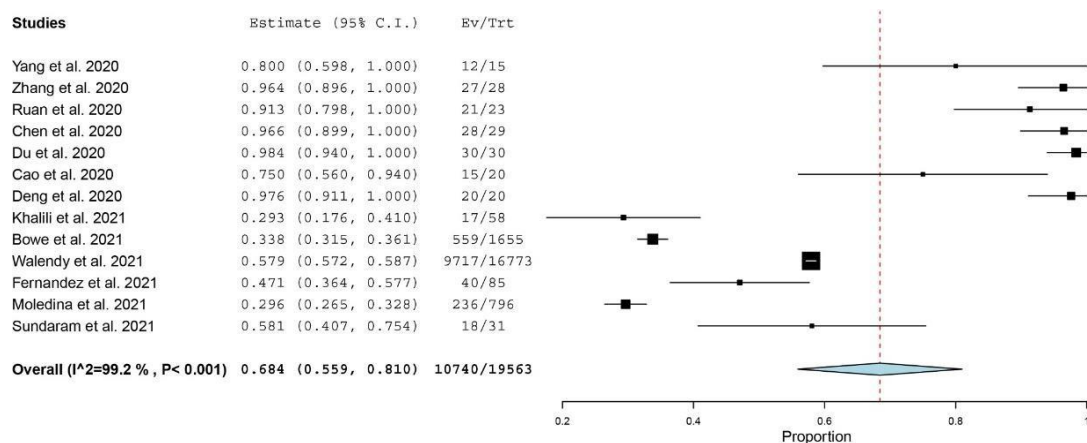
Acute Kidney Injury in Adults due to COVID-19 infection: A Systematic Review and Meta-Analysis



D.



E.



F.

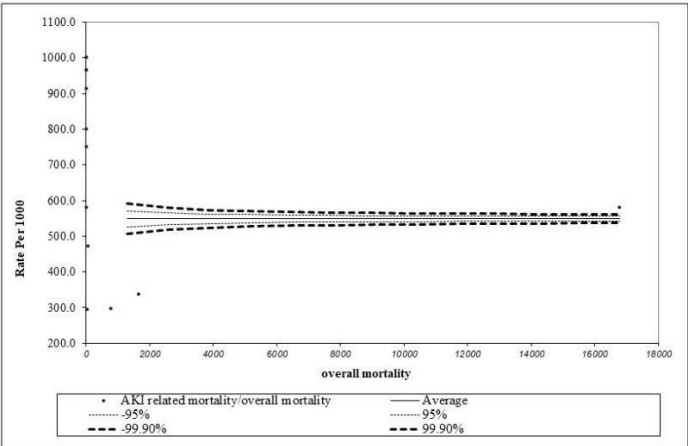
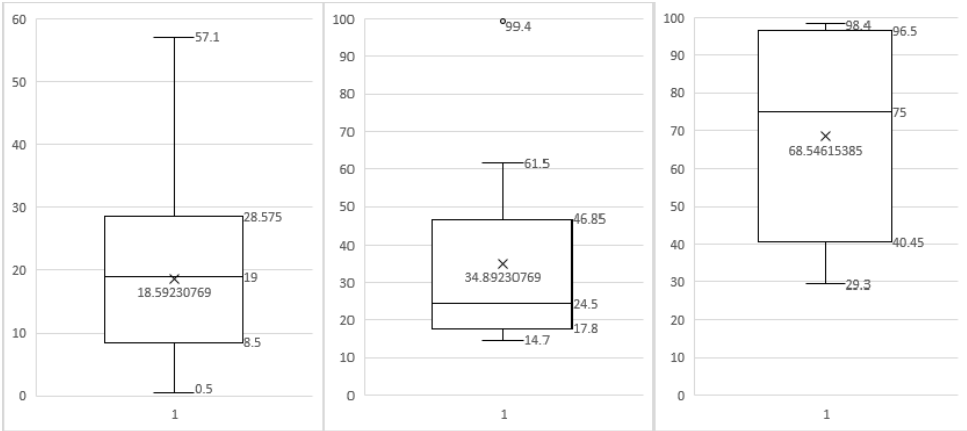


Figure 4: Box plot distribution of AKI incidence, overall mortality, and AKI-related death in COVID-19 infection in the adult (a, b, c) respectively from different studies. The circular dots represent the outliers.





Genetic Basis of Biofilm Formation and Spread of Nosocomial Infections

Snehashis Koley and Mandira Mukherjee

Abstract

Microbial communities that adhere to surfaces are referred to as biofilms. A major feature of the biofilm is the self-produced extracellular polymeric substances (EPS) which mainly consists of polysaccharides, nucleic acids (extracellular DNA), and proteins that leads to their compact association which confers remarkable resistance to conventional biocides, antimicrobial treatments, and immune defense responses in the host. Biofilms cause a wide range of sub-acute or chronic infections that are difficult to eradicate. Formation of these sessile microbial communities on a wide variety of medical devices and their inherent resistance to antimicrobial agents play an important role in dissemination of two thirds of nosocomial infections where the infection was acquired by patients' at hospital settings. Nosocomial infections like ventilator associated pneumonia (VAP), lower respiratory tract infections, pulmonary infections, prosthetic heart valve infections (endocarditis), catheter-associated urinary tract infections (CAUTIs), and catheter-related blood stream infections (CRBSIs) were reported to be transmitted by bacterial and fungal biofilms in hospital wards and critical care units (CCU). The opportunistic pathogens that account for medical device related nosocomial infections include *Pseudomonas aeruginosa*, *Escherichia coli*, *Enterococcus spp.*, *Klebsiella pneumoniae*, *Acinetobacter spp.*, *Staphylococcus spp.*, *Serratia marcescens*, *Proteus mirabilis*, *Streptococcus mutans* and the fungi *Candida albicans*, *Aspergillus fumigates*, *Cryptococcus neoformans*, *Trichosporon spp.*, *Coccidioides spp.*, *Pneumocystis spp.* Recent genomic studies have identified several genes and gene products variably expressed during biofilm development in most of these microbes. This chapter describes the biofilm associated genes that were studied in detail in different opportunistic medically important bacteria and fungi based on explicit literature review. Growth conditions of different strains of the biofilm producers were tabulated with detailed information on the methodology to explore the genetic basis of biofilm development.

Keywords Extracellular polymorphic substances, Bacterial biofilms, Fungal biofilms, Medical device associated nosocomial infection, Differential expression of biofilm related genes

1 Introduction

Nosocomial infection or hospital acquired infection was one of the leading causes of medical complication during extended hospital stay that adds to the enhanced medical expenditure and uncontrolled rate of mortality. About 60–70% of nosocomial infections

were associated with microbial biofilms on most type of implanted medical devices like prosthetic heart valves, orthopedic implants, intravascular catheters, artificial hearts, left ventricular assist devices, cardiac implants, vascular prostheses, cerebrospinal fluid shunts, urinary catheters, ocular prostheses, contact lenses, and intrauterine contraceptive devices. Reports from different nations indicated high prevalence of the aforementioned biofilm related nosocomial infection [1]. Both commensal and pathogenic microorganisms were involved in biofilm formation and their presence had important implications for patients, as they were also significantly less susceptible to antibiotics.

In prosthetic valve endocarditis biofilms were generated on prosthetic heart valves and surrounded tissues. *Streptococcus* species, namely *S. aureus*, *S. epidermidis*, and other Gram-negative *Bacillus*, *Enterococcus*, and *Candida spp.* were found to be the causative agents. During the time of implantation of mechanical valves, tissue damage may occur, and fibrin and platelet accumulation which facilitated microbes to colonize and form biofilms. Patient on ventilation support reported to have ventilator associated pneumonia (VAP) after 48–72 h due to formation of biofilm on the ventilator assist devices and endotracheal tubes (ETT) [2]. Risk of developing VAP after incubation increased by 6–20 fold, and showed significantly higher mortality rates (24–76%) [3]. Based on the risk of infection with MDR pathogens, VAP were classified as either early-onset (<5 days of hospitalization) and late-onset (≥5 days of hospitalization). ETT which was reported as a factor in the acquisition of VAP [4–6] has also been found to proliferate biofilms within 24 h duration [7]. Numerous microorganisms including MRSA, *K. pneumoniae*, *P. aeruginosa*, *E. coli* were reported to colonize ETT in the form of a biofilm. Urinary catheters usually made of latex or silicon were used during surgical operations [8] for urine generations and excretion from the body. Open system catheters, where urine was collected on an open collection center led to very high chance of contamination which accounted as one of the common causes of urinary tract infection (UTI). However, closed system catheters, where urine was collected in a plastic bag led to reduced chances for UTI [9] but the risk of development of catheter-associated urinary tract infections (CAUTI) in patients increased approximately by 10% each day. Contamination in the urine stored within the drainage bag was found to be a huge source of bacteria, which further can develop the infection. *E. coli*, *S. epidermidis*, *Enterococcus faecalis*, *P. aeruginosa*, *Proteus mirabilis*, *K. pneumoniae*, and other Gram-negative bacteria were found to be associated with biofilm formation [10] in the urinary catheter that causes CAUTI. Central venous catheters were utilized to deliver nutritional fluids, medications, blood products and were the most common surface available for biofilm formation universally. Microbial colonization and

biofilm formation could occur as early as 1 day after the catheter insertion in a population of adult cancer patients [11] but the duration of catheterization had an important impact on the degree of biofilm formation. Biofilm generally formed on the external surface of the short-term catheters whereas in the lumen of the long-term catheters which were found to be the common cause of Catheter-related blood stream infections (CRBSIs). Growth of the microorganisms depend on the nature of the fluid administered through the catheter, i.e. intravenous fluid provided sustained growth for gram-negative bacteria [12, 13]. Wound infection that appears due to contamination caused by microorganisms from patient's skin after any surgery [14] was termed as surgical site infection (SSI). Most commonly associated microorganisms were *S. aureus*, *Corynebacterium spp.* followed by *Bacillus spp.* and *S. epidermidis* [15]. Biofilm production was found to be the primary cause of SSIs and produced severe medical complications.

Biofilms were defined as complex communities of the microorganisms that can attach to both abiotic and biotic surfaces. A major feature of the biofilm was the self-produced gelatinous extracellular polymeric substances (EPS) [16, 17] which forms a three-dimensional cell and polymer matrix [18]. EPS mainly consists of polysaccharides, nucleic acids (extracellular DNA), and proteins, which helped to protect the microorganisms from external threats, including immune system components and antimicrobials [19].

The mechanism of biofilm development in bacteria and fungi was very similar with some distinct differences in their structural elements. Bacterial biofilm formation was generally initiated by (1) primary contact/attachment of microbes to the surface where the bacteria adhered to the surface through their attachments like pili and flagella which provide strength to the interaction between the microbes and surface, they may also get attached through other physical forces, namely van der Waal's forces, electrostatic interactions. Other factors, namely adhesion (attachment of microbes to surface) and cohesion (interaction within the cells), solid-liquid interface [20, 21] had important roles in biofilm formation. Bacterial adhesion could be further divided into primary or docking stage and the secondary or locking stage [22]. (2) Micro-colony formation: After a stable attachment of microbes to biotic or abiotic surface, multiplication by cell division initiated, through particular chemical signaling within the extracellular polymeric substances (EPS), leading to the formation of micro-colonies [23]. Generally these bacterial colonies contain different types of micro-communities, which coordinated with each other and played an important role in the exchange of substrates, distribution of metabolic products, and excretion of end-products [24]. (3) Maturation and establishment of the architecture of the biofilm: In this stage cell-to-cell communications were initiated [25], resulting in secretion of autoinducer molecules that facilitated quorum sensing

[26]. Certain genes were expressed whose products helped in the formation of EPS. After the formation of EPS, interstitial voids were formed, filled with water, and acted as circulatory system [27]. (4) Detachment/dispersion of the biofilm: Microbial Biofilms underwent rapid multiplication to convert from sessile to motile form and then detachment occur naturally [23]. Those bacteria which were unable to produce EPS disperse either directly or via mechanical stress into the environment [28]. During detachment these microbial communities produced different saccharolytic enzymes which helped the microbe to find a new surface. *Escherichia coli* produced *N*-acetyl-heparosan lyase, *Pseudomonas aeruginosa*, and *Pseudomonas fluorescens* produced alginate lyase and *Streptococcus equi* produced hyaluronidase for the lysis of the EPS [29].

The process of fungal biofilm development were mostly studied in yeast that included multiple stages; (1) adsorption of yeast cells to a surface termed as initial adhesion, (2) basal layer yeast formation through the early development of hyphae and extracellular matrix, (3) biofilm maturation that contained a significant number of yeast, hyphae, pseudohyphae, extracellular matrix, and water channels for nutrient movement, and (4) cell dispersion. Studies were limited for filamentous fungi and a proposed model for biofilm formation in filamentous fungi reported [30] the following stages (1) propagule adsorption that included spores, hyphal fragments or sporangia deposition on surfaces, (2) active attachment through adhesive substances that were secreted from spores which helped these fungi to attach, (3) micro-colony formation in which hyphal branching and apical elongation occurred and production of EPS in helped to adhere to the surface, (4) initial maturation by the formation of compact hyphal network that included multiple layering by adhesion between two hyphae with generation of water channel, (5) maturation that included formation of fruiting bodies, sporogenous cells, and other survival structures, and finally (6) spore dispersal that led to detached cells which act as new propagules.

The underlying genetic mechanisms involved in biofilm development in opportunistic pathogenic bacteria such as *Pseudomonas aeruginosa*, *Escherichia coli*, *Enterococcus spp.*, *Klebsiella pneumoniae*, *Acinetobacter baumannii*, *Staphylococcus aureus*, *Serratia marcescens*, *Proteus mirabilis*, *Streptococcus mutans*, and fungi *Candida albicans*, *Aspergillus fumigates*, *Cryptococcus neoformans*, *Trichosporon spp.*, *Coccidioides spp.*, *Pneumocystis spp.* were initiated by differential gene expression that resulted in cascade of events thus favoring the process of biofilm development.

Furthermore two fungi *Trichosporon asahii* and *Pneumocystis jirovecii* were also reported as opportunistic pathogens to humans. They were found to produce biofilms but till date no genetic information were available on biofilm formation by these

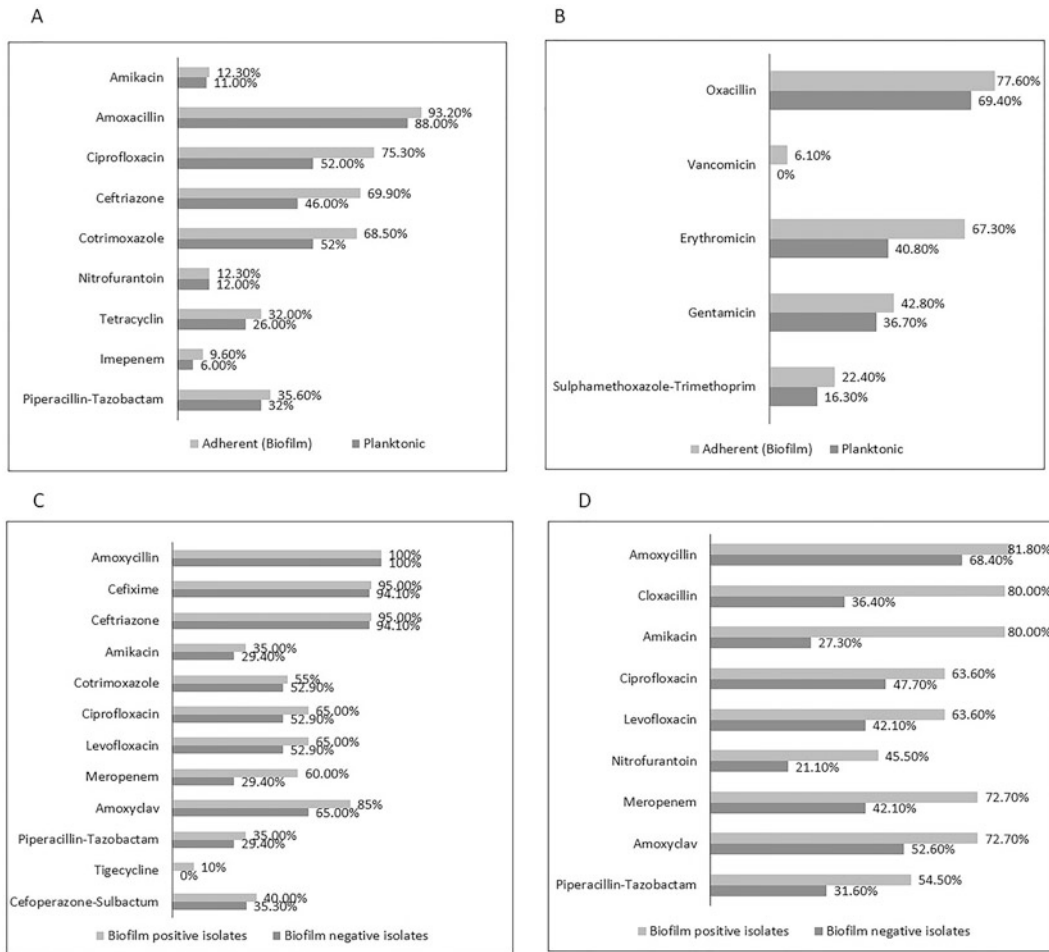


Fig. 1 Antibiotic-resistant profiles in planktonic and biofilm producing (a) *E. coli* [108], (b) *Staphylococcus spp.* [109], (c) Gram-negative isolates, and (d) Gram-positive isolates, respectively [110]

pathogens. *Trichosporon asahii* was reported to be the third most common etiological agent of fungemia [107] in patients with hematological malignancies, extensive burns, solid tumors, AIDS, etc. *Pneumocystis jirovecii* caused pneumonia in patients suffering from immunocompromised disease such as HIV-AIDS and in people receiving immunosuppressive therapies.

Several reports indicated a distinct difference of antibiotic resistance pattern among the biofilm producers compared to the biofilm non-producing microbes which leads to ineffective therapy that was one of the major causes of chronic infections (Fig. 1).

Mechanism of resistance against antimicrobials of biofilm communities was extensively explored. Reports indicated that biofilm production imparts (i) incomplete and/or gentle penetration of antibiotics into the microbes due to their rigid surface (mushroom

like or tower like) architecture. (ii) Altered microenvironment in the biofilm, i.e. high level of protein synthesis and metabolic activity at the surface and low level and slow or absence of growth in the center may be an additional reason for reduced susceptibility against the antibiotics. Moreover high oxygen concentration at the surface but very low (anaerobic conditions) in the center of the biofilm may also cause inhibitory effect on penetration of drug molecules. (iii) Furthermore EPS provided tolerance against aminoglycosides in biofilm community. Uptake of resistant genes by horizontal gene transfer significantly enhanced the mutation frequency of biofilm-growing microorganism compared to their planktonic population and this physiological condition helped in developing resistance against multiple antibiotics (multidrug resistance; MDR) by means of traditional resistance mechanisms against β -lactam antibiotics, aminoglycosides, and fluoroquinolones. (iv) Nevertheless in a bacterial community, bacteria communicate with each other by the synthesis of several signaling molecules. Presence of critical concentrations of bacteria in a limited space in the environment activate the quorum sensing (QS) genes that further influence the development of bacterial biofilms and also provide tolerance against antibiotic therapy [111, 112].

2 Materials and Methods

2.1 Microbial Strains and Culture Conditions

2.2 Genetic Study

2.2.1 Molecular Detection of Biofilm Related Genes

Polymerase Chain Reaction (PCR), a common technique for amplification and identification of a specific gene sequences, was used in the study of biofilm related genes. Using genomic DNA or total DNA as template, PCR assays were performed in a reaction volume of 20 μ L that consists of varied concentration of DNA template, 10 pmol of specific forward and reverse primer each for specific biofilm genes, 1X PCR buffer, 10 mM dNTP mix, 50 mM $MgCl_2$, and 2.0 U Taq DNA polymerase. Conditions generally for the PCR were initial denaturation at 94 °C for 5 min, followed by 30/35 cycles of denaturation at 94 °C for 30 s/1 min, annealing temperature for each gene for 30 s/1 min, an extension at 72 °C for 1 kb/min which was dependent on the size of the respective gene, followed by a final extension at 72 °C for 5–10 min. Positive and negative controls were all included in all PCR assays.

2.2.2 Functional Complementation

Transposon mutagenesis and gene knockout study was performed to assign functional role of several genes in microbial biofilm. Genes were amplified by PCR from the genomic DNA isolated from the

microorganism and then ligated onto specific restriction site of appropriate shuttle vector to explore their functional role.

2.2.3 *Biofilm Related Gene Expression*

Real Time-PCR assay was performed to detect the quantitative expression of the biofilm related genes. The overexpression or downregulation of genes related to the biofilm formation were monitored. RNA was isolated from the microbial sample using RNA extraction protocol. DNA contamination were removed by treatment with RNase free DNaseI. RNA samples were quantified spectrophotometrically at 260 nm. Purified total RNA was precipitated with ethanol and stored at -80°C until further use. RNA was transcribed into cDNA using reverse transcriptase enzyme and was directly used as template for Real Time PCR using specific primers with respect to genes related to biofilm formation.

3 Interpretation

A major focus of this chapter has been laid to address the various methods used for the detection of the biofilm related genes in opportunistic medically important pathogens that play role in the dissemination of nosocomial infection. Several genes related to virulence of the pathogens were found to control the different steps of biofilm growth. The biofilm genes and their role had been studied explicitly and published successfully from a wide array of opportunistic pathogens (Table 1). Microbial strains and growth conditions constitutes a very important criteria that must be documented to perform these studies at the molecular level (Table 2). PCR followed by transposon mutagenesis and gene knockout studies were promiscuous techniques that were explored in several studies to understand the role of respective biofilm genes at the molecular level. This chapter provides genetic information based on literature survey into the present data available on biofilm genes from different opportunistic pathogens and the experimental details of the molecular studies executed (Tables 3 and 4).

Genes that were expressed in adherent pathogens or were regulated by the quorum sensing system were successfully investigated by quantitative Real Time-PCR method (Table 5). This method directly facilitated comparison between the expression of the different genes under biofilm and planktonic form. Additionally the transcriptional heterogeneity investigated could contribute to the further understanding of microbial biofilm. These findings may create a major step in the future research on the genetic basis of biofilm development in the opportunistic pathogens that cause nosocomial infection and pose difficulty in clinical management.

Table 1
Biofilm related genes in different opportunistic pathogens

Microorganisms	Genes and operons involved in Biofilm formation	Role of the gene	Reference
<i>Pseudomonas aeruginosa</i>	<i>pilA</i>	Type IV pili constructed from PilA helps in surface adhesion	[31]
	<i>algR</i>	Regulates <i>pilA</i> expression	
	<i>fimU-pilVWXYZIY2E</i> operon	Major prepilins PilY1 and PilY2—role in fimbrial assembly and biosynthesis	[32, 33]
	Lectins PA-IL and PA-IIL	Role in intercellular adhesion	[34]
	<i>pslA-O</i> and <i>pelA-G</i>	Encodes exopolysaccharides Psl and Pel that helps in adhesion and maturation of biofilm	[35]
	<i>algACD</i> operon	Regulates the production of GDP-mannuronic acid, foundation molecule for alginate synthesis; thus regulate the production of alginic acid, a major constituent of slime	[36]
	<i>las</i> based quorum sensing system transcribed by <i>lasR</i> and <i>lasI</i>	<i>lasI</i> enzyme, produced by <i>lasI</i> directs the synthesis of autoinducer—III, and when threshold value is reached, autoinducer binds to <i>lasR</i> (encoded by <i>lasR</i>), resulting in production of several biofilm genes	[37]
	<i>rhl</i> based quorum sensing system transcribed by <i>rhlRI</i> operon	Responsible for the production of amphiphilic biosurfactant—rhamnolipids (heat stable hemolysin), helps in maintaining macrocolonies and fluid-filled channels in the latter stages of biofilm development	[38, 39]
	<i>pqs</i> quorum sensing system	Required for the production of <i>rhl</i> -dependent exoproducts Required for the activation of <i>lasR</i>	[40]
<i>Escherichia coli</i>	<i>fim</i> operon	<i>fimA</i> to <i>fimH</i> located in a single large operon and controlled by an invertible 314-bp switch element located upstream of <i>fimA</i> and flanked by inverted repeats. The inversion mediated by FimE and FimB. Promotes adhesion, important for biofilm formation	[41]
	<i>csgBA</i> operon	Encodes structural components of curli which promotes adhesion to extracellular matrix proteins	[42, 43]
	<i>csgDEFG</i> operon	Encodes transcriptional regulator (CsgD) and curli export machinery (CsgEFG)	[43]

(continued)

Table 1
(continued)

Microorganisms	Genes and operons involved in Biofilm formation	Role of the gene	Reference
	<i>ompR</i> allele (<i>ompR234</i>)	Leads to OmpR dependent activation of <i>csyD</i> promoter, leading to curli production and biofilm production	[44]
	Chromosomal <i>omp85</i> gene	Encodes Omp85 protein which play an important role in biofilm development	[45]
	<i>flu</i> gene (Antigen 43)	Increased expression associated with biofilm formation and biofilm maturation on abiotic surfaces and eukaryotic cells	[46]
	<i>aidA</i> and <i>tibA</i>	Produce two autotransporter proteins AidA and TibA respectively, involved in virulence and bacterial adhesion to different eukaryotic cells	[47]
	<i>yfaL</i> , <i>yeeJ</i> , <i>ypjA</i> , <i>ycgV</i>	Uncharacterized genes having structural similarity with Ag43, role in building biofilm when expressed from a induced promoter	[48, 49]
<i>Enterococcus</i> spp.	<i>agg</i>	Encodes Aggregation (Agg) protein which is involved in adherence to eukaryotic cells	[50]
	<i>efaA</i> (specific for <i>Enterococcus faecalis</i>)	Produces Enterococcus fecal is endocarditis-associated antigen A, involved in adhesion	[51]
	<i>ace</i>	Produces ace that promotes conditional adherence to collagen and laminin	
	<i>bopABCD</i> operon	Bop (biofilm on plastic) have a putative maltose metabolism function, regulated by <i>fsr</i> , important for biofilm formation	
	<i>ebpABC</i>	Pili which has an important role in biofilm formation, it's components are encoded by endocarditis and biofilm associated pili genetic locus (EbpABC)	
	<i>srt</i> gene	Shortage encoding gene, role in encoding pili component	[52]
	<i>fsc</i> locus (<i>fscA</i> , <i>fscB</i> , and <i>fscC</i> genes)	Fecal streptococci regulator locus, part of quorum sensing system. FscA and FscC constitute a two component system, in which FscC acts as histidine kinase sensor and FscA acts as response regulator. FscB regulates <i>gelE</i> gene	[53]

(continued)

Table 1
(continued)

Microorganisms	Genes and operons involved in Biofilm formation	Role of the gene	Reference
	<i>gelE</i>	Encodes zinc-metalloprotease gelatinase, regulated by <i>ftr</i> locus, have role in biofilm formation	[54]
<i>Klebsiella pneumonia</i>	<i>fim</i> operon	Encodes type 1 fimbriae, which is required for fimbrial structure and assembly. Regulated by phase variation	[55]
	<i>mrkA</i> and <i>mrkD</i> gene	MrkA type 3 fimbriae mediate biofilm formation on major biotic and abiotic surfaces in the presence of MrkD type 3 fimbrial adhesin	[56]
	<i>ecpABCDE</i> operon	Encodes ECP during adhesion and play an important role in facilitating biofilm formation	[57]
	<i>treC</i> and <i>sugE</i>	Modulate CPS production and affect biofilm formation	[58]
<i>Acinetobacter baumannii</i>	<i>bap</i> loci	Encodes biofilm associated protein (Bap) homologue involved in intercellular adhesion. Main functional region constitutes of highly conserved seven tandem repeats	[59, 60]
	<i>csuAB-A-B-C-D-E</i> operon	Production and assembly of pili, transcription. <i>csuE</i> has major role in biofilm formation	[61]
	<i>bfmR</i>	Regulate <i>csuAB-A-B-C-D-E</i> operon	[61]
	<i>bla_{PER-1}</i> and <i>ompA</i>	<i>bla_{PER-1}</i> has been identified to form biofilm in clinical isolates. <i>ompA</i> produces outer membrane protein A (OmpA), which has a partial role in biofilm formation on abiotic surface	[62]
<i>Staphylococcus aureus</i>	<i>icaADBC</i> operon	PIA which promotes interaction between bacterial cells, synthesized by four proteins IcaA, IcaD, IcaB and IcaC. IcaC involved in the formation of long oligomers. IcaB deacylate PIA/PNAS resulting in promoting in negatively charged cell surface and positively charged polymers	[63–65]
	<i>eno</i> , <i>ebps</i> , <i>fib</i>	Encodes microbial surface components recognizing adhesive matrix molecules (MSCRAMM's) that are reported to have a role in biofilm formation	[66]

(continued)

Table 1
(continued)

Microorganisms	Genes and operons involved in Biofilm formation	Role of the gene	Reference
	<i>eno</i>	Encodes α -enolase, expressed at the surface of the bacterial wall, bind laminin and acts as plasminogen receptor. By the binding of bacterial cells to laminin, α -enolase allowed bacterial cell adherence to ECM	[67]
	<i>ebps</i>	Encodes elastin binding protein (EbpS). EbpS helped in binding of <i>S. aureus</i> in the N-terminal region of elastin (a major component of elastic fiber ECM)	[68]
	<i>fib</i>	Encodes a glycoprotein called fibrinogen binding protein (fib), present in blood, mediated platelet adherence and aggregation at wound site. Ability of <i>S. aureus</i> to adhere to fibrinogen which was usually deposited on implanted biomaterials, thus endorsing infections in wounds and foreign body	[69]
	<i>atlA and atlE</i>	They encode surface localized proteins or autolysins AtlA and AtlE that mediate initial attachment by binding to hydrophobic surfaces	[70]
	<i>dlt operon or tagO</i>	Involved in Teichoic acid (TA) and Lipoteichoic acid (LTA) synthesis; they have a role in initial bacterial adherence to host cells	[71]
	<i>cna</i> gene	Encodes collagen adhesin	[72]
	<i>clfA</i> gene	Encodes MSCRAMM clumping factor A, helps in fibrinogen binding	
	<i>fnbA and fnbB</i>	Encodes fibronectin binding protein	
	<i>sasG</i> gene	Encodes surface protein G, role in adherence	[73]
<i>Serratia marcescens</i>	<i>swrI and swrR</i>	SwrI predominantly synthesizes N-butanoyl-L-homoserine lactone (C ₄ -HSL), bind to SwrR, and affect the expression of at least 28 proteins. Role in producing thicker biofilm for a longer period of time	[74]
	<i>bsmA and bsmB</i>	Quorum sensing controlled gene, BsmB is necessary for activating aggregation whereas BsmA is necessary to control the size of the aggregation. Regulate the biofilm structure	[75]

(continued)

Table 1
(continued)

Microorganisms	Genes and operons involved in Biofilm formation	Role of the gene	Reference
	<i>fimA</i>	Type 1 fimbrial adhesin gene, helps in attaching to immortalized corneal epithelial cells	[74]
	<i>oxyR</i>	Conservative bacterial transformation factor that has a regulatory role in oxidative stress response, it has a role in primary attachment of the cells to a surface	[76]
<i>Proteus mirabilis</i>	<i>Esp</i>	Produces enzymes responsible for biofilm formation	[77]
	<i>rsbA</i>	Quorum sensing gene regulates swarming manner. Facilitates biofilm formation	[78]
	<i>atfA and atfC</i>	Part of ATF fimbriae, important role in adhesion and biofilm formation on abiotic surface	
<i>Streptococcus mutans</i>	<i>spaP and fapI</i>	Produces surface-associated protein (SapP) and fimbriae associated protein (FapI), have been found to act as high-affinity adhesins, and they play an important role in the initiation of biofilm formation	[79, 80]
	<i>brpA</i>	Encodes biofilm regulatory protein which is basically a surface-associated polypeptide has role in biofilm formation on abiotic surfaces	[81]
	<i>Sgp</i>	Produces regulatory G protein (SGP) which is essential for cell growth, has also been found to be involved in biofilm formation	[82]
	<i>Dgk</i>	Codes for undecaprenol kinase activity, which play an important role in stress response, also has role in biofilm formation as signal transducer	
	<i>comCDE</i> quorum sensing system	<i>comC</i> produce a complete-stimulating peptide (CSP) producer. <i>comDE</i> encodes a two component transduction system which specifically senses and responds to CSP. This operon has a role in biofilm formation	[83]

(continued)

Table 1
(continued)

Microorganisms	Genes and operons involved in Biofilm formation	Role of the gene	Reference
<i>Candida albicans</i>	<i>ALS1</i>	Helps to adhere to vascular endothelial cell monolayers	[84]
	<i>ALS2</i>	Adhesion to buccal epithelial cells, fibronectin or laminin	
	<i>ALS3</i>	Adhesion to endothelial cells, buccal epithelial cells and FaDu monolayers	
	<i>ALS5</i>	Adhesion to endothelial cells, buccal and FaDu epithelial cells, fibronectin, laminin, gelatin and to type IV collagen	[85]
	<i>ALS6</i>	Adhesion to gelatin	[86]
	<i>ALS9</i>	Adhesion to endothelial cell	[87]
	<i>Eap1</i>	Encodes enhanced adherence to polystyrene 1; a cell wall protein that included a signal peptide, a GPI anchor site, which resulted in adhesion to human epithelial cells, under the regulation of <i>EFG</i> gene	[88]
	<i>FLO8 and FLO9</i>	Flocculation genes that has an impact on the expression of <i>Eap1</i> encoded cell wall protein	[88]
	<i>Hwp1</i>	Hyphal Wall Protein 1 produced cell surface protein expressed only on hyphae that promoted binding to oral epithelial cells. Expression of HWP1 was dependent upon transcription factor Bcr1. <i>Hwp1</i> was partially required for biofilm formation in vitro but absolutely required for in vivo	[89]
	<i>Rbt1</i>	Related to family of hypha-associated cell surface proteins and proven to be essential for adhesiveness to polystyrene	[90]
	<i>YWP1</i>	Produces yeast wall protein 1 or Pga24, another cell wall protein, critical for the dispersion of yeast cells from biofilm	[91]
	<i>MP65</i> gene	Produces cell wall mannoprotein Mp65p— Important role on the stability of the cell wall, adherence to epithelial cells and formation of biofilms	[92]
	<i>Pra1</i> pH regulated antigen	Produces specific fibrinogen binding protein, <i>Pra1p</i> that act as surface receptors in adhesio	[93]

(continued)

Table 1
(continued)

Microorganisms	Genes and operons involved in Biofilm formation	Role of the gene	Reference
	<i>GAL102</i> , <i>PMT</i> (protein mannosyltransferase) gene families	Role in protein mannosylation, thus governs adherence	[94, 95]
	<i>sun41</i> and <i>pga1</i>	Cell wall non-adhesin genes, roles in cell wall integrity	[96]
	<i>FKS1</i> gene	Responsible for cell wall β -1,3 glucan synthesis, provide resistance to fluconazole	[97]
<i>Aspergillus fumigatus</i>	<i>cspA</i> gene	Encodes a cell wall protein, contained a putative leader sequence and specific GPI modification site, that resulted in adhesion to ECM	[98]
	<i>uge3</i>	Produces Uge3p which is cytoplasmic UDP-glucose-4-epimerase, governed the synthesis of UDP- <i>N</i> -acetylgalactosamine from UDP- <i>N</i> -acetylglucosamine and UDP-galactose from UDP-glucose in GAG biosynthesis which plays a role in formation of biofilm	[99]
	<i>agd3</i>	Produces Agd3p which is necessary for the deacetylation of the GalNac residues	[100]
	<i>ega3</i>	Encodes an α -1,4-galactosaminidase, involved in carbohydrate biosynthesis which play a role in the formation of biofilm	[101, 102]
	<i>gtb3</i>	Encodes a large integral membrane glycosyltransferase, involvement in carbohydrate biosynthesis that is related to biofilm production	
	<i>sph3</i>	Encodes a spherulin-4 protein (glycoside hydrolase) which play a role in biofilm formation	
	<i>rodA</i> and <i>rodB</i> gene	Encode two hydrophobins RodAp and RodBp whose upregulation related to biofilm formation	
	<i>pks/alb1</i>	Part of a cluster of six genes which encoded a polyketide synthase, which had a role in biofilm formation	[103]
	<i>medA</i>	Produces a developmentally regulated protein MedAp, a temporal modifier of	

(continued)

Table 1
(continued)

Microorganisms	Genes and operons involved in Biofilm formation	Role of the gene	Reference
		expression of core conidiation genes, had an important role in biofilm formation on glass and plastic abiotic surfaces	
<i>Cryptococcus neoformans</i>	<i>CAP59</i> , <i>CAP64</i> , <i>CAP60</i> , and <i>CAP10</i>	Related to the formation of capsule, which led the formation of biofilms	[104]
	<i>LACI</i> gene	Increased expression of laccase involved in biofilm formation	[105]
	<i>UREI</i> gene	Produces a metallo-enzyme urease, catalyzed the hydrolysis of urea to ammonia and carbamate, expressed increasingly in biofilm condition	[106]

Table 2
Growth conditions of the microorganisms

Microorganisms	Strains	Growth conditions	Reference
Bacteria			
<i>Pseudomonas aeruginosa</i>	PAO1	37 °C overnight in shaking condition in Luria Bertani medium or M63-arginine (minimal) medium	[31, 35]
	PA14		
	ZK2870		
<i>Escherichia coli</i>	K-12	37 °C overnight in shaking condition in Luria Bertani medium	[41]
	MG1655		
	TG1		
	JM109		
	BL21		
	DH5α		
<i>Enterococcus faecalis</i>	OG1RF	In brain heart infusion (BHI) at 37 °C overnight	[50]
	ATCC29212		
<i>Klebsiella pneumonia</i>	C3091	BHI medium.	[56]
	IA565	In L-agar or GCAA agar at 37 °C overnight	
	43,816		
<i>Acinetobacter baumannii</i>	ATCC19606	Mueller Hinton (MH) broth at 37 °C overnight	[59]
	307–0294		

(continued)

Table 2
(continued)

Microorganisms	Strains	Growth conditions	Reference
<i>Staphylococcus aureus</i>	UAMS-1 RN4220 8325-4	Tryptic soy broth at 37 °C overnight with 0.5% glucose, constant aeration	[66]
<i>Serratia marcescens</i>	MG1	Lysogeny broth. For swarming and swimming assay Helvick medium	[75]
<i>Streptococcus mutans</i>	GS-5	Todd-Hewitt broth (THB) or chemically defined medium (CDM)	[83]
Fungi			
<i>Candida albicans</i>	SC5314 CA-1 3153A NGY152	Standard yeast culture media and filamentous growth media	[88]
<i>Aspergillus fumigatus</i>	Af293	Yeast extract peptone dextrose (YPD) broth/potato dextrose agar (PDA) at 37 °C	[98, 102]
<i>Cryptococcus neoformans</i> var. <i>grubii</i>	ATCC90112	Saboraud dextrose broth with shaking (200 rpm) at 37 °C	[105]
<i>Cryptococcus neoformans</i> var. <i>gattii</i>	ATCC 56990		
<i>Trichosporon ashaii</i>	ATCC201110 MPU 105	YPD broth, Saboraud dextrose agar	[107]

Table 3
PCR primers used to detect biofilm related genes in different microorganisms

Genes and primers	References
<p>For construction of <i>csyD::uidA</i> chromosomal fusion, template MG1655 chromosomal DNA, primers C1 (5'-CGAATAATCTTGCGGTCGACAAGCAGG-3') and C2 (5'-GAAAGTGCCGCAAGGAGCTCTAACG-3')</p> <p>For overproduction of OmpR and OmpR234 protein, template MG1655 and MG1655 <i>ompR234</i>, primer R1 (5'-AGTACAAACCATGGAAGAGAACTAC-3') and R2 (5'-CTTCGTACGCGAAAGCTTTATTAAACTG-3')</p> <p>The <i>csyB</i> promoter region containing DNA probe was obtained by PCR amplification from pCSG4 using primers D4 (5'-CTGTCTGAAG CTTTTTGATAGCGGAAAACGG-3') and D5 (5'-CACCTGGACCTGGTC GTACATTTAA-3')</p>	[43]
<p>1st fragment from 5'-<i>agn43</i> with following primers: 1-Kpn (5'-GAACCTGTCGGTACCGATGCCCTCCC-3') and 2-BamHI (5'-CGGGATCC GTTGCCACTGTACCGGGCTTGACGACC-3')</p> <p>2nd fragment from 3'-<i>agn43</i> with following primers: 3-BamHI (5'-CGGGATCCAC AACTGCAGTATACCTGGCAGGG-3') and 4-XbaI (5'-GCTCTAGAAGGTCAC ATTCAGTGTGGC-3')</p>	[46]
<p><i>agg</i> gene (413 bp) FP: (5'-CTTGGACACGACCCATGAT-3'), RP: (5'-AGAAAGAACATCACCACGAGC-3')</p> <p><i>efnA</i> gene (706 bp) FP: (5'-GACAGACCCTCACGAATATG-3'), RP: (5'-CCAGTTCATCATGCTGTAGTA-3')</p> <p><i>ace</i> gene (615 bp) FP: (5'-GAATGACCGAGAACGATGGC-3'), RP: (5'-CTTGATGTTGGCCTGCTTCC-3')</p> <p><i>bop</i> gene (312 bp) FP: (5'-GATCGTCTTCGCCATAGTAGG-3'), RP: (5'-ATACACAACAGCCCTTGGCT-3')</p> <p><i>ebpA</i> gene (613 bp) FP: (5'-CCATTTGCAGAAGCAAGAATG-3'), RP: (5'-GAGTGAAAGTTCCTCCTCTAG-3')</p> <p><i>ebpB</i> gene (504 bp) FP: (5'-CATTAGCAGAGGCATCGCAA-3'), RP: (5'-CAAGTGGTGGTAAGTCATAGG-3')</p> <p><i>ebpC</i> gene (487 bp) FP: (5'-CTGCTACGAATATGGTGGTG-3'), RP: (5'-GGTGTGTTGATTGTTTGCCTC-3')</p> <p><i>srt</i> gene (612 bp) FP: (5'-GTATCCTTTTGTAGCGATGC-3'), RP: (5'-TGTCCTCGAACTAATAACCGA-3')</p> <p><i>frrA</i> gene (474 bp) FP: (5'-CGTTCCGTCTCTCATAGTTA-3'), RP: (5'-GCAGGATTTGAGGTTGCTAA-3')</p> <p><i>frrB</i> gene (428 bp) FP: (5'-TAATCTAGGCTTAGTTCCAC-3'), RP: (5'-CTAAATGGCTCTGTCGTCTAG-3')</p> <p><i>frrC</i> gene (716 bp) FP: (5'-GTGTTTTTGATTCGCCAGAGA-3'), RP: (5'-TATAACAATCCCCAACCGTG-3')</p> <p><i>gelE</i> gene (704 bp) FP: (5'-GGTGAAGAAGTTACTCTGAC-3'), RP: (5'-GGTATT GAGTTATGAGGGGC-3')</p>	[51]
<p><i>ecpA</i> gene (477 bp) FP: (5'-GCAACAGCCAAAAAAGACACC-3'), RP: (5'-CAGTTCGACGCGACCTGG-3')</p> <p><i>mrkD</i> (757 bp) FP: (5'-CTGACGCTTTTATTGGCTTAATGGCGC-3'), RP: (5'-CTACTAAACGAAAAGACCGGAAATTCTGC-3')</p> <p><i>mrkA</i> (498 bp) FP: (5'-CGGTAAAGTTACCGACGTATCTTGTACTG-3'), RP: (5'-GTTACCACCGGTGTGGTTAACAGC-3')</p>	[57]

(continued)

Table 3
(continued)

Genes and primers	References
Parental allele of <i>bfmR</i> amplified by PCR using primers, 2065 (5'-CGCGGATCCGCGTTGCTTGCATCGTAACG-3'), 2066 (5'-CGCGGATCCGCG AATGCAGCAAC ATCTCCG-3') <i>csuAB</i> region was amplified by PCR using primers, 5'-CsuAB-BamHI (5'-CGGGA TCCGCTGTTACTGGTCAGGTTGACG-3') and 3'-CsuAB-EcoRI (5'-GGAATTC ATAATCGCCTTGTGCTTTTGGTG-3')	[61]
<i>atlA</i> and <i>atlE</i> genes were amplified using PCR, primers used were as follows: <i>atl1</i> : 5'-AAATTGCTCTTGCGTTGTCA-3', <i>atl2</i> : 5'-CAGTTGCCACTGC TCGAATA-3'; <i>atl</i> R-Cmp_for: 5'GCGTGATCAAAAACCATAACG-3', <i>atl</i> R-Cmp_rev: 5'-TGT GTGCACAACGACACTAAA-3'	[70]
<i>Esp</i> gene (955 bp) were amplified using conventional PCR, primers used were as follows, F: 5'-TTGCTAATGCTAGTCCACGACC-3', R: 5'-GCGTCAACAC TTGCATTGCCGAA-3'	[77]
<i>rsbA</i> gene (467 bp) were amplified, using primers such as: <i>rsbAF</i> : 5'-CCA GACTAGCGCAGGAAGTT-3', <i>rsbAR</i> : 5'-ATGGGTGTCTGTCTGCTCTCA-3'	[113]
<i>aftA</i> gene (382 bp) and <i>atfC</i> gene (469 bp) amplified using conventional PCR and primers used as follows: F: 5'-ATAATTTCTAGACCTGCCCTAGCA-3', R: 5'-TGCTTGGATCCGTAATTTTAAACG-3', and F: 5'-AGAAAGGGATCCTACA AATTAA-3', F-'ATAGCATGCATTTAAATTGCC-3'	[114]

Table 4
Genes and gene constructs used in the functional complementation study

Gene constructs	Reference
DNA fragments containing <i>pilW</i> (PA4552) or <i>pilY1</i> (PA4554) genes amplified from genomic DNA of <i>Pseudomonas aeruginosa</i> TBCF10839 and ligated into the <i>Bgl</i> III- and <i>Eco</i> RI-site of shuttle vector pME6010. Introduction of plasmid constructs into strains TBCF10839 PA4554:: Tn5	[31]
pEH110B containing 9 kb <i>Eco</i> RI-HindIII fragment subcloned into BluescriptII KS ⁺ . pCK54, pSK9, pCRV35, pStRV20, and pNcRB19 were subcloned from pEH110B using convenient restriction enzyme. In all of these constructs orientation of the insert is such that <i>pilS/pilR</i> would be under the control of Bluescript T7 promoter	[115]
Gene deletion strategy used to construct chromosomal deletion mutants in strains PA14 and ZK2870. <i>DpelA</i> mutant of ZK2870 obtained by crossing in the <i>DpelA</i> pEX18Gm plasmid containing 579 bp from the 5' region of the gene and the 829 bp from the 3' region of the gene amplified from PA14. Resulting <i>pelA</i> deletion contains first 52 codons fused in frame with the last 194 codons	[35]
Incomplete ORF (~209 bp), identified distal to <i>lasR</i> , named ORF2. 703 bp probe encompassing an <i>Eco</i> RV- <i>Eco</i> RI fragment from pMJG1.7 used to screen a sub genomic library of PAO1. A 5.4 kb <i>Eco</i> RV fragment identified, isolated and subcloned into pBluescriptII KS ⁺ to construct pJMC30. Cloned insert further subcloned into a 1.8 kb <i>Eco</i> RI fragment and a 4.0 kb <i>Cla</i> I fragment. These were inserted into pBluescriptII KS ⁺ to construct pJMC31 and pJMC32, respectively	[37]

(continued)

Table 4
(continued)

Gene constructs	Reference
Wild-type PAO1 and mutant <i>rhlA::Tn5</i> used. Plasmid pSMC21 (GFP ⁺ Ap ^r Kn ^r) expressed <i>gfp</i> , used to label the strains, and plasmid pMH520 contains a <i>rhlA::gfp</i> transcriptional fusion	[39]
PAO1, MPAO1, PAO1seq used and chromosomal transposon insertion mutations were transferred between strains by transformation. Recipient strains carrying a plasmid encoding phage lambda red recombination functions were electroporated with chromosomal DNA isolated from donor strains, with selection for transposon antibiotic-resistant transformants. Transformants were cured of the plasmid carrying lambda red prior to further analysis. <i>E.coli</i> DH5α used for plasmid construction and SM10λ <i>pir</i> for conjugal suicide plasmid delivery. For pLG10 construction, cosmid 122 first digested with <i>Hind</i> III and <i>Nhe</i> I. 10,301 bp <i>phnAB</i> containing fragment from this digestion was gel purified and DNA joined to the gel purified 4532 bp fragment from pUC18 cleaved with <i>Hind</i> III and <i>Xba</i> I	[116]
Plasmids used: pCSG4, pCP994, pKK <i>KompR</i> , pKK <i>KompR</i> 234, pCal-n-CpxR, pBC <i>csg</i> and pBC <i>csgD::uidA-kan</i> . <i>ompR</i> 234 mutations were transferred using its genetic linkage (50% construction) with <i>malA</i> , followed by screening of adherent transductants. Transductions of <i>rpoS::Tn10</i> allele obtained. To obtain a <i>csgD::uidA</i> chromosomal fusion, a 3642 bp DNA fragment corresponding to the whole <i>csg</i> region amplified from MG1655. PCR fragment digested with <i>Sal</i> I and <i>Sac</i> I restriction sites, cloned into corresponding sites of vector pBC to give pBC <i>csg</i> . 3.8-kb <i>Sma</i> I fragment containing <i>uidA-kan</i> cassette (pN496) was cloned into unique <i>Eco</i> RV site of the <i>csgD</i> gene carried by pBC <i>csg</i> , producing pBC <i>csgD::uidA</i>	[43]
To generate <i>agn43::cam</i> mutation, three DNA fragments were used. Fragments 1 and 2 were generated by PCR amplification of 5'- <i>agn43</i> and 3'- <i>agn43</i> followed by restriction digestion by <i>Kpn</i> I– <i>Bam</i> HI, and <i>Xba</i> I– <i>Bam</i> HI, respectively. 3rd fragment was generated by <i>Bam</i> HI digestion of plasmid pNK2884. These fragments ligated together into pUC19, resulting chloramphenicol-resistant plasmid in the following orientation: <i>agn43-5'::cat::agn43-3'</i>	[46]
<i>E.coli</i> MS427 genetically marked by insertion of <i>gfp</i> mut3b* into the chromosomal attachment site of bacteriophage λ. <i>gfp</i> mut3b* containing a NotI fragment from pOS32 was ligated to the <i>bla-attP</i> -containing NotI fragment of pLDR11. Ligation mixture was transformed into MS427 (pLDR8) cells expressing λ Int. Correct chromosomal insertion of <i>gfp</i> mut3b* into an ampicillin-resistant, green fluorescent transformant (OS56) was verified by PCR	[47]
mini-Tn5 element carried on a pUT plasmid in <i>E.coli</i> SM10(λ <i>pir</i>) used as a donor to introduce the transposon to the Amp ^r <i>K. pneumoniae</i> 43,816 strain.	[56]
Genomic DNA of bacteria extracted, digested with PstI and self-ligated with T4DNA ligase. The fragments having both transposon ends and flanking region of insertion site were amplified by inverse PCR with primers Km4180F: 5'-GTTTCATTGATGCTCGATG-3' and Km2921R: 5'-GTACCGAGCTCGAATTCGGC-3'. Flanking regions of target genes <i>treC</i> , <i>treB</i> , <i>sugE</i> and <i>wza</i> were amplified with gene specific primers and resulting fragments were cloned into temperature sensitive vector pKO2-Km, containing Kan ^r gene and <i>sacB</i> gene for positive and negative selection. Resulting plasmid transformed into strain NTH-K2044 and plated at restrictive temperature (43 °C) to force integration of plasmid into bacterial chromosome by single crossover	[58]

(continued)

Table 4
(continued)

Gene constructs	Reference
EZ-Tn5 Kan-2 Transposomes were electroporated into electro-component <i>A. baumannii</i> 207-0294, prepared by washing log phase bacteria three times with ice-cold sterile ultrapure water and resuspending them in ice-cold sterile 10% glycerol	[59]
Amplified PCR product (<i>bfmR</i>) ligated into pCRBlunt II TOPO and transformed into <i>E.coli</i> Top10 cells. DNA isolated from pMU287 and digested with <i>Bam</i> HI, fragment was ligated into the cognate site of the <i>A. baumannii</i> — <i>E.coli</i> shuttle vector, pWH1266. Amplified amplicon (for <i>csuAB</i>) ligated to <i>Bam</i> HI- and <i>Eco</i> RI-digested pGEX4T-2 and resulting plasmid, pCWD33, transformed into <i>E.coli</i> BL21 cells	[61]
Shotgun ligating <i>Bam</i> HI digested chromosomal DNA into pBluescriptII SK. Clones bearing inserts carrying the Tn5 kanamycin ^R marker and chromosomal DNA were selected and sequenced Plasmids pBsmA, pBsmAOp, pBsmB constructed amplifying <i>bsmA</i> , <i>bsmA-nifS</i> operon and <i>bsmB</i> from <i>S. liquefaciens</i> MG1 using primers F2ML (5'-TTACCCACC AGAAGCTTGAAGG-3') (<i>Hind</i> III), and R2ML (5'-CCAGGTTGGCTCTAGATTT CCC-3') (<i>Xba</i> I), primers F2ML and R7ML (5'-ATCGTCATGGTCTAGAAGGTCG-3') (<i>Xba</i> I), and primers F5ML (5'-CTGGCAACATATCTAGATTACCC-3') (<i>Xba</i> I) and R4ML (5'-GGTTCGGTGAGAATTCAGGAG-3') (<i>Eco</i> RI), respectively. Plasmid pBluescript II SK and PCR amplified regions digested with corresponding RE sites engineered into primers and purified and fragments were ligated into pBluescript II SK to obtain pML 001 (<i>bsmA</i>), pML002 (<i>bsmB</i>), pML003 (<i>bsmA-nifS</i> operon). pBRGm constructed and inserts from these three plasmids transferred to obtains pBsmA, pBsmB, and pBsmAOp, respectively	[75]
Targeted mutagenesis of <i>oxyR</i> carried out using single-crossover strategy. A426-bp internal fragment of <i>oxyR</i> amplified, cloned into pCR2.1 and subcloned into pMQ118, a suicide vector in <i>S. marcescens</i> . Resulting plasmid pRMQS133 was introduced into <i>S. marcescens</i> via conjugation and verified by PCR. Resulting <i>oxyR</i> -2 mutation had a duplication and had pMQ118 inserted at 435 bp. pRMQS140 is a medium-copy-number shuttle plasmid bearing a wild-type copy of <i>oxyR</i> and the adjacent gene <i>prgL</i> . The <i>S. marcescens</i> DNA amplified and cloned into pMQ131 using yeast in vivo cloning. Using yeast in vivo cloning, pRMQS143, a p15a-based shuttle plasmid bearing a wild-type <i>oxyR</i> ORF under control of <i>P_{BAD}</i> promoter, was made. The <i>oxyR</i> gene amplified from wild-type <i>S. marcescens</i> WT-D strain and recombined into pMQ125 under <i>P_{BAD}</i> promoter control	[76]
Isogenic mutant of <i>S. mutans</i> NG8 lacking the major cell surface-associated P1 was constructed by insertional inactivation of <i>spaP</i> gene, this strain was named as <i>S. mutans</i> 834. Biofilm production from these two types of strains compared	[79]
To make comC mutant SMCC-L1, pComC-KO plasmid DNA was transformed into <i>S. mutans</i> BM71, prior to linearization of plasmid by <i>Sca</i> I digestion to disrupt beta-lactamase gene. Transformed colonies were selected on THYE-erythromycin agar plates and then confirmed by a rapid PCR using the existing primers and strategy. The knockout mutant of <i>comD</i> and <i>comE</i> were, respectively, generated by transforming pComD-Ko (pVA8912 harboring a 292-bp internal comD fragment Em ^r) and pComE-KO (pVA8912 harboring a 462-bp internal come fragment Em ^r) into <i>S. mutans</i> wild-type strain BM71, chromosomal DNA was isolated from transformants selected on THYE-erythromycin agar plates to determine the presence of <i>erm</i> gene at the desired loci by PCR. Result confirmed by inactivation of the <i>comC</i> ,	[83]

(continued)

Table 4
(continued)

Gene constructs	Reference
<i>comD</i> , <i>comE</i> genes with resultant mutants designated SMCC-L1, SMCD-L1, and SMCE-1, respectively	
<i>ALS</i> genes and fragments for DNA sequencing amplified using proofreading polymerases. Fragments were ligated onto pCRBlunt. pDDB57 contains a amplifiable copy of a deletion cassette encoding <i>URA3</i> selectable marker. Deletion cassette for <i>ALS3</i> and <i>ALS1</i> produced, primers mentioned in Zhao et al. 2004. PCR produced deletion cassettes purified, extracted. CAI4 strain used as parent for mutant construction. Genomic DNA isolated from transformants	[84]
PCR disruption used to replace <i>FLO8</i> and <i>FLO11</i> in both MATa and MAT α Σ 1278b cells with kanMX G418 resistance or <i>HIS3</i> marker. Relative to start site, <i>FLO8</i> (+1 to +2400) and <i>FLO11</i> (−26 to +4170) deleted. To overexpress <i>EAP1</i> , <i>C. albicans</i> <i>URA3</i> obtained as a <i>SacII</i> - <i>XbaI</i> fragment from pDDB57 and inserted into <i>SacII</i> / <i>XbaI</i> -digested pBluescript KS(+) to generate pAU1. 1.1 kb region upstream of <i>ACT1</i> from <i>C. albicans</i> SC5314 genomic DNA amplified by PCR and cloned into the <i>KpnI</i> and <i>XhoI</i> sites of pAU1 and pAU2. Entire ORF of <i>EAP1</i> flanked by an upstream <i>ClaI</i> site and a downstream <i>SmaI</i> . Resulting construct (pAU3) linearized by cutting in the <i>EAP1</i> ORF DNA with <i>PstI</i> to direct integration to the native <i>EAP1</i> locus	[88]
Construction of CAH7-1A1E2 (<i>hwp1/hwp1</i>), CAHR3 (<i>hwp1/HWP1</i>), CAI4-URA3 (reference strain), CAYF178U (<i>als3/als3</i>), CAYC2YF1U (<i>als1/als1</i>), FJS2 (<i>hrr1/hrr1</i>), FJS5 (<i>cht2/cht2</i>), FJS6 (<i>ece1/ece1</i>), and FJS8 (<i>rht5/rht5</i>) as per Nobile et al. 2006 instructions. CJN1222 (<i>bcrl/bcrl TEF1-HWP1</i>) constructed using template plasmid pCJN498 and primers HWP1-F-OE-Ag-NAT-Ag-TEF1p: (5'-TAC ATCAACTGGATGTTATTTGCATCTACTACTATAAGCTCAAACAAATTATC TTTCAAAAATGTTATAATTAACAAGTCATCTATAATTCTTTGGATCC ATCAAGCTTGCCTCGTCCCC-3') and HWP1-R-OE-Ag-NAT-Ag-TEF1p: (5'-CTTCCTCTGTTTCAC CTTGACCGTCTACCTGTGGGACAGTGGCCCCAATTGATAACATGTAATAA GCGATAGCAATAAGTTGAGCAGTTGATAATCTCATTATAAAA TGTATACTTAGAA-3').	[89]
Two allelic coding sequences amplified from BWP17 g-DNA using primer, RBT1AttBIATG: 5'-GGGACAAGTTTGTACAAAAAGCAGGCTCAACTATGA GATTTGCAACTGC-3' and RBT1AttB22098R 5'-GGGACCACTTTGTACAAGAA AGCTGGGTACTTCGAATGAAGAGACTGAAGC-3', cloned in pBC542 vector. To express Rbt1 variants lacking the N-terminal domain, two different fragments produced—(a) Rbt1 signal peptide using RBT1XbaATG: 5'-CCCTCTAGACTATGA GATTTGCAACTGCC-3' and RBT1Nhe60R: 5'-CCCCTAGCCTCAGTGGATA AAATGTAG-3' and (b) Rbt1 C-terminal sequence using RBT1Xba805: 5'-CCCTCT AGAGACTGTCAATGTGACCCCC-3' and RBT1Xho2090R: 5'-CCCCTCGAGGA AGAGACTGAAGCAATAGTG-3'. After restriction with <i>NheI</i> and <i>XbaI</i> and further ligation of the two fragments, final products digested with <i>XbaI</i> and <i>XhoI</i> and cloned in pBC542 vector at the <i>XbaI</i> and <i>XhoI</i> unique sites. Recombinant plasmids were sequenced and transferred into BY4742 as well as pBC542 used as negative control. Two overexpressing strains OExRBT1SL and OExRBT1FL corresponding, respectively, to the expression of a short <i>RBT1</i> allele and a long <i>RBT1</i> allele under the <i>TEF1</i> promoter were obtained	[90]
Both alleles of <i>YWPI</i> disrupted by homologous recombination of transforming DNA cassettes. PCR amplicons were transfected into <i>C. albicans</i> strains BWP17 by the use	[91]

(continued)

Table 4
(continued)

Gene constructs	Reference
of lithium acetate. <i>YWPI</i> allele 1 and allele 2 were disrupted with an amplicon containing ARG4 and recyclable <i>URA3-dpl</i> cassette. <i>YWPI</i> , <i>HIS1</i> , and <i>URA3</i> were amplified by PCR from <i>C. albicans</i> 3153A genomic DNA. Amplicons included 999 bp 5' and 852 bp 3' from coding sequence of <i>YWPI</i> , 231 bp 5' and 51 bp 3' from <i>HIS1</i> and 435 bp 5' and 141 bp 3' from <i>URA3</i> . <i>HIS1</i> and <i>YWPI</i> amplicons were cloned in pGEM-T and pGEM-T easy. A <i>NotI</i> restriction fragment containing <i>YWPI</i> was cloned into a unique <i>NotI</i> site in the <i>HIS1</i> plasmid for combination of <i>YWPI</i> and <i>HIS1</i> in the same plasmid, after removal of a unique <i>NsiI</i> site from pGEM-T; resulting in 50 bp vector sequence between <i>HIS1</i> and <i>YWPI</i> . Prior to transformation, plasmids were linearized at a unique <i>NruI</i> site in <i>HIS1</i> or <i>NsiI</i> site in <i>YWPI</i>	
<i>GAL102</i> amplified with the CaputGAL10(f): 5'-GGGATCCCAACTTGACCTTAA AGG-3' and CaputGAL10(r): 5'-CAGTTCATGGCAAGGGAACC-3' primers. Fragment cloned in pGEM-Teasy vector to construct pVM602. pVM603 constructed by cloning of pYES2. pMS643 constructed by cloning <i>BamHI/XhoI</i> insert from pVM603 in the same sites in pPS180. Construct obtained used to transform <i>S. cerevisiae gal10</i> deletion strain, pJB5. To express CaGal102 in E.coli, the only CUG codon in Gal102 was converted to other serine encoding codon to compensate for alternative genetic code in <i>C. albicans</i>	[94]
<i>SUN41</i> was deleted in <i>C. albicans</i> strain SC5314 by FLIP mediated, site-specific recombination where one pair of sequences flanking the <i>SUN41</i> coding sequence amplified by PCR using primers orf6.2071_FLR1a_ApaI (5'-GCTGGGGCCCCAACCCTGTGGCATATGAA-3') and orf6.2071_FLR1a_XhoI (5'-CCGCTCGAGTGCTGGAAGTACTGCACATAATTT-3') for FLR1; orf6.2071_FLR2_NotI (5'-ATAAGAATGCGGCCGCACCCCTTTTTCTTCTTCCTT-3') and orf6.2071_FLR2_SacII (5'-TCCCCGCGGACCGAAAAATCTTTGGCAGA-3') for FLR2. FLR1 was cloned into the vector after <i>ApaI</i> and <i>XhoI</i> digestion, and FLR2 was cloned after <i>NotI</i> and <i>SacII</i> digestion, resulting in the plasmid pSFS2A-sun1a-2. <i>SUN41</i> open reading frame, including 1031 bp upstream, was PCR amplified with the primers orf6.2071_FLR1a_ApaI and 2071_end_rev_XhoI (5'-CCGCTCGAGGG AAGAAGAGAAAAAGGGGTATC-3') and cloned together with FLR2 into pSFS1A using the restriction sites <i>ApaI/XhoI</i> and <i>NotI/SacII</i> for FLR2	[96]
Strains were constructed from BWP17 and reference strain DAY185. Heterozygous deletion mutant <i>FKS1/fks1Δ</i> was constructed by PCR product-directed disruption using template plasmid pFA-URA3 and primers FKS1-S1 and FKS1-S2. Deletion was confirmed by PCR with primer sets (FKS1-G1, U2 and U3, FKS1-G4). Overexpression strain <i>TDH3-FKS1</i> was constructed by transforming Day185 with PCR products from template pCJN542 and primers FKS1-F-TDH3-OE and FKS1-R-TDH3-OE	[97]
To generate $\Delta cspA$ mutant strain, based on <i>A. fumigatus cspA</i> sequence, primers designed to amplify <i>cspA</i> LB and RB region. Primers for <i>cspA</i> LB: 5'-GCGGTATT GTTGTAAGGTCG-3' and 5'-GTGGAGTCGCTTGATGTTT-3'. The primers for <i>cspA</i> RB were 5'-GCTGGTATCTGGGTTGTCAT-3' and 5'-ACTTTGAGCGTCTC CTCTG-3'. The <i>cspA</i> LB and <i>cspA</i> RB fragments were ligated into the upstream and downstream regions of the hygromycin B phosphotransferase resistance gene (<i>hph</i>) in the pXEH vector, respectively, generating	[98]

(continued)

Table 4
(continued)

Gene constructs	Reference
plasmid pXEH- $\Delta cspA$. An <i>A. fumigatus</i> Af 293 $\Delta cspA$ mutant strain was then generated using the pXEH- $\Delta cspA$ vector by <i>A. tumefaciens</i> -mediated transformation (ATMT)	
Plasmid pAN7.1 modified for gateway [®] use by digestion with <i>Bmg</i> BI or <i>Nae</i> I followed by fusion of an <i>attR</i> :: <i>ccdB</i> target sequence at the site of each digestion using the gateway [®] vector conversion system, to generate plasmids pHY and pYG. To generate the disruption constructs, 1 kb of the flanking sequences of <i>uge3</i> was amplified by PCR from Af293 genomic DNA using primers U1: 5'-CACCAAGGTTTACTATTTCTAGTGGATGG-3', U2: 5'-CGAGGACGATA TGCTCAGG-3' and U3: 5'-CACCTTTTCATTTTGGTATGGCGT-3', U4: 5'-CGTGTCTGCTTTGGACTTGA-3' to generate fragments FS1 and FS4 respectively. The resulting PCR products were then cloned into pENTR-D-TOPOH entry plasmid. A LR recombination allowed recombination of pENTR::FS1 with pHY, and of pENTR::FS4 with pYG, resulting in the fusion of each flanking sequence with the hph cassette in plasmids pHY and pYG plasmids. Finally, the DNA fragments for transformation were generated by PCR, using the primers U1, HY: 5'-CAACCACGGCCTCCAGAAGAAGA-3' with pHY::FS1 and U4, YG: 5'-GCGA GAGCCTGACCTATTGCATCT-3' with pYG::FS4	[99]

Table 5
Gene expression of by Real Time PCR

NTUH-K2044 wild-type strain and mutants harvested, total RNA converted into cDNA using Superscript [®] II Reverse Transcriptase. Gene expression levels monitored by RT-PCR. Expression of <i>treC</i> , <i>treB</i> , and <i>wza</i> genes were analyzed using RT-PCR and primers used as follows. <i>treB</i> -F: 5'-CCCGTTTGCGCTTTGTG-3', <i>treB</i> -R: 5'-ATGCGCAGCTGCTCAATCT-3'; <i>treC</i> -RF: 5'-CCGACAGCGGGCAG TATT-3', <i>treC</i> -R: 5'-CGCCGGATTCTCCAGTT-3'; (<i>wza</i>) KP3720-RF: 5'-GTCAGGTACGCCAGGATATCG-3', KP3720-RR: 5'-CATCAACC TGAGGGCT TTCAA-3'	[58]
Transcriptional analysis performed using RT-PCR kit and primers used were as follows: 5' region of <i>bap</i> : 5'-TCATACGTCTGAAAAATGGCGAG-3'; 5' region of <i>bap</i> (for cDNA strand): 5'-CATCAAGTGCTACTGTCCGGCG-3'; 3' region of <i>bap</i> : 5'-CAGATGTGCCTCATTTGTCCG-3'; 3' region of <i>bap</i> (for cDNA strand): 5'-CCTGTATTCACTCCTTGACCAGCAG-3'	[59]
cDNA synthesized from total RNA of the isolates were used as templates and primers were: <i>blap_{ER-1}</i> gene (FP 5'-ATGAATGTCAATTATAAAAGC-3'; RP 5'-AA TTTGGGCTTAGGGCAAGAAA) and 16S rRNA (FP 5'-TGGCTCAGATTGAA CGCTGGCGGC-3'; RP 5'-TACCTTGTTACGACTTCACCCCA-3')	[62]
Quantification of <i>icaA</i> , <i>icaD</i> , <i>eno</i> , <i>ebps</i> and <i>fib</i> genes were performed using RT-PCR, primers (F: forward and R: reverse) and probes (P) were as follows: <i>icaA</i> F: 5'-CAATACTATTTTCGGGTGTCTTCACTCT-3', R: 5'-CAAGAAACTG CAATATCTTCGGTAATCAT-3', P: 5'-FAM-CCCAGTAGCCAACATC-NFQ-3' <i>icaD</i> F: 5'-TCAAGCCCAGACAGAGGAATA-3', R: 5'-ACACGATATAGCGA TAAGTGCTGTTT-3', P: 5'-FAM-CCCAACGCTAAAATC-NFQ-3'	[66]

(continued)

Table 5
(continued)

eno F: 5'-AAACTGCCGTAGGTGACGAA-3', R: 5'-TGTTTCAACAGCATCTT CAGTACCTT-3', P: 5'-FAM-TTCGCTCCTAAATTTG-NFQ-3'	
ebps F: 5'-ACATTCAAATGACGCTCAAAACAAAAGT-3', R: 5'-CTTATCTT GAGACGCTTATCCTCAGT-3', P: 5'-FAM-CAAGGCGAATAACTC G-NFQ-3'	
fib F: 5'-GAATATGGTGCACGTCCACAATT-3', R: 5'-AAGATTTTGAGCTTG AATCAATTTTGTCTTTTT-3', P: 5'-FAM-TCGCTGCTGGTTTA TT-NFQ-3'	
Quantification of <i>atlA</i> and <i>atlE</i> were performed using RT-PCR, using primer sets, <i>atlR_for</i> : 5'-GTGAATAGAAGATTTGGACAACG-3', <i>atlR_rev</i> : 5'-TGTACGTG CTTGATCAGTCAAA-3'; <i>SAatlFOR</i> : 5'-AAGCAGCTGAGACGACACAA-3', <i>SAatlREV</i> : 5'-TTGCTGTTTTTGGTTGGACA-3'	[70]
Quantification of <i>clfA</i> , <i>cna</i> , <i>fnbA</i> , <i>fnbB</i> were performed using RT-PCR, using primer sets as follows, <i>clfA</i> F: 5'-ATTGGCGTGGCTTCAGTGCT-3', R: 5'-CGTT TCTTCCGTAGTTGCATTTG-3'; <i>cna</i> F: 5'-AAAGCGTTGCCTAGTGGAGA-3', R: 5'-AGTGCCTTCCCAAACCTTTT-3', <i>fnbA</i> F: 5'-ATCAGCAGATGTAGCGG AAG-3', R: 5'-TTTAGTACCGCTCGTTGTCC-3'; <i>fnbB</i> F: 5'-AAGAAGCACCG AAAACTGTG-3', R: 5'-TCTCTGCAACTGCTGTAACG-3'	[72]
RT-qPCR was performed in yeast and hypha forms to measure <i>RBT1</i> expression in two overexpressing strains. Expression levels of <i>RBT1</i> in the two cell forms were determined using primers <i>RBT1qFb</i> 5'-TCAATGCCGCATTTGTCGTG TCT-3' and <i>RBT1qRB</i> 5'-AAGGCCAGGTTCAATTGGACAG-3' in the two overexpressing strains	[90]
Quantitative expression of <i>Mp65</i> was determined by RT-PCR starting from total RNA of <i>C. albicans</i> NGY152 (wild type) and RLVA96 (<i>mp65Δ</i>). Primers for the target gene <i>MP65</i> are, <i>MP65f</i> : 5'-TGTTGTTGTCACTATTGGTAATGG-3', and <i>MP65r</i> : 5'-CGGCAGCAGAAGAAGAAGC-3', and reference gene <i>ACT1</i> are, <i>ACT1f</i> : 5'-CGATAACGGTTCTGGTATG-3' and <i>ACT1r</i> : 5'-CCTTGATGTCTT GGTCTAC-3'	[117]
RT-PCR performed for <i>SUN41</i> (orf19.3642) using following primer, <i>FP</i> : 5'-GGTGCTGCTGGATCTTATGG-3', <i>RP</i> : 5'-CCCAAAGAGTATGAGCAAATT GT-3', and probe 59	[96]
RNA isolated using hot phenol method using liquid nitrogen and Total RNA used for genome wide expression profiling through genotypic technology	[94]
RNA isolation and RT-PCR for <i>FKSI</i> gene, data represented as transcript fold-change normalized to a constitutive reference gene transcript (<i>ACT1</i>) and relative to reference strain	[97]
Levels of <i>cspA</i> mRNA transcript measured using RT-PCR. The primers for <i>cspA</i> were 5'-ATGATGCTCCACCTGACCT-3', 5'-AAGTCGGAACCAGAGGAT-3'. The primers for GAPDH were 5'-ATTCCTTCTCTCAACGGC-3', 5'-ACAACAT CGTCCTCAGTG-3'	[98]
In vitro expression of the <i>uge3</i> gene was quantified by RT-PCR, primers used: 5'-GCTGTTAGCCTCCCAGTACC-3' and 5'-GGACTTGGTCGTACCCCAT-3'	[99]
RT-PCR for different genes in <i>C. neoformans</i> were performed, using the following primers, <i>CAP59</i> F: 5'-GATCTGGGAGCGCTGTAGAC-3', R: 3'-TCTCTGCTC GTCGGTATCCT-5'; <i>LAC1</i> F: 5'-GCCATCAGTCAGGCAGTT-3', R: 3'-TCGG CCATGGAATTGGAAT-5'; <i>URE1</i> F: 5'-TCGTATCGGTGAAGTCGTCACT-3', R: 3'-GGACCACGGAATTGCTTCAT-5'; <i>GADPH</i> F: 5'-TTTCCCGCGACTTTTTT G-3', R: 3'-TCGCAGCCGAGTCTACGAT-5'.	[106]
For <i>C. gattii</i> , primer sets are as follows: <i>CAP59</i> F: 5'-CCTCCATATCCTCGACCT CA-3', R: 3'-AGTTGGACCACGTTTCTTG-5'; <i>LAC1</i> F: 5'-TCCCTACGAGAG CACATTGGT-3', R: 3'-CCCCTGCCCCCATGTC-5'; <i>URE1</i> F: 5'-GCCGGACG TCATTGACTTTT-3', R: 3'-CCC CAGTCGTTGGTCCAA-5'	

Moreover risk of medical complications in biofilm associated nosocomial infection due to reduced antimicrobial susceptibility demands intricate characterization of biofilm associated genes to decipher alternate therapeutics to combat the dissemination of nosocomial infection caused by microbial biofilms.

Acknowledgement

The authors would like to express their deepest gratitude to Director, Calcutta School of Tropical Medicine, Kolkata, West Bengal for his kind support. The authors would also want to thank Dr. Moupriya Nag, Assistant Professor, and Prof. Dibyajit Lahiri, Assistant Professor, UEM, Kolkata, West Bengal for the invitation to write this chapter.

References

1. CDC progress report (2018). <https://www.cdc.gov/hai/data/portal/progress-report.html>
2. Diaz E, Rodríguez AH, Rello J (2005) Ventilator-associated pneumonia: issues related to the artificial airway. *Respir Care* 50:900–909
3. Chastre J, Fagon JY (2002) Ventilator-associated pneumonia. *Am J Respir Crit Care Med* 165:867–903
4. Ramirez P, Ferrer M, Torres A (2007) Prevention measures for ventilator-associated pneumonia: a new focus on the endotracheal tube. *Curr Opin Infect Dis* 20:190–197
5. Depuydt P, Benoit D, Vogelaers D, Decruyenaere J, Vandijck D, Claeys G, Verschraegen G, Blot S (2008) Systematic surveillance cultures as a tool to predict involvement of multidrug antibiotic resistant bacteria in ventilator-associated pneumonia. *Intensive Care Med* 34:675–682
6. Amin A (2009) Clinical and economic consequences of ventilator-associated pneumonia. *Clin Infect Dis* 49(Suppl. 1):S36–S43
7. Bauer TT, Torres A, Ferrer R, Heyer CM, Schultze-Werninghaus G, Rasche K (2002) Biofilm formation in endotracheal tubes. Association between pneumonia and the persistence of pathogens. *Monaldi Arch Chest Dis* 57:84–87
8. Kaye D, Hessen M (1994) Infections associated with foreign bodies in the urinary tract. In: Kaye D (ed) *Infections associated with indwelling medical devices*, 2nd edn. American Society for Microbiology, Washington, pp 291–307
9. Kokare CR, Chakraborty S, Khopade AN, Mahadik KR (2009) Biofilm: importance and applications. *Indian J Biotechnol* 8:159–168
10. Stickler DJ (1996) Bacterial biofilms and the encrustation of urethral catheters. *Biofouling* 9:293–305
11. Anaissie E, Samonis G, Kontoyiannis D, Costerton J, Sabharwal U, Bodey G, Raad I (1995) Role of catheter colonization and infrequent hematogenous seeding in catheter-related infections. *Eur J Clin Microbiol Infect Dis* 14:134–137
12. Maki DG, Mermel LA (1998) Infections due to infusion therapy. In: Bennett JV, Brachman PS (eds) *Hospital infections*, 4th edn. Lippincott-Raven, Philadelphia, pp 689–724
13. Donlan R, Murga R, Carson L (1999) Growing biofilms in intravenous fluids. In: Wimpenny J, Gilbert P, Walker J, Brading M, Bayston R (eds) *Biofilms, the good, the bad, and the ugly*. Presented at the fourth meeting of the Biofilm Club; Powys, UK. British Biofilm Club, Powys, pp 23–29
14. Kathju S, Nistico L, Hall-Stoodley L, Post JC, Ehrlich GD, Stoodley P (2009) Chronic surgical site infection due to suture associated polymicrobial biofilm. *Surg Infect* 10:457–461
15. Edmiston CE, Jr McBain AJ, Roberts C, Leaper D (2015) Clinical and microbiological aspects of biofilm-associated surgical site infections. *Adv Exp Med Biol* 830:47–67

16. Percival SL, Suleman L, Vuotto C, Donelli G (2015) Healthcare-associated infections, medical devices and biofilms: risk, tolerance and control. *J Med Microbiol* 64:323–334
17. Lindsay D, von Holy A (2006) Bacterial biofilms within the clinical setting: what healthcare professionals should know. *J Hosp Infect* 64:313–325
18. Bryers JD (2008) Medical biofilms. *Biotechnol Bioeng* 100:1–18
19. Percival SL, Thomas JG, Williams DW (2010) Biofilms and bacterial imbalances in chronic wounds: anti-Koch. *Int Wound J* 7:169–175
20. Maric S, Vranes J (2007) Characteristics and significance of microbial biofilm formation. *Period Bilgor* 109:115–121
21. Garrett TR, Bhakoo M, Zhang Z (2008) Bacterial adhesion and biofilms on surfaces. *Prog Nat Sci* 18:1049–1056
22. Dunne WM (2002) Bacterial adhesion: seen any good biofilms lately? *Clin Microbiol Rev* 15:155–166
23. Costerton JW, Stewart PS, Greenberg EP (1999) Bacterial biofilms: a common cause of persistent infections. *Science* 284:1318–1322
24. Davey ME, O'toole GA (2000) Microbial biofilms: from ecology to molecular genetics. *Microbiol Mol Biol Rev* 64:847–867
25. Davies DG, Parsek MR, Pearson JP, Iglewski BH, Costerton JW, Greenberg EP (1998) The involvement of cell-to-cell signals in the development of a bacterial biofilm. *Science* 280(5361):295–298
26. Federle MJ, Bassler BL (2003) Interspecies communication in bacteria. *J Clin Invest* 112:1291–1299
27. Parsek MR, Singh PK (2003) Bacterial biofilms: an emerging link to disease pathogenesis. *Annu Rev Microbiol* 57:677–701
28. Baselga R, Albizu I, Amorena B (1994) *Staphylococcus aureus* capsule and slime as virulence factors in ruminant mastitis: a review. *Vet Microbiol* 39:195–204
29. Sutherland IW (1999) Polysaccharases for microbial exopolysaccharides. *Carbohydr Polym* 38:319–328
30. Harding MW, Marques LL, Howard RJ, Olson ME (2009) Can filamentous fungi form biofilms? *Trends Microbiol* 17:475–480
31. Bohn YS, Brandes G, Rakhimova E, Horatzek S, Salunkhe P, Munder A, van Barneveld A, Jordan D, Bredenbruch F, Haussler S et al (2009) Multiple roles of *Pseudomonas aeruginosa* TBCF10839 PilY1 in motility, transport and infection. *Mol Microbiol* 71:730–747
32. Mattick JS (2002) Type IV pili and twitching motility. *Annu Rev Microbiol* 56:289–314
33. Alm RA, Hallinan JP, Watson AA, Mattick JS (1996) Fimbrial biogenesis genes of *Pseudomonas aeruginosa*: *pilW* and *pilX* increase the similarity of type 4 fimbriae to the GSP protein-secretion systems and *pilY1* encodes a gonococcal PilC homologue. *Mol Microbiol* 22:161–173
34. Wentworth JS, Austin FE, Garber N, Gilboa-Garber N, Paterson CA, Doyle RJ (1991) Cytoplasmic lectins contribute to the adhesion of *Pseudomonas aeruginosa*. *Biofouling* 4:99–104
35. Friedman L, Kolter R (2004) Two genetic loci produce distinct carbohydrate-rich structural components of the *Pseudomonas aeruginosa* biofilm matrix. *J Bacteriol* 186:4457–4465
36. May TB, Shinabarger D, Maharaj R, Kato J, Chu L, DeVault JD, Roychoudhury S, Zielinski NA, Berry A, Rothmel RK (1991) Alginate synthesis by *Pseudomonas aeruginosa*: a key pathogenic factor in chronic pulmonary infections of cystic fibrosis patients. *Clin Microbiol Rev* 4:191–206
37. Passador L, Cook JM, Gambello MJ, Rust L, Iglewski BH (1993) Expression of *Pseudomonas aeruginosa* virulence genes requires cell-to-cell communication. *Science* 260:1127–1130
38. Ochsner UA, Reiser J (1995) Autoinducer-mediated regulation of rhamnolipid biosurfactant synthesis in *Pseudomonas aeruginosa*. *Proc Natl Acad Sci U S A* 92:6424–6428
39. Davey ME, Caiazza NC, O'Toole GA (2003) Rhamnolipid surfactant production affects biofilm architecture in *Pseudomonas aeruginosa* PAO1. *J Bacteriol* 185:1027–1036
40. Diggle SP, Cornelis P, Williams P, Camara M (2006) 4-quinolone signalling in *Pseudomonas aeruginosa*: old molecules, new perspectives. *Int J Med Microbiol* 296:83–91
41. Prüß MB, Besemann C, Denton A, Wolfe AJA (2006) Complex transcription network controls the early stages of biofilm development by *Escherichia coli*. *J Bacteriol* 188:3731–3739
42. Ben Nasr A, Olsen A, Sjobring U, Muller-Esterl W, Bjorck L (1996) Assembly of human contact phase proteins and release of bradykinin at the surface of curli-expressing *Escherichia coli*. *Mol Microbiol* 20:927–935
43. Prigent-Combaret C, Brombacher E, Vidal O, Ambert A, Lejeune P, Landini P, Dorel C (2001) Complex regulatory network

- controls initial adhesion and biofilm formation in *Escherichia coli* via regulation of the *csgD* gene. *J Bacteriol* 183:7213–7223
44. Vidal O, Longin R, Prigent-Combaret C, Dorel C, Hooreman M, Lejeune P (1998) Isolation of an *Escherichia coli* K-12 mutant strain able to form biofilms on inert surfaces: involvement of a new *ompR* allele that increases curli expression. *J Bacteriol* 180:2442–2449
 45. Voulhoux R, Bos MP, Geurtsen J, Mols M, Tommassen J (2003) Role of a highly conserved bacterial protein in outer membrane protein assembly. *Science* 299:262–265
 46. Danese PN, Pratt LA, Dove SL, Kolter R (2000) The outer membrane protein, antigen 43, mediates cell-to-cell interactions within *Escherichia coli* biofilms. *Mol Microbiol* 37:424–432
 47. Sherlock O, Verjborg RM, Klemm P (2005) The TibA adhesin/invasion from Enterotoxigenic *Escherichia coli* is self-recognizing and induces bacterial aggregation and biofilm formation. *Infect Immunol* 73:1954–1963
 48. Cucarella C, Solano C, Valle J, Amorena B, Lasa I, Penades JR (2001) Bap, a *Staphylococcus aureus* surface protein involved in biofilm formation. *J Bacteriol* 183:2888–2896
 49. Latasa C, Roux A, Toledo-Arana A, Ghigo JM, Gamazo C, Penades JR, Lasa I (2005) BapA, a large secreted protein required for biofilm formation and host colonization of *Salmonella enterica serovar enteritidis*. *Mol Microbiol* 58:1322–1339
 50. Eaton TJ, Gasson MJ (2001) Molecular screening of enterococcus virulence determinants and potential for genetic exchange between food and medical isolates. *Appl Environ Microbiol* 67:1628–1635
 51. Hashem YA, Amin HM, Essam TM, Yassin AS, Aziz RK (2017) Biofilm formation in enterococci: genotype-phenotype correlations and inhibition by vancomycin. *Sci Rep* 7:5733
 52. Stępień-Pyśniak D, Hauschild T, Kosikowska U, Dec M, Urban-Chmiel R (2019) Biofilm formation capacity and presence of virulence factors among commensal *Enterococcus spp.* from wild birds. *Sci Rep* 9:11204
 53. Sifri CD, Mylonakis E, Singh KV, Qin X, Garzin DA, Murray BE et al (2002) Virulence effect of *Enterococcus faecalis* protease genes and the quorum-sensing locus *fsr* in *Caenorhabditis elegans* and mice. *Infect Immun* 70:5647–5650
 54. Hancock LE, Perego M (2004) The *Enterococcus faecalis* *fsr* two-component system controls biofilm development through production of gelatinase. *J Bacteriol* 186:5629–5639
 55. Kline KA, Dodson KW, Caparon MG, Hultgren SJ (2010) A tale of two pili: assembly and function of pili in bacteria. *Trends Microbiol* 18:224–232
 56. Langstraat J, Bohse M, Clegg S (2001) Type 3 fimbrial shaft (MrkA) of *Klebsiella pneumoniae*, but not the fimbrial adhesin (MrkD), facilitates biofilm formation. *Infect Immun* 69:5805–5812
 57. Alcántar-Curiel MD, Blackburn D, Saldaña Z, Gayosso-Vázquez C, Iovine NM, de la Cruz MA, Girón JA (2013) Multi-functional analysis of *Klebsiella pneumoniae* fimbrial types in adherence and biofilm formation. *Virulence* 4:129–138
 58. Wu MC, Lin TL, Hsieh PF, Yang HC, Wang JT (2011) Isolation of genes involved in biofilm formation of a *Klebsiella pneumoniae* strain causing pyogenic liver abscess. *PLoS One* 6:e23500
 59. Loehfelm TW, Luke NR, Campagnari AA (2008) Identification and characterization of an *Acinetobacter baumannii* biofilm-associated protein. *J Bacteriol* 190:1036–1044
 60. Rahbar MR, Rasooli I, Mousavi Gargari S, Amani J, Fattahian Y (2010) In silico analysis of antibody triggering biofilm associated protein in *Acinetobacter baumannii*. *J Theor Biol* 266:275–290
 61. Tomaras AP, Flagler MJ, Dorsey CW, Gaddy JA, Actis LA (2008) Characterization of a two component regulatory system from *Acinetobacter baumannii* that controls biofilm formation and cellular morphology. *Microbiology* 154:3398–3409
 62. Lee HW, Kim J, Lee JC, Lee YC, Seol SY (2008) Capacity of multidrug-resistant clinical isolates of *Acinetobacter baumannii* to form biofilm and adhere to epithelial cell surfaces. *Clin Microbiol Infect* 14:49–54
 63. Cerca N, Jefferson KK, Maira-Litrán T, Pier DB, Kelly-Quintos C, Goldmann DA, Azeredo J, Pier GB (2007) Molecular basis for preferential protective efficacy of antibodies directed to the poorly acetylated form of staphylococcal poly-N-acetyl- β -(1-6)-glucosamine. *Infect Immun* 75:3406–3413
 64. Agarwal A, Jain A (2013) Glucose & sodium chloride induced biofilm production & *ica* operon in clinical isolates of staphylococci. *Indian J Med Res* 138:262–266

65. Cue D, Lei MG, Lee CY (2012) Genetic regulation of the intercellular adhesion locus in staphylococci. *Front Cell Infect Microbiol* 2:38
66. Kot B, Sytykiewicz H, Sprawka I (2018) Expression of the biofilm-associated genes in methicillin-resistant *Staphylococcus aureus* in biofilm and planktonic conditions. *Int J Mol Sci* 19:3487
67. Carneiro CR, Postol E, Nomizo R, Reis LF, Brentani RR (2004) Identification of enolase as a laminin-binding protein on the surface of *Staphylococcus aureus*. *Microbes Infect* 6:604–606
68. Downer R, Roche F, Park PW, Mecham RP, Foster TJ (2002) The elastin-binding protein of *Staphylococcus aureus* (EbpS) is expressed at the cell surface as an integral membrane protein and not as a cell wall-associated protein. *J Biol Chem* 277:243–225
69. Hartford OM, Wann ER, Höök M, Foster TJ (2001) Identification of residues in the *Staphylococcus aureus* fibrinogen-binding MSCRAMM clumping factor A (ClfA) that are important for ligand binding. *J Biol Chem* 276:2466–2473
70. Houston P, Rowe SE, Pozzi C, Waters EM, O’Gara JP (2011) Essential role for the major autolysin in the fibronectin-binding protein-mediated *Staphylococcus aureus* biofilm phenotype. *Infect Immun* 79:1153–1165
71. Vergara-Irigaray M, Maira-Litran T, Merino N, Pier GB, Penades JR, Lasa I (2008) Wall teichoic acids are dispensable for anchoring the PNAG exopolysaccharide to the *Staphylococcus aureus* cell surface. *Microbiology* 154:865–877
72. Kannappan A, Gowrishankar S, Srinivasan R, Pandian SK, Ravi AV (2017) Antibiofilm activity of *Vetiveria zizanioides* root extract against methicillin-resistant *Staphylococcus aureus*. *Microb Pathog* 110:313–324
73. Corrigan RM, Rigby D, Handley P, Foster TJ (2007) The role of *Staphylococcus aureus* surface protein SasG in adherence and biofilm formation. *Microbiology* 153:2435–2446
74. Labbate M, Zhu H, Thung L, Bandara R, Larsen MR, Willcox MDP, Givskov M, Rice SA, Kjelleberg S (2007) Quorum-sensing regulation of adhesion in *Serratia marcescens* MG1 is surface dependent. *J Bacteriol* 189:2702–2711
75. Labbate M, Queck SY, Koh KS, Rice SA, Givskov M, Kjelleberg S (2004) Quorum sensing-controlled biofilm development in *Serratia liquifaciens* MG1. *J Bacteriol* 186:692–698
76. Shanks RMQ, Stella NA, Kalivoda EJ, Doe MR, O’Dee DM, Lathrop KL, Guo FL, Nau GJ (2007) A *Serratia marcescens* OxyR homolog mediates surface attachment and biofilm formation. *J Bacteriol* 189:7262–7272
77. Sayal RA, Alkharasani NMF, Alsadawi AA, Alquaraishi (2018) Molecular study of biofilm and some antibiotic resistance gene in *Proteus mirabilis* isolated from children with UTI patients in Al-Najaf governorate. *J Pharm Sci Res* 8:1986–1990
78. Hussein EI, Al-Batayneh K, Masadeh MM, Dahadhah FW, Zoubi MSA, Aljabali AA et al (2020) Assessment of pathogenic potential, virulent genes profile, and antibiotic susceptibility of *proteus mirabilis* from urinary tract infection. *Int J Microbiol* 2020:1–5
79. Bowen WH, Schilling K, Giertsen E, Pearson S, Lee SF, Bleiweis A, Beeman D (1991) Role of a cell surface-associated protein in adherence and dental caries. *Infect Immun* 59:4604–4609
80. Froeliger EH, Fives-Taylor P (2001) *Streptococcus parasanguis* fimbria-associated adhesin Fap1 is required for biofilm formation. *Infect Immun* 69:2512–2519
81. Wen ZT, Burne RA (2002) Functional genomics approach to identifying genes required for biofilm development by *Streptococcus mutans*. *Appl Environ Microbiol* 68:1196–1203
82. Yoshida A, Kuramitsu HK (2002) Multiple *Streptococcus mutans* genes are involved in biofilm formation. *Appl Environ Microbiol* 68:6283–6291
83. Li YH, Tang N, Aspiras MB, Lau CYP, Lee JH, Ellen RP, Cvitkovitch DG (2002) A quorum-sensing signaling system essential for genetic competence in *Streptococcus mutans* is involved in biofilm formation. *J Bacteriol* 184:2699–2708
84. Zhao X, Oh S-H, Cheng G et al (2004) ALS3 and ALS8 represent a single locus that encodes a *Candida albicans* adhesin; functional comparison between Als3p and Als1p. *Microbiology* 150:2415–2428
85. Gaur NK, Klotz SA, Henderson RL (1999) Overexpression of the *Candida albicans* *ALA1* gene in *Saccharomyces cerevisiae* results in aggregation following attachment of yeast cells to extracellular matrix proteins, adherence properties similar to those of *Candida albicans*. *Infect Immun* 67:6040–6047
86. Sheppard DC, Yeaman MR, Welch WH et al (2004) Functional and structural diversity in the Als protein family of *Candida albicans*. *J Biol Chem* 279:30480–30489

87. Zhao X, Oh S-H, Hoyer LL (2007) Unequal contribution of *ALS9* alleles to adhesion between *Candida albicans* and vascular endothelial cells. *Microbiology* 153 (Pt 7):2342–2350
88. Li F, Palecek SP (2003) EAP1, a *Candida albicans* gene involved in binding human epithelial cells. *Eukaryot Cell* 2:1266–1273
89. Nobile CJ, Nett JE, Andes DR, Mitchell AP (2006) Function of *Candida albicans* adhesin Hwp1 in biofilm formation. *Eukaryot Cell* 5:1604–1610
90. Monniot C, Boisrame A, Da Costa G, Chauvel M, Sautour M, Bounoux ME, Bellon-Fontaine MN, Dalle F, d'Enfert C, Richard ML (2013) Rbt1 protein domains analysis in *Candida albicans* brings insights into hyphal surface modifications and Rbt1 potential role during adhesion and biofilm formation. *PLoS One* 8:e82395
91. Granger BL, Flenniken ML, Davis DA, Mitchell AP, Cutler JE (2005) Yeast wall protein 1 of *Candida albicans*. *Microbiology* 151:1631–1644
92. Sandini S, Stringaro A, Arancia S, Colone M, Mondello F, Murtas S, Girolamo A, Mastrangelo N, De Bernardis F (2011) The MP65 gene is required for cell wall integrity, adherence to epithelial cells and biofilm formation in *Candida albicans*. *BMC Microbiol* 11:106
93. Chaffin WL (2008) *Candida albicans* cell wall proteins. *Microbiol Mol Biol Rev* 72:495–544
94. Sen M, Shah B, Rakshit S, Singh V, Padmanabhan B, Ponnusamy M, Pari K, Vishwakarma R, Nandi D, Sadhale PP (2011) UDP-glucose 4, 6-dehydratase activity plays an important role in maintaining cell wall integrity and virulence of *Candida albicans*. *PLoS Pathog* 7:e1002384
95. Peltroche-Llacsahuanga H, Goyard S, d'Enfert C, Prill SK, Ernst JF (2006) Protein O-mannosyltransferase isoforms regulate biofilm formation in *Candida albicans*. *Antimicrob Agents Chemother* 50:3488–3491
96. Hiller E, Heine S, Brunner H, Rupp S (2007) *Candida albicans* Sun41p, a putative glycosidase, is involved in morphogenesis, cell wall biogenesis, and biofilm formation. *Eukaryot Cell* 6:2056–2065
97. Nett JE, Sanchez H, Cain MT, Andes DR (2010) Genetic basis of *Candida* biofilm resistance due to drug-sequestering matrix glucan. *J Infect Dis* 202:171–175
98. Fan Z, Li Z, Xu Z, Li H, Li L, Ning C, Ma L, Xie X, Wang G, Yu H (2015) cspA influences biofilm formation and drug resistance in pathogenic fungus *Aspergillus fumigatus*. *Biomed Res Int* 2015:1–9
99. Gravelat FN, Beauvais A, Liu H, Lee MJ, Snarr BD, Chen D, Xu W, Kravtsov I, Hoareau CM, Vanier G, Urb M, Campoli P, Al-Abdallah Q, Lehoux M, Chabot JC (2013) *Aspergillus* galactosaminogalactan mediates adherence to host constituents and conceals hyphal β -glucan from the immune system. *PLoS Pathog* 9:e1003575
100. Lee MJ, Gravelat FN, Cerone RP, Baptista SD, Campoli PV, Choe SI, Kravtsov I, Vinogradov E, Creuzenet C, Liu H, Berghuis AM, Latge JP, Filler SG, Fontaine T, Sheppard DC (2014) Overlapping and distinct roles of *Aspergillus fumigatus* UDP-glucose 4-epimerases in galactose metabolism and the synthesis of galactose-containing cell wall polysaccharides. *J Biol Chem* 289:1243–1256
101. Bamford NC, Snarr BD, Gravelat FN, Little DJ, Lee MJ, Zacharias CA, Chabot JC, Geller AM, Baptista SD, Baker P, Robinson H, Howell PL, Sheppard DC (2015) Sph3 is a glycoside hydrolase required for the biosynthesis of galactosaminogalactan in *Aspergillus fumigatus*. *J Biol Chem* 290:27438–27450
102. Bamford NC, Mauff FL, Loon JCV, Ostapska H, Snarr BD, Zhang Y, Kitova EN, Klassen JS, Codée JDC, Sheppard DC, Howell PL (2020) Structural and biochemical characterization of the exopolysaccharide deacetylase Agd3 required for *Aspergillus fumigatus* biofilm formation. *Nat Commun* 11:2450
103. Kaur S, Singh S (2014) Biofilm formation by *Aspergillus fumigatus*. *Med Mycol* 52:2–9
104. Chang YC, Penoyer LA, Kwon-Chung KJ (1997) The second capsule gene of *Cryptococcus neoformans*, CAP64, is essential for virulence. *Infect Immun* 64:1977–1983
105. Zhu X, Gibbons J, Garcia-Rivera J, Casadevall A, Williamson PR (2001) Laccase of *Cryptococcus neoformans* is a cell wall-associated virulence factor. *Infect Immun* 69:5589–5596
106. Benaducci T, Sardi JDCO, Lourencetti NMS, Scorzoni L, Gullo FP, Rossi SA, Derissi JB, de Azevedo Prata MC, Fusco-Almeida AM, Mendes-Giannini MJS (2016) Virulence of *Cryptococcus sp.* biofilms in vitro and in vivo using *Galleria mellonella* as an alternative model. *Front Microbiol* 7:290
107. Kurakado S, Chiba R, Sato C, Matsumoto Y, Sugita T (2020) N,N,N',N'-tetrakis(2-pyridylmethyl) ethylenediamine, a zinc chelator,

- inhibits biofilm and hyphal formation in *Trichosporon asahii*. *BMC Res Notes* 13:142
108. Raya S, Belbase A, Dhakal L, Prajapati KG, Baidya R, Bimali NK (2019) In-vitro biofilm formation and antimicrobial resistance of *Escherichia coli* in diabetic and nondiabetic patients. *Biomed Res Int* 2019:1–8
 109. Oliveira AD, Pereira VC, Pinheiro L, Riboli DM, Martins KB, Da Cunha MRDS (2016) Antimicrobial resistance profile of planktonic and biofilm cells of *Staphylococcus aureus* and coagulase-negative staphylococci. *Int J Mol Sci* 17:1423
 110. Mishra SK, Basukala P, Basukala O, Parajuli K, Pokhrel BM, Rijal BP (2014) Detection of biofilm production and antibiotic resistance pattern in clinical isolates from indwelling medical devices. *Curr Microbiol* 70:128–134
 111. Høiby N, Bjarnsholt T, Givskov M, Molin S, Ciofu O (2010) Antibiotic resistance of bacterial biofilms. *Int J Antimicrob Agents* 35:322–332
 112. Sharma D, Misba L, Khan AU (2019) Antibiotics versus biofilm: an emerging battleground in microbial communities. *Antimicrob Resist Infect Control* 8:76
 113. Badi SA, Norouzy J, Sepahi AA (2014) Detection RsbA gene's band & effect of miristic acid in virulence of *Proteus mirabilis* isolated from urinary tract infection. *Iran J Public Health* 43:210
 114. Zunino P, Geymonat L, Alllen AG, Legnani-Fajardo C, Maskell DJ (2000) Virulence of *Proteus mirabilis* ATF isogenic mutant is not impaired in a mouse model of ascending urinary tract infection. *FEMS Immunol Med Microbiol* 29(2):137–143
 115. Hobbs M, Collie ESR, Free PD, Livingston SP, Mattick JS (1993) PilS and PilR, a two-component transcriptional regulatory system controlling expression of type 4 fimbriae in *Pseudomonas aeruginosa*. *Mol Microbiol* 7:669–682
 116. Gallagher LA, McKnight SL, Kuznetsova MS, Pesci EC, Manoil C (2002) Functions required for extracellular quinolone signaling by *Pseudomonas aeruginosa*. *J Bacteriol* 184:6472–6480
 117. Sandini S, Stringaro A, Arancia S, Colone M, Mondello F, Murtas S et al (2011) The MP65 gene is required for cell wall integrity, adherence to epithelial cells and biofilm formation in *Candida albicans*. *BMC Microbiol* 11:106

3 Quorum Sensing in Gram-Negative Bacteria

Snehashis Koley, Ambar Bose, and Mandira Mukherjee

DOI: 10.1201/9781003300557-3

3.1 INTRODUCTION

Quorum sensing (QS) was defined as the regulation of gene expression in response to variations in cell-population density. The different steps in QS included (i) synthesis and release of extracellular signal molecules known as autoinducers (AI); (ii) activation of a specific receptor present in the cytoplasm or in the membrane on reaching a certain threshold concentration of the AIs; and (iii) regulation of expression of genes in the QS regulon (1). Thus quorum sensing empowers cells in a population to function in harmony and conduct the different cellular activities collectively.

Gram-negative bacteria synthesize and release acyl-homoserine lactones (AHLs) or other chemical molecules whose production depends on S-adenosylmethionine (SAM) as a substrate which freely diffuses across the inner and outer membranes. These chemical compounds, the autoinducers (AIs), and are grouped as AI-1 type. In addition, another type of AI, called AI-2, which is a furanosyl borate diester, was detected in *Vibrio harveyi*, a free-living bioluminescent Gram-negative marine bacterium (2). A third, autoinducer-3 (AI-3), derived from threonine dehydrogenase (Tdh) products and “abortive” tRNA synthetase reactions, was first detected in enterohaemorrhagic *Escherichia coli* (EHEC), which regulated its virulence (3).

Incidence of QS was observed among intraspecies as well as interspecies Gram-negative bacteria. Co-culture systems of *V. harveyi* and *E. coli* demonstrated that AI-2 production by one species regulated gene expression in the other (4–6). Moreover, in another study, *P. aeruginosa* cell culture supernatant was found to be capable of mediating cell death of *E. coli* through a QS-facilitated process (7).

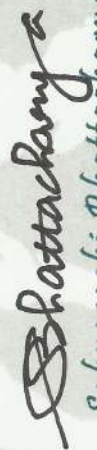
QS, in most of the Gram-negative bacteria, utilizes a LuxI (AI synthase)/LuxR (transcriptional regulator) type of system (1). There are varied homologues of the AI synthase (LuxI type) and the transcriptional regulator across the different species of the Gram-negative bacteria which actively used QS, suggesting a high degree of evolutionary conservation. Unlike quorum sensing by homoserine lactone autoinducers, AI-2 is a one-of-a-kind, ‘universal’ signal that might be employed by a wide range of bacteria for intra- and interspecies communication. In *E. coli*, *Salmonella typhimurium*, *V. harveyi*, and *V. cholerae*, evidence suggested that the biosynthetic pathway and biochemical intermediates in AI-2 production were identical, which further supported the idea that QS mediated by AI-2 production facilitated both intra- and interspecies communication (6) In this chapter focus on the quorum sensing circuits in the different species of disease-causing Gram-negative bacteria, their mechanism of synthesis, and action at the molecular level.



Certificate of Participation

This is to certify that **Snehashis Koley**, School of Tropical **Medicine, Kolkata** has participated and delivered an oral presentation entitled "*Prophages : An Alternative Therapy for Recurrent Urinary Tract Infection*" in the "6th India Biodiversity Meet 2019 (International Conference)", held at Indian Statistical Institute, Kolkata, from 14th ~ 16th February, 2019.


Abhishek Mukherjee
Organising Secretary


Sabyasachi Bhattacharya
Head, AERU, ISI


6th INDIA BIODIVERSITY MEET 2019
International Conference
14 -16 FEBRUARY, 2019

**Biospectrum 2020
International Conference on Biotechnology
& Biological Sciences**



Certificate of Presentation

This is to certify that Ms. Arunita Ghosh, Mr. Debojyoty Bandyopadhyay, Mr. Snehashis Koley, Dr. Mandira Mukherjee Of School of Tropical Medicine presented paper titled Uropathogenic Escherichia coli in India- An overview on recent research advancements and trends In Biospectrum held from 19th to 21st November 2020.

Prof. Dr. Sajal DasGupta
Vice Chancellor UEMK

Prof. Dr. Satyajit Chakrabarti
Conference Co-Chair

Prof. Dr. Susmita Mukherjee
HOD, Dept. of Biotechnology



CERTIFICATE

OF PRESENTATION

INTERNATIONAL CONFERENCE ON

'Technological Innovations in Agriculture, Life Sciences, AND Food & Nutrition - ICALF 2023'

Organized by
Swami Vivekananda University

This is to certify that Prof./Dr./Mr./Mrs. Snehashis Koley
of School of Tropical Medicine, Kolkata
has presented the paper titled Acute Kidney Injury: Meta-Analysis
held at Swami Vivekananda University (SVU) Barrackpore Campus during 27th-28th February 2023.

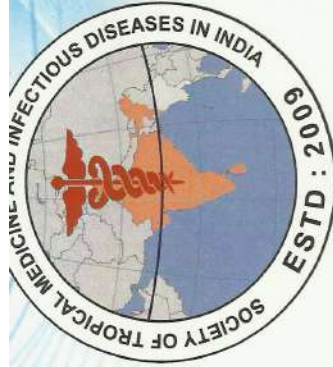
Subrata Kumar Dey
Prof.(Dr.) Subrata Kumar Dey
Vice Chancellor, SVU

Saurabh Adhikari
Mr. Saurabh Adhikari
Chief Operating Officer, SVU

Pink Nath
Prof.(Dr.) Pink Nath
Registrar, SVU

Sankar
Dr. Tanmoy Sarkar
HOD, Agriculture
(Joint Convener ICALF 2023)

Pritha Pal
Dr. Pritha Pal
HOD, Microbiology
(Joint Convener ICALF 2023)



Certificate of Attendance

CME 7
*on Tropical
& Infectious Diseases*

SOCIETY OF TROPICAL MEDICINE AND INFECTIOUS DISEASES IN INDIA

*This is to certify that..... **Snehashis Koley**.....
attended The CME 7 on Tropical and Infectious Diseases organised by the
Society of Tropical Medicine and Infectious Diseases in India
held on 11th June, 2017 as a delegate.*

We wish him/her success in life.

Arindam Naskar

Dr. Arindam Naskar
Organising Secretary

Rama Prasad Goswami

Dr. Rama Prasad Goswami
Chairperson



Certificate of Attendance

**SOCIETY OF TROPICAL MEDICINE
AND INFECTIOUS DISEASES IN INDIA**

This is to certify that *Snehashis Koley*
attended the CME 9 held on 18th August, 2019
at Oberoi Grand Hotel, Kolkata.

We wish him / her success in life.

.....
Organising Secretary
Dr. Amartya Kumar Misra

Rama Prosad Goswami
Organising Chairperson
Dr. Rama Prosad Goswami

Workshop and hands on training on Biomedical techniques



Organised by

**DEPARTMENT OF BIOCHEMISTRY AND MEDICAL BIOTECHNOLOGY
CALCUTTA SCHOOL OF TROPICAL MEDICINE
KOLKATA**

Certificate of Participation

This is to certify that Mr. / Ms. Snehadip Koley of School Of Tropical Medicine has participated in the "Workshop and hands on training on Biomedical techniques" during February 13th to February 15th, 2017 sponsored by Department of Biotechnology, Government of West Bengal under BOOST-II scheme 2014-2015.

Nandita Basu

Prof. Nandita Basu
Director
Calcutta School of Tropical Medicine
Kolkata

Bibhuti Saha

Prof. Bibhuti Saha
Dean of Student Affairs
Calcutta School of Tropical Medicine
Kolkata

Mandira Mukherjee

Dr. Mandira Mukherjee
Head,
Dept. of Biochemistry & Medical Biotechnology
Calcutta School of Tropical Medicine,
Kolkata